Novel roles for cytokinin in the responses to high light and circadian stress

Dissertation

zur Erlangung des akademischen Grades

des Doktors der Naturwissenschaften (Dr. rer. nat.)

eingereicht im Fachbereich Biologie, Chemie, Pharmazie

der Freien Universität Berlin

vorgelegt von

Silvia Nitschke

aus Brandenburg an der Havel

2014

Diese Arbeit wurde von Januar 2009 bis November 2014 unter der Leitung von Prof. Dr. Thomas Schmülling am Institut für Biologie/Angewandte Genetik der Freien Universität Berlin angefertigt.

1. Gutachter: Prof. Dr. Thomas Schmülling

2. Gutachter: Prof. Dr. Wolfgang Schuster

Disputation am 10.03.2015

Table of contents

List of tables

List of figures

List of abbreviations

A	Absorbance
AAO3	*ABSCISIC ALDEHYDE OXIDASE 3*
ABA	Abscisic acid
ABA	*ABA DEFICIENT*
ACD6	*ACCELERATED CELL DEATH 6*
ACT2	*ACTIN 2*
AHK	*ARABIDOPSIS HISTIDINE KINASE*
AOC2	*ALLENE OXIDE CYCLASE 2*
AOS	*ALLENE OXIDE CYCLASE 2*
APS	Ammonium persulfate
APX	Ascorbate peroxidase
AS	Alternative splicing
ASC	Ascorbate; ascorbic acid
ARR	*ARABIDOPSIS RESPONSE REGULATOR*
ATP	Adenosine triphosphate
BAP1	*BON ASSOCIATION PROTEIN 1*
BFN1	*BIFUNCTIONAL NUCLEASE 1*
BI1	*BAX INHIBITOR 1*
bp	Base pair(s)
BSA	Bovine serum albumin
°C	Degree Celsius
Ca^{2+}	Calcium ion
CAB2	*CHLOROPHYLL A/B BINDING PROTEIN 2*
CaMV	Cauliflower mosaic virus
CAPS	Cleaved amplified polymorphic sequence
CAT2	*CATALASE 2*
CCA1	*CIRCADIAN CLOCK ASSOCIATED 1*
cDNA	Complementary DNA
CHE	*CCA1 HIKING EXPEDITION*
$^3Chl^*$	Excited triplet chlorophyll
CI51	*51 KDA SUBUNIT OF COMPLEX I*
CKX	*CYTOKININ OXIDASE/DEHYDROGENASE*
CL	Continuous light (In most cases it refers to the "standard regime" of 32 hours CL.)
COI1	*CORONATINE-INSENSITIVE 1*
Col-0	Ecotype/accession Columbia-0
COR47	*COLD-REGULATED 47*
CRE1	*CYTOKININ RESPONSE 1* (=*AHK4*)
CRF	*CYTOKININ RESPONSE FACTOR*
Ct	Threshold cycle
CTP	*C-TERMINAL PROCESSING PEPTIDASE*
cZ	*cis*-zeatin
D	Dark (period); deuterium (only in chapter 2.10.1)
DEGP	*DEG PROTEASE*

DHA	Dehydroascorbate
DHAR	Dehydroascorbate reductase
DMAPP	Dimethylallyl diphosphate
DMSO	Dimethyl sulfoxide
DNA	Desoxyribonucleic acid
DNase	Desoxyribonuclease
dNTP	Desoxyribonucleoside-tri-phosphate
DTT	Dithiothreitol
DW	Dry weight
e.g.	*exempli gratia* (Latin: for example)
EC	Evening complex
EDS1	*ENHANCED DISEASE SUSCEPTIBILITY 1*
EDTA	Ethylenediaminetetraacetic acid
ELF	*EARLY FLOWERING*
EMS	Ethyl methanesulfonate
ER	Endoplasmic reticulum
ERF1	*ETHYLENE RESPONSE FACTOR 1*
ESI	Electrospray ionization
et al.	*et alii* (Latin: and others)
F1, F2, F3…	First, second, third… filial generation after a cross
Fe	Iron
FER1	*FERRITIN 1*
Fig./Figs.	Figure/figures
FTSH	*FTSH PROTEASE*
F_v/F_m	Maximum quantum efficiency of photosystem II photochemistry
FW	Fresh weight
g	Gram
GOI	Gene of interest
GR	Glutathione reductase
GSH	Reduced glutathione
GSSG	Oxidized glutathione
GSR	General stress response
h	Hour
H_2O_2	Hydrogen peroxide
HEPES	4-(2-Hydroxyethyl)piperazineethanesulfonic acid
HL	High light
HOTE	Hydroxyoctadecatrienoic acid
HPLC-MS	High performance liquid chromatography-mass spectrometry
HR	Hypersensitive response
i.e.	*id est* (Latin: that is)
ICS1	*ISOCHORISMATE SYNTHASE 1*
Ile	Isoleucine
iP	Isopentenyl adenine
IPT	Isopentenyltransferase
JA	Jasmonic acid
JAR1	*JASMONATE-RESISTANT 1*

JAZ	*JASMONATE ZIM DOMAIN*
KMD	*KISS ME DEADLY*
KOR1	*KORRIGAN 1*
L	Light (period); lincomycin (only in Fig. 3.3)
LD	Long-day (light/dark: 16 h/8 h)
L*er*	Ecotype/accession Landsberg *erecta*
Leu	Leucine
LHY	*LATE ELONGATED HYPOCOTYL*
LOX	*LIPOXYGENASE*
LPO	Lipid peroxidation
LUC	Luciferase
LUX (*PCL1*)	*LUX ARRHYTHMO* (*PHYTOCLOCK 1*)
m	Meter
MCP2D	*METACASPASE 2D*
MDA	Malondialdehyde
MDHAR	Monodehydroascorbate reductase
MeJA	Methyl jasmonate
MES	2-(*N*-morpholino)ethanesulfonic acid
min	Minute
mRNA	Messenger RNA
MS	Murashige and Skoog
MYC2 (*JIN1*)	*JASMONATE-INSENSITIVE 1*
n	Random sample
NAD(P)H	Reduced nicotinamide adenine dinucleotide (phosphate)
NBT	Nitroblue-tetrazolium
NDHI	Encodes subunit of the chloroplast NAD(P)H dehydrogenase complex
NPQ	Non-photochemical quenching
NPR	*NONEXPRESSOR OF PR GENES*
$^1O_2$	Singlet oxygen
$O_2^{\bullet -}$	Superoxide anion radical
OPC	Oxo-pentenyl-cyclopentane
OPDA	Oxo-phytodienoic acid
OPR3	*OPDA REDUCTASE 3*
ORA59	*OCTADECANOID-RESPONSIVE ARABIDOPSIS 59*
ORAC	Oxygen radical antioxidant capacity
p	Probability (p value)
PCD	Programmed cell death
PCESR	Plant core environmental stress response
PHY	*PHYTOCHROME*
POX	Peroxidase
PP2AA2	*PROTEIN PHOSPHATASE 2A SUBUNIT A2*
ppm	Parts per million
PR	*PATHOGENESIS-RELATED GENE*
PRR	*PSEUDO RESPONSE REGULATOR*
PSII	Photosystem II
PSBA	*PHOTOSYSTEM II REACTION CENTER PROTEIN A* (encoding the D1 protein)

PUFA	Polyunsaturated fatty acid
qRT-PCR	Quantitative reverse transcription polymerase chain reaction
RBCL	Large subunit of ribulose-1,5-bisphosphate carboxylase/oxygenase (RuBisCO)
RBOH	*RESPIRATORY BURST OXIDASE HOMOLOGUES*
RD29B	*RESPONSIVE TO DESSICATION 29B*
RNA	Ribonucleic acid
RNase	Ribonuclease
ROCK	*REPRESSOR OF CYTOKININ DEFICIENCY*
ROS	Reactive oxygen species
ROX	6-Carboxyl-X-rhodamine
rpm	Rounds per minute
RPS3	Encodes a chloroplast ribosomal protein S3, a constituent of the small subunit of the ribosomal complex
RT	Room temperature
sec	second
SA	Salicylic acid
SAG12	*SENESCENCE-ASSOCIATED GENE 12*
SAM	Shoot apical meristem
SAND (*MON1*)	*MONENSIN SENSITIVITY 1* (encoding a SAND family protein)
SCF	SKP1/Cullin/F-box
SD	Short-day (light/dark: 8 h/16 h)
SDS	Sodium dodecyl sulfate
SE	Standard error
SID1	*SALICYLIC ACID INDUCTION DEFICIENT 1*
SOD	Superoxide dismutase
TAFII15	*TBP-ASSOCIATED FACTOR II 15*
TBA	Thiobarbituric acid
T-DNA	Transfer DNA
TEMED	*N*,*N*,*N*′,*N*′-Tetramethylethane-1,2-diamine
TIC	*TIME FOR COFFEE*
TOC1	*TIMING OF CAB EXPRESSION 1* (= *PRR1*)
tRNA	Transfer RNA
tZ	*trans*-zeatin
U	Unit
UBC10	*UBIQUITIN-CONJUGATING ENZYME 10*
UV	Ultraviolet
vs.	*versus* (Latin: in comparison with)
Ws	Ecotype/accession Wassilewskija
WT	Wild type (if not stated otherwise, Col-0)
ZAT12 (*RHL41*)	*RESPONSIVE TO HIGH LIGHT 41* (encoding a zinc-finger transcription factor)
ZTL	*ZEITLUPE*

1 Introduction

As the title of my thesis reveals, the role of cytokinin has been investigated under two different kinds of stress, high light and "circadian stress". In contrast to high light stress which is a well-characterized form of abiotic stress, "circadian stress" was a previously unknown phenomenon that was newly discovered in the course of this work. Circadian stress regimes negatively affect the circadian clock, influence the reactive oxygen species gene network as well as the jasmonic acid pathway, and can cause a cell death phenotype. Therefore, the following chapters will deal with a number of topics, including cytokinin and high light stress, but also the circadian clock, reactive oxygen species, programmed cell death, and jasmonic acid. The circadian clock section, however, will be the major part of the Introduction due to its high complexity and, moreover, high relevance for many aspects of this work.

1.1 Cytokinin

Cytokinins belong to a major class of plant hormones and regulate various aspects of growth and development. The great number of cytokinin-regulated processes reflects how multifunctional cytokinins are being involved in regulating cell division, shoot initiation and growth, apical dominance, sink-source relationships, leaf senescence, nutrient uptake, phyllotaxis as well as vascular, gametophyte, and embryonic development (Werner and Schmülling, 2009; Hwang *et al.*, 2012; Kieber and Schaller, 2014). Even a role for cytokinins during adverse environmental conditions, either of biotic or of abiotic origin, is emerging more and more (Ha *et al.*, 2012; O'Brien and Benková, 2013). The following sections will give an overview of cytokinin synthesis, metabolism, and signaling. Moreover, suppressors of the cytokinin deficieny syndrome as well as the role of cytokinin in light-regulated processes and under abiotic stresses will be briefly introduced.

1.1.1 Cytokinin synthesis

Cytokinins are derived from the compound adenine and are distinguished by their differences in N^6 substitutions at the purine ring and the specific modifications on these side chains as well as by differences in the modifications at the N^3, N^7, and N^9 position (e.g. ribose or ribose-phosphate at N^9 forming ribonucleosides or -nucleotides, respectively). Depending on the chemical structure of the N^6-attached side chain, cytokinins are classified as isoprenoid or aromatic cytokinins. The most abundant forms carry an isoprenoid substitution, including isopentenyl (iP)-type and zeatin-type cytokinins. The hydroxylation of the isopentenyl side chain in the zeatin-type can occur on either of the methyl groups, which results in the *cis* or *trans* configurated *cis*-zeatin (cZ) or *trans*-zeatin (tZ), respectively (Mok and Mok, 2001; Sakakibara, 2006). The iP- and tZ-type cytokinins are the major and most active forms, while cZ-type cytokinins were thought to be of minor importance in *Arabidopsis* (Spíchal *et al.*, 2004; Romanov *et al.*, 2006; Heyl *et al.*, 2012; Miyawaki *et al.*, 2006). However, a more recent study revealed that cZ-type cytokinins play an important role in primary root growth and vascular

development since cZ-deficient *Arabidopsis* plants (*ipt2,9*) develop shorter primary roots with aberrant vasculature (Köllmer *et al.*, 2014).

The central enzymes of cytokinin metabolism have been identified in *Arabidopsis*. The initial and rate-limiting step is catalyzed by isopentenyltransferases (IPTs) using the isopentenyl precursor dimethylallyl diphosphate (DMAPP) and either adenosine phosphate (IPT1, IPT3, and IPT4-8) or tRNA (IPT2 and IPT9) as substrate (Kakimoto *et al.*, 2001; Takei *et al.*, 2001; Miyawaki *et al.*, 2006). The different *IPT* genes display tissue-specific expression patterns, but together their expression domains are distributed throughout the whole plant, including below-ground and above-ground organs (Miyawaki *et al.*, 2004; Takei *et al.*, 2004a). The proteins also differ in terms of subcellular localization (Kasahara *et al.*, 2004). Kasahara and colleagues could show that IPT1, IPT3, IPT5 and IPT8 are localized in the chloroplast suggesting that cytokinin biosynthesis, in large part, occurs in plastids. The same study revealed that IPT2 and IPT4 are localized in the cytosol, while IPT7 is located in mitochondria. Intriguingly, the localization of IPT3 is dependent on its modification by farnesylation (Galichet *et al.*, 2008). Farnesylation directs IPT3 to the nucleus and the cytosol despite the presence of an N-terminal chloroplast transit peptide which was described by Kasahara *et al.* (2004). Only the non-farnesylated IPT3 protein is located in the plastids. The modification influences not only the protein localization but also the catalytic activity: the farnesylated IPT3 produces more iP and the non-farnesylated protein more tZ. Moreover, the farnesyl acceptor site is essential for its general enzymatic activity (Galichet *et al.*, 2008). In *Arabidopsis IPT3*, *IPT5*, and *IPT7* are the most highly expressed *IPT* genes during the vegetative phase, while *IPT1* expression is also present but at a low level (Miyawaki *et al.*, 2006). Miyawaki and colleagues studied the corresponding mutant plants and found that the respective IPT enzymes act in a highly redundant fashion. The *ipt3,5,7* triple and *ipt1,3,5,7* quadruple mutants exhibited strong effects on shoot and root phenotypes, as characterized by retarded shoot and enhanced root growth, respectively (Miyawaki *et al.*, 2006). However, a closer look on the respective single and double mutants also revealed distinct (lateral root) phenotypes in these plants (Chang *et al.*, 2013).

The formation of cZ entirely depends on the prenylation of tRNA by one of the two tRNA-IPTs and is completed by subsequent hydrolysis (Miyawaki *et al.*, 2006). In contrast, adenosine phosphate-IPTs catalyze the formation of iP-ribonucleotides either as tri-, di- or monophosphate (iPRTP, iPRDP, or iPRMP). The corresponding tZ-ribonucleotides are generated by hydroxylation of the isopentenyl side chain in the iP-forms which is catalyzed by CYP735As, cytochrome P450 monooxygenases (Takei *et al.*, 2004b). Nucleoside monophosphates (either iPRMP or tZRMP) can be directly converted into the biologically active free nucleobases (iP and tZ) by the LONELY GUY (LOG) family of cytokinin ribonucleoside monophosphate phosphoribohydrolase enzymes which catalyze the production of the majority of free nucleobases in *Arabidopsis* (Kurakawa *et al.*, 2007; Kuroha *et al.*, 2009; Tokunaga *et al.*, 2012).

1.1.2 Cytokinin metabolism

The abundance of biologically active cytokinins is not only modulated by their *de novo* synthesis. A second option is to reduce the amount of active cytokinins. This is mainly achieved by their degradation or inactivation. The degradation of cytokinins is completely irreversible and catalyzed by cytokinin oxidases/dehydrogenases (CKXs). The inactivation occurs by conjugation to sugars by glycosyltransferases (UGTs) and can be transient or stable.

1.1.2.1 Cytokinin inactivation by conjugation

Cytokinins can be *N*-glycosylated at the N^3, N^7, and N^9 position of the purine ring, while *O*-glycosylation takes place at the hydroxyl group in the isoprenoid side chain of zeatin-type cytokinins (Sakakibara, 2006). The *O*-glucosides can be converted into active cytokinins by β-glucosidases, suggesting that the *O*-glucosylated cytokinins represent inactive storage forms of the hormone (Brzobohaty *et al.*, 1993). Since *N*-glucosides are resistant to glucosidases, it is assumed that *N*-modifications represent the irreversibly inactive cytokinins (Mok and Mok, 2001; Sakakibara, 2006).

1.1.2.2 Cytokinin degradation by CKX enzymes

Cytokinins are catabolized in a single FAD-dependent enzymatic step by CKX enzymes. In this reaction the N^6-attached side chain is removed yielding adenine or adenosine as well as the corresponding aldehyde (Brownlee *et al.*, 1975; McGaw and Horgan, 1983; Bilyeu *et al.*, 2001). The *Arabidopsis* genome contains seven *CKX* genes (*CKX1*-*CKX7*) (Bilyeu *et al.*, 2001; Schmülling *et al.*, 2003; Werner *et al.*, 2003). Interestingly, CKX2 and CKX4 show high substrate specificity for iP and tZ and their nucleosides, while other CKX isoforms, such as CKX1 or CKX3, show preferences for the degradation of cytokinin glucosides or nucleotides, respectively (Galuszka *et al.*, 2007; Kowalska *et al.*, 2010).

The different CKX isoforms not only differ in their biochemical properties (Galuszka *et al.*, 2007; Kowalska *et al.*, 2010), they also show distinct patterns of expression and subcellular localizations (Werner *et al.*, 2003; Werner *et al.*, 2006; Köllmer *et al.*, 2014). The individual *CKX* genes are expressed in various tissues and during different developmental stages in the shoot and root. The overall expression levels of all *CKX* genes in *Arabidopsis* are very low (Werner *et al.*, 2006) but the expression of several *CKX* genes is induced rapidly upon cytokinin treatment (Brenner *et al.*, 2012; Bhargava *et al.*, 2013). Their expression domains are small and partially overlap with the expression domains of *IPT* genes, suggesting a strict regulation between cytokinin synthesis and degradation in these areas to enable cytokinin responses that are locally restricted, i.e. paracrine or autocrine (Werner *et al.*, 2006). On the other hand, *CKX6* is expressed in the vasculature, which suggests a function in the regulation of cytokinin as a long-distance signal (Werner *et al.*, 2003). CKX7 is located in the cytosol (Köllmer *et al.*, 2014). CKX1 and CKX3 were found to be located in the vacuole (Werner *et al.*, 2003), although more recent data indicate CKX1 localization in the endoplasmic reticulum (ER) (unpublished results, Dr. Henriette Weber). CKX2 and CKX4 to CKX6 are very likely located extracellularly in the apoplast following secretion through the secretory pathway (Bilyeu *et al.*, 2001; Werner *et al.*, 2001; 2003).

The 35S promoter-driven overexpression of *CKX* genes has been used as a tool to study the consequences of cytokinin deficiency for physiological and developmental processes. It provided a lot of insight into cytokinin-dependent mechanisms in tobacco and *Arabidopsis* (Werner *et al.*, 2001; 2003). In *Arabidopsis* the overexpression of *CKX1*, *CKX3*, and *CKX5* leads to the most severe shoot phenotypes, while the phenotypes are somewhat less pronounced in *CKX2*, *CKX4*, and *CKX6* overexpressors. However, qualitatively the phenotypic changes are very similar for all *CKX* genes. The most obvious phenotypic changes are a retarded development of smaller shoots due to the diminished activity of apical meristems and leaf primordia as well as enhanced primary root growth and lateral root formation (Werner *et al.*, 2003). These different responses reflect the opposite roles of cytokinin during shoot and root development. This is similar to the phenotypes of the *ipt3,5,7 and ipt1,3,5,7* multiple mutants (see 1.1.1) and indicates positive regulation of shoot growth and negative regulation of root growth by cytokinin. The combination of all aberrant phenotypic traits in *CKX* overexpressing cytokinin-deficient plants is defined as cytokinin deficiency syndrome.

1.1.3 Cytokinin signaling

The cytokinin status of a plant is not only defined by the amount of cytokinin present. It is just as decisive how cytokinin is perceived, how efficient the signal is transmitted into the cell or cytoplasm and how well it is transduced and interpreted as an appropriate signal for the cell.

The cytokinin signal is transduced by a multistep phosphorelay mechanism which shares commonalities with the bacterial two-component system (TCS). The simple TCS in bacteria literally consists of two components and involves only one phosporelay. The higher complexity in cytokinin signaling is characterized by a higher number of participating components and hence more phosphorelay steps (Hwang *et al.*, 2002; Kieber and Schaller, 2014). Therefore, it comprises more targets to precisely regulate the intensity of the signal and, moreover, enables a much higher amplification of the original stimulus.

A schematic model of the cytokinin signaling cascade is shown in Figure 1.1. In *Arabidopsis*, the phosphorelay is initiated by the autophosphorylation of histidine kinase receptors (AHKs) at a histidine residue in their protein kinase domain (red) in response to cytokinin recognition. The phosphoryl group is transferred intramolecularly to an aspartate residue of the receptor receiver domain (green) and further relayed to histidine phosphotransfer proteins (AHPs). Among the six *AHP* genes *AHP6* encodes a pseudo-phosphotransfer protein which lacks the conserved histidine residue. It inhibits the phosphorelay presumably by interacting with activated receptors and/or response regulators and is, therefore, a negative regulator of cytokinin signaling (Mähönen *et al.*, 2006; Bishopp *et al.*, 2011). The other AHP family members transmit the signal (the phosphoryl group) to B-type response regulators (ARRs), which is the last of four sequential phosphorylation events. Once activated by phosphorylation, B-type ARRs act as transcription factors and bind with their C-terminal DNA-binding domain (turquoise) to promoter regions of cytokinin target genes. Among the target genes are A-type *ARR* genes, which encode proteins resembling B-type ARRs having a phospho-accepting receiver domain but lacking the DNA-binding domain. Therefore, they can compete with B-type ARRs for the phosphoryl

residue from AHPs by directly interacting with them (Dortay *et al.*, 2006). Hence, they cause feedback inhibition by interfering with AHP-mediated signaling (Werner and Schmülling, 2009).

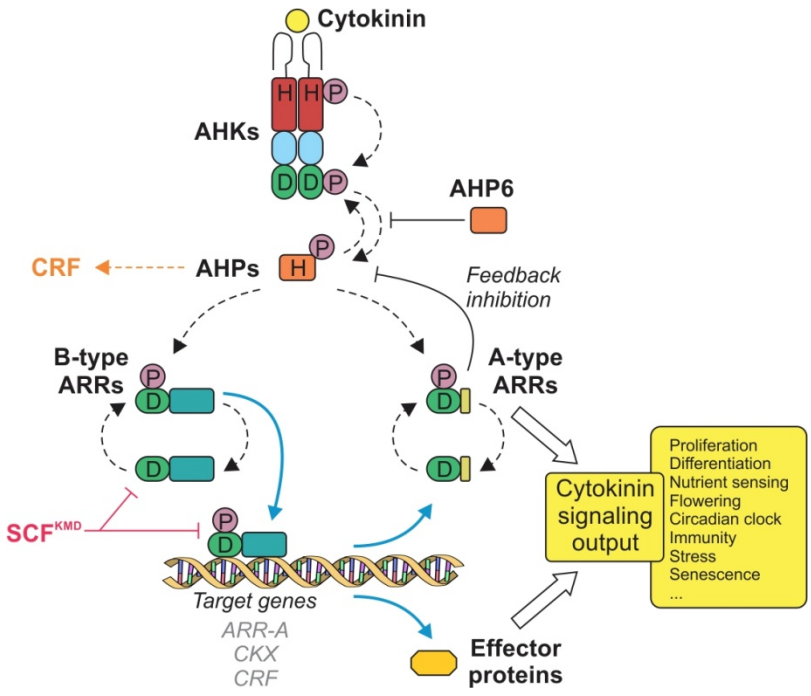

Figure 1.1: Schematic overview of the cytokinin signaling pathway in *Arabidopsis*.

Biologically active cytokinins bind to the CHASE domain of histidine kinase receptors (AHKs) which results in the autophosphorylation of a histidine (H) residue in the protein kinase domain (red). The phosphoryl group is relayed intramolecularly to an aspartate (D) residue in the receptor receiver domain (green) and then to a conserved H residue of the histidine phosphotransfer proteins (AHPs). AHP proteins transfer the phosphoryl group to B-type or A-type response regulators (ARRs). An exception is AHP6, a pseudo-phosphotransfer protein that lacks the conserved H residue and inhibits the phosphorelay. Once activated by phosphorylation, B-type ARRs act as transcription factors binding with their C-terminal DNA-binding domain (turquoise) to promoter regions of target genes including A-type *ARR* genes (*ARR-A*) and other cytokinin-related genes (e.g. *CKX* and *CRF* genes). Cytokinin response factors (CRFs) act in an additional branch of cytokinin signaling parallel to that of B-type ARRs modulating overlapping and unique target genes (Rashotte *et al.*, 2006). One function of the A-type ARRs is to repress signaling in a negative feedback loop. Together with other effector proteins, they determine the signaling output of the pathway. The abundance of B-type ARR proteins is controlled by the ubiquitin proteasome pathway using KISS ME DEADLY (KMD) F-box proteins (Kim *et al.*, 2013). The figure has been adapted from Werner and Schmülling (2009). SCF, SKP1/Cullin/F-box; *CKX*, *CYTOKININ OXIDASE/DEHYDROGENASE*.

1.1.3.1 Cytokinin receptors

The cytokinin receptor family in *Arabidopsis* is composed of three histidine kinases: AHK2, AHK3 (Hwang and Sheen, 2001), and CRE1/AHK4 (also called WOL; Mähönen *et al.*, 2000; Inoue *et al.*, 2001; Yamada *et al.*, 2001; Suzuki *et al.*, 2001; Ueguchi *et al.*, 2001b). They are mainly localized in the ER (Wulfetange *et al.*, 2011; Caesar *et al.*, 2011), presumably oriented in a way that signal perception takes places within the ER and the signal transduction cascade is initiated at the cytosolic part of the receptor. Expression of all three receptor genes can be detected in all organs throughout the plant, albeit with different abundances (Nishimura *et al.*, 2004; Higuchi *et al.*, 2004). *CRE1/AHK4* is mainly expressed in the root, especially in the vasculature and in pericycle cells (Mähönen *et al.*, 2000; Higuchi *et al.*, 2004). Weaker *CRE1/AHK4* expression can be detected also in various shoot tissues, most pronounced in restricted areas of the shoot apical meristem (Gordon *et al.*, 2009;

Chickarmane *et al.*, 2012). In contrast, *AHK2* and *AHK3* genes are more highly expressed in aerial parts, including leaf veins, petioles, inflorescence stems, flowers, and siliques. *AHK3* is rather ubiquitously expressed, e.g. in the whole leaf and also in roots, while *AHK2* exhibits only moderate expression in the root (Nishimura *et al.*, 2004; Higuchi *et al.*, 2004).

There is functional redundancy among the three *AHK* genes, which is consistent with the large overlap in the expression sites of the receptor genes. An indication for the redundant action of the receptors during physiological and developmental processes is the observation that single and even some double receptor mutants do not show strong plant phenotypes, whereas the triple mutants are severely impaired in their development, including extreme dwarfism and infertility (Nishimura *et al.*, 2004; Higuchi *et al.*, 2004; Riefler *et al.*, 2006). Nevertheless, there are also some specific functions which could be attributed to single receptors. For instance, CRE1/AHK4 is of great importance for primary root growth as well as for plant regeneration in tissue culture (Inoue *et al.*, 2001; Higuchi *et al.*, 2004; Nishimura *et al.*, 2004). In contrast, AHK3 plays a predominant role in shoot-related aspects of plant development, including shoot and leaf growth, photomorphogenesis, and leaf senescence (Nishimura *et al.*, 2004; Riefler *et al.*, 2006; Kim *et al.*, 2006). Although AHK2 does not seem to act alone, it strongly contributes to many AHK3-mediated responses, which can be deduced from the enhanced phenotypes in *ahk2 ahk3* double mutants as compared with *ahk3* single mutants. Combined loss of AHK2 and AHK3 leads to the most prominent changes in vegetative growth, especially of shoot development. The result is a dwarfed phenotype which is not observed in the other double receptor mutants (Nishimura *et al.*, 2004; Riefler *et al.*, 2006).

All receptors bind bioactive cytokinins with high affinity and exhibit low affinity for adenine itself or inactive conjugates. However, they show differences in their relative affinities for bioactive cytokinins. For instance, AHK3 shows a high affinity for tZ, but a relatively low affinity for iP, while CRE1/AHK4 and AHK2 both exhibit a high affinity for tZ and iP (Spíchal *et al.*, 2004; Romanov *et al.*, 2006; Stolz *et al.*, 2011). This is interesting because tZ and iP might have specific roles in root-to-shoot communication (Hirose *et al.*, 2008; Matsumoto-Kitano *et al.*, 2008; Kudo *et al.*, 2010). Since AHK3 is predominantly expressed in leaves, it might specifically perceive long-distance cytokinin signals in the form of xylem-transported tZ from the roots (Heyl *et al.*, 2012).

1.1.3.2 Response regulators

The *Arabidopsis* genome encodes 23 functional ARRs which are divided into three groups (type A, B, and C). As outlined above (see 1.1.3; Fig. 1.1) A-type and B-type ARRs are involved in cytokinin signaling. There are 11 B-type *ARR* genes, *ARR1*, *ARR2*, *ARR10-ARR14* and *ARR18-ARR21* and 10 A-type *ARR* genes, *ARR3-ARR9* and *ARR15-ARR17*, in *Arabidopsis* (Heyl and Schmülling, 2003; Kieber and Schaller, 2014).

Genetic analyses based on loss-of-function mutations indicate that the five B-type ARRs ARR1, ARR2, ARR10, ARR11, and ARR12 play predominant roles in cytokinin signaling (Mason *et al.*, 2005; Yokoyama *et al.*, 2007; Ishida *et al.*, 2008a). As with other components in the cytokinin signaling pathway, there is high functional redundancy in this gene family. Substantial defects in cytokinin-

dependent developmental processes are only observed in multiple mutant combinations. One exception is ARR2, which plays an important role in the cytokinin-dependent delay of leaf senescence (Kim *et al.*, 2006) and the support of salicylic acid (SA) signaling by cytokinin (Choi *et al.*, 2010). However, apart from that, ARR1, ARR10, and ARR12 together regulate the majority of typical cytokinin responses (Mason *et al.*, 2005; Ishida *et al.*, 2008a; Agyros *et al.*, 2008). *arr1,10,12* triple mutants exhibit a strongly reduced shoot development, aborted primary root growth, enlarged seed size, and defects in female gametophyte development (Ishida *et al.*, 2008a; Agyros *et al.*, 2008; Cheng *et al.*, 2013), phenotypes that are reminiscent of the *ahk* receptor triple mutants (Higuchi *et al.*, 2004; Nishimura *et al.*, 2004; Riefler *et al.*, 2006). The potential action of B-type ARRs is not only controlled by their activation through phosphorylation. Another mechanism to regulate their function is the control of their abundance. B-type ARR proteins are degraded by the ubiquitin proteasome pathway (Kim *et al.*, 2012; Kim *et al.*, 2013). In this regard, cytokinin signaling exhibits similarities to other hormonal pathways such as those for auxin, jasmonic acid, gibberellins, and ethylene, in which key transcriptional regulators undergo proteasomal degradation (Santner and Estelle, 2010). The degradation is controlled by the SKP1/Cullin/F-box protein (SCF) E3 ubiquitin ligase complex in which the specificity for ARRs is determined by the four-member family of F-box proteins KISS ME DEADLY (KMD) (Kim *et al.*, 2013 and indicated in Fig. 1.1).

The A-type *ARR* genes belong to the target genes of B-type ARRs and, consistently, their promoters contain B-type ARR binding sites, which were shown to be crucial for induction by cytokinin (Taniguchi *et al.*, 2007; Ramireddy *et al.*, 2013). Therefore, A-type *ARRs* are primary response genes in the cytokinin signaling cascade which are rapidly upregulated by cytokinin, some showing induction already after 10-15 minutes (D'Agostino *et al.*, 2000; Rashotte *et al.*, 2003; Brenner *et al.*, 2005). Moreover, they are among the genes with the most robust changes in expression levels in response to cytokinin as revealed by meta-analyses of multiple microarray datasets (Brenner *et al.*, 2012; Bhargava *et al.*, 2013). Due to their strong regulation by cytokinin, A-type *ARR* promoters were used for the construction of reporter lines to monitor cytokinin signaling (D'Agostino *et al.*, 2000; Hwang and Sheen, 2001). Meanwhile, these reporter lines are progressively replaced by the more sensitive and specific TCS-GFP reporter, which uses concatemers of the sole core binding site of A-type *ARR* promoters (Müller and Sheen, 2008; Zürcher *et al.*, 2013).

Genetic analyses indicate that ARR3-ARR9 and ARR15 function as negative regulators of cytokinin signaling (Kiba *et al.*, 2003; To *et al.*, 2004; 2007; Leibfried *et al.*, 2005; Lee *et al.*, 2007a). They show a high functional overlap which is in part due to the fact that they exhibit high similarities in their amino acid sequences (D'Agostino *et al.*, 2000). Only double or higher-order mutants significantly reflect the negative effect of A-type ARRs on cytokinin responses, as they exhibit increased cytokinin sensitivity in common cytokinin assays (To *et al.*, 2004). These mutants show also a higher sensitivity in terms of cytokinin-regulated gene expression (To *et al.*, 2004), while the overexpression of *ARR7* for example has a repressive effect on various groups of cytokinin-regulated genes (Lee *et al.*, 2007a). This negative effect, as described above, is due to the ability of A-type ARRs to receive phosphoryl groups, thereby competing with the true transcriptional regulators, the B-type ARRs. But cytokinin not only arranges the inhibition of its own signal by transcriptional regulation of A-type ARRs. Once the

multistep phosphorelay is initiated by cytokinin, A-type ARR proteins are stabilized in a phosphorylation-dependent manner, increasing their abundance (To *et al.*, 2007).

The ability to regulate cytokinin signaling in a positive and negative manner is crucial to ensure the spatiotemporal precision needed for diverse physiological and developmental processes regulated by the hormone. The negative regulation not only serves to prevent continued activation of the cytokinin pathway, it is also decisive for the modulation of cytokinin sensitivity to allow responses to varying cytokinin concentrations in different tissues or under changing conditions.

In addition to the B-type ARR-dependent branch of cytokinin signaling, at least one additional branch exists. It comprises another class of transcription factors; the cytokinin response factors (CRFs). CRFs belong to a family of six closely related APETALA2 (AP2) transcription factors. Three CRFs (CRF2, CRF5, and CRF6) are upregulated by cytokinin (as indicated in Fig. 1.1), which is B-type ARR-dependent. All six CRFs rapidly translocate to the nucleus in response to cytokinin treatment, which is solely dependent on AHKs and AHPs. This relocalization of CRF proteins defines a branch point in the cytokinin TCS transduction pathway (Rashotte *et al.*, 2006; Fig. 1.1). The connection of CRFs with the cytokinin TCS was underpinned by interaction studies (Cutcliffe *et al.*, 2011), revealing direct interactions with AHPs. CRFs affect unique target genes as well as a set of cytokinin-responsive genes that largely overlaps with B-type ARR targets (Rashotte *et al.*, 2006).

1.1.4 Suppressors of the cytokinin deficiency syndrome

In order to identify genes which are involved in the development of the cytokinin deficiency syndrome in *CKX1* overexpressing plants a suppressor EMS mutagenesis screen was conducted by Dr. I. Bartrina (Bartrina, 2006). Mutants were isolated based on the reversion of the stunted shoot phenotype which is characteristic for *35S:CKX1* transgenic plants and were called *repressors of cytokinin deficiency* (*rock*). So far only the strongest *CKX1* suppressor mutants (*rock1* to *rock4)* were further characterized and the mutated loci identified *via* map-based cloning.

The *rock1* mutation (line #120; Bartrina, 2006) leads to a recessive loss-of-function allele of *AT5G65000*. This *ROCK1* gene was predicted to encode a nucleotide sugar transporter. Indeed, nucleotide sugars could be transported by ROCK1. The data further revealed that ROCK1 plays a role in the glycosylation of CKX proteins in the ER which is important for their activity. The *ROCK1* loss-of-function was shown to reduce the CKX activity, thereby counteracting the *CKX1* overexpression and increasing the cytokinin content (Niemann, 2013).

Furthermore, it was revealed that *rock2* and *rock3* plants (lines #205 and #608; Bartrina, 2006) carry mutations in the *AHK2* and *AHK3* receptor genes, respectively. Both are dominant gain-of-function alleles that lead to constitutive activity of the respective receptor. Hence, the cytokinin deficiency in *35S:CKX1* plants could be circumvented by cytokinin-independent activation of cytokinin signaling (Jensen, 2013).

Lastly, the *rock4* mutation (line #29; Bartrina, 2006) leads to a dominant gain-of-function allele of the *IPT3* gene. The mutation causes a premature stop codon which results in a truncated IPT3 protein version (Jensen, 2013) which lacks the predicted farnesylation site described by Galichet *et al.* (2008).

1.1.5 Cytokinin, light, and abiotic stresses

Cytokinin influences several light-regulated processes. Exogenous cytokinin or endogenously elevated cytokinin levels can partially mimic photomorphogenesis in etiolated seedlings (Chory *et al.,* 1994; Lochmanová *et al*., 2008) which is mediated by functional cytokinin signaling through the transcription factors ARR1, ARR10 and ARR12 (Argyros *et al*., 2008). A direct link between light and cytokinin signaling was revealed by the interaction between PHYTOCHROME B (PHYB) and ARR4 stabilizing the active Pfr-form of PHYB (Sweere *et al.*, 2001). Moreover, cytokinin acts as a signal for photosynthetic acclimation to canopy light gradients (Boonman *et al.*, 2007) and shade-induced leaf growth arrest (Carabelli *et al.*, 2007). Exogenous application of cytokinin stimulates the transition from etioplast to chloroplast in detached leaves and cell cultures, increases the rate of grana and stroma lamella and extends the life span of chloroplasts (Parthier, 1979; Čatský *et al.*, 1993; Mok, 1994; Chernyad'ev, 2000; Synková *et al*., 2006). The cytokinin receptor triple mutant as well as the B-type *ARR* triple mutant *arr1,10,12* exhibit reduced chlorophyll levels, consistent with the positive function of cytokinin in chloroplast development and maintenance (Riefler *et al.*, 2006; Argyros *et al*., 2008). Furthermore, cytokinin influences photosynthesis and related processes (Kusnetsov *et al.,* 1998; Synková *et al*., 1999; Yaronskaya *et al.*, 2006; Cortleven and Valcke, 2012) which is at least partially due to control of gene expression (Rashotte *et al*., 2003; Brenner *et al*., 2005; Zubo *et al*., 2005; 2008).

Recent research has provided evidence that cytokinins are also involved in stress responses (Argueso *et al.*, 2009; Ha *et al*., 2012; O'Brien and Benková, 2013). For instance, cytokinins are known to induce an antioxidant protection mechanism in chloroplasts (Procházková *et al*., 2008) and alter the transcript levels of many stress-inducible genes (Rashotte *et al.*, 2003; Brenner *et al.*, 2005; Brenner and Schmülling, 2012; Brenner *et al*., 2012; Bhargava *et al*., 2013). Several reports revealed a role for cytokinins during drought, cold, salt, and osmotic stress (Tran *et al*., 2007; 2010; Rivero *et al.,* 2007; Jeon *et al.*, 2010; Nishiyama *et al.*, 2011a; 2013; Kang *et al.*, 2013; Jeon and Kim, 2013; Macková *et al*., 2013) which in part was shown to be linked to a crosstalk between cytokinin and abscisic acid (Tran *et al.*, 2007; Nishiyama *et al.*, 2011a; Ha *et al.*, 2012). However, a role for cytokinin during light stress has not yet been described.

1.2 Plants under high light stress

During their life cycle, plants are subjected to continuously changing environmental conditions, including various stress factors. Abiotic stresses such as heat, drought, cold, salt, osmotic, high light (HL), or mechanical stress can severely affect plant development, growth, fertility, and productivity. One of the multiple consequences under several environmental stresses is photoinhibition, the inhibition of the activity of photosystem II (PSII) (Murata *et al.*, 2007). Photoinhibition results in the reduction of the photosynthetic capacity, thereby limiting plant growth and productivity (Takahashi and

Badger, 2011). The extent of photoinhibition is determined by the balance between the rate of photodamage to PSII and the rate of its repair (Takahashi and Murata, 2008). Interestingly, stress factors, such as cold, heat, high salinity, and oxidative stress accelerate photoinhibition by inhibiting PSII repair (Murata *et al.*, 2007; Takahashi and Murata, 2008), while excessive light absorption under HL stress causes both direct photodamage and the impairment of the repair cycle (Tyystjärvi, 2008; Takahashi and Badger, 2011).

1.2.1 Light as stress factor

1.2.1.1 High light stress causes photoinhibition

Light is the driving force of photosynthesis which enables the conversion of light energy into chemical energy through the photosynthetic transport of electrons within the thylakoid membranes. This chemical energy is then used for the fixation of carbon dioxide (CO_2) in the Calvin cycle. These photosynthetic processes yield molecular oxygen (O_2) and glucose and are, therefore, indispensable for life on earth. However, light acts as stress factor at the same time, causing photoinhibition (Barber and Andersson, 1992; Aro *et al.*, 1993; Adir *et al.*, 2003; Yamamoto *et al.*, 2008).

An excess of light present under HL stress causes severe photodamage to PSII, especially to the highly vulnerable reaction center protein D1 (Aro *et al.*, 1993; 2005). It has been demonstrated that light-induced photodamage is strictly proportional to light intensity (Tyystjärvi and Aro, 1996). If the rate of photodamage exceeds the rate of repair, the result is photoinhibition (Nishiyama *et al.*, 2006). Therefore, a high rate of PSII (especially D1) repair is required which involves D1 degradation, its removal from the damaged PSII complex, and its replacement by *de novo* synthesis (Aro *et al.*, 1993; 2005; Kato and Sakamoto, 2009; see 1.2.1.2). However, under HL the rate of repair is not high enough to fully prevent photoinhibition (Nishiyama *et al.*, 2006). It is even depressed due to the inhibition of D1 *de novo* synthesis and reactive oxygen species (ROS), which are metabolic byproducts of photosynthesis, are thought to be the major reason for that (Takahashi and Badger, 2011). Under HL, the excess of light energy leads to an amplification of ROS production, including singlet oxygen ($^1O_2$), the superoxide anion radical ($O_2^{\bullet -}$), and hydrogen peroxide (H_2O_2) (Apel and Hirt, 2004; Krieger-Liszkay, 2005; Gill and Tuteja, 2010; for more details on ROS production see chapter 1.4.1). Although it is still controversial whether photodamage to PSII can at least in part be attributed to a direct action of ROS, especially to $^1O_2$ (Krieger-Liszkay *et al.*, 2008; Edelman and Mattoo, 2008; Tyystjärvi, 2008; Takahashi and Badger, 2011), it seems that the main consequence of increased ROS levels under HL stress is the suppression of PSII protein synthesis, including D1 (Nishiyama *et al.*, 2006; Takahashi and Murata, 2008; Tyystjärvi, 2008; Takahashi and Badger, 2011). Therefore, light-induced ROS production strongly accelerates photoinhibition by interfering with PSII repair. In conclusion, under HL photoinhibition is caused by both, increased photodamage to PSII and reduced PSII (D1) repair.

1.2.1.2 Photo-protective mechanisms

Plants have developed a large array of mechanisms for the protection against the detrimental effects of light. D1 repair is one of the most important mechanisms protecting the plant from photoinhibition. A high rate of D1 turnover is indispensable, especially under HL conditions because of the unavoidable photodamage. Damaged D1 proteins are continuously degraded and replaced by *de novo* synthesized D1 in a process called the D1 repair cycle (Aro *et al.*, 1993; 2005; Baena-González and Aro, 2002; Munné-Bosch *et al.*, 2013). This cycle consists of several steps (Kato and Sakamoto, 2009; Takahashi and Badger, 2011): (1) migration of the damaged PSII from the grana to the stroma lamellae and partial disassembly of PSII, (2) proteolytic degradation of the damaged D1 protein by FTSH and DEG proteases, (3) *de novo* synthesis of precursor D1 protein (preD1) encoded by the *PSBA* gene of the chloroplast genome and co-translational insertion into the thylakoid membrane, (4) maturation of preD1 by C-terminal processing catalyzed by the C-terminal processing peptidase (CTP), and (5) migration to the grana thylakoids and reassembly to a fully functional PSII complex.

In order to avoid oxidative stress, enzymatic and non-enzymatic ROS scavenging systems are active to protect plants against photoinhibition and minimize the inhibition of D1 repair (Nishiyama *et al.*, 2001; 2006; Takahashi and Badger, 2011). For example, in chloroplasts membrane-bound tocopherols and carotenoids efficiently scavenge $^1O_2$ at PSII, while superoxide dismutase (SOD) and ascorbate peroxidase (APX) play an important role in degrading $O_2^{\bullet -}$ and H_2O_2, respectively (Triantaphylidès and Havaux, 2009; Gill and Tuteja, 2010; Sharma *et al.*, 2012). A more detailed overview of the ROS scavenging system in plants is given elsewhere (see 1.4.2).

An efficient D1 repair and a functional ROS scavenging system do not suffice under HL conditions. To avoid net photoinhibition, plants have additional photo-protection mechanisms such as light avoidance (e.g. leaf and chloroplast movements), cyclic electron flow, the photorespiratory pathway, and the dissipation of excess light energy as thermal energy (Takahashi and Badger, 2011). The latter process is also known as non-photochemical quenching (NPQ) and involves the xanthophyll class of carotenoids (Jahns and Holzwarth, 2012). Especially zeaxanthin which is formed in the so-called xanthophyll cycle from violaxanthin *via* antheraxanthin under light is a key player in the dissipation of excess light energy as heat (Demmig-Adams and Adams, 1996; Niyogi *et al.*, 1998). NPQ reduces photodamage (Li *et al.*, 2002; Sarvikas *et al.*, 2006) and efficiently prevents the formation of $^1O_2$ by quenching the first excited singlet state of chlorophyll ($^1Chl^*$), which can be directly converted to excited triplet chlorophyll ($^3Chl^*$) acting as efficient photosensitizer resulting in $^1O_2$ generation (Triantaphylidès and Havaux, 2009; Jahns and Holzwarth, 2012).

Taken together, the multitude of photo-protective mechanisms emphasizes the relevance of photoinhibition and the importance of counteraction to ensure proper plant performance.

1.3 The circadian clock

This chapter focuses on the circadian clock, its relevance for plant fitness as well as its features and characteristics. Moreover, the molecular clock mechanism in *Arabidopsis* will be described and

examples for clock input and output pathways will be given. The ultimate section deals with the interplay between circadian timekeeping and phytohormone pathways and, in more detail, with the current knowledge of the crosstalk between the circadian oscillator and cytokinin.

1.3.1 The circadian clock enhances plant fitness

The circadian clock synchronizes internal events with external cues. As internal molecular timekeeper it measures the periodic changes in the environment, including daily or seasonal fluctuations, and is reset on a daily basis (McClung, 2011; Nagel and Kay, 2012; Carré and Veflingstad, 2013; Sanchez and Yanovsky, 2013). Once consonant with the environmental cycles, it can precisely coordinate diverse physiological and developmental processes in a time-of-day- or time-of-year-specific manner, thereby optimizing organismal biology and thus enhancing fitness (Green *et al.*, 2002; Michael *et al.*, 2003a; Dodd *et al.*, 2005; Graf *et al.*, 2010; Yerushalmi *et al.*, 2011; Lai *et al.*, 2012).

The consequences of circadian dysfunction on health and diseases are under active investigation in human research. The close connection between disrupted circadian rhythms and cancer, diabetes, cardiovascular dysfunction, sleep disorders and mental illnesses underpins the enormous relevance of precisely "ticking" clocks for human health. Even healthy individuals can be confronted with the negative effects of desynchronized circadian clocks during jet lag or shift work (Gillette *et al.*, 2013).

Similarly, plant circadian clocks which are consonant with the environmental cycles also promote fitness and survival (Resco *et al.*, 2009; Yerushalmi and Green, 2009). Key traits for plant fitness, including seed germination, gas exchange, growth and flowering, are under clock control (Yakir *et al.*, 2007a; Resco *et al.*, 2009). The study of plants with impaired clock function has yielded experimental evidence that correctly regulated circadian timing confers an adaptive advantage. Indeed, a functioning circadian clock is decisive for the onset of flowering and general viability. Plants with clocks that are impaired in the ability to properly anticipate daily changes in the environment show dramatic shifts in flowering time (either too early or extremely late) and have low-viability phenotypes under certain photoperiods (Green *et al.*, 2002; Nagel and Kay, 2012). Furthermore, it has been demonstrated that plants with clocks that match the environmental light-dark cycle have increased chlorophyll contents and an enhanced photosynthetic capacity. This has been suggested to cause higher biomass accumulation and better survival in these plants (Dodd *et al.*, 2005). It has also been shown that accurate circadian timing enables an optimized rate of starch degradation during the night which ensures optimal carbon utilization and hence continued growth during nighttime (Graf *et al.*, 2010; Graf and Smith, 2011). In a recent study, a genetically heterogenous F2 population was generated segregating for the *prr5* and *prr9* allele which confer circadian rhythms shorter or longer, respectively, than the normal 24-hour periodicity. These F2 plants were grown under short or long light-dark cycles (T-cycles, light-dark cycles with a period different from 24 hours) of 20 and 28 hours, respectively, under different "competition strengths" (different seedling densities). Among the resulting F3 seedlings the frequency of the *prr9* allele was higher in the progeny of F2 plants grown under 28-hour cycles but significantly decreased in the progeny of F2 plants competing under 20-hour cycles (Yerushalmi *et al.*, 2011). Dodd and colleagues have shown a similar fitness benefit for clock mutants

under T-cycles that matched their internal rhythm. The short-period mutant (*toc1*) outcompeted the long-period mutant (*ztl*) under short T-cycles and the opposite was observed under long T-cycles (Dodd *et al.*, 2005; for explanations of clock parameters such as "period" see 1.3.3). Intriguingly, altered clock function contributes to increased growth, called hybrid vigor or heterosis, observed in hybrids and allopolyploids (Ni *et al.*, 2009). There is also growing evidence that the function of the circadian clock is crucial for the modulation of biotic and abiotic stress responses (Roden and Ingle, 2009; Sanchez *et al.*, 2011). For instance, the circadian clock optimizes jasmonate-mediated defense against herbivory (Goodspeed *et al.*, 2012; Goodspeed *et al.*, 2013) and coordinates the timing of plant immune responses (Wang *et al.*, 2011; Zhang *et al.*, 2013). It controls cold-responsive genes, thereby determining cold acclimation and freezing tolerance (Bieniawska *et al.*, 2008; Dong *et al.*, 2011), and is also important under drought (Legnaioli *et al.*, 2009), salt, and osmotic stress (Kant *et al.*, 2008; Nakamichi *et al.*, 2009). More recently, the circadian clock has been shown to regulate reactive oxygen species (ROS) homeostasis and oxidative stress responses (Lai *et al.*, 2012).

1.3.2 Commonalities between circadian systems of diverse species

The clock components are not conserved between different kingdoms of life, i.e. the molecular architecture of the core oscillator in plants is completely different from that in fungi, insects, and mammals (Young and Kay, 2001; Heintzen and Liu, 2007; Mohawk *et al.*, 2012; Pokhilko *et al.*, 2012). In higher plants the circadian oscillator is even more complex than that of other circadian systems, since multiple clock components are members of multigene families with partially redundant functions. Nevertheless, circadian clocks exhibit remarkably similar properties across all organisms studied (Carré and Veflingstad, 2013): 1) Circadian rhythms persist even in the absence of environmental cues (free run; e.g. constant light or darkness) which means that they are endogenously generated and self-sustaining. 2) They show temperature compensation which means that the periodicity (i.e. the pace) of the rhythm remains relatively constant across a wide range of ambient temperatures. 3) Clocks are entrained by strong environmental signals (e.g. light-dark or temperature cycles), i.e. clock-driven rhythms are responsive to resetting stimuli and thereby synchronized with the environment. 4) The ability of the environment to reset the clock is dependent on the precise time of day because this resetting response to stimuli is itself under circadian control. Thus, it is "gated" by the circadian clock which means that the circadian clock regulates its own sensitivity to environmental stimuli in a time-of-day-specific manner (McClung, 2006; Harmer, 2009).

1.3.3 Analysis of circadian rhythms – some characteristics and definitions

Before molecular and genetic processes within the circadian clock network were unravelled, rhythmic parameters such as leaf movements served to study the performance of the core oscillator in plants. These movements were not merely responses to environmental cycles since they persisted under constant conditions and exhibited periods of only approximately 24 hours, which established the term "circadian" ("circa", about; "dies", day) (McClung, 2006; Harmer, 2009). A breakthrough for chronobiological research in plants was the establishment of *Arabidopsis thaliana* as model plant as well as the observation that the light-harvesting *CHLOROPHYLL A/B BINDING PROTEIN* (*CAB*; also

called *LHCB*) gene and also other genes are under circadian control (McClung, 2006). Another important milestone was the use of the firefly luciferase (*LUC*) gene as reporter of clock gene expression (e.g. *CAB2*), a powerful tool for the discovery of clock mutants by analyzing alterations in bioluminescence rhythms (Millar *et al.*, 1995a; 1995b).

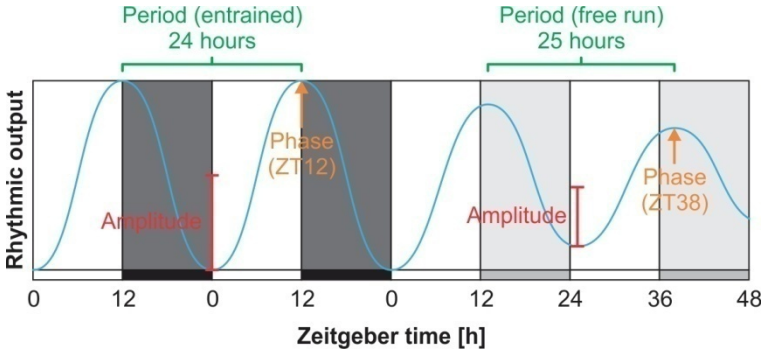

Figure 1.2: Rhythmic outputs from the circadian clock can be described by mathematical parameters.
An idealized rhythmic clock output is depicted (blue) in light-dark cycles (entraining conditions, white and dark gray) and constant light (free-running conditions, white and light gray). The entrained period of this output is exactly 24 hours, while in constant conditions the free-running period of 25 hours is revealed. The phase refers to a specific point in the cycle and is often expressed as zeitgeber time (ZT) counting from the last entraining stimulus (zeitgeber). The amplitude of the rhythm is defined as one-half the peak-to-trough distance (adapted from Harmer, 2009).

Bioluminescence rhythms as well as other rhythmic parameters are usually studied under constant conditions after the clock has been entrained to 24-hour rhythms of diurnal cycles (e.g. 12 h light/12 h dark). These so-called free-running conditions enable to distinguish between diurnal rhythms which are solely driven by the entraining environmental cycles and circadian rhythms which are endogenously generated and self-sustaining (as defined in 1.3.2). Hence, only rhythms that persist in the free run are circadian rhythms, are clock-driven and therefore reflect clock performance. Circadian rhythms often exhibit oscillation patterns similar to sinusoidal waves and can be described by mathematical terms such as period, phase, and amplitude (Fig. 1.2; McClung, 2006; Hanano *et al.*, 2006; Harmer, 2009). The "period" is defined as the time that is required for one complete cycle and usually refers to the distance between peaks. Under entraining conditions, which synchronize the circadian clock with the environment on a regular basis, the period matches the environmental cycle which is usually 24 hours. In contrast, the non-24-hour periodicity of the endogenous circadian clock is revealed under free-running conditions which lack synchronizing stimuli. The "phase" refers to a specific point in the cycle (e.g. the peak or the trough) and is commonly expressed as a specific time of day, often defined as zeitgeber time (ZT). Zeitgeber is German for "time giver", which is an entraining environmental signal such as light that resets the clock to synchronize the internal timing with the surrounding world. The dark-to-light transition at dawn is such a zeitgeber and is usually defined as ZT0. The "amplitude" in most cases is defined as one-half the peak-to-trough distance and reflects the robustness of the oscillation wave. In some studies, "2 amplitudes" or "peak-to-trough ratios" are measured to express the absolute change, maxima to minima, within the oscillation wave.

The free run not only helps identifying genes that are clock-regulated. It is also applied, as already mentioned above, to measure clock outputs such as *CAB2* oscillations to screen for clock mutants and/or further characterize the relevance of a certain allele for clock function. Among the genes, that

are frequently used to study the clock output and hence monitor clock performance are also *CAT2 or CAT3* (Zhong and McClung, 1996; Zhong *et al.*, 1998; Michael *et al.*, 2003b) and *CCR2*/*GRP7* (Strayer *et al.*, 2000; Doyle *et al.*, 2002). A gene is considered to encode a core oscillator component if its loss-of-function or overexpression results in a severe lack of clock precision such as strong changes in periodicity (i.e. short- or long-period phenotypes) or even arrhythmicity (i.e. the circadian oscillations are strongly irregular or even completely abolished) (Nagel and Kay, 2012). Another key test for an oscillator component is derived from the prediction that its abundance should determine the phase (McClung, 2011). Indeed, pulses of *Arabidopsis* clock components, driven by an inducible promoter, shift the phase of the clock (Knowles *et al.*, 2008).

1.3.4 Organization of the plant circadian system

Initially, the circadian system was defined as unidirectional path, made of three modules: 1) Clock input pathways that reset the clock, which include entrainment signals such as light and temperature; 2) the central circadian clock or oscillator that generates circadian rhythms, and 3) clock output pathways, including clock-driven rhythmic changes in transcript or protein abundances, the control of enzymatic activities, alterations in metabolic levels, which affect a magnitude of developmental and physiological processes. However, this is an oversimplified model. Increasing evidence instead suggests that the circadian system is a complex, interconnected, and reciprocally regulated network. The core oscillator consists of multiple coupled feedback loops. Clock-driven rhythms (e.g. oscillating gene expression) have multiple roles, determining oscillator function itself as well as acting in clock input and output pathways. Clock outputs often feedback to the oscillator, serving as an input signal thereby modulating the function of the central oscillator. Input pathways regulate clock components and directly affect clock outputs, but the perception of the input signals is modulated by the circadian clock in a process called gating (Harmer, 2009; Pruneda-Paz and Kay, 2010). Gating mechanisms are not only involved in setting the susceptibility of the clock to certain inputs to a specific time of day. Gating is a widely used mechanism by which the clock operates to vary the intensity of responses to stimuli of equal strength applied at a different time of day. Among the processes which are "gated" (modulated; i.e. the "gate" is either closed or open for a certain pathway) by the circadian clock are stomatal movements, low-temperature as well as hormonal responses (Hotta *et al.*, 2007; Robertson *et al.*, 2009).

1.3.5 The molecular clock mechanism

Circadian systems in eukaryotes, although comprised of species-specific components, share similarities in the basic organization. In general, the core oscillator is composed of interconnected feedback loops, comprising transcription-based interactions in which reciprocal regulation is accomplished by positive and negative regulators. In *Arabidopsis*, the transcriptional feedback loops are well characterized and are a critical part of the oscillatory mechanism. Nevertheless, their coupling with post-transcriptional, post-translational, and chromatin modifications also plays an important role (McClung, 2011; Nagel and Kay, 2012; Carré and Veflingstad, 2013).

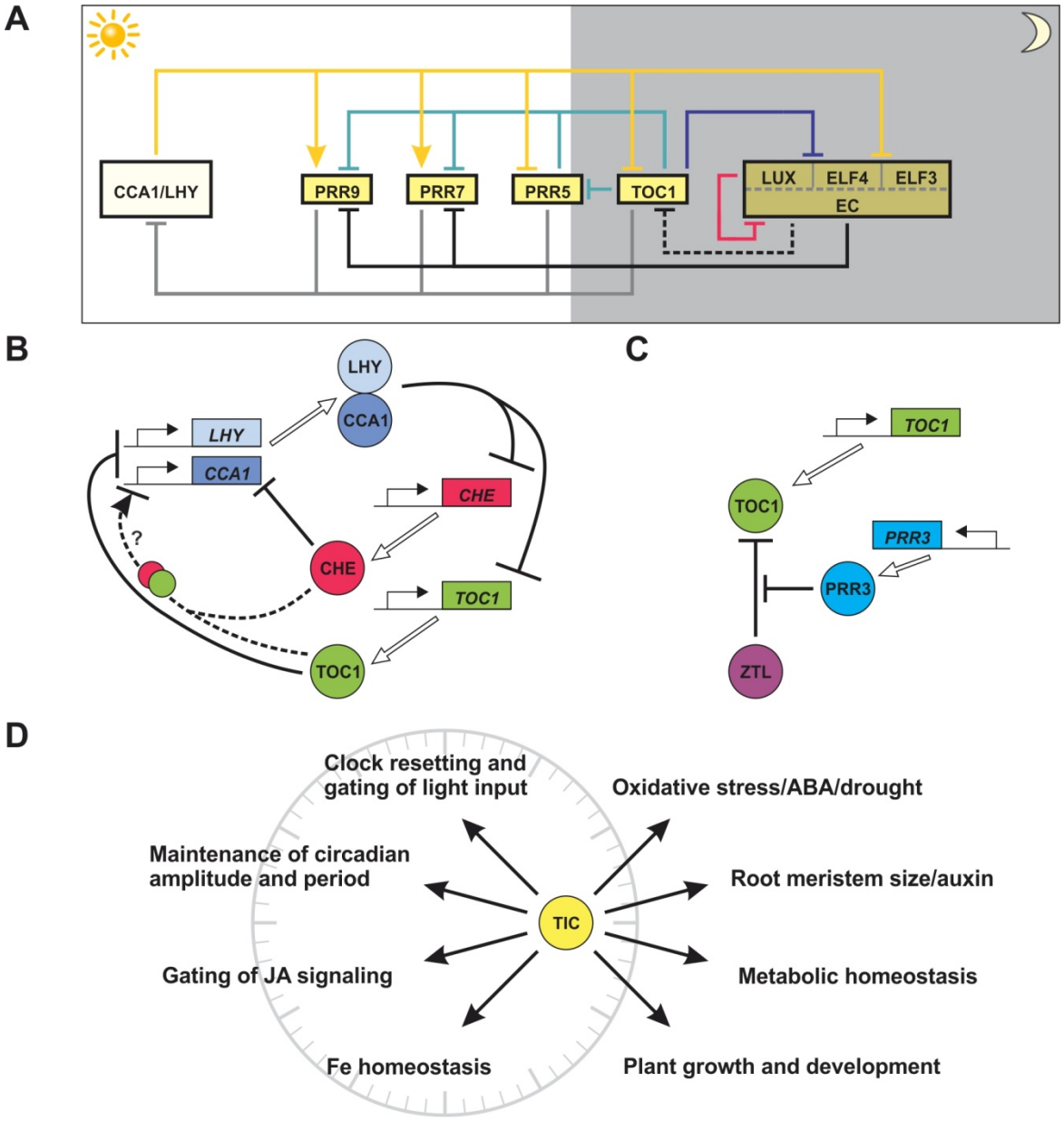

Figure 1.3: The plant circadian clock and associated components.

A, The transcriptional network of the plant circadian clock. At dawn *CCA1* and *LHY* are expressed simultaneously acting to induce *PRR7* and *PRR9* as well as to repress *TOC1* and *PRR5* expression (yellow lines). During the course of the day *CCA1* and *LHY* expression is inhibited through the action of *PRR9*, *PRR7*, *PRR5*, and *PRR1*/*TOC1* that are sequentially expressed (gray lines). During the night the expression of the *PRR* genes is shut down through the action of the evening complex (EC) which is comprised of ELF3, ELF4, and LUX proteins (black lines) which enables *CCA1*/*LHY* transcription to rise again at the following dawn. The effect of the EC on *TOC1* may be indirect (indicated by a dashed line). The latter components of the PRR cascade act repressive onto the earlier ones enabling their temporal separation and expression as consecutive waves (turquoise lines). The EC inhibits its own action forming an evening-specific, direct autoregulatory loop to ensure only transient EC activity (pink line). The EC also feeds back to its own expression *via* TOC1 (blue line) (adapted from Carré and Veflingstad, 2013). **B**-**D**, Additional clock and clock-associated components. CHE is a clock component forming an additional feedback loop within the clock. *CHE* expression is repressed by CCA1 and LHY and CHE represses *CCA1* expression. The precise role of the TOC1-CHE protein-protein interaction is not clear (**B**). PRR3 belongs to the family of pseudo response regulators and regulates TOC1 abundance in the leaf vasculature preventing ZTL-mediated proteasomal degradation of TOC1 (**C**). TIC is a clock-associated component that influences clock performance and clock-controlled processes (indicated by the schematic clock) as well as redox and metabolic homeostasis, plant growth and development (**D**). All abbreviations used here are explained in the list at the beginning of this work.

1.3.5.1 Interconnected transcriptional circuits within the Arabidopsis clock

So far, more than 20 clock or clock-associated components have been identified in *Arabidopsis* (Hsu and Harmer, 2014). Recent studies enabled to incorporate many of the known regulators of circadian rhythms into comprehensive clock models (Pokhilko, 2012; Nagel and Kay, 2012; Carré and Veflingstad, 2013; Hsu and Harmer, 2014). However, although the current models are already quite complex and combine a variety of experimental data, they are still very limited in representing the full complexity of the clock network. Some components could not yet be fit into the clock circuitry. Moreover, certain regulatory mechanisms (i.e. other than transcription-based regulations) are not integrated leading to an oversimplification of the network (Bujdoso and Davis, 2013; McClung, 2014). The clock model depicted in Figure 1.3A is also far from complete. It illustrates the main and well established connections within the core oscillator, emphasizing the transcriptional relationships.

1.3.5.2 The morning genes CCA1 and LHY

CIRCADIAN CLOCK ASSOCIATED 1 (CCA1) and LATE ELONGATED HYPOCOTYL (LHY) are closely related members of the REVEILLE (RVE) family of MYB transcription factors. All 11 family members share the sequence motif SHAQKYF within their DNA-binding domains which enables binding at the evening element (EE; AAAATATCT) in promoter regions of target genes (Rawat *et al.*, 2009). Both transcription factors, CCA1 and LHY, are morning-phased clock components. Their transcript levels peak simultaneously early around dawn, and protein levels follow with a lag of approximately two hours (Wang and Tobin, 1998; Schaffer *et al.*, 1998; Kim *et al.*, 2003). Their loss-of-function results in short-period phenotypes, and overexpression of both genes confers arrhythmicity in multiple outputs and represses the expression of both the endogenous *CCA1* and *LHY* genes (Wang and Tobin, 1998; Green and Tobin, 1999; Schaffer *et al.*, 1998; Fowler *et al.*, 1999; Alabadí *et al.*, 2002; Mizoguchi *et al.*, 2002). Interestingly, the lack of both components leads to even more pronounced phenotypes, including even shorter periodicity than in either single mutant or rather arrhythmicity for some outputs (Alabadí *et al.*, 2002; Mizoguchi *et al.*, 2002). This clearly points to a synergistic function of CCA1 and LHY within the core oscillator. Indeed, they not only form homodimers, they also physically interact with each other to form heterodimers (Lu *et al.*, 2009; Yakir *et al.*, 2009) and specifically bind to a cis-element, the EE, within the *TIMING OF CAB EXPRESSION 1* (*TOC1)* promoter to directly repress *TOC1* expression (Alabadí *et al.*, 2001; Perales and Más, 2007).

1.3.5.3 The evening gene TOC1

TOC1 belongs to the family of pseudo response regulators (see 1.3.5.4.) and is also a core oscillator of the circadian network since its action is required for proper clock function. It is an evening-phased component and its loss-of-function also results in a short-period phenotype, while overexpression of *TOC1* leads to arrhythmic clock outputs (Millar *et al.*, 1995a; Strayer *et al.*, 2000; Makino *et al.*, 2002; Más *et al.*, 2003a). Together with TOC1, CCA1 and LHY form the central feedback loop of the oscillator. The role of TOC1 within this core loop has been revisited in three recent studies (Huang *et al.*, 2012; Gendron *et al.*, 2012; Pokhilko *et al.*, 2012). By presenting compelling experimental evidence and

revised computational modeling these studies conclusively showed that TOC1 is not an activator of *CCA1* and *LHY* as originally assumed (Locke *et al.*, 2005; Pokhilko *et al.*, 2010) but extensively acts as a circadian transcriptional repressor. Many TOC1 targets were identified by genome-wide chromatin immunoprecipitation sequencing (ChIP-seq), among them *CCA1* as well as *LHY*. Interestingly, TOC1 binding peaked in antiphase to target gene expression, suggesting a repressive function of TOC1 (Huang *et al.*, 2012). In fact, elevated *TOC1* expression (by ethanol- or hormone-dependent induction) repressed *CCA1* and *LHY* expression (Gendron *et al.*, 2012; Huang *et al.*, 2012) and TOC1 binding to the *CCA1* promoter was shown *in vitro* and *in vivo* (Gendron *et al.*, 2012). Hence, the CCA1/LHY-TOC1 core model has been completely revised to a central oscillator loop which is entirely based on transcriptional repression (Fig. 1.3A; Pokhilko *et al.*, 2012; Nagel and Kay, 2012; Carré and Veflingstad, 2013).

1.3.5.4 The pseudo response regulator family

TOC1 is only one member of the PSEUDO RESPONSE REGULATOR (PRR) family that plays an important role in the circadian clock (Farré and Liu, 2013). The transcript expression of *CCA1*/*LHY* is followed by that of five *PRR* genes. *PRR9* transcript abundance peaks early in the morning and *PRR7*, *PRR5*, *PRR3* and *TOC1* (*PRR1*) transcript levels rise sequentially over the course of the day, also known as circadian waves of *PRR* expression (Matsushika *et al.*, 2000; 2002). PRR protein levels (including TOC1) exhibit also a diurnal and circadian rhythm with their peak expression following their respective transcript expression with a slight lag (Fujiwara *et al.*, 2008). Loss-of-function of each of the *PRR* genes leads to a changed periodicity of circadian rhythms. For instance, *prr9* and *prr7* single mutants display a long-period phenotype, whereas *prr5* mutant plants exhibit shortening of circadian periods (Eriksson *et al.*, 2003; Ito *et al.*, 2003; Michael *et al.*, 2003a; Yamamoto *et al.*, 2003). Furthermore, *prr9 prr7* double mutants show extreme period lengthening, much stronger than could be accounted for by an additive effect, combined with a late flowering phenotype, indicating functional redundancy of both components (Farré *et al.*, 2005; Nakamichi et al., 2005b; Salomé and McClung, 2005a). PRR9 and PRR7 repress *CCA1*/*LHY* expression (Nakamichi *et al.*, 2010) which in turn positively regulate *PRR9* and *PRR7* expression (Farré *et al.*, 2005), forming the so-called morning loop. The repression of *CCA1*/*LHY* is thought to be the main function of PRR proteins within the oscillator. PRR5 also has this repressive function (Nakamichi *et al.*, 2010; Nakamichi *et al.*, 2012). Therefore, *CCA1* and *LHY* are repressed by the consecutive waves of PRR9, PRR7, PRR5, and TOC1 expression from early daytime until midnight (Fig. 1.3A). The lack of PRR9, PRR7, and PRR5 in the corresponding triple mutant results in constitutively high expression of both *CCA1* and *LHY* (Nakamichi *et al.*, 2005b), which is even slightly higher in the *prr9 prr7 prr5 toc1* quadruple mutant (Yamashino *et al.*, 2008). Moreover, the triple and quadruple mutant both flower extremely late (under long-day and short-day conditions) and exhibit severe arrhythmia which involves the abolishment of circadian and, intriguingly, also several diurnal rhythms (Nakamichi *et al.*, 2005b; Yamashino *et al.*, 2008). Yamashino and colleagues showed increased *PRR5* expression levels in a *cca1 lhy* double mutant, which indicates that, similar to *TOC1*, *PRR5* may be repressed by CCA1 and LHY. Interestingly, backward inhibition from later activated PRRs onto earlier expressed *PRR* genes is thought to be important for temporal separation of *PRR*

expression, i.e. it enables their expression as consecutive waves (Carré and Veflingstad, 2013). Due to its restricted spatial expression in the vasculature PRR3 is often excluded in descriptions of the oscillator mechanism and is much less studied than the other four PRR family members. Nevertheless, its role within the circadian clock will be described separately below (see 1.3.5.6).

1.3.5.5 The evening complex formed by LUX, ELF3, and ELF4

Proper regulation of *CCA1* and *LHY* requires additional evening-phased clock components, including LUX ARRHYTHMO/PHYTOCLOCK 1 (LUX/PCL1), EARLY FLOWERING 3 (ELF3), and ELF4 (McClung, 2011; Pokhilko *et al.*, 2012; Nagel and Kay, 2012). These three components exhibit diurnal and circadian rhythmic oscillations and are expressed from the evening throughout the night, whereas the *LUX* expression pattern is temporally largely overlapping with that of *TOC1* (Liu *et al.*, 2001; Doyle *et al.*, 2002; Hazen *et al.*, 2005; Dixon *et al.*, 2011; Carré and Veflingstad, 2013). They interact with each other to form the evening complex (EC) (Nusinow *et al.*, 2011; Chow *et al.*, 2012). The lack of any member of the EC causes an arrhythmicity phenotype which strongly supports their importance as clock components within the so-called evening loop.

The analysis of the respective mutants further revealed that they are all crucial for high-amplitude diurnal and circadian rhythms of both *CCA1* and *LHY* (Doyle *et al.*, 2002; Hazen *et al.*, 2005; Kolmos *et al.*, 2009; Dixon *et al,* 2011). The positive regulation of *CCA1*/*LHY* is achieved by an indirect mechanism. ELF3 and ELF4 associate with LUX in order to bind to target promoters (Dixon *et al.*, 2011; Chow *et al.*, 2012; Herrero *et al.*, 2012; Nagel and Kay, 2012). LUX is a MYB-like GARP transcription factor (Hazen *et al.*, 2005; Onai and Ishiura, 2005) which binds to the LUX binding site (LBS; GATA/TCG) in the *PRR9* and its own promoter inhibiting the expression (Dixon *et al.*, 2011; Helfer *et al.*, 2011; Chow *et al.*, 2012). It is believed that the repression of *PRR9*, *PRR7*, and *TOC1* by the EC leads to the derepression of *CCA1*/*LHY* thereby indirectly promoting their expression (Carré and Veflingstad, 2013). *PRR9* and *PRR7* expression are elevated in *elf3* mutants at time points when the EC components usually peak (Dixon *et al.*, 2011). Also the expression of *TOC1* is upregulated in EC mutants (Kikis *et al.*, 2005; McWatters *et al.*, 2007; Dixon *et al.*, 2011). Therefore, the EC is thought to downregulate *TOC1* expression. However, it is not yet clear if the downregulation is achieved directly or indirectly (indicated by dashed line in Fig. 1.3A). The *TOC1* promoter contains two LBS motifs supporting the idea of direct repression but an association of EC components with the *TOC1* promoter could not be shown so far (Kolmos *et al.*, 2009; Dixon *et al.*, 2011; Helfer *et al.*, 2011; Carré and Veflingstad, 2013). LUX represses itself, as already mentioned, and probably also *ELF4* (Helfer *et al.*, 2011). The ability to repress its own components in an evening-specific autoinhibitory loop may be important to ensure only transient EC activity (Carré and Veflingstad, 2013). *LUX* and *ELF4* were also among the TOC1 target genes identified by ChIP-Seq experiments (Huang *et al.*, 2012). Therefore, the EC may regulate its own expression also indirectly *via* TOC1 (Carré and Veflingstad, 2013). Lastly, also CCA1/LHY inhibit the EC by repressing *LUX*, *ELF3*, and *ELF4* expression through binding to EE or CBS (CCA1-binding site; AAA/CAATCT) motifs within their promoters (Hazen *et al.*, 2005; Kikis *et al.*, 2005; Li *et al.*, 2011; Lu *et al.*, 2012; Nagel and Kay, 2012). Since they act during the night the EC components are considered to be key regulators of nocturnal gene expression. Furthermore, the EC

supports the anticipation of dawn by promoting the expression of the morning genes *CCA1* and *LHY* (Pokhilko *et al.*, 2012).

1.3.5.6 Other indispensable clock- or clock-associated genes

In the following, three components will be described that were not integrated into the core oscillator model shown in Figure 1.3A but are also important for clock function. CCA1 HIKING EXPEDITION (CHE), a TCP transcription factor (also known as TCP21), was identified as clock component involved in the central loop (Fig. 1.3B; Pruneda-Paz *et al.*, 2009). It was shown to bind to the *CCA1* promoter repressing *CCA1* expression. Moreover, a direct interaction with TOC1 was revealed although the precise role of this protein-protein interaction remains to be elucidated (indicated by a question mark in Fig. 1.3B). In addition, it is not clear yet under which conditions CHE acts to regulate *CCA1* expression. The *CHE* promoter contains a CBS (AAAAATCT), to which CCA1 as well as LHY can bind and repress *CHE*. Consistent with its role as clock component, *CHE* additionally shows a partial functional redundancy with *LHY* since the short-period phenotype in a *lhy* single mutant could be significantly enhanced by additional *CHE* loss-of-function (Pruneda-Paz *et al.*, 2009).

PRR3 is often disregarded in current clock models and, therefore, also missing in the clock model depicted in Figure 1.3A because the corresponding gene is only expressed in leaf vascular tissue (Para *et al.*, 2007). However, its function as vascular regulator of TOC1 has been shown (Para *et al.*, 2007) and is summarized in a scheme (Fig. 1.3C). TOC1 stability is controlled by targeted proteasomal degradation through interaction with the F-box protein ZEITLUPE (ZTL) (Más *et al.*, 2003b). This post-translational regulation is important for circadian function and timing. PRR3 prevents ZTL-mediated TOC1 degradation by phosphorylation-dependent binding to the ZTL-interacting domain of TOC1, resulting in an increased amplitude of TOC1 oscillation waves (Para *et al.*, 2007; Fujiwara *et al.*, 2008). Temporally, *PRR3* expression largely overlaps with *TOC1* expression (Matsushika *et al.*, 2000; 2002; Fujiwara *et al.*, 2008). *PRR3* loss-of-function leads to reduced TOC1 accumulation and results in a short-period phenotype, which is most pronounced for the cycling of genes that are specifically expressed in the leaf vasculature (Michael *et al.*, 2003a; Para *et al.*, 2007). Moreover, loss-of-function of both *PRR3* and *TOC1* results in clock phenotypes that are highly similar to that of the *toc1* mutant alone, which reveals that *TOC1* is epistatic to *PRR3* (Para *et al.*, 2007). In contrast, *PRR3* overexpression strongly raised TOC1 protein levels and additionally results in slightly longer periodicity and delayed flowering under long-day (LD) conditions (Murakami *et al.*, 2004; Para *et al.*, 2007). A flowering phenotype, as already mentioned above (see 1.3.1), is often associated with clock dysfunction and, furthermore, indicates an involvement in daylength responses.

TIME FOR COFFEE (TIC) is a nuclear regulator of the circadian clock and, additionally, has multiple other functions important for general plant homeostasis (Fig. 1.3D). TIC is necessary for maintaining the circadian period and amplitude of oscillator and hence clock output gene expression and is of particular importance for high-amplitude rhythmic expression of *LHY* (Hall *et al.*, 2003; Ding *et al.*, 2007) TIC is involved in the gating of light input into the oscillator and resets the clock during the second half of the night prior to dawn. Neither its abundance nor its subcellular localization is regulated

by the circadian clock. *TIC* transcripts and proteins are constitutively expressed and proteins localize to the nucleus. The mechanism by which TIC confers proper rhythmicity is unknown (Hall *et al.*, 2003; Ding *et al.*, 2007). In addition, TIC is a regulator of iron (Fe) homeostasis and regulates the expression of Fe-responsive genes such as *FERRITIN 1* (*FER1*) (Duc *et al.*, 2009). Several recent studies have demonstrated how tightly linked the circadian clock and Fe homeostasis are, being reciprocally regulated (Hong *et al.*, 2013b; Chen *et al.*, 2013b; Salomé *et al.*, 2013). TIC is involved in the clock-regulated gating of jasmonic acid (JA) signaling (Shin *et al.*, 2012). Moreover, TIC has functions in regulating plant growth and development (Sanchez-Villarreal *et al.*, 2013). The lack of *TIC* leads for instance to an altered plastochron and late flowering. Furthermore, *tic* plants are hypersensitive to oxidative stress due to a perturbed redox homeostasis. They are also hypersensitive to abscisic acid (ABA) which confers tolerance to drought stress. Their metabolic homeostasis is dramatically disturbed as reflected by a perturbed carbohydrate accumulation and altered amino acid profiles (Sanchez-Villarreal *et al.*, 2013). Lastly, TIC controls root meristem size by influencing auxin accumulation (Hong *et al.*, 2013a).

1.3.6 Clock input pathways

Chronobiologists study clock performance usually under constant conditions. However, in their natural habitats plants are confronted with a cycling environment. To ensure fitness and survival (see 1.3.1) plants need to optimally anticipate daily changes in order to appropriately regulate physiological and developmental processes in a time-of-day-specific manner. Therefore, the circadian timekeeping machinery gets synchronized with the external environment on a daily basis, called entrainment. The most prominent daily changes include light-dark and temperature cycles, which are the predominant input signals for the oscillator. Both light and temperature act as zeitgebers and set the phase of the clock every cycle in order to adjust the internal rhythm (Millar, 2004; Salomé and McClung, 2005b). To study the ability of light or temperature to reset the phase of the circadian clock so-called phase response curves (PRCs) are recorded. After entrainment to a particular light-dark regime plants are released into constant conditions. Subsequently, subsets of plants receive light or temperature pulses at different times (every few hours) during the subjective day or night in the free run. Phase adjustments (either an advance or a delay) are measured by monitoring the oscillations of clock genes or clock output genes such as *CAB2* or *CCR2*/*GRP7* (Salomé and McClung, 2005b; Hotta *et al.*, 2007).

1.3.6.1 Entrainment by light

Interestingly, the sensitivity to light is gated by the circadian clock which means that light pulses applied during constant conditions change the phase of circadian rhythms to a different extent dependent on the (subjective) time of day. PRCs in response to light pulses show a delay of the phase around dusk and during the early subjective night and an advance of the phase during the latter part of the subjective night. Intriguingly, a "dead zone" without phase changes can be observed during the course of the day, which means that the metaphorical gate is closed to prevent light from constantly resetting the clock during the middle part of the day. This is crucial because light-dark transitions around dusk and dawn give the most valuable information about the time of day while the presence of

light during the course of the day does not confer any information about the time (Devlin and Kay, 2001; McWatters and Devlin, 2011). The gating of light inputs, therefore, enables a high sensitivity of the clock to dawn and dusk signals. This is required for proper entrainment by light and crucial for the integration of daylength information into the oscillator especially during seasonal transitions (Devlin, 2002; Gardner *et al.*, 2006; McWatters and Devlin, 2011).

In diurnal organisms such as *Arabidopsis*, phase advances in response to light signals predominate over phase delays. Therefore, the speed of the oscillator increases under continuous light due to shortening of periodicity (Devlin, 2002). The free-running period of the circadian clock even further decreases as light intensity increases. This is known as Aschoff's rule (Aschoff, 1979) and is probably due to a continuous readjustment of phase as a result of more phase advances than delays (Devlin, 2002). It is thought very likely that the accuracy of synchronization and the maintenance of circadian rhythms rely on both phase responses to transient signals and continuous resetting mechanisms (Gardner *et al.*, 2006).

The resetting mechanism of the clock by light requires the perception of light quality and quantity. Among the common photoreceptors both phytochromes and cryptochromes are important for light input into the oscillator (Frankhauser and Staiger, 2002). In *Arabidopsis*, there are five phytochromes (PHYA-PHYE) which respond to red and far-red light (Nagy and Schäfer, 2002; Quail, 2002) and two cryptochromes (CRY1 and CRY2) sensing blue light (Lin, 2002). Evidence for their involvement comes from the observation that photoreceptor mutants show lengthening of circadian periods under various intensities of red and blue light, respectively (Somers *et al.*, 1998; Devlin and Kay, 2000). This means that a reduced light input causes period lengthening, which is in line with Aschoff's rule describing the inverse relationship between period length and light intensity. Intriguingly, PHYs and CRYs are not only responsible for light input they are also rhythmic outputs of the clock. Their transcript accumulations exhibit diurnal and circadian rhythms (Tóth *et al.*, 2001). Although the phases of maximum expression differ between the photoreceptor genes there is a clear overrepresentation of peak expression in the morning and the evening, respectively. This incidence is thought to be one aspect contributing to the rhythmic sensitivity of the clock to light (Gardner *et al.*, 2006; McWatters and Devlin, 2011).

Interestingly, clock function in *PHY* and *CRY* mutants is only affected under continuous light conditions but not in constant darkness (Devlin and Kay, 2000). This underpins their importance for light signaling and light input into the clock (Jones, 2009), but at the same time it also indicates that they are very unlikely oscillator components themselves (Hotta *et al.*, 2007; Jones, 2009). Moreover, in nature, plants are not exposed to only red or blue light. Strikingly, even the photoreceptor quadruple mutant *cry1 cry2 phyA phyB* exhibits robust diurnal and circadian rhythms of leaf movement under white light, although the morphology of this mutant is reminiscent of an etiolated wild-type seedling reflecting – despite exposure to light – severely compromised light perception (Yanovsky *et al.*, 2000). The same persistence of rhythmicity under continuous white light was also observed in the *PHY* quintuple mutant (Strasser *et al.*, 2010). In conclusion, these data indicate that the photoreceptors are important for the light input pathway but are not required for a functional oscillator neither are they

part of the core circadian clock. However, it is not unconceivable that the remaining PHY or CRY receptors play a role in clock regulation under white light in the respective higher-order mutants.

But how are the light signals transduced to the oscillator? In order to reset the circadian clock oscillator components need to be affected by light (Millar, 2004). This transduction mechanism is still poorly understood. Indeed, light can affect oscillator components on different levels. The transcript levels of the *CCA1*, *LHY*, *PRR9*, *PRR7*, *ELF4* and *GIGANTEA* (*GI*) genes are upregulated by light (Hotta *et al.*, 2007; Jones, 2009) and photoreceptor signaling pathways mediate their induction (Kikis *et al.*, 2005; Pruneda-Paz and Kay, 2010). There are also studies which report about light-regulated transcript stability (for *CCA1*; Yakir *et al.*, 2007b), light-regulated translation (for LHY; Kim *et al.*, 2003) and light-dependent protein stability (for TOC1 and PRR5; Más *et al.*, 2003b; Kiba *et al.*, 2007; Kim *et al.*, 2007). The latter example involves ZTL and is very interesting because ZTL is itself a clock component with light-sensing properties and was, therefore, defined as circadian photoreceptor. Under (blue) light ZTL interacts with GI, while in darkness (after dusk) the interaction partners dissociate and ZTL is free to act as an F-box protein targeting TOC1 and PRR5 for proteasomal degradation (Más *et al.*, 2003b; Kiba *et al.*, 2007; Kim *et al.*, 2007). There are additional clock components for which a role in the light input pathway has been identified. Among them are ELF3, ELF4, and TIC, all of them being involved in the gating of light responses as described in more detail in the following sections.

As already mentioned before (see 1.3.5.5), loss of ELF3 leads to a severe arrhythmicity phenotype. However, this phenotype is conditional because it is observed in continuous light while *elf3* plants are still rhythmic in constant darkness (Hicks *et al.*, 1996; Covington *et al.*, 2001). The overexpression of *ELF3* results in period lengthening which led to the conclusion that ELF3 might function as a negative regulator of light input into the clock (Covington *et al.*, 2001). Moreover, it was shown that the clock in the *elf3-1* loss-of-function mutant stops at subjective dusk during free-running conditions (McWatters *et al.*, 2000) which causes the arrhythmicity in the subjective night. Therefore, ELF3 is proposed to be crucial for the maintenance of circadian rhythms especially as daylength increases towards summer (McWatters and Devlin, 2011). Another indication that daylength sensing is dramatically impaired in *elf3* mutants is the fact that they flower early under LD and short-day (SD) conditions (Zagotta *et al.*, 1992; 1996). Additionally, ELF3 is thought to be a so-called gate-keeper, attenuating light inputs during the night, which is in accordance with its phasing (maximal expression) in wild-type plants (Salomé and McClung, 2005b).

The *elf4* mutant is also defective in circadian gating. *ELF4* loss-of-function leads to similar phenotypes compared with those of *elf3* mutants. Arrhythmia is also observed in the absence of light-dark cycles. However, under continuous light arrhythmicity is reached later than in *elf3* plants (after one cycle) and, moreover, *elf4* mutants show impaired maintenance and accuracy also under constant darkness. ELF4 also acts predominantly during the dark period and loss-of-function results in an "open gate" (sensitivity to resetting light stimuli) especially during the subjective night, when the gate is closed in the wild type. Hence, ELF4 is also a gate-keeper. Furthermore, analyses of *elf4* plants under different light-dark cycles indicated impaired anticipation of dawn and its defect in daylength sensing is also

revealed by its early flowering phenotype under SD conditions (Doyle *et al.*, 2002; McWatters *et al.*, 2007).

Both ELF3 and ELF4 are necessary for light-induced expression of *CCA1* and *LHY* (Kikis *et al.*, 2005). The fact that *CCA1* and *LHY* expression is light-regulated on different levels, as described above, points already to their relevance for entrainment by light. Their importance for the resetting of the circadian clock was further demonstrated by ethanol-inducible pulses of their expression. These pulses of expression are sufficient to induce phase shifts and the resulting PRCs display the common shape as described in the beginning of this chapter (Knowles *et al.*, 2008). Interestingly, *cca1 lhy* double mutants are rhythmic under light-dark cycles showing proper entrainment (Kim *et al.*, 2003; Yamashino *et al.*, 2008; Dixon *et al.*, 2011), but the *cca1 lhy elf3* triple mutant exhibits a severe disruption of diurnal rhythms (Dixon *et al.*, 2011). This clearly underlines the important role of ELF3 for the entrainment by light but also indicates the relevance of a functional evening loop, including the EC (Pokhilko *et al.*, 2012).

As introduced above (see 1.3.5.6), TIC is a clock-associated component with multiple functions. Mutation of *TIC* also leads to a compromised circadian gating of light responses (Hall *et al.*, 2003) abeit somewhat less pronounced than in *elf3* plants (McWatters *et al.*, 2000). Similar to the *elf3* mutants the clock in *tic* mutants stops following release to continuous light. However, this does not occur at dusk as in *elf3* plants but in the mid to late subjective night (Hall *et al.*, 2003) which indicates that TIC acts in the second half of the night to maintain rhythmicity. *tic* single mutants still show anticipation of dawn and are not completely arrhythmic although the amplitude, accuracy and/or periods of circadian rhythms are markedly affected especially for *CCA1* and even more pronounced for *LHY* (Hall *et al.*, 2003; Ding *et al.*, 2007). Both morning genes are already strongly misregulated in *tic* single mutants (i.e. they show a strongly dampened expression and almost complete arrhythmia for *LHY*) under long photoperiods (Ding *et al.*, 2007). However, in combination with *ELF3* or *ELF4* loss-of-function the phenotypes of *tic* mutants are extremely aggravated. The corresponding double mutants (*elf3 tic*, *elf4 tic*) become immediately arrhythmic once they are transferred to continuous light. Moreover, they completely lack anticipation of dawn and dusk under diurnal conditions (Hall *et al.*, 2003; Ding *et al.*, 2007). This combinatorial effect is probably due to a functional overlap between TIC and the two EC components, which usually act at different circadian times (Ding *et al.*, 2007).

Another gene family is known to be involved in the light input pathway, the PRR family. As described above (see 1.3.5.4), both *prr9* and *prr7* mutants exhibit long-period phenotypes which are strongly enhanced in *prr9 prr7* double mutants (Farré *et al.*, 2005; Nakamichi et al., 2005b; Salomé and McClung, 2005a). This indicates a function in the transmission of light signals to the circadian clock following Aschoff's rule. Interestingly, plants lacking the function of multiple *PRR* genes (e.g. *prr9 prr7 prr5* and *prr9 prr7 prr5 toc1*) show strongly impaired diurnal rhythms for *CCA1*, *GI*, *RVE1*, *TOC1*, and *PRR3* being arrhythmic (or constitutive). This, together with the compromised inhibition of hypocotyl elongation in the presence of light, leads to the conclusion that the light signaling pathway is severely attenuated in these plants since they show such a pronounced light insensitivity (Nakamichi *et al.*, 2005b; Ito *et al.*, 2007; Yamashino *et al.*, 2008).

1.3.6.2 Entrainment by temperature and temperature compensation

The circadian clock is also entrained by temperature cycles with amplitudes of at least 4 °C (Salomé and McClung, 2005b). The warm periods correspond to the "day" and the cold periods to the "night". The larger the temperature steps the stronger the amplitudes of the resulting rhythms (McWatters and Devlin, 2011). The entrainment by temperature shares commonalities with the resetting by light. It is also gated by the circadian clock and can be studied by PRCs resulting in very similar phase response curves. However, it is rather difficult to study temperature entrainment because so many biochemical processes are temperature-sensitive (Millar, 2004; Gardner *et al.*, 2006; Hotta *et al.*, 2007).

Although temperature affects biochemical reactions, the periodicity of the clock is largely unaffected by temperature changes in the physiological range (from 12 to 27 °C in *Arabidopsis*; Hotta *et al.*, 2007). This is called temperature compensation and is an important feature of biological clocks. It would be fatal if the clock, as internal timekeeper, would increase its pace in the same way as biochemical reactions do increase their rate with increasing temperatures (McWatters and Devlin, 2011). There is limited understanding of the mechanism behind this phenomenon. It is known that the amplitudes and peak levels of the oscillator components *CCA1*, *LHY*, and *GI* are crucial (Gould *et al.*, 2006). Additionally, PRR9 and PRR7 play a role in temperature compensation by regulating *CCA1* and *LHY* (Salomé *et al.*, 2010).

Interestingly, really low temperatures have a negative effect on the circadian oscillator and on clock-driven rhythmic gene expression. The amplitude of oscillator gene cycling is dramatically reduced and oscillations of output genes get disrupted at 4 °C under diurnal (light-dark) conditions. Furthermore, complete arrhythmicity is observed at 4 °C under free-running (constant light) conditions (Bieniawska *et al.*, 2008). These results not only show that temperature can affect the functionality of the circadian clock, but also indicate that the circadian clock reaches its limits to properly compensate for temperature changes at very low temperatures.

1.3.7 Clock output pathways

1.3.7.1 Regulation of developmental and physiological processes by the circadian clock

The circadian clock drives rhythmicity of many biological events throughout the life cycle of a plant. Rhythmic leaf movements are only one among many clock-regulated processes – termed clock outputs. During development from the seed to a seed-producing flowering plant, the clock influences germination and growth. Moreover, it controls the reproductive development by determining the transition from vegetative to reproductive growth in a daylength-dependent manner as well as the efficiency of pollination by regulating flower opening (Yakir *et al.*, 2007a; de Montaigu *et al.*, 2010; Hsu and Harmer, 2014). Furthermore, many cellular physiological and metabolic processes are under clock control, including stomatal opening, photosynthesis, starch metabolism, redox homeostasis, abiotic and biotic stress responses, and hormonal signaling (Adams and Carré, 2011; Sanchez *et al.*, 2011; Haydon *et al.*, 2013a; Hsu and Harmer, 2014).

1.3.7.2 Transcriptional control as important mechanism for regulating outputs

The general pervasiveness of the circadian clock in plants and, in particular, its tremendous effect on the transcriptome are reflected by estimates that it regulates 30 to 40 % of all genes in *Arabidopsis* (Harmer *et al.*, 2000; Michael and McClung, 2003; Covington *et al.*, 2008). Intriguingly, about 90 % of the *Arabidopsis* transcripts cycle under at least one condition, including diurnal (different photo- or thermocycles) and circadian conditions. The most cycling genes could be identified under diurnal conditions of SD photocycles, while fewer transcripts oscillate in LD photocycles (53 % versus 38 %; Michael *et al.*, 2008b).

As transcriptional regulation also forms the basis of the oscillator mechanism itself, it is considered as one of the most important levels of circadian output control. It requires the action of several oscillator components which function as transcription factors modulating oscillatory patterns of many target (or output) genes (Adams and Carré, 2011). The phase-specific expression of output genes is gene-specific as well as setting-dependent (photocycles, thermocycles, and circadian conditions) which already indicates that multiple factors determine the timing of clock-driven rhythmic gene expression. Certainly, the time-of-day-specificity in output gene expression is widely achieved by time-of-day-specific expression of oscillator genes that encode activating and/or repressing transcription factors such as CCA1, LHY, LUX, and TOC1 (Harmer and Kay, 2005; Perales and Más, 2007; Helfer *et al.*, 2011; Gendron *et al.*, 2012; Huang *et al.*, 2012). Their abundance or activity is not solely determined by transcriptional regulation. Both, abundance and activity are also extensively modulated on post-transcriptional and post-translational level (Staiger and Green, 2011; McClung, 2011; Nagel and Kay, 2012). This includes, for instance, the control of transcript stability, alternative splicing events (which can result in nonsense-mediated mRNA decay), protein modification (e.g. phosphorylation) and degradation *via* the ubiquitin proteasome pathway. Moreover, cyclic changes in the chromatin structure stongly affect the accessibility of transcription factor binding sites in the promoter regions of target genes. For example, rhythmic transcription of *TOC1* could be linked to rhythmic histone acetylation at the promoter, which is associated with open chromatin structure (Perales and Más, 2007). It is thought that epigenetic modifications not only play a decisive role in oscillator but also in output gene expression since they are closely associated with gene expression in general (Gardner *et al.*, 2011). Moreover, several examples in mammals point to their impact on the circadian system and clock-regulated transcription, while the study of chromatin changes in correlation with circadian function is in its infancy in plants (Michael *et al.*, 2008b; McClung, 2011). In addition to the presence or absence of transcription factors, the timing of output gene expression is determined by specific circadian clock regulatory elements (CCREs) in the output gene promoter regions. A number of *cis*-regulatory elements which confer phase-specific transcription have already been identified. These comprise the previously mentioned EE and CBS (see 1.3.5) but also the G-box (CACGTG), GATA element (TATC), morning element (ME; AACCACAC), protein box (PBX; ATGGGCC) and the telomere-box and starch-box (TBX; AAACCCT and SBX; AAGCCC). These *cis*-regulatory elements were separated into three "phase modules": ME/G-box, EE/GATA, and PBX/TBX/SBX, associated with dawn-, evening-, and midnight-specific gene expression, respectively (Michael *et al.*, 2008b; Hubbard *et al.*, 2009). Specific flanking sequences and/or combinations of different CCREs might enable to produce

every possible phase of gene expression during the course of the day (Harmer and Kay, 2005; Covington *et al.*, 2008; Michael *et al.*, 2008b).

Transcriptome analyses revealed that the genes of many fundamental biological pathways are clock-regulated, i.e. they cycle under circadian (constant) conditions (Harmer *et al.*, 2000; Covington *et al.*, 2008). It is believed that the high amount of processes under clock control is achieved by regulating key transcripts (encoding key transcription factors or rate-limiting enzymes) rather than transcripts of the entire pathway (Harmer *et al.*, 2000). Circadian microarray datasets, for instance, demonstrate clock regulation of transcripts involved in photosynthesis, starch metabolism, redox balance, cold responses, hormonal responses, phenylpropanoid (anthocyanin and flavonoid) synthesis, and isoprenoid metabolism (Harmer *et al.*, 2000; Covington *et al.*, 2008). The latter relies on the methylerythritol phosphate (MEP) pathway which is limiting for the accumulation of chlorophylls, carotenoids, tocopherols, gibberellins, and ABA (Covington *et al.*, 2008). Since the MEP pathway also provides the isoprenoid precursor DMAPP, it is even conceivable that the circadian clock might influence the synthesis of iP- and tZ-type cytokinins, which predominantly derive from DMAPP produced from the MEP pathway (Kasahara *et al.*, 2004).

The expression of chlorophyll and phenylpropanoid biosynthesis genes peaks at the end of the night or in the early morning. Photosynthesis genes show maximal expression around midday. Starch synthesis genes peak at dawn, while starch degradation-related transcripts peak at dusk or during the subjective night. The same is true for cold-responsive genes, which also exhibit maximal expression in the evening, whereas heat-responsive genes are expressed in antiphase, rising in the morning (Harmer, 2000; Smith *et al.*, 2004; Lu *et al.*, 2005; Covington *et al.*, 2008). These are only a few examples for clock-regulated time-of-day-specific gene expression which enables proper anticipation of dawn or dusk, ensures optimal functioning as well as temporal separation of different biological pathways and/or appropriate responses to day- or nighttime cues. Interestingly, 68 % of the clock-controlled genes are linked to stress regulation (Kreps *et al.*, 2002), including genes with roles under cold, heat, salt, drought, ROS, and osmotic stress (Harmer *et al.*, 2000; Kreps *et al.*, 2002; Covington *et al.*, 2008). The fact that the circadian clock strongly influences key biological pathways and also stress responses on the transcriptional level clearly indicates how crucial the circadian phase is when performing differential expression analysis. Several reports confirm the time-of-day-dependence of transcriptional responses (Espinoza *et al.*, 2008; Kilian *et al.*, 2012; Lai *et al.*, 2012; Hsu and Harmer, 2012).

Hormone-associated genes (e.g. synthesis or response genes) were also found to be highly rhythmic under diurnal conditions (Covington *et al.*, 2008; Michael *et al.*, 2008a; Mizuno and Yamashino, 2008). Of course, diurnal regulation does not necessarily mean circadian regulation because it can be the consequence of multiple environmental cues. Therefore, Covington *et al.* (2008) analyzed the overlap between clock-regulated and hormone-induced genes and, strikingly, a significant enrichment of circadian regulation was found for all sets of hormone response genes tested (35 to 61 %). Although transcript levels do not always correlate with the protein abundance or activity the extensive regulation of hormone-associated transcripts by the clock clearly points to a pervasive influence of the clock on

virtually every hormone pathway. Consistent with that, many studies confirmed the vast effect of the circadian clock on many phytohormones by modulating their levels and signaling (see next chapter, 1.3.8). Since hormones affect many if not all of the known circadian-controlled processes clock regulation of hormonal pathways is thought to be an indispensable way to control a multitude of output pathways (Yakir *et al.*, 2007a; Robertson *et al.*, 2009; McWatters and Devlin, 2011).

Of course, there are many alternative and/or additional possibilities to control certain clock output pathways. The circadian clock for example also regulates enzyme activities, drives protein as well as metabolite oscillations, and generates rhythms of Ca^{2+} fluxes (Farré and Weise, 2012; Haydon *et al.*, 2013a). Through the interplay of all these mechanisms, the oscillator temporally coordinates, fine-tunes, and gates a high number of specific biological processes – the clock outputs. At the same time it gets continuously synchronized with the changing environment and internal cues *via* input pathways, including output signals which feedback to the clock (Harmer, 2009). Besides its fundamental roles in plant development and physiology, the enrichment of clock-regulated hormone- and stress-associated genes strongly indicates that, in addition, the circadian system modulates a significant amount of hormone and stress pathways. This very likely contributes to the adaptive advantage which is conferred by a resonant (properly phased) circadian clock (Covington *et al.*, 2008).

1.3.8 The interplay between circadian timekeeping and phytohormones

As outlined above, the circadian clock controls output pathways by utilizing rhythmic hormone signaling. The production of basically all major phytohormones oscillates under diurnal and/or circadian conditions, including ABA, auxin, brassinosteroids, cytokinin, ethylene, gibberellins, JA, and SA (Jouve *et al.*, 1999; Thain *et al.*, 2004; Nováková *et al.*, 2005; Bancos *et al.*, 2006; Fukushima *et al.*, 2009; Rawat *et al.*, 2009; Arana *et al.*, 2011; Goodspeed *et al.*, 2012). A high number of phytohormone-related gene products are cycling under diurnal and/or circadian conditions (Covington *et al.*, 2008; Michael *et al.*, 2008a; Mizuno and Yamashino, 2008). Mizuno and Yamashino (2008) reported that especially ABA- and methyl jasmonate-responsive genes cycle diurnally. This view has been further expanded by Michael *et al.* (2008a) who showed extensive oscillations of many major "phytohormone genes" (as they termed them, including biosynthesis, catabolism, receptor, and signaling genes). They found that cytokinin and ethylene genes are overrepresented during the dark period, whereas brassinosteroid, gibberellin, auxin, and ABA gene expression is enriched at or around dawn under SD photocycles. Lastly, Covington *et al.* (2008) evaluated the amount of hormone-responsive genes which are under clock control with the result that, strikingly, about 40 % of the genes of each hormone class are circadian-regulated.

One impressive example for an extensive orchestration of phytohormone-related gene expression by the circadian clock is related to the coincidence mechanism of hypocotyl growth. Especially the hormone-related genes with peak abundance at or around dawn could be linked to the dawn- and SD-specific hypocotyl elongation, including in particular ABA, auxin, gibberellin, and brassinosteroid genes (Michael *et al.*, 2008a). This growth response is due to a coincidence mechanism which depends on accurate hormonal action as a result of proper integration of internal (circadian rhythm) and external

(photoperiod/light signaling) cues. More recently, a more refined coincidence model was proposed in which the circadian clock regulates PIF4 protein abundance in a photoperiod-dependent manner which in turn regulates hormone-associated genes – identified as PIF4 targets – to eventually promote hypocotyl elongation (Nomoto *et al.*, 2012).

Additionally, the circadian clock has profound effects on hormonal pathways by gating the sensitivity to hormonal inputs. The circadian oscillator regulates ABA signaling (Legnaioli *et al.*, 2009; Castells *et al.*, 2010; Seung *et al.*, 2012) and controls the timing and intensitiy of auxin responses (Covington and Harmer, 2007; Rawat *et al.*, 2009). Furthermore, circadian oscillation of gibberellin signaling (Arana *et al.*, 2011) and time-of-day regulation of JA signaling by the clock (Shin *et al.*, 2012) have been reported recently.

Strikingly, hormonal pathways are not only outputs of the circadian clock. Hormone signaling can also act as input signal for the core oscillator. Auxin, for instance, regulates circadian amplitude and clock precision, while brassinosteroids and ABA modulate circadian periodicity (Hanano *et al.*, 2006). Furthermore, ABA induces the core oscillator gene *TOC1* (Legnaioli *et al.*, 2009). In the following section, present knowledge concerning the crosstalk between the circadian clock and the cytokinin pathway will be summarized.

1.3.8.1 The circadian clock and cytokinin

Cytokinin has also specific effects on the circadian system. Cytokinin treatment leads to phase delays (by one to three hours) in different circadian rhythms, such as *CCA1*, *LHY*, *TOC1*, *CAB2*, *CAT3*, and *CCR2*/*GRP7* oscillations (Hanano *et al.*, 2006; Zheng *et al.*, 2006). This phase delay is more pronounced in constant darkness compared with continuous light conditions (for *CCR2*; Hanano *et al.*, 2006). Interestingly, dose-dependent effects were observed by Salomé *et al.* (2006) characterized by a delayed phase in response to high and an advanced phase in response to lower cytokinin concentrations. The phase effect by cytokinin is dependent on ARR4 and PHYB (Hanano *et al.*, 2006; Zheng *et al.*, 2006). In terms of phase modulation, the *arr4* and *phyB* mutants are insensitive to cytokinin (Zheng *et al.*, 2006), whereas *ARR4* overexpressing plants exhibit hypersensitivity to cytokinin with regard to the circadian phase delay (although they do not show any circadian phenotype without cytokinin application). The introduction of a *PHYB* mutation completely eliminates this strong phase phenotype, clearly demonstrating that *PHYB* is epistatic to *ARR4* in this cytokinin-mediated input (Hanano *et al.*, 2006). Moreover, *arr3,4* double mutants exhibit an advanced phase (Salomé *et al.*, 2006) similar to *phyB* mutants under white light (Salomé *et al.*, 2002). Therefore, it is thought that the phase-adjusting cytokinin-input to the clock is integrated as follows: 1) Cytokinin activates *ARR3* and *ARR4* which act redundantly. 2) ARR4 interacts with PHYB which stabilizes the active Pfr-form of PHYB, as reported by Sweere *et al.* (2001). 3) Finally, PHYB signaling acts on clock gene expression in a phase-dependent manner (Hanano *et al.*, 2006; Salomé *et al.*, 2006).

In contrast to its effects on the phase, circadian periodicity is not very strongly affected by cytokinin treatment (Hanano *et al.*, 2006; Salomé *et al.*, 2006; Zheng *et al.*, 2006). This is at least true for constant light conditions. However, Hanano *et al.* (2006) reported interesting effects of cytokinin on

periodicity under constant darkness. Under these circadian conditions cytokinin causes significant period shortening of *CCR2*/*GRP7* rhythms. In addition, cytokinin supports rhythmicity of *CAB2* expression under dark conditions, which otherwise (without cytokinin) gets usually dampened very quickly. Hence, cytokinin treatment leads to a sustained precision in periodicity for this clock output, which exhibits an extremely high variance concerning period length due to the loss of rhythmicity without cytokinin (Hanano *et al.*, 2006).

Additionally, a pronounced long-period phenotype was found in *arr3,4* double mutants, which has been observed to a similar extent in the *arr3,4,5,6* quadruple mutant. The long periodicity is completely abolished by additional mutation of *ARR8* and *ARR9* in the *arr3,4,8,9* as well as the *arr3,4,5,6,8,9* mutant (Salomé *et al.*, 2006). The authors concluded that this long-period phenotype is independent of active PHYB, because it could be observed under all light conditions including blue light as well as under continuous darkness when PHYB is not active. Another important conclusion was that the long periodicity in *arr3,4* and *arr3,4,5,6* plants is established in a cytokinin-independent manner. One reason to assume this was that the period phenotype did not correlate with the increasing cytokinin sensitivity observed due to an increasing number of mutated A-type *ARR* genes. Secondly, the introduction of a genomic copy of *ARR5* into *arr3,4,5,6* plants did not rescue this circadian phenotype although it restored the cytokinin responsiveness in root elongation assays (To *et al.*, 2004). Furthermore, period phenotypes of a few cytokinin-associated mutant or transgenic plants were analyzed. The *cre1 ahk3* double mutant exhibits no altered period for leaf movements. Moreover, plants overexpressing *ARR4*, *ARR5*, *ARR6*, and *ARR9* also show no period phenotype for this circadian output (Salomé *et al.*, 2006).

Cytokinin also affects oscillator and output gene expression. It induces the morning genes *CCA1* and *LHY*, as well as the output gene *CAB2*, while repressing the evening-phased *TOC1* gene (Zheng *et al.*, 2006). The cytokinin effect on clock gene expression seems to be gated since another study shows that *CCA1* is induced by cytokinin only in the evening, but not in the morning and *vice versa* for *GI* and *TOC1* (Hanano *et al.*, 2006). Additionally, the *PRR* genes *PRR9* and *PRR5* were shown to be upregulated in response to cytokinin (Brenner *et al.*, 2005). On the contrary, Salomé *et al.* concluded that cytokinins do not influence the expression of clock genes after exploring available microarray data (Salomé *et al.*, 2006). Intriguingly, the same lack of cytokinin-dependent clock gene regulation might be concluded from recent meta-analyses of several microarray datasets which yielded lists of strongly cytokinin-regulated transcripts, not including many (if at all) oscillator genes (Brenner *et al.*, 2012; Bhargava *et al.*, 2013).

Data on the regulation of the cytokinin pathway by the circadian clock, as clock output, are limited. Cytokinin levels fluctuate under diurnal conditions in tobacco leaves with peak levels around midday (Nováková *et al.*, 2005). However, in *Arabidopsis*, potential oscillations in cytokinin production and/or cytokinin degradation await elucidation. As already described above, the circadian clock strongly regulates a multitude of hormone-responsive genes, including cytokinin-related transcripts. Among the analyzed genes that are upregulated by cytokinin 38 % were found to be clock-regulated, while it was 45 % of the tested genes usually downregulated by cytokinin (Covington *et al.*, 2008). For both groups

of circadian-regulated genes phases of maximal expression were determined. Interestingly, cytokinin-induced genes exhibit phase enrichment during the subjective night before midnight, while most of the cytokinin-repressed genes peak during the subjective day before midday. Among the A-type *ARRs*, *ARR9* was found to oscillate diurnally under SD and LD photocycles, peaking in the morning, although the increase in *ARR9* expression already starts earlier, in the second half of the night, under SD conditions (Michael *et al.*, 2008a; Ishida *et al.*, 2008b). It is the only cytokinin-associated gene for which circadian control of peak expression was proven genetically by analyzing the *ARR9* expression pattern in the *cca1 lhy toc1* triple mutant (Ishida *et al.*, 2008b). For *ARR4:LUC* reporter lines bioluminescence rhythms were shown under circadian conditions in phase with *TOC1* oscillations, although the authors concluded that *ARR4* is unlikely to be under strong circadian control because of the weak amplitudes (Salomé *et al.*, 2006). Among the *CKX* genes, only *CKX5* exhibits dawn- and SD-specific peak expression (Nomoto *et al.*, 2012). Furthermore, an interesting link that the circadian clock might regulate cytokinin signaling comes from the observation that clock mutants (affected in *CCA1* and/or *LHY* function) show altered cytokinin responses in root elongation, hypocotyl growth and tissue culture (Zheng *et al.*, 2006). *CCA1* or *LHY* gain-of-function alleles caused hypersensitivity towards cytokinin, while the *cca1 lhy* loss-of-function double mutant exhibited reduced sensitivity in these assays. This led to the conclusion that the core oscillator might directly or indirectly modulate cytokinin signaling.

1.4 Reactive oxygen species

Life in an oxygen-rich world implicates the potential risk of oxidative stress. Molecular oxygen in its triplet ground state ($^3O_2$; usually referred to as O_2) is relatively stable compared with its reactive forms, the reactive oxygen species (ROS), including the hydroxyl radical ($HO^\bullet$), superoxide anion radical ($O_2^{\bullet-}$), hydrogen peroxide (H_2O_2), and singlet oxygen ($^1O_2$) (Apel and Hirt, 2004; Mittler *et al.*, 2004). The following chapters will give an overview of ROS production, scavenging, and signaling.

1.4.1 Production of reactive oxygen species

ROS production occurs in all cellular compartments, including chloroplasts, peroxisomes, and mitochondria as well as extracellularly in the apoplast under various stress conditions or in response to developmental signals (Gechev *et al.*, 2006; Mhamdi *et al.*, 2010; Juvany *et al.*, 2013; Wrzaczek *et al.*, 2013). In light the chloroplasts and peroxisomes are the main ROS producers in plants. In contrast, in the darkness and in non-green tissues, mitochondria are the main source of ROS generation (Gill and Tuteja, 2010; Wrzaczek *et al.*, 2013). Exposure to stress can cause a drastic increase of ROS production, leading to oxidative stress. This harmful role of ROS made them well-known as toxic byproducts of aerobic metabolism (Apel and Hirt, 2004; Mittler *et al.*, 2004). However, ROS can also be actively produced by enzymes and play an important role as signaling molecules, acting locally or across long distances (Gechev *et al.*, 2006; Mittler *et al.*, 2011).

In chloroplasts light not only drives photosynthesis, but causes ROS production at the same time due to the high input of energy. In plants $^1O_2$ is produced by photosensitizers such as chlorophylls and

their precursors (Krieger-Liszkay, 2005; Triantaphylidès and Havaux, 2009). In the light-harvesting antenna complexes (LHCs) and photosystem II (PSII), excited triplet chlorophylls ($^3Chl^*$) act as photosensitizers, producing $^1O_2$ by transferring excitation energy to O_2 (Triantaphylidès and Havaux, 2009; Fischer *et al.*, 2013). In photosystem I (PSI), the reduction of O_2 leads to the formation of $O_2^{\bullet-}$ which can be converted into H_2O_2 and $HO^\bullet$ (Apel and Hirt, 2004; Gill and Tuteja, 2010).

As mentioned above, ROS can also be produced by enzymes, including glycolate oxidase, xanthine oxidase, and different peroxidases (Mhamdi *et al.*, 2010; Wrzaczek *et al.*, 2013). Key players in the network of ROS producing enzymes are the respiratory burst oxidase homologues (RBOHs), also called NADPH oxidases, which are plasma membrane-localized proteins (Suzuki *et al.*, 2011). They catalyze the generation of $O_2^{\bullet-}$ followed by the rapid dismutation to H_2O_2 in the apoplast, thereby contributing to a great number of developmental and physiological processes as well as to responses under biotic and abiotic stresses (Torres and Dangl, 2005; Suzuki *et al.*, 2011).

1.4.2 The ROS scavenging system

Since ROS are highly reactive and potentially toxic O_2-derived intermediates they can affect many cellular functions by damaging nucleic acids, oxidizing proteins, and causing lipid peroxidation (LPO) at high concentrations (Gill and Tuteja, 2010; Sharma *et al.*, 2012). The oxidation of polyunsaturated fatty acids (PUFAs) during LPO additionally gives rise to harmful reactive species such as malondialdehyde (MDA), thereby even enhancing cytotoxicity (Gill and Tuteja, 2010). It is essential to strictly control ROS levels in order to avoid oxidative stress which might even induce cell death, but also to ensure accurate ROS dynamics important for their signaling role at low or moderate concentrations (Gechev *et al.*, 2006; Mittler *et al.*, 2011; Sharma *et al.*, 2012). Therefore, plants have developed a sophisticated ROS scavenging system, comprised of enzymatic and non-enzymatic mechanisms. These mechanisms enable them to efficiently reduce ROS levels and to maintain ROS homeostasis (Asada, 2006; Sharma *et al.*, 2012).

Major enzymatic scavengers of plants include superoxide dismutase (SOD) as well as the enzymes of the Halliwell-Asada pathway (also called water-water or ascorbate-glutathione cycle), including ascorbate peroxidase (APX), monodehydroascorbate reductase (MDHAR), dehydroascorbate reductase (DHAR), and glutathione reductase (GR) which detoxify $O_2^{\bullet-}$ and H_2O_2 (Asada, 2006; Foyer and Noctor, 2011; Sharma *et al.*, 2012). Moreover, catalases (CAT) are also crucial for the degradation of H_2O_2 (Mhamdi *et al.*, 2010).

Non-enzymatic scavengers comprise the hydrophilic low molecular weight antioxidants ascorbate (ASC) and glutathione (GSH) as well as the lipophilic tocopherols and carotenoids. While ASC and GSH are decisive for the detoxification of $O_2^{\bullet-}$ and H_2O_2, in part because of their participation in the Halliwell-Asada pathway (Asada, 2006; Gill and Tuteja, 2010; Sharma *et al.*, 2012), tocopherols and carotenoids are indispensable for the scavenging of lipid-derived reactive species and especially for the quenching of $^1O_2$ (Havaux *et al.*, 2005; Triantaphylidès and Havaux, 2009; Gill and Tuteja, 2010). Moreover, carotenoids such as the xanthophyll lutein not only deactivate $^1O_2$, but also efficiently quench $^3Chl^*$, thereby eliminating the main source for $^1O_2$ production (Dall'Osto *et al.*, 2006; Gill and

Tuteja, 2010; Sharma *et al.*, 2012). Additionally, the xanthophyll class of carotenoids, especially zeaxanthin, plays an important role in the thermal dissipation of excess light energy (non-photochemical quenching), which is also strongly reducing light-induced ROS generation (Murata *et al.*, 2012; Jahns and Holzwarth, 2012).

1.4.3 ROS signaling

ROS act as signaling molecules in many different processes. The diversity of these processes is determined by multiple factors, including their chemical identity, the site of production, the intensity of the signal (dose-dependent effect), pre-conditions (priming by previous stresses), and the developmental stage (Gechev *et al.*, 2006; Mittler *et al.*, 2011; Schmitt *et al.*, 2014). Another important factor which confers ROS specificity is the interaction with other signaling molecules such as nitric oxide, lipid-derived signals, and plant hormones (Gechev *et al.*, 2006).

Through their extensive interplay with hormonal pathways, ROS participate in multiple physiological and developmental processes. They control stomatal closure, gravitropism, germination, lignin biosynthesis, programmed cell death, hypersensitive responses, and osmotic stress (Mittler *et al.*, 2011; Sharma *et al.*, 2012).

The ability of ROS to influence the expression of a great number of genes discloses their specificity since specific "transcriptomic footprints" have been identified for $O_2^{\bullet-}$, H_2O_2, and $^1O_2$ (Gadjev *et al.*, 2006). *FER1* was revealed as H_2O_2-specific and *BON ASSOCIATION PROTEIN 1* (*BAP1*) as $^1O_2$-specific marker gene, just to mention two well-known examples (op den Camp *et al.*, 2003; Ochsenbein *et al.*, 2006). Moreover, different stress treatments cause distinct responses regarding scavenging gene expression indicating that unique ROS signatures are needed under specific stress conditions, such as cold, heat, high light (HL), or drought (Mittler *et al.*, 2004). The strong overrepresentation of stress-related genes in the sets of ROS-responsive transcripts also points to the importance of ROS as mediators of biotic and abiotic stress responses (Gadjev *et al.*, 2006; Ochsenbein *et al.*, 2006; Miller *et al.*, 2008). Among the highly upregulated genes are heat shock, AP2/ERF, MYB and WRKY transcription factor genes, as well as mitogen-activated-protein kinase (MAPK) genes which all play pivotal roles in stress pathways (Mittler *et al.*, 2004; Gadjev *et al.*, 2006).

Furthermore, a number of zinc-finger transcription factor genes (called *ZAT*), including *ZAT12*, are strongly induced by ROS. Interestingly, *ZAT12* is not only upregulated by $O_2^{\bullet-}$, H_2O_2, and $^1O_2$ (Gechev *et al.*, 2006), it is also highly responsive to a multitude of biotic and abiotic stress treatments, including cold, heat, light stress, and pathogen infection (Rizhsky *et al.*, 2004; Vogel *et al.*, 2005; Davletova *et al.*, 2005). Since *ZAT12* is activated under almost all adverse environmental conditions, it belongs to the plant core environmental stress response (PCESR) genes (Kilian *et al.*, 2012; Hahn *et al.*, 2013). Similarly, together with *BAP1*, it was identified as rapid wounding response (RWR) gene which, due their large overlap with biotic and abiotic stress response genes, were discussed as so-called general stress response (GSR) genes of *Arabidopsis* (Walley *et al.*, 2007). Overexpression of *ZAT12* leads to higher tolerance to cold, oxidative stress (including light stress), and osmotic stress, while *ZAT12* loss-of-function leads to an increased sensitivity to salinity, osmotic, and heat stress

(Davletova *et al.*, 2005; Miller *et al.*, 2008). Therefore, *ZAT12* is a good example highlighting the relationship between ROS, the activation of ROS-responsive genes, and their implication in acclimation responses.

1.5 Programmed cell death

The term programmed cell death (PCD) is used to describe forms of cell death that are triggered by active cellular events, involving changes in cell metabolism and the activation of signaling pathways. Thus, controlled genetically regulated mechanisms lead to an active cell suicide. The possibility to activate PCD in specific cells without affecting the surrounding tissue is recognized as a key mechanism in development and defense both in plant and animal systems. (de Pinto *et al.*, 2012; Lord and Gunawardena, 2012; Cai *et al.*, 2014).

1.5.1 Programmed cell death in plants

Apoptosis was the first form of PCD to be discovered and characterized in animals. Therefore, plant PCD has often been investigated in comparison with the best-known animal process (de Pinto *et al.*, 2012; Lord and Gunawardena, 2012). Although some of the apoptosis hallmarks can be observed in plants, including increased vesicle formation, cytoplasmic condensation, nuclear and chromatin condensation, and DNA fragmentation (laddering) (de Pinto *et al.*, 2012; Lord and Gunawardena, 2012) plant PCD is not synonymous with apoptosis (van Doorn *et al.*, 2011; van Doorn, 2011). Firstly, "apoptotic features" such as chromatin condensation and DNA fragmentation are not specific to apoptosis and can also be detected during necrosis and autophagy, the other two forms of PCD in the animal system as well as in different forms of plant PCD (Kroemer *et al.*, 2009; van Doorn *et al.*, 2011; de Pinto *et al.*, 2012). Secondly, the key defining features of apoptosis are completely missing in plant PCD, namely the formation of apoptotic bodies as well as their engulfment *via* phagocytosis followed by their degradation within the adjacent cells which is due to the presence of cell walls and the absence of phagocytes (van Doorn *et al.*, 2011; van Doorn, 2011).

In order to be able to distinguish different forms of PCD, other plant-specific criteria were defined, mainly based on histological observations. van Doorn (2011) describes two broad categories of plant PCD that are distinguished at the moment, called autolytic and non-autolytic PCD. The autolytic cell death is characterized by tonoplast rupture and rapid clearance of the cytoplasm, involving the release of hydrolases from collapsed vacuoles as well as autophagy-like processes. It mainly occurs during plant development and after mild abiotic stress. The non-autolytic form is mainly found during PCD that is triggered by plant-pathogen interactions, including hypersensitive response (HR)-related PCD. It can include tonoplast rupture which is, however, not followed by rapid clearance of the cytoplasm, completely lacks tonoplast rupture, or cell death occurs prior to vacuole collapse (van Doorn, 2011).

Another classification is based on the cause of PCD, which categorizes into developmentally regulated and environmentally induced PCD (Lord and Gunawardena, 2012). Prominent examples of PCD during development include the deletion of the embryonic suspensor, anther dehiscence, xylem differentiation, leaf senescence, flower senescence, and leaf morphogenesis. Environmentally induced

PCD is usually a consequence of adverse external cues, including abiotic (e.g. heat, ozone, and hypoxia) and biotic stresses (de Pinto *et al.*, 2012; Lord and Gunawardena, 2012). A good example for the latter is the already mentioned HR-related PCD. HR cell death is one of the best-studied forms of PCD in plants and the result of an incompatible plant-pathogen interaction (Coll *et al.*, 2011). It involves a localized cell death response at the site of infection which limits pathogen spread thereby protecting the surrounding tissues from infection (Greenberg, 1996). Although the advantage of PCD seems very obvious for HR cell death or the controlled death of specific cells during many developmental processes, it is, however, not always clear in several cases of abiotic stress-induced PCD (de Pinto *et al.*, 2012).

Despite the great number of examples, the biochemistry and genetics underlying plant PCD are not well understood (van Doorn, 2011). The extensive comparison with the animal system yielded limited but, nevertheless, valuable information concerning PCD regulators (de Pinto *et al.*, 2012; Lord and Gunawardena, 2012). For instance, caspases play an important role during controlled cell suicide in mammals. True caspases could not be identified in plants. However, caspase-like proteases (CLPs) have been identified in plant systems, including vacuolar processing enzymes (VPEs) and metacaspases (MCs/MCPs). VPEs possess caspase-like activity and are described as "executors" of cell death, being involved in developmental and pathogen-induced cell death (Hara-Nishimura *et al.*, 2005; Hara-Nishimura and Hatsugai, 2011). The second group of CLPs is divided into two classes, type I (MC1-3/MCP1A-C) and type II MCs/MCPs (MC4-9/MCP2A-F). Members of both classes were shown to be involved in the control of PCD in response to biotic and abiotic stresses (He *et al.*, 2008; Watanabe and Lam, 2011; Coll *et al.*, 2010).

Another intensively studied PCD regulator is Bax Inhibitor 1 (BI1). BI1 was originally isolated from a human cDNA library, based on its ability to block cell death in yeast induced by ectopic expression of the mouse Bax protein that acts pro-apoptotic. Although no counterparts of mammalian Bax have been found in plants, BI1 is a highly conserved ER-localized protein also found in plants and is able to suppress Bax toxicity *in planta* (Kawai-Yamada *et al.*, 2001; 2004; Ishikawa *et al.*, 2011). Plant *BI1* is expressed in diverse tissue types and its expression is upregulated during senescence and under various stress conditions (Watanabe and Lam, 2009). In *Arabidopsis*, similar to other plant species, *BI1* overexpression leads to attenuated PCD, whereas loss-of-function results in accelerated progression of PCD in response to multiple abiotic and biotic stimuli (Watanabe and Lam, 2006; 2008). It has been proposed that BI1 suppresses cell death downstream of ROS generation (Kawai-Yamada *et al.*, 2004) and at least in part by maintaining calcium (Ca^{2+}) homeostasis (Ihara-Ohori *et al.*, 2007).

Interestingly, a number of plant ROS scavenging enzymes, including APX and SOD, have been isolated as "Bax Inhibitors" in a cDNA library screen because they were also able to suppress Bax toxicity in yeast (Watanabe and Lam, 2009; Ishikawa *et al.*, 2011). Indeed, an impairment of H_2O_2-degrading enzymes, including catalases, has been reported for various kinds of plant PCD (de Pinto *et al.*, 2012). A decrease in ROS scavenging results in increased ROS levels pointing to a critical function of ROS in PCD processes. In fact, ROS play a key role in the induction, signaling, and execution of plant cell death and an oxidative burst was found to be associated with various kinds of PCD (Van Breusegem

and Dat, 2006; Gechev *et al.*, 2006; 2010; Gadjev *et al.*, 2008; de Pinto *et al.*, 2012). During PCD the ROS signal is often amplified by the induction of ROS producing enzymes such as NADPH oxidases (RBOHs) and/or, as indicated above, the inhibition of ROS scavenging enzymes (Gechev *et al.*, 2010). PCD can be triggered by different types of ROS, including $O_2^{\bullet-}$, H_2O_2, and $^1O_2$ (Van Breusegem and Dat, 2006; Gadjev *et al.*, 2008; Gechev *et al.*, 2010). It has been shown that the different ROS can activate distinct signaling pathways (Gadjev *et al.*, 2006; 2008; Laloi *et al.*, 2007; Kim and Apel, 2013). Downstream events in response to high ROS concentrations involve MAPK cascades, alterations in cytosolic Ca^{2+} levels, activation of ion channels, and changes in the redox state of the cell. This provokes a global transcriptional reprogramming, involving the induction of ROS-specific transcription factors, cell death-specific nucleases and proteases (e.g. MCs/MCPs) – and eventually PCD (Gechev *et al.*, 2010).

Strikingly, the environmental and physiological context is of great importance for the outcome of ROS-related redox signaling and PCD regulation (Love *et al.*, 2008; Gechev *et al.*, 2010; Mhamdi *et al.*, 2010). For instance, growth of the oxidative stress signaling mutant *cat2* in different light-dark regimes revealed that the photoperiod is a critical determinant of the oxidative stress response and the associated cell death phenotype (Queval *et al.*, 2007). Moreover, the timing and the intensity of oxidative stress, in addition to the chemical nature of ROS, determine which specific response (e.g. PCD) is activated or if it is activated at all (de Pinto *et al.*, 2006; 2012). There are examples showing that either ROS alone are not sufficient to induce PCD or that a specific ROS pathway is modulated by another signaling molecule or pathway. For instance, bacterial mutants which fail to induce cell death still caused an oxidative burst in tobacco suspension cells (Greenberg, 1996). Elevated ROS levels in *Arabidopsis* plants expressing the death-promoting Bax protein were not abrogated in *BI1* overexpressing plants although plant cell death was strongly attenuated (Ishikawa *et al.*, 2011). Low activities of both peroxisomal CAT and cytosolic APX in tobacco and *Arabidopsis* plants surprisingly show less severe stress symptoms than plants lacking only one antioxidant enzyme. In both plant species the lack of *APX1* reduced or even rescued cell death phenotypes of *CAT*-deficient plants (Rhizhsky *et al.*, 2002; Vanderauwera *et al.*, 2011). Additionally, there are examples which show a crosstalk between distinct ROS pathways, revealing an antagonism between $^1O_2$- and $O_2^{\bullet-}$/H_2O_2-induced responses (Kim and Apel, 2013). For example, in the *flu* mutant the overexpression of the H_2O_2-degrading thylakoid-specific *APX* further aggravates $^1O_2$-dependent growth inhibition and PCD (Laloi *et al.*, 2007).

Furthermore, as in many plant processes an extensive interplay exists between ROS and other signaling molecules such as hormones in the control of PCD (Overmyer *et al.*, 2003; 2005; Danon *et al.*, 2005; Gadjev *et al.*, 2008). Especially stress hormones such as ET, JA, and SA are known to be important for ROS-dependent cell death (Overmyer *et al.*, 2003; 2005; Danon *et al.*, 2005). There is evidence that ROS (H_2O_2) can induce the accumulation of plant hormones such as ET, JA, and SA, placing hormonal signaling downstream of the ROS signal. However, there are also examples that reveal ROS as secondary messengers in hormonal pathways (Karuppanapandian *et al.*, 2011). Hence, the relationship between ROS and hormones is characterized by complex feed-back and feed-forward

interactions which modulate multiple plant processes, including PCD (Overmyer *et al.*, 2003; Mittler *et al.*, 2004).

In the next chapter, two prominent forms of plant PCD, leaf senescence and HR cell death, will be briefly addressed, especially taking into account ROS and phytohormones as active players during these cell death programs.

1.5.2 Leaf senescence and HR cell death – a role for ROS and hormones in a genetically controlled PCD program

Both leaf senescence and HR cell death are well-studied forms of plant PCD occurring in leaves (Wang *et al.*, 2013). Leaf senescence is an age-dependent process occurring at the final stage of leaf development and is intimately associated with senescence on the organismal level in *Arabidopsis* which in the end leads to the death of the whole plant (Lim *et al.*, 2007). In this genetically coordinated process, leaf cells undergo orderly changes in cell structure, metabolism, and gene expression. It includes yellowing of the leaves (chlorosis) caused by the degradation of chlorophylls, the hydrolysis of membrane lipids and proteins, and the remobilization of macromolecules (Lim *et al.*, 2007; Khanna-Chopra, 2011). Furthermore, it is accompanied by extensive changes in gene expression, including decreased expression of photosynthesis-associated genes (e.g. *CAB2*) and the induction of senescence-associated genes (*SAGs*) such as *SAG12* (Lim *et al.*, 2007). Leaf senescence is influenced by both internal and environmental signals. The internal factors include age-derived signals, ROS, and hormones, whereas external cues can be biotic or abiotic stresses, which influence ROS levels and hormonal responses and usually accelerate senescence (Lim *et al.*, 2007; Khanna-Chopra, 2011; Jibran *et al.*, 2013). Hormones do not only integrate environmental cues but also developmental cues. Therefore, they are of great importance for the timing and progression of senescence. All classical plant hormones have been described to modulate leaf senescence. For instance, senescence can be accelerated by ET, JA, ABA, and SA, and delayed by auxin, gibberellin, and cytokinin (Schippers *et al.*, 2007; Jibran *et al.*, 2013; Khan *et al.*, 2014). Senescence-promoting hormones such as ET, JA, and SA accumulate while senescence-delaying hormones such as cytokinin decrease in senescing leaves (He *et al.*, 2002; Lim *et al.*, 2007; Seltmann *et al.*, 2010; Khan *et al.*, 2014). Intriguingly, overexpression of *BI1* delays methyl jasmonate (MeJA)-induced leaf senescence by suppressing the cytosolic Ca^{2+}-dependent activation of MAPK6, which is one example revealing the involvement of an active PCD program during leaf senescence (Yue *et al.*, 2012). Furthermore, hormones positively regulate senescence by activating stress-related genes, the expression of *SAGs,* and by interacting with the ROS signaling network (Lim *et al.*, 2007; Khanna-Chopra, 2011; Wu *et al.*, 2012). However, the capability to induce senescence strongly depends on the developmental stage. Leaves need to "acquire the competence to senesce" in order to be able to respond to senescence-inducing signals (Jibran *et al.*, 2013; Thomas, 2013). A well-studied example is the age dependence of senescence inducibility by ethylene. Ethylene can induce senescence only after the leaves have passed the transition from juvenility to maturity (Jing *et al.*, 2002; 2005; Thomas, 2013). One group of mutants that are impaired in the proper timing of senescence is called *onset of leaf death* (*old*). Many *old* mutants display early senescence phenotypes and show enhanced ethylene responses (Jing *et al.*, 2002; 2005).

old1 is allelic to *cpr5* (*constitutive expression of PR genes 5*) a lesion mimic mutant (LMM) (Bowling *et al.*, 1997; Jing *et al.*, 2007). Interestingly, *old1/cpr5* mutant plants show two independent forms of PCD, the premature senescence and HR-like spontaneous lesions both of which are linked to the overproduction of $O_2^{\bullet-}$ (Bowling *et al.*, 1997; Jing *et al.*, 2008). ROS accumulation as well as the induction of many ROS-related genes could already be detected in presymptomatic *cpr5* mutants (Bowling *et al.*, 1997; Jing *et al.*, 2008) which indicates that ROS generation and a disturbed cellular redox balance are closely linked to the following cell death events (Jing *et al.*, 2008). Indeed, ROS (H_2O_2) have been shown to accumulate in senescing leaves, while ROS scavenging enzymes (e.g. *CAT2*) are downregulated in parallel (Smykowski *et al.*, 2010; Bieker *et al.*, 2012; Wang *et al.*, 2013). Furthermore, many *SAG* genes are ROS-inducible (Navabpour *et al.*, 2003) and senescence-associated *NAC* genes were found to be rapidly and strongly induced by H_2O_2 treatment (Balazadeh *et al.*, 2011). Ferritins belong to the ROS gene network and play a crucial role during oxidative stress and ROS detoxification (Ravet *et al.*, 2009; Briat *et al.*, 2010). *FER1* loss-of-function causes earlier onset of age-dependent leaf senescence which has been linked to its detoxifying function that is required when ROS accumulate during senescence (Murgia *et al.*, 2007). Together, these data strongly support the idea that ROS act as signals to promote senescence (Jing and Nam, 2012; Wang *et al.*, 2013).

During HR, a biphasic burst of ROS occurs which is thought to be decisive for the induction of HR cell death. Several enzymatic systems contribute to the overproduction of ROS, including peroxidases, oxalate and amine oxidases as well as NADPH oxidases (Levine *et al.*, 1994; de Pinto *et al.*, 2012). NADPH oxidase-dependent ROS production is crucial for the regulation of HR development, HR cell death, and systemic immunity (Torres *et al.*, 2002; 2005; Suzuki *et al.*, 2011). In order to unravel signaling pathways involved in cell death, LMMs which exhibit abnormal cell death phenotypes and spontaneous lesion formation were extensively studied (Lorrain *et al.*, 2003). For instance, in two *Arabidopsis* mutants, *lsd1* (*lesion-stimulating disease 1*) and *rcd1* (*radical-induced cell death 1*), elevated ROS levels have been shown to be necessary and sufficient to induce spreading of cell death (Van Breusegem and Dat, 2006). The fact that LMMs such as *lsd1* activate HR and form lesions in the absence of any pathogen underlines the presence of genetically regulated PCD programs (Greenberg, 1996). Hormonal pathways also play an important role in HR cell death, especially SA signaling which involves the induction of PR (pathogenesis-related) proteins. While JA has been shown to widely act antagonistically to SA and *vice versa* (Brooks *et al.*, 2005; Zheng *et al.*, 2012; Pieterse *et al.*, 2012; Van der Does *et al.*, 2013), cytokinin supports SA signaling (Choi *et al.*, 2010; Robert-Seilaniantz *et al.*, 2011). Moreover, SA acts synergistically with ROS to drive HR (Foyer and Noctor, 2005; Coll *et al.*, 2011). Many LMMs exhibit constitutively active SA signaling (Lorrain *et al.*, 2003). In addition, the disease resistance signaling components *EDS1* (*ENHANCED DISEASE SUSCEPTIBILITY 1*) and *PAD4* (*PHYTOALEXIN-DEFICIENT 4*) are essential regulators of cell death pathways and regulate a ROS- and SA-dependent signal amplification loop (Lorrain *et al.*, 2003; Coll *et al.*, 2011). The ROS-responsive gene *BAP1* and its homolog *BAP2* exhibit overlapping functions in suppressing PCD, including HR cell death, thereby containing ROS-induced cell death (Yang *et al.*, 2007). Interestingly, a very recent study revealed that HR cell death is controlled by the circadian clock which further emphasizes how diverse the influences on PCD processes are (Korneli *et al.*, 2014).

1.6 Jasmonic acid

The plant hormone jasmonic acid (JA) belongs to the broad class of oxylipins which are lipid-derived signaling molecules (Browse, 2009a; Wasternack and Kombrink, 2010; Dave and Graham, 2012). JA controls plant growth and development as well as responses to biotic and abiotic stresses. Many developmental processes such as seed germination, seedling development, trichome formation, root growth, flower development, seed development, and senescence are regulated by JA (Wasternack and Hause, 2013; Wasternack, 2014). Especially its impact on fertility is well-known since many JA synthesis and signaling mutants are male sterile (Browse, 2009b; Acosta and Farmer, 2010). However, its function as stress hormone is also well-studied, in particular the key role of JA in plant defenses against herbivores and against necrotrophic pathogens as well as the regulation of wound responses (Wasternack *et al.*, 2006; Acosta and Farmer, 2010; Pieterse *et al.*, 2012; Wasternack, 2014). In the following two chapters current knowledge on JA synthesis and signaling will be summarized.

1.6.1 JA synthesis

JA synthesis is divided into three steps, the initiation, completion, and biochemical diversification, and takes place in several cellular compartments (Acosta and Farmer, 2010). The initiation of JA synthesis occurs in plastids. Polyunsaturated fatty acids (PUFAs), namely hexadecatrienoic acid (C16:3) or α-linolenic acid (C18:3) which are abundant in chloroplast membranes, are the initial substrates which get enzymatically oxygenated by 13-lipoxygenases (13-LOXs) to form fatty acid hydroperoxides (Schaller and Stintzi, 2009; Gfeller *et al.*, 2010). *Arabidopsis* has four 13-LOX isoforms, LOX2, LOX3, LOX4, and LOX6 (Bannenberg *et al.*, 2009). All four 13-LOX forms contribute to JA formation (Wasternack and Hause, 2013). LOX2 is of great importance for wound-induced JA formation (Bell *et al.*, 1995) and LOX3 and LOX4 have been shown to act redundantly in JA synthesis ensuring male fertility (Caldelari *et al.*, 2011). The resulting 13-hydroperoxide forms are the substrates for allene oxide synthase (AOS) which generates unstable allene oxide intermediates which further undergo enzyme-directed cyclization mediated by allene oxide cyclase (AOC) to form cyclopentenones (Gfeller *et al.*, 2010; Wasternack and Kombrink, 2010). The cyclopentenones are called dinor-OPDA (dinor-oxo-phytodienoic acid; C16:3-derived) and OPDA (C18:3-derived) and are the end-products of the initial step of JA synthesis in the chloroplast (Gfeller *et al.*, 2010; Acosta and Farmer, 2010). They are JA precursors, but also themselves biologically active signaling compounds (Dave and Graham, 2012; Wasternack *et al.*, 2013). The completion of JA synthesis occurs in peroxisomes where the AOS- and AOC-catalyzed products dinor-OPDA and OPDA are reduced to cyclopentanones followed by β-oxidation to finally form JA. This series of peroxisomal reactions begins with the enzyme OPDA reductase 3 (OPR3) and involves several intermediate JA precursors, OPC-8, OPC-6, and OPC-4 which are oxo-pentenyl-cyclopentanes (OPCs) with 8-, 6-, and 4-carbon chains, respectively (Schaller and Stintzi, 2009; Gfeller *et al.*, 2010; Wasternack and Kombrink, 2010). After β-oxidation JA is transported to the cytosol where its biochemical diversification takes place. The numerous metabolic conversions include hydroxylation, O-glucosylation, methylation, amino acid-conjugation, and sulfation (Kombrink, 2012; Wasternack and Hause, 2013). The conjugation of JA with amino acids such as isoleucine, however, is the most important reaction that is catalyzed by JAR1 (JASMONATE-RESISTANT 1) (Staswick *et al.*,

2002; Staswick and Tiryaki, 2004; Suza and Staswick, 2008). It yields the bioactive jasmonate JA-Ile which is the major ligand for the JA receptor complex (Fonseca *et al.*, 2009; Wasternack and Hause, 2013; see 1.6.2). In the *jar1* mutant, the JA-Ile levels are drastically reduced and most JA responses are impaired (Suza and Staswick, 2008; Browse, 2009b; Kombrink, 2012). However, residual low levels of JA-Ile can be detected in *jar1* which are sufficient to retain fertility (Kombrink, 2012) pointing to additional low activity JA-conjugating enzymes (Suza and Staswick, 2008).

1.6.2 JA signaling

JA signaling takes place in the nucleus and relies on the ubiquitin proteasome system (Acosta and Farmer, 2010; Santner and Estelle, 2010; Pérez and Goossens, 2013; Wasternack and Hause, 2013). One mutant of particular importance for the understanding of JA signaling is *coi1* (*coronatine-insensitive 1*) which is impaired in every aspect of JA signal transduction and response (Feys *et al.*, 1994; Wasternack, 2007; Browse, 2009b). COI1 is an F-box protein (Xie *et al.*, 1998) and is part of a functional SCF complex (SCF^{COI1}) (Lorenzo and Solano, 2005) that targets the transcriptional repressors JAZ (JASMONATE ZIM DOMAIN) for proteasomal degradation (Chini *et al.*, 2007; Thines *et al.*, 2007; Yan *et al.*, 2007). In the presence of JA-Ile, the most biologically active ligand, COI1 and JAZ associate and form the COI1-JAZ co-receptor complex (Katsir *et al.*, 2008; Fonseca *et al.*, 2009; Sheard *et al.*, 2010; Wasternack and Hause, 2013). This allows the hormone-dependent degradation of JAZ proteins which, in turn, releases positively acting transcription factors (e.g. MYC2) and hence enables the transcription of JA response genes (Wasternack and Hause, 2013). The *Arabidopsis* genome contains 12 *JAZ* genes (*JAZ1-JAZ12*) (Chung *et al.*, 2009; Kazan and Manners, 2012). Eight of them, including *JAZ1*, are strongly induced by JA (Thines *et al.*, 2007; Browse, 2009a). In addition to the *JAZ* genes, transcription factor genes such as *MYC2*, and also JA synthesis genes, including *LOXs*, *AOS*, *AOC*, and *OPR3* belong to the immediate-early genes in response to JA, in parallel to defense-specific genes such as *PDF1.2* (*PLANT DEFENSIN 1.2*) or *VSP2* (*VEGETATIVE STORAGE PROTEIN 2*) (Chung *et al.*, 2008; Browse, 2009a; Wasternack and Hause, 2013). The activation of JA synthesis genes by JA signaling results in a positive feedback loop amplifying the JA signal (Wasternack, 2007; Browse, 2009a).

In *Arabidopsis*, two major branches of the JA signaling pathway are recognized, the MYC and the ERF branch (Lorenzo *et al.*, 2004; Pieterse *et al.*, 2012; Wasternack and Hause, 2013). The MYC branch is controlled by MYC-type bHLH (basic helix-loop-helix) transcription factors such as MYC2 and is activated by herbivorous insects or mechanical wounding leading to the expression of MYC branch marker genes (e.g. *VSP2*) (Lorenzo *et al.*, 2004; Lorenzo and Solano, 2005; Pieterse *et al.*, 2012). The ERF branch of the JA pathway requires both JA and ethylene signaling (Lorenzo and Solano, 2005; Pieterse *et al.*, 2012). It involves the ethylene-stabilized transcription factors EIN3/EIL1 (ETHYLENE-INSENSITIVE 3, EIN3-LIKE 1) which interact with JAZ proteins and are released upon proteasomal JAZ degradation. EIN3/EIL1 activate the transcription of specific *APETALA2/ETHYLENE RESPONSE FACTOR* (*ERF*) transcription factor genes, including *ERF1* and *ORA59* (*OCTADECANOID-RESPONSIVE ARABIDOPSIS 59*) which activate ERF branch marker genes (e.g. *PDF1.2*) important for defenses against necrotrophic pathogens (Pieterse *et al.*, 2012; Wasternack and Hause, 2013). Both JA

signaling branches are antagonistically regulated. ERF1 positively regulates the ERF branch, thereby promoting resistance to necrotrophic pathogens, but negatively regulates the MYC branch. In contrast, the effects of MYC2 are opposite to those of ERF1 (Lorenzo *et al.*, 2004; Lorenzo and Solano, 2005; Pieterse *et al.*, 2012). However, MYC2 has recently emerged as a master regulator of JA signaling. Thus, MYC2 is not solely coordinating JA-mediated defense responses by differentially regulating both branches of JA signaling. The crosstalk between JA signaling and other phytohormone pathways as well as the interactions between JA signaling and light, phytochrome signaling, and the circadian clock are also known to be regulated by MYC2 (Kazan and Manners, 2013).

1.7 Research objectives and work flow

The aim of the present work was to elucidate the role of cytokinin in the responses to HL and circadian stress. Recent research already provided evidence that cytokinin is an important regulator under adverse environmental conditions. However, a role for cytokinin during light stress had not been studied and several observations in pre-tests suggested that plants with a reduced cytokinin status (i.e. *35S:CKX4* and *ahk2 ahk3*) are more sensitive to this kind of stress than wild-type plants.

In order to study the potential involvement of cytokinin in the light stress response, suitable experimental conditions had to be defined. Light intensities of ~1000 µmol m^{-2} s^{-1} were chosen as stressor and, moreover, a detached leaf assay was established to enable a higher throughput. Since HL stress causes photoinhibition the decrease in F_v/F_m ratios, reflecting the reduction of PSII maximum quantum efficiency, served as measure of the severity of stress. To find out which cytokinin receptor mediates the protective function of cytokinin, single and double receptor mutants were studied under HL stress. Photoinhibition is a consequence of increased photodamage, especially affecting the PSII reaction center protein D1, and/or decreased D1 repair. Therefore, PSII recovery analysis was performed, D1 protein abundance determined, and transcript levels of genes encoding D1 and proteases of the D1 repair cycle were analyzed to evaluate the contribution of a compromised D1 repair cycle. In addition, the degree of photodamage had to be tested. For that the D1 repair cycle needed to be blocked (e.g. by lincomycin) in order to exclusively monitor the impact of photodamage, measuring F_v/F_m ratios as well as the D1 protein abundance. Lastly, photo-protective mechanisms such as non-enzymatic and enzymatic scavenging systems were examined to find potential targets for cytokinin action.

The second part of this work dealt with a previously unknown phenomenon termed "circadian stress". Prolongation of the light period resulted in a pronounced cell death phenotype in plants with a reduced cytokinin status. A high number of transgenic and mutant plants with an altered cytokinin status were analyzed to confirm a role for cytokinin and to unravel the function of specific synthesis and signaling genes of the cytokinin pathway in this novel stress response.

Interestingly, the initiation of cell death was rather delayed, not occurring during the light treatment but depending also on the presence and duration of the following dark period. Therefore, it was ruled out that the cell death development was part of a light stress response. Instead, it was suggested that the change in the light-dark regime negatively affected the circadian clock resulting in "circadian

stress" that triggered the cell death response. Different light-dark-temperature regimes were used to prove this hypothesis. Furthermore, transcript profiles were recorded to uncover if the onset of the stress response in cytokinin-deficient plants on the molecular level coincided with a change in circadian oscillator and clock output gene expression compared with the expression in wild-type plants. Since this was the case, it was hypothesized that mutants that are impaired in circadian clock function might also exhibit a cell death phenotype in response to circadian stress. Several clock mutants as well as hybrids with cytokinin-deficient plants were analyzed regarding their circadian stress response.

The classical stress hormones ABA, SA, and JA have been shown to play roles under stressful environmental conditions as well as during cell death. Therefore, it was tested if they might contribute to the stress and cell death phenotypes in cytokinin-deficient plants. For that, the transcript levels of the corresponding synthesis and response genes were examined and the respective phytohormone levels were determined. Since these experiments pointed to an involvement of the JA pathway, genetic crosses were carried out between cytokinin-deficient plants and JA synthesis and signaling mutants, respectively. The resulting hybrids were also analyzed regarding their response to circadian stress. Other important regulators of cell death are ROS. Transcript analyses pointed to a strong increase in oxidative stress accompanying cell death initiation and progression in cytokinin-deficient plants. In order to elucidate the contribution of ROS to the cell death phenotype following circadian stress in more detail, lipid peroxidation was measured by different means to evaluate oxidative stress. Moreover, H_2O_2 levels were determined and the role of ROS-producing NADPH oxidases RBOHD and RBOHF were examined.

2 Material & Methods

2.1 Databases and software

The databases and softwares used in the present study are listed in Table 1.

Table 1: Databases and software.

Name	Company, reference, or internet link	Purpose of use
ABRC	*Arabidopsis* Biological Resource Centre (https://abrc.osu.edu/)	Ordering *Arabidopsis* seeds
Applied Biosystems 7500 Software v2.0.6	Applied Biosystems/Life Technologies	Quantitative RT-PCR (qRT-PCR)
CorelDRAW	Corel Corporation	Figure design
DIURNAL	Mockler *et al.*, 2007 (http://diurnal.mocklerlab.org/)	Identification of genes with diurnal and circadian expression
eFP Browser	Winter *et al.*, 2007 (http://bbc.botany.utoronto.ca/efp/cgi-bin/efpWeb.cgi)	Developmental and stress-induced gene expression patterns (color-coded)
Excel	Microsoft Office	Calculations and graph design
geNorm	Vandesompele *et al.*, 2002	Search for the most stable reference genes for qRT-PCR
ImageJ	Abràmoff *et al.*, 2004	Image analysis
NASC	The European *Arabidopsis* Stock Centre (http://arabidopsis.info/)	Ordering *Arabidopsis* seeds
NCBI	The National Center for Biotechnology Information (http://www.ncbi.nlm.nih.gov/)	Literature (PubMed), BLAST and others
NEBcutter	New England BioLabs Inc. (http://tools.neb.com/NEBcutter2/)	Search for restriction sites
NetPrimer	PREMIER Biosoft	Primer quality assessment
Primer3	BioTools, University of Massachusetts Medical School (http://biotools.umassmed.edu/bioapps/primer3_www.cgi)	Primer design
Shimadzu Class VP 6.14 Software	Shimadzu	Analysis of antioxidants
SIGnAL	Salk Institute Genomic Analysis Laboratory (http://signal.salk.edu/cgi-bin/tdnaexpress), Alonso *et al.*, 2003	Search for *Arabidopsis* T-DNA insertion mutants
TAIR	The *Arabidopsis* Information Resource (http://www.arabidopsis.org/)	*Arabidopsis* gene information search

2.2 Kits

Kits that were used in this work are listed in Table 2.

Table 2: Kits.

Name	Manufacturer and Cat. No.	Purpose of use
Amplex Red Hydrogen Peroxide/Peroxidase Assay Kit	Invitrogen/Life Technologies, Cat. No. A22188	Quantification of the H_2O_2 content in *Arabidopsis* leaves
NucleoSpin RNA Plant	Macherey-Nagel, Cat. No. 740949.250	RNA isolation and purification from plant tissue
RNeasy Mini Kit	Qiagen, Cat. No. 74106	RNA purification

RNeasy Plant Mini Kit	Qiagen, Cat. No. 74904	RNA isolation and purification from plant tissue
SuperSignal West Pico Chemiluminescent Substrate	Thermo Scientific, Cat. No. 34080	Immuno-detection
QIAshredder	Qiagen, Cat. No. 79656	RNA extraction
QIAquick Gel Extraction Kit	Qiagen, Cat. No. 28704	DNA gel extraction
QIAquick PCR Purification Kit	Qiagen, Cat. No. 28104	PCR purification

2.3 Enzymes

Table 3 contains information about all enzymes that were used in this study in addition to the ones included in the Kits listed in Table 2.

Table 3: Enzymes.

Name	Manufacturer and Cat. No.	Purpose of use
α-Amylase	Roche, Cat. No. 10102814001	Starch quantification
Amyloglucosidase	Sigma-Aldrich, Cat. No. 10113	Starch quantification
Ascorbate oxidase	Sigma-Aldrich, Cat. No. A0157	MDHAR activity
DNase (RNase-Free Set)	Qiagen, Cat. No. 79254	DNase digestion during RNA purification
Glucose-6-phosphate-dehydrogenase (G6PDH)	Roche, Cat. No. 10127671001	Starch quantification
Hexokinase (HK)	Sigma-Aldrich, Cat. No. H5625 Roche, Cat. No. 11426362001	Starch quantification
Immolase DNA Polymerase	Bioline, Cat. No. BIO-21047	qRT-PCR
Restriction enzymes	Fermentas/Thermo Scientific or New England BioLabs	Restriction digestion for genotyping (CAPS marker)
Superoxide dismutase (SOD)	Sigma-Aldrich, Cat. No. S8409	SOD activity
SuperScript III Reverse Transcriptase	Invitrogen/Life Technologies, Cat. No. 18080-044	cDNA synthesis
Taq DNA Polymerase	AG Schuster Institute of Biology/Applied Genetics, FU Berlin	PCR analysis for genotyping

2.4 *Arabidopsis thaliana* plants

If not stated otherwise *Arabidopsis thaliana* ecotype Columbia-0 (Col-0) was used as the wild type (WT) in this study. In specific experiments the accessions C24, Landsberg *erecta* (L*er*), and Wassilewskija (Ws) were tested regarding their circadian stress response.

In Table 4 all mutant and transgenic *Arabidopsis* plants that were used throughout this work are listed.

Table 4: Mutant and transgenic *Arabidopsis* plants.

Name[1)]	References	Source[2)]/Comments
Cytokinin-related		
arr2-1 (*arr2*), GK-269G01	--	Dr. Eva Hellmann, FU Berlin (currently at the University of Helsinki, Finland)
arr1-3 arr12-1 (*arr1,12*) *arr10-5 arr12-1* (*arr10,12*)	Mason *et al.*, 2005; Ishida *et al.*, 2008a	Dr. Eswarayya Ramireddy, FU Berlin
arr3 arr4 (*arr3,4*)	To *et al.*, 2004; Salomé *et al.*, 2006	N25271

35S:CKX1 *35S:CKX2* *35S:CKX4*	Werner *et al.*, 2003	Prof. Dr. Tomáš Werner, FU Berlin
cre1-2 (*cre1*) *ahk2-5* (*ahk2*) *ahk3-7* (*ahk3*) *cre1-2 ahk2-5* (*cre1 ahk2*) *cre1-2 ahk3-7* (*cre1 ahk3*) *ahk2-5 ahk3-7* (*ahk2 ahk3*)	Riefler *et al.*, 2006	Dr. Michael Riefler, FU Berlin
ipt3-2 (*ipt3*) *ipt5-2* (*ipt5*) *ipt7-1* (*ipt7*) *ipt3-2 ipt5-2* (*ipt3,5*) *ipt3-2 ipt7-1* (*ipt3,7*) *ipt3-2 ipt5-2 ipt7-1* (*ipt3,5,7*)	Miyawaki *et al.*, 2006; Chang *et al.*, 2013	Prof. Dr. Tatsuo Kakimoto, Osaka University (Japan)
rock1 35S:CKX1 *rock2 35S:CKX1* *rock3 35S:CKX1* *rock4 35S:CKX1*	Bartrina, 2006; Jensen, 2013; Niemann, 2013	Dr. Michael Niemann (*rock1*), Dr. Helen Jensen (*rock2* and *rock3*), and Dr. Isabel Bartrina (*rock4*), FU Berlin
Clock-related		
cca1-1	Green and Tobin, 1999 (Ws background); Yakir *et al.*, 2009 (backcrossed six times to Col-0)	Prof. Dr. Rachel Green, The Hebrew University (Jerusalem, Israel)
lhy-11 *cca1-1 lhy-11*	Mizoguchi *et al.*, 2002 (L*er* background); Ito *et al.*, 2007; Niwa *et al.*, 2007 (backcrossed four times to Columbia)	Prof. Dr. Takeshi Mizuno, Nagoya University (Japan)
CCA1ox (*35S:CCA1*) *TOC1ox* (*35S:TOC1*)	Wang and Tobin, 1998 Makino *et al.*, 2002	Prof. Dr. Takeshi Mizuno, Nagoya University (Japan)
lhy-20, SALK_031092 *cca1-1 lhy-20*[3)]	Michael *et al.*, 2003a; Salomé *et al.*, 2010 This study	N531092 --
toc1-101	Kaczorowski, 2004; Kikis *et al.*, 2005	Prof. Dr. C. Robertson McClung, Darmouth College (Hanover, New Hampshire, USA)
35S:CKX4 toc1-101[3)] *ahk2 ahk3 toc1-101*[3)]	This study	--
elf3-8 *elf3-9*	Hicks *et al.*, 2001	N3794 N3795
elf4-101, SAIL_1244_G01	Khanna *et al.*, 2003	Dr. Jos Schippers, RWTH Aachen University
lux-1	Hazen *et al.*, 2005	Dr. Jos Schippers, RWTH Aachen University (plus corresponding C24 wild-type seeds)
prr3-1, SALK_090261 (*prr3*) *prr5-3*, SALK_064538 (*prr5*) *prr7-3*, SALK_030430 (*prr7*) *prr9-1*, SALK_007551 (*prr9*)	Michael *et al.*, 2003a; Salomé and McClung, 2005a	N666702 N670849 N678316 N657486
prr7-3 prr5-1 (*prr7 prr5*); additionally contains *TOC1:LUC* conferring BASTA-resistance	Michael *et al.*, 2003a; Salomé and McClung, 2005a	Dr. Patrice Salomé, Max Planck Institute for Developmental Biology (Tübingen)
prr9-1 prr5-3 (*prr9 prr5*)[3)]	This study	Derived from crosses between *prr9-1 prr7-3* and *prr5-3*
prr9-1 prr7-3 (*prr9 prr7*)	Salomé and McClung, 2005a	Prof. Dr. C. Robertson McClung, Darmouth College (Hanover, New Hampshire, USA)
prr9-1 prr7-3 prr5-3 *(prr9 prr7 prr5)*[3)]	This study	Derived from crosses between *prr9-1 prr7-3* and *prr5-3*
tic-2, SAIL_753_E03	Ding *et al.*, 2007	N861195
che-2, SAIL_1284_G12	Pruneda-Paz *et al.*, 2009	N847874

JA-/SA-related		
coi1, SALK_035548	Maruta *et al.*, 2011	N535548
coi1 ahk2 ahk3[3)]	This study	Silencing of *CKX4* overexpression in *coi1 35S:CKX4* hybrids
jar1-1	Staswick *et al.*, 1992; 2002	N8072
jar1-1 ahk2 ahk3[3)] *jar1-1 35S:CKX4*[3)]	This study	--
myc2-3/jin1-8, SALK_061267	Lorenzo *et al.*, 2004; Shin *et al.*, 2012	N656547 Silencing of *CKX4* overexpression in *myc2-3 35S:CKX4* hybrids; genetic linkage between *MYC2* and *AHK3*
npr1-1 *npr1-2*	Cao *et al.*, 1997	N3726 N3801
Light perception, ROS-related, and others		
phyA-211 (*phyA*) *phyB-9* (*phyB*)	Reed *et al.*, 1994 (*y18*) Reed *et al.*, 1993 (*hy3-EMS142*)	Stefanie Zintl, FU Berlin (in Columbia background)
rbohD-3 *rbohF-3* *rbohDF*	Torres *et al.*, 2002	N9555 N9557 N9558
ahk2 ahk3 rbohD-3[3)] *ahk2 ahk3 rbohF-3*[3)] *35S:CKX4 rbohD-3*[3)] *35S:CKX4 rbohF-3*[3)]	This study	Derived from crosses between *rbohDF* and *ahk2 ahk3* or *35S:CKX4* (cytokinin-deficient *rbohDF* plants died off starting around bolting time)
ctpa1, SAIL_169_G01	Yin *et al.*, 2008	N860483

1) Written in parentheses are the names used throughout this study
2) NASC ID if ordered from stock centre or seeds kindly provided by the indicated researcher
3) Generated in this study

2.5 Growth conditions for *Arabidopsis thaliana* plants

2.5.1 Growth temperature, light intensity, and daylength (photoperiod)

For the majority of experiments *Arabidopsis* plants were grown under SD conditions (light/dark: 8 h/16 h) in a phytochamber at 22 °C and light intensities of 120-170 µmol m^{-2} s^{-1}. LD conditions (light/dark: 16 h/8 h) were used for genotyping, genetic crosses, and propagation (in the greenhouse), or segregation analyses (growth chamber/culture room). Under the LD rhythm plants were exposed to temperature cycles (light/dark: 22 °C/18 °C).

2.5.2 In vitro culture

Arabidopsis seedlings were grown under sterile conditions on solid medium (see Table 5) for segregation analyses (hybrids carrying the *35S:CKX4* transgene), pre-selection (for selection of *coi1* homozygotes), and "bulk" genotyping (verification of genotyping results in the subsequent generation using two pools of 10 to 20 seedlings per genotype, medium without supplements).

Seeds were surface-sterilized by soaking and shaking for 5 min in 70 % ethanol with the addition of 0.01 % Triton X-100. Afterwards seeds were rinsed two to three times with 70 % ethanol under a clean bench and finally transferred (by pipetting) onto a sterile filter paper in a Petri dish. The dried seeds were then transferred onto the medium using sterile toothpicks. After the seeds were sown on

medium the Petri dishes were either loosely sealed with plastic wrap (for segregation analysis in the growth chamber/culture room) or sealed with Leukopor tape (for pre-selection in the SD phytochamber under rather unsterile conditions). After stratification (4 °C) for two days, the Petri plates were transferred to growth conditions.

Table 5: Plant culture medium.

MS medium[1)] supplemented with hygromycin[2)] or MeJA[3)]	
Components	**Concentration**
MS basal salt mixture	4.3 g/L
MES	0.5 g/L
Sucrose	10 g/L (1 %)
Phytagel	9 g/L
pH 5.7 (adjusted with 1N KOH)	
Hygromycin (50 mg/mL)	300 µL/L (15 mg/L)
MeJA (4.36 M) diluted to 25 mM working solution (in DMSO)	1 mL/L (25 µM)

1) Murashige and Skoog, 1962
2) Segregation analysis for selection of homozygous *35S:CKX4* transgenic plants; added after autoclaving
3) Pre-selection of *coi1* homozygotes from a segregating population; added after autoclaving

2.5.3 Growth on soil

Arabidopsis seeds were sown on thoroughly watered "sowing soil" (2:2:1, Soil Type P:Soil Type T:Sand), stratified at 4 °C for two days, and then transferred to the greenhouse (LD) or the phytochamber (SD). For the first two days the plant trays were covered with a clear plastic dome to protect seeds and germinating seedlings from desiccation. After about two weeks plantlets were singled out. In the phytochamber plants further grew on "sowing soil" and in the greenhouse they were transferred to soil containing Perligran G instead of sand. Soil-grown plants were used for HL as well as circadian stress treatments (see also 2.6).

2.6 Light stress and light-dark-temperature regimes

2.6.1 HL stress treatment

HL experiments (~1,000 µmol m^{-2} s^{-1}, Percival AR66L, Percival Scientific) were mainly performed with detached leaves of four-week-old SD-grown plants (one experiment with whole plants, Fig. 3.1B). True leaves 5, 6, and/or 7 were used and marked prior to the experiment (~1 week) with toothpicks of different colors. Leaves were detached using scissors and transferred to Petri dishes with water using featherweight forceps to minimize wounding of the petioles. Control leaves remained in SD conditions. Continuous light (CL, ~150 µmol m^{-2} s^{-1}) treatments either at growth temperature (22 °C) or in combination with cold (10 °C) were also performed in a growth chamber.

2.6.2 Circadian stress treatment – changes in the light-dark-temperature regime

The different light-dark-temperature regimes used for the circadian stress project have been accomplished by combining phytochambers and growth chambers that were programmed to the regime/rhythm of interest. For experiments with a high number of different conditions in parallel (e.g. shown in Figs. 3.16 and 3.19) plant trays were transferred into the respective conditions manually during the experiment.

If not stated otherwise, five- to six-week-old SD-grown plants were used. The standard temperature was 22 °C and the standard circadian stress regime used in this work was 32 hours of CL treatment (see Fig. 3.6A, "32 h L/16 h D") later always referred to as "CL treatment". Alternative regimes are explained in the respective figures and the corresponding (main) text. The light intensity during the light periods was always adjusted to ~150 µmol m^{-2} s^{-1} to keep it similar to the prior growth conditions (SD) which was especially important for cold treatments (10 °C) because the cold temperature dramatically decreased the efficiency of the tubes/lamps. For subsequent analyses affected leaves (e.g. from treated *ahk2 ahk3* and *35S:CKX4* plants) and leaves of the same developmental stage (e.g. from treated wild-type or control plants) were chosen, respectively. For most experiments which required the harvest of leaf material only distal halves of these leaves were harvested corresponding to the most affected parts in cytokinin-deficient plants (exceptions: F_v/F_m, HOTE, FW, ion leakage, and starch analyses; whole leaves were used for these experiments). Harvests that took place during the dark period (e.g. kinetics experiment; see Fig. 3.23A) were carried out under green (control) light exposure.

2.7 Genetic crosses

To perform genetic crosses, the female parent was prepared first. Two to three flower buds were selected in which the tips of the petals were barely visible and before the anthers began to release pollen. Siliques, leaves, younger flower buds, and open flowers in the close proximity as well as sepals, petals, and all six stamens on the selected flower buds were removed using a small pair of scissors and precision clamping tweezers, respectively. It was visually confirmed (under the binocular) that no pollen has been deposited yet on the stigma and that the pistil was fully intact. After emasculation of the flower buds of the female parent the male parent was chosen. A newly opened flower was selected with anthers that were dehiscent. The complete flower was removed by squeezing near the pedicel with tweezers. The female parent was pollinated by taking the fully open flower of the male parent and brushing the anthers over the bare stigma of the female parent. By visual inspection (under the binocular) it was confirmed that the stigma was covered with pollen. Crosses were successful when siliques started elongating after two to three days. Seeds from the respective siliques were harvested (collection in small paper bags) and used for propagation. Segregation analyses and genotyping were carried out using the F2 and F3 progeny, respectively.

2.8 Nucleic acid methods

2.8.1 Quantification of transcript abundance via quantitative RT-PCR

2.8.1.1 Isolation and purification of total RNA

Arabidopsis leaf material for the extraction of total RNA was shockfrozen in liquid nitrogen in 2 mL-microcentrifuge tubes containing two steel beads and ground in pre-cooled (liquid nitrogen) adapters using a Retsch mill (Retsch Mixer Mill MM2000). For qRT-PCR analysis on HL samples (Fig. 3.2) and on CL samples for endpoint analysis (one day after CL treatment; Fig. 3.12) total RNA from leaf material (~100 mg) was extracted using the TRIzol method (for details see below) followed by RNA purification using the RNeasy Mini Kit (Table 2) according to the manufacturer's protocol including the on-column DNase (Table 3) digestion. For all other qRT-PCR experiments the total RNA from leaf material (< 100 mg, to obtain higher yields) was extracted and purified using Kits only (either NucleoSpin RNA Plant, RNeasy Plant Mini Kit, or a combination of QIAshredder and RNeasy Mini Kit; see Table 2) always including on-column DNase digestion and according to the manufacturer's protocol.

For the HL experiment leaves 5, 6, and 7 were pooled. For the CL (circadian stress) experiments the distal halves of affected leaves from treated cytokinin-deficient plants (e.g. *ahk2 ahk3* and/or *35S:CKX4*) and the distal halves of leaves of the same developmental stage from other treated (e.g. wild type) or control plants were harvested (as described in 2.6.2).

In the following the TRIzol method is described. 1 mL TRIzol reagent (see Table 6) was added to the frozen leaf material and samples were immediately vortexed (until completely thawed and homogenous). The samples were incubated for 5 min at RT and then centrifuged for 5 min at 16,000 x g and 4 °C. The supernatants were transferred into new 2 mL-microcentrifuge tubes and 400 µL of chloroform/isoamyl alcohol (24:1) were added. The samples were vortexed (until homogenous) and again incubated for 5 min at RT followed by centrifugation (15 min, 16,000 x g, 4 °C). The upper phase (600-700 µL) of the supernatant was transferred into a new 1.5 mL-microcentrifuge tube. 300-350 µL (1/2 volume) of isopropyl alcohol and 300-350 µL (1/2 volume) of high salt solution (1.2 M sodium chloride, 800 mM sodium citrate) were added. The mixture was inverted until it was clear again and then incubated for 10 min at RT. Afterwards the samples were centrifuged for 10 min at 12,000 x g and 4 °C. The supernatant was completely removed and discarded. 900 µL of 75 % ethanol were added to the RNA pellet followed by short vortexing and centrifugation (5 min, 7,500 x g, 4 °C). This ethanol washing step was repeated a second time. The RNA pellet was dried at RT and dissolved on a heating block for 5 min at 60 °C in 30 µL of RNase-free water.

In order check the quality and quantity of the isolated RNA the RNA samples were measured photometrically at 260, 280 and 230 nm using the NanoDrop ND-1000 spectrophotometer with the RNA-40 program. The RNA was considered clean if the ratios of 260/280 and 260/230 were both > 2. Equal amounts of starting material (1 µg RNA) were used for cDNA synthesis (see 2.8.1.2).

Table 6: TRIzol reagent.

Components	Concentration
Phenol	38 %
4 M guanidinium thiocyanate	800 mM
4 M ammonium thiocyanate	400 mM
3 M sodium acetate, pH 5	100 mM
50 % glycerol	5 %
Always freshly prepared	

2.8.1.2 cDNA synthesis

For cDNA synthesis 1 µg RNA (see 2.8.1.1) and SuperScript III Reverse Transcriptase (see Table 3) were used. First, mix 1 (Table 7) was incubated for 5 min at 65 °C and then immediately placed on ice for at least 2 min. Mix 2 was prepared as a master-mix for all reactions and 5.5 µL of this mixture were added to mix 1. This reaction mixture was incubated for 5 min at 25 °C, 60 min at 50 °C, and 15 min at 70 °C. After cDNA synthesis the cDNA was diluted 1:10 and then used for qRT-PCR (see 2.8.1.4).

Table 7: Reaction mixture for cDNA synthesis with SuperScript III.

Mix 1		Mix 2	
Components	**Volume [µL]**	**Components**	**Volume [µL]**
50 µM oligo dT primer	1	5x first strand buffer	4
50 µM N9 random primer	1.8	0.1 M DTT	1
RNA	x (1 µg)	200 U/µL SuperScript III	0.5
5 mM dNTPs	2	--	--
water	ad 14.5	--	--

2.8.1.3 Primer design for qRT-PCR analysis

All primer pairs were designed using the Primer3 software (see Table 1) under the following conditions: optimum Tm at 60 °C, GC content between 20 % and 80 %, product size 100-200 bp. Then all primers found were checked using BLASTN (TAIR) and NetPrimer (see Table 1) to confirm their specificity (Blast) and to evaluate their quality (NetPrimer: rating 100 %, exclusion of hairpins, self-, and cross-dimers). Suitable primer pairs were ordered from Invitrogen/Life Technologies. In Table 8 all primers that were used for qRT-PCR in this work are listed and subgrouped in primers for genes of interest (GOI) and primers for reference genes.

Table 8: Primer sequences for qRT-PCR.

Gene	AGI number	Forward Primer	Reverse Primer
Genes of interest (GOI)			
*AAO3**	AT2G27150	TGCTTATGGTCTCGGTATGG	TAACGGCTTCACAACTGCTC
*ABA1**	AT5G67030	TTTGTTTCTTCGGATGTTGG	GAATGGCTTCCTCCTCAGTC
ABA2	AT1G52340	TAGTGTGGGAGGTGTTGTGG	CAAATGAGCCAAAGCGAGT
ACD6	AT4G14400	GGACCGTGAAGTGAGGAAGT	GATGCTCCGTATGAAAGACAAG

AOC2	AT3G25770	CGACACAGCCCCAAGATT	GATGACGACGCAGAGACCT
*AOS**	AT5G42650	CCCTTTTCCGATTTCTCTCC	AACGGTCTTTGATTGGTCCTAC
ARR4	AT1G10470	CCGTTGACTATCTCGCCT	CGACGTCAACACGTCATC
ARR5	AT3G48100	CTACTCGCAGCTAAAACGC	GCCGAAAGAATCAGGACA
ARR7	AT1G19050	CTTGGAACCAATCTGCTCTC	ATCATCGACGGCAAGAAC
ARR9	AT3G57040	GATAGAGCACGTCCTAGATTCG	CTGCATTCCCTACTGAAACC
ARR16	AT2G40670	TCAGGAGGTTCTTGTTCGTCTT	AACCCAAATACTCCAATGC
BAP1	AT3G61190	CCAGAGATTACGGCGCGTGTT	TACAGACCCCAAACCGGAACTCC
BFN1	AT1G11190	GCCGGACCAGCACATGTAGT	TAAGAGCAGGCTTGGTCGGGA
BI1	AT5G47120	GCTCTTGTGGCGTCTGCCTT	AAGGGGCCAACAGAAGCACC
CAB2	AT1G29920	AGAGGCCGAGGACTTGCTTTAC	GCCAATCTTCCGTTCTTGAGC
CAT2	AT4G35090	CCGCCTGCTGTCTGTTCT	AATCGTTCTTGCCTCTCTGGT
CCA1	AT2G46830	AGCAACGTGAAAGGTGGACTGAG	GCGCTTGACCCATAGCTACACC
CHE	AT5G08330	GAAGACGACCACGAACCAC	ACCCTAAAACCCTAATCAAACAAG
*CKX5**	AT1G75450	CGACTCGTCAGAACAGCTTAC	GTTACGCCGTGGTTCATT
COI1	AT2G39940	ACAAGGAATGGAGGACGAAG	GGCGGAAGTCACAGAGGT
COR47	AT1G20440	CGATGAAGAAGGTGAGGAAAA	GGGATGGTAGTGGAAACTGG
CTP homolog	AT3G57680	TGTTTGTGACGGTGGCTA	AGCAATGGAACCGAACTG
CTP homolog	AT4G17740	ACAGTTGCTCGATATGAAACAC	CTTGATTGAGATAACAAGCAGC
CTP homolog	AT5G46390	TATCCCTGAACTTCCACCTC	CATTAGTAGCAGCAACGGAG
DEGP5	AT4G18370	GGGTAGTAAGTGGGTTGGGAAG	TGTCAATGGGAATGGCAAA
DEGP8	AT5G39830	CCCGAAACTCTCCTGAAACC	AAATCCAACACCCGCAGA
EDS1	AT3G48090	CAAGCTTCTGTGGAAATGGCTGTG	ATGTCACACAACGAGGCTCAAGG
ELF3	AT2G25930	AACAGCAACAGCCAACAAAG	GTCACTCCTCCCCCATCTCT
ELF4	AT2G40080	AGGCAGAGCAGGGAGAGG	GGTGATTGTCGTTGACTTGTTG
ERF1	AT3G23240	TTCCGATCAAATCCGTAAGC	CCGAGCCAAACCCTAATACC
FER1	AT5G01600	CAACGGTGACCACACGCCTT	ACGAGAGTGCGTTTGAGGCC
FTSH1	AT1G50250	CGCTAGCTTTAGCTGTAGTGG	ATCCTTCTGGGAGATCCG
FTSH2	AT2G30950	GAGAAAGAAACTATTGGCGGT	TGATGCTGGAGTTGTCGT
FTSH5	AT5G42270	GGAGTGCCGTTCTTTTCGT	CATCATTTCCACCACCCATC
FTSH8	AT1G06430	TGTGCCCTTCTTTTCCATCT	TCCAGTTCCTCTTTGCCTACC
ICS1	AT1G74710	CGTCGTTCGGTTACAGGTT	CCGTTTCCGTTCTCGTTAG
JAZ1	AT1G19180	CCCAACACCATTGACAGAAC	CTAAACCGAGCCACGACA
LHY	AT1G01060	CAACGAAACAGGTAAGTGGCGACA	TGCGTGGAAATGCCAAGGGT
LOX3	AT1G17420	ACGTTGTCGTACTGGTCGCC	GTCTCGTGGCACATACATAGGTAATG
LOX4	AT1G72520	AAGGTCTCCCTGCTGATCTCAT	AAGCCCATGTGGTTGTGTTG
LUX	AT3G46640	GCTCATCATCTTCACAAACCA	CTTCGTCGCTTGGTAATCC
MCP2D	AT1G79340	AACCCGCTATGCAGACACACG	CAGTTGGTTTCCCCGCTGGA
MYC2	AT1G32640	CAGAGAAACTCCAAATCAAGAACC	CAACGCCGACATCAACCT
OPR3	AT2G06050	GAGACATGACGGCGGCACAA	AATACTCTGCCAACGCCGCG
ORA59	AT1G06160	CGGAAGATGGAGAATGTGAAT	GACGAAGAAGATGAATAGGAGGA
PR1	AT2G14610	ATGCAGTGGGACGAGAGGGT	AACCCACATGTTCACGGCGG
PR5	AT1G75040	ATCATCACCCACAGCACAGAGACA	CCAGACGGTGGTAGGGCAATTG
PRR3	AT5G60100	TGGGAGTAGTGGTGGTTTGAG	ATTGATTTGAAGGCGAGGTG
PRR5	AT5G24470	GAATGAAGCGAAAGGACAGA	GATTGGACTTGACGAACGAA

PRR7	AT5G02810	CATCGTTTCAGCCTTTACCC	CATTCCTCCAGCATTCATACC
PRR9	AT2G46790	TATGGGGGAGATTGTGGTTT	GGCAGTGATGATTTGACGAG
PSBA	ATCG00020	CGAAAGCGAAAGCCTATG	GTTGCGGTCAATAAGGTAGG
RBOHD	AT5G47910	CGGGATAGTCGTCGGTGTT	TTCCATCGGCTCATAGGTGT
*RBOHF**	AT1G64060	AGAATACAGCACAGGAAGCAAC	GAGAGCAGAACGAGCATCAC
RD29B	AT5G52300	TGGAGGAGGAGGAGAGAAGA	TTACCACCGAGCCAAGAAGT
SAG12	AT5G45890	TCTGGTGTGTTCACTGGAGAGT	ATCCGTTAGTAGATTCGCCGTA
SID1	AT4G39030	GGTTCGTTCTCGTCGGATT	TTCTTGACATTGGTGCCTGA
TIC	AT3G22380	TATGACGACGGAGGTGTAGG	ATTGTTGTGGCTGTGATGGT
TOC1	AT5G61380	TTGGTCACCGGCAGGAAATCC	ACTGACCCTTAACGCGGGGT
ZAT12	AT5G59820	CGCTTTGTCGTCTGGATTG	AGCAGCCCCACTCTCGTT
Reference genes			
ACT2	AT3G18780	CTTGCACCAAGCAGCATGAA	CCGATCCAGACACTGTACTTCCTT
CI51	AT5G08530	TTTCGTCTCCATGGCACCCG	TGAGTCTTTTCCGGAGGCGGA
KOR1	AT5G49720	GGGTGTGAGACCAGAAGATTAG	TGTGGTAAAGTAACCCACCC
MCP2D	AT1G79340	see above (GOI)	see above (GOI)
NDHI	ATCG01090	CAATCAACAACAGGCAAATC	GGAGTGCCGTTCTTTTCGT
PP2AA2	AT3G25800	CCATTAGATCTTGTCTCTCTGCT	GACAAAACCCGTACCGAG
RPS3	ATCG00800	TTGAAGATAAACCCCGAAGA	ACGGATTGGAAATTCTGGTA
SAND	AT2G28390	CAGATTCGAGGTCTTCTCCT	GTGTGGCTACCATCAGAGACT
TAFII15	AT4G31720	GAATCACGGCCAACAATC	ACTCTTAGCCAAGTAGTGCTCC
UBC10	AT5G53300	CCATGGGCTAAATGGAAA	TTCATTTGGTCCTGTCTTCAG

1) Abbreviations of gene names are explained in the list at the beginning of this work.

* These primers were used in a 600 nM final concentration instead of the standard 300 nM (see 2.8.1.4).

2.8.1.4 Quantitative reverse transcription PCR (qRT-PCR)

qRT-PCR analysis was performed with the 7500 Fast Real-Time PCR System (Applied Biosystems/Life Technologies) using SYBR green I as DNA-binding dye, ROX as internal reference dye, and Immolase (see Table 3) as hot-start DNA polymerase. The composition of one reaction mixture is listed in Table 9.

Table 9: Reaction mixture for qRT-PCR.

Components	Volume [µL]	Final concentration
10x Immolase buffer	2	1x
50 mM $MgCl_2$	0.8	2 mM
5 mM dNTPs	0.4	100 µM
10x SYBR Green I	0.2	0.1x
25 µM ROX	0.04	50 nM
50 µM forward primer	0.12/0.24	300 nM/600 nM
50 µM reverse primer	0.12/0.24	300 nM/600 nM
Immolase (5 U/µL)	0.04	0.01 U
water	ad 19	--
Template (1:10 diluted cDNA)	1	1:200 diluted

All components excluding the diluted cDNA (template) were mixed as a master-mix for all reactions and 19 µL of that master-mix were added to each well of the 96-well plate which already contained the template or water as no template control.

For the PCR reaction the "FAST" cycling setup was used (Applied Biosystems 7500 Software, see Table 1). After heat activation of the DNA polymerase (95 °C, 15 min) 40 PCR cycles followed comprised of denaturation (95 °C, 5 sec), annealing (55 °C, 15 sec), and elongation (72 °C, 10 sec). Finally, a dissociation curve was generated to check for specificity of the amplification.

Primer efficiency was tested for all primer pairs that were designed. For that a cDNA mix of all cDNA samples (1:10 diluted) of one experimental setup was prepared of which a dilution series was made using two-fold (first five) and four-fold (last two) dilutions. These diluted cDNA samples together with the 1:10 diluted cDNA mix (as highest template concentration) were measured in technical triplicates and duplicates, respectively, using the standard PCR program (see above). Primer efficiency (E in %) was calculated as $E = 10^{-1/slope} \times 100$ plotting the logarithm of the dilutions (1, 0.5, 0.25, 0.125, 0.0625, 0.0156, 0.00391, and 0.000977) on the X axis and the Ct (threshold cycle, output of detection system) values on the Y axis. Primers were defined as suitable if the efficiency was ≥ 86 %.

For each experimental setup the relative expression of candidate reference genes was determined for all cDNA samples *via* qRT-PCR at first. The resulting Ct values were transformed into $2^{-\Delta Ct}$ ($\Delta Ct = Ct_{sample} - Ct_{min}$; Ct_{min} = lowest Ct value) which were implemented into geNorm (see Table 1; Vandesompele *et al.*, 2002). By using the geNorm algorithm the most stable reference genes within the tested set of candidate genes could be identified. At least two reference genes were selected for each setup. They are always indicated in the respective figure legends (for primer sequences see Table 8).

The reference gene data were used for the normalization of the expression values derived from GOI analysis. For that a normalization factor (NF) was calculated for each sample as the geometric mean of the $2^{-\Delta Ct}$ values of all reference genes determined. The relative expression of GOI was then calculated as $2^{-\Delta Ct}$ (GOI)/NF. If not stated otherwise these relative expression values were normalized to the wild-type control which was set to 1.

2.8.2 Genotyping of Arabidopsis plants

2.8.2.1 Genotyping strategies

Plants were genotyped after ordering seeds from NASC or in the F2 and F3 generation following genetic crosses. However, in some cases homozygous plants could be selected by phenotypic characteristics as for example *tic-2* (dark green serrated leaves, late flowering) or *elf3* and *lux* (long hypocotyls, long petioles, early flowering), or homozygous plants were identified by selection on MeJA-containing medium (*coi1*) or segregation analysis (*35S:CKX4*) (see also 2.5.2).

Two different strategies were pursued for PCR-based genotyping. Insertional mutants (mostly carrying T-DNA insertions) were genotyped *via* PCR using two primer pairs, one pair flanking the insertion and used to amplify the wild-type allele and one pair comprised of a gene-specific and a insertion (T-DNA)-

specific primer used to amplify the mutant allele. In Table 10 all insertion-specific primers that were used are listed and Table 11 contains all gene-specific primer pairs and information about the primer combination for detecting the respective mutant alleles.

Table 10: Insertion-specific primers used in this study.

Name[1)]	Primer	Purpose of use
D4_CKX4ox (D4)	CAGAATTGAAAGCAAATATCA	Genotyping of *35S:CKX4* plants (D4 binds to the terminator sequence of the transgene)
dSpm transposon insertion (dSpm1)[2)]	CTTATTTCAGTAAGAGTGTGGGGTTTTGG	Genotyping of *rbohF-3*
dSpm transposon insertion (dSpm11)[2)]	GGTGCAGCAAAACCCACACTTTTACTTC	Genotyping of *rbohD-3*
Feldmann-T-DNA-LB (F_T-DNA)[3)]	GATGCACTCGAAATCAGCCAATTTTAGAC	Genotyping of *cca1-1* (derived from the Feldmann T-DNA collection)
GABI-Kat (GABI)	CCCATTTGGACGTGTAGACAC	Genotyping of GABI-Kat lines
IT-LB1 (SAIL)	GCCTTTTCAGAAATGGATAAATAGCCTTGCTTCC	Genotyping of SAIL lines
SALK LBb1.3 (SALK)	ATTTTGCCGATTTCGGAAC	Genotyping of SALK lines

1) Written in parentheses are the names used in Table 11
2) Tissier *et al.*, 1999
3) Krysan *et al.*, 1996

Table 11: Primer sequences for genotyping of insertional mutants.

Mutant	Primer sequences[1)] wild-type allele	Product size [bp]	Primer combination mutant allele (see also Table 10)	Annealing [°C]
ahk2-5	F-GCAAGAGGCTTTAGCTCCAA R-TTGCCCGTAAGATGTTTTCA	672	F + SAIL (650 bp)	55
ahk3-7	F-CCTTGTTGCCTCTCGAACTC R-CGCAAGCTATGGAGAAGAGG	558	R + GABI (450 bp)	55
arr3	F-CCTGGAATGACTGGATACGA R-AGTTCCTTCGTGAGCAAAGAG	716	F + SALK (ca. 650 bp)	55
arr4	F-CTGAAACAGGAATCGTCCAA R-TATTACACGGCATCCCAGAA	583	R + SALK (ca. 600 bp)	55
cca1-1	F-TGTCCAGATAAGAAGTCACGCTCAGAAA R-TTTATTCATGGAGGATGCAGCAGAGA	914	F + F_T-DNA (ca. 250 bp)	65
che-2	F-CATATCGTGTGGGGGTCA R-TTACTCACTGCTCCGTCGTT	917	R + SAIL (ca. 500 bp)	55
35S:CKX4	**--**	--	F (GCTTAACATCTTTGTCCC) + D4 (700 bp)	55
coi1	F-TGATTCCATCGTCCCACTT R-TTGAACCATCTCCGACACAC	394	R + SALK (ca. 250 bp)	55
ctpa1	F-ACTCACAGCGTTTTCACAGG R-CGTGCTCAGCGACCATAA	978	F + SAIL (ca. 580 bp)	55
elf4-101	F-CCTCTACCCAATCACTTCACAG R-ACCATCGTGACCGTTCTTC F*-GGAAGAAAAAGTTGGGAGGA[2)]	530 (F + R)	F* + SAIL (ca. 650 bp)	55
lhy-20	F-GAGAGCGATGGACTGAGGA R-TTTTCGGGGTAGAGATGATAGAG	795	R + SALK (ca. 500 bp)	55
myc2-3/ jin1-8	F-GACGGATACGGAATGGTTTT R-GTTTGCTGGCTTTCTTCCTC	853	F + SALK (ca. 550 bp)	55
toc1-101	F-GAT**TTTGATCTTGTGGGAT**CTG[3)] R-TCTTTTCATTGGCTCATGGT	360	-- (see Table 12)	55
prr3-1	F-GCTGAGTTAGGCTCCAGAAGA R-GCGAGAAAGAGAATGAGAGAGG	835	F + SALK (ca. 550 bp)	55
prr5-1/ prr5-3	F-GCAAACCTATGTACCAAACAGA R-TTCCGACGTGATAACTTTCC	874	R + SALK (ca. 300 bp, *prr5-1*) (ca. 600 bp, *prr5-3*)	55

prr7-3	F-GGGTTTATGGCTGTGTTTTG R-ATGTTCCGACGAGATTTGTG	623	F + SALK (ca. 400 bp)	55
prr9-1	F-CATCACTGCCCTTCTTCGT R-CGTTTTTCCTCATTGGTTTG	484	F + SALK (ca. 400 bp)	55
rbohD-3	F-TGGACTGGCATTGTGATGGTTGTG R-CGGGAGCTGATGTGATTGAGAAAGG	702	R + dSpm11 (ca. 750 bp)	65
rbohF-3	F-GGTGCTGGTGGTGGTTTGGTG R-TGAGCGAAATCGGAGCGATAGATG	218	R + dSpm1 (ca. 200 bp)	65

1) F: forward primer; R: reverse primer
2) F* primer only for T-DNA-specific PCR
3) Bold: 16 bp-deletion in *toc1-101*

Mutants carrying a point mutation (derived from EMS mutagenesis) or a deletion (*toc1-101*) were genotyped using so-called CAPS markers. The deletion and point mutations caused cleaved amplified polymorphic sequences (CAPS), which means that they result in differences in the restriction fragment lengths because a restriction site was created or abolished, respectively, by the mutation. For that approach a DNA fragment was amplified *via* PCR that contained the polymorphic site and the PCR product was digested with a specific restriction enzyme (see Table 12 and 2.8.2.6).

Table 12: Genotyping using CAPS markers.

Mutant	Primer pair	Restriction enzyme	Wild-type allele/ mutant allele [bp][1)]	Mutation, reference[2)]
jar1-1	CAATGGAAACGCTACTGACC CGGGACTACAGGAAGGAGAC	*Hpy*188III	221, 411/632	Ser112Phe (TCT→TTT)
npr1-1	TGCGTGTGCTCTTCATTTC ATCGTTTCCCGAGTTCCA	*Hin*1II	115, 98, 200, 377/213, 200, 377	His334Tyr (CAT→TAT)
npr1-2	CCTGATGTATCTGCTCT GCTTAATGCAGATGGTG	*Nsb*I/*Fsp*I	330, 134/464	Cys150Tyr (TGC→TAC) (Zang and Shapiro, 2002)
toc1-101	CAATGGCTAAGGGTATGAAGATG CAGTAACAGCAAGAGAAGAAGTGG	*Bst*YI/*Psu*I	47, 494, 288/47, 782	16 bp-deletion (nt 466-481 from ATG)

1) DNA fragment lengths after digestion with the specified restriction enzyme
2) Reference for CAPS marker

2.8.2.2 Extraction of genomic DNA from Arabidopsis

Plant material (e.g. 1-2 young leaves or 10-20 seedlings) was shockfrozen in liquid nitrogen in 1.5 mL-microcentrifuge tubes containing two steel beads and ground in pre-cooled (liquid nitrogen) adapters using a Retsch mill. 400 µL of the extraction buffer (200 mM Tris/HCl pH 7.5, 250 mM NaCl, 25 mM EDTA, 0.5 % SDS) were added to the plant powder and the mixture was thorougly vortexed. The sample was centrifuged in a microcentrifuge for 3 min at 13,000 rpm and 300 µL of the supernatant was transferred into a fresh 1.5 mL-microcentrifuge tube. 300 µL of isopropyl alcohol were added, the sample was vortexed, incubated at RT for at least 2 min, and then centrifuged again (5 min, 10,000 rpm). The supernatant was discarded and the pellet washed with 300 µL 70 % ethanol. After another centrifugation step (5 min, 10,000 rpm) the supernatant was discarded and the pellet dried at RT. 40 µL water were added to the dried pellet. The samples were kept at least for 1 hour at 4 °C (mostly overnight) until used for PCR analysis.

2.8.2.3 PCR analysis

Standard PCR analysis was performed using genomic DNA extracts (see 2.8.2.2) in order to genotype *Arabidopsis* plants. For amplification thermostable DNA polymerase from *Thermus aquaticus* (*Taq*, see Table 3) was used and 10x *Taq* PCR buffer consisted of 500 mM KCl, 100 mM Tris/HCl pH 9, and 1 % Triton X-100. The composition of a typical PCR reaction mixture (20 µL) is shown in Table 13.

Table 13: PCR reaction mixture.

Components	Volume [µL]	Final concentration
10x *Taq* PCR buffer	2	1x
100 mM $MgCl_2$	0.4	2 mM
5 mM dNTPs	0.8	200 µM
50 µM forward primer	0. 25	625 nM
50 µM reverse primer	0. 25	625 nM
Taq DNA polymerase	0.5	--
water	ad 19/18.5	--
Template (undiluted DNA extract)	1/1.5	--

Primer pairs were designed as described in chapter 2.8.1.3. The desired product size of course changed and depended on the specific approach (Tables 11 and 12, see 2.8.2.1). After the initial denaturation step (95 °C, 5 min) 40 PCR cycles followed comprised of denaturation (95 °C, 15 sec), annealing (55-65 °C, 40 sec), and elongation (72 °C, 1 min/kb). The final elongation step (at 72 °C) was twice as long as the amplicon-specific elongation time.

2.8.2.4 Agarose gel electrophoresis

After standard PCR (see 2.8.2.3) or restriction digestion (see 2.8.2.6) agarose gel electrophoresis was performed in order to separate DNA fragments by size. Prior to electrophoresis the samples were mixed with the suitable amount of 10x gel loading buffer (30 % glycerol, 0.25 % bromophenol blue, 0.25 % xylene cyanol). Depending on the expected DNA size 0.8-2.0 % agarose (in TAE) were used. The 1x TAE buffer (electrophoresis buffer) consisted of 40 mM Tris, 20 mM acetic acid, and 1 mM EDTA pH 8). In most cases the 100 bp DNA ladder P-805 (100-1000 bp, MBBL) was used as molecular weight marker for DNA size determination. DNA was visualized by staining with ethidium bromide (0.3 µg/mL gel) or RedSafe (iNtRON Biotechnology, Inc., 1x concentration) using an ultraviolet (UV) transilluminator (SynGene Bioimaging system, Merck).

2.8.2.5 Purification of PCR products

PCR products were either purified by direct PCR cleanup or by gel extraction using the respective "QIAquick" kits from Qiagen (see Table 2) and following the manufacturer's protocol. After that DNA concentration was measured photometrically using the NanoDrop ND-1000 spectrophotometer with the predefined DNA-50 program.

2.8.2.6 Restriction digestion

Restriction enzymes for genotyping using CAPS markers (see 2.8.2.1) were purchased from Fermentas/Thermo Scientific or New England BioLabs and used with the supplied buffers. A typical reaction mixture consisted of 50-500 ng DNA, 5-10 U of the restriction enzyme, 1x of the recommended reaction buffer and water to a final volume of 30 µL. The reaction mixture was incubated at the specified temperature for at least 3 hours, sometimes overnight. Afterwards the restriction enzyme was inactivated by heat as recommended by the manufacturer.

2.9 Protein methods

2.9.1 Protein extraction

After HL treatment (see 2.6.1) ~100 mg or 150-200 mg leaf material (pooled leaves 5, 6, and 7) were harvested for D1 protein blot analysis (see 2.9.3-2.9.5) or the analysis of scavenging enzyme activities (see 2.10.3), respectively. The shockfrozen material was homogenized using a Retsch mill in pre-cooled (liquid nitrogen) adapters using two steel beads.

For D1 protein blot analysis 500 µL of protein extraction buffer were added to the homogenized leaf material. The buffer consisted of 150 mM NaCl, 100 mM Tris/HCl pH 7, 1 % Triton X-100 and prior to use the recommended amount of protease inhibitor cocktail tablets (1 tablet/10 mL, Roche, Cat. No. 11836170001) was added. After the samples have been thoroughly vortexed they were further homogenized using an ultrasonic homogenizer (Sonopuls HD 2070, Bandelin Electronic). After that the samples were centrifuged for 10 min at 10,000 x g and 4 °C and the supernatants were used to measure the concentration of protein and, subsequently, for protein blot analysis.

For enzyme measurements 1000 µL of ice-cold extraction buffer were added to the homogenized leaf material. The buffer consisted of 50 mM MES pH 6, 2 mM $CaCl_2$, 40 mM KCl, and 1 mM ascorbic acid and was always freshly prepared. After thorough vortexing the samples were centrifuged for 20 min at 16,000 x g and 4 °C. The centrifugation step was repeated (for 10 min) after taking the supernatant. The obtained supernatants were analyzed regarding their scavenging enzyme activities as fast as possible. Afterwards the protein concentrations were determined for each sample in aliquots that were taken immediately after the extraction.

2.9.2 Determination of protein concentrations

For D1 protein blot analysis (see 2.9.3-2.9.5) protein concentrations were determined according to Bradford (1976) and for the analysis of scavenging enzyme activities (see 2.10.3) the determination of total protein was carried out according to Lowry *et al.* (1951). Both methods have been adapted to microplates using a microplate reader (PowerWave HT microplate spectrophotometer, BioTek). Moreover, both methods required a BSA (bovine serum albumin) standard curve. Therefore, BSA dilution series were prepared using a 1 mg/mL stock solution (Bradford: 0.5, 0.25, 0.125, 0.05, 0.025, and 0.01 mg/mL; Lowry: 0.75, 0.5, 0.25, 0.125, and 0.05 mg/mL). Water was used as blank. Standards, samples, and blanks were measured in triplicates.

For Bradford analysis Bradford reagent (Bio-Rad) was diluted 1:5 with water. 200 µL of the diluted Bradford reagent were added to 10 µL of BSA standard, blank, or sample (see 2.9.1) which was diluted 1:20 or 1:30. The mixture was incubated for 15 min at RT before measuring at 595 nm. For Lowry analysis 80 µL of water were added to 20 µl of BSA standard, blank, or sample (see also 2.9.1) which was diluted 1:5. Then 200 µL of Biuret reagent (Sigma-Aldrich) were added and everything was mixed using the shake option (20 sec) of the microplate reader. After incubation for 10-15 min at RT 10 µL of 2 N Folin & Ciocalteu's reagent (Sigma-Aldrich) were added, everything was mixed again for 20 sec, followed by an incubation of 30 min at RT. Finally, the absorbance was measured at 660 nm. In order to calculate the protein concentration in the samples linear regression analysis was performed using the values of the BSA standards (blank values always substracted) to obtain the equation for the standard curve.

2.9.3 SDS polyacrylamide gel electophoresis (SDS-PAGE) and protein blotting

For D1 protein blot analysis proteins were separated by size using denaturing SDS-PAGE. For that SDS polyacrylamide gels consisting of two layers were prepared. The upper layer (stacking gel) contained 4.5 % acrylamide and lower layer (separating, or resolving, gel) contained 14 % acrylamide (see Table 14).

Table 14: Reaction mixture for two SDS polyacrylamide mini-gels.

Components, separating gel (14 %, 10 mL)	Volume [µL]	Components, stacking gel (4.5 %, 6 mL)	Volume [µL]
water	3,892	water	4,100
40 % acryl-bisacrylamide	3,500	40 % acryl-bisacrylamide	675
1.5 M Tris/HCl pH 9	2,500	0.5 M Tris/HCl pH 6.8	1,149
20 % SDS[1)]	50	20 % SDS[1)]	30
10 % APS[2)]	50	10 % APS[2)]	40
TEMED[3)]	8	TEMED[3)]	5

1) SDS, sodium dodecyl sulfate
2) APS, ammonium persulfate
3) TEMED, *N*,*N*,*N*',*N*'-tetramethylethane-1,2-diamine

Gels were prepared and electrophoresis was performed using the Hoefer Mighty Small II System. The electrophoresis buffer was prepared as a 10x stock solution which consisted of 1.92 M glycine, 0.25 M Tris, and 1 % SDS (pH 8.3). Samples (see 2.9.1) were prepared by adding the adequate amount of 4x loading buffer (40 % glycerol, 264 mM Tris [using 1 M Tris/HCl pH 6.8], 8 % SDS, 5 % 2-mercaptoethanol, and a small spatula tip bromophenol blue) and water. The samples were heat-treated for 5 min at 95 °C and then a specific volume (corresponding to 3.5-7 µg total protein) loaded onto the stacking gel. As protein molecular weight marker PageRuler Prestained Protein Ladder (Fermentas/Thermo Scientific, 3 µL) was used. Gel electrophoresis was performed using 20 mA (constant) per gel until sufficiently separated (visualized by prestained marker).

The protein blotting was performed using the Mini Trans-Blot Electrophoretic Transfer Cell System (Bio-Rad). For that gels were equilibrated for 15 min in the blotting buffer (192 mM glycine, 25 mM Tris). Meanwhile, the PVDF membrane (Immobilon-P Membrane, Cat. No. IPVH00010, pore size 0.45 µm,

EMD Millipore) was activated with methanol (30 sec), rinsed with water (2 min) and equilibrated in the blotting buffer. Also foam (fiber) pads and Whatman papers (grade 3MM Chr, Cat. No. 3030917) were pre-soaked in the blotting buffer. The blotting sandwich (in the direction of transfer: cathode, foam pad, 2 Whatman papers, gel, PVDF membrane, 2 Whatman papers, foam pad, anode) was inserted into the blotting module and blotting was carried out overnight at 4 °C using 45-50 mA (constant). Successful transfer was verified when prestained protein marker was visible on the PVDF membrane.

2.9.4 Ponceau S staining

After overnight blotting the PVDF membrane was stained using Ponceau S solution (Fluka) to check if equal amounts of protein were loaded. The PVDF membrane was washed 2x 5 min with 1x TBS-T (10x: 0.25 M Tris/HCl pH 7.4, 1.5 M NaCl, 30 mM KCl, 0.5 % Tween-20) before it was stained in a Ponceau S bath for 5 min. Pictures were taken (membranes were put in a transparent plastic bag and scanned) to document the protein loading. For that the protein bands corresponding to the large subunit of ribulose-1,5-bisphosphate carboxylase/oxygenase (RBCL) were compared. After documentation the membranes were de-stained in 0.1 M NaOH for 1 min, and then rinsed in water for 3-5 min.

2.9.5 Immuno-detection

After Ponceau S staining (see 2.9.4) the PVDF membranes were washed for 5 min in 1x TBS-T. The blots were then blocked for ~2 h in 7 % Skim Milk (Fluka/Sigma-Aldrich, in 1x TBS-T) at RT. Afterwards the primary antibody (anti-D1, Agrisera, Cat. No. AS05084) was added to the blocking solution obtaining a 1:30,000 dilution. An incubation at RT for 1 h followed. Before blots were incubated with the secondary antibody (goat anti-rabbit IgG peroxidase conjugate, EMD Millipore, Cat. No. DC03L) for 1 h at RT in the blocking solution (also 1:30,000 diluted), they were washed for 15 min (3x 5 min) in 1x TBS-T. After the incubation with the secondary antibody the same washing procedure was carried out, followed by immuno-detection using the SuperSignal West Pico Chemiluminescent Substrate Kit (see Table 2) according to the manufacturer's instructions. After incubation with the ECL substrate an X-ray film (Kodak X-Omat) was used to detect the chemiluminescence (exposure time varied, 5 sec to 5 min). The quantification of independent experiments (n = 3 in Fig. 3.2B and n = 4 in Fig. 3.3C) was performed with ImageJ (see Table 1).

2.10 Analysis of physiological parameters

2.10.1 Determination of phytohormones by HPLC-MS/MS

Phytohormone measurements were carried out in collaboration with Prof. Dr. Ivo Feussner and Dr. Tim Iven (Albrecht-von-Haller-Institute for Plant Sciences, University of Göttingen). Leaf material (400-500 mg) was harvested at the indicated time points (Fig. 3.45A, see also 2.6.2) and sent to Göttingen on dry ice.

The extraction was performed with some modifications as described for lipids (Matyash *et al.*, 2008). 100 mg fresh (setup 1, see Fig. 3.45A) or 10 mg freeze dried plant tissue (setup 2, see Fig. 3.45A) was extracted adding 0.75 mL of methanol and the following internal standards: 10 ng D_4-salicylic acid (D_4-SA), 10 ng D_6-abscisic acid (D_6-ABA) (both from CDN Isotopes), 10 ng D_6-jasmonic acid (D_6-JA), 30 ng D_5-oxo-phytodienoic acid (D_5-OPDA), 10-ng D_3-jasmonyl-leucine (D_3-JA-Leu) (all three kindly provided by Otto Miersch, Halle/Saale, Germany). After mixing, 2.5 mL of methyl-tert-butyl ether (MTBE) were added and the extract was shaken for 1 h at 4 °C. Phase separation was achieved by addition of 0.6 mL water, incubation for 10 min at RT and centrifugation at 450 x g for 15 min. The upper phase was collected and the lower phase was re-extracted with 0.7 mL methanol/water (3:2.5, v/v) and 1.3 mL MTBE, followed by incubation and centrifugation as described above. The combined upper phases were dried under streaming nitrogen and resuspended in 100 µL of acetonitrile/water/acetic acid (20:80:0.1, v/v/v).

The analysis was carried out as described earlier (Ternes *et al.*, 2011) using an Agilent 1100 HPLC system (Agilent) coupled by an ESI chip ion source (TriVersa NanoMate, Advion BioSciences) to an Applied Biosystems 3200 triple quadrupole/linear ion trap mass spectrometer (Life Technologies). Briefly, a scheduled multiple reaction monitoring (MRM) detection in negative and positive ionisation mode was performed applying the following MS instrument parameters:

m/z 137→93 for SA with declustering potential (DP) of -25 V, entrance potential (EP) of -6 V and collision energy (CE) of -20 eV; *m/z* 141→97 for D_4-SA with DP of -25 V, EP of -6 V and CE of -22 eV; *m/z* 209→59 for JA with DP of -30 V, EP of -4.5 V and CE of -24 eV; *m/z* 293→225 for OPC-8 with DP of -80 V, EP of -4.5 V and CE of -30 eV; *m/z* 265→221 for OPC-6 with DP of -50 V, EP of -6 V and CE of -24 eV; *m/z* 237→165 for OPC-4 with DP of -45 V, EP of -6 V and CE of -24 eV; *m/z* 215→59 for D_6-JA with DP of -35 V, EP of -8.5 V and CE of -24 eV; *m/z* 322→130 for jasmonyl isoleucine/leucine (JA-Ile/-Leu) with DP of -45 V, EP of -5 V and CE of -28 eV; *m/z* 325→133 for D_3-JA-Leu with DP of -65 V, EP of -4 V and CE of -30 eV; *m/z* 263→153 for ABA with DP of -35 V, EP of -4 V and CE of -14 eV; *m/z* 269→159 for D_6-ABA with DP of -30 V, EP of -5 V and CE of -16 eV; *m/z* 291→165 for OPDA with DP of -50 V, EP of -5 V and CE of -26 eV; *m/z* 263→165 for dinor-OPDA with DP of -40 V, EP of -5 V and CE of -20 eV; *m/z* 296→170 for D_5-OPDA with DP of -65 V, with EP of -4 V and CE of -28 eV.

Quantification was carried out using a calibration curve of intensity (m/z) ratios of [unlabeled]/[deuterium-labeled] *versus* molar amounts of unlabeled (0.3-1000 pmol). Calibration was performed for the following pairs of unlabeled/deuterium-labeled standards: SA with D_4-SA; JA, OPC-8, OPC-6, and OPC-4 with D_6-JA; JA-Ile/-Leu with D_3-JA-Leu; ABA with D_6-ABA; OPDA and dinor-OPDA with D_5-OPDA.

2.10.2 Starch quantification

The quantification of starch in leaf material was performed according to Smith and Zeeman (2006) with slight modifications. The leaf material (70-90 mg) was harvested into 1.5 mL-microcentrifuge screw-capped tubes (Sarstedt, Cat. No. 72.607.772 [tubes], 65.716 [caps]), frozen in liquid nitrogen

and ground using a Retsch mill in pre-cooled (liquid N_2) adapters using two steel beads. For starch extraction/solubilization 775 µL of 0.2 M KOH were added to each sample and incubated for 1 h at 95 °C using a thermomixer (Eppendorf) under continuous agitation. After incubation samples were cooled down to RT and centrifuged at 16,000 x g for 10 min at RT. 300 µL of the supernatant were transferred into a fresh 1.5 mL-microcentrifuge tube and 100 µL of 1 M acetic acid were added to acidify the sample (pH between 5 and 6). The starch needs to be digested to obtain glucose which can be determined using an enzymatic optical glucose assay. For that, 50 µL of the neutralized, solubilized starch solution are mixed with 50 µL of an enzyme mix containing amyloglucosidase (AMG, 1 U, see Table 3) and α-amylase (α-AMY, 2 U, see Table 3) in 50 mM Na-acetate buffer pH 4.75. The reaction mixture was incubated at 37 °C (optimal for α-AMY) for 1 h and overnight at 55 °C (optimal for AMG). The reaction was stopped by heat treatment (5 min, 95 °C) and subsequently centrifuged at 16,000 x g for 10 min.

5-20 µL of the supernatants (digested starch samples) and 5 µL of the glucose standards (6, 4, 2, 1, 0.4, and 0.1 mM), respectively, were used for the enzymatic optical glucose determination using a microplate reader (PowerWave HT microplate spectrophotometer, BioTek). The required amount of water was added to obtain 20 µL sample/standard volume. Then 140 µL of the glucose-6-phosphate-dehydrogenase (G6PDH) mix were added and the absorbance was measured at 340 nm until a plateau was reached (ca. 5 min) to obtain A_{start}. The G6PDH mix (for 10 samples) was prepared as follows: 20 µL of the G6PDH suspension (0.7 U/µL) were centrifuged for 10 min at 4 °C and 14,000 x g. To the G6PDH pellet 10 µL of a 200 mM ATP solution, 10 µL of a 120 mM NADP solution (Roche, Cat. No. 10128040001), and 1380 µL 100 mM imidazole buffer pH 6.9 with HCl (containing 1.5 mM $MgCl_2$) were added. In order to measure the starch-derived glucose 5 µL of a hexokinase (HK) mix were added and the absorbance was again measured at 340 nm for 30-50 min (depending on the amount of glucose) until a second plateau was reached (A_{end}). For the HK mix (for 10 samples) 8 µL of a hexokinase suspension (1.5 U/µL) were centrifuged at 14,000 x g for 10 min at 4 °C and 50 µL of the imidazole buffer (see above) were added to the HK pellet.

For calculation ΔA was determined for the samples and the standards by substracting A_{start} from A_{end} which was then corrected by substraction of ΔA_{blank}. The amount of glucose in the samples was calculated using the equation from the glucose standard curve. The starch content in mg/g FW was calculated using the molar mass of glucosyl residues in starch (162.1 g/mol).

2.10.3 Analysis of scavenging enzyme activities

Activities of the scavenging enzymes ascorbate peroxidase (APX; EC 1.11.1.11), monodehydro-ascorbate reductase (MDHAR; EC 1.6.5.4), dehydroascorbate reductase (DHAR; EC 1.8.5.1), and glutathione reductase (GR; EC 1.8.1.7) were measured as described in Murshed *et al*. (2008). Peroxidase activity (POX; EC 1.11.1) was measured according to Kar and Mishra (1976) and superoxide dismutase (SOD; EC 1.15.1.1) activity according to Dhindsa *et al*., 1981 with slight modifications. Proteins were extracted as described in chapter 2.9.1 and protein concentrations

determined using the Lowry method (see 2.9.2). In Table 15 the protocols for APX, MDHAR, DHAR, GR, and POX measurements are listed.

Table 15: Protocols for the determination of enzyme activities.

	APX	MDHAR	DHAR	GR	POX
Reaction buffer (RB)	50 mM K-phosphate buffer pH 7, 0.6 mM ASC*	50 mM HEPES pH 7.6, 2.5 mM ASC*, 0.25 mM NADH*	50 mM HEPES pH 7, 0.1 mM EDTA, 1.25 mM GSH*	50 mM HEPES pH 8, 0.5 mM EDTA, 0.25 mM NADPH*	50 mM K-phosphate buffer, 16 mM pyrogallol
RB volume per well [µL]	170	185	170	160	180
Extract volume [µL][1)]	20	10	20	30	10
Substrate (stock concentration)	H_2O_2 (254 mM)	Ascorbate oxidase (80 U/mL)	DHA* (8 mM)	GSSG* (20 mM)	H_2O_2 (254 mM)
Substrate volume [µL] (final concentration)[2)]	10 (12.7 mM)	5 (0.4 U/well)	10 (0.4 mM)	10 (1 mM)	10 (12.7 mM)
Wavelength [nm]	290[3)]	340	265[3)]	340	430
Extinction coefficient ε [mM^{-1} cm^{-1}]	2.8	6.22	14	6.22	2.47
ΔA/min (slope)	negative	negative	positive	negative	positive

1) Prior to the addition of the substrate non-specific reactions were measured for 6 min for MDHAR, GR, and POX.

2) After addition of the substrate specific reactions were measured for 6 min for MDHAR, GR, and POX. For APX and DHAR the substrate was added immediately and the reaction was measured for 6 min and additional blank measurements were carried out in parallel using 20 µL more RB instead of the sample.)

3) Measurement in UV-transmitting plates (Costar, Cat. No. 3635), all other reactions were measured in standard microplates (Sarstedt, Cat. No. 82.1581)

* ASC, ascorbate; DHA, dehydroascorbate; GSH, glutathione; GSSG, oxidized glutathione; NAD(P)H, reduced nicotinamide adenine dinucleotide (phosphate)

All enzyme measurements were carried out at least in triplicates and have been adapted to microplates (standard and UV plates, see Table 15) using a microplate reader (PowerWave HT microplate spectrophotometer, BioTek) and a final volume of 200 µL. In order to determine the path length (b) for the calculation of the respective enzyme activities, a path length correction factor (b_{corr}) was determined for both microplate types first. For that the absorbance (A) of water was measured at 977 nm and 900 nm, respectively, in a cuvette with b = 1 cm as well as in wells of the microplates that were used filled with 200 µL water. b_{corr} was calculated with the following equation and resulted in b_{corr} = 0.61 for the standard plates and b_{corr} = 0.58 for the UV plates.

$$b_{corr} = \frac{\Delta A_{977-900nm}\,(well)}{\Delta A_{977-900nm}\,(cuvette)}$$

In order to calculate the enzyme activity (as substrate turnover in mmol per L and min) in the samples all absorbance values (derived from the 6-min kinetics) were plotted and a linear regression analysis was performed to obtain the slopes. For MDHAR, GR, and POX measurements the slope from the non-specific reaction was substracted from the slope from the specific reaction. For APX and DHAR measurements the blank values were substracted from the sample slopes. The resulting corrected slope (ΔA/min) was used for calculating the activity using the following equation:

$$Activity\left(\frac{mmol}{L \times min}\right) = \frac{\Delta A}{min} \times \frac{1}{\varepsilon \times b_{corr}} \times \frac{V_t}{V_s}$$

ΔA/min = Change in absorbance per minute (corrected slope, see text above)

ε = Extinction coefficient [mM^{-1} cm^{-1}]

V_t = Total extract volume (1000 µL)

V_s = Sample volume (see Table 15)

The activity was expressed per mg protein and, therefore, divided by the protein concentration (c_{prot}).

$$\frac{Activity}{mg\ protein}\left(\frac{\mu mol}{mg \times min}\right) = Activity\left(\frac{mmol}{L \times min}\right) \div c_{prot}\left(\frac{mg}{mL}\right)$$

The activity of SOD was determined by measuring its ability to inhibit the photochemical reduction of nitroblue-tetrazolium (NBT) to formazan (blue color). The reaction mixture consisted of 50 mM K-phosphate buffer (pH 7.8), 933 µM methionine, 75 µM NBT, 0.1 mM EDTA, and 10 µM riboflavin. Either 970 µL of the reaction mixture were added to 30 µL sample (leaf extract, see 2.9.1), vortexed, and divided into wells of the microplate using 200 µL per well (at least in triplicates) or the reaction mixture was directly pipetted into the wells (200 µL per well) as blank. Two identical microplates including samples and blanks were prepared. One was HL-treated (see 2.6.1) for 30 sec to 2 min (avoiding overcoloration, samples should be less blue than blanks) and the second plate was kept in darkness and served as control. After HL treatment both plates were measured at 550 nm. Absorbance values of the HL-treated samples and blanks were corrected by substraction with the respective control values (dark). The inhibition of formazan formation was calculated in percent (blanks served as reference with maximal reduction of NBT). In parallel SOD standards (see Table 3) were measured on the same plates (6 U/well resulting in ~76 % inhibition) and SOD activity was calculated based on the equation of the standard curve and expressed per mg protein.

2.10.4 Analysis of antioxidants and antioxidant capacity

2.10.4.1 Oxygen radical antioxidant capacity (ORAC) assay

The ORAC assay was performed by Dr. Anne Cortleven (FU Berlin) and conducted as described by Gillespie *et al*. (2007).

2.10.4.2 Determination of carotenoids by HPLC

Carotenoids were extracted and analyzed by HPLC applying the method of Thayer and Björkman (1990). These experiments were performed by Dr. Anne Cortleven (FU Berlin) in collaboration with Prof. Dr. Bernhard Grimm (Humboldt University, Berlin).

2.10.4.3 Determination of tocopherols by HPLC

Tocopherol measurements were carried out in collaboration with Prof. Dr. Han Asard and Hamada AbdElgawad (University of Antwerp, Belgium). For that, ~200 mg leaf material (pooled leaves 5, 6, and 7) were harvested and shockfrozen (sent to Antwerp on dry ice). The material was quickly ground using a MagNa Lyzer Instrument (Roche). Hexane was used to extract tocopherols followed by

centrifugation and filtration. Dimethyltocol (5 ppm) was added to each sample as internal standard and tocopherols were determined by normal-phase HPLC using a Partisil 5 µm PAC column (250 mm x 4.6 mm, Shimadzu) with an isocratic flow of 1.5 mL min^{-1}. Hexane containing 8 % tetrahydrofuran was used as elution buffer. Fluorescence was detected with a Shimadzu spectrofluorometric detector RF-10A (excitation wavelength 290 nm, emission wavelength 330 nm). Data were analyzed using the Shimadzu Class VP 6.14 software.

2.10.4.4 Glutathione and ascorbate measurements via reversed-phase HPLC

The determination of glutathione and ascorbate was carried out in collaboration with Prof. Dr. Han Asard and Hamada AbdElgawad (University of Antwerp, Belgium) according to Potters *et al.* (2004). Leaf material (~200 mg, pooled leaves 5, 6, and 7) was harvested and shockfrozen (sent to Antwerp on dry ice). Dr. Anne Cortleven and I participated in the measurements in Antwerp. The material was quickly ground using a MagNa Lyzer Instrument (Roche). Samples were kept frozen during grinding to prevent oxidation. 1 mL ice-cold 6 % (w/v) meta-phosphoric acid was added and samples were thawed on ice followed by centrifugation at 12,000 x g and 4 °C for 15 min. The resulting supernatant was kept on ice until HPLC analysis.

In order to measure GSH and ASC (reduced forms) 100 µL of the supernatant were added to 300 µL of the eluent (2 mM KCl, pH 2.5 adjusted with H_3PO_4). For total glutathione and ascorbate (GSH plus GSSG and ASC and DHA, respectively) measurements aliquots of the leaf extracts (100 µL) were reduced using 200 mM DTT/400 mM Tris solution (50 µL, final pH between 6 and 7, checked in random samples) in the dark for 15 min at RT. After incubation 250 µL of the eluent were added. Antioxidants were separated on a Polaris C18-A reversed-phase HPLC column (100 mm x 4.6 mm, 3 µm particle size, 40 °C, Varian) with an isocratic flow of 1 mL min^{-1} of the eluent. Antioxidants were quantified using a custom-made electrochemical detector and the purity and identity of the peaks were confirmed using an in-line diodearray detector (DAD, SPD-M10AVP, Shimadzu). Data were analyzed using the Shimadzu Class VP 6.14 software. The concentrations of the reduced forms as well as the total amount of antioxidant were calculated using a standard curve created by known concentrations of GSH and ASC, respectively. The amount of the oxidized forms (GSSG or DHA, respectively) was measured indirectly and calculated as the difference between the total concentrations of antioxidants in the DTT-reduced fraction and the concentration in the sample without reduction (reduced forms).

2.10.5 Determination of oxidative stress

2.10.5.1 Lipid peroxidation

Lipid peroxidation (LPO) as a consequence of oxidative stress was measured by four different means. 1) Thermoluminescence was measured in leaf discs using a custom-made apparatus that has been described previously (Havaux, 2003). The amplitude of the thermoluminescence band peaking at ~135 °C can be used as an index of LPO (Havaux, 2003; Ducruet, 2003). The samples were slowly heated from 25 °C to 150 °C at a rate of 6 °C min^{-1}.

2) Photon emission associated with LPO called autoluminescence (Havaux *et al*., 2006) was imaged at RT using a highly sensitive charge coupled device (CCD) camera (VersArray LN/CCD 1340-1300B, Roper Scientific), with a liquid N_2-cooled sensor to enable measurement of faint light by signal integration as described in Havaux *et al.* (2009). For these autoluminescence measurements, circadian stress (CL-) treated plants were dark-adapted for 2 h before imaging, to allow chlorophyll luminescence to fade away.

3) Hydroxyoctadecatrienoic acid (HOTE) isomers were analyzed as a measure of LPO/oxidative stress (Montillet *et al.*, 2004). Leaf material (700-800 mg, pooled leaves 5, 6, and 7) was harvested and shockfrozen. The frozen leaf tissue was ground with mortar and pestle. Subsequently, 500 mg of the leaf material were used for the extraction of lipids. After extraction, ROS- and LOX-induced LPO were determined as described in Havaux *et al.* (2009).

The thermoluminescence and autoluminescence as well as the HOTE measurements were performed in collaboration with Prof. Dr. Michel Havaux (CEA Cadarache, Saint-Paul-lès-Durance, France). For the HOTE measurements Dr. Anne Cortleven and I conducted the experiment, carried out the sampling, and sent the frozen samples (on dry ice) to Saint-Paul-lès-Durance.

4) MDA (malondialdehyde) as secondary end product of the oxidation of polyunsaturated fatty acids (PUFAs) was quantified as index of LPO according to Heath and Packer (1968) with slight modifications. MDA reacts with thiobarbituric acid (TBA) and can be estimated spectrophotometrically by measuring at 532 nm. This method has been adapted to microplates using a microplate reader (PowerWave HT microplate spectrophotometer, BioTek). Leaf material (45-55 mg) was ground using a Retsch mill in pre-cooled adapters (liquid N_2) using two steel beads. 650 µL of 0.1 % TCA (trichloroacetic acid) were added to the ground material followed by thorough vortexing. The mixture was centrifuged at 13,200 rpm (using a microcentrifuge) for 10 min at RT. 125 µL of the supernatant or of 0.1 % TCA (as blank) were transferred into a fresh 2 mL-microcentrifuge screw-capped tube (Sarstedt, Cat. No. 72.693) and 500 µL of TBA solution (4x volume, 0.5 % TBA in 20 % TCA) were added, and mixed by vortexing. The reaction mixture was incubated at 95 °C for 30 min, cooled down on ice quickly (4 min), and centrifuged at 13,200 rpm for 10 min and 4 °C. 170 µL of the sample (or blank) were measured (at least in duplicates) using Greiner 96-well plates (Greiner, Cat. No. 675101, 170 µL = path length of 1 cm). The absorbance was measured at 532 nm (specific) and 600 nm (non-specific) and the extinction coefficient $\varepsilon = 155\ mM^{-1}\ cm^{-1}$ was used for calculating the amount (in nmol) of MDA per fresh weight.

2.10.5.2 Hydrogen peroxide (H_2O_2) content

For H_2O_2 measurements 40-55 mg leaf material (see also 2.6.2) was harvested, shockfrozen, and ground using a Retsch mill in pre-cooled adapters (liquid N_2) using two steel beads. The H_2O_2 content in the samples was determined using the Amplex Red Hydrogen Peroxide/Peroxidase Assay Kit (see Table 2) according to the manufacturer's instructions. I carried out the treatments and the subsequent sampling, while the measurements were conducted by Dr. Anne Cortleven (FU Berlin).

2.10.6 Evaluation of other stress and cell death parameters

2.10.6.1 Chlorophyll fluorescence ratio F_v/F_m

The F_v/F_m ratio, reflecting the photosystem II maximum quantum efficiency (Baker, 2008), was measured in order to determine the extent of photoinhibition after HL treatment or following circadian stress regimes as a measure of stress and the severity of cell death, respectively. For that pulse-amplitude-modulated (PAM) measurements were carried out using the chlorophyll fluorometer FluorCam (Photon Systems Instruments). Plants were dark-adapted for 20-30 min. After dark-adaptation the minimum fluorescence emission signal F_0 was recorded first, followed by the recording of the maximum fluorescence yield F_m that was induced by a saturating light pulse (1500 µmol m^{-2} s^{-1}). The variable fluorescence F_v is defined as the difference F_m - F_0. Therefore, $F_v/F_m = (F_m - F_0)/F_m$. For HL experiments (see 2.6.1) detached leaves and defined leaves of whole plants (still attached) were measured. For circadian stress experiments whole plants were treated with a certain light-dark-temperature regime (see 2.6.2) and leaves were detached (floating on water in Petri dishes) prior to dark-adaptation for PAM measurements.

For lincomycin treatment detached leaves (leaf 6) were incubated for 3 h floating on 1 mM lincomycin (Sigma-Aldrich) to block chloroplast protein synthesis or on water at 10-20 µmol m^{-2} s^{-1} light intensity and 22 °C. To ensure proper uptake of the solution the ends of the petioles had to be covered with solution and were also cut again under solution to prevent airlocks. Incubated leaves were HL-treated (see 2.6.1) or kept under growth light as controls (see 2.5.1) for 3 h. F_v/F_m ratios were measured afterwards.

For photosystem II recovery analysis F_v/F_m ratios were measured after 24 h HL as well as after 24 h and 48 h relaxation, respectively. Petri dishes with detached leaves were transferred to control (SD) conditions for recovery/relaxation after HL treatment.

2.10.6.2 Quantification of necroses

If not stated otherwise necrotic leaves were counted at least 4 h after the end of the dark period which induced the cell death phenotype following CL treatment (circadian stress). At this stage the necrotic lesions were already visible, albeit not dried off (as seen on the pictures that were taken one or two days later), and were observed together with water-soaked lesions (see 2.10.6.4 for fresh weight analysis). Necrotic leaves were only counted among the mature leaves that were fully expanded and given as percentage of all mature leaves because the total amount of leaves varied among the mutant and transgenic plants that were investigated.

2.10.6.3 Ion leakage

Ion leakage indicating loss of membrane integrity due to cell death progression was measured in leaves of circadian stress-treated (CL) and control plants according to Watanabe and Lam (2006) with slight modifications. Taking leaf discs was not an option because cutting the discs damaged the already limp CL-treated leaves even more. Therefore, whole leaves were detached (equal amounts of treated

and control leaves, 4-6 leaves of wild-type and 8-12 leaves of cytokinin-deficient plants) at the indicated time points and incubated in a defined volume of water (12 mL) in a small Petri dish for 4 hours at RT. After incubation the conductivity of the water was measured using a conductivity meter (EC-Controller, Stelzner). Since the leaf size strongly differs between wild-type and cytokinin-deficient *ahk2 ahk3* and *35S:CKX4* plants ion leakage was expressed as percent of control, setting the respective control values to 100 %.

2.10.6.4 Fresh weight analysis

The formation of water-soaked lesions accompanied cell death progression leading to loss of fresh weight (FW). For each sample 4 leaves of the wild type, 8-10 leaves of *35S:CKX4* and *ahk2 ahk3* plants were detached, weighed, and the FW per leaf determined. Finally, the FW per leaf was expressed as percent of control, setting the control values to 100 %.

2.11 Contributions

I worked together with Dr. Anne Cortleven on the HL project. At the beginning of this year we published the results as co-first authors (Cortleven and Nitschke *et al.*, 2014). She performed the ORAC assay as well as the carotenoid analysis which was carried out in collaboration with Prof. Dr. Bernhard Grimm (Humboldt University, Berlin). Nevertheless, these data have been included here to provide this essential information in the framework of my thesis. We equally contributed to the generation of all other results shown in the HL section (3.1). My own contribution is specified in Table 16.

Table 16: Contributions to the results shown in the HL section (chapter 3.1).

Figures	My part*	Dr. Anne Cortleven*
3.1	C, D, E, F	B, F
3.2	A, B (optimization, blot shown), C, D, and F (primer design, pre-tests)	B (repetition, quantification), C-F (qRT-PCR results shown)
3.3	A, B, C (optimization, blot shown)	C (repetition, quantification)
3.4	D, E, F	A-F
3.5	A-F	A-F

* Capital letters refer to the respective figure panels.

Tocopherol, glutathione, and ascorbate measurements were performed in collaboration with Prof. Dr. Han Asard and Hamada AbdElgawad (University of Antwerp, Belgium) (see also 2.10.4.3-2.10.4.4).

Hamada AbdElgawad (University of Antwerp, Belgium) also helped with the optimization of the enzyme (activity) measurements.

The thermoluminescence, autoluminescence, and HOTE measurements were performed in collaboration with Prof. Dr. Michel Havaux (CEA Cadarache, Saint-Paul-lès-Durance, France) (see also 2.10.5.1).

The phytohormone measurements were carried out in collaboration with Prof. Dr. Ivo Feussner and Dr. Tim Iven (Albrecht-von-Haller-Institute for Plant Sciences, University of Göttingen) (see also 2.10.1).

The H_2O_2 measurements using the Amplex Red Kit (see Table 2) were conducted by Dr. Anne Cortleven (FU Berlin) after I performed the treatments and the subsequent sampling (see also 2.10.5.2).

Prof. Dr. Tatsuo Kakimoto, Prof. Dr. Takeshi Mizuno, Prof. Dr. Rachel Green, Prof. Dr. C. Robertson McClung, Dr. Jos Schippers, and Dr. Patrice Salomé kindly provided seeds of mutant and transgenic plants that were used for the circadian stress project (see Table 4).

3 Results

3.1 Plants with a reduced cytokinin status are more sensitive to high light stress

3.1.1 HL treatment causes stronger photoinhibition in plants with a reduced cytokinin status

Plants are photosynthetic organisms and utilize light to drive photosynthesis. However, at the same time they need to cope with the detrimental effects an excess of excitation energy can have. In their natural environments plants are often subjected to sudden increases in light intensity. Therefore, a proper light stress response including a great variety of photoprotective mechanisms is indispensable to prevent strong photodamage, which results in photoinhibition – the light-induced reduction of the photosynthetic capacity (see 1.2.1).

Several observations suggested that plants with a reduced cytokinin status might be more sensitive to light stress than wild-type plants. The cytokinin receptor double mutant *ahk2 ahk3* and *35S:CKX4* transgenic plants appeared to be particularly sensitive. Therefore, these plants were selected and exposed to defined HL stress conditions in order to analyze their light stress response. The corresponding results (chapter 3.1) were obtained in collaboration with Dr. Anne Cortleven. My own contribution is specified in Table 16 (see 2.11).

After growing plants under SD conditions for about four weeks they were exposed to HL intensities (~1000 µmol m^{-2} s^{-1}) for 24 hours. Immediately after the HL treatment the PSII maximum quantum efficiency (F_v/F_m) was determined by chlorophyll fluorescence imaging as indicated in Fig. 3.1A. A strong decrease in F_v/F_m ratios was measured in HL-treated cytokinin-deficient plants (*35S*:*CKX4* and *ahk2 ahk3*), while wild-type plants showed a much weaker response (Fig. 3.1B). The stronger stress-induced decline in F_v/F_m revealed that HL caused stronger photoinhibition in plants with a reduced cytokinin status.

In order to investigate the role of cytokinin during HL stress in more detail, further experiments were carried out with detached leaves to enable a higher throughput. Similar to the experiments performed on whole plants, HL treatment triggered a stronger reduction of F_v/F_m ratios in cytokinin-deficient leaves compared with wild-type leaves. Defined leaves were analyzed (leaf 4 to 9, data only shown for leaf 5 to 7) and the stronger light stress response was detectable in all tested leaves (Fig. 3.1C and data not shown). However, older leaves generally tended to show a more pronounced stress response. Importantly, the stress response was due to the HL treatment itself and not caused by the lack of the dark period, as continuous moderate light (CL, instead of HL) did not result in the reduction of F_v/F_m values (Fig. 3.1D). Kinetics of the HL stress response (measured as F_v/F_m) revealed that the divergence between cytokinin-deficient and wild-type plants already started after 3 h HL treatment, but the difference was more pronounced after 12 h and 24 h HL, respectively (Fig. 3.1E).

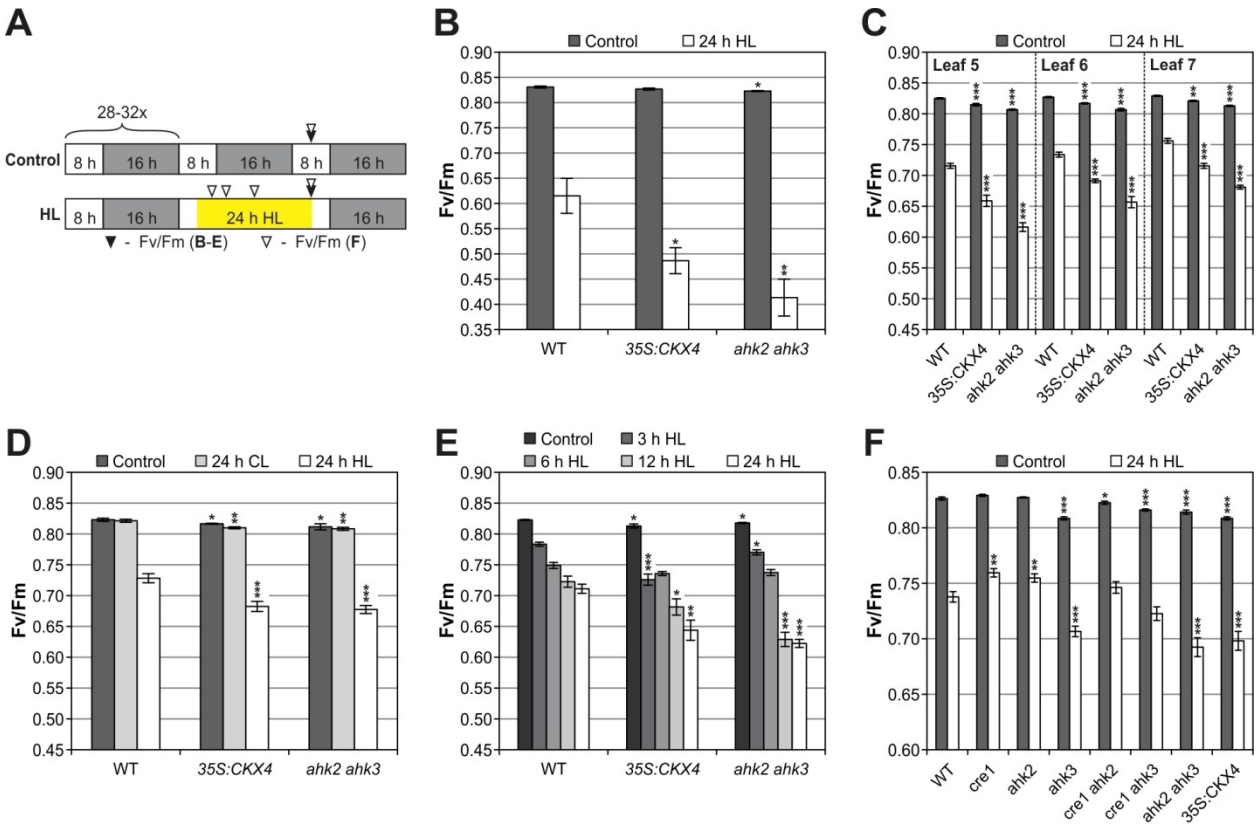

Figure 3.1: Plants with a reduced cytokinin status are more sensitive to high light treatment.

A, Schematic overview of the experimental design in **B**-**F**. Four-week-old plants were continuously grown under SD conditions or exposed to a 24-hour HL regime. White, light period; gray, dark period; yellow, HL (~1000 µmol m^{-2} s^{-1}); arrowheads indicate sampling points. **B**, Stress-induced decrease in F_v/F_m ratios (photosystem II maximum quantum efficiency) corresponding to the inhibition of photosystem II in whole plants (leaf 6) after 24 h HL (n = 6). **C**, F_v/F_m ratios in control and HL-treated detached leaves 5, 6, and 7 (n = 8). **D**, F_v/F_m ratios of detached leaf 7 directly after 24 h light treatment (continuous moderate light (CL) or HL) (n = 8). **E**, F_v/F_m ratios of detached leaf 6 after different HL exposure times (n = 8). **F**, F_v/F_m ratios of detached leaf 6 of different cytokinin receptor single and double mutants (n = 15). Asterisks indicate significant differences compared with the respective wild type (*t* test: *, $p < 0.05$; **, $p < 0.01$; ***, $p < 0.001$). Error bars represent SE.

To study the contribution of the different cytokinin receptors in mediating the light stress response, all single (*cre1, ahk2, ahk3*) and the corresponding double (*cre1 ahk2*, *cre1 ahk3*, *ahk2 ahk3*) cytokinin receptor mutants were analyzed after 24 h of HL treatment (Fig. 3.1F). Mutation of *AHK2* and/or *CRE1/AHK4* alone did not cause a decrease in photosynthetic efficiency of PSII (F_v/F_m) compared with the wild type, while a significant decrease in PSII efficiency was observed in *ahk3* mutants. The decrease in F_v/F_m was even a bit stronger in the *ahk2 ahk3* double receptor mutants, which could not be observed in the other double receptor mutants. This indicates that the AHK3 receptor is the key mediator in this light stress response, while AHK2 has an accessory function.

3.1.2 The D1 protein level is strongly reduced by light stress in plants with a reduced cytokinin status

The stronger photoinhibition of cytokinin-deficient plants after exposure to HL could be either the consequence of a hampered D1 repair cycle or a higher degree of photodamage (i.e. damaged PSII

proteins) or both (see 1.2.1.1). PSII is able to recover from light stress. The recovery can be monitored by the increase in F_v/F_m ratios during relaxation under control conditions (in this case SD rhythm). In *35S:CKX4* and *ahk2 ahk3* plants, the recovery capacity was attenuated compared with the wild type, as indicated by significantly lower F_v/F_m values after 24 and 48 hours of relaxation (Fig. 3.2A). F_v/F_m ratios did not return to initial levels in these plants, which was the case for wild-type plants after 48 hours of relaxation. The lack of full recovery indicates that the photodamage could not be properly repaired, which might be due to a compromised D1 repair or a partially irreversible damage.

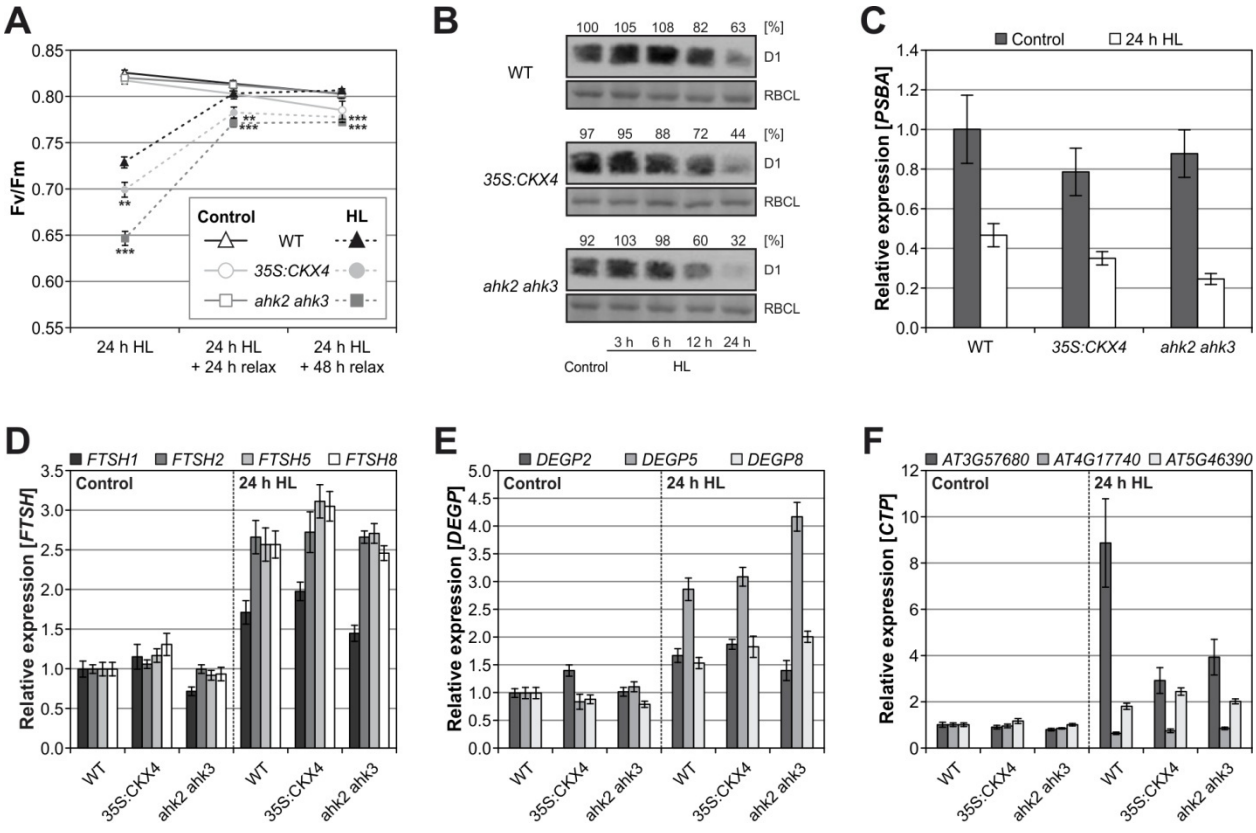

Figure 3.2: Effect of high light treatment on the functionality, protein and transcript levels of genes encoding D1 and proteases of the D1 repair cycle.

Defined leaves of four-week-old SD-grown plants were detached and subjected to 24 hours of HL treatment (for schematic overview see Fig. 3.1A). **A**, F_v/F_m ratios of leaf 6 after 24 h HL and after 24 h and 48 h relaxation, respectively (n = 22). Asterisks indicate significant differences compared with the respective wild type (*t* test: **, $p < 0.01$; ***, $p < 0.001$). **B**, Determination of the D1 protein levels by western blot analysis. Proteins were extracted from pooled leaves 5, 6 and 7 after different durations of HL. Percentages above the blots indicate the relative D1 protein levels compared with the wild-type control (mean of three independent experiments). One representative blot is shown. **C**-**F**, Expression levels of *PSBA* (**C**; encoding D1), *FTSH* (**D**), *DEGP* (**E**), and *CTP* (**F**) genes recorded by qRT-PCR analysis. Data represent the mean of eight biological replicates and are expressed as relative values compared with the corresponding wild type, which was set to 1. *NDHI* and *RPS3* (**C**) as well as *ACT2*, *KOR1*, and *TAFII15* (**D**-**F**) served as reference genes. Error bars represent SE. RBCL, large subunit of RuBisCO. Abbreviations of gene names are explained in the list at the beginning of this work.

The D1 protein is the most vulnerable component of PSII and its replacement by newly synthesized functional D1 protein is required to avoid or attenuate photoinhibition (see 1.2.1.2). Therefore, the D1 protein abundance was determined. In case of a reduced repair and/or a stronger photodamage in plants with a reduced cytokinin status, a clear difference to wild type should be detectable. The D1

protein level was investigated by protein blot analysis (Fig. 3.2B). D1 protein levels were almost unchanged in all genotypes after 3 to 6 h HL treatment. However, after longer HL treatment, the D1 protein level was stronger diminished in leaves of *35S:CKX4* and *ahk2 ahk3* plants in comparison with leaves of wild-type plants. The strongest difference in D1 protein abundance between the cytokinin-deficient and wild-type plants was noted after 24 h HL. In wild type, 63 % of the initial D1 protein level was retained, while only 32 % and 44 % of the D1 protein level compared with the wild-type control were left in *35S:CKX4* and *ahk2 ahk3*, respectively. The stronger degree of D1 degradation/damage clearly demonstrates an imbalance between photodamage and repair in plants with a reduced cytokinin status. This is consistent with the kinetics of F_v/F_m reduction shown in Fig. 3.1E, revealing the largest differences after 12 h and 24 h HL treatment.

Additionally, transcript levels of the *PSBA* gene encoding the D1 protein and various genes encoding proteins of the D1 repair cycle were analyzed. After 24 h HL the transcript level of *PSBA* was slightly stronger decreased in leaves of both *35S:CKX4* and *ahk2 ahk3* plants compared with leaves of the wild type (Fig. 3.2C). Next, it was analyzed whether the expression of genes involved in the D1 repair cycle such as *FTSH* (*FTSH1, FTSH2, FTSH5* and *FTSH8*; Fig. 3.2D), *DEGP* (*DEGP5* and *DEGP8*; Fig. 3.2E) and *CTP* homologs (*AT3G57680*, *AT4G17740*, and *AT5G46390*; Fig 3.2F) was altered in plants with a lowered cytokinin status. *FTSH* and *DEGP* encode proteases involved in D1 degradation (Kato and Sakamoto, 2009). Most of these transcripts were induced upon HL treatment but generally the basic steady state mRNA levels and the degree of induction were similar in cytokinin-deficient and wild-type plants. One exception was *DEGP5*, which was slightly stronger induced in *ahk2 ahk3* mutants in comparison with the wild type and *35S:CKX4* (Fig. 3.2E). Three *Arabidopsis* genes (*AT3G57680*, *AT4G17740*, and *AT5G46390*) have been predicted to encode *CTP* homologs (Satoh and Yamamoto, 2007; Yin *et al.*, 2008) based on the similarity of their amino acid sequences with the C-terminal processing peptidase encoded by the cyanobacterial *CtpA* gene, which is required for maturation of the D1 protein. Among these, *AT3G57680* showed a strong (9-fold) induction in leaves of wild-type plants in response to HL stress (Fig. 3.2F). *AT5G46390* showed a slight induction (2-fold), while the third homolog did not respond to HL treatment. The transcript levels of the latter two genes were comparable between cytokinin-deficient and wild-type plants. However, in contrast to the strong upregulation of *AT3G57680* in wild type, cytokinin-deficient plants only showed a 3- to 4-fold induction (Fig. 3.2F). In order to explore if this limited induction in plants with a reduced cytokinin status might be causal for the HL stress phenotype, the HL response of the corresponding *ctpa1* mutant (Yin *et al.*, 2008) was analyzed. This mutant behaved like wild type (data not shown) which indicates that AT3G57680 has no important function in the light stress response and that its differential expression is likely not the reason for the HL phenotype in cytokinin-deficient plants.

3.1.3 Photodamage is increased in plants with a reduced cytokinin status

To evaluate whether an increased photodamage contributes to the light stress phenotype in cytokinin-deficient plants, the D1 repair cycle was inhibited. When the PSII repair is blocked, the photoinhibition that is measured solely reflects the photodamage and, hence, enables to exclusively monitor the damage to PSII. A reduced D1 repair activity can be achieved by exposure to low temperatures

(Grennan and Ort, 2007; Mohanty *et al.*, 2007). Alternatively, the repair cycle can be completely blocked by application of lincomycin, an antibiotic which inhibits plastid protein synthesis (Takahashi and Badger, 2011). Both treatments caused a strong decrease of the F_v/F_m ratios in all genotypes, demonstrating the importance of the D1 repair cycle for protection against HL stress (Fig. 3.3A-B). However, the reduction of F_v/F_m was significantly stronger in *35S:CKX4* and *ahk2 ahk3*, revealing that cytokinin-deficient plants undergo a higher degree of photodamage. In accordance to this, the analysis of D1 protein levels in samples of the lincomycin experiment confirmed the stronger photodamage in cytokinin-deficient plants (Fig. 3.3C). After 3 hours of HL in the presence of lincomycin the D1 protein abundance in cytokinin-deficient plants was reduced to about 50 % compared with the HL/L-treated wild type reflecting the stronger impairment.

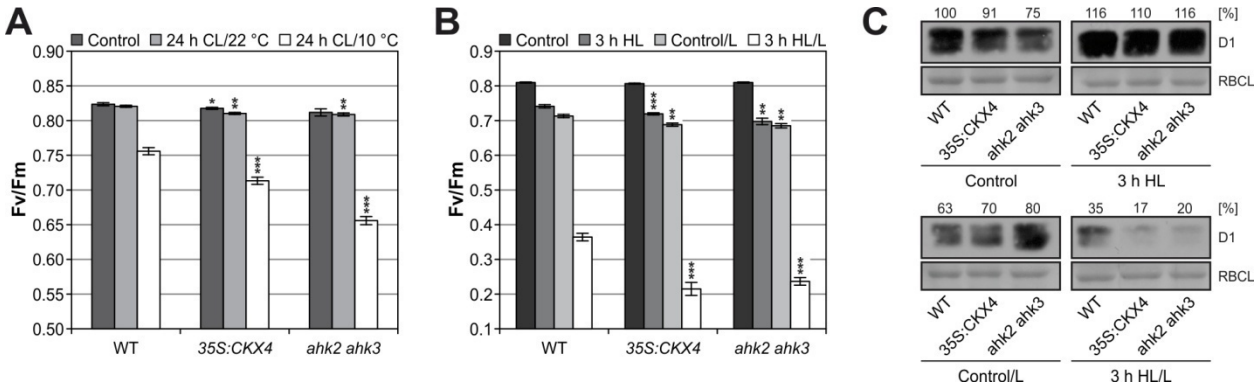

Figure 3.3: Photodamage is increased in plants with a reduced cytokinin status.

A-**B**, Photochemical efficiency F_v/F_m was measured in detached leaves of four-week-old SD-grown plants. F_v/F_m ratios of leaf 7 exposed to a 24-hour continuous moderate light treatment (CL) at 22 °C and 10 °C, respectively (**A**; n = 8). F_v/F_m ratios of leaf 6 subjected to 3 hours of HL in the absence or presence of 1 mM lincomycin (L) (**B**; n = 8). C, Determination of the D1 protein levels in leaf material (pooled leaves 5, 6, and 7) derived from the experiment shown in **B** by western blot analysis. Percentages above the blots indicate the relative D1 protein levels compared with the wild-type control (mean of four independent experiments). One representative blot is shown. Asterisks indicate significant differences compared with the respective wild type (*t* test: *, $p < 0.05$; **, $p < 0.01$; ***, $p < 0.001$). Error bars represent SE. RBCL, large subunit of RuBisCO.

In conclusion, the data above indicate that the damaging impact of light is more severe in cytokinin-deficient plants. The result is an elevated level of photodamage. This, together with the lack of full repair (see recovery analysis; Fig. 3.2A), provides a good explanation for the higher sensitivity towards HL stress in cytokinin-deficient plants.

3.1.4 Plants with a reduced cytokinin status show reduced ROS scavenging capacity

It is well-known that photo-oxidative stress, provoked by elevated levels of ROS, accelerates photoinhibition (see 1.2.1.1). A reduced efficiency of ROS scavenging can be responsible for that, especially under conditions that favor ROS production such as HL stress. To test this, the total antioxidant capacity was determined by using the oxygen radical antioxidant capacity (ORAC) assay. This initial experiment indicated that *35S:CKX4* and *ahk2 ahk3* plants had about 20 to 30 % lower total antioxidant capacity after HL stress compared with the wild type (Fig. 3.4A).

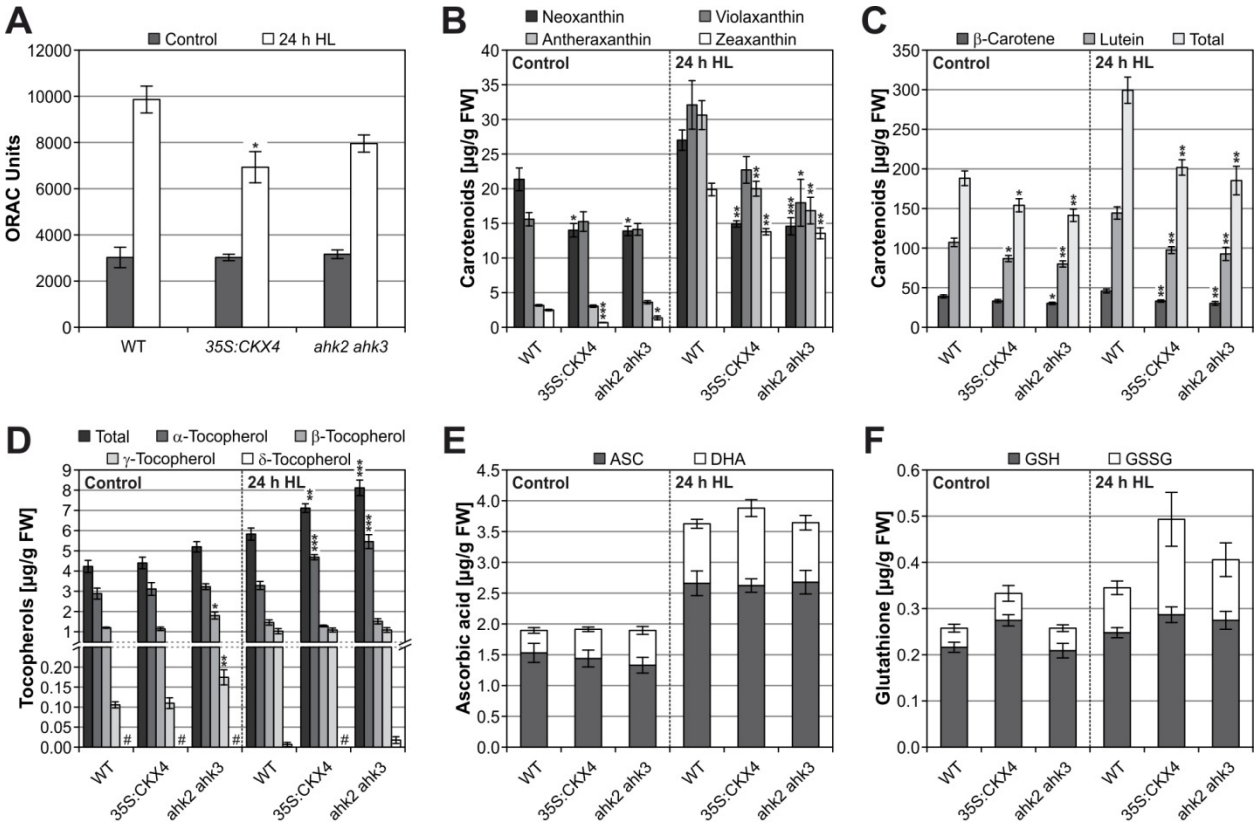

Figure 3.4: Antioxidant capacity in plants with a reduced cytokinin status after high light treatment.

Detached leaves (leaf 5, 6, and 7 pooled) of four-week-old SD-grown plants were subjected to 24 hours of HL treatment (for schematic overview see Fig. 3.1A). **A**, Total antioxidant capacity expressed as ORAC (oxygen radical absorbance capacity) units (µmol Trolox equivalents/g fresh weight) (n = 3). **B**-**D**, Lipophilic antioxidant contents. Xanthophyll pigments of the xanthophyll cycle and neoxanthin (**B**; n = 4), beta-carotene and lutein as well as the total carotenoid levels, (**C**; n = 4), and the tocopherol content (**D**; n = 8; #, not detected). **E**-**F**, Hydrophilic antioxidant contents. Ascorbic acid (**E**) and glutathione (**F**) (ASC, ascorbate; DHA, dehydroascorbate; GSH, reduced glutathione; GSSG, oxidized glutathione; n = 12). Asterisks indicate significant differences compared with the respective wild type (*t* test: *, $p < 0.05$; **, $p < 0.01$; ***, $p < 0.001$). Error bars represent SE. The carotenoid measurements were performed in collaboration with Prof. Dr. Bernhard Grimm and tocopherol, ascorbic acid, and glutathione experiments in collaboration with Prof. Dr. Han Asard and Hamada AbdElgawad (see 2.11).

Based on this observation, different ROS scavenging mechanisms (see 1.4.2), both non-enzymatic and enzymatic, that are typically used for photo-protection during HL stress were investigated in more detail. First, the contents of lipophilic antioxidants, carotenoids and tocopherols, were determined. Already under control conditions, most of the carotenoids of the xanthophyll class were found to be less abundant in cytokinin-deficient plants (Fig. 3.4B, neoxanthin and zeaxanthin; Fig. 3.4C, lutein). The deficiency in xanthophylls was even more pronounced after HL treatment due to a limited HL-induced increase in plants with a reduced cytokinin status. Therefore, cytokinin-deficient plants had even 30 to 45 % less xanthophylls compared with the wild type after HL treatment (Fig. 3.4B-C). Carotenoids, especially xanthophylls, are crucial for NPQ, the thermal dissipation of excess light energy under HL and the quenching of $^3Chl^*$ and $^1O_2$ (Gill and Tuteja, 2010; Jahns and Holzwarth, 2012). Additionally, within the carotene class of carotenoids β-carotene plays a central role in the deactivation of $^1O_2$ in the PSII reaction center (Telfer, 2014). Interestingly, also the abundance of β-carotene was significantly lower (~30 %) in cytokinin-deficient plants compared with wild-type plants after the HL

regime (Fig. 3.4C). Together, these results reveal an overall deficiency in carotenoids in both *35S:CKX4* and *ahk2 ahk3* plants (see also total carotenoid content in Fig. 3.4C). This might lead to a compromised energy dissipation mechanism and a reduced $^3Chl^*$ and $^1O_2$ quenching capacity in these plants.

As a second group of lipophilic antioxidants, tocopherols were analyzed (Fig. 3.4D). The total tocopherol content was increased in *35S:CKX4* and *ahk2 ahk3* plants above the wild-type level after HL treatment, which was due to the elevation of α-tocopherol. This might be an attempt to compensate for the lack of antioxidant protection by carotenoids and/or simply reflects the higher degree of light stress in cytokinin-deficient plants.

Furthermore, the contents of hydrophilic antioxidants, namely ascorbate and glutathione, were determined. Ascorbate levels increased after HL treatment, revealing an adaptive response to the light stress, but the increase was similar in both cytokinin-deficient and wild-type plants (Fig. 3.4E). The total glutathione levels increased only slightly after HL exposure, while especially the oxidized form GSSG was highest in *35S:CKX4* plants, albeit not statistically significant (Fig. 3.4F).

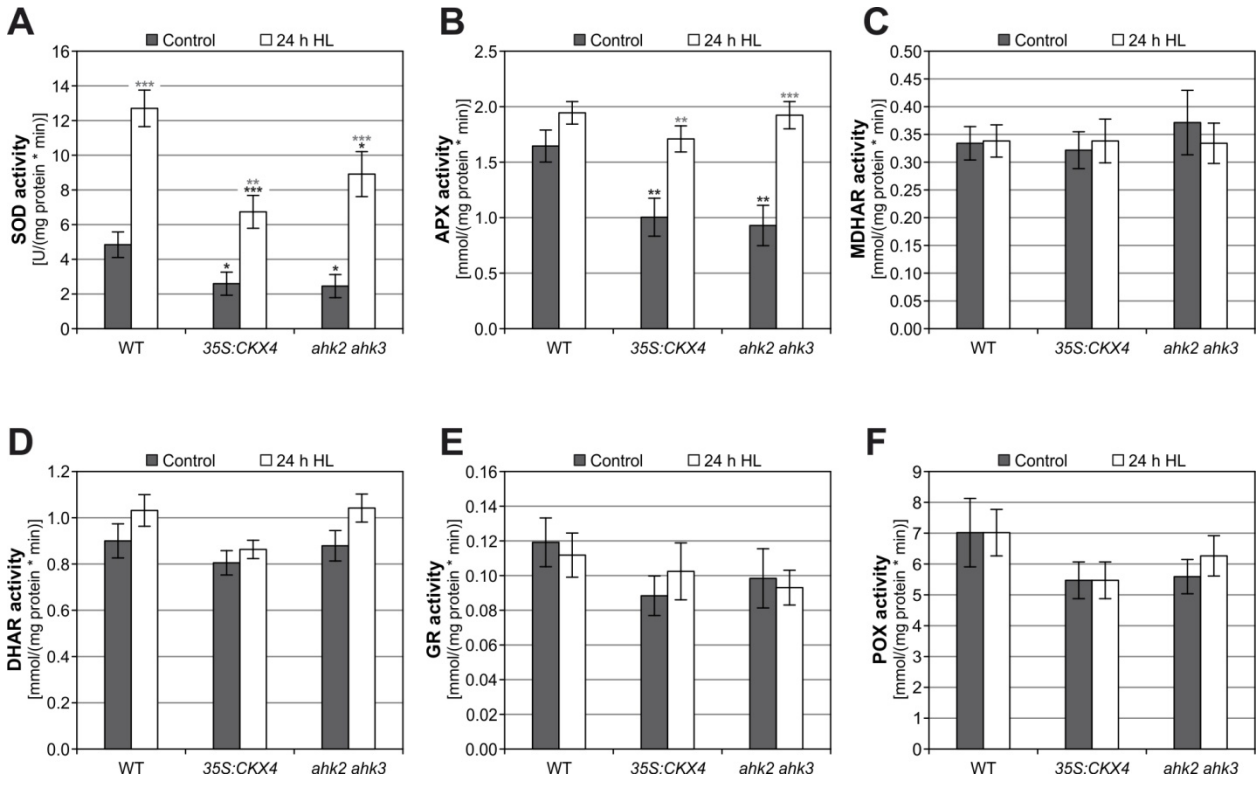

Figure 3.5: Scavenging enzyme activities in plants with a reduced cytokinin status after high light treatment.
Detached leaves (leaf 5, 6, and 7 pooled) of four-week-old SD-grown plants were subjected to 24 hours of HL treatment (for schematic overview see Fig. 3.1A). **A**, Superoxide dismutase (SOD). **B**, Ascorbate peroxidase (APX). **C**, Monodehydroascorbate reductase (MDHAR). **D**, Dehydroascorbate reductase (DHAR). **E**, Glutathione reductase (GR). **F**, Peroxidase (POX). Asterisks indicate significant differences compared with the respective wild type (black) and with the corresponding control (gray) (*t* test: *, $p < 0.05$; **, $p < 0.01$; ***, $p < 0.001$). Error bars represent SE (n = 12).

Next, the focus was on enzymatic scavenging mechanisms. Therefore, the enzyme activities of superoxide dismutase (SOD), enzymes of the Halliwell-Asada pathway, including ascorbate peroxidase (APX), monodehydroascorbate reductase (MDHAR), dehydroascorbate reductase (DHAR) and glutathione reductase (GR), as well as the activity of peroxidase (POX) were analyzed (Fig. 3.5). Only the SOD and APX activities were altered upon HL exposure and showed significant differences between the genotypes (Fig. 3.5A-B). Interestingly, *35S:CKX4* and *ahk2 ahk3* plants displayed a significant reduction of SOD and APX activities (by about 2-fold) under control conditions. This either reflects already a deficiency in the regulation of scavenging enzymes under control conditions, or the reduced activities indicate that cytokinin-deficient plants encounter less oxidative stress under moderate light (control) conditions. After HL treatment, the APX activity increased only slightly in wild-type plants, while it increased much stronger (1.7- and 2-fold, respectively) in both *35S:CKX4* and *ahk2 ahk3* plants (Fig. 3.5B). The SOD activities in HL-treated wild-type and *35S:CKX4* plants increased by 2.5-fold, and *ahk2 ahk3* mutants had even a 3.5-fold increase in the SOD activity. However, the overall SOD activity in plants with a reduced cytokinin status remained significantly lower compared to wild-type plants (Fig. 3.5A).

In the following sections, the results of the second project are presented and described. This part of the work deals with a previously unknown phenomenon – a drastic stress response conferred by changes in the light-dark regime.

3.2 A normal cytokinin status is essential for a proper response to changes in light-dark regimes

Plants are confronted with a multitude of environmental conditions that require an appropriate response. Daily or seasonal fluctuations in light are among the challenges plants have to deal with. Of course, this includes changes in light intensities, which may vary over several orders of magnitude. But it also includes changes in the duration of light periods. The integration of internal and external cues is crucial for proper adaptation to these ever-changing light conditions enabling optimal function and timing of light-dependent processes such as photosynthesis, growth responses and flowering (Dodd *et al.*, 2005; Hotta *et al.*, 2007; Covington *et al.*, 2008; McWatters and Devlin, 2011). In this regard, it was intriguing to observe that plants with a reduced cytokinin status developed necroses upon substantial changes in the light-dark regime while wild-type plants remained largely unaffected suggesting an adaptive advantage conferred by cytokinin.

3.2.1 Plants with a reduced cytokinin status are sensitive to changes in the light-dark regime

The transfer of SD-adapted plants to LD conditions (Fig. 3.6A; "16 h L/8 h D") repeatedly resulted in the formation of necrotic leaves in *35S:CKX4* and to a lesser extent in *ahk2 ahk3* plants after one LD cycle whereas no or only very few necroses could be detected in control (kept in SD rhythm) and wild-type plants, respectively (Fig. 3.6B-C).

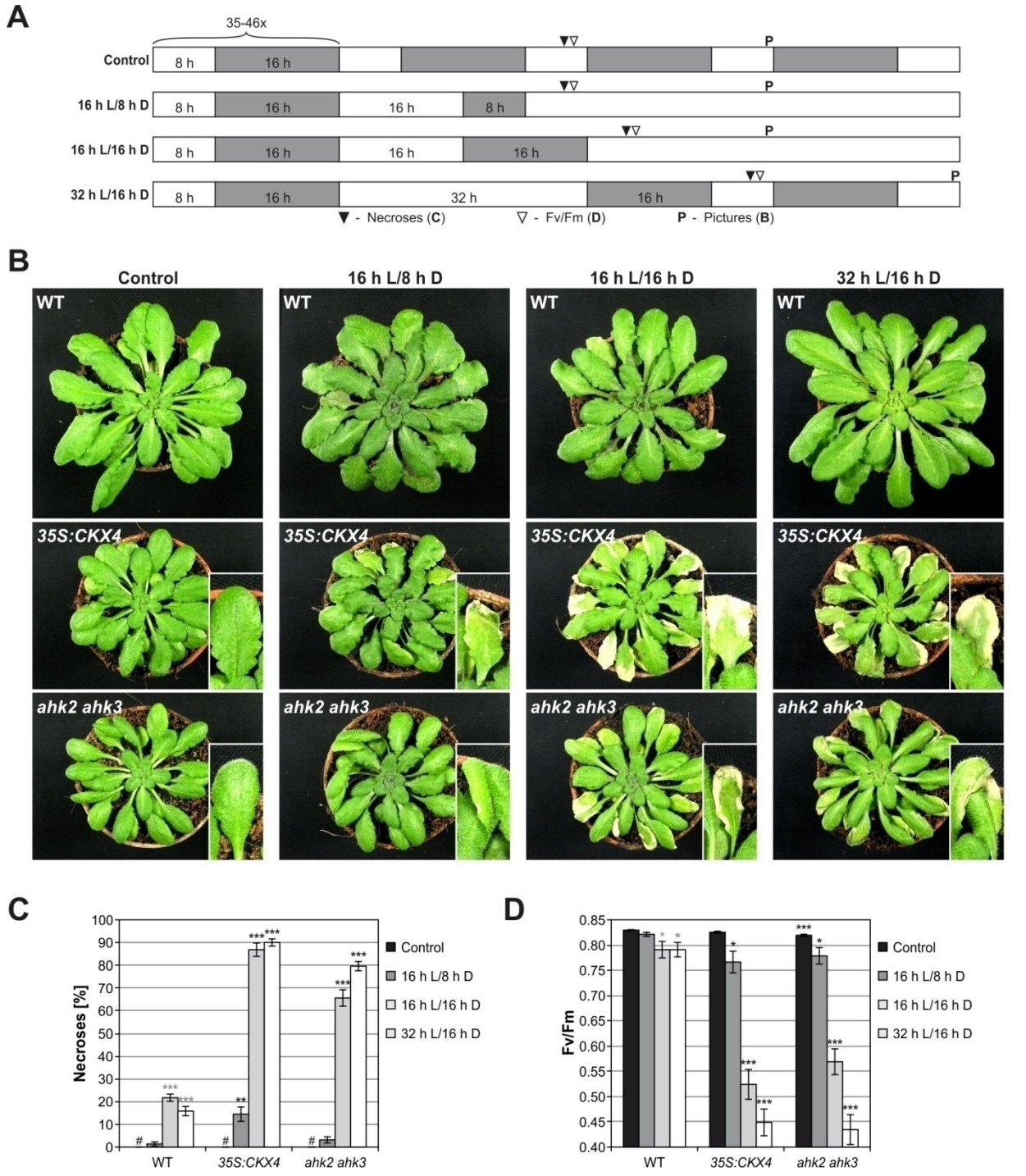

Figure 3.6: Plants with a reduced cytokinin status are sensitive to changes in the light-dark regime.

A, Schematic overview of the experimental design. Plants were grown under SD conditions for five to six weeks prior to the exposure to changed light-dark regimes. White, light period (L); gray, dark period (D). **B**, Phenotype of representative plants after respective treatments. Pictures were taken at the time points indicated in (**A**). Inserts give representative examples of leaves showing the necrotic phenotype. **C**, Photosystem II maximum quantum efficiency, as measured by the chlorophyll fluorescence ratio F_v/F_m in representative and/or affected leaves (n = 12). **D**, Percentage of necrotic leaves counted in mature leaves five hours after the end of the dark period as indicated by an open triangle in (**A**) (n = 10; #, not detected). Asterisks indicate significant differences compared with the respective wild types (black) and with the corresponding control (gray, for wild type only) (*t* test: *, $p < 0.05$; **, $p < 0.01$; ***, $p < 0.001$). Error bars represent SE.

Additionally, chlorophyll fluorescence measurements were carried out, more precisely F_v/F_m ratios were determined. The F_v/F_m ratio is not only useful to study photoinhibition under light stress (see 3.1) but is also widely used as a measure of stress in leaves since photosynthetic performance decreases under various stresses (Baker, 2008; see 1.2). As a matter of fact, F_v/F_m values significantly decreased in leaves of *35S:CKX4* and *ahk2 ahk3* upon imposing the "16 h L/8 h D" regime clearly demonstrating that this caused a stressed state (Fig. 3.6D). Subsequently, more changes in light-dark regimes were tested (Fig. 3.6A; "16 h L/16 h D" and "32 h L/16 h D"). These experiments revealed that further extension of the light period as well as prolongation of the dark period dramatically increased the stress phenotype. The percentage of necrotic leaves increased up to 90 % in *35S:CKX4* and up to 80 % in *ahk2 ahk3* of all mature leaves (Fig. 3.6C). In addition, the necrotic area was profoundly enlarged as the inserts indicate in Figure 3.6B. Wild-type plants also developed necroses under these conditions (up to 20 %), though lesser and smaller ones, which was reflected by only slight but significant decreases in F_v/F_m ratios compared with the controls. In contrast, the treated cytokinin-deficient plants exhibited an enormous reduction in F_v/F_m under both regimes (Fig. 3.6D). In order to analyze the observed phenotype in more detail the 32-hour light regime (referred to as continuous light [CL] treatment in the following) was chosen as "standard regime". Besides a strong and remarkably reproducible phenotype this regime offers a condition which is easy to accomplish and that comprises a reduced complexity compared with the "16 h L/16 h D" regime. It also includes a prolonged light treatment but the following dark period is resonant (in-phase) with the nights under control (SD) conditions which is not the case for the "16 h L/16 h D" regime.

3.2.2 The cytokinin receptors CRE1/AHK4, AHK2, and AHK3 mediate the response to the CL regime

To further evaluate the hypothesis that cytokinin plays a role in proper adaptation to changes in light-dark regimes more mutant and transgenic plants with an altered cytokinin status were tested under the aforementioned CL conditions. As described above, *ahk2 ahk3* mutants developed necroses after CL treatment. Therefore, one attempt was to study the contribution of the different cytokinin receptors more explicitly under these conditions. For that purpose single and double receptor mutants (Riefler *et al.*, 2006) were analyzed and compared with the response of *ahk2 ahk3* and *35S:CKX4* plants (Fig. 3.7). Mutation of *CRE1/AHK4* and/or *AHK2* alone did not cause the formation of necroses while the single *ahk3* mutant exhibited a necrotic phenotype clearly distinguishable from wild type but weaker than in *ahk2 ahk3* or *35S:CKX4* (Fig. 3.7A-B; for controls see Appendix Fig. A.1). Interestingly, a rather severe phenotype, even stronger than in *ahk2 ahk3* and *35S:CKX4*, could be detected in the *cre1 ahk3* double mutant although *cre1* and *cre1 ahk2* plants behaved like wild type. The stress-induced decrease in F_v/F_m shown in Figure 3.7C correlated well with the severity of the necrotic phenotype except for *cre1 ahk3* which exhibited a much stronger reduction in F_v/F_m ratios. However, although these plants had only a few more affected leaves per plant the affected areas were much larger compared with *ahk2 ahk3* covering the leaves more or less completely while they were more restricted to the margins in *ahk2 ahk3*. These results clearly demonstrate that the AHK3 receptor is the key mediator in this adaptive response to changed light-dark regimes. Nonetheless, AHK2 and

CRE1/AHK4 play accessory roles acting only in combination with the AHK3 receptor under the tested conditions. Noteworthy, *cre1* has a rather synergistic effect on *AHK3* loss-of-function revealing a quite strong cooperative function for CRE1/AHK4.

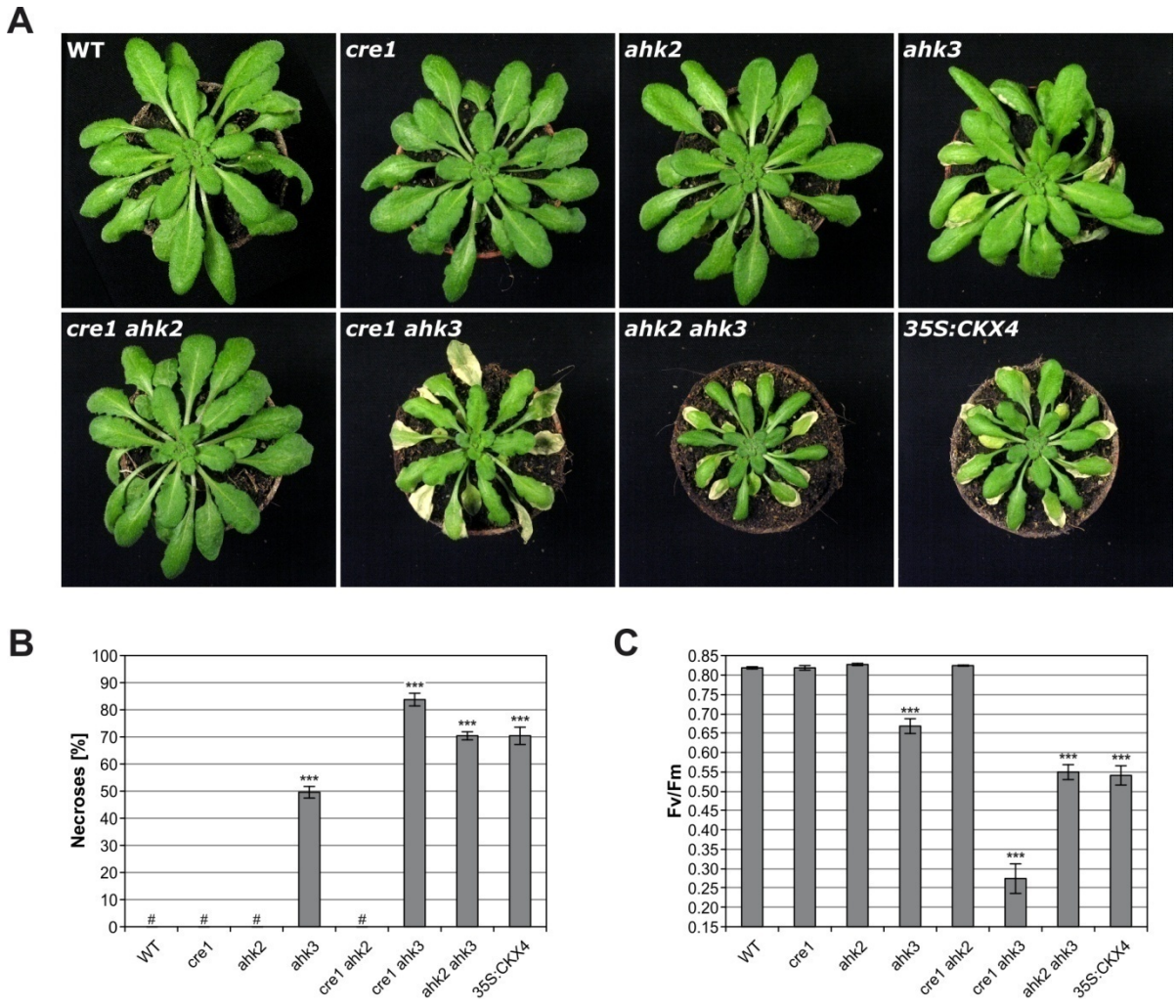

Figure 3.7: Redundant action of the cytokinin receptors CRE1/AHK4, AHK2, and AHK3 in mediating the response to changed day-night rhythms.

A, Pictures show cytokinin receptor single and double mutants in comparison with wild-type and *35S:CKX4* transgenic plants. Plants were grown for five weeks under SD conditions, subjected to 32 hours of CL and transferred back into SD conditions afterwards. Pictures were taken two days after CL treatment and are representative for the observed phenotypes. **B**, Percentage of necrotic leaves counted in mature leaves one day after CL treatment (n = 10; #, not detected). **C**, Stress-induced decrease in F_v/F_m ratios corresponding to the inhibition of photosystem II measured one day after CL treatment (n = 10 [*ahk2*, *cre1 ahk2*]; n = 11 [*cre1*, *cre1 ahk3*]; n = 12 [WT, *ahk3*, *ahk2 ahk3*, *35S:CKX4*]). Experimental design corresponds to "32 h L/16 h D" in Fig. 3.6A. Control plants remained continuously in the SD rhythm and were not affected (for pictures see Appendix Fig. A.1). Asterisks indicate significant differences compared with wild type (*t* test: ***, $p < 0.001$). Error bars represent SE.

3.2.3 Cytokinin oxidase/dehydrogenase overexpressors and 35S:CKX1 suppressor mutants under CL conditions

Next, additional *CKX* overexpressing plants (Werner *et al.*, 2003) and suppressor mutants of the *35S:CKX1*-induced cytokinin deficiency phenotype (called *rock*; Bartrina, 2006; Jensen, 2013; Niemann, 2013; see 1.1.4) were analyzed. Constitutive expression of *CKX1* and *CKX2*, in addition to

CKX4, resulted in a necrotic phenotype after CL treatment (Fig. 3.8A; for controls see Appendix Fig. A.2) revealing yet another indication that the proper response to CL is cytokinin-dependent.

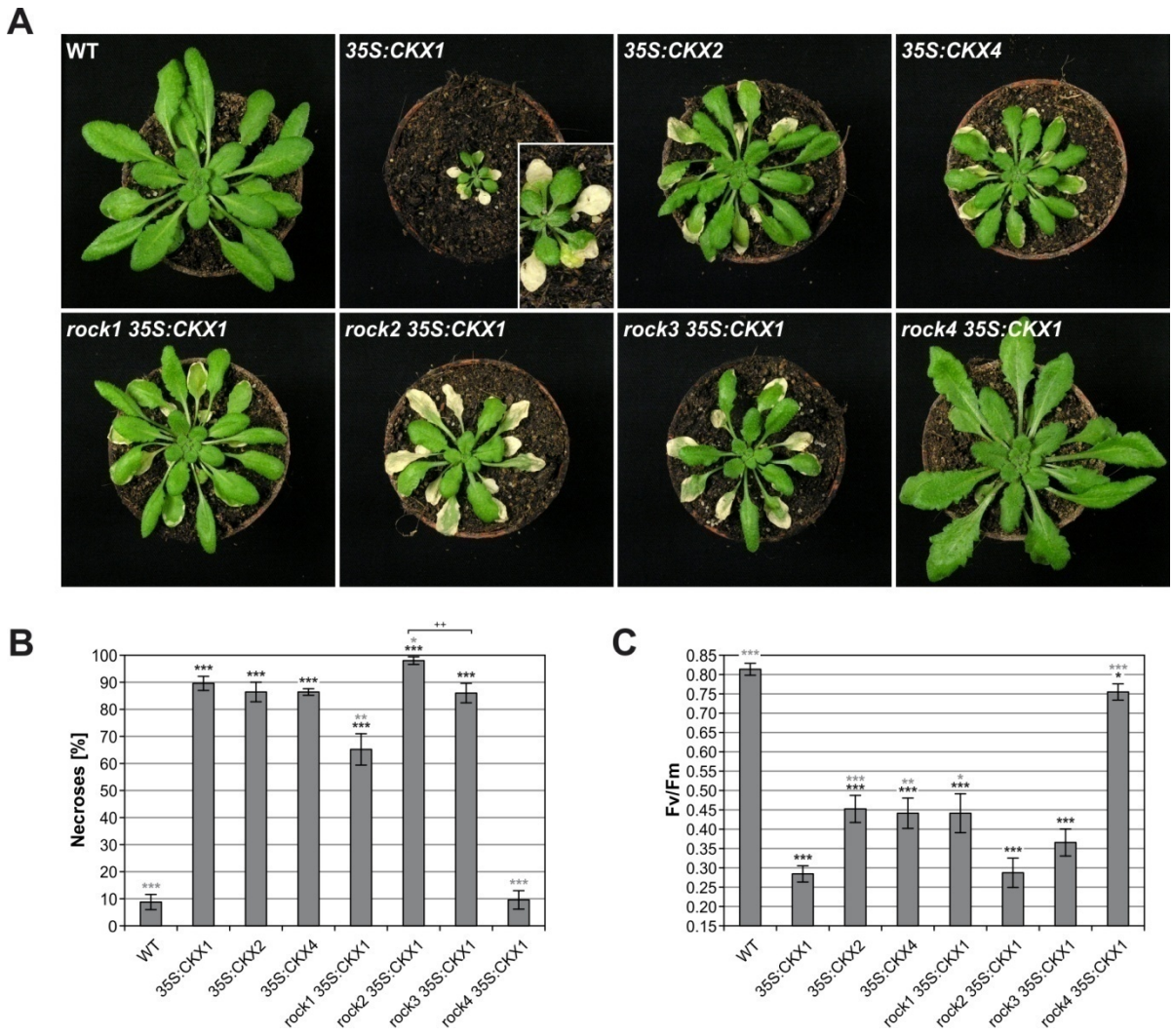

Figure 3.8: The necrotic phenotype displayed by cytokinin-deficient *CKX* overexpressing plants after continuous light treatment is partially reversed in *rock* mutants.

A, Different cytokinin oxidase/dehydrogenase (*CKX*) overexpressing transgenic plants (*35S:CKX1*, *35S:CKX2*, and *35S:CKX4*) and *35S:CKX1* suppressor mutants (called *rock*) which to a different extent suppress the morphological consequences of the cytokinin deficiency syndrome are depicted in comparison with wild type. Plants were grown for six weeks under SD conditions, subjected to 32 hours of CL and transferred back into SD conditions afterwards. Pictures were taken three days after CL treatment and are representative for the observed phenotypes. **B**, Percentage of necrotic leaves counted in mature leaves one day after CL treatment (n = 8 [WT, *35S:CKX2*]; n = 10 [*35S:CKX4*, *rock1/35S:CKX1*, *rock2/35S:CKX1*]; n = 12 [*35S:CKX1*, *rock3/35S:CKX1*, *rock4/35S:CKX1*]). **C**, Stress-induced decrease in F_v/F_m ratios corresponding to the inhibition of photosystem II measured one day after CL treatment (n = 12). Experimental design corresponds to "32 h L/16 h D" in Fig. 3.6A. Control plants remained continuously in the SD rhythm and were not affected (for pictures see Appendix Fig. A.2). Asterisks or plus signs indicate significant differences compared with wild type (black) and with *35S:CKX1* (gray) or between *rock2/35S:CKX1* and *rock3/35S:CKX1* (plus signs) (*t* test: *, $p < 0.05$; **, $p < 0.01$; ***, $p < 0.001$; $^{++}$, $p < 0.01$). Error bars represent SE.

While the amount of necrotic leaves per plant was similar in all *CKX* overexpressors (Fig. 3.8B) the dimension of necroses and hence the degree of stress was not. *35S:CKX1* exhibited the most severe stress phenotype as indicated by a pronounced decrease in F_v/F_m whereas both *35S:CKX2* and

35S:CKX4 showed an intermediate response between *35S:CKX1* and wild-type plants (Fig. 3.8C). The stunted shoot phenotype of *35S:CKX1* plants due to their cytokinin deficiency could be reversed by different *rock* mutations (see above). Thus, the question arose if the necrotic phenotype of *35:CKX1* plants could also be reversed in plants additionally carrying *rock* mutations. In fact, *rock1* and *rock4* mutations caused partial or almost full reversion, respectively, reflected by a decrease in the percentage of necrotic leaves to an intermediate or wild-type level (Fig. 3.8B) and F_v/F_m values similar to *35S:CKX4* or close to wild-type levels, respectively (Fig. 3.8C). In contrast, the *rock2* mutation did not lead to an improved phenotype. Instead, the amount of necroses was slightly increased in *rock2 35S:CKX1* compared with *35S:CKX1* (Fig. 3.8B). Plants carrying the *rock3* mutation leading to an AHK3 receptor gain-of-function repeatedly tended to show partial reversion compared with *35S:CKX1* and *rock2 35S:CKX1* plants. Though this reversion was not significant in most cases it nevertheless reconfirmed the role of AHK3 for this response. It might be worth noticing that *rock3* plants in the wild-type background behaved like wild type (data not shown) indicating that the necrotic phenotype observed in *rock3 35S:CKX1* plants is solely due to *CKX1* overexpression. Taken together, the compromised response to changed light-dark regimes caused by cytokinin deficiency could indeed be at least partially reversed through the presence of *rock* alleles (exception *rock2;* tendency *rock3*).

3.2.4 Isopentenyltransferases redundantly act to provide a sufficient cytokinin content for a proper response to changed light-dark regimes

In the following, cytokinin synthesis *ipt* mutants (Miyawaki *et al.*, 2006) were analyzed under CL conditions. The aim was to obtain an additional proof for the relevance of a sufficient cytokinin content for proper adaptation to changes in light-dark regimes. Pretests revealed that the triple mutant *ipt3,5,7* exhibited a dramatic necrotic phenotype reflected by 100 % necroses. Thus, all mature leaves were affected thereby exceeding all other mutants described so far. Therefore, in order to find out if the lack of a specific IPT isoform is responsible for the CL phenotype or if the effect in *ipt3,5,7* plants is additive or synergistic due to the lack of several cytokinin producing enzymes the corresponding single and double mutants were examined and compared with *ipt3,5,7* after CL treatment. Figure 3.9 demonstrates that the *IPT* genes act redundantly in the CL response. The single mutants developed only a few necroses (Fig. 3.9A-B; for controls see Appendix Fig. A.3), while the double mutants showed an intermediate necrotic phenotype between single mutants and triple knockout. A similar pattern was observed for the stress-induced decrease in F_v/F_m ratios after CL treatment (Fig. 3.9C).

3.2.5 The contribution of B-type ARRs in the adaptive response to altered light-dark regimes

Eventually, experiments were performed to unravel a role for specific B-type ARRs, transcription factors mediating the cytokinin signal to downstream targets (see 1.1.3.2). The results show that ARR2 and a combination of ARR10 and ARR12 are important for a proper response to changed light-dark regimes as reflected by necrotic leaves formed after CL treatment (Fig. 3.10A; for controls see Appendix Fig. A.4). Nevertheless, one has to note that their loss-of-function had a considerably smaller effect than constitutive *CKX4* expression (Fig. 3.10B-C). The simultaneous mutation of *ARR1* and

ARR12 resulted in slight changes compared with the wild type although these were not statistically significant. Due to the strong functional redundancy among B-type ARRs (Argyros *et al.*, 2008; Ishida *et al.*, 2008a) it would have been advantageous to test higher-order mutants. However, an attempt to analyze *arr1,10,12* mutants failed because these plants had profound difficulties to grow under SD conditions.

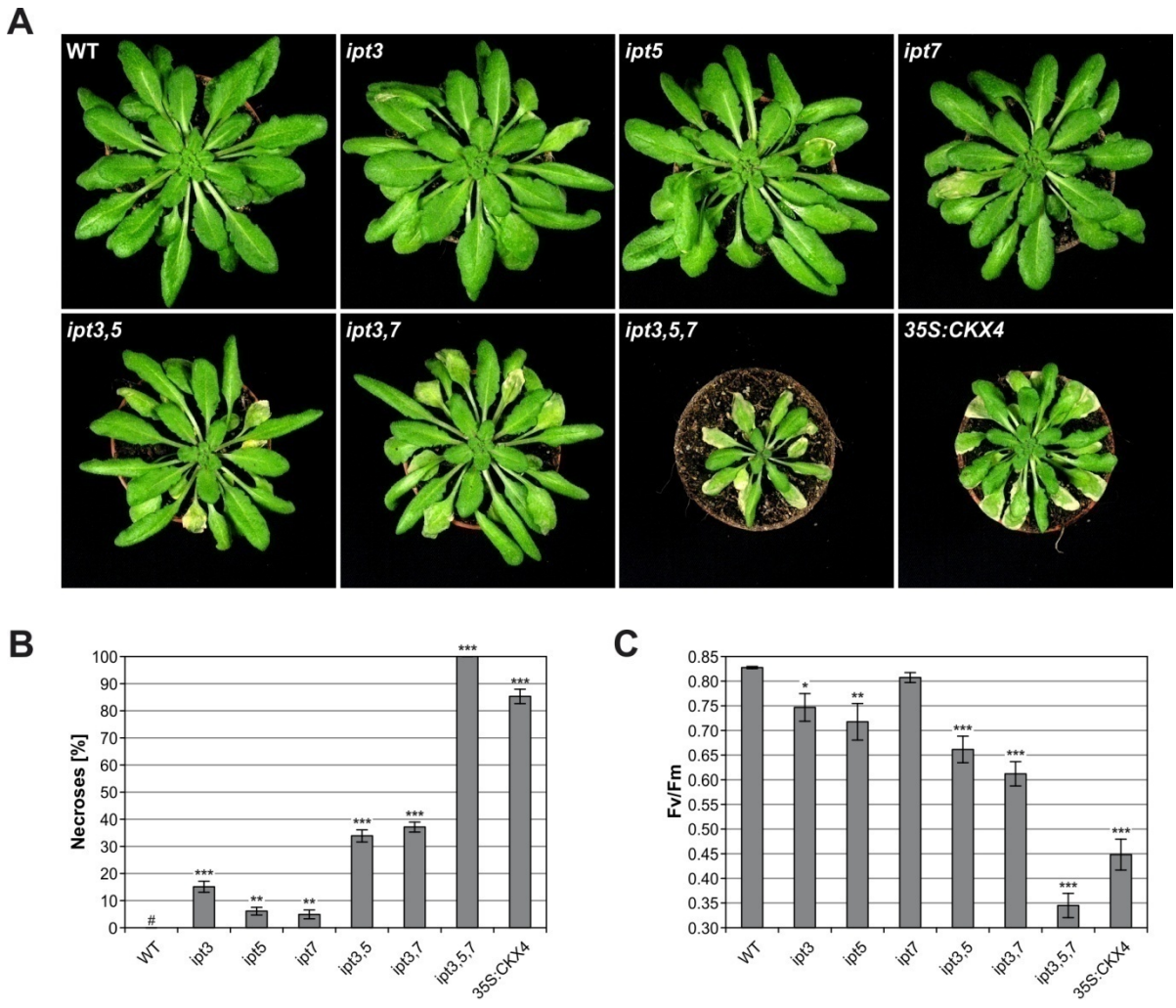

Figure 3.9: The isopentenyltransferase genes *IPT3*, *IPT5*, and *IPT7*, important for cytokinin synthesis, are required for a proper response to changes in light-dark regimes.

A, Pictures show *ipt* single, double, and triple mutants in comparison with wild-type and *35S:CKX4* transgenic plants. Six-week-old plants were subjected to 32 hours of CL and transferred back into SD conditions afterwards. Pictures were taken two days after CL treatment and are representative for the observed phenotypes. **B**, Quantification of necrotic leaves (as percentage of all mature leaves) one day after CL treatment (n = 14; #, not detected). **C**, Stress-induced decrease in F_v/F_m ratios corresponding to the inhibition of photosystem II measured one day after CL treatment (n = 16). Experimental design corresponds to "32 h L/16 h D" in Fig. 3.6A. Control plants remained in the SD rhythm and were not affected (for pictures see Appendix Fig. A.3). Asterisks indicate significant differences compared with wild type (*t* test: *, $p < 0.05$; **, $p < 0.01$; ***, $p < 0.001$). Error bars represent SE.

Collectively, the results described in this chapter clearly point to a so far unknown role of cytokinin in the adaptive response to changes in light-dark regimes and a redundant action of several cytokinin

synthesis and signaling genes. This function is evidently of great importance since many of the plants with a reduced cytokinin status developed strong leaf necroses – a cell death phenotype.

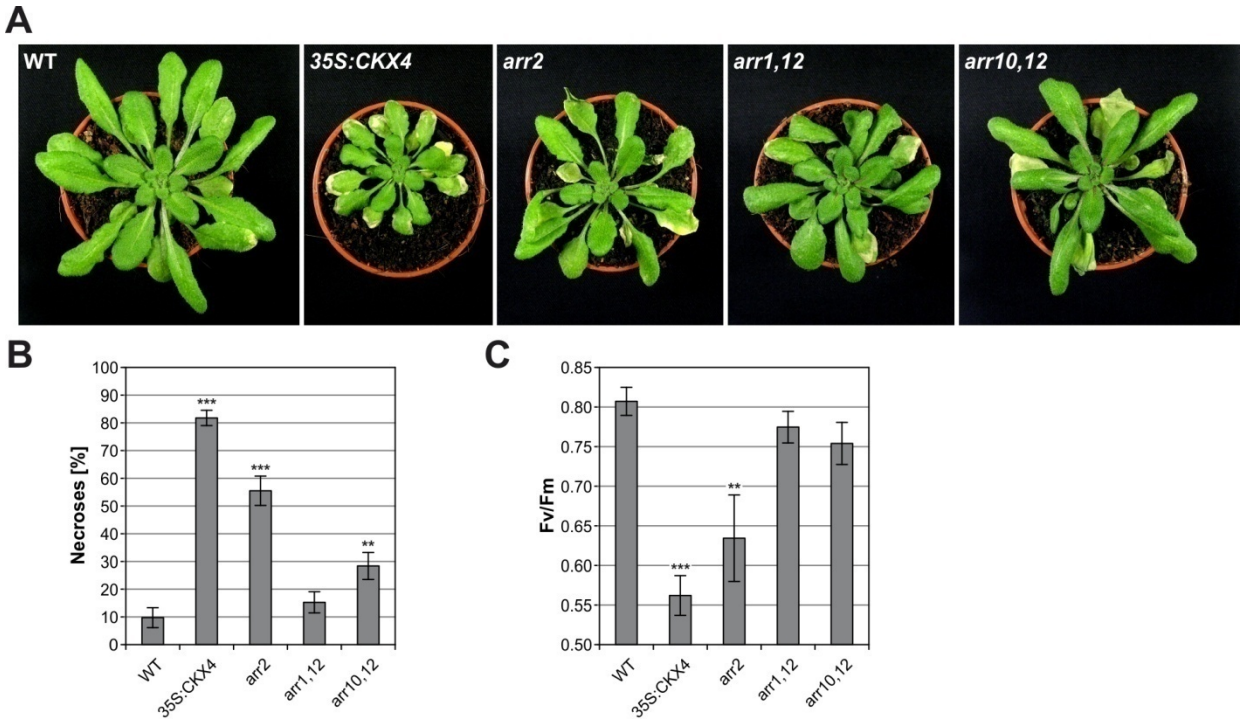

Figure 3.10: The role of B-type response regulators in the response to altered light-dark cycles.

A, Pictures show B-type *arr* mutants (*arr2*; *arr1,12*; *arr10,12*) in comparison with wild-type and *35S:CKX4* transgenic plants. Six-week-old plants were subjected to 32 hours of CL and transferred back into SD conditions afterwards. Pictures were taken two days after CL treatment and are representative for the observed phenotypes. **B**, Quantification of necrotic leaves (as percentage of all mature leaves) one day after CL treatment (n = 10). **C**, Stress-induced decrease in F_v/F_m ratios corresponding to the inhibition of photosystem II measured one day after CL treatment (n = 12). Experimental design corresponds to "32 h L/16 h D" in Fig. 3.6A. Control plants remained in the SD rhythm and were not affected (for pictures see Appendix Fig. A.4). Asterisks indicate significant differences compared with wild type (*t* test: **, $p < 0.01$; ***, $p < 0.001$). Error bars represent SE.

3.3 Further characterization of the cell death phenotype in plants with a reduced cytokinin status

3.3.1 Induction of lipid peroxidation and formation of water-soaked lesions in cytokinin-deficient plants after CL treatment

ROS are produced as both active signaling components and toxic byproducts during development and various stresses (see 1.4.1). If stress conditions persist, ROS levels increase resulting in oxidative stress (Mittler *et al.*, 2004; Apel and Hirt, 2004). One immediate consequence of oxidative stress is the oxidation of lipids, called lipid peroxidation (LPO). Therefore, LPO was analyzed in order to map oxidative stress in cytokinin-deficient plants one day after CL treatment. This was achieved by three different means: autoluminescence and thermoluminescence imaging (Havaux, 2003; Ducruet, 2003; Havaux *et al.*, 2006), and the quantification of hydroxyoctadecatrienoic acid (HOTE) isomers which enables to distinguish between ROS- and lipoxygenase (LOX)-mediated LPO (Montillet *et al.*, 2004).

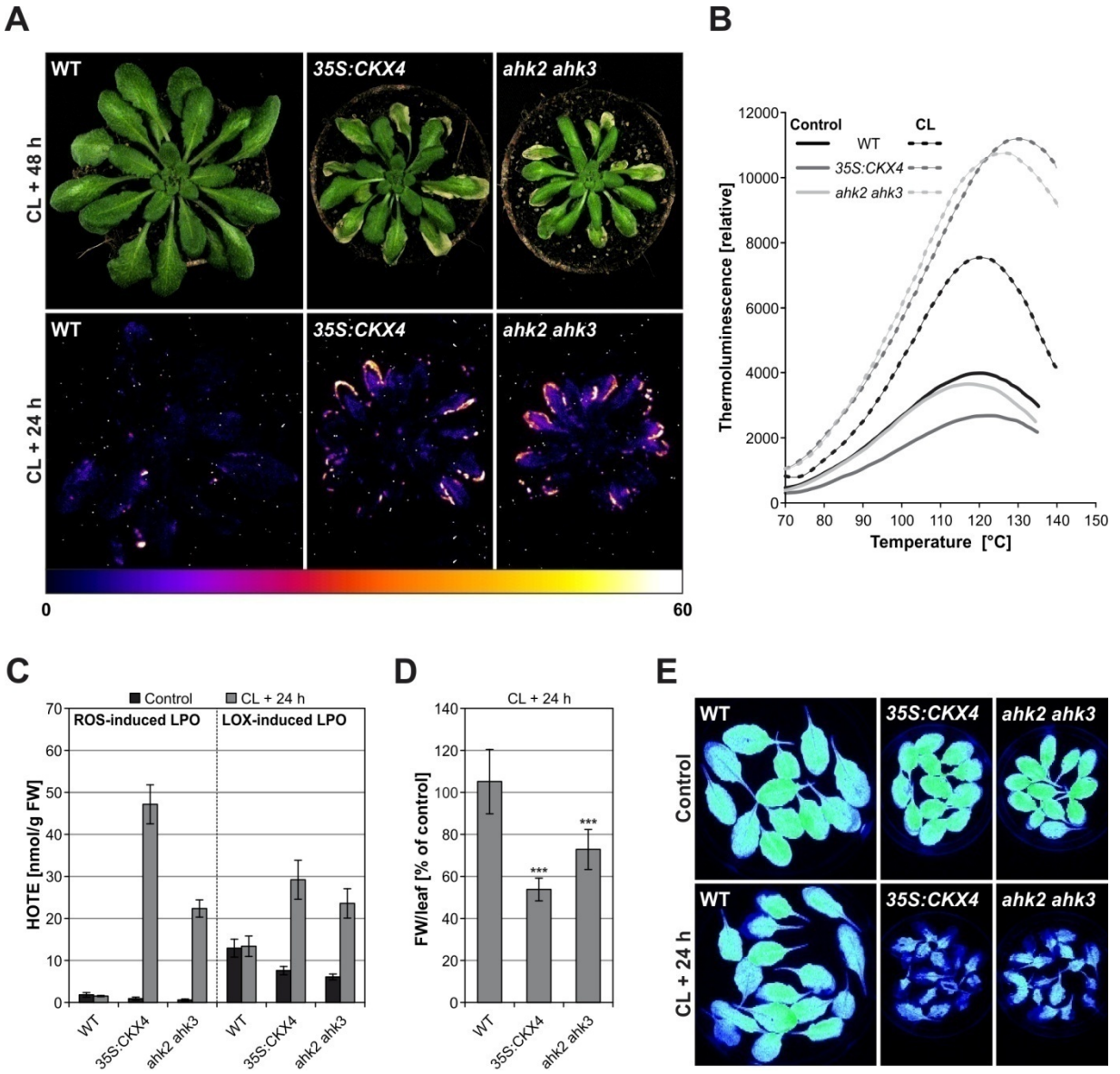

Figure 3.11: The induction of lipid peroxidation and the formation of water-soaked lesions are characteristics of the cell death response in cytokinin-deficient plants after continuous light treatment.

A-B, Increased oxidative stress in cytokinin-deficient plants one day after CL treatment reflected by autoluminescence (**A**, bottom row) and elevated thermoluminescence (**B**). Pictures of plants taken two days after CL treatment (**A**, top row) show the presence of necroses in the areas of highest autoluminescence measured one day earlier (**A**, bottom row). **C**, Analysis of ROS- and LOX-induced LPO by detection of the corresponding HOTE (hydroxyoctadecatrienoic acid) isomers one day after CL treatment (n = 4). **D**, Decrease in fresh weight (FW) per leaf (as per cent of respective controls [set to 100 %]) analyzed one day after CL treatment reflecting limpness of the leaves due to formation of water-soaked lesions (n = 10; each sample consisted of four [WT] or eight to ten [*35S:CKX4*, *ahk2 ahk3*] leaves). **E**, Chlorophyll fluorescence of leaves detached one day after CL treatment exhibits a similar but inverse pattern compared with the autoluminescence images. The light regimes correspond to "Control" and "32 h L/16 h D" in Fig. 3.6A. Asterisks indicate significant differences compared with wild type (*t* test: ***, $p < 0.001$). Error bars represent SE. The autoluminescence and thermoluminescence as well as the HOTE measurements were performed in collaboration with Prof. Dr. Michel Havaux (see 2.11).

The stress caused by CL treatment led to a pronounced LPO in both *35S:CKX4* and *ahk2 ahk3* plants while wild type was not or only slightly affected. This was reflected by the increase in both autoluminescence (Fig. 3.11A, bottom row) and thermoluminescence (Fig. 3.11B) as well as by the increase in HOTE levels (Fig. 3.11C). The latter provided evidence that LPO was induced by both ROS

and LOX because ROS- and LOX-derived moieties could be detected among the extracted HOTE isomers. Surprisingly, cytokinin-deficient control plants tended to exhibit less LPO compared with wild-type controls (Fig. 3.11C). The severe stress in cytokinin-deficient plants was also hallmarked by a strong loss of fresh weight (Fig. 3.11D). It was reduced down to 55 or 70 % of the controls, respectively, in *35S:CKX4* and *ahk2 ahk3*, while it was not altered in wild-type leaves. In the literature limp leaves in combination with cell death progression are referred to as water-soaked lesions and are usually observed during disease-associated (HR) cell death following pathogen attack (Greenberg *et al.*, 2000; Katagiri *et al.*, 2002; Su'udi *et al.*, 2011; Ishiga *et al.*, 2011). Sometimes the whole leaf, in extreme cases also including the petiole, turned limp, whereas the necrotic lesions were more restricted to the margins of the leaf. While the limp parts recovered from the "water-soaked" phenotype within the following 24 hours the necrotic lesions particularly emitting light visualized by the autoluminescence measurements (Fig. 3.11A, bottom row) were conform with the necrotic parts still visible one day later (Fig. 3.11A, top row). Interestingly, the same patterns, albeit inversed, were observed by imaging the decrease of chlorophyll fluorescence (Fig. 3.11E). This result further validated the F_v/F_m measurements as suitable method for assessing the stress after CL treatment.

3.3.2 Changes in transcript levels of stress- and cell death-associated genes accompany cell death progression in cytokinin-deficient plants

In line with the phenotypically visible cell death progression a large set of genes was differentially expressed. Some of the results are depicted in Figure 3.12. Samples for quantitative RT-PCR (qRT-PCR) analysis were harvested one day after CL treatment (Fig. 3.12A). Corresponding to the results shown in Figure 3.11 the expression analysis of oxidative stress marker genes *BAP1* and *ZAT12* (see 1.4.3) revealed a dramatic increase of oxidative stress in CL-treated cytokinin-deficient plants while wild type only showed a marginal elevation of *BAP1* and *ZAT12* expression compared with control levels (Fig. 3.12B). It should also be noted, that *ZAT12* levels were, though only slightly, increased up to 8- and 7-fold, respectively, in *35S:CKX4* and *ahk2 ahk3* plants under control conditions at the end of the SD light period. Since senescence is one well-studied form of programmed cell death in plants (Lim *et al.*, 2007, see 1.5.2) the response of senescence-associated genes was examined. All three genes tested exhibited profound changes in expression levels in plants with a reduced cytokinin status after CL treatment (Fig. 3.12B). The levels of *BIFUNCTIONAL NUCLEASE 1* (*BFN1*) and senescence marker gene *SAG12* were strongly elevated. In contrast, the *CAB2* gene, encoding a chlorophyll binding protein, was 43- and 32-fold downregulated in CL-treated *35S:CKX4* and *ahk2 ahk3* plants, respectively, compared with the wild-type control. This is in accordance with the loss of chlorophyll during cell death progression. Additionally, *LOX3* and *LOX4* were upregulated in cytokinin-deficient plants in response to CL and are most likely involved in the LOX-induced LPO described above (Fig. 3.12D). However, a slight induction of both genes could also be detected in wild type. Cell death marker genes *MCP2D* and *BI1* (see 1.5.1) were upregulated exclusively in CL-treated cytokinin-deficient plants confirming cell death progression also on the molecular level (Fig. 3.12E). In order to find out whether the lesions formed after CL treatment mimic the pathogen-inducible HR, SA signaling and defense gene expression (*PR1* and *EDS1*, respectively) known to be linked to HR cell death (see

1.5.2) was studied (Fig. 3.12F). The results indicate a possible involvement of SA signaling in the execution of CL-dependent cell death because *PR1* was substantially induced in affected cytokinin-deficient plants. In contrast, *EDS1* transcript levels which are induced in response to pathogen attack or SA treatment (Falk *et al.*, 1999; Feys *et al.*, 2001) were not changed excluding the EDS1/PAD4 pathway in this response.

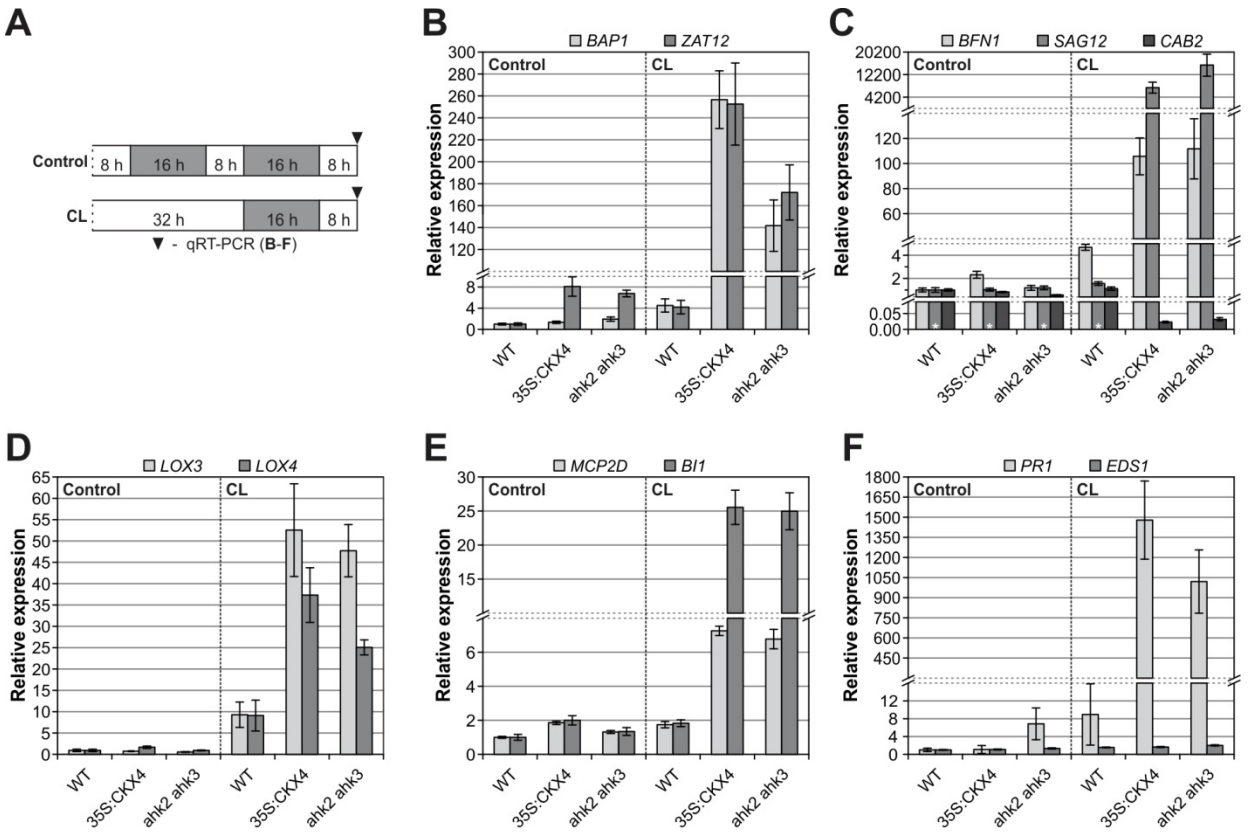

Figure 3.12: Cell death progression in cytokinin-deficient plants after continuous light treatment is accompanied by strong changes in stress- and cell death-associated transcript levels.

A, The scheme represents the experimental setup in **B**-**F**. White, light period; gray, dark period. Plants were grown under SD conditions for six weeks. Control plants remained in the SD rhythm while a subset of plants was subjected to 32 hours of CL. Leaf samples for qRT-PCR were collected after one SD following CL treatment. Transcript levels of numerous genes were dramatically altered in plants with a reduced cytokinin status in response to CL treatment including oxidative stress marker genes (**B**); senescence-associated genes (**C**); lipoxygenase genes (**D**); cell death marker genes (**E**), and SA signaling (*PR1*) and defense (*EDS1*) genes (**F**). Data represent the mean and SE values of six biological replicates. For *SAG12* no transcripts could be detected in the controls and in CL-treated wild type (**C**, marked by asterisks). A threshold cycle (Ct) of 40 was assumed in order to calculate relative expression values for CL-treated *35S:CKX4* and *ahk2 ahk3*. Expression levels are normalized to the respective wild-type control, which was set to 1. *PP2AA2*, *SAND*, and *UBC10* served as reference genes. Abbreviations of gene names are explained in the list at the beginning of this work.

3.3.3 Age-dependent cell death in cytokinin-deficient plants in response to the CL regime

It is apparent on all pictures of plants showing the cell death phenotype that only mature leaves were subject to cell death while young developing leaves looked unaffected (see 3.2). The question arose if only mature leaves of cytokinin-deficient plants exhibited the molecular stress phenotype described in Figure 3.12 or if young leaves of the same plants were also affected on the molecular level but perhaps below a threshold required to transform the stress response into a "death signal". To answer that

question another qRT-PCR analysis was performed, this time on samples harvested already 16 hours after CL treatment (Fig. 3.13A) because it was evident that the water-soaked and necrotic lesions were already visible at that time. Moreover, young developing leaves were examined in addition to the so far analyzed mature leaves (Fig. 3.13B). Intriguingly, none of the tested genes displayed a differential expression in young leaves after CL treatment. Oxidative stress marker genes *BAP1* and *ZAT12* were exclusively upregulated in mature leaves (Fig. 3.13C-D). Consistent with this result, a decreased *CAB2* expression indicating loss of chlorophyll and an increased *BI1* expression closely connected to cell death progression were noted only in mature leaves of cytokinin-deficient plants after CL treatment (Fig. 3.13E-F).

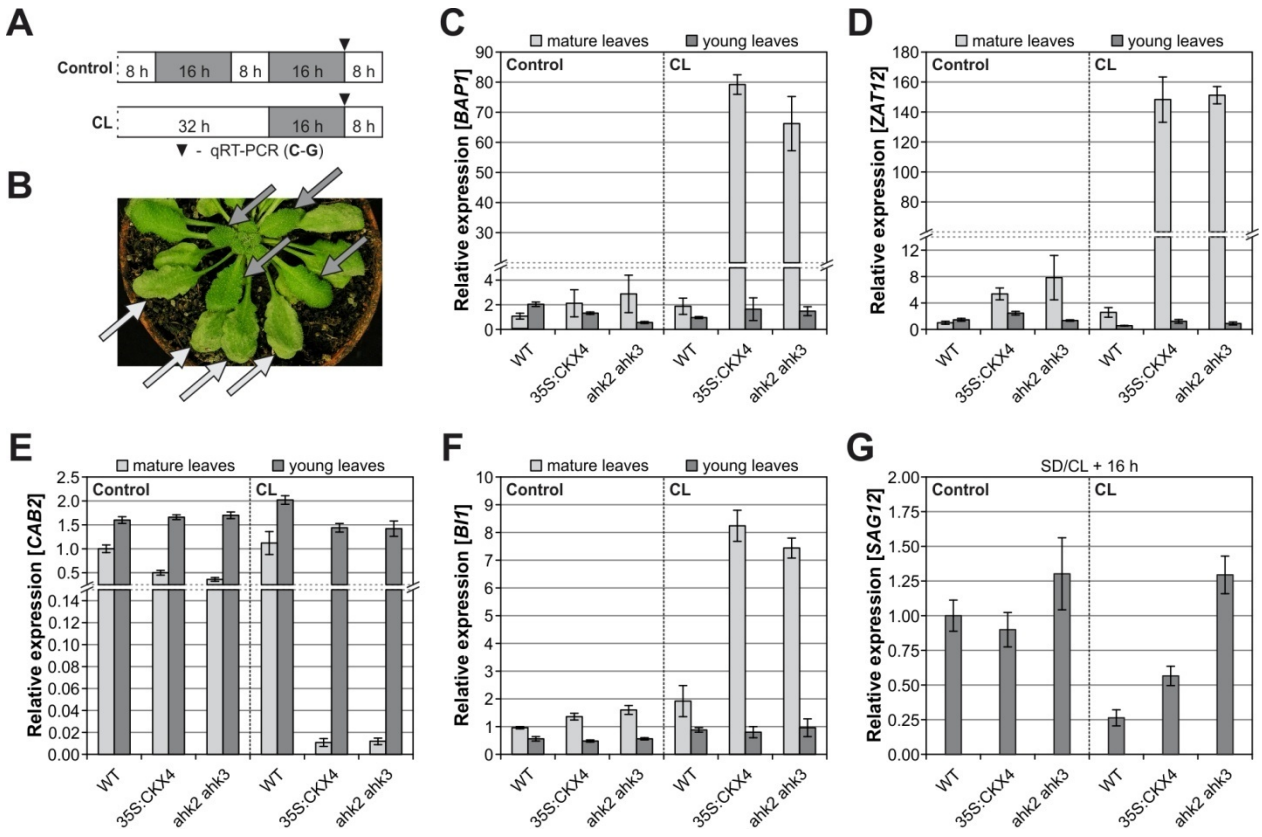

Figure 3.13: The stress response presumably causing the cell death is exclusively initiated in mature leaves.

A, Schematic overview of the experimental design. White, light period; gray, dark period. The light regime corresponds to the one described in Fig. 3.12, except that the samples for qRT-PCR were collected already 16 hours after CL treatment in this setup. **B**, Cell death phenotype in a *35S:CKX4* transgenic plant at the end of the night following CL treatment. Arrows point to affected mature leaves (light gray) and to unaffected young leaves (dark gray), respectively, which correspond to the sampled material in (**C**-**F**). For control and CL-treated wild-type plants leaves of the corresponding developmental stage were chosen. **C-F**, Transcript levels in mature and young leaves at the end of a 16-hour dark period following CL treatment or during a normal SD rhythm. The expression levels of *BAP1* (**C**), *ZAT12* (**D**), *CAB2* (**E**), and *BI1* (**F**) are shown. **G**, Expression levels of *SAG12* only in mature leaves 16 hours after CL treatment. Data represent the mean and SE values of four biological replicates and are expressed as relative values compared with wild-type control/mature leaves, which was set to 1. *PP2AA2* and *MCP2D* served as reference genes. Abbreviations of gene names are explained in the list at the beginning of this work.

These results clearly demonstrate that young leaves were completely unaffected concerning stress and cell death responses. This leads to the conclusion that a certain developmental stage might be essential to acquire the competence to sense and/or respond to stress caused by the changed light-

dark regime. This assumption was further supported by the fact that the cell death phenotype was increasing with plant age indicating a gradual increase in leaf sensitivity and/or responsiveness. Seedlings did not exhibit necroses in response to CL, while three- or four-week-old plants displayed a distinct but still weak phenotype (data not shown). Five- to six-week-old plants which were used for all experiments in this study were most sensitive towards changes in light-dark regimes showing a remarkably reproducible and strong phenotype. An age-dependent cell death might suggest a process resembling senescence (Lim *et al.*, 2007). However, the cell death phenotype during senescence looks different being characterized by the chlorosis (yellowing) of leaves, which was not visible after CL. Besides, the *SAG12* gene, which is highly linked to senescence (Gan and Amasino, 1995), was not upregulated 16 hours after CL (Fig. 3.13G), although lesions were already visible and even though it was found to be strongly induced at a later stage of cell death progression (see Fig. 3.12C). Therefore, the data collectively point to an age-dependent cell death which is distinct from senescence but may depend on the acquisition of a similar competence stage.

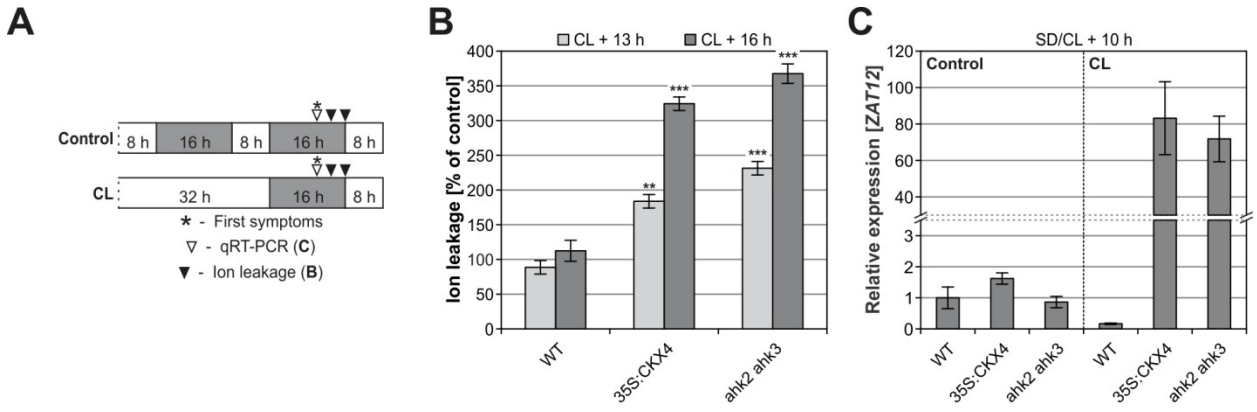

Figure 3.14: Cell death is established during the dark period following continuous light treatment.

A, Schematic overview of the experimental design. White, light period; gray, dark period. The light regime corresponds to the one described in Fig. 3.12. The time points for the respective measurements are indicated. First symptoms, leaves start to go limp. **B**, Ion leakage indicating loss of membrane integrity due to cell death progression at different time points following CL treatment. Conductivity values are expressed as per cent of control (set to 100 %) (n = 4). **C**, Transcript level of the oxidative stress marker gene *ZAT12* after 10 hours of dark period following CL treatment (n = 4). Expression levels are normalized to the wild-type control, which was set to 1. *CI51* and *PP2AA2* served as reference genes. Asterisks indicate significant differences compared with respective wild types (*t* test: **, $p < 0.01$; ***, $p < 0.001$). Error bars represent SE.

3.3.4 Cell death in cytokinin-deficient plants manifests itself during the dark period following the CL treatment

Since the cell death was already initiated in the morning following CL treatment (see Fig. 3.13) it was assumed that the cell death as well as the stress preceding and causing it already started during the 16-hour dark period directly following the CL treatment. In order to provide proof of this hypothesis ion leakage was recorded as a measure for cell death during (after 13 h) and at the end (after 16 h) of the night (Fig. 3.14A-B). An increase in ion leakage caused by a loss of membrane integrity was only measured in CL-treated cytokinin-deficient plants revealing already progressing cell death. This increase was already detectable after 13 hours of darkness indicating that the onset of cell death occurred indeed during the night. This implies that the stress acting as the "death signal" must have

started even earlier during the night. In fact, a pronounced stress response could already be detected after 10 hours of darkness reflected by strongly elevated *ZAT12* levels (Fig. 3.14C) coinciding with the first signs of limpness especially in *35S:CKX4* (see Fig. 3.14A, "First symptoms"). However, the reason for this pronounced stress response was not elucidated so far.

3.4 Light stress *versus* "circadian stress" – light-dark regimes provide insight

In the previous section it was shown that the oxidative stress response and the resulting cell death were already present during the dark period following CL treatment. Although it is evident that the changes in the light-dark regime somehow caused this stress response the precise trigger was not identified yet. In order to better understand cause and effect in this stress response plants were subjected to additional light-dark regimes.

3.4.1 The CL response is distinct from a light stress response

The most obvious explanation seemed to be that the prolonged light period caused a light stress response. This would imply that a stress response should be detectable directly after the CL treatment and might be even enhanced after further extension of light treatment. To test this hypothesis, plants were exposed to increasing periods of light and F_v/F_m ratios were determined after 32, 56, and 80 hours as well as after 5 and 8 days of light. None of the extended light treatments produced a stress response in wild-type or *35S:CKX4* and *ahk2 ahk3* plants as reflected by F_v/F_m values above 0.8 for all measurements (Fig. 3.15A). Only by interruption of the extended light periods with a 16-hour dark treatment after 32 or 56 hours of CL, respectively (Fig. 3.15B), cell death was initiated in plants with a reduced cytokinin status. In contrast, plants under prolonged CL remained completely unaffected (Fig. 3.15C). Even after four days of CL the cell death phenotype could be provoked by a 16-hour dark period (data not shown). Consequently, it seems that the precise duration of CL was rather secondary for the outcome. The amount of necrotic leaves was quite similar after 32 or 56 hours of CL (Fig. 3.15D) although the affected areas tended to be somewhat larger in cytokinin-deficient plants after 56 hours of CL as reflected by a stronger stress-induced decrease in F_v/F_m ratios (Fig. 3.15E).

Taken together, these results clearly demonstrate that the dark period succeeding the CL is decisive for the observed phenotype since CL alone was not sufficient to induce the stress response. This result clearly excludes the light stress hypothesis. On the other hand, one should consider that although the prolonged light treatment alone did not suffice to elicit stress within the plants, it still was crucial for the phenotype since a 16-hour SD night usually does not result in the initiation of cell death (see controls). Altogether, the data in Figure 3.15 rule out light stress *per se* and further support the idea that the overall disruption of the day-night rhythm caused the phenotype.

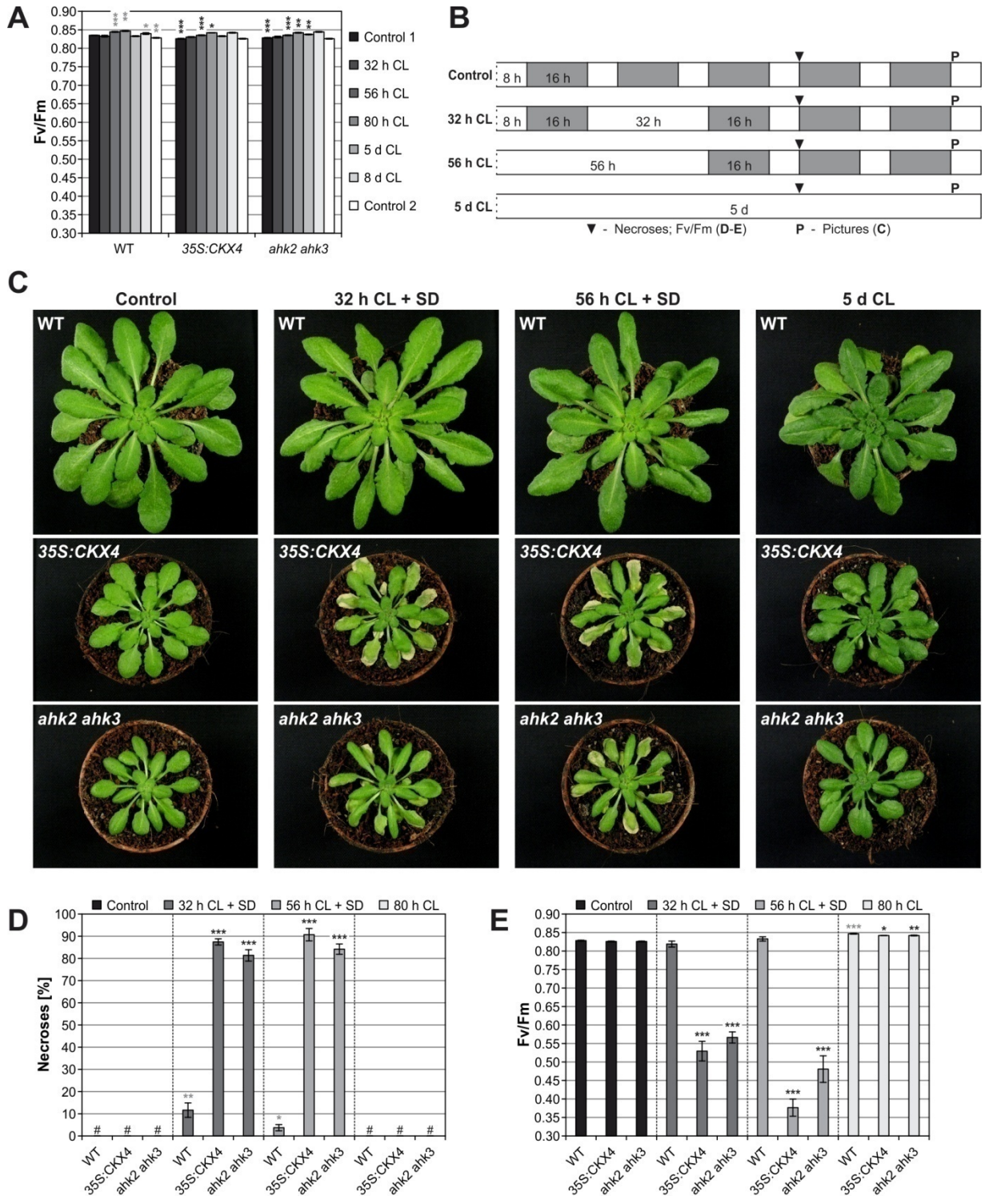

Figure 3.15: Continuous light alone is not sufficient to induce the cell death phenotype – a succeeding dark period is indispensable.

Figure 3.15 continued.

A, Five-week-old SD-adapted plants were either kept under SD conditions (controls) or subjected to prolonged CL treatments of different durations. To measure possible stress responses F_v/F_m ratios were determined at the time points designated in the legend (n = 12; Control 1, simultaneously with "32 h CL"; Control 2, simultaneously with "8 d CL"). **B**, Scheme representing the experimental setup for **C**-**E**. White, light period; gray, dark period. Prior to the experiment all plants were grown under SD rhythm for five weeks. In parallel to the SD controls, plants were subjected to a 32- or 56-hour CL treatment followed by SD rhythm or exposed to 5 days of CL. **C**, Representative phenotypes of all investigated genotypes after respective treatments. Pictures were taken at the time points indicated in (**B**). **D**-**E**, The percentage of necrotic leaves counted in all mature leaves (**D**; n = 10; #, not detected) and the stress-induced decrease in F_v/F_m ratios (**E**; n = 12) were determined at the time points indicated in (**B**). Asterisks indicate significant differences compared with the respective wild types (black) and with the corresponding control (gray, for wild type only) (*t* test: *, $p < 0.05$; **, $p < 0.01$; ***, $p < 0.001$). Error bars represent SE.

3.4.2 Cell death in cytokinin-deficient plants after CL treatment is dependent on a long dark period succeeding the extended light regime

Next, the question was asked whether a minimum duration of darkness following CL was required to induce the necrotic phenotype. Thus, SD-adapted plants were exposed to the standard CL treatment and subjected to different night lengths (2.5, 5, 7.5, 10 and 16 hours) afterwards (Fig. 3.16A). The results indicate that the critical night length is between 5 and 7.5 hours (Fig. 3.16B-C), because "2.5 h D" and "5 h D" plants remained completely healthy, while cell death could already be observed in cytokinin-deficient plants exposed to 7.5 hours of darkness. Interestingly, plants did not respond in an "all-or-none" manner. Rather, a gradual increase in the amount of necroses (Fig. 3.16B) and decrease in F_v/F_m (Fig. 3.16C) was discovered in response to increasing night lengths. Therefore, the most severe phenotype was observed after 16 hours of night. Accordingly, it seems that plants did not anticipate a long night as they could only cope with short nights. Nevertheless, it is astonishing that they were forced into cell death instead of simply re-acclimating to a normal SD night to which they were adapted before. Furthermore, it is notable that short nights did not fully reverse the phenotype. Cytokinin-deficient "2.5 h D" and "5 h D" plants also initiated cell death in response to a 16-hour dark period one day later while continued CL could prevent this (Fig. 3.16C-D). Even the rather weak phenotype of "7.5 h D" plants was transformed into a quite strong cell death phenotype (especially in *35S:CKX4* plants) after an extended dark treatment. Plants with a reduced cytokinin status tended to show a more severe response after a delayed long night ("2.5 h D/16 h D" and "5 h D/16 h D") compared with an immediate one ("16 h D"). This trend was even more pronounced in wild-type plants which exhibited a significant increase in the amount of necrotic leaves under these conditions (Fig. 3.16D). As stated above, cytokinin-deficient plants seemed to anticipate only short nights in response to CL. Obviously, CL treatment changed internal settings towards long days and/or short nights in these plants since they could not master long dark periods anymore regardless of their onset. Therefore, the response to CL appears to be a precisely regulated and apparently irreversible adaptive response. Moreover, the results again confirm the requirement of a long night for the cell death phenotype.

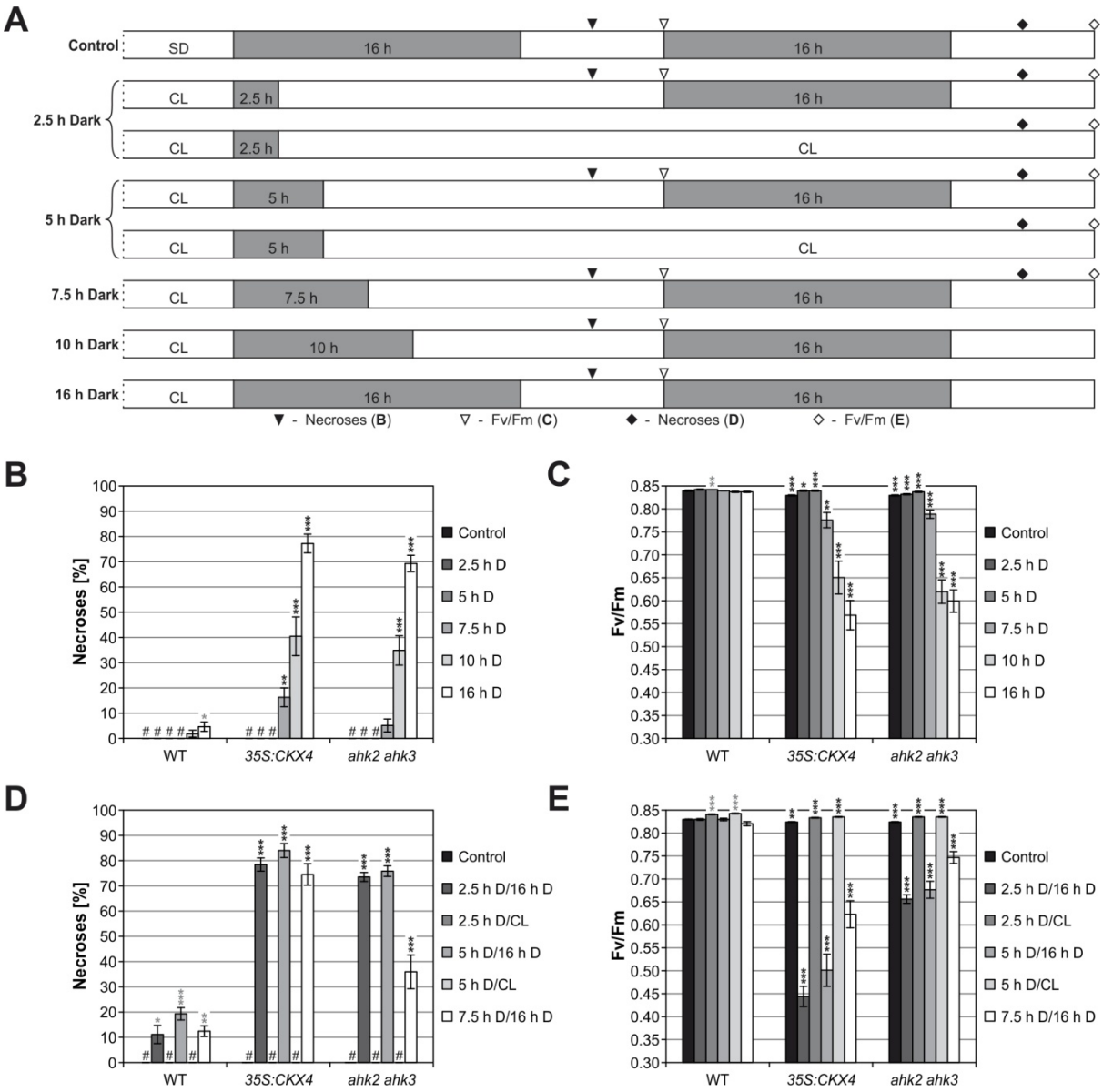

Figure 3.16: The duration of dark periods following continuous light is decisive for the severity of cell death.

A, Schematic overview about the design of the experiments shown in **B**-**E**. White, light period; gray, dark period. Prior to the experiment all plants were grown under SD conditions for five weeks. **B**-**C**, The percentage of necrotic leaves counted in all mature leaves (**B**; n = 10; #, not detected) and the stress-induced decrease in F_v/F_m ratios (**C**; n = 14) were determined after plants were subjected to different durations of dark periods (D) following 32 hours of CL (as indicated in **B**). **D**-**E**, Necroses and F_v/F_m ratios were determined as in **B** and **C**, respectively. In this case, the measurements were performed one day later after plants were additionally exposed to a 16-hour dark period or kept under CL. Asterisks indicate significant differences compared with the respective wild types (black) and with the corresponding control (gray, for wild type only) (*t* test: *, $p < 0.05$; **, $p < 0.01$; ***, $p < 0.001$). Error bars represent SE.

3.4.3 Prolonged dark periods alone are not sufficient to induce the cell death phenotype

Does an unexpectedly long night exceeding the 16-hour SD night equally cause cell death in cytokinin-deficient plants without prior CL treatment? To test this, SD nights were extended up to 48 hours (Fig. 3.17A). But this did not result in a cell death phenotype (Fig. 3.17B). After 24 hours of darkness no stress response was measured. Minor decreases in F_v/F_m ratios could be detected to a similar extent in all investigated genotypes after 48 hours of darkness (Fig. 3.17C). However, plants had almost fully

recovered two days after the prolonged dark treatment ("48 h D + L"). Taken together, long nights trigger cell death in plants with a reduced cytokinin status only when following a prolonged light period but are rather effectless without preceding CL treatment.

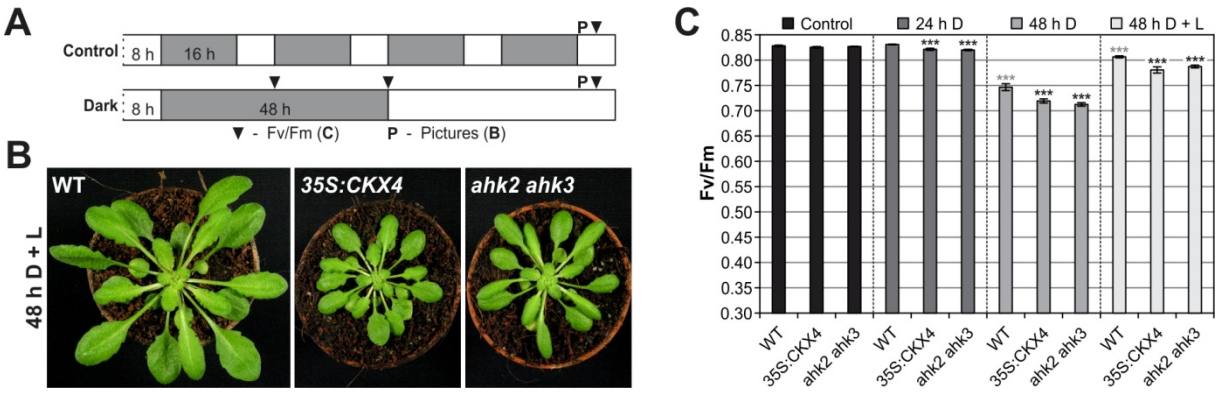

Figure 3.17: Prolonged dark periods without prior continuous light treatment do not cause the cell death phenotype.

A, The scheme represents the experimental setup for **B**-**C**. White, light period; gray, dark period. **B**, Absence of necroses in leaves of all genotypes in response to prolonged dark treatment. **C**, Chlorophyll fluorescence ratio F_v/F_m after prolonged dark periods (D) and after relaxation (L, light) from 48 hours of darkness (n = 12). Plants were five weeks old and continuously grown under SD conditions before the experiment started. Asterisks indicate significant differences compared with the respective wild types (black) and with the corresponding control (gray, for wild type only) (*t* test: ***, $p < 0.001$). Error bars represent SE.

3.4.4 Cell death is unlikely caused by a limited carbohydrate availability

Since the CL-dependent cell death is initiated during a long night period the idea arose that the phenotype might be caused by carbon starvation. It is already known that the rate of nocturnal starch degradation is regulated by the circadian clock (Graf *et al.*, 2010). Hence, a misregulated utilization of starch due to the disrupted day-night-rhythm might cause a decrease in carbohydrate availability in the second half of the night. This possibility was examined by quantification of the starch content directly after the CL treatment and at the end of the following dark period. These data were compared with the contents in controls after a SD light and dark period, respectively (Fig. 3.18A). After CL treatment the starch content was considerably increased by about 5- to 6-fold in all investigated genotypes, presumably resulting from the prolongation of photosynthetic carbon fixation (Fig. 3.18B). While control plants reached quite low levels of starch at the end of the SD night CL-treated plants only utilized about half of the accumulated starch during the night period and thus still exhibited high carbon availability. The rate of starch degradation/utilization was even accelerated in CL-treated plants since they used about double as much starch compared with the control plants during nighttime. These data show that a lack of carbohydrate availability was very unlikely the cause for the necrotic phenotype after CL.

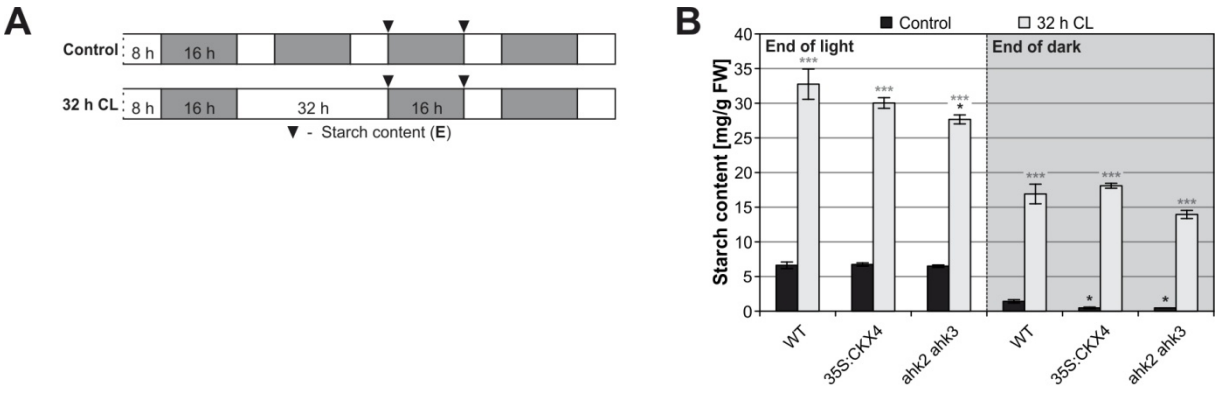

Figure 3.18: Cell death is unlikely caused by a limited carbohydrate availability during the long night following the continuous light regime.

A, The scheme indicates the light regime and the time points at which samples for starch measurements were collected. White, light period; gray, dark period. **B**, Starch content at the end of light and dark periods during a SD (controls) and a 32-hour CL regime followed by a 16-hour night (n = 5 [*35S:CKX4*, *ahk2 ahk3*]; n = 6 [WT]). Plants were five weeks old and continuously grown under SD conditions before the experiment started. Asterisks indicate significant differences compared with the respective wild types (black) and with the corresponding controls (gray) (*t* test: *, $p < 0.05$; ***, $p < 0.001$). Error bars represent SE.

3.4.5 A substantial prolongation of the light period is essential for the cell death response

Next, plants were subjected to different "CL" periods from 12 to 32 hours always succeeded by a 16-hour dark period (Fig. 3.19A). These regimes enabled to identify a critical length of CL required for the induction of cell death. Furthermore, they provided a possibility to study the potential impact of the phase/subjective time at the end of the different CL periods. In addition, they could provide an indication whether a gradual decrease in clock performance/precision during prolonged free-running (constant) conditions might be decisive for the phenotype. If so, longer CL treatments should be more detrimental. This hypothesis was excluded right away due to the fact that all cytokinin-deficient plants subjected to 16 hours of CL or more exhibited a similar necrotic phenotype (Fig. 3.19B). This is in accordance with the results already shown in Figure 3.6 ("16 h L/16 h D" *versus* "32 h L/16 h D") and also in line with the outcome after 32 and 56 h CL, respectively, which represented no compelling difference (see Fig. 3.15B-E). Additionally, these data rule out a primary influence of the T-cycle length (see 1.3.1) and also exclude a strong impact of the subjective time at the end of the light treatment. Interestingly, the 12-hour CL regime caused an intermediate cell death phenotype in plants with a reduced cytokinin status. This indicates that the critical length was already reached although a further extension of light seemed to be required for a more pronounced phenotype. Nevertheless, it was intriguing to observe again (see also Fig. 3.6) that already such small alterations and shifts in the day-night rhythm resulted in detectable necroses (Fig. 3.19C) and significant decreases in F_v/F_m (Fig. 3.19D) in cytokinin-deficient plants.

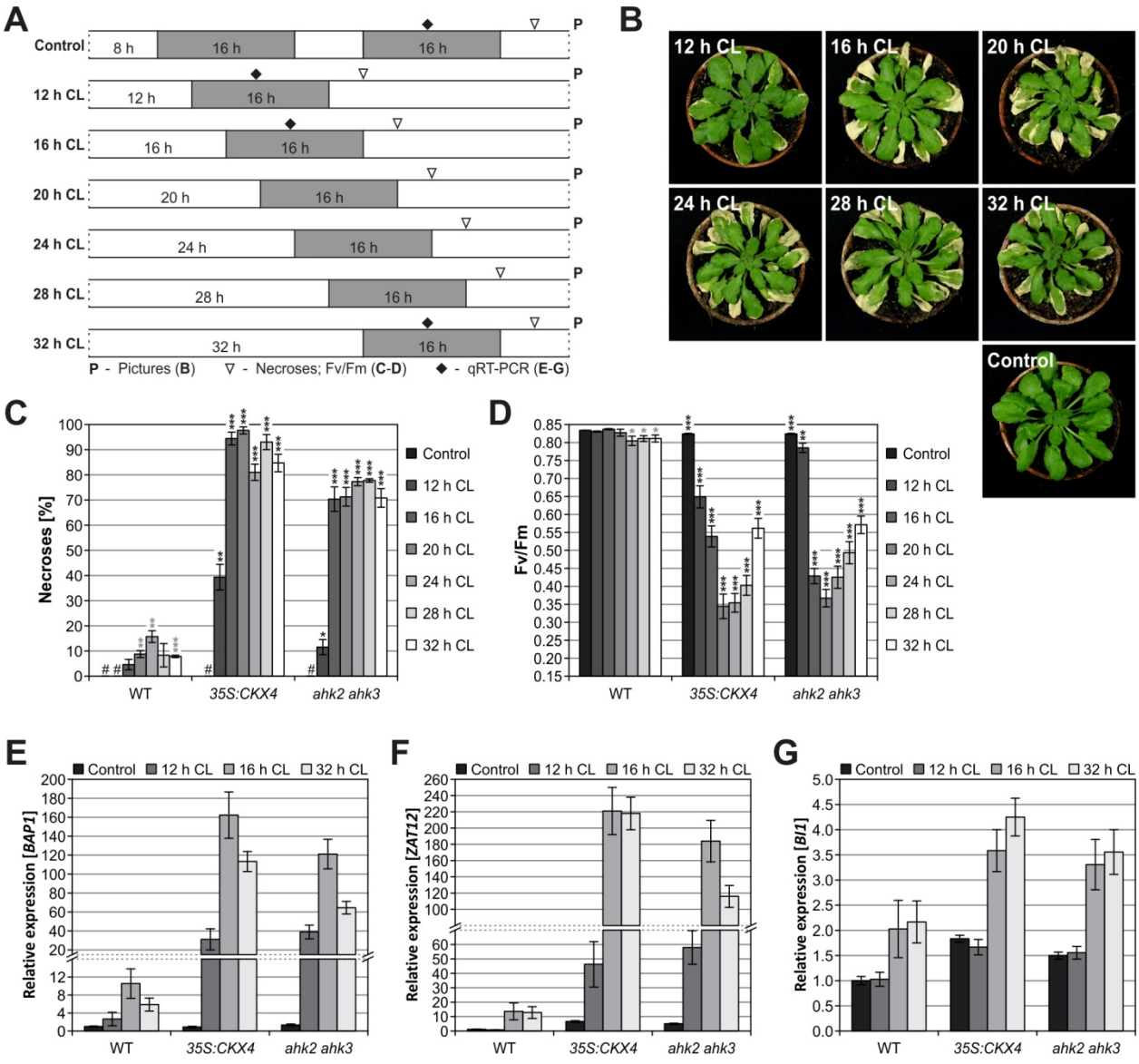

Figure 3.19: The cell death phenotype, in conjunction with the molecular stress response, is triggered by a substantial extension of the light period.

A, Schematic representation of experimental setups in **B**-**G**. White, light period; gray, dark period. Six-week-old SD-adapted plants were either kept under SD conditions (controls) or subjected to prolonged CL treatments of different durations followed by a 16-hour dark period. **B**, Images show *35S:CKX4* transgenic plants exemplary for the phenotypes observed in plants with a reduced cytokinin status after different durations of CL. Pictures were taken one day after the graphically designated regimes as indicated by the dotted lines in (**A**). **C**-**D**, The percentage of necrotic leaves counted in all mature leaves (**C**; n = 5; #, not detected) and the stress-induced decrease in F_v/F_m ratios (**D**; n = 12) were determined 20 hours (including a 16-hour dark period) after exposure to different durations of CL as indicated in (**A**). **E**-**G**, Transcript levels of the oxidative stress marker genes *BAP1* (**E**) and *ZAT12* (**F**) and the cell death marker gene *BI1* (**G**) after 7.5 hours of darkness during a normal SD (control) or following different CL durations (12, 16, and 32 hours) (n = 4). Expression levels are normalized to the respective wild-type control, which was set to 1. *PP2AA2* and *MCP2D* served as reference genes. Asterisks indicate significant differences compared with the respective wild types (black) and with the corresponding control (gray, for wild type only) (*t* test: *, $p < 0.05$; **, $p < 0.01$; ***, $p < 0.001$). Error bars represent SE. Abbreviations of gene names are explained in the list at the beginning of this work.

In the following, the question was asked if the intermediate phenotype in response to the 12-hour CL regime would also be reflected on the molecular level. For that purpose, a qRT-PCR analysis was performed on "12 h CL" samples and compared with "16 h CL" and "32 h CL" samples (sampling point

is indicated in Fig. 3.19A). The induction of oxidative stress and cell death marker genes (*BAP1*/*ZAT12*, and *BI1*, respectively) served as molecular indicators for a stress and cell death phenotype (Fig. 3.19E-G). As expected, oxidative stress marker genes were induced to an intermediate level in "12 h CL" plants with a reduced cytokinin status while much higher levels were reached after longer periods of CL (Fig. 3.19E-F), which is in line with the visible differences between cell death phenotypes. However, after "12 h CL" the *BI1* expression in cytokinin-deficient plants was not elevated above control levels, corresponding with the small and rather few lesions in these plants (Fig. 3.19G). Wild-type plants showed a very mild form of cell death after longer CL periods (Fig. 3.19C) which was similarly reflected on the molecular level in "16 h CL" and "32 h CL" samples.

Collectively, the results described so far clearly demonstrate that the exposure to aberrant light-dark regimes was the fundamental problem for plants with a reduced cytokinin status and not merely prolonged light or dark periods. Thus, an involvement of the circadian clock seemed obvious. Since it is the timekeeper which synchronizes internal cues with the external environment a desynchronization of the clock might have caused the stress response.

3.4.6 Temperature cycles partially substitute for the lacking light-dark cycle during CL

So far, plants were only subjected to altered light-dark regimes. In the next experiment the influence of temperature was tested in addition. Since temperature is also an important entrainment factor serving as input signal for the circadian clock (McWatters *et al.*, 2000; Michael *et al.*, 2003b; Mizuno *et al.*, 2014; see 1.3.6.2) it was hypothesized that temperature cycles might partially or fully substitute for the lacking light-dark cycle during CL. Therefore, plants were exposed to two kinds of CL treatments (Fig. 3.20A), one at a constant temperature (22 °C) as before and the other including a temperature cycle characterized by decreased temperature at subjective night (22/10/22 °C). Indeed, the temperature regime could at least in part mimic the missing light-dark cycle since the CL-dependent phenotype in cytokinin-deficient plants could be strongly reversed (Fig. 3.20B), although duration and intensity of CL were unchanged. The percentage of necrotic leaves was dramatically reduced (Fig. 3.20C) and the F_v/F_m ratios decreased only slightly in response to temperature cycles (Fig. 3.20D), especially in *ahk2 ahk3* plants which almost behaved like wild type. These findings strongly support the idea that a desynchronization of the circadian clock in plants with a reduced cytokinin status might have caused the profound stress response upon changed light-dark regimes.

3.4.7 Entrainment conditions determine the severity of cell death after CL treatment

The fact that conditions preceding the CL treatment were decisive for the outcome provided a further indication for a connection to the circadian clock. Entrainment to SD and LD photoperiods prior to CL treatment as well as entrainment to permanent CL prior to a 16-hour dark period led to strikingly different results (for experimental design see Fig. 3.21A). Compared with the standard CL regime where plants were entrained to SD conditions ("SD/CL/SD", Fig. 3.21B-C), LD-adapted cytokinin-deficient plants ("LD/CL/SD") displayed an alleviated cell death phenotype as reflected by less necroses and a smaller reduction of F_v/F_m ratios (Fig. 3.21D-E). Interestingly, the transfer of LD-grown

plants to SD conditions ("LD/SD") led to a very weak phenotype which was marked by only a few necrotic leaves. The opposite regime induced a somewhat stronger effect (see Fig. 3.6, "16 h L/8 h D"). Plants with a reduced cytokinin status did not exhibit a pronounced phenotype after entrainment to CL irrespective of the onset of the "unexpected" dark period (Fig. 3.21F-G). On the contrary, wild-type plants were significantly (but rather weakly) affected in this experimental setup. The fact that entrainment to CL prevents a pronounced cell death phenotype in cytokinin-deficient plants demonstrates that the synchronization/adaptation to light-dark cycles (SD > LD) prior to CL is crucial for the outcome. Moreover, the different entrainments revealed that the phenotype inversely correlated with the length of light periods prior to CL and/or the 16-hour night.

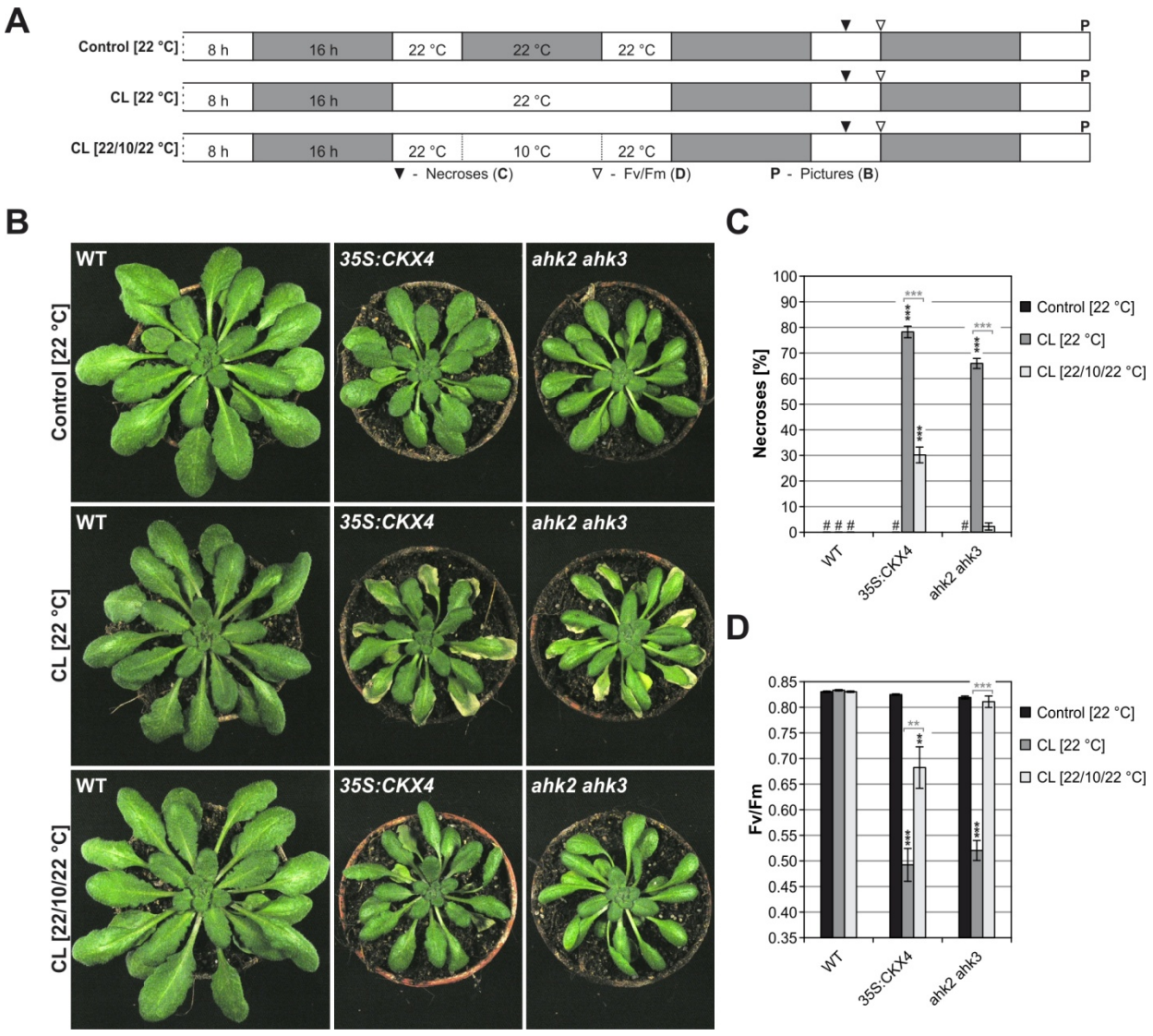

Figure 3.20: Temperature cycles partially substitute for the lacking light-dark cycle during continuous light.

A, The scheme illustrates the light-dark and temperature cycles six-week-old SD-adapted plants were exposed to. White, light period; gray, dark period. Plants were constantly grown at 22 °C before the treatments. **B**, Representative phenotypes observed after different light-dark and/or temperature cycles indicated in (**A**). Pictures were taken two days after CL treatment. **C**-**D**, The percentage of necrotic leaves counted in all mature leaves (**C**; n = 10; #, not detected) and the stress-induced decrease in F_v/F_m ratios (**D**; n = 12). Asterisks indicate significant differences compared with respective wild types (black) and between the two CL treatments (gray) (*t* test: **, $p < 0.01$; ***, $p < 0.001$). Error bars represent SE.

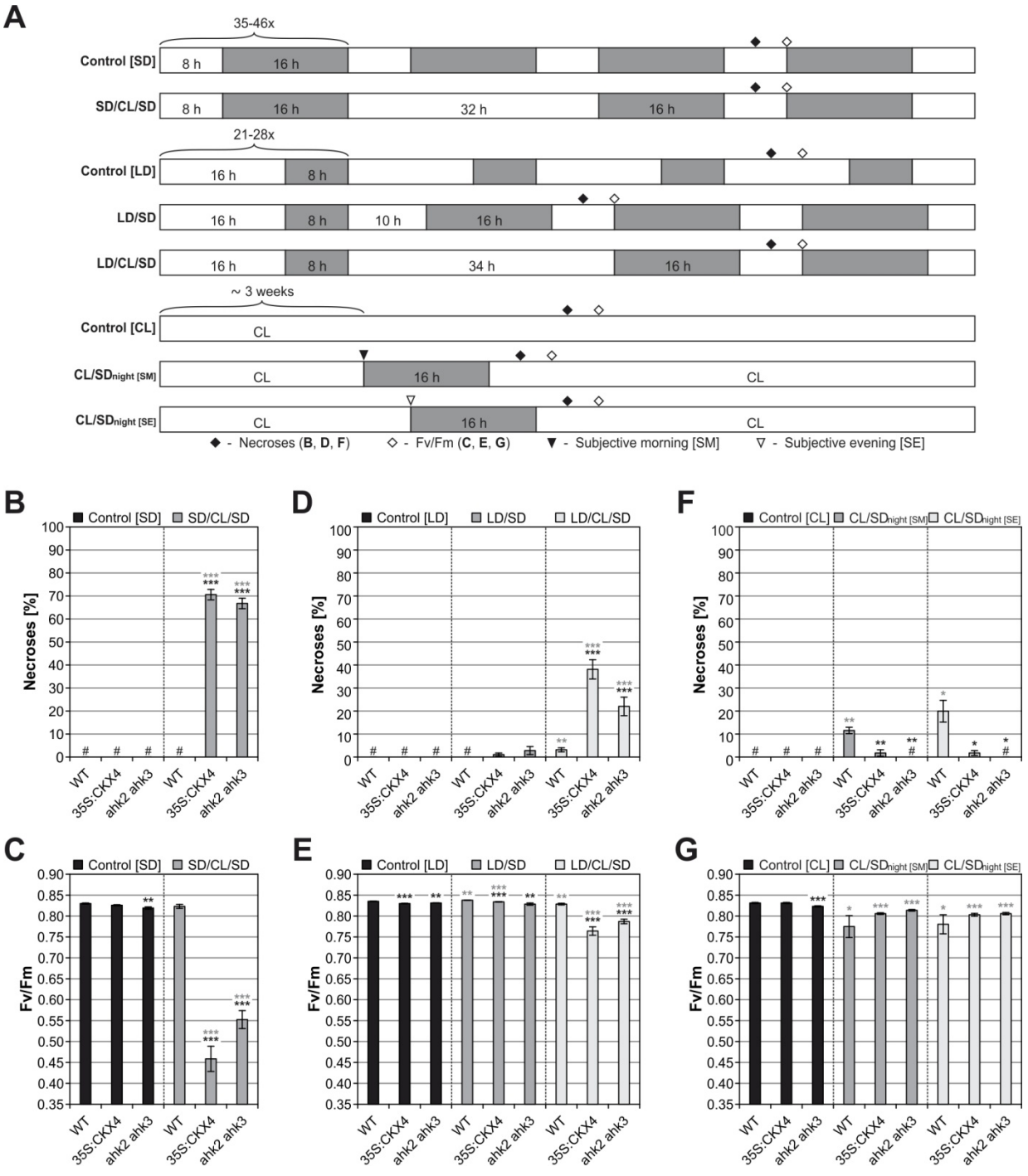

Figure 3.21: The entrainment prior to continuous light is a determining factor for the severity of cell death.

A, Schematic representation of the experimental design in **B**-**G**. White, light period; gray, dark period. Plants were entrained to SD, LD or CL conditions. The duration of each entrainment prior to the respective treatment is indicated. SD- and LD-adapted plants were subjected to CL followed by SD conditions. Additionally, LD-grown plants were directly transferred to the SD rhythm. CL-adapted plants were exposed once to a 16-hour night starting at different times of the subjective day; at the subjective morning (SM) or evening (SE). **B**-**G**, Analysis of the response to altered light-dark regimes after different entraining conditions. The percentage of necrotic leaves counted in all mature leaves (**B**, **D**, **F**; #, not detected) and the stress-induced decrease in F_v/F_m ratios (**C**, **E**, **G**) were recorded. Consequences of SD (**B**, n = 12; **C**, n = 10), LD (**D**, n = 15; **E**, n = 10), and CL entrainment (**F**, n = 20; **G**, n = 7) are shown. Asterisks indicate significant differences compared with the respective wild types (black) and with the corresponding controls (gray) (*t* test: *, $p < 0.05$; **, $p < 0.01$; ***, $p < 0.001$). Error bars represent SE.

Altogether, the results described in this chapter show that the severity of cell death in cytokinin-deficient plants is determined by the interplay of entrainment, treatment and post-treatment regime, which is summarized in a scheme (Fig. 3.22). Only if each of the three elements contributes in a cell-death-promoting way (marked in green) cell death is induced. This implies a rather complex circuitry of events necessary for cell death initiation. The factors that modulate the cell death phenotype (light, dark, and temperature) have in common that they feed input information about the time of day into the circadian clock (see 1.3.6). The duration of each factor and their sequential combination is decisive for the outcome which gives compelling evidence that the circadian clock is involved in this response. Therefore, the data argue for a substantial modulation or even disturbance of internal timekeeping caused by a changed light-dark regime. In conclusion, this points to a previously unknown phenomenon coined here "circadian stress".

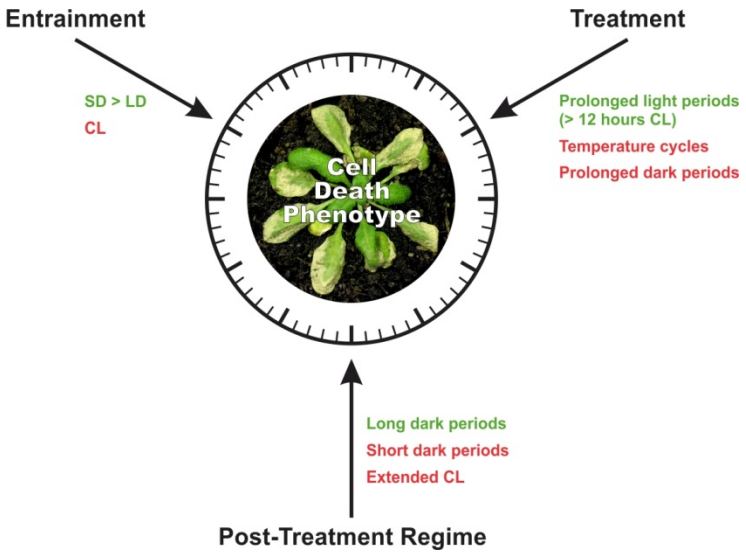

Figure 3.22: The cell death phenotype in plants with a reduced cytokinin status is modulated by the interplay of three different factors – entrainment, treatment, and post-treatment regime.

The picture in the center represents the cell death phenotype in plants with a reduced cytokinin status after CL treatment (*ipt3,5,7* is displayed). The severity of that phenotype is influenced by the entraining conditions, the treatment itself, and the post-treatment regime; marked by arrows. Positive (green) or non-inducing/diminishing (red) factors for the development of cell death are summarized adjacent to the respective arrows. Each of the conditions highlighted in green is not sufficient alone but the sequential combination of them necessary for the induction of the cell death phenotype. The schematic image of the clock implies the suggested hypothesis that all of the listed factors are also input signals for the circadian clock, thereby either modulating or even disturbing its action. Thus, a disrupted resonance with the environment due to a disrupted circadian clock might cause the stress response arguing for a previously unknown phenomenon called "circadian stress".

3.5 Analysis of circadian clock and clock output gene expression after CL treatment

3.5.1 Expression profiles of oxidative stress and cell death marker genes following the CL regime

In order to further prove the "circadian stress" hypothesis, changes in transcriptional expression patterns of central oscillator genes and circadian clock output genes had to be examined. To be able to evaluate a possible connection between a desynchronized circadian clock and the stress response,

kinetics of oxidative stress and cell death marker gene expression in response to "circadian stress" was assessed first.

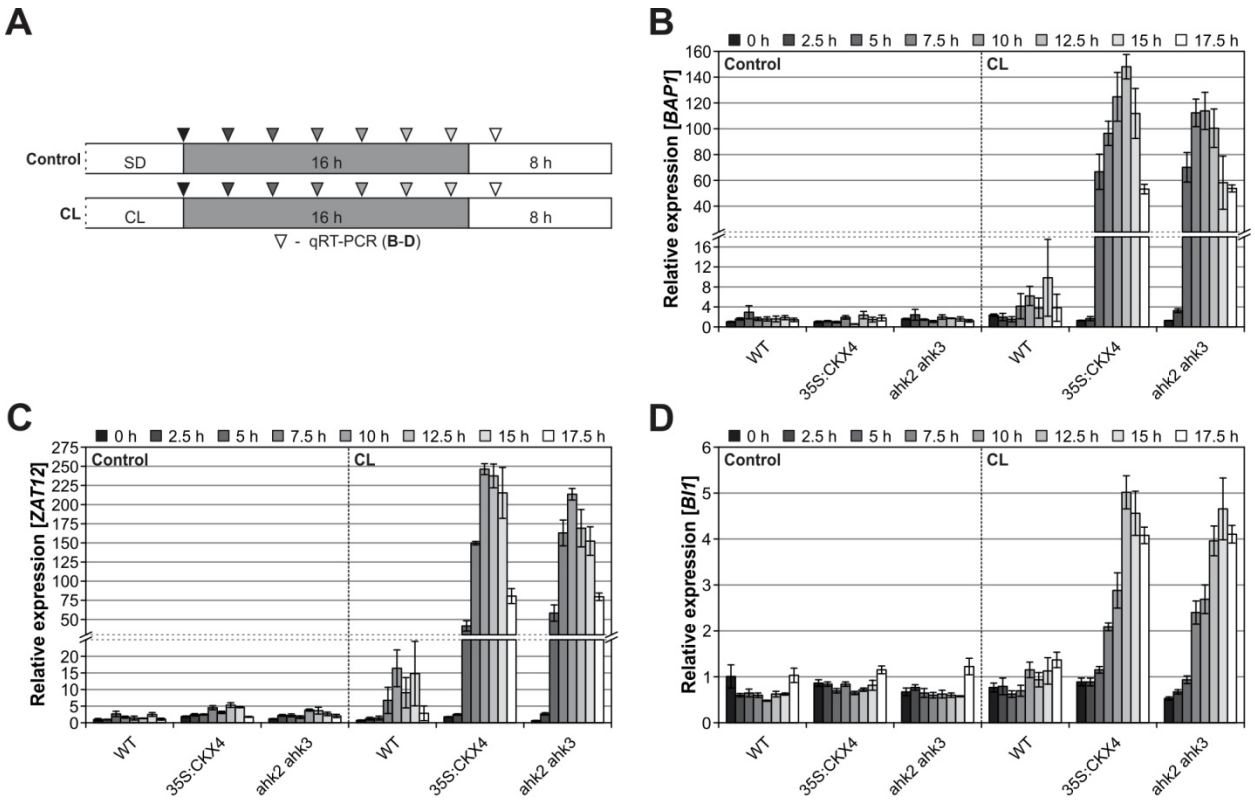

Figure 3.23: Oxidative stress marker genes *BAP1* and *ZAT12* and cell death marker gene *BI1* are strongly induced in cytokinin-deficient plants during the dark period following continuous light treatment.

A, The scheme represents the experimental setup in **B**-**D**. White, light period; gray, dark period. Plants were grown under SD conditions for six weeks. Control plants remained in the SD rhythm while a subset of plants was subjected to 32 hours of CL. Leaf samples were collected in a 2.5-hour time interval starting directly after a normal SD light period or CL (0 h) and ending 17.5 hours later. Kinetics of gene expression were analyzed *via* qRT-PCR. Transcript levels of oxidative stress marker genes *BAP1* and *ZAT12* (**B**-**C**) and cell death marker gene *BI1* (**D**) were determined. Data represent the mean and SE values of four biological replicates and are expressed as relative values compared with the respective wild-type control (0 h), which was set to 1. *PP2AA2* and *MCP2D* served as reference genes.

For that purpose, leaf samples were harvested during the night following CL treatment in a 2.5-hour time interval starting directly at the end of the CL regime. The transcriptional expression patterns after CL treatment were analyzed by qRT-PCR and compared with the kinetics during a normal SD night (Fig. 3.23A). The results clearly show that a very strong stress response was induced in *35S:CKX4* and *ahk2 ahk3* plants during the night after CL treatment as reflected by strongly elevated *BAP1* and *ZAT12* transcript levels (Fig. 3.23B-C). This acute stress response was initiated after "5 h" of darkness and was not present in control plants. CL-treated wild-type plants displayed a small stress response which was characterized by a slight increase in *BAP1* and *ZAT12* expression levels starting after "7.5 h" of darkness. This indicates that the wild type also encountered stress due to changes in the day-night rhythm albeit to a limited extent, which is in line with the weak necrotic phenotype observed in several experiments (see 3.4). Even under control conditions cytokinin-deficient plants tended to express more *ZAT12* compared with wild-type plants, which is consistent with previous results (see Figs. 3.12B;

3.13D; 3.19F). Interestingly, the expression patterns in CL-treated cytokinin-deficient plants are reminiscent of an oscillation wave for both genes although peak levels were reached at different time points. The expression kinetics of the cell death marker gene *BI1* revealed an elevated expression exclusively in CL-treated *35S:CKX4* and *ahk2 ahk3* plants conform to their cell death phenotype (Fig. 3.23D). The (molecular) cell death response was somewhat delayed compared with the stress response hallmarked by induced stress marker genes. More precisely, differential expression of *BI1* started one time point later after "7.5 h". This indicates that the initiation of cell death was the consequence of the preceding stress. Moreover, it could be confirmed that cell death was induced during the night following CL treatment, which is in accordance with the conclusions drawn from Figure 3.14. In addition, the expression of oxidative stress marker genes was not elevated directly after CL giving further evidence that a light stress response can be ruled out.

3.5.2 Perturbation of CCA1/LHY gene expression patterns in response to CL treatment

If a desynchronization between internal and external cues due to a disturbed circadian oscillator was responsible for the stress response, a CL-dependent alteration in oscillator gene expression would be expected. Therefore, core genes of the circadian clock were analyzed (see 1.3.5). The transcript abundance of *CCA1* and *LHY* was comparable between the genotypes under control (SD) conditions (Fig. 3.24A-B). Their expression kinetics was characterized by low transcript levels at the end of the SD light period ("0 h") and the beginning of the dark phase ("2.5 h" to "7.5 h"), respectively. Around midnight both *CCA1* and *LHY* levels started to increase reaching their expression peak close to dawn (at "15 h") in anticipation of the next morning. The peak-to-trough ratios within the selected SD period were equally high in all investigated genotypes (≥ 2000) reflecting robust oscillations.

In contrast, CL treatment caused dampened *CCA1* and *LHY* oscillations in wild-type and even more pronounced in cytokinin-deficient plants. While reduced peak-to-trough ratios of ~40 were recorded in wild type, these ratios were even lower in *35S:CKX4* (11 [*CCA1*]; 6 [*LHY*]) and *ahk2 ahk3* (25 [*CCA1*]; 12 [*LHY*]) reflecting strongly impaired oscillations. One reason for the reduced amplitudes was the incidence of abnormally high expression levels at subjective dusk ("0 h") and during the early night ("2.5 h" to "7.5 h") in all genotypes after CL. On the one hand, this might reflect a light response of the light-regulated transcription factor genes *CCA1* and *LHY* caused by the prolonged light treatment (see 1.3.6.1). On the other hand, this might as well reflect a decreased precision in clock performance caused by the free run (CL) conditions which reduced the capability to properly anticipate dusk. Another reason for the overall decrease in amplitudes was the alleviated increase in *CCA1* and *LHY* expression during the second half of the night. CL-treated wild-type plants displayed an advanced (at "12.5 h" instead of "15 h") and reduced morning peak. The reduction of maximum expression in wild type was reflected by a peak-to-peak ratio of ~2 between control and CL conditions for both genes. This effect was dramatically enhanced in *35S:CKX4* (7 [*CCA1*]; 14 [*LHY*]) and *ahk2 ahk3* (7 [*CCA1*]; 10 [*LHY*]) plants. They even completely failed to generate distinct morning peaks revealing an insufficient anticipation of dawn in these plants.

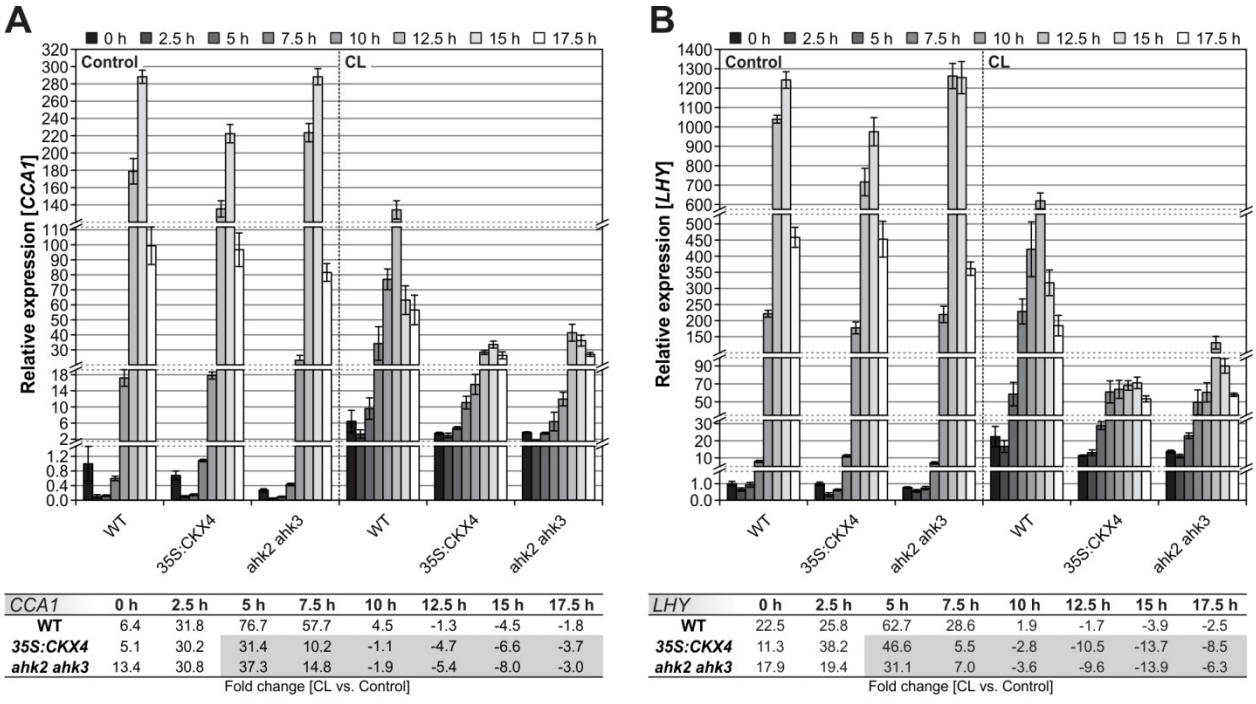

CCA1	0 h	2.5 h	5 h	7.5 h	10 h	12.5 h	15 h	17.5 h
WT	6.4	31.8	76.7	57.7	4.5	-1.3	-4.5	-1.8
35S:CKX4	5.1	30.2	31.4	10.2	-1.1	-4.7	-6.6	-3.7
ahk2 ahk3	13.4	30.8	37.3	14.8	-1.9	-5.4	-8.0	-3.0

Fold change [CL vs. Control]

LHY	0 h	2.5 h	5 h	7.5 h	10 h	12.5 h	15 h	17.5 h
WT	22.5	25.8	62.7	28.6	1.9	-1.7	-3.9	-2.5
35S:CKX4	11.3	38.2	46.6	5.5	-2.8	-10.5	-13.7	-8.5
ahk2 ahk3	17.9	19.4	31.1	7.0	-3.6	-9.6	-13.9	-6.3

Fold change [CL vs. Control]

TOC1	0 h	2.5 h	5 h	7.5 h	10 h	12.5 h	15 h	17.5 h
WT	-1.8	-1.4	1.1	-1.6	-4.2	-2.1	3.1	3.4
35S:CKX4	-1.2	-1.2	-1.2	-1.1	-1.3	3.0	6.7	4.7
ahk2 ahk3	-1.2	-1.3	-1.6	-1.1	-1.4	1.8	5.2	3.2

Fold change [CL vs. Control]

CHE	0 h	2.5 h	5 h	7.5 h	10 h	12.5 h	15 h	17.5 h
WT	1.4	-1.5	1.3	-1.5	-1.4	1.0	1.3	1.2
35S:CKX4	1.3	-1.2	-1.6	-1.4	-9.4	-15.9	-74.5	-450.8
ahk2 ahk3	1.7	-1.1	-1.6	-6.1	-6.0	-7.3	-81.3	-102.5

Fold change [CL vs. Control]

Figure 3.24: Kinetics of circadian clock gene expression during the dark period following continuous light treatment.

A-**D**, Kinetics of transcript abundances for the morning-expressed genes *CCA1* and *LHY* (**A**-**B**), the evening-expressed gene *TOC1* (**C**), and the oscillator gene *CHE* (**D**) in a 2.5-hour time interval starting directly after SD or CL (0 h) and ending 17.5 hours later. The experimental setup corresponds to the one explained in Fig. 3.23 (for a schematic overview see Fig. 3.23A). Data in graphs represent the mean and SE values of four biological replicates and are expressed as relative values compared with the respective wild-type control (0 h), which was set to 1. *PP2AA2* and *MCP2D* served as reference genes. To facilitate the evaluation of CL-dependent changes in relative expression levels between the genotypes tables have been inserted below each panel displaying the respective fold changes [CL *versus* corresponding control]. Highlighted in gray, most prominent CL-induced divergences in cytokinin-deficient plants compared with the wild type.

It is notable that the divergence of *CCA1*/*LHY* expression between wild-type and cytokinin-deficient plants after CL treatment started already after "5 h" of darkness coinciding with the upregulation of

stress marker genes (see Fig. 3.23B-C). The expression in wild type was already about 2-fold higher at that time point and increased stronger during the following 7.5 hours compared with the cytokinin-deficient plants. This divergence, starting at "5 h", is also reflected by the fold changes displayed in the tables inserted into Fig. 3.24A-B.

Taken together, the expression data of the central oscillator genes *CCA1* and *LHY* give compelling evidence that the changed light-dark regime negatively affects oscillations within the core of the circadian clock. Therefore, it can be concluded that "circadian stress" is a suitable term to describe the plant response after CL. Furthermore, plants with a reduced cytokinin status exhibited an even more pronounced circadian stress phenotype than wild-type plants. This phenotype was characterized by a strongly diminished increase in *CCA1* and *LHY* expression levels coinciding with the activated stress response. Thus, the cell death phenotype and the preceding stress response in cytokinin-deficient plants appear to be closely linked to a disrupted oscillator gene expression.

3.5.3 CL treatment results in disturbed TOC1 and CHE expression profiles

Next, the evening-expressed gene *TOC1*, which is also a core oscillator component of the *Arabidopsis* clock (see 1.3.5.3), was analyzed (Fig. 3.24C). Its expression is usually repressed by the morning-phased gene products CCA1 and LHY (Alabadí *et al.*, 2001). The results clearly demonstrate this relationship. As the levels of *CCA1* and *LHY* rose during the course of the night in the controls, *TOC1* levels fell. In accordance with the reduced increase in *CCA1* and *LHY* expression after CL treatment, *TOC1* repression was alleviated. This led to higher *TOC1* levels in CL-treated cytokinin-deficient plants in the second half of the night (see corresponding table in Fig. 3.24C). Subsequently, the oscillator gene *CHE* (see 1.3.5.6), which is also involved in the central circadian loop, was examined (Fig. 3.24D). While the expression profiles of controls and CL-treated wild type were largely similar, the expression pattern was extremely different in CL-treated plants with a reduced cytokinin status. *CHE* levels drastically decreased by more than 100-fold (see table in Fig. 3.24D).

Together, the results in Figure 3.24 show extensive changes in oscillator gene expression after CL treatment. The changes were more severe in cytokinin-deficient plants reflecting stronger circadian stress. Due to the coincidence between the onset of the (molecular) stress response and the highly attenuated morning-gene expression in plants with a reduced cytokinin status, a predominant role of CCA1 and LHY may be suggested.

3.5.4 Disruption of circadian output rhythms in cytokinin-deficient plants after CL treatment

A desynchronization between endogenous and external rhythms has been shown in the previous sections. But how should this be responsible for the detected stress response? A requirement would be that the circadian oscillator was sufficiently disrupted to produce impaired output signals. To test this, the expression patterns of the genes *CAB2* (Fig. 3.25A), *CAT2* (Fig. 3.25B), and *FER1* (Fig. 3.25C) were determined because they are well-known to be regulated by the circadian clock and, hence, can

be used to examine clock performance (Millar and Kay, 1991; Zhong and McClung, 1996; Duc *et al.*, 2009; Hong *et al.*, 2013b).

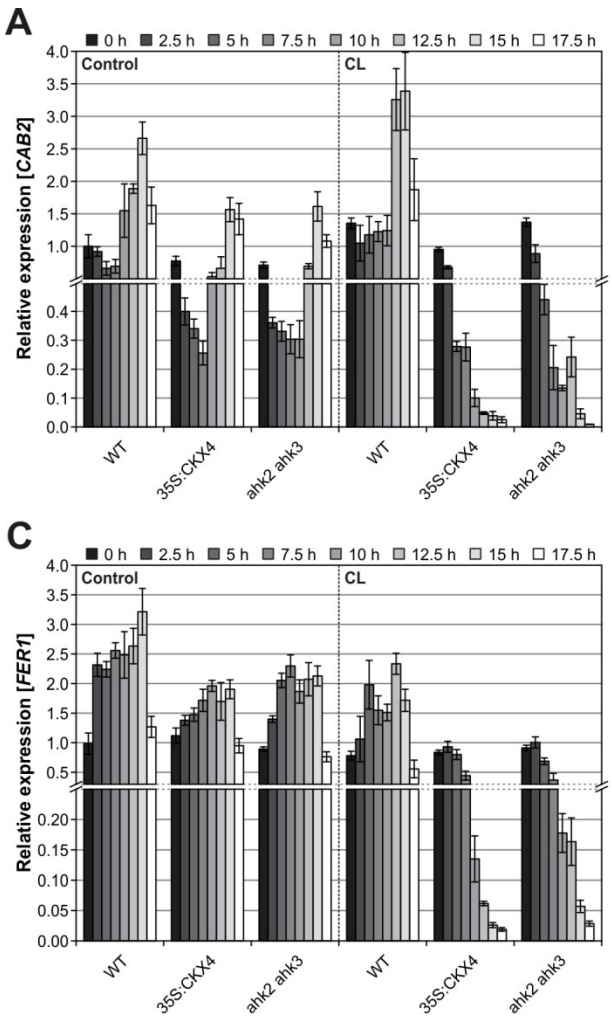

D

CAB2	0 h	2.5 h	5 h	7.5 h	10 h	12.5 h	15 h	17.5 h
WT	1.3	1.2	1.8	1.8	-1.3	1.7	1.3	1.1
35S:CKX4	1.2	1.7	-1.2	1.1	-5.3	-13.9	-39.2	-54.6
ahk2 ahk3	1.9	2.5	1.3	-1.5	-2.3	-2.9	-35.7	-116.7

CAT2	0 h	2.5 h	5 h	7.5 h	10 h	12.5 h	15 h	17.5 h
WT	1.9	1.1	1.7	2.0	-1.5	-1.4	-2.6	-2.7
35S:CKX4	2.6	2.2	1.8	-1.4	-6.4	-15.5	-23.0	-46.5
ahk2 ahk3	2.7	1.4	-1.2	-2.5	-6.1	-16.3	-47.1	-50.5

FER1	0 h	2.5 h	5 h	7.5 h	10 h	12.5 h	15 h	17.5 h
WT	-1.3	-2.2	-1.1	-1.7	-1.6	-1.1	-1.9	-2.3
35S:CKX4	-1.3	-1.5	-1.9	-3.9	-14.6	-27.5	-74.0	-49.1
ahk2 ahk3	1.0	-1.4	-3.0	-6.1	-10.6	-12.7	-37.6	-26.3

Fold change [CL vs. Control]

Figure 3.25: Kinetics of circadian clock output gene expression during the dark period following continuous light treatment.

A-**C**, Kinetics of transcript abundances for the clock-regulated genes *CAB2* (**A**), *CAT2* (**B**), and *FER1* (**C**) in a 2.5-hour time interval starting directly after SD or CL (0 h) and ending 17.5 hours later. The experimental setup corresponds to the one explained in Fig. 3.23 (for a schematic overview see Fig. 3.23A). Data represent the mean and SE values of four biological replicates and are expressed as relative values compared with the respective wild-type control (0 h), which was set to 1. *PP2AA2* and *MCP2D* served as reference genes. **D**, Tables display the respective fold changes for each gene [CL *versus* corresponding control] to facilitate the evaluation of CL-dependent changes in relative expression levels between the genotypes. Highlighted in gray, most prominent CL-induced divergences in cytokinin-deficient plants compared with the wild type.

CAB2 and *CAT2* usually exhibit their peak expression in the morning. Accordingly, a morning-specific maximum in expression was detected under control conditions and in CL-treated wild-type plants (Fig. 3.25A-B). The maximum expression of *CAT2* was somewhat reduced in the CL-treated wild type compared with the wild-type control, indicating already a slight alteration in this circadian output. However, the circadian regulation of both genes was drastically affected in CL-treated cytokinin-deficient plants. The transcript levels did not only fail to accumulate in anticipation of the next

morning, the genes were rather expressed in anti-phase compared with the controls and were diminished to very low expression levels towards the end of the night. A similar decrease in expression was detected for *FER1* (Fig. 3.25C). The corresponding tables in Figure 3.25D also show that all three clock-regulated genes strongly decreased in their expression (down to 50- to 100-fold) in cytokinin-deficient plants while the wild type remained largely unaffected, especially during the second half of the night following CL. These results show that the degree of circadian stress is indeed refected by the extent of altered *CAB2*, *CAT2*, and *FER1* regulation. This implies, that the circadian desynchrony after CL treatment as indicated by the disturbed core oscillator was strong enough to affect clock-regulated gene expression and to cause a disturbed clock output.

3.5.5 Expression profiles of cytokinin-associated genes under SD and after CL conditions

Similar analyses as above were conducted for a set of cytokinin-associated genes (Fig. 3.26). So far, *ARR9* was described as oscillating gene among A-type *ARR* genes (Ishida *et al.*, 2008b) and only *CKX5* was shown to exhibit dawn- and SD-specific peak expression among *CKX* genes (Nomoto *et al.*, 2012). Both were predicted by using DIURNAL (http://diurnal.mocklerlab.org/), an online tool which enables to identify cycling genes by screening different sets of microarray time course data (Mockler *et al.*, 2007). In this work, DIURNAL was used to search for further A-type *ARR* candidate genes which oscillate particularly under SD conditions. Indeed, additional genes could be identified, namely *ARR4* (rather weakly), *ARR5*, *ARR7*, and *ARR16*. Interestingly, all of these cytokinin-associated cycling genes exhibit their maximum expression during or at the end of the SD night, which was shown to be critical for cell death initiation after CL treatment.

By using the samples of the same time course experiment outlined above (see Fig. 3.23A) the nocturnal or dawn-specific phasing could be confirmed for all tested genes in the wild-type controls (Fig. 3.26). In these plants peak-to-trough ratios of ~3 for *ARR4* (Fig. 3.26A), *ARR5* (Fig. 3.26B), and *ARR7* (Fig. 3.26C) expression were recorded, while the ratios were even higher for *ARR9* (Fig. 3.26D; ~9), *ARR16* (Fig. 3.26E; ~13), and *CKX5* (Fig. 3.26F; ~7). Surprisingly, this diurnal rhythm was impaired in both *35S:CKX4* and *ahk2 ahk3* control plants. The expression of these genes either exhibited no distinct peak sometimes being characterized by rather irregular expression patterns (Fig. 3.26A-C) or the phasing was correct but oscillations were dampened as reflected by reduced peak-to-trough ratios compared with the wild type (Fig. 3.26D-F). This clearly demonstrates that the cytokinin status influences the oscillation of cytokinin-associated genes.

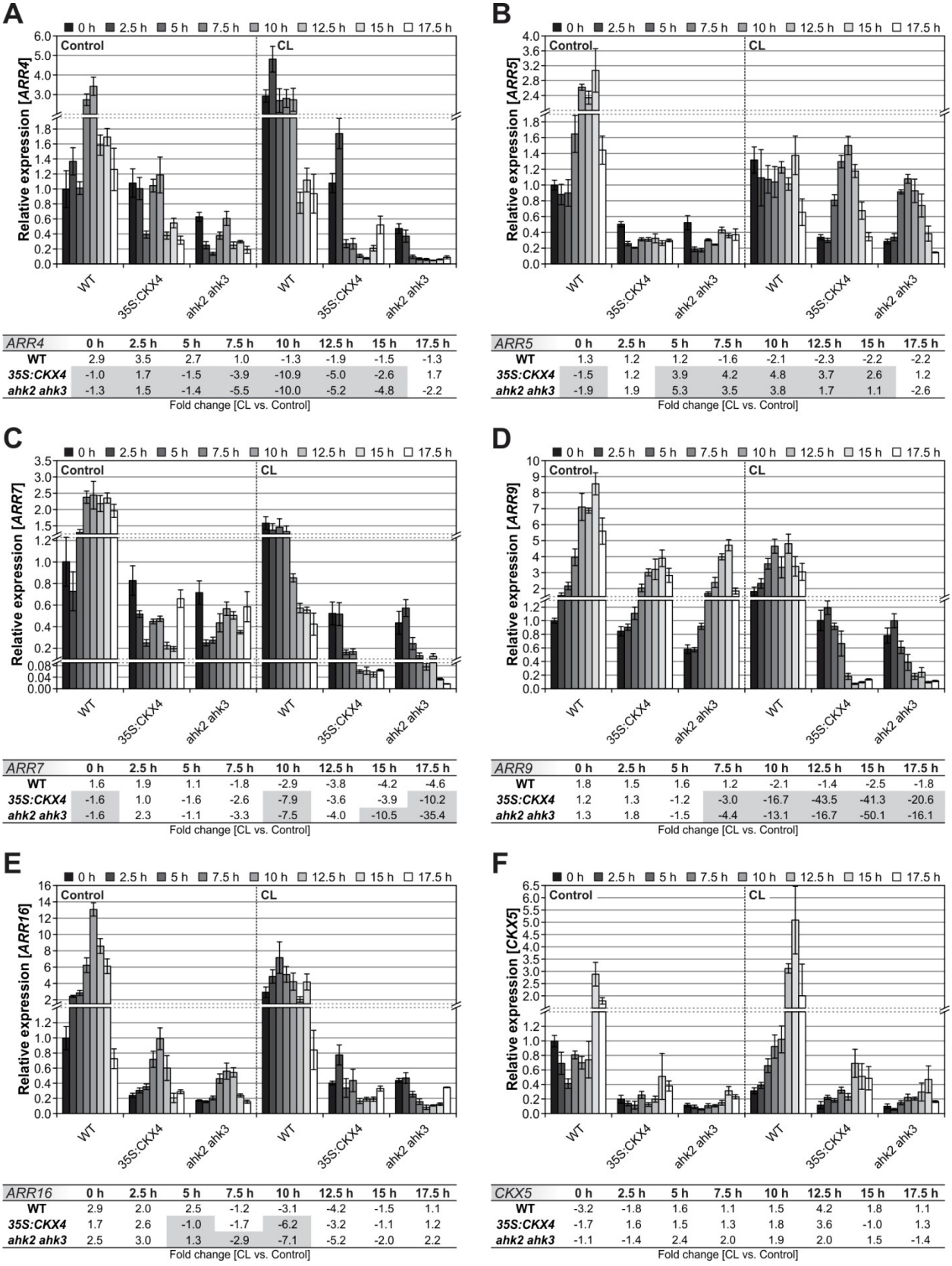

ARR4	0 h	2.5 h	5 h	7.5 h	10 h	12.5 h	15 h	17.5 h
WT	2.9	3.5	2.7	1.0	-1.3	-1.9	-1.5	-1.3
35S:CKX4	-1.0	1.7	-1.5	-3.9	-10.9	-5.0	-2.6	1.7
ahk2 ahk3	-1.3	1.5	-1.4	-5.5	-10.0	-5.2	-4.8	-2.2

Fold change [CL vs. Control]

ARR5	0 h	2.5 h	5 h	7.5 h	10 h	12.5 h	15 h	17.5 h
WT	1.3	1.2	1.2	-1.6	-2.1	-2.3	-2.2	-2.2
35S:CKX4	-1.5	1.2	3.9	4.2	4.8	3.7	2.6	1.2
ahk2 ahk3	-1.9	1.9	5.3	3.5	3.8	1.7	1.1	-2.6

Fold change [CL vs. Control]

ARR7	0 h	2.5 h	5 h	7.5 h	10 h	12.5 h	15 h	17.5 h
WT	1.6	1.9	1.1	-1.8	-2.9	-3.8	-4.2	-4.6
35S:CKX4	-1.6	1.0	-1.6	-2.6	-7.9	-3.6	-3.9	-10.2
ahk2 ahk3	-1.6	2.3	-1.1	-3.3	-7.5	-4.0	-10.5	-35.4

Fold change [CL vs. Control]

ARR9	0 h	2.5 h	5 h	7.5 h	10 h	12.5 h	15 h	17.5 h
WT	1.8	1.5	1.6	1.2	-2.1	-1.4	-2.5	-1.8
35S:CKX4	1.2	1.3	-1.2	-3.0	-16.7	-43.5	-41.3	-20.6
ahk2 ahk3	1.3	1.8	-1.5	-4.4	-13.1	-16.7	-50.1	-16.1

Fold change [CL vs. Control]

ARR16	0 h	2.5 h	5 h	7.5 h	10 h	12.5 h	15 h	17.5 h
WT	2.9	2.0	2.5	-1.2	-3.1	-4.2	-1.5	1.1
35S:CKX4	1.7	2.6	-1.0	-1.7	-6.2	-3.2	-1.1	1.2
ahk2 ahk3	2.5	3.0	1.3	-2.9	-7.1	-5.2	-2.0	2.2

Fold change [CL vs. Control]

CKX5	0 h	2.5 h	5 h	7.5 h	10 h	12.5 h	15 h	17.5 h
WT	-3.2	-1.8	1.6	1.1	1.5	4.2	1.8	1.1
35S:CKX4	-1.7	1.6	1.5	1.3	1.8	3.6	-1.0	1.3
ahk2 ahk3	-1.1	-1.4	2.4	2.0	1.9	2.0	1.5	-1.4

Fold change [CL vs. Control]

Figure 3.26: Kinetics of A-type *ARR* and *CKX5* gene expression during the dark period following continuous light treatment.

Figure 3.26 continued.

A-**D**, Kinetics of transcript abundances for *ARR4* (**A**), *ARR5* (**B**), *ARR7* (**C**), *ARR9* (**D**), *ARR16* (**E**) and *CKX5* (**F**) in a 2.5-hour time interval starting directly after SD or CL (0 h) and ending 17.5 hours later. The experimental setup corresponds to the one explained in Fig. 3.23 (for a schematic overview see Fig. 3.23A). DIURNAL (http://diurnal.mocklerlab.org/) was used to identify cycling cytokinin-related genes under SD conditions. The genes selected for this experiment showed a rhythmic expression pattern. The peak-to-trough ratio was > 2 (except for *ARR4*, ratio of ~ 1.8). Data in graphs represent the mean and SE values of four biological replicates and are expressed as relative values compared with the respective wild-type control (0 h), which was set to 1. *PP2AA2* and *MCP2D* were used as reference genes. Additionally, tables have been inserted into each panel displaying the respective fold changes [CL *versus* corresponding control] to facilitate the evaluation of CL-dependent changes in relative expression levels between the genotypes. Highlighted in gray, most prominent CL-induced divergences in cytokinin-deficient plants compared with the wild type.

The differences already under control conditions made it difficult to evaluate the CL-induced changes in transcript abundances for each genotype. Therefore, the fold changes between the expression levels after CL and the respective control levels were determined (see corresponding tables in Fig. 3.26 below each graph). These data showed that the changes in *CKX5* expression after CL treatment were marginal and, moreover, similar in all investigated genotypes. Greater changes could be detected for *ARR7* expression, which were slightly stronger in cytokinin-deficient plants compared with wild-type plants. However, CL treatment led to more dramatically changed *ARR4*, *ARR5*, *ARR9*, and *ARR16* expression in plants with a reduced cytokinin status. The CL regime caused oscillating *ARR5* expression in *35S:CKX4* and *ahk2 ahk3* which was absent under SD rhythm, while the inverse effect was visible for *ARR16* – together pointing to a clear misregulation. The *ARR4* and *ARR9* expression patterns in *35S:CKX4* and *ahk2 ahk3* were characterized by a strong down-regulation of these genes which was not detectable in wild type. Since the cycling of *ARR9* expression was shown to be under clock control (Ishida *et al.*, 2008b) the disrupted expression in cytokinin-deficient plants after CL treatment reflects an impaired circadian regulation. Therefore, this result marks circadian stress in these plants similar to the outcome in Figure 3.25. Together, the data in Fig. 3.26 demonstrate that the cytokinin status already has an impact on the cycling of *ARR* and *CKX5* gene expression under control conditions. Furthermore, a disturbed clock performance especially in cytokinin-deficient plants under circadian stress also affected the cycling behavior of these genes. Collectively, these results lead to the hypothesis that cytokinin might serve as an input signal modulating clock precision to fine-tune the time-of-day-specific circadian regulation of CK-associated (and probably other) genes.

Since A-type *ARR* genes are direct targets of cytokinin signaling they are often used to study the cytokinin response on the molecular level (Rashotte *et al.*, 2003; Brenner *et al.*, 2005). Therefore, the question arose if an increased cytokinin response could be detected in CL-treated wild-type plants which, due to their higher cytokinin status, coped better with circadian stress conditions. For that, especially the first half of the night was of interest because the stress response further leading to cell death was induced during that time (see Fig. 3.23B-C).

The CL-dependent changes in *ARR5*, *ARR7*, *ARR9*, and *ARR16* transcript abundances did not indicate strong differences between the genotypes in the expression of these response genes directly after CL or in the early night (see tables in Fig. 3.26B-E; "0 h" to "5 h"). A transient increase in cytokinin action might be deduced from a CL-induced increase in *ARR4* expression in wild type (see table in Fig. 3.26A; "0 h" to "5 h"). However, the overall increase (by about 3-fold) was not very pronounced and might only be part of the general disturbance of clock-regulated gene expression in response to circadian

stress. Thus, it seems that it is not a transient cytokinin signal but a generally high cytokinin status which prevents a high degree of circadian stress in wild-type plants.

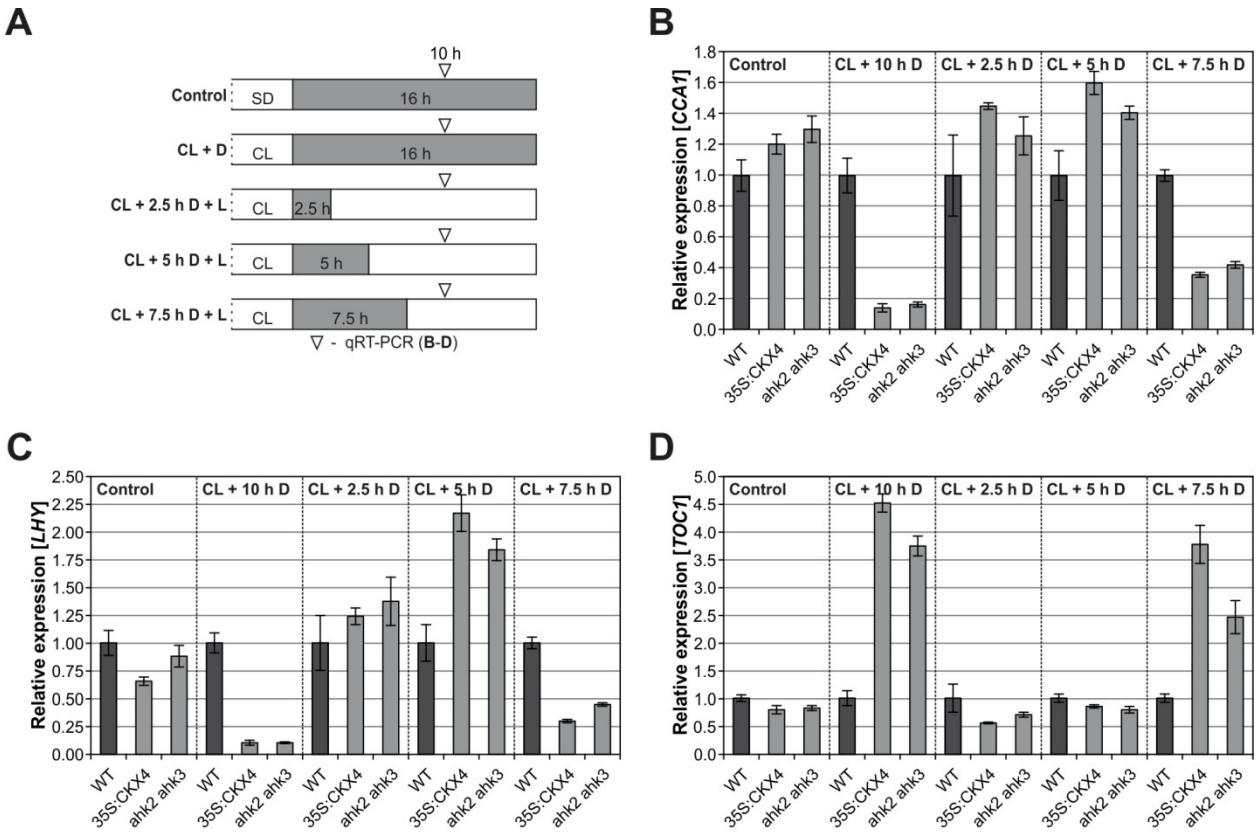

Figure 3.27: Re-entrainment of the circadian clock as demonstrated by the light-dependent resetting of the core oscillator might be crucial for the circumvention of cell death after short nights.

A, Schematic overview of the experimental design for **B**-**D**. White, light period; gray, dark period. Prior to the experiment all plants were grown under SD rhythm for six weeks. Control plants remained in the SD rhythm while a subset of plants was subjected to 32 hours of CL. In addition to prolonged darkness following the CL treatment plants were also exposed to shorter dark periods (2.5, 5, and 7.5 h) terminated by the premature onset of light periods. Leaf samples for qRT-PCR were collected ten hours after CL or a SD light period, respectively. It was examined if the molecular phenotype in cytokinin-deficient plants after CL (followed by a long dark period) as defined by repression of *CCA1* and *LHY* expression (**B**-**C**) and elevation of *TOC1* expression (**D**) could be reversed by short nights and the earlier onset of light, respectively. Data represent the mean and SE values of four biological replicates and are expressed as relative values compared with the respective wild type (dark gray columns), all of which were set to 1. *PP2AA2* and *MCP2D* served as reference genes.

3.5.6 Relationship between circadian stress and cell death

The correlation between the disrupted oscillator gene expression and the stress and cell death response led to the hypothesis that the cell death might be triggered by the circadian stress. To further evaluate this hypothesis it had to be ruled out that the perturbation of the clock core gene expression in cytokinin-deficient plants was already determined by the CL treatment itself irrespective of the following events. As described in Figure 3.16 short nights (2.5 and 5 hours) following CL treatment could prevent cell death initiation while intermediate night lengths (7.5 hours) led to intermediate cell death phenotypes. Accordingly, it was investigated if the changes in oscillator gene expression were also detectable after short or intermediate nights following CL treatment or if the perturbation in oscillator gene expression was restricted to long cell death-inducing nights (Fig. 3.27A). Strikingly, in

cytokinin-deficient plants *CCA1* and *LHY* transcript levels reached or even slightly exceeded wild-type levels after short nights while they were minimal after long nights (standard regime) and intermediate after intermediate nights (Fig. 3.27B-C). The same, though inverse, was observed for *TOC1* expression (Fig. 3.27D). First of all, these results show that the earlier onset of light periods after short nights resulted in a re-entrainment of the circadian clock as demonstrated by the light-dependent resetting of the core oscillator. Thus, the reversion of the cell death phenotype could indeed be correlated to a proper gene expression of the core oscillator. In conclusion, this indicates that the degree of circadian stress detected on the molecular level (i.e. the disrupted oscillator gene expression) determines the severity of the cell death phenotype.

However, the question arose if the opposite could be true, meaning that the initiation of cell death caused the circadian stress. One counter-argument is that the disturbance of the core oscillator coincided with the onset of the stress response but started prior to cell death initiation (see Figs. 3.14, 3.23 and 3.24). Nevertheless, it was analyzed if a perturbed clock gene expression was solely detectable in mature leaves undergoing cell death or also in phenotypically unaffected young leaves of the same plants. For that, the same experimental setting was used as described in Figure 3.13 which already showed that molecular stress and cell death responses were present only in mature (affected) leaves 16 hours after CL treatment. However, both *CCA1* and *LHY* expression were similarly reduced in young and mature leaves following the CL regime (Fig. 3.28A-B). The same was observed for the elevation of *TOC1* expression in all samples after CL treatment (Fig. 3.28C). This demonstrates that the whole plant's circadian clock was affected by the changed light-dark regime. Since circadian stress could also be detected in unaffected young leaves, the data indicate that the circadian stress is due to the changed light-dark regime and not to the cell death.

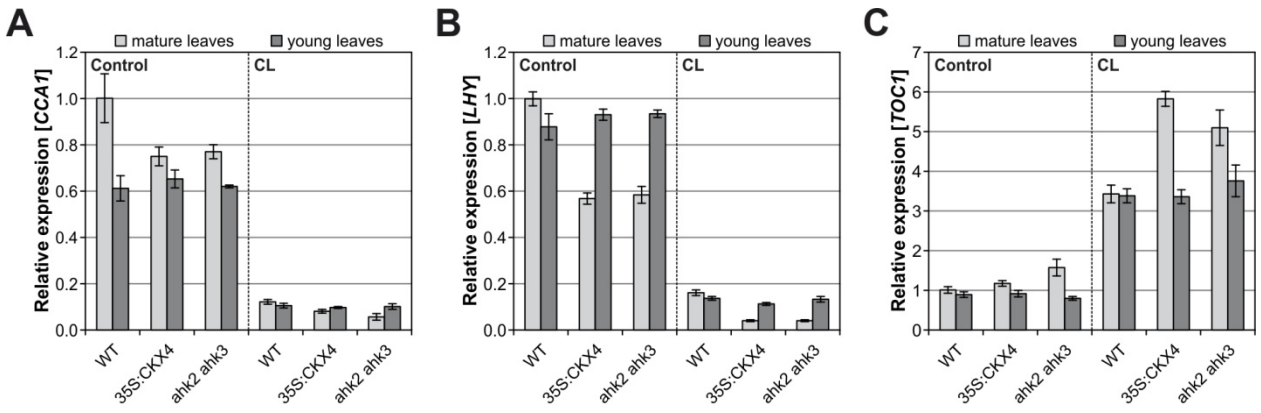

Figure 3.28: The whole plant is affected by circadian stress since the expression of core oscillator genes is disrupted in all aerial parts and not only in mature leaves undergoing cell death progression.

A-**D**, Plants were grown under SD conditions for six weeks. Control plants remained in the SD rhythm while the other plants were subjected to 32 hours of CL. Leaf samples for qRT-PCR were collected at the end of the 16-hour dark period following CL treatment or a normal SD (the experimental design corresponds to the one explained in Fig. 3.13A-B). The alteration in expression of the core oscillator genes *CCA1* (**A**), *LHY* (**B**), and *TOC1* (**C**) in response to CL treatment was similar in mature and young leaves, respectively. Data represent the mean and SE values of four biological replicates and are expressed as relative values compared with wild-type control/mature leaves, which was set to 1. *PP2AA2* and *MCP2D* were used as reference genes.

3.6 Specific clock components are indispensable for a proper response to changed light-dark regimes

The previous chapter focused on proving the "circadian stress" hypothesis in general and the data described above clearly demonstrated that a reduced cytokinin status resulted in a disturbance of the circadian clock after CL treatment. The following experiments addressed the question which factors might mediate/promote the interaction between cytokinin and the clock and, more specifically, which clock components might be involved in the cytokinin-dependent adaptive response to changed light-dark regimes.

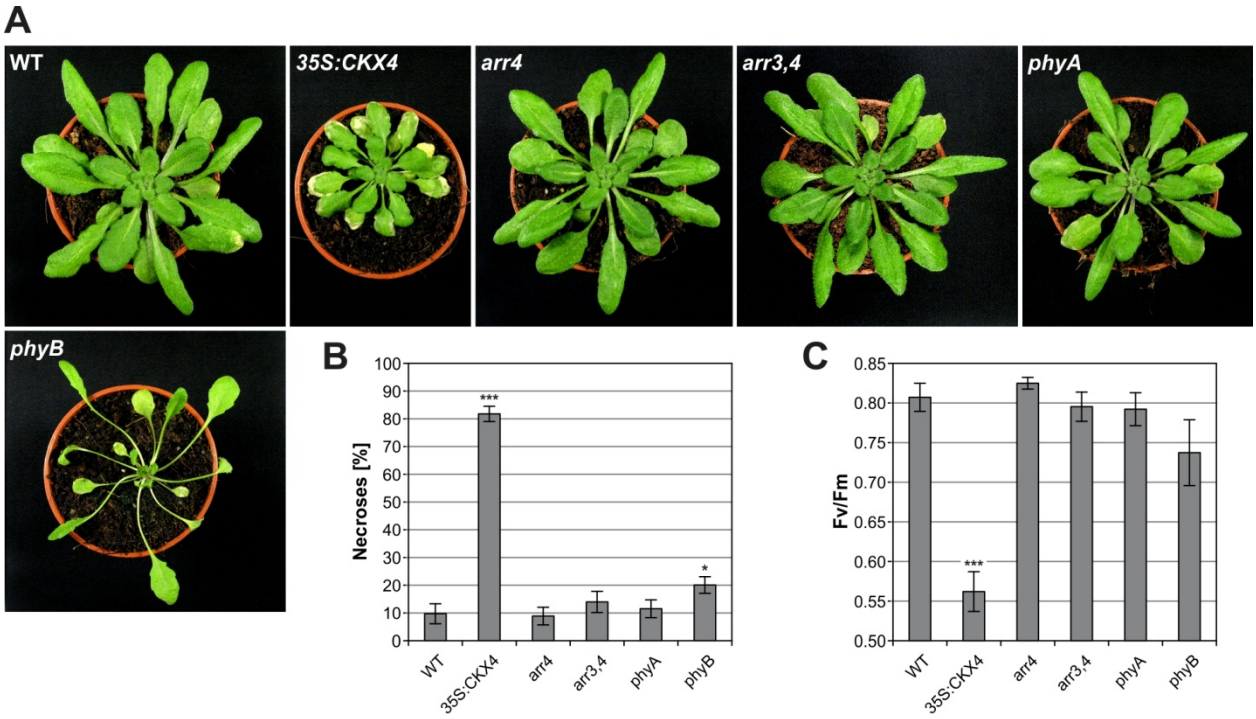

Figure 3.29: The A-type response regulators ARR3 and ARR4 and the photoreceptors PHYA and PHYB are no major players in the response to altered light-dark cycles.

A, Pictures show six-week-old A-type ARR (*arr4* and *arr3,4*) and phytochrome mutants (*phyA* and *phyB*) in comparison with the wild type and *35S:CKX4*. Plants were subjected to 32 hours of CL and transferred back into SD conditions afterwards. Pictures were taken two days after CL treatment and are representative for the observed phenotypes. **B**-**C**, The percentage of necrotic leaves counted in all mature leaves (**B**; n = 10) and the stress-induced decrease in F_v/F_m ratios (**C**; n = 12) measured one day after CL treatment. Experimental design corresponds to "32 h L/16 h D" in Fig. 3.6A. Control plants remained in the SD rhythm and were not affected (for pictures see Appendix Fig. A.5). Asterisks indicate significant differences compared with wild type (*t* test: *, $p < 0.05$; ***, $p < 0.001$). Error bars represent SE.

3.6.1 ARR3, ARR4 and PHYB play no predominant role in the CL response

In the literature one can find models which describe how cytokinin or cytokinin-related signaling components may act on the circadian clock, ascribing a role to ARR4 (and ARR3) and involving the photoreceptor PHYB (Hanano *et al.*, 2006; Salomé *et al.*, 2006; Zheng *et al.*, 2006; see 1.3.8.1). Hence, *arr4* and *arr3,4* as well as *phyA* and *phyB* mutants were analyzed after CL treatment to either confirm or exclude their connection to the CL response. The mutant phenotypes after CL treatment rather argue against an involvement of these factors (Fig. 3.29A; for controls see Appendix Fig. A.5).

All mutants appeared largely unaffected compared with *35S:CKX4* transgenic plants as was confirmed by quantification of necroses (Fig. 3.29B). Solely the mutation of *PHYB* led to an increase in the number of necrotic leaves (by about 10 %) in comparison with the wild type. A trend towards higher stress could also be deduced from a slight decrease in F_v/F_m ratios in *phyB* mutants (Fig. 3.29C). However, the overall effect in *phyB* mutants was small or even completely absent in some experiments (data not shown). Therefore, a predominant role for PHYB in the integration of the cytokinin signal to the circadian clock in response to CL treatment can be ruled out. The same conclusion can be drawn for ARR3 and ARR4 although their involvement might be masked by functional redundancy with other A-type ARRs.

3.6.2 Plants lacking proper CCA1/LHY expression or function also exhibit cell death following CL treatment

In order to unravel the contribution of specific components of the core oscillator (see 1.3.5) in the adaptive response to changed light-dark regimes different mutant and transgenic lines changed in CCA1 and/or LHY function or abundance were tested for their response to CL treatment. The expression profiles of *CCA1* and *LHY* after CL treatment (see Fig. 3.24) clearly showed strongly attenuated expression of these clock genes in cytokinin-deficient plants. This not only reflected circadian stress *per se*. It also suggested that the adaptive advantage conferred by cytokinin was achieved by supporting *CCA1* and *LHY* expression and that a pronounced deficiency in expression of both genes could be decisive for the cell death phenotype.

By analyzing *cca1-1 lhy-11* double loss-of-function mutants it could indeed be confirmed that both genes play an important role in the response to changed light-dark regimes (Fig. 3.30). These plants exhibited a strong cell death phenotype after CL treatment (Fig. 3.30A; for controls see Appendix Fig. A.6A) which was comparable with the CL responses of *35S:CKX4* and *ahk2 ahk3* plants. The stress phenotype was characterized by high percentages of necrotic leaves (Fig. 3.30B) and pronounced decreases in F_v/F_m ratios (Fig. 3.30C). Visible, though not statistically significant, effects could also be observed in the single T-DNA insertion lines *cca1-1* and *lhy-20*. This indicates a redundant action of both oscillator genes in the response to changing light-dark conditions. Intriguingly, the *lhy-11* single mutant exhibited a pronounced cell death phenotype which was almost as strong as in the double mutant *cca1-1 lhy-11*. This seems rather contradictory. However, it should be noted that the genetic background in *lhy-11* is different from that in *lhy-20*. While *lhy-20* is a T-DNA insertion allele (Michael *et al.*, 2003a), the *lhy-11* mutation was introduced into the already existing *lhy-1* line (originally called *lhy*; Schaffer *et al.*, 1998) *via* EMS mutagenesis. The *lhy-1* allele is dominant and causes *LHY* overexpression. The mutagenized population was used to screen for suppressors of *lhy-1* namely *lhy* loss-of-function mutants. Three intragenic suppressors were found; *lhy-11*, *lhy-12*, and *lhy-13* (Mizoguchi, 2002) all carrying mutations within the *LHY* coding region resulting in the lack of functional LHY proteins. Interestingly, Mizoguchi and colleagues could show (exemplary for *lhy-12*) that the *LHY* mRNA abundance was still constantly high and, moreover, there are studies pointing to a regulatory role of *LHY* transcripts (Schaffer *et al.*, 1998; Kim *et al.*, 2003; see also 4.2.4.1).

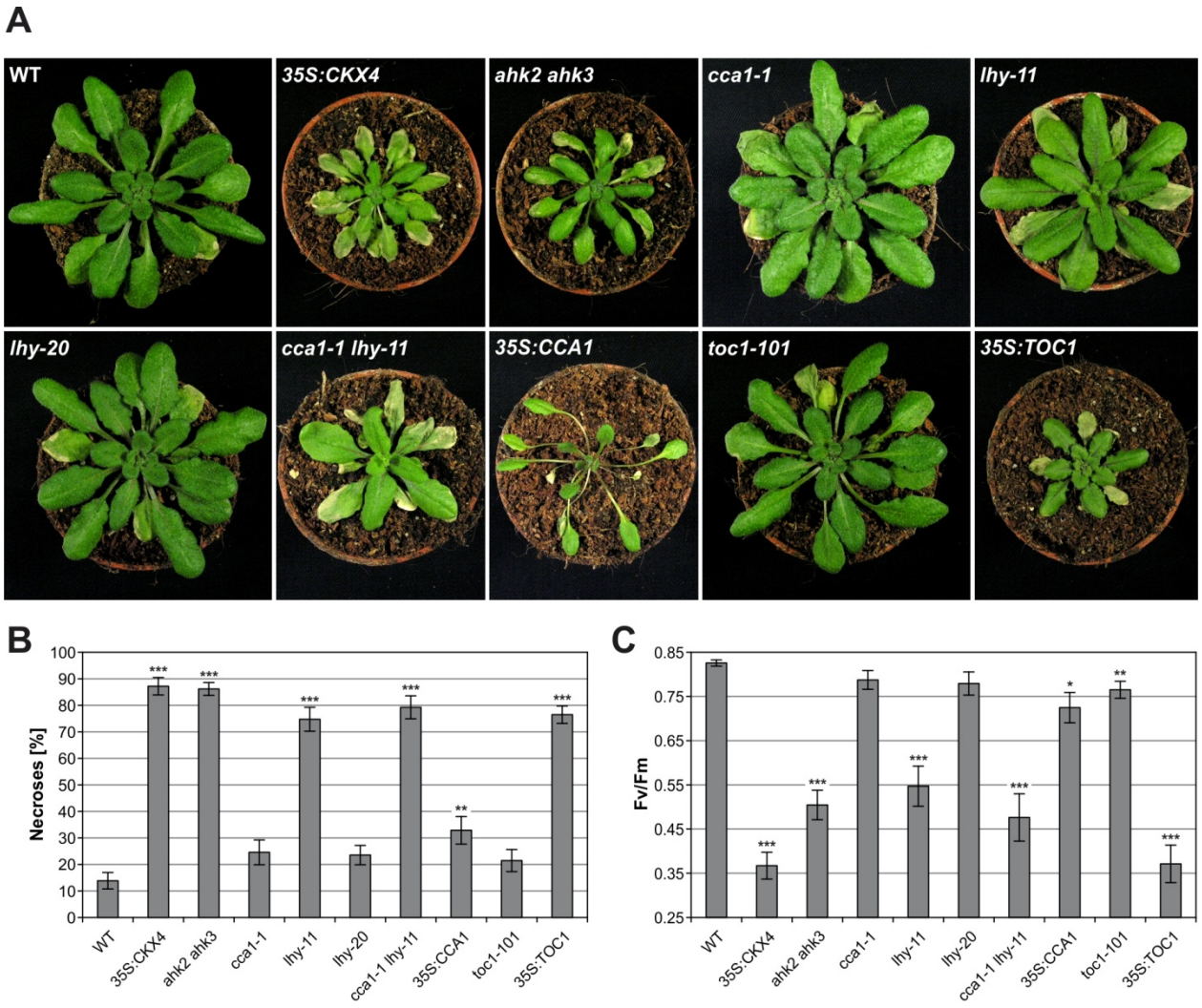

Figure 3.30: Loss-of-function and/or constitutive expression of oscillator components also confers the cell death phenotype after continuous light treatment.

A, Pictures showing the response to CL treatment in single or double mutants of the oscillator components *CCA1*, *LHY*, and *TOC1* as well as in overexpression lines for *CCA1* and *TOC1* in comparison with wild-type and cytokinin-deficient plants. Five-week-old SD-grown plants were subjected to 32 hours of CL and transferred back into SD rhythm afterwards while control plants remained in SD rhythm continuously and were not affected (for pictures see Appendix Fig. A.6). Pictures were taken two days after CL treatment and are representative for the observed phenotypes. **B**-**C**, The percentage of necrotic leaves counted in all mature leaves (**B**; n = 11) and the stress-induced decrease in F_v/F_m ratios (**C**; n = 15) measured one day after CL treatment. Experimental design corresponds to "32 h L/16 h D" shown in Fig. 3.6A. Asterisks indicate significant differences compared with wild type (*t* test: *, $p < 0.05$; **, $p < 0.01$; ***, $p < 0.001$). Error bars represent SE.

Beyond that, the *lhy-1* mutant was originally in the L*er* background (Schaffer, 1998). The *cca1-1 lhy-11* mutant (Mizoguchi *et al.*, 2002) was backcrossed four times into the Columbia background (Ito *et al.*, 2007). However, some phenotypical characteristics were still reminiscent of the L*er* background. Therefore, L*er* plants were also tested under CL conditions. They behaved like Col-0 (see Appendix Fig. A.6B-C). The same was done for the Ws accession, because the *cca1-1* mutant was derived from that accession (Green and Tobin, 1999) and has then also been introduced into Col-0 *via* backcrossing (six times; Yakir *et al.*, 2009). Interestingly, Ws plants were even less sensitive than Col-0 plants. No necroses and also no decreases in F_v/F_m ratios were detected (see Appendix

Fig. A.6B-C). Therefore, it can be concluded that none of the different ecotype backgrounds contributed to a high sensitivity towards circadian stress or to the differences between *lhy* alleles after CL treatment.

In order to confirm the relevance of a simultaneous *CCA1* and *LHY* mutation on the observed cell death phenotype, *cca1-1* mutants were also crossed with *lhy-20* mutants in this study. Since homozygous plants were not yet available at the end of this work the segregating progeny has been phenotypically analyzed and genotyped after exposure to the CL regime. The strongest cell death phenotypes could be correlated to homozygous double mutants (data not shown). These results support the idea that the combined action of CCA1 and LHY plays a predominant role in this adaptive response to changed light-dark regimes. However, it is notable that the phenotype of the identified *cca1-1 lhy-20* mutants seemed to be somewhat less pronounced than in *cca1-1 lhy-11* plants, which indicates that *lhy-11* might indeed be the stronger allele in this context.

Lastly, *CCA1* overexpressing plants (*35S:CCA1*) were tested for their phenotype after CL treatment (Fig. 3.30). The constitutive expression of *CCA1* has profound consequences for the clock performance. It leads to a strong arrhythmicity phenotype (abolished circadian rhythms under constant conditions) and the repression of both the endogenous *CCA1* gene and the *LHY* gene (Wang and Tobin, 1998). Despite their strongly impaired clock function, *35S:CCA1* plants exhibited only a weak cell death phenotype after CL treatment (Fig. 3.30A-C). This, on the one hand, indicates that high levels of *CCA1* (transcripts and proteins) which are present in these plants (Wang and Tobin, 1998) are rather protective and that the degree of arrhythmicity is not decisive under circadian stress conditions. The weak but reproducible phenotype, on the other hand, could at least in part be explained by the severely reduced expression of *LHY* transcripts and proteins in these plants (Wang and Tobin, 1998; Daniel *et al.*, 2004).

3.6.3 The elevation of TOC1 expression alone is not decisive for cell death in cytokinin-deficient plants

To study the contribution of TOC1, a third oscillator component, *toc1-101* and *35S:TOC1* plants were also examined regarding their response to the circadian stress regime (Fig. 3.30A-C). The *toc1-101* loss-of-function mutant exhibited only a weak cell death phenotype which resembled the outcome for *cca1-1* and *lhy-20* single mutants. The constitutive expression of *TOC1* in *35S:TOC1* plants, however, caused a strong cell death phenotype comparable with cytokinin-deficient and *cca1-1 lhy-11* plants.

The question arose if the influence of TOC1 was stronger than deduced from the expression profiles shown in Figure 3.24C. The expression patterns were characterized by increased transcript levels in cytokinin-deficient plants at the end of the night following CL treatment. In order to clarify if a high *TOC1* expression itself – observed in cytokinin-deficient plants after CL treatment and continuously present in *35S:TOC1* plants – is decisive for the circadian stress response, the *toc1-101* allele was introduced into *35S:CKX4* and *ahk2 ahk3* plants, respectively. If the high *TOC1* expression caused the circadian stress resulting in cell death, the phenotypes of *35S:CKX4* and *ahk2 ahk3* plants should be reversed by introgression of the *toc1-101* loss-of-function allele. As Figure 3.31 shows the contrary

was observed. The cell death phenotypes of cytokinin-deficient *toc1-101* mutants were further aggravated (Fig. 3.31A; for controls see Appendix Fig. A.7). This view was corroborated by significantly increased numbers of necrotic leaves (Fig. 3.31B) as well as significantly decreased F_v/F_m ratios in plants addictionally carrying the *toc1-101* allele (Fig. 3.31C). This is consistent with the fact that the *toc1-101* single mutant exhibited a somewhat stronger phenotype compared with the wild type which already indicates a rather amplifying effect of *toc1* loss-of-function for the CL response. Collectively, the data demonstrate that the high expression of *TOC1* in cytokinin-deficient plants after CL treatment was not critical for the cell death phenotype under circadian stress but was presumably only the consequence of the attenuated *CCA1*/*LHY* expression. But why do *35S:TOC1* plants exhibit a pronounced cell death phenotype after CL treatment? It is known, that *CCA1*/*LHY* diurnal and circadian rhythms are strongly dampened in *TOC1* overexpressing plants (Makino *et al.*, 2002; Gendron *et al.*, 2012; Huang *et al.*, 2012). Therefore, it seems plausible that also in this case the reduced expression of these two morning-phased genes caused the strong CL-dependent cell death phenotype.

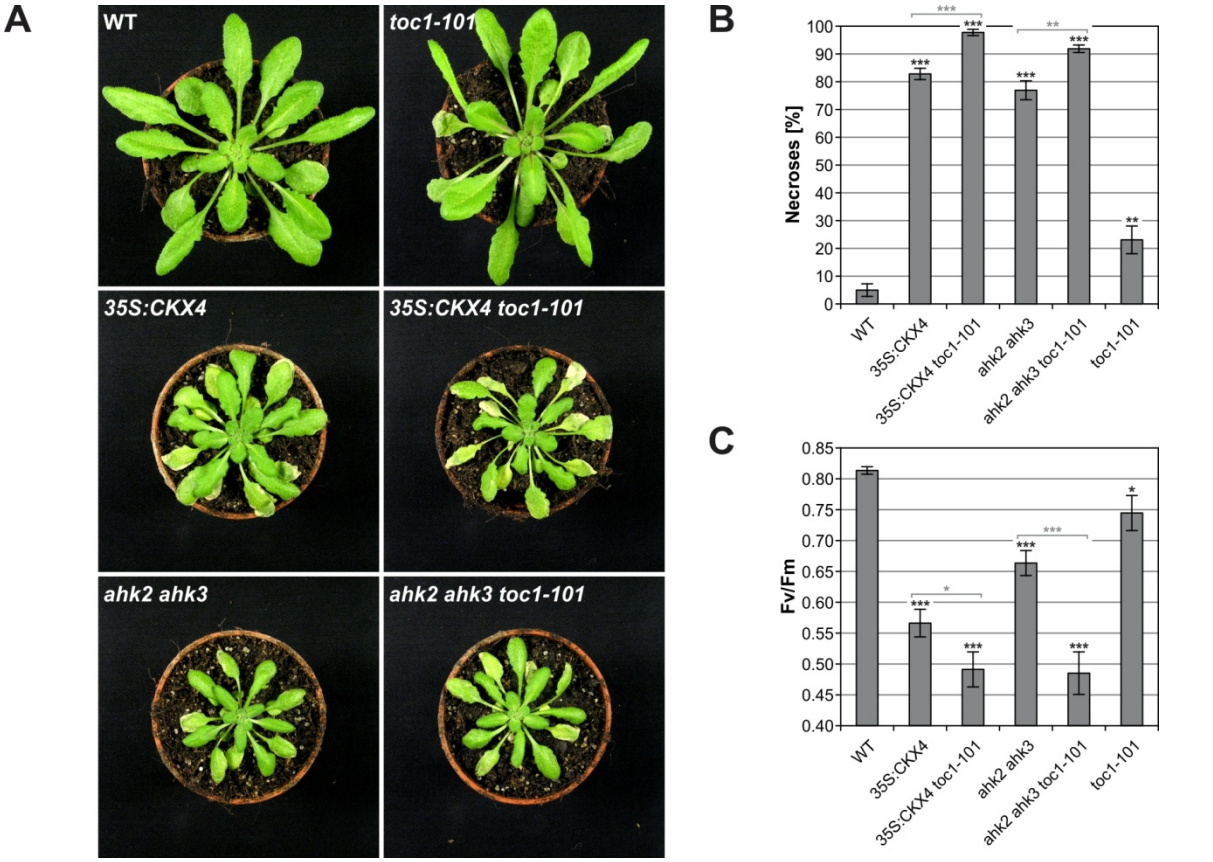

Figure 3.31: The *toc1-101* loss-of-function allele causes an aggravated cell death phenotype in cytokinin-deficient plants after continuous light treatment.

A, Plants with a reduced cytokinin status (*35S:CKX4* and *ahk2 ahk3*) in wild-type and *toc1-101* background. Five-week-old SD-grown plants were subjected to 32 hours of CL and transferred back into SD rhythm afterwards while control plants remained in SD rhythm continuously and were not affected (for pictures see Appendix Fig. A.7). Pictures were taken two days after CL treatment and are representative for the observed phenotypes. **B**-**C**, The percentage of necrotic leaves counted in all mature leaves (**B**; n = 11) and the stress-induced decrease in F_v/F_m ratios (**C**; n = 16) measured one day after CL treatment. Experimental design corresponds to "32 h L/16 h D" shown in Fig. 3.6A. Asterisks indicate significant differences compared with wild type (black) and between cytokinin-deficient plants in wild-type or *toc1-101* background (gray) (*t* test: *, $p < 0.05$; **, $p < 0.01$; ***, $p < 0.001$). Error bars represent SE.

3.6.4 Involvement of the evening complex in the CL response

Proper regulation of *CCA1* and *LHY* requires additional evening-expressed clock genes, including *ELF3*, *ELF4*, and *LUX*, which together form the so-called evening complex (EC) (Nusinow *et al.*, 2011; see 1.3.5.5). The EC is necessary for high-amplitude diurnal and circadian rhythms of both morning genes (Doyle *et al.*, 2002; Hazen *et al.*, 2005; Kolmos *et al.*, 2009; Dixon *et al,* 2011). Therefore, the analysis of the corresponding mutants provides a further tool to study the consequences of a diminished *CCA1*/*LHY* expression under circadian stress. But it also unravels if the EC itself might be involved in the response to changed light-dark regimes. The night period following the CL treatment was critical for the CL-dependent cell death (see Fig. 3.15). Since the EC is described as key regulator of nocturnal clock gene expression (Pokhilko *et al.*, 2012), this observation could be explained by a perturbation of the EC. As a matter of fact, the mutation of each EC component led to a cell death phenotype in response to the CL regime (Fig. 3.32). The cell death phenotype following CL treatment was strongly induced in the presence of both tested *elf3* mutant alleles, *elf3-8* and *elf3-9* (Fig. 3.32A; for controls see Appendix Fig. A.8A). It was also very pronounced in the *lux-1* mutant, while an intermediate phenotype was observed in *elf4-101* plants (Fig. 3.32B; for controls see Appendix Fig. A.8B). The quantification of necrotic leaves confirmed this view (Fig. 3.32C-D). The stronger reduction of F_v/F_m ratios in *elf3* and *lux-1* plants further gave evidence that the cell death was more severe compared with *35S:CKX4* transgenic plants, although the percentage of affected leaves was similar (Fig. 3.32E-F). In contrast, the decrease in F_v/F_m values was rather comparable between *elf4-101* and *35S:CKX4* plants but the total number of necrotic leaves was much smaller in *elf4-101*. This reflects a comparable extent of cell death when considering only the leaf level. Since *lux-1* plants are in the C24 background, a control experiment with the corresponding C24 accession was carried out. The pictures show that CL-treated C24 plants developed some chloroses (see Appendix Fig. A.8C). Counting the chloroses, although looking somewhat different, as necroses resulted in about 10 % more necroses in C24 plants compared with Col-0 plants (see Appendix Fig. A.8D). However, one can deduce from the F_v/F_m ratios that the overall stress was comparable between the wild types (see Appendix Fig. A.8E), confirming the strong impact of the *lux-1* allele itself. Altogether, the results clearly demonstrate that a perturbation of the EC causes a cell death phenotype after the CL regime. Therefore, it is evident that an impaired EC can contribute to the overall circadian stress under changing light-dark regimes. The question is whether this is the case in plants with a reduced cytokinin status.

In order to uncover the potential involvement of the EC in the establishment of the cell death phenotype in cytokinin-deficient plants the transcript expression patterns of its three components were recorded after CL treatment and compared with the profiles from plants under control (SD) conditions (for experimental design see Fig. 3.23A). It is well-known that *ELF3*, *ELF4*, and *LUX* gene expression are under circadian control as reflected by their sustained oscillation under constant light (Dixon *et al.*, 2011; Doyle *et al.*, 2002; Hazen *et al.*, 2005). Therefore, it had to be examined if the accurate cycling of these genes was perturbed due to cytokinin deficiency and/or circadian stress.

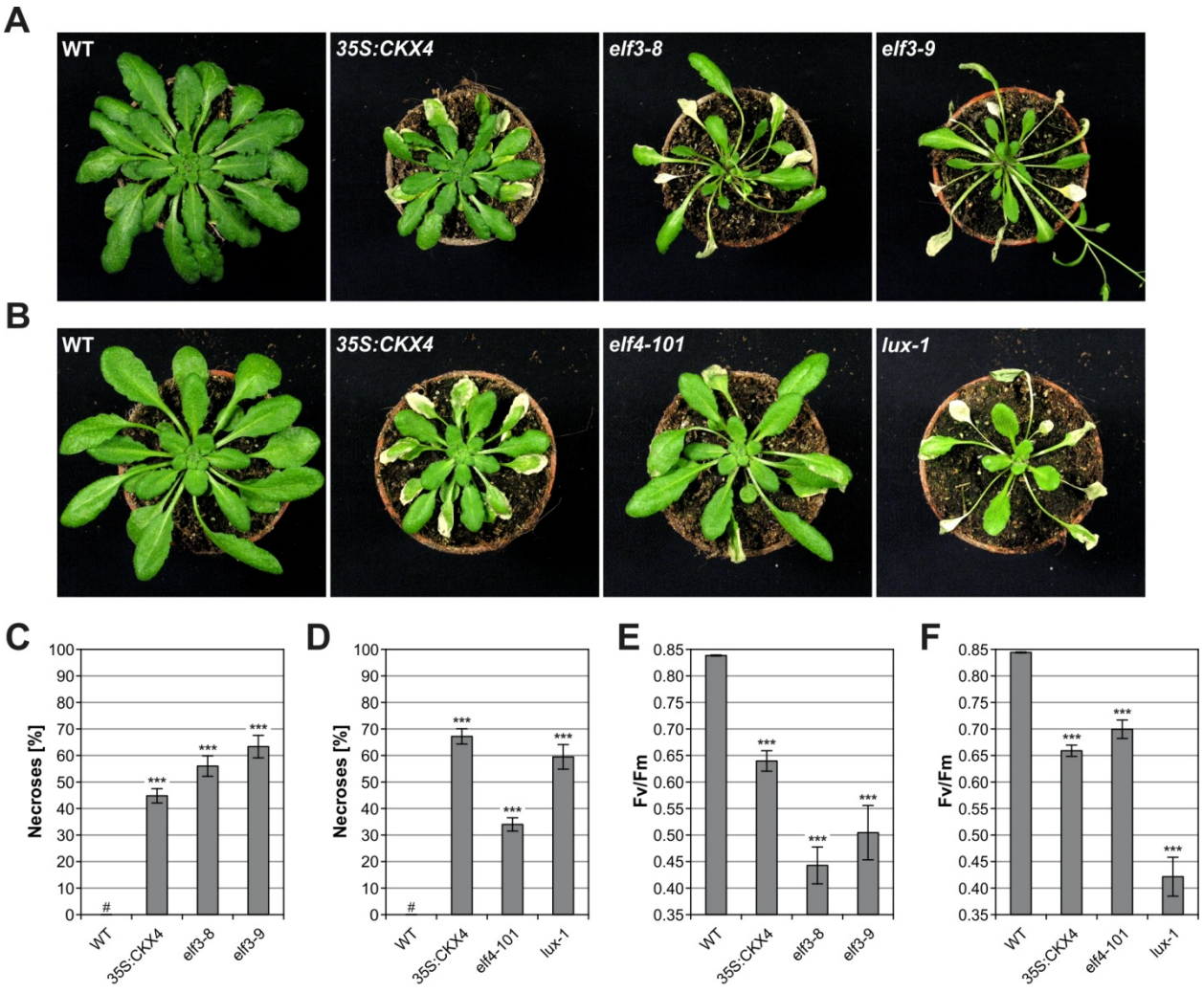

Figure 3.32: Mutants compromised in the evening complex also exhibit the cell death phenotype after continuous light treatment.

A-**B**, Plants carrying mutations in the EC components *ELF3*, *ELF4*, or *LUX* compared with wild-type and *35S:CKX4* transgenic plants. Six- or five-week-old (**A** and **B**, respectively) SD-grown plants were subjected to 32 hours of CL and transferred back into SD rhythm. Control plants remained in SD rhythm continuously and were not affected (for pictures see Appendix Fig. A.8). Pictures were taken three days after CL treatment and are representative for the observed phenotypes. **C**-**D**, The percentage of necrotic leaves counted in all mature leaves measured one day after CL treatment (**C**, n = 14; **D**, n = 10; #, not detected). **E**-**F**, The stress-induced decrease in F_v/F_m ratios measured directly after quantification of necroses (n = 11). Experimental design corresponds to "32 h L/16 h D" shown in Fig. 3.6A. Asterisks indicate significant differences compared with wild type (*t* test: ***, $p < 0.001$). Error bars represent SE.

The kinetics of *ELF3* expression in control plants looked similar between the genotypes and was characterized by generally high transcript abundances at nighttime with peak expression around midnight (Fig. 3.33A). Although the maximum expression was advanced and reduced by about 2-fold in CL-treated wild-type plants, it could still be observed. On the contrary, actual peak expression was absent in cytokinin-deficient plants after CL treatment. Moreover, *ELF3* expression started to decrease after end of CL treatment reaching the minimum shortly after midnight (at "10 h"). The difference between wild-type and cytokinin-deficient plants in response to CL is also underlined by the CL-dependent fold changes in *ELF3* expression (see corresponding table in Fig. 3.33D). *ELF3* expression was 2- to 3-fold lower in *35S:CKX4* and *ahk2 ahk3* plants after "5 h" of darkness following CL

treatment compared with the respective controls and further decreased at later time points. Thus, the divergence to wild type started already at "5 h", which temporally corresponds to the divergence observed for *CCA1*/*LHY* expression (see Fig. 3.24A-B) and to the induction of stress marker genes (see Fig. 3.23B-C).

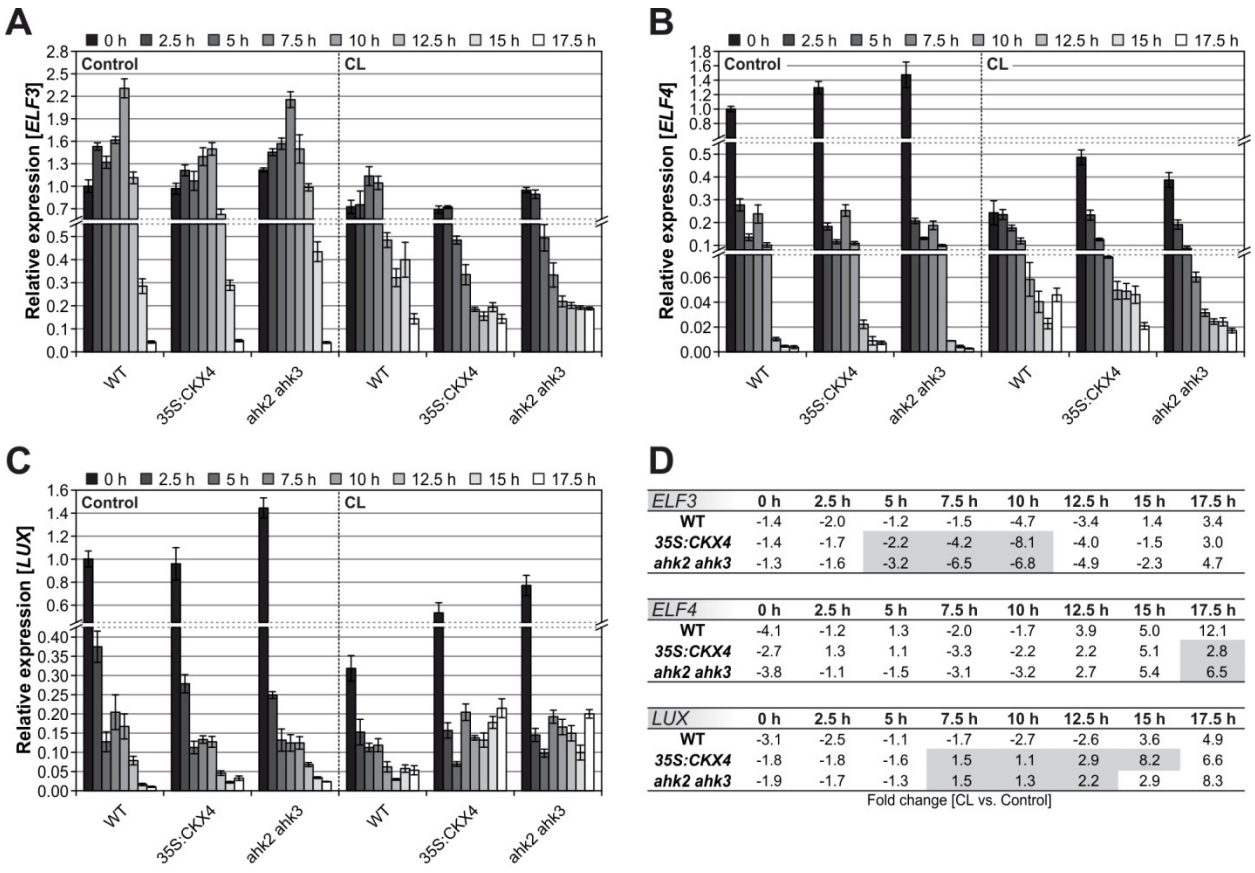

ELF3	0 h	2.5 h	5 h	7.5 h	10 h	12.5 h	15 h	17.5 h
WT	-1.4	-2.0	-1.2	-1.5	-4.7	-3.4	1.4	3.4
35S:CKX4	-1.4	-1.7	-2.2	-4.2	-8.1	-4.0	-1.5	3.0
ahk2 ahk3	-1.3	-1.6	-3.2	-6.5	-6.8	-4.9	-2.3	4.7

ELF4	0 h	2.5 h	5 h	7.5 h	10 h	12.5 h	15 h	17.5 h
WT	-4.1	-1.2	1.3	-2.0	-1.7	3.9	5.0	12.1
35S:CKX4	-2.7	1.3	1.1	-3.3	-2.2	2.2	5.1	2.8
ahk2 ahk3	-3.8	-1.1	-1.5	-3.1	-3.2	2.7	5.4	6.5

LUX	0 h	2.5 h	5 h	7.5 h	10 h	12.5 h	15 h	17.5 h
WT	-3.1	-2.5	-1.1	-1.7	-2.7	-2.6	3.6	4.9
35S:CKX4	-1.8	-1.8	-1.6	1.5	1.1	2.9	8.2	6.6
ahk2 ahk3	-1.9	-1.7	-1.3	1.5	1.3	2.2	2.9	8.3

Fold change [CL vs. Control]

Figure 3.33: Expression profile of genes encoding components of the evening complex during the dark period following continuous light treatment.

A-**C**, Kinetics of transcript abundances for *ELF3* (**A**), *ELF4* (**B**), and *LUX* (**C**) in a 2.5-hour time interval starting directly after SD or CL (0 h) and ending 17.5 hours later. The experimental setup corresponds to the one explained in Fig. 3.23 (for a schematic overview see Fig. 3.23A). Data represent the mean and SE values of four biological replicates and are expressed as relative values compared with the respective wild-type control (0 h), which was set to 1. *PP2AA2* and *MCP2D* served as reference genes. **D**, Tables display the respective fold changes for each gene [CL *versus* corresponding control] to facilitate the evaluation of CL-dependent changes in relative expression levels between the genotypes. Highlighted in gray, most prominent CL-induced divergences in cytokinin-deficient plants compared with the wild type.

In contrast to the differences seen in *ELF3* expression, the differences between the genotypes were marginal for *ELF4* expression under control and after CL conditions (Fig. 3.33B and corresponding table in Fig. 3.33D). Interestingly, the *ELF4* transcript levels increased in all genotypes during the late night after CL treatment compared with the controls. A CL-dependent increase in abundance was also recorded for *LUX* expression, although this time a bit more pronounced in CL-treated cytokinin-deficient plants (Fig. 3.33C and corresponding table in Fig. 3.33D). This is consistent with the current clock model which includes a negative feedback from CCA1/LHY to the EC (Pokhilko *et al.*, 2012; see Fig. 1.3A). Similar to *TOC1* expression (see Fig. 3.24C) *LUX* expression was elevated at the end of the

night especially in cytokinin-deficient plants pointing to a derepression as a consequence of the attenuated *CCA1*/*LHY* expression after CL treatment. Although the same mechanism is assumed for *ELF3* regulation by CCA1/LHY, the *ELF3* expression profiles did not reflect this connection. Rather the opposite was observed. The alleviated expression of *CCA1*/*LHY* coincided with a reduced *ELF3* expression after CL treatment. This, together with the results from the mutant analysis, implies that ELF3 might be the limiting factor for proper EC function under these conditions. Hence, the deficiency in *ELF3* expression might preclude the proper regulation of both *CCA1* and *LHY* due to a nonfunctional EC.

3.6.5 A role for CHE and TIC in the response to CL treatment

Since the oscillator gene *CHE* was strongly down-regulated in response to CL treatment (see Fig. 3.24D) the question arose if the cell death phenotype could also be observed in plants carrying a *CHE* loss-of-function allele. Two independent T-DNA insertion lines were described which both exhibit only reduced and not completely abolished *CHE* expression (Pruneda-Paz *et al.*, 2009). The stronger line, *che-2*, was tested in this study. The observed cell death phenotype of *che-2* plants was intermediate between wild-type and *35S:CKX4* plants (Fig. 3.34A; for controls see Appendix Fig. A.9A). This was equally reflected by the percentage of necrotic leaves (Fig. 3.34B) as well as the reduction in F_v/F_m ratios (Fig. 3.34C). Therefore, the results indicate that CHE plays a role in the circadian stress response. The intermediate phenotype might be due to the incomplete knockout of *CHE* or could imply that CHE modulates the circadian stress response only to a certain extent. The expression profile in Figure 3.24D already indicated that the reduction of *CHE* expression is rather a cell death-accompanying than an inducing event because the divergence between wild-type and cytokinin-deficient plants started after "10 h" of darkness when cell death was already initiated.

The clock-associated component TIC (see 1.3.5.6) was also tested concerning its involvement in the response to changing light-dark regimes. Two facts draw the attention towards this protein. It functions in the mid to late subjective night enabling the sensing of dawn (Hall *et al.*, 2003) and it was shown to be important under oxidative stress conditions (Sanchez-Villarreal, 2010; Sanchez-Villarreal *et al.*, 2013). Similar to *che-2* plants also *tic-2* plants exhibited an intermediate cell death phenotype (Fig. 3.34D-F; for controls see Appendix Fig. A.9B), which points to a contribution of TIC in this response. In contrast to the core oscillator genes *CCA1*, *LHY*, and *TOC1*, which displayed a perturbed expression in the whole plant after CL treatment (see Fig. 3.28A-C), *TIC* expression was only decreased in the affected mature leaves of cytokinin-deficient plants (see Fig. 3.34G). This observation links *TIC* misexpression to the cell death progression in plants with a reduced cytokinin status.

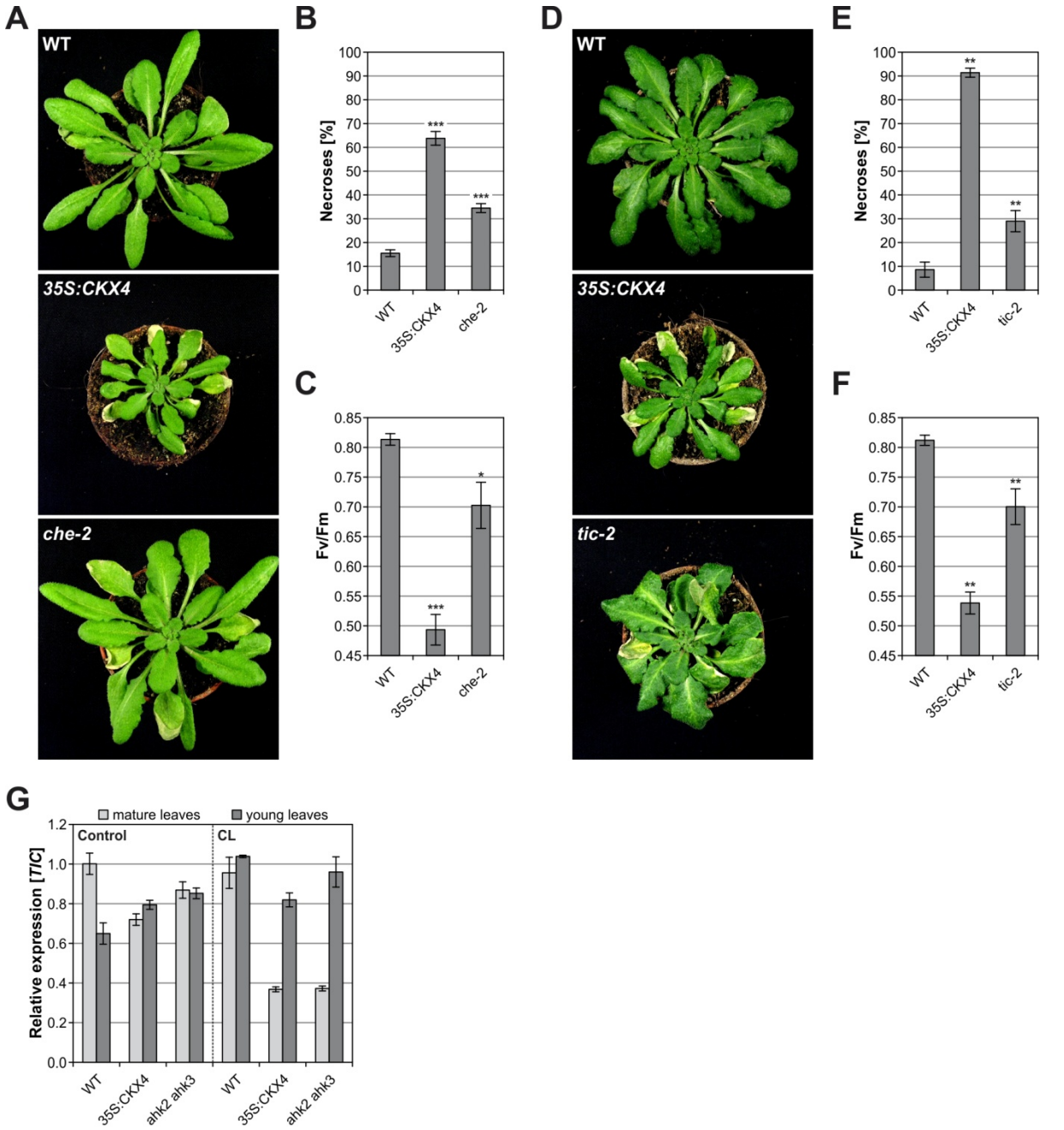

Figure 3.34: Clock and clock-associated components CHE and TIC play a role in development of the cell death phenotype after continuous light treatment.

A and **D**, Plants carrying mutations in the oscillator gene *CHE* (**A**) and the clock-associated component *TIC* (**D**) compared with *35S:CKX4* and wild type. Five- or six-week-old (**A** and **D**, respectively) SD-grown plants were subjected to 32 hours of CL and transferred back into SD rhythm. Control plants remained in SD rhythm continuously and were not affected (for pictures see Appendix Fig. A.9). Pictures were taken three days after CL treatment and are representative for the observed phenotypes. **B** and **E**, The percentage of necrotic leaves counted in all mature leaves measured one day after CL treatment (n = 10). **C** and **F**, The stress-induced decrease in F_v/F_m ratios measured directly after quantification of necroses (**C**, n = 16; **F**, n = 15). Experimental design corresponds to "32 h L/16 h D" shown in Fig. 3.6A. **G**, Transcript levels of the clock-associated gene *TIC* in mature and young leaves at the end of the 16-hour night following a normal SD light period or CL (for experimental design see Fig. 3.13A-B). Expression levels are normalized to wild-type control/mature leaves, which was set to 1 (n = 4). *PP2AA2* and *MCP2D* were used as reference genes. Asterisks indicate significant differences compared with wild type (*t* test: *, $p < 0.05$; **, $p < 0.01$; ***, $p < 0.001$). Error bars represent SE.

3.6.6 Cytokinin-deficient, cca1-1 lhy-11, and elf3-9 plants exhibit highly similar molecular phenotypes following the CL regime

The data described above clearly provide evidence that especially the proper expression (sufficient levels and cycling) of the clock morning elements *CCA1* and *LHY* was critical under circadian stress imposed by changed light-dark regimes. This could be confirmed by the occurrence of a cell death phenotype in *cca1-1 lhy-11* double mutants and was further substantiated by the strong effects in EC mutants, especially *elf3* and *lux*, after CL treatment. In the following, the molecular phenotype of *cca1-1 lhy-11* and *elf3-9* plants was investigated. The main interest was whether the perturbations in gene expression which were observed in cytokinin-deficient plants following the CL regime would be similarly detectable in these clock mutants.

The transcript abundance of oscillator and clock output gene expression in *cca1-1 lhy-11* and *elf3-9* was examined after "12.5 h" of darkness in SD-grown plants and following CL conditions (Fig. 3.35A). At this time point the most pronounced differences regarding *CCA1*/*LHY* expression were recorded after CL treatment between wild-type and cytokinin-deficient plants (see Fig. 3.24A-B). The already described CL-dependent changes in nocturnal *CCA1*/*LHY* expression could be reproduced for wild type and *35S:CKX4* in this experiment (Fig. 3.35B-C). While the wild type exhibited only a 2-fold decrease in the expression of both morning-phased genes in response to CL treatment, *35S:CKX4* showed even a 5- or 10-fold decrease, respectively. The *CCA1* transcript data in Figure 3.35B for *cca1-1 lhy-11* were consistent with the fact that *cca1-1* is a null allele (Green and Tobin, 1999). In contrast, an overexpression of *LHY* was detected in the double *cca1-1 lhy-11* mutant (Fig. 3.35C) although *lhy-11* is a loss-of-function allele (Mizoguchi *et al.*, 2002). However, this is in accordance with what has been shown for *lhy-12* plants which also exhibit constantly high *LHY* transcript levels coding for nonfunctional LHY proteins (Mizoguchi *et al.*, 2002). Under control conditions a 6-fold higher expression level compared with the wild type was detected at "12.5 h" (Fig. 3.35C). At this time point *LHY* was already close to its peak expression (see wild-type control in Fig. 3.24B). Earlier, after "7.5 h" of darkness, the relative expression levels of *LHY* were similarly high in *cca1-1 lhy-11* plants but were 200- to 300-fold higher compared with the wild type due to the sustained *LHY* oscillations in wild-type plants (data not shown). This reveals that *LHY* transcript levels were indeed constantly high in plants carrying the *lhy-11* allele. Nevertheless, it should be noted that *cca1-1 lhy-11* plants lack CCA1 and LHY proteins because they are absent in *cca1-1* (Green and Tobin, 1999) and *lhy-11* plants (Kim *et al.*, 2003), respectively. Concerning *elf3-9*, a reduced *CCA1* and *LHY* expression was detected already under control conditions. This is in agreement with the results from *elf3-4* plants by Dixon *et al.* (2011) and consistent with the well-known positive effect of the EC on the expression of both morning genes (Nagel and Kay, 2012; Pokhilko *et al.*, 2012). Interestingly, the *CCA1* and *LHY* levels in *elf3-9* further decreased after CL treatment reaching similar or even lower absolute levels, respectively, compared with *35S:CKX4* plants. The overall fold change was slightly smaller than in *35S:CKX4* probably due to the already low expression under control conditions. Together, *35S:CKX4*, *cca1-1 lhy-11*, and *elf3-9* plants either exhibit a reduced *CCA1*/*LHY* expression in response to the CL regime (*35S:CKX4* and *elf3-9*) or are generally impaired in CCA1/LHY functionality (*cca1-1 lhy-11*), thereby lacking sufficient nighttime expression of both genes.

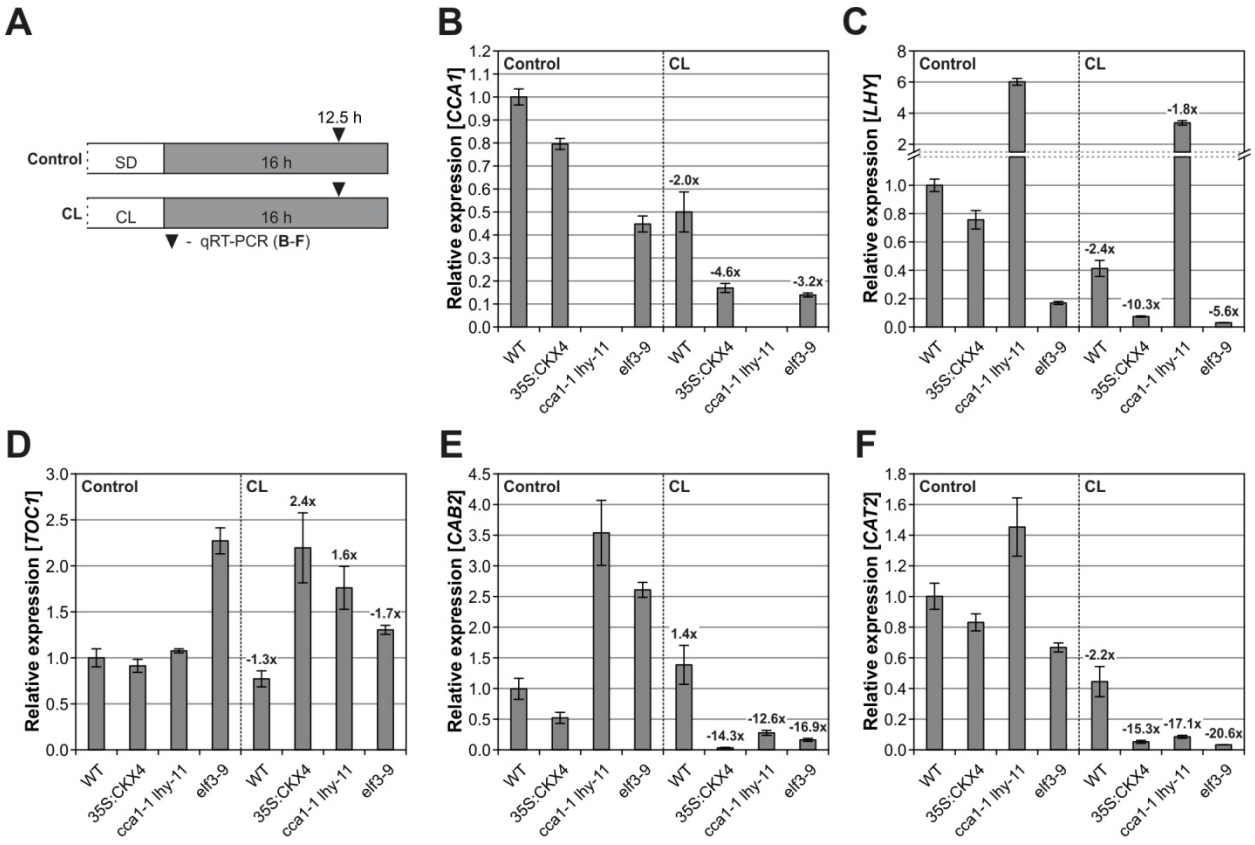

Figure 3.35: The clock mutants *cca1-1 lhy-11* and *elf3-9* are also affected in oscillator and clock output gene expression in response to the continuous light regime.

A, The scheme represents the experimental setup for **B**-**F**. White, light period; gray, dark period. Six-week-old SD-grown plants were exposed to 32 hours of CL and transferred back into SD rhythm. Control plants remained in SD rhythm continuously. Leaf samples for qRT-PCR were collected during the dark period following CL or a normal SD light period (after 12.5 hours), the time point at which the molecular phenotype observed in *35S:CKX4* concerning oscillator and output gene expression was very pronounced (for comparison see Fig. 3.24 and 3.25). Transcript levels of the oscillator genes *CCA1*, *LHY*, and *TOC1* (**B**-**D**) and the clock output genes *CAB2* and *CAT2* (**E**-**F**) were determined. Data represent the mean and SE values of four biological replicates and are expressed as relative values compared with the wild-type control, which was set to 1. *PP2AA2* and *MCP2D* were used as reference genes. CL-dependent changes in relative expression levels are displayed as fold changes [CL *versus* corresponding control] in each CL panel.

The *TOC1* expression analysis confirmed the elevated expression in *35S:CKX4* plants "12.5 h" after CL treatment (Fig. 3.35D; see also Fig. 3.24C). The same trend was detected in CL-treated *cca1-1 lhy-11* plants. The *elf3-9* mutant behaved somewhat differently regarding *TOC1* transcript abundance. Already under control (SD) conditions the *TOC1* levels were increased which corresponds to the slightly higher nighttime expression of *TOC1* in *elf3-4* plants also described by Dixon *et al.* (2011). Although still higher than in wild-type plants the *TOC1* levels did not increase upon CL treatment in *elf3-9* compared with control conditions. However, as shown by the mutation of *TOC1* in the cytokinin-deficient background (see Fig. 3.31) the elevation of *TOC1* levels in plants with a reduced cytokinin status was not crucial for the circadian stress response. More critical was the overall perturbation of the core oscillator, especially the morning genes *CCA1* and *LHY*, which led to a severely disturbed clock output (see Fig. 3.25). Although the impairment of CCA1 and LHY action as explained above was caused by different means in the investigated plants, the disruption of the clock output was strikingly similar

(Fig. 3.35E-F). The *CAB2* as well as the *CAT2* transcript levels were reduced to the same extent in *35S:CKX4* and in *cca1-1 lhy-11* and *elf3-9* plants, which hallmarks the malfunction of the circadian clock in response to CL treatment.

An additional earlier time point ("7.5 h") was integrated into the next set of graphs in order to evaluate if the kinetics/onset of the stress response was comparable between cytokinin-deficient plants and the clock mutants after CL treatment (Fig. 3.36A). The strong elevation in transcript abundances of oxidative stress marker genes *BAP1* and *ZAT12* already after "7.5 h" of darkness following CL treatment indeed indicated that the onset and degree of the stress response was similar in *35S:CKX4* and the clock mutants (Fig. 3.36B-C). However, the expression reached a slightly higher level in *35S:CKX4* plants after "12.5 h" of darkness. In agreement with the previous results CL-treated wild-type plants also exhibited a (molecular) stress phenotype, albeit rather weak. The transcript abundance of the cell death marker gene *BI1* was also slightly elevated in the CL-treated wild type (Fig. 3.36D). But these levels were definitely exceeded in *35S:CKX4* plants and the clock mutants in the late night ("12.5 h") following CL conditions which indicates cell death progression. Earlier, at "7.5 h" the *BI1* transcript levels already tended to be increased in comparison with the wild type. This was particularly the case in the clock mutants which is consistent with the previous observation that the cell death was initiated around "7.5 h" after CL treatment (see Fig. 3.19G and 3.23D; sometimes more pronounced after "10 h", see Fig. 3.44C). Interestingly, the transcript abundance of the previously introduced gene *TIC* (see Fig. 3.34D-G) was similarly decreased in the clock mutants as in *35S:CKX4* plants after CL treatment (Fig. 3.36E). Even more intriguingly, also the A-type *ARR* genes *ARR4*, *ARR7*, *ARR9*, and *ARR16* were reduced in their expression levels in response to the CL regime in the clock mutants (Fig. 3.36F-I). In Figure 3.26 the CL-dependent misregulation of several cytokinin-associated genes, including the ones shown here, were depicted. These results revealed that the proper cycling of these genes was influenced by the cytokinin status and the circadian clock performance. Therefore, it was surprising to observe that the misexpression of these *ARRs* after CL treatment was independent of an altered cytokinin status. In all cases the relative decrease was even more pronounced in the clock mutants compared with *35S:CKX4* plants (see corresponding tables in Fig. 3.36J). But the *ARR* levels in the clock mutants under control conditions were comparable to or even higher than in the wild type reflecting a normal cytokinin status. This emphasizes the importance of the circadian clock for cytokinin-associated gene expression and points to a time-of-day-specific regulation by the oscillator (gating).

Taken together, the results in Figure 3.35 and 3.36 clearly demonstrate that the reduced action of CCA1/LHY at nighttime following CL treatment results in a very similar molecular phenotype in cytokinin-deficient and *cca1-1 lhy-11* or *elf3-9* plants. In other words, the circadian stress phenotype after CL treatment is caused by an insufficient clock performance – either directly due to defects in the circadian clock itself or indirectly due to lacking input signals conferred by cytokinin signaling. Therefore, these data further underline the connection of cytokinin and the circadian clock in the response to changing light-dark regimes.

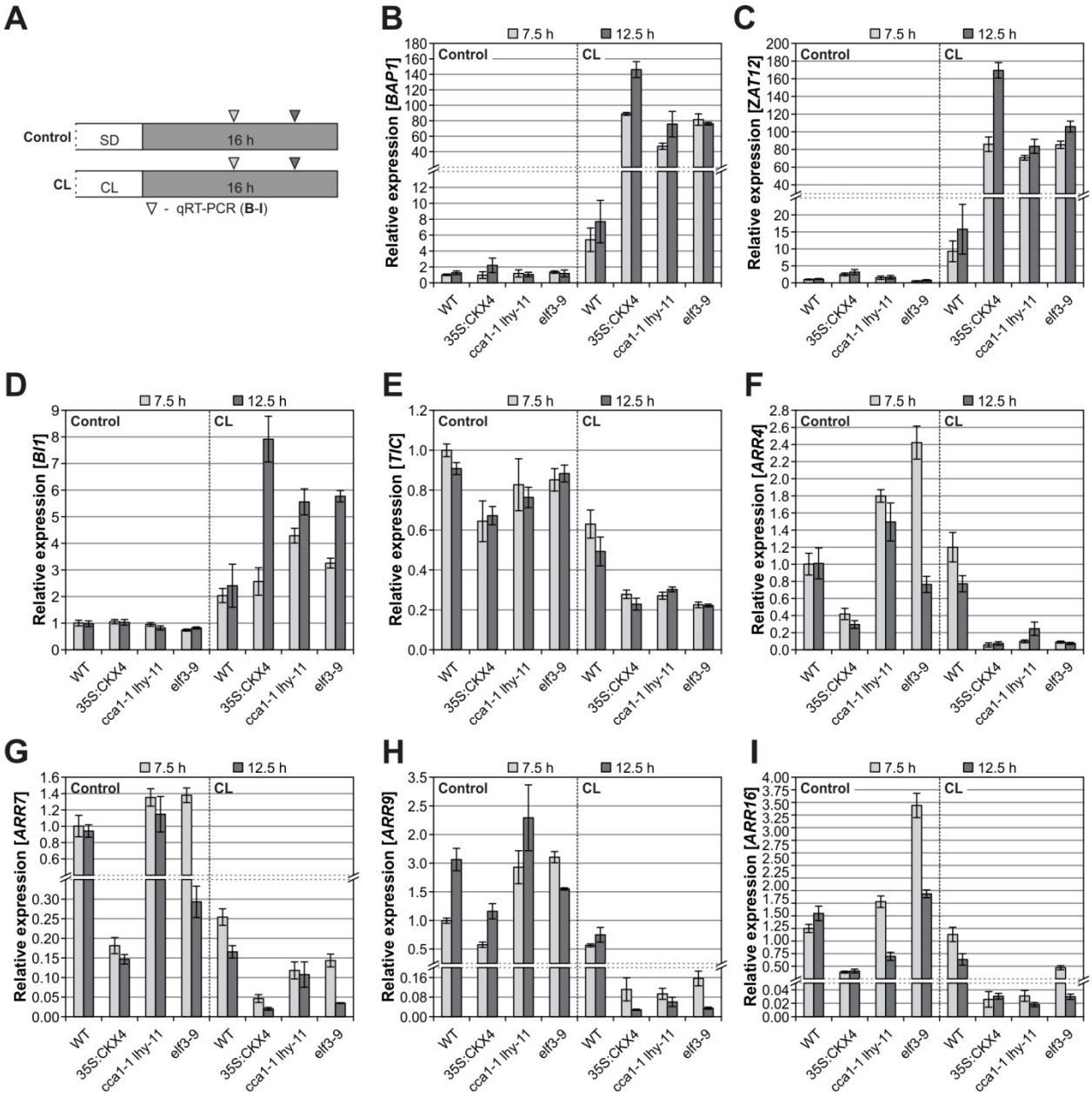

J

	BAP1		ZAT12		BI1		TIC		ARR4		ARR7		ARR9		ARR16	
	7.5 h	12.5 h	7.5 h	12.5 h	7.5 h	12.5 h	7.5 h	12.5 h	7.5 h	12.5 h	7.5 h	12.5 h	7.5 h	12.5 h	7.5 h	12.5 h
WT	5.4	6.2	9.3	14.0	2.1	2.4	-1.6	-1.8	1.2	-1.3	-3.9	-5.7	-1.8	-2.7	-1.1	-3.4
35S:CKX4	92.1	65.7	34.2	53.5	2.4	7.6	-2.3	-2.9	-7.6	-3.8	-3.9	-7.4	-5.1	-40.8	-5.4	-5.2
cca1-1 lhy-11	39.2	73.0	47.8	50.2	4.4	6.7	-3.0	-2.5	-18.4	-6.0	-11.4	-10.6	-20.7	-46.2	-49.5	-24.8
elf3-9	59.8	64.6	147.0	135.3	4.4	7.1	-3.8	-4.0	-27.4	-9.9	-9.7	-8.4	-13.5	-44.4	-15.3	-56.6

Fold change [CL vs. Control]

Figure 3.36: The clock mutants *cca1-1 lhy-11* and *elf3-9* display a highly similar molecular phenotype compared with *35S:CKX4* plants after continuous light treatment.

A, Schematic overview of the experimental design for **B**-**J**. White, light period; gray, dark period. The setup corresponds to the one shown in Fig. 3.35, except that samples for qRT-PCR were collected at an additional time point (after 7.5 hours). Transcript levels of oxidative stress marker genes *BAP1* and *ZAT12* (**B**-**C**), cell death marker gene *BI1* (**D**), clock-associated gene *TIC* (**E**), and A-type *ARR* genes *ARR4*, *ARR7*, *ARR9*, and *ARR16* (**F**-**I**) were determined. Data represent the mean and SE values of four biological replicates and are expressed as relative values compared with wild-type control (7.5 h), which was set to 1. *PP2AA2* and *MCP2D* served as reference genes. **J**, Tables display the respective fold changes for each gene [CL *versus* corresponding control] to facilitate the evaluation of CL-dependent changes in relative expression levels between the genotypes. Highlighted in gray, CL-induced divergences compared with the wild type; gray intensity reflects extent of divergence.

3.6.7 Contribution of pseudo-response regulator genes to the cell death phenotype after CL treatment

The pseudo-response regulators PRR9, PRR7, PRR5, and PRR3 belong to a five-member family together with TOC1 (identical to PRR1). They are components of the circadian clock and are essential for the function of the central oscillator (Matsushika *et al.*, 2000; Michael *et al.*, 2003a; Nakamichi *et al.*, 2005a; 2005b; 2010; Para *et al.*, 2007; Yamashino *et al.*, 2008; see 1.3.5.4). Thus, their involvement in the response to changing light-dark regimes was also examined. First of all, *prr* single and double mutants as well as the triple mutant *prr9 prr7 prr5* were subjected to CL conditions. Strikingly, although the triple mutant is known to have severe clock defects, including an arrhythmia phenotype (Nakamichi *et al.*, 2005b) the strongest CL response could be detected for the *prr3* single knockout (Fig. 3.37A-C). The cell death phenotype was intermediate between wild-type and *35S:CKX4* plants (Fig. 3.37A; for controls see Appendix Fig. A.10) as also reflected by the percentage of necrotic leaves (Fig. 3.37B) and the stress-induced decrease in F_v/F_m ratios (Fig. 3.37C). While *prr5* plants behaved like wild type all the other investigated mutants, including the triple knockout, tended to be less sensitive than wild type to the CL regime, which was deduced from the lower percentage of necroses (Fig. 3.37B). However, the lowest sensitivity to circadian stress was observed for *prr9* plants. In all experiments these plants either formed no necroses or only very rarely and were less affected than the wild-type plants. Together, the results point to a negative function of PRR9 under circadian stress conditions and indicate that the loss of PRR3 contributes to the cell death phenotype after CL treatment.

All PRRs of the so-called "PRR1/TOC1 quintet" are subjected to diurnal and circadian rhythms at the level of transcription (Matsushika *et al.*, 2000). In order to investigate if PRRs are also involved in the response of cytokinin-deficient plants to the CL regime, *PRR* gene expression profiles were recorded and analyzed (Fig. 3.38, for experimental design see Fig. 3.23A). Indeed, changes in transcript abundances were observed in all genotypes and for all tested *PRR* genes after CL treatment (Fig. 3.38A-D) reflecting the influence of the altered light-dark regime on clock-regulated gene expression. To examine potential differences in CL-dependent changes in *PRR* expression between wild-type and cytokinin-deficient plants the CL-induced fold changes were analyzed (see corresponding tables in Fig. 3.38A-D). Most prominent effects were found for *PRR3* (Fig. 3.38A). Usually *PRR3* expression peaks around dusk and subsequently the transcript levels continuously decrease reaching the minimum of expression in the morning (Matsushika *et al.*, 2000). The same pattern was detected for *PRR3* under control conditions used here (Fig. 3.38A). Interestingly, the gradual reduction of transcript abundance at nighttime was accelerated in cytokinin-deficient plants after CL treatment. Even more intriguing, the divergence to wild type started after "5 h" of darkness, coinciding with the induction of the stress response (see Fig. 3.23) and the divergence of *CCA1*/*LHY* (see Fig. 3.24) and *ELF3* (see Fig. 3.33) expression. The divergence of *PRR3* expression started with a 3- to 4-fold decrease in cytokinin-deficient plants ("5 h") and was even more pronounced later with an about 20-fold CL-induced change (see table in Fig. 3.38A). In contrast, the maximum CL-induced change detected in wild-type plants was only a 3-fold decrease ("10 h"). These differences support the idea

that a lack of *PRR3* expression might contribute to the overall cell death phenotype in cytokinin-deficient plants in response to the CL regime.

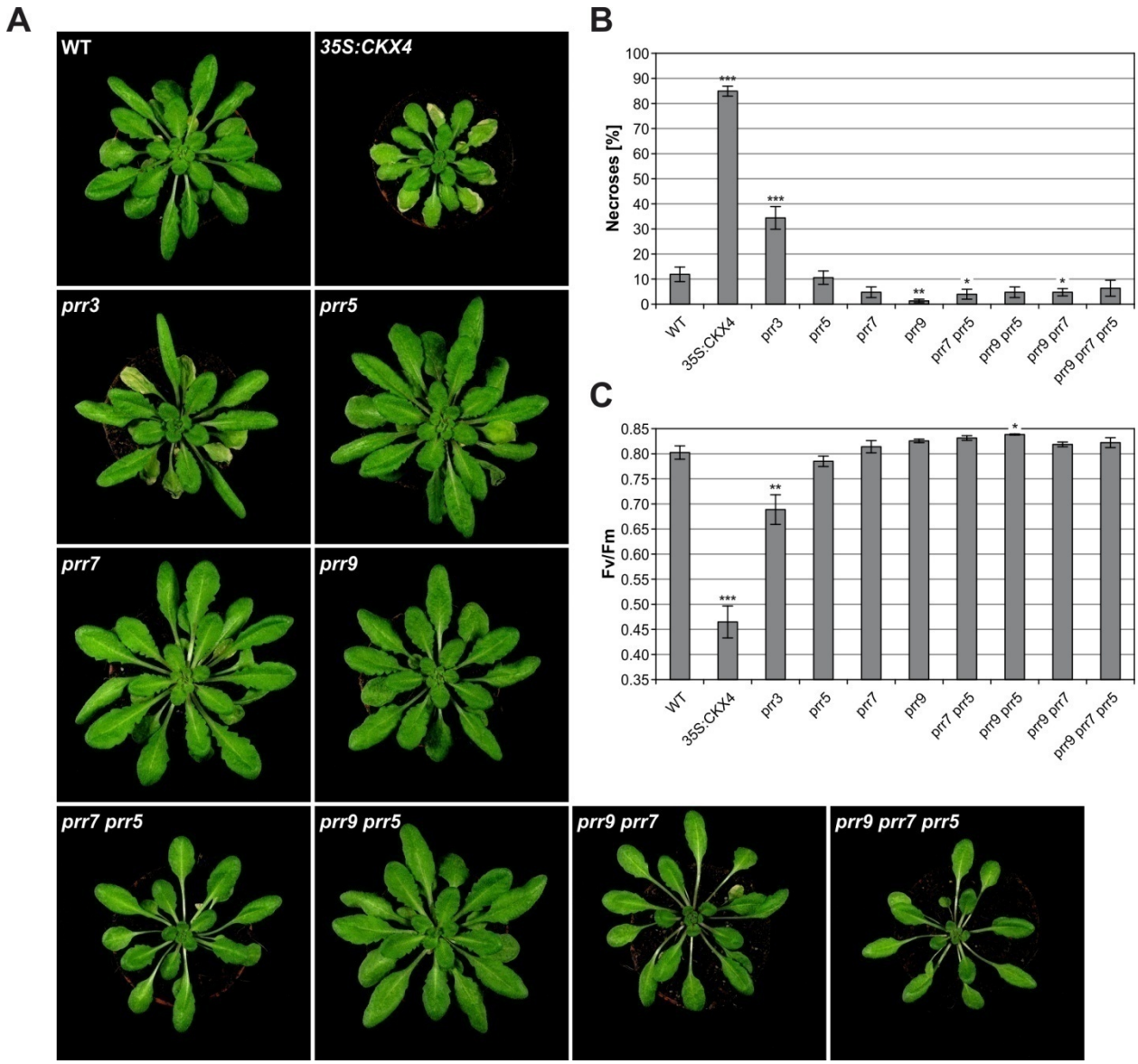

Figure 3.37: Contribution of pseudo-response regulators (PRRs) to the cell death phenotype after CL treatment.

A-**C**, CL response of single, double, and triple *prr* mutants in comparison with wild type and *35S:CKX4*. Six-week-old SD-grown plants were subjected to 32 hours of CL and transferred back into SD rhythm. Control plants remained in SD rhythm continuously and were not affected (for pictures see Appendix Fig. A.10). Pictures were taken two days after CL treatment and are representative for the observed phenotypes. **B**-**C**, The percentage of necrotic leaves counted in all mature leaves (**B**; n = 11) and the stress-induced decrease in F_v/F_m ratios (**C**; n = 12) measured one day after CL treatment. Experimental design corresponds to "32 h L/16 h D" shown in Fig. 3.6A. Asterisks indicate significant differences compared with wild type (*t* test: *, $p < 0.05$; **, $p < 0.01$; ***, $p < 0.001$). Error bars represent SE.

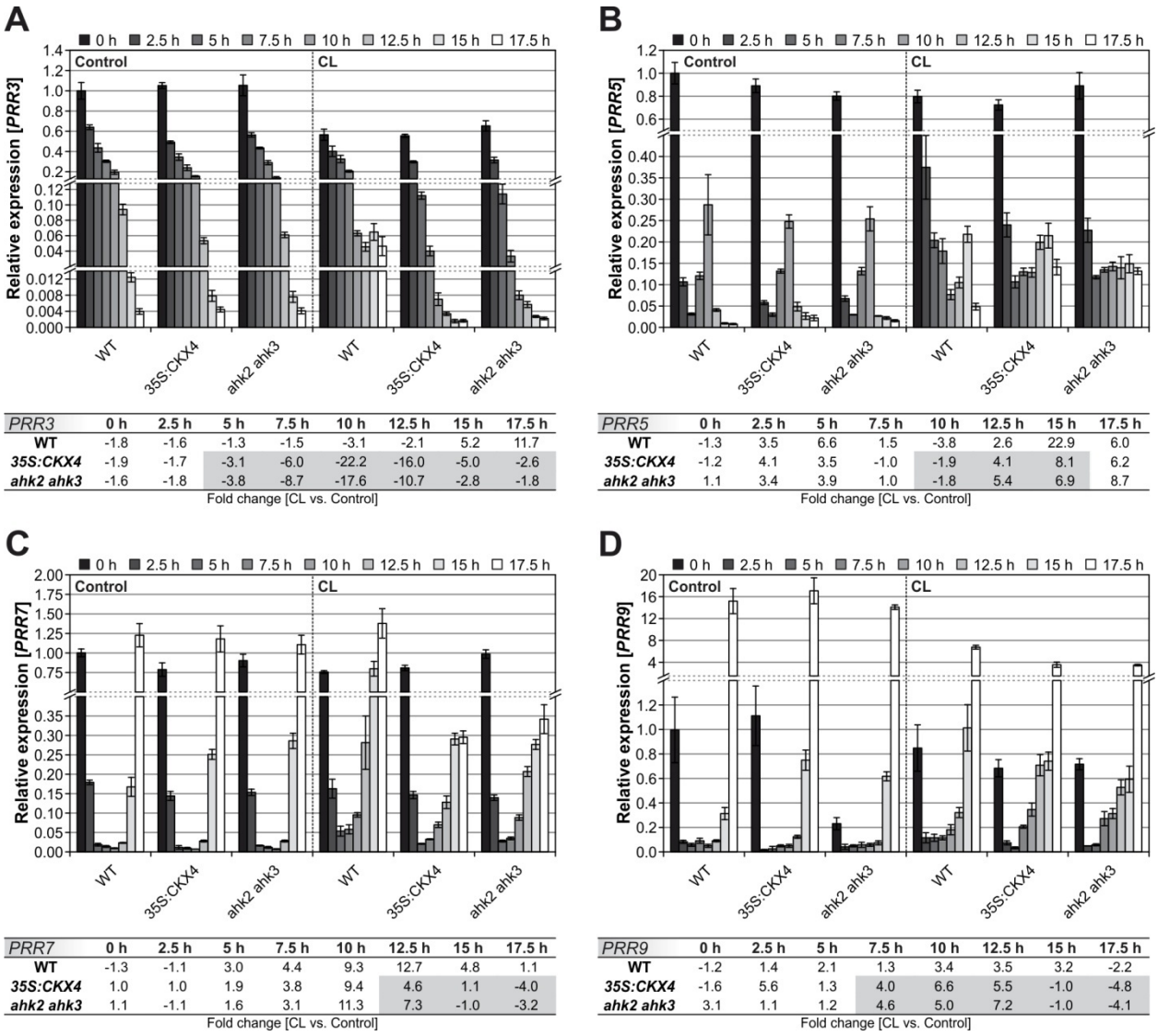

PRR3	0 h	2.5 h	5 h	7.5 h	10 h	12.5 h	15 h	17.5 h
WT	-1.8	-1.6	-1.3	-1.5	-3.1	-2.1	5.2	11.7
35S:CKX4	-1.9	-1.7	-3.1	-6.0	-22.2	-16.0	-5.0	-2.6
ahk2 ahk3	-1.6	-1.8	-3.8	-8.7	-17.6	-10.7	-2.8	-1.8

Fold change [CL vs. Control]

PRR5	0 h	2.5 h	5 h	7.5 h	10 h	12.5 h	15 h	17.5 h
WT	-1.3	3.5	6.6	1.5	-3.8	2.6	22.9	6.0
35S:CKX4	-1.2	4.1	3.5	-1.0	-1.9	4.1	8.1	6.2
ahk2 ahk3	1.1	3.4	3.9	1.0	-1.8	5.4	6.9	8.7

Fold change [CL vs. Control]

PRR7	0 h	2.5 h	5 h	7.5 h	10 h	12.5 h	15 h	17.5 h
WT	-1.3	-1.1	3.0	4.4	9.3	12.7	4.8	1.1
35S:CKX4	1.0	1.0	1.9	3.8	9.4	4.6	1.1	-4.0
ahk2 ahk3	1.1	-1.1	1.6	3.1	11.3	7.3	-1.0	-3.2

Fold change [CL vs. Control]

PRR9	0 h	2.5 h	5 h	7.5 h	10 h	12.5 h	15 h	17.5 h
WT	-1.2	1.4	2.1	1.3	3.4	3.5	3.2	-2.2
35S:CKX4	-1.6	5.6	1.3	4.0	6.6	5.5	-1.0	-4.8
ahk2 ahk3	3.1	1.1	1.2	4.6	5.0	7.2	-1.0	-4.1

Fold change [CL vs. Control]

Figure 3.38: Expression profiles of pseudo-response regulator genes are altered in response to circadian stress.

A-**D**, Kinetics of transcript abundances for the *PRR* genes *PRR3* (**A**), *PRR5* (**B**), *PRR7* (**C**), and *PRR9* (**D**) in a 2.5-hour time interval starting directly after SD or CL (0 h) and ending 17.5 hours later. The experimental setup corresponds to the one explained in Fig. 3.23 (for a schematic overview see Fig. 3.23A). Data in graphs represent the mean and SE values of four biological replicates and are expressed as relative values compared with the respective wild-type control (0 h), which was set to 1. *PP2AA2* and *MCP2D* were used as reference genes. To facilitate the evaluation of CL-dependent changes in relative expression levels between the genotypes tables have been inserted below each panel displaying the respective fold changes [CL *versus* corresponding control]. Highlighted in gray, CL-induced divergences in cytokinin-deficient plants compared with the wild type; gray intensity reflects extent of divergence.

The expression profiles of *PRR5* and *PRR7* did not reveal strong differences between wild type and plants with a reduced cytokinin status under control and also after CL treatment (Fig. 3.38B-C). At the end of the night following the CL regime (last three time points; see table in Fig. 3.38C) a higher expression of *PRR7* was observed in wild-type plants compared with cytokinin-deficient plants. This result correlates with the advanced and higher *CCA1*/*LHY* expression in these plants (see Fig. 3.24A-B) because CCA1 and LHY support the expression of *PRR7* by directly binding to its promoter (Farré *et al.*, 2005). Although CCA1/LHY promote *PRR9* expression in a similar manner, the *PRR9* expression pattern

does not reflect this relationship (Fig. 3.38D). Cytokinin-deficient plants rather show an increased *PRR9* abundance compared with the wild type ("7.5 h" to "12.5 h") after CL treatment (see corresponding table in Fig. 3.38D) although *CCA1* and *LHY* expression were attenuated (see Fig. 3.24A-B). This increase in *PRR9* levels coincided with the strongest differences in *CCA1*/*LHY* expression between wild-type and cytokinin-deficient plants (see Fig. 3.24) and succeeded the decreased *ELF3* abundance in *35S:CKX4* and *ahk2 ahk3* plants (see Fig. 3.33). The *prr9* mutant analysis pointed to a negative function of PRR9 in the response to changed light-dark regimes (see Fig. 3.37). Therefore, one could conclude that the increased *PRR9* expression in cytokinin-deficient plants might contribute to the circadian stress.

3.7 The role of the JA pathway and ROS homeostasis in the development of cell death in response to circadian stress

3.7.1 Synthesis and response gene expression of the classical stress hormones ABA, SA, and JA

The circadian clock of plants with a reduced cytokinin status is perturbed in response to substantial changes in the light-dark regime. The desynchronization of the core oscillator coincided with the induction of a severe stress response eventually leading to cell death initiation. In order to unravel which signaling pathways might mediate the stress and succeeding cell death responses, qRT-PCR analyses were performed to determine synthesis and response gene expression of the classical stress hormones ABA, SA, and JA.

The first visible symptoms (limp leaves especially in *35S:CKX4* plants) were detectable after "10 h" of darkness following CL treatment (see Fig. 3.14). Therefore, the sampling for qRT-PCR analysis started at that time point. In addition, leaf samples were harvested two and four hours later after "12 h" and "14 h" (Fig. 3.39A). Since several studies revealed a crosstalk between cytokinin and ABA during stress (Tran *et al.*, 2007; Nishiyama *et al.*, 2011a; Ha *et al.*, 2012), ABA-associated genes were investigated first. The expression of ABA synthesis genes was not dramatically altered among the genotypes or in response to the CL regime (Fig. 3.39B-D). While *AAO3* (Fig. 3.39B) tended to be higher expressed in cytokinin-deficient plants after CL treatment, the opposite tendency was observed for *ABA1* (Fig. 3.39C) and *ABA2* (Fig. 3.39D). But the overall changes were marginal. The results for the ABA response genes looked somewhat different. Indeed, differential expression patterns between wild-type and cytokinin-deficient plants were detected after CL treatment, being characterized by higher transcript levels of *RD29B* (Fig. 3.39E) and *COR47* (Fig. 3.39F) in *35S:CKX4* and *ahk2 ahk3* plants. However, the transcript levels of both genes reached even higher or similar levels in *35S:CKX4* control plants. Therefore, the detected differences after the CL regime are unlikely causal for the cell death phenotype, as cell death was not initiated in control plants.

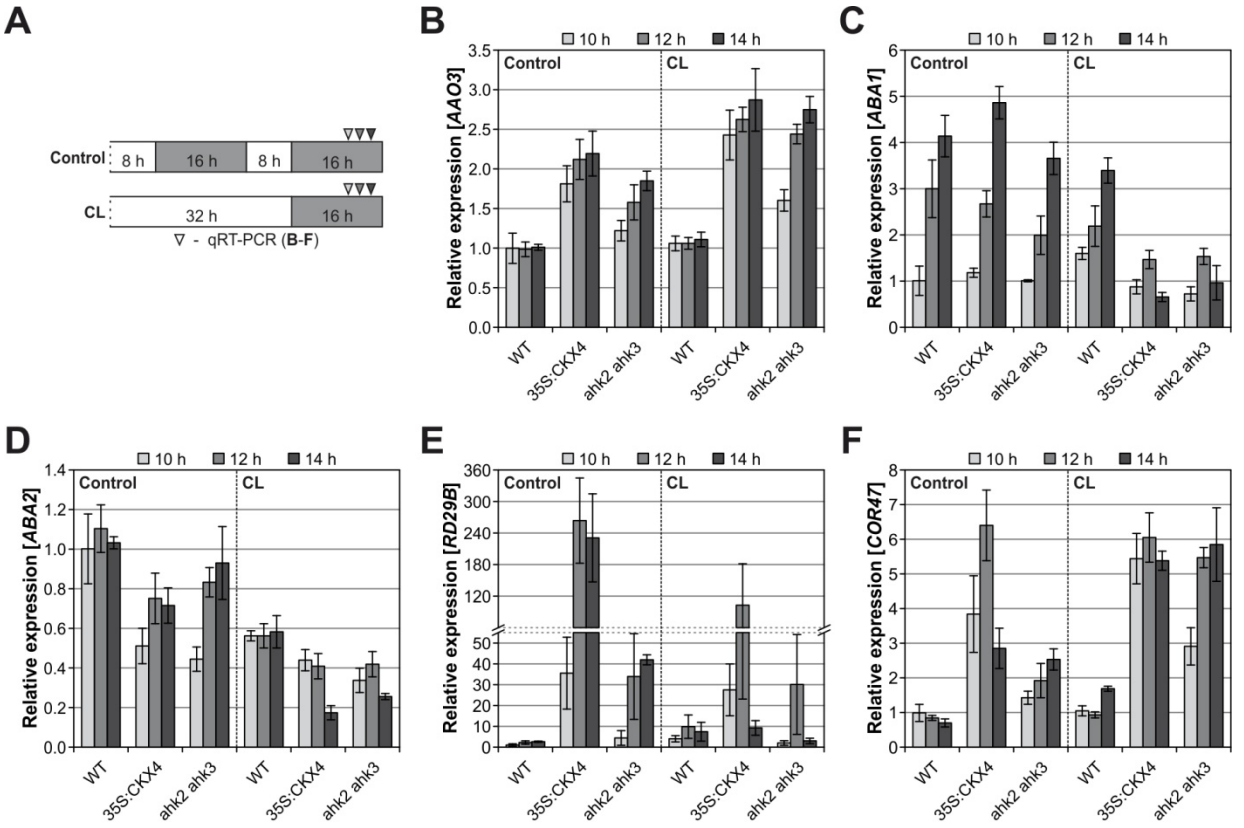

Figure 3.39: Expression of abscisic acid synthesis and response genes following continuous light treatment.

A, The scheme represents the experimental setup in **B**-**F**. White, light period; gray, dark period. Plants were grown under SD rhythm for six weeks prior to the indicated treatment. Leaf samples for qRT-PCR analysis were collected 10, 12, and 14 hours of darkness following CL treatment or a normal SD light period, respectively. Transcript levels of ABA synthesis genes *AAO3*, *ABA1*, and *ABA2* (**B**-**D**) and ABA response genes *RD29B* and *COR47* (**E**-**F**) were determined. Data represent the mean and SE values of four biological replicates and are expressed as relative values compared with the 10-hour wild-type control, which was set to 1. *CI51* and *PP2AA2* were used as reference genes. Abbreviations of gene names are explained in the list at the beginning of this work.

Secondly, SA synthesis and response gene expression was investigated because SA is known to be involved in different forms of cell death (see 1.5.2) and, moreover, a strong increase in *PR1* expression has already been shown for late stages of cell death progression in this work (see Fig. 3.12F). Although both tested SA synthesis genes were clearly induced in cytokinin-deficient plants in comparison with the wild type after CL treatment (Fig. 3.40A-B), the transcript levels of SA response genes showed the opposite pattern (Fig. 3.40C-E). The differences in expression patterns were especially pronounced for *PR1* (Fig. 3.40D) and *PR5* (Fig. 3.40E). In CL-treated wild-type plants both genes were strongly upregulated in comparison with CL-treated *35S:CKX4* and *ahk2 ahk3* plants. It is known that cytokinin can positively regulate SA signaling (Choi *et al.*, 2010). Therefore, the hypothesis arose that the support of SA signaling due to functional cytokinin signaling in wild-type plants might be protective under circadian stress.

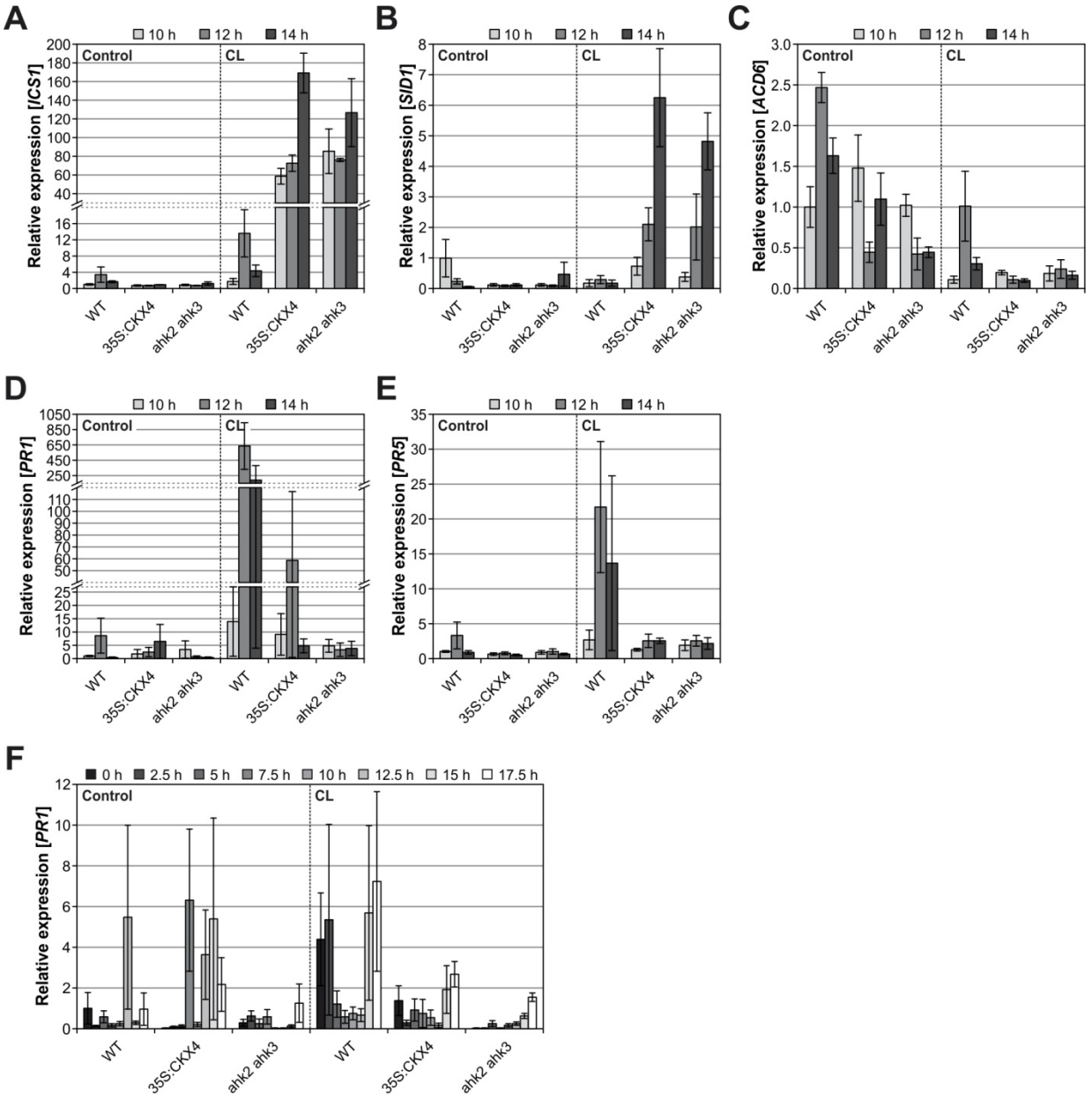

Figure 3.40: Expression of salicylic acid synthesis and response genes following continuous light treatment.

A-**E**, Transcript levels of SA-associated genes in six-week-old plants after 10, 12, and 14 hours of darkness following CL treatment or a normal SD light period, respectively (as indicated in Fig. 3.39A). The expression levels of SA synthesis genes *ICS1* and *SID1* (**A**-**B**) and SA response genes *ACD6*, *PR1*, and *PR5* (**C**-**E**) were determined. **F**, Kinetics of the *PR1* transcript abundance in a 2.5-hour time interval starting directly after CL or a normal SD light period (0h) and ending 17.5 hours later (for a schematic overview see Fig. 3.23A). All data represent the mean and SE values of four biological replicates and are expressed as relative values compared with the respective wild-type control, which was set to 1 (**A**-**E**, 10-hour wild-type control; **F**, 0-hour wild-type control). *CI51* and *PP2AA2* (**A**-**E**) as well as *PP2AA2* and *MCP2D* (**F**) were used as reference genes. Abbreviations of gene names are explained in the list at the beginning of this work.

To further evaluate this hypothesis, the complete expression profile of the *PR1* gene was recorded during the dark period following a normal SD light period (controls) or CL treatment (for experimental design see Fig. 3.23A). The *PR1* expression kinetics revealed that the transcript abundance was highly variable, even under control conditions (Fig. 3.40F), while the cell death phenotype was strongly

reproducible and specific. Since SA-related transcript abundances could not be reliably correlated to the cell death phenotype, these results did not support the hypothesis that the SA pathway might be decisive for the cell death phenomenon. Moreover, SA signaling mutants, *npr1-1* and *npr1-2* (Cao *et al.*, 1997), were tested for the cell death phenotype after CL treatment. If proper SA signaling was protective, these mutants should develop necroses in response to the CL regime. Both mutants were not affected (data not shown). Therefore, the hypothesis has been largely disproven.

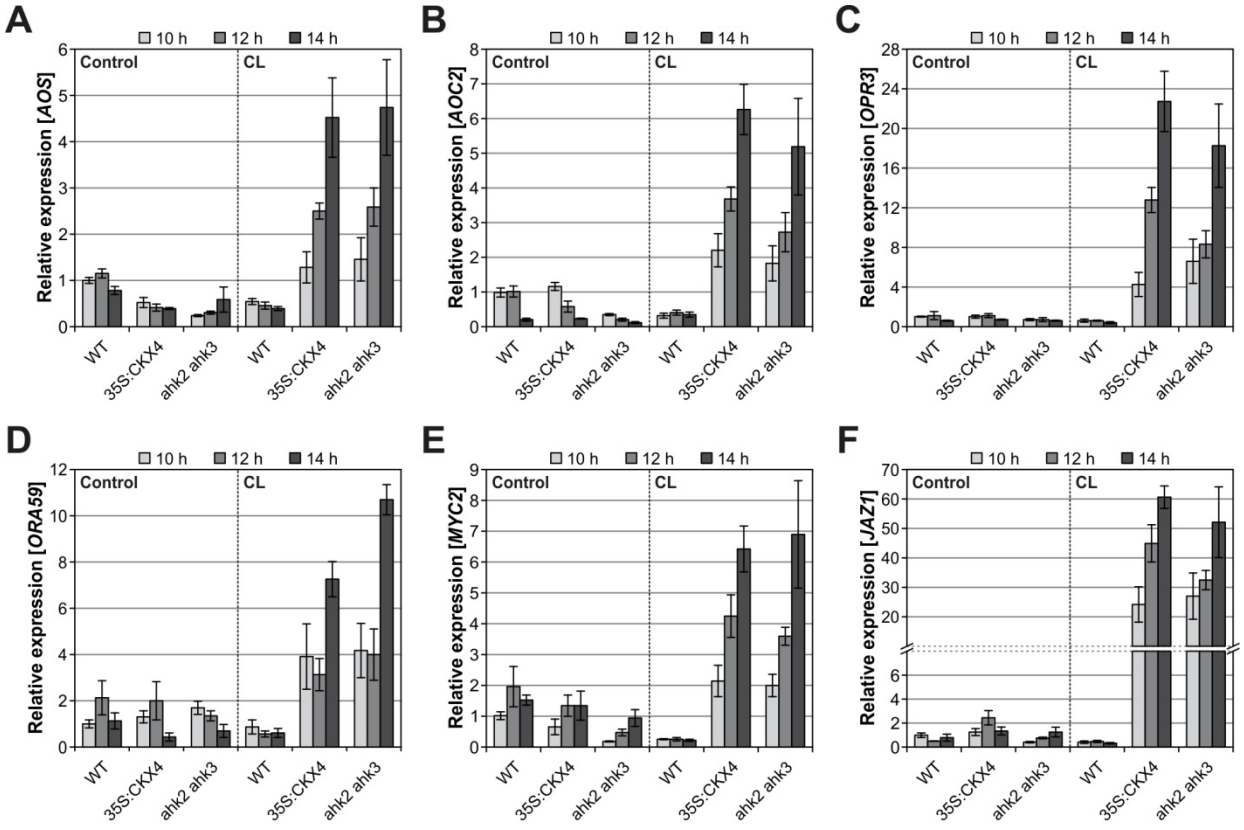

Figure 3.41: Expression of jasmonic acid synthesis and response genes following continuous light treatment.
A-**F**, Transcript levels of JA-associated genes in six-week-old plants after 10, 12, and 14 hours of darkness following CL treatment or a normal SD light period, respectively (as indicated in Fig. 3.39A). The expression levels of JA synthesis genes *AOS*, *AOC2*, and *OPR3* (**A**-**C**) and JA response genes *ORA59*, *MYC2*, and *JAZ1* (**D**-**F**) were determined. Data represent the mean and SE values of four biological replicates and are expressed as relative values compared with the respective 10-hour wild-type control, which was set to 1. *CI51* and *PP2AA2* were used as reference genes. Abbreviations of gene names are explained in the list at the beginning of this work.

Lastly, JA synthesis and response gene expression was analyzed using the same experimental setup as for ABA- and SA-related genes (see Fig. 3.39A). Intriguingly, all tested synthesis (Fig. 3.41A-C) and response genes (Fig. 3.41D-F) exhibited highly similar expression patterns and were exclusively upregulated in cytokinin-deficient plants after CL treatment. In order to find out whether the changes in transcript levels of JA-associated genes coincide with the onset of the molecular stress response in *35S:CKX4* and *ahk2 ahk3* plants following the CL regime, the expression kinetics of several JA-related genes was recorded (Fig. 3.42; for CL-induced fold changes see tables in Appendix Fig. A.11). The stress marker genes *BAP1* and *ZAT12* were already induced after "5 h" of darkness following CL

treatment (see Fig. 3.23B-C). Strikingly, the same was true for the tested JA synthesis genes *LOX3*, *LOX4*, and *OPR3* (Fig. 3.42A-C).

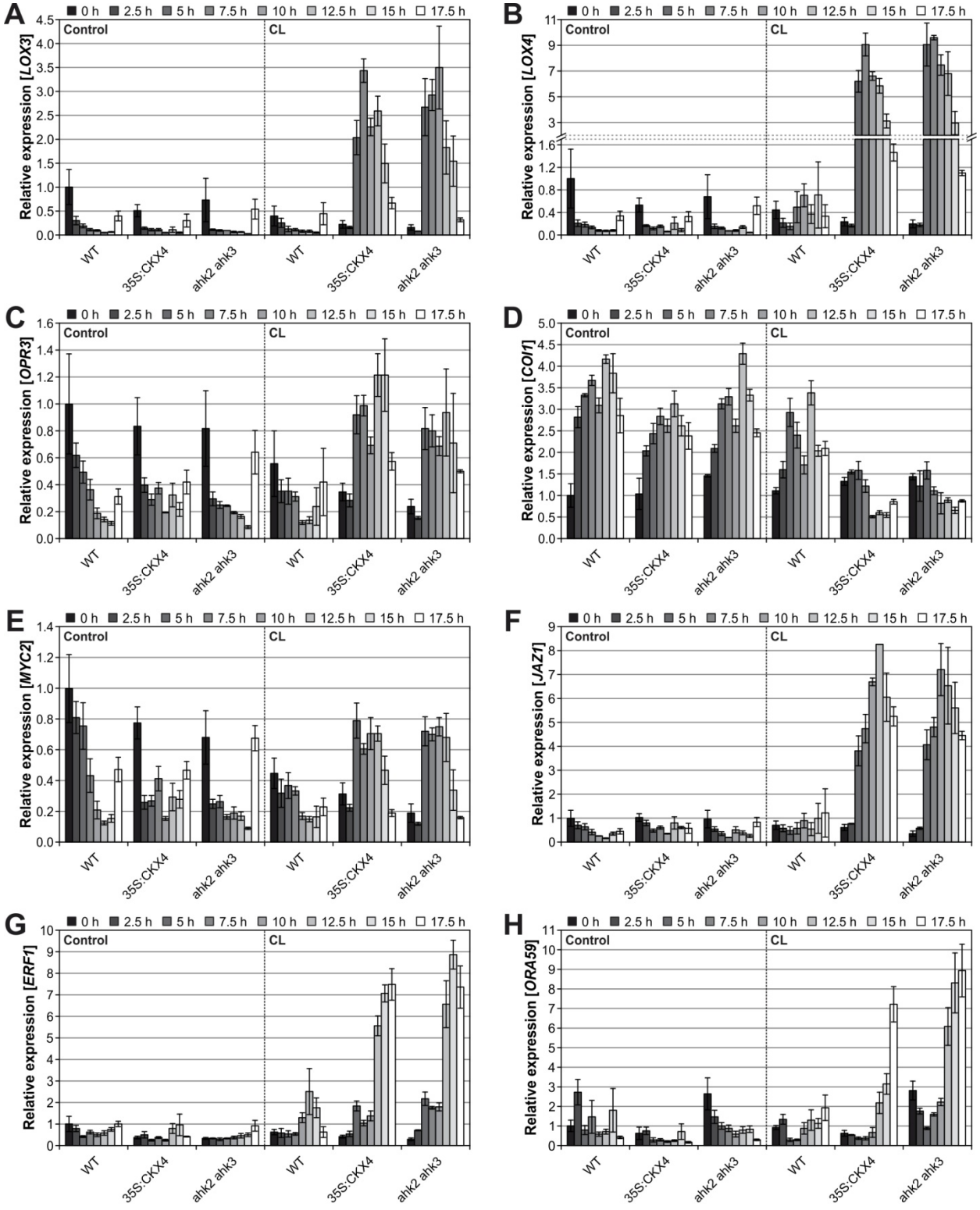

Figure 3.42: Jasmonic acid synthesis and response genes are strongly induced in cytokinin-deficient plants during the dark period following continuous light treatment.

Figure 3.42 continued.

A-**H**, Kinetics of JA-related transcript levels in a 2.5-hour time interval starting directly after SD or CL (0h) and ending 17.5 hours later (for a schematic overview see Fig. 3.23A). The expression levels of JA synthesis genes *LOX3* (**A**), *LOX4* (**B**), and *OPR3* (**C**) as well as the JA receptor gene *COI1* (**D**) were recorded. Moreover, two classes of JA response genes were analyzed: *MYC2* (**E**) and *JAZ1* (**F**) belonging to the MYC branch and the transcription factor genes *ERF1* (**G**) and *ORA59* (**H**) involved in the ERF branch of JA signaling. All data represent the mean and SE values of four biological replicates and are expressed as relative values compared with the respective 0-hour wild-type control, which was set to 1. *PP2AA2* and *MCP2D* served as reference genes. Abbreviations of gene names are explained in the list at the beginning of this work. For corresponding fold-change tables see Appendix (Fig. A.11).

The JA receptor gene *COI1* was also investigated (Fig. 3.42D). It was already shown that *COI1* transcript abundance oscillates under diurnal conditions correlating with rhythmic JA responses (Shin *et al.*, 2012). Moreover, Shin and colleagues have shown that *COI1* expression was downregulated by JA treatment. Therefore, it was interesting to observe, that cytokinin-deficient plants exhibited a reduced *COI1* expression after CL treatment especially during the second half of the night (Fig. 3.42D), while *COI1* levels in control and CL-treated wild-type plants followed an oscillation wave peaking around that time. Together, the increase in JA synthesis gene expression and the attenuated *COI1* expression suggested an elevated JA content presumably activating JA signaling in CL-treated cytokinin-deficient plants. Indeed, the expression profiles of MYC branch JA response genes *MYC2* and *JAZ1* indicated an activation of JA signaling in these plants (Fig. 3.42E-F). Additionally, the induction of these genes also started after "5 h" of darkness following CL treatment coinciding with the onset of the molecular stress response (see Fig. 3.23B-C) and the divergence in core oscillator gene expression (see Fig. 3.24A-B). *MYC2* has been shown to display minimal expression during the night starting to decrease at dusk under diurnal conditions (Shin *et al.*, 2012). Interestingly, this nighttime repression was not only confirmed for *MYC2* (Fig. 3.42E) but seemed to be a universal phenomenon which was observed in wild-type control plants for all JA synthesis and response genes shown in Figure 3.42A-F (excluding *COI1*). The maximal decrease in expression was characterized by fold changes between 7- and 19-fold in these plants (between "0 h" and "12.5 h"/"15 h"). While the oscillations of these genes were very precise in the wild-type control, several small alterations compared with the wild type could be observed in the cytokinin-deficient control plants (being more frequently in *35S:CKX4*).

Together, the results point to a connection between the stress and cell death responses triggered by CL treatment and the activation of JA signaling. They further indicate that the circadian stress causes a complete inversion of the normal (control) oscillation waves of JA-associated gene expression due to the desynchronized circadian clock. The link between circadian stress and a misregulated JA-related gene expression was in part also observed in CL-treated wild-type plants. The wild type also encounters circadian stress, albeit to a much weaker extent (e.g. see Fig. 3.19). In line with that, small perturbations in JA-related gene expression after CL treatment were detected compared with the respective wild-type control, most pronounced for *LOX4* and *JAZ1* (Fig. 3.42B and F). This further supports the hypothesis that circadian stress affects proper JA-associated gene expression.

In contrast, the transcription factor genes *ERF1* and *ORA59*, belonging to the ERF branch of JA signaling (see 1.6.2), did not exhibit a distinct rhythmic expression under control conditions (Fig. 3.42G-H). Furthermore, both genes were induced in cytokinin-deficient plants after CL treatment, though highly pronounced rather at later time points (starting at "12.5 h"). These data indicate that

the ERF branch of JA signaling was probably activated at later stages during cell death progression and that this might be a secondary event.

3.7.2 The activation of the JA pathway is linked to a perturbed circadian clock and is abolished after resetting of the oscillator

To further corroborate the hypothesis that the circadian clock is linked to JA-associated gene expression, *JAZ1* and *MYC2* transcript levels were exemplarily determined in clock mutants in response to circadian stress. For qRT-PCR analysis, the same experimental setting was used as described in Figure 3.36 in order to explore gene expression after "7.5 h" and "12.5 h" of darkness following CL treatment or a normal SD light period (Fig. 3.43A). Consistent with the previous results (see Fig. 3.42), the transcript levels of *JAZ1* as well as of *MYC2* were elevated in *35S:CKX4* plants in response to the CL regime at each time point tested, indicating an activated JA pathway. Both JA response genes were also induced in *cca1-1 lhy-11* and *elf3-9* plants (Fig. 3.43B-C). The overall increase in transcript abundance was slightly smaller than in *35S:CKX4* plants. In comparison with the respective controls the *JAZ1* and *MYC2* transcript abundances increased by about 8- to 15-fold and 2- to 4-fold in the clock mutants, while a 14- to 20-fold and about 5-fold increase was observed in *CKX4* overexpressing plants, respectively (see corresponding table in Fig. 3.43D). In contrast, *MYC2* expression was even slightly decreased in the CL-treated wild type (Fig. 3.43C). Hence, the data reveal that the disturbance of the core oscillator in the investigated clock mutants could largely mimic the effect of cytokinin deficiency after exposure to changed light-dark regimes also in terms of JA-related gene expression.

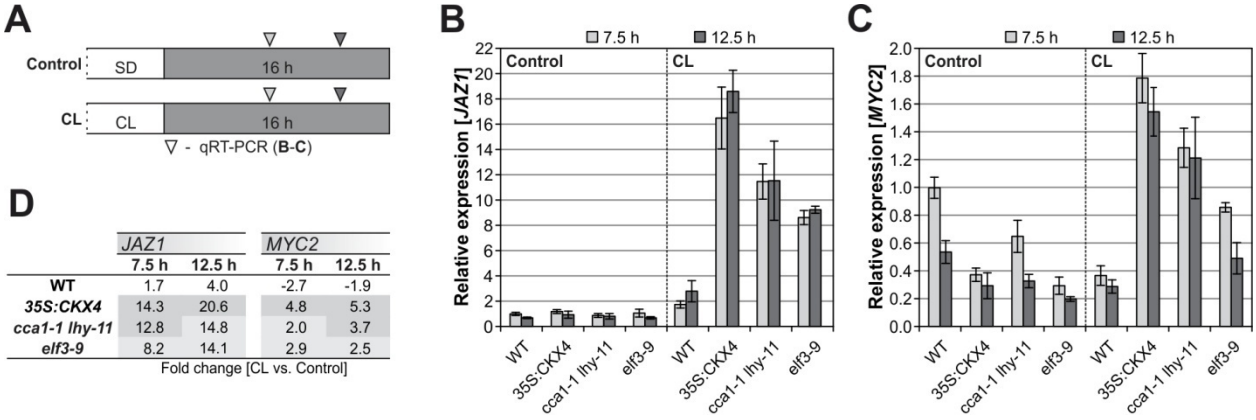

D

	JAZ1		MYC2	
	7.5 h	12.5 h	7.5 h	12.5 h
WT	1.7	4.0	-2.7	-1.9
35S:CKX4	14.3	20.6	4.8	5.3
cca1-1 lhy-11	12.8	14.8	2.0	3.7
elf3-9	8.2	14.1	2.9	2.5

Fold change [CL vs. Control]

Figure 3.43: The continuous light response in clock mutants is also characterized by an induction of jasmonic acid response genes.

A, Schematic overview of the experimental design for **B**-**D**. White, light period; gray, dark period. The setup corresponds to the one shown in Figure 3.36. Prior to the experiment all plants were grown under SD rhythm for six weeks. Samples for qRT-PCR analysis were collected after 7.5 and 12.5 hours of darkness following CL treatment or a normal SD light period. Transcript levels of the JA response genes *JAZ1* (**B**) and *MYC2* (**C**) were determined in the clock mutants *cca1-1 lhy-11* and *elf3-9* and in *35S:CKX4* and wild-type plants. Data represent the mean and SE values of four biological replicates and are expressed as relative values compared with the 7.5-hour wild-type control, which was set to 1. *PP2AA2* and *MCP2D* served as reference genes. **D**, Tables display the respective fold changes [CL *versus* corresponding control] to facilitate the evaluation of CL-dependent changes in relative expression levels between the genotypes. Highlighted in gray, CL-induced divergences compared with the wild type; gray intensity reflects the extent of divergence.

The following approaches, shown in Figure 3.44, were used to prove the link between an activated JA response and a perturbed circadian clock but also to unravel the potential connection between JA and the development of cell death. First, *JAZ1* expression was analyzed in young and mature leaves using the same experimental setup as explained in Figure 3.13. Similar to the expression of oxidative stress marker genes (see Fig. 3.13C-D), *JAZ1* was solely induced in mature leaves which undergo cell death progression after CL treatment, while no upregulation was detected in unaffected young leaves (Fig. 3.44B). This observation already points to a possible connection between JA and cell death under these conditions.

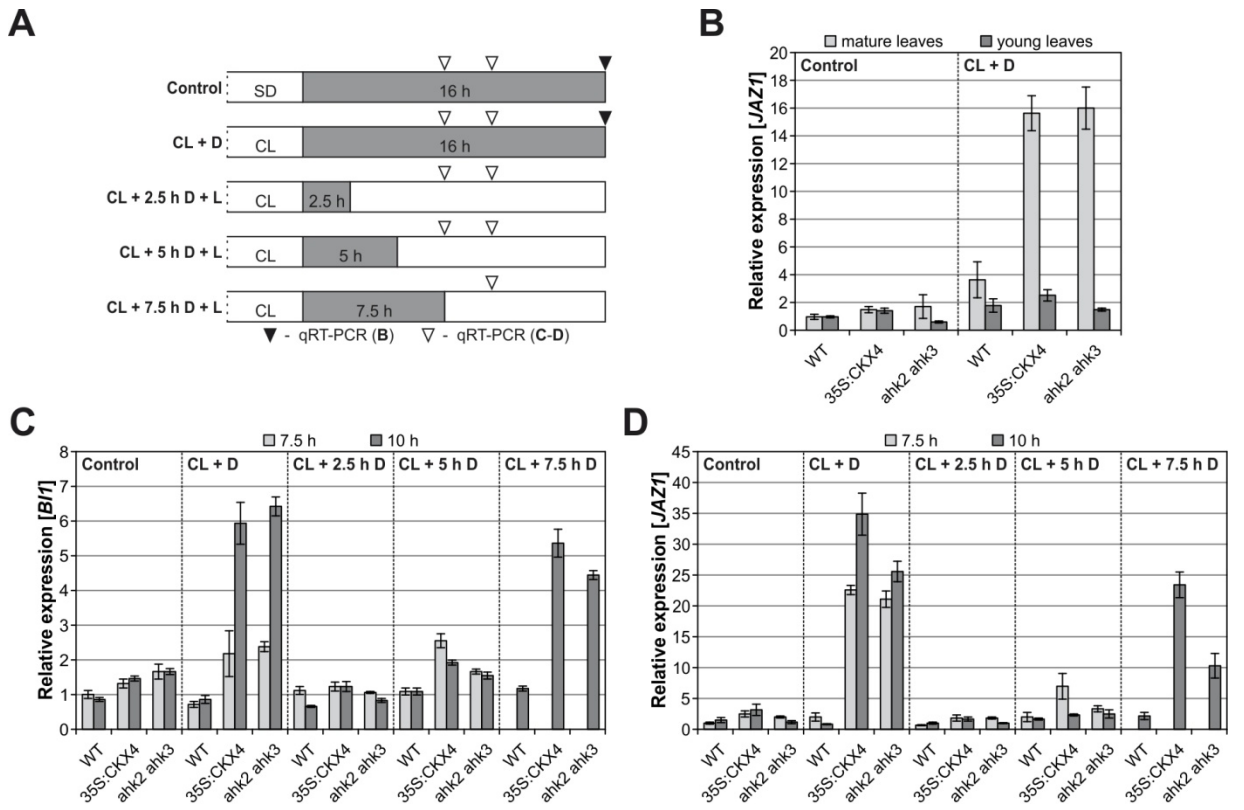

Figure 3.44: Re-entrainment of the circadian clock by earlier onset of light periods prevents cell death and the jasmonic acid response after short nights.

A, Schematic overview of the experimental design for **B**-**D**. White, light period; gray, dark period; "D", darkness. Prior to the indicated treatments all plants were grown under SD rhythm for six weeks. Leaf samples for qRT-PCR analysis were collected 16 hours (**B**) or 7.5 and 10 hours (**C**-**D**) after a SD light period or CL treatment, respectively. *JAZ1* expression was induced in CL-treated mature leaves of cytokinin-deficient plants (**B**; for the experimental design see also Fig. 3.13A-B). In addition to prolonged darkness following the SD or CL plants were also exposed to shorter dark periods (2.5, 5, and 7.5 h) following the CL regime. It was examined if the reversion of the cell death phenotype after short nights could be correlated to a rescue of the molecular phenotype concerning *BI1* (**C**; cell death marker) and *JAZ1* (**D**; JA response) expression. All data represent the mean and SE values of four biological replicates and are expressed as relative values compared with the respective wild-type control (**B**, mature leaves; **C**-**D**, 7.5 h), all of which were set to 1. *PP2AA2* and *MCP2D* were used as reference genes.

As demonstrated by previous experiments, cell death was not induced after short nights (2.5 and 5 hours) following CL treatment, while intermediate night lengths (7.5 hours) led to intermediate cell death phenotypes (see Fig. 3.16). Furthermore, the absence of cell death could be

correlated with the re-entrainment of the circadian clock by the earlier onset of light periods, which reset the expression of the core oscillator genes *CCA1*, *LHY*, and *TOC1*, especially after short nights (see Fig. 3.27). Consequently, the same experimental setup, this time including an additional time point ("7.5 h"; Fig. 3.44A), was used to analyze *BI1* and *JAZ1* expression after different night lengths (Fig. 3.44C-D). Elevated *BI1* transcript levels correlated with the initiation of cell death in the investigated plants (see Figs. 3.19G, 3.23D, and 3.36D). Accordingly, at "10 h" the *BI1* transcript abundance was strongly elevated in cytokinin-deficient plants after long or intermediate nights, but not after short nights that did not induce cell death (Fig. 3.44C). This indicates that a "point of no return" for cell death initiation is reached only after prolonged dark treatments. A small trend towards increased *BI1* transcript levels was observed in cytokinin-deficient plants (especially *35S:CKX4*) at "7.5 h" after "CL + 5 h D", indicating that a critical night length was almost reached. Similarly, *JAZ1* transcripts were also slightly elevated in these samples but were decreased again at "10 h", 5 hours after the re-start of light (Fig. 3.44D). Interestingly, *JAZ1* expression levels in *35S:CKX4* plants were even 10-fold increased directly after 5 hours of darkness following the CL regime (data not shown). This clearly demonstrates that the change in gene expression had already started (consistent with the results shown in Fig. 3.42F). However, instead of being further increased, as observed after prolonged darkness ("CL + D"), the earlier onset of light treatment resulted in a consecutive downregulation of *JAZ1* expression ("CL + 5 h D"; Fig. 3.44D). Therefore, the lowered *JAZ1* expression correlated with the rescue of the plants. Another indication that the *JAZ1* transcript abundance reflected the severity of the visually inspected phenotype was the complete lack of induction after 2.5 hours of darkness and the occurrence of intermediate levels after 7.5 hours of darkness.

JAZ1 transcript levels not only reflected well the severity of the visually inspected cell death (see Fig. 3.16B-C) but, strikingly, could also be correlated with the degree of clock resetting (see Fig. 3.27). Therefore, the data described in this section support the hypothesis that the circadian desynchronization of both clock mutants and cytokinin-deficient plants in response to the circadian stress regime determined the extent of JA responses which likely contributed to the cell death phenotype. Together, these results point to an interconnection between clock performance, the control of stress/JA responses and the occurrence of cell death.

3.7.3 Phytohormone measurements reveal strong alterations in JA metabolite levels

Phytohormone measurements were conducted in order to evaluate whether the profiles of synthesis and response gene expression (see 3.7.1) correspond with the respective phytohormone contents. Therefore, the ABA, SA, and JA levels were determined in two different setups. Setup 1 comprised time points corresponding to early stages of stress responses, including cell death initiation, while setup 2 comprised early and late stages of cell death progression (as indicated in Fig. 3.45A). Due to the loss of fresh weight accompanying cell death progression in cytokinin-deficient plants, the hormone levels of setup 2 were expressed per dry weight in order to avoid biased results based on altered fresh weights (setup 1, amount per fresh weight). Thus, the absolute values cannot be directly compared between both setups.

The ABA levels were slightly increased in cytokinin-deficient plants after 7.5 and 10 hours of darkness following CL treatment, while no alterations were detected at earlier time points (Fig. 3.45B). Therefore, the ABA content could not be linked to the induction of stress response genes which started already after 5 hours of darkness (see Fig. 3.23B-C). Moreover, the elevated ABA levels after 10 hours of darkness in response to the CL regime were not detected in setup 2 (Fig. 3.45C). No further increase in the ABA content was observed for later time points corresponding to late stages of cell death progression. Therefore, changes in the ABA content do not correlate with the stress and cell death phenotype in cytokinin-deficient plants in response to circadian stress, which is consistent with the results for ABA synthesis and response gene expression.

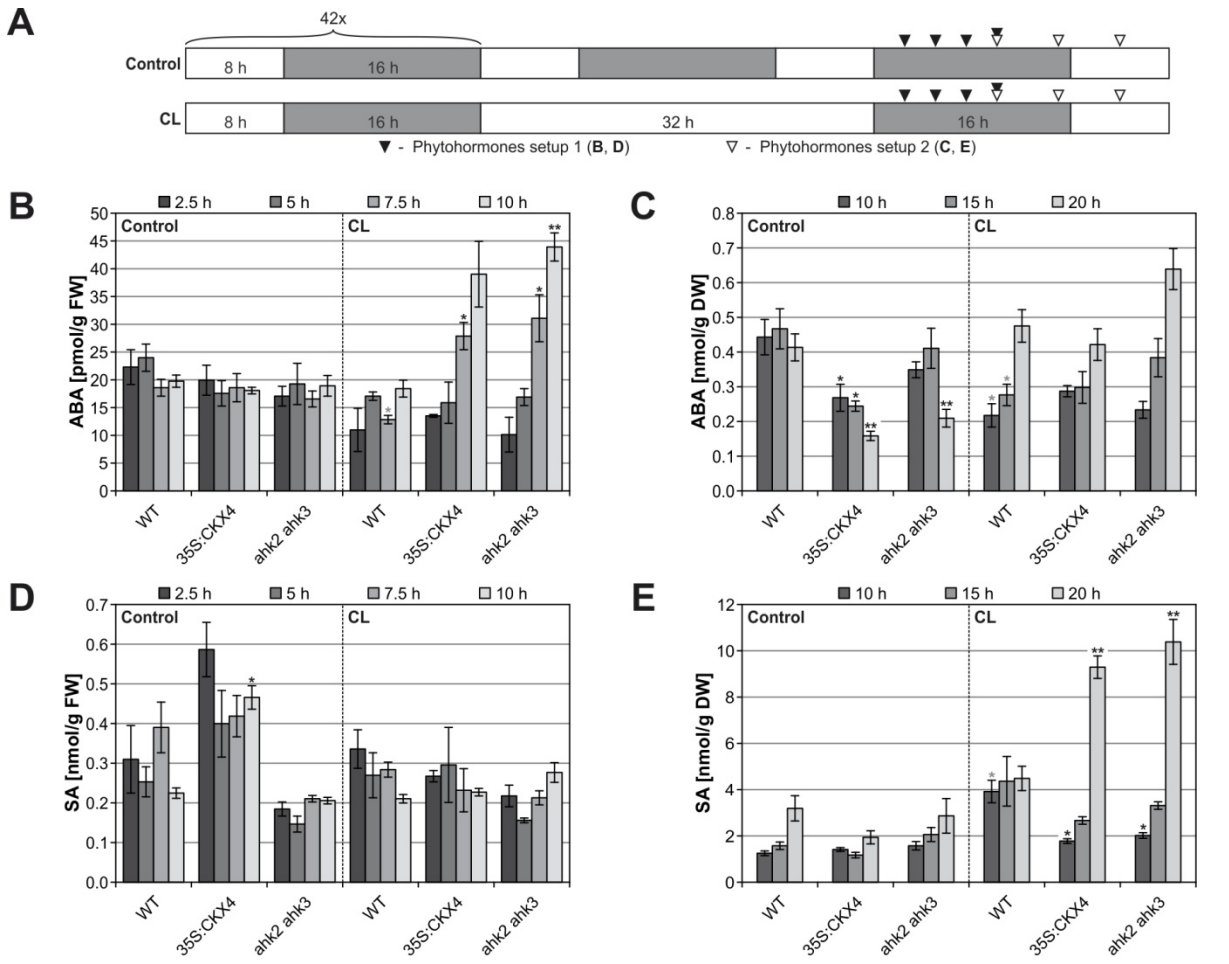

Figure 3.45: Abscisic acid and salicylic acid content after continuous light treatment at early and late stages of the stress and cell death response.

A, Representation of the experimental design. Plants were grown under SD conditions for six weeks. Control plants remained in the SD rhythm while a subset of plants was subjected to the CL treatment. Leaf samples for phytohormone measurements were collected for two different setups as indicated in the scheme. Setup 1 comprises four time points which correspond to early stages of the stress response, including cell death initiation. In contrast, setup 2 comprises three time points corresponding to early (10 h) and late stages (15 and 20 h) of cell death progression. **B** and **D**, ABA and SA content, respectively, per fresh weight (FW) in samples of setup 1 (as indicated in **A**). **C** and **E**, ABA and SA content, respectively, per dry weight (DW) in samples of setup 2 (see **A**). Asterisks indicate significant differences compared with the respective wild types (black) and with the corresponding controls (gray, for wild type only) (*t* test: *, $p < 0.05$; **, $p < 0.01$). Error bars represent SE (setup 1, n = 3; setup 2, n = 4). The phytohormone measurements were performed in collaboration with Prof. Dr. Ivo Feussner and Dr. Tim Iven (see 2.11).

Similarly, SA measurements also did not reveal strong increases in the SA content (Fig. 3.45D-E), which could attribute the stress and cell death responses in cytokinin-deficient plants to activated SA signaling or would explain the increased SA responses in the CL-treated wild type (concluded from the induction of *PR1* and *PR5*; see Fig. 3.40D-E). Only at "20 h" after CL treatment, rather late in cell death progression, SA levels were significantly increased in cytokinin-deficient plants (Fig. 3.45E). Therefore, SA might be involved in the process of cell death at later stages under these conditions which is also in accordance with the highly induced *PR1* gene expression 24 hours after CL treatment (see Fig. 3.12F).

Since the strong changes in JA synthesis and response genes pointed to a highly activated JA pathway in cytokinin-deficient plants upon circadian stress treatment (see Figs. 3.41 and 3.42), it was of particular interest to study if and eventually when JA levels rise to activate or enhance JA signaling. The gene expression profiles in cytokinin-deficient plants revealed that the JA response was already induced at "5 h" after CL treatment (see Fig. 3.42E-F). The obvious explanation would have been that a prior elevation in JA levels has caused this molecular JA response. Surprisingly, this was not the case. The results for setup 1, comprising the early time points following the CL regime (for experimental design see Fig. 3.45A), revealed that a rise of the JA and JA-Ile/-Leu content in comparison with the respective controls was not detectable until "10 h" after CL treatment (Fig. 3.46A-B). The amino acid conjugates JA-Ile and JA-Leu could not be separated with the used method. Therefore, JA-Ile/-Leu (Fig. 3.46B) reflects a mixture of both compounds comprising the biologically active JA-Ile. Similar results were obtained for JA precursors such as dinor-OPDA and OPC-6 (data not shown). The data clearly demonstrate that the activation of the JA response genes preceded the actual increase in JA metabolites. Hence, the results indicate that the activation of JA response genes was not caused by an increase in JA (JA-Ile) levels and either occurred in a JA-independent fashion or reflects an enhanced JA responsiveness. The *BI1* expression profiles (see Fig. 3.23D) together with the re-entrainment experiments (see Figs. 3.16B-C and 3.44C) indicated that a "point of no return" for cell death initiation was reached after 7.5 hours of darkness following the CL regime. This led to the conclusion that the induction of cell death preceded and, hence, did not depend on increased JA (JA-Ile) levels.

The increase in JA and JA-Ile/-Leu levels coincided with the first symptoms of cell death that were visible at "10 h" (Figs. 3.14A and 3.46A-B). The increased JA and JA-Ile/-Leu content at "10 h" was highly reproducible and conform with the increased levels of JA precursors in setup 2 (Fig. 3.46C-I; for setup see Fig. 3.45A). Interestingly, JA (Fig. 3.46C), its conjugates (Fig. 3.46D), and its precursors (Fig. 3.46E-I) accumulated to high levels at later time points ("15 h" and "20 h") after CL treatment. Hence, the accumulation of JA metabolites coincided with the phenotypically visible cell death phenotype and was strongly pronounced at late stages of cell death development. Therefore, these results indicate that the newly synthesized JA (JA-Ile) contributes to cell death progression under these conditions.

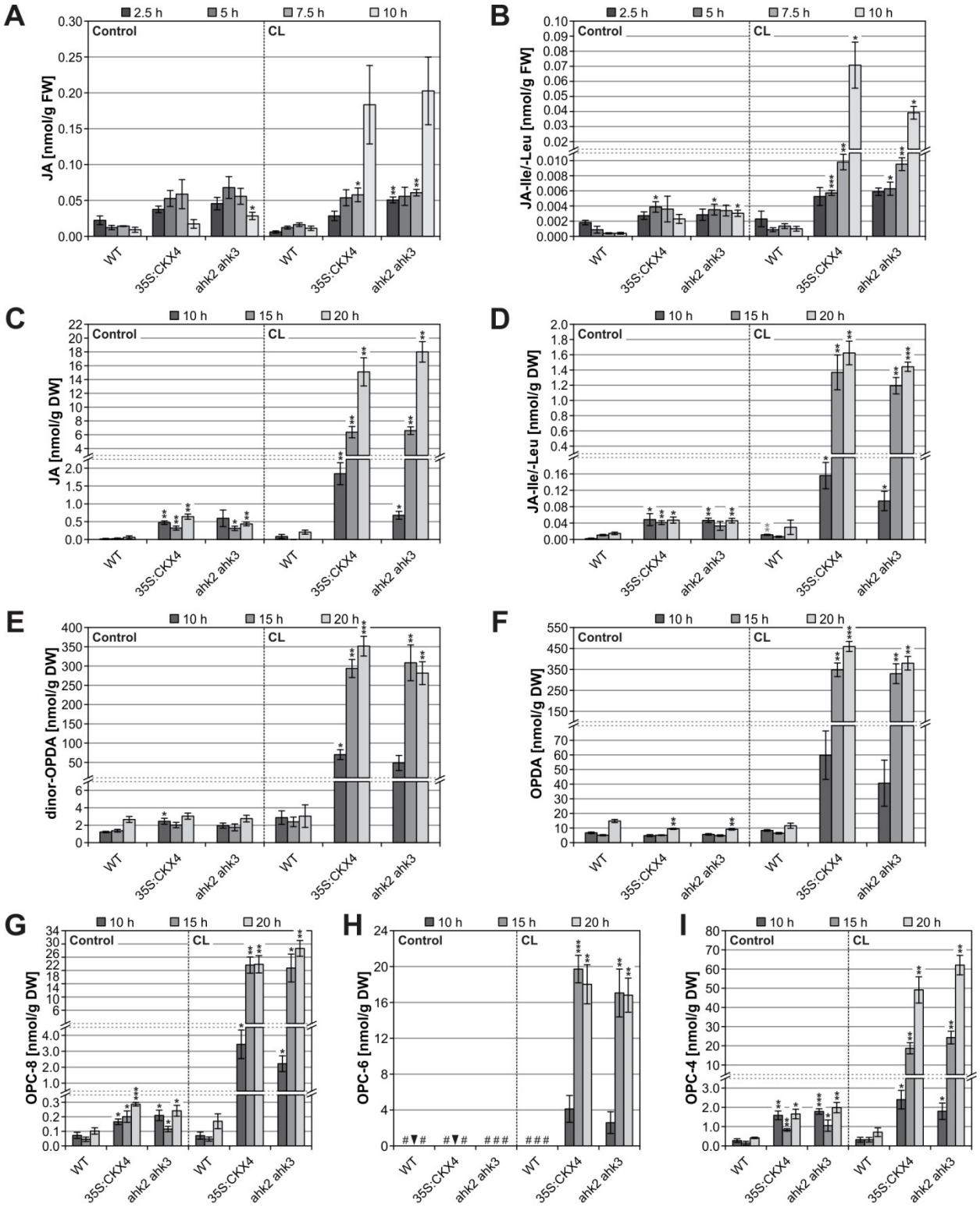

Figure 3.46: Cell death progression in cytokinin-deficient plants following the continuous light regime is accompanied by accumulation of jasmonic acid metabolites.

Figure 3.46 continued.

A-I, Content of JA, its precursors and conjugates in plants with a reduced cytokinin status in comparison with the wild type (experimental design depicted and described in Fig. 3.45). **A**-**D**, JA and JA conjugate levels per fresh weight (FW; **A**-**B**) and per dry weight (DW; **C**-**D**) measured in samples of setup 1 (n = 3) and setup 2 (n = 4), respectively (as indicated in Fig. 3.45A). **E**-**I**, JA precursor levels after 10, 15, and 20 hours of darkness following CL treatment (setup 2). Dinor-OPDA and OPDA originating from hexadecatrienoic (C16:3) and α-linolenic (C18:3) acid, respectively (**E**-**F**), are further reduced to OPCs with 8-, 6-, or 4-carbon chains (**G**-**I**), which undergo fatty acid β-oxidation to finally form JA (n = 4). #, not detected; arrowheads, content < 0.01 nmol/g DW (**H**). Asterisks indicate significant differences compared with the respective wild types (black) and with the corresponding controls (gray, for wild type only) (*t* test: *, $p < 0.05$; **, $p < 0.01$; ***, $p < 0.001$). Error bars represent SE. The phytohormone measurements were performed in collaboration with Prof. Dr. Ivo Feussner and Dr. Tim Iven (see 2.11).

In addition to the strong changes in JA metabolite levels after CL treatment, elevated JA metabolite levels compared with the wild type were also detected in cytokinin-deficient plants under control conditions. Compared with the wild-type controls, JA levels were 10- to 30-fold higher in *35S:CKX4* and 7- to 40-fold higher in *ahk2 ahk3* control plants (Fig. 3.46C). Similarly, JA conjugates, including the biologically active JA-Ile derivative, were increased 3- to 25-fold in cytokinin-deficient control plants compared with the respective wild type (Fig. 3.46D). Strikingly, this difference between wild-type and cytokinin-deficient control plants was not found for the AOS- and AOC-catalyzed products dinor-OPDA and OPDA (Fig. 3.46E-F), which are early biosynthetic intermediates during JA synthesis (see 1.6.1). However, it was detectable for OPC-8 (Fig. 3.46G) and OPC-4 (Fig. 3.46I; OPC-6 levels were not detectable in the control plants), respectively. Comparable results were obtained in control plants of setup 1 (Fig. 3.46A-B and data not shown), which indicates that the formation of OPCs during JA synthesis might be differentially regulated in cytokinin-deficient plants compared with the wild type.

Collectively, the JA metabolite data confirm that a relationship between the cytokinin status and JA exists under circadian stress but also under control (SD) conditions indicating a suppressive function of cytokinin on JA synthesis.

3.7.4 JA synthesis and signaling mutants under CL treatment

The results described in the previous sections indicated that the JA pathway was activated in plants with a reduced cytokinin status in response to circadian stress conditions. Genetic crosses between cytokinin-deficient plants and the JA synthesis and signaling mutants *jar1-1*, *jin1-8/myc2-3*, and *coi1*, respectively, were carried out to evaluate the potential function of JA signaling in determining the onset and/or severity of cell death in response to the CL regime. The *jin1-8*/*myc2-3* allele (SALK_061267) led to the silencing of *CKX4* overexpression (as indicated by a uniformly reversed shoot phenotype in the F2 generation), which was probably due to a copy of the CaMV 35S promoter in the SALK T-DNA (Daxinger *et al.*, 2008). Due to genetic linkage between *AHK3* and *JIN1*/*MYC2*, the generation of *ahk2 ahk3 jin1-8*/*myc2-3* plants was also compromised. Therefore, the contribution of JIN1/MYC2, a key player in JA signaling (see 1.6.2), could not be analyzed by using this approach.

In contrast, the genetic crosses with the *jar1-1* mutant were straightforward and plants homozygous for all loci could be identified. The cell death phenotype of plants with a reduced cytokinin status was strongly reversed in the *jar1-1* background (Fig. 3.47A; for controls see Appendix Fig. A.12). The percentage of necroses was significantly reduced (Fig. 3.47B) and the stress-induced decrease in F_v/F_m ratios significantly diminished (Fig. 3.47C) in cytokinin-deficient *jar1-1* mutants compared with the

JAR1 wild-type counterparts. The *jar1-1* single mutant behaved like the wild type. These results clearly demonstrate that an activated JA pathway promotes cell death progression. The *JAR1* mutation causes a deficiency in the biologically active JA conjugate JA-Ile (Suza and Staswick, 2008; see 1.6.1). Therefore, it can be concluded that JA-Ile-dependent signaling determines the severity of cell death in cytokinin-deficient plants.

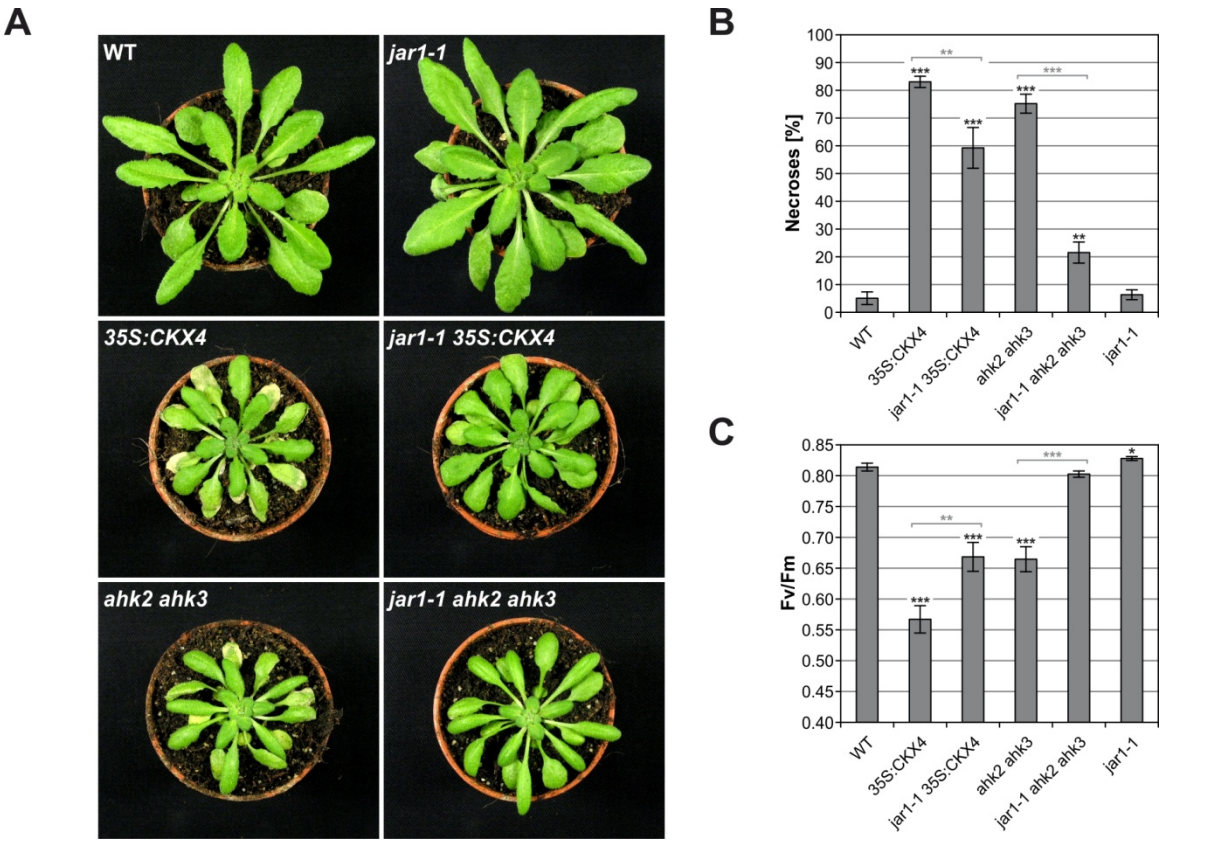

Figure 3.47: The cell death phenotype in cytokinin-deficient plants after continuous light treatment is partially rescued in the *jar1-1* background.

A, Plants with a reduced cytokinin status (*35S:CKX4* and *ahk2 ahk3*) in wild-type and *jar1-1* background. Five-week-old SD-grown plants were subjected to CL treatment and transferred back into SD rhythm afterwards while control plants remained in SD rhythm continuously and were not affected (for pictures see Appendix Fig. A.12). Pictures were taken two days after CL treatment and are representative for the observed phenotypes. **B**-**C**, The percentage of necrotic leaves counted in all mature leaves (**B**; n = 10) and the stress-induced decrease in F_v/F_m ratios (**C**; n = 16) measured one day after CL treatment. Experimental design corresponds to "32 h L/16 h D" in Fig. 3.6A. Asterisks indicate significant differences compared with wild type (black) and between cytokinin-deficient plants in wild-type or *jar1-1* background (gray) (*t* test: *, $p < 0.05$; **, $p < 0.01$; ***, $p < 0.001$). Error bars represent SE.

COI1 is a crucial part of the JAZ-COI1 co-receptor complex which binds JA-Ile (see 1.6.2). To study the consequences of an impaired JA signaling, also *coi1* mutants were crossed with *35S:CKX4* and *ahk2 ahk3*. Unfortunately, only *coi1 ahk2 ahk3* plants could be tested under CL treatment because the presence of the *coi1* allele (SALK_035548) also silenced the 35S promoter-driven *CKX4* transgene expression. Moreover, homozygous *coi1* plants had to be selected on MS medium containing 25 µM MeJA from a population segregating for *coi1* because homozygous plants developed no seeds due to male sterility. Together with wild-type and *ahk2 ahk3* plants (grown on MS medium without MeJA) all

seedlings were potted into soil about two weeks after germination. Strikingly, no difference concerning the cell death phenotype was observed in *coi1 ahk2 ahk3* triple mutants compared with the *ahk2 ahk3* double knockout (Fig. 3.48A; for controls see Appendix Fig. A.13). Neither the percentage of necroses nor the F_v/F_m ratios differed significantly between these plants one day after CL treatment (Fig. 3.48B-C).

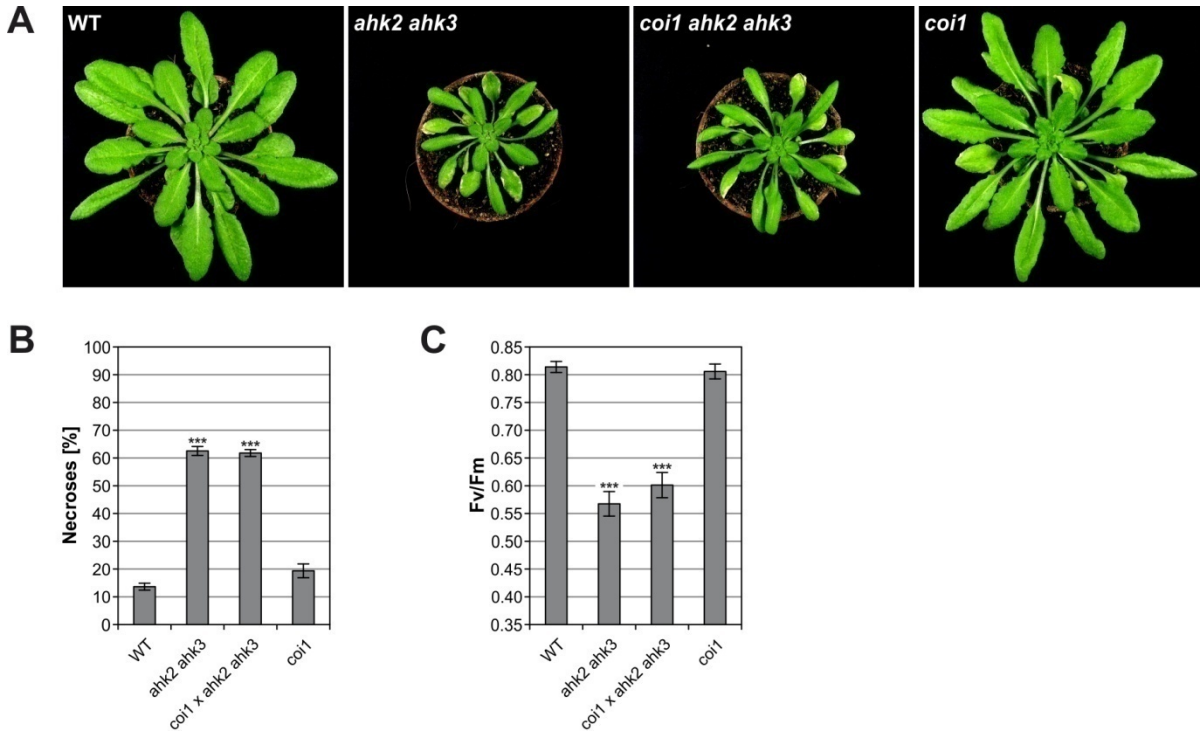

Figure 3.48: The cell death phenotype in *ahk2 ahk3* plants after continuous light treatment is not reversed in the *coi1* background.

A, Cytokinin receptor double mutant *ahk2 ahk3* in wild-type and *coi1* background. Homozygous *coi1* plants (for *coi1* and *coi1 ahk2 ahk3*) were selected by their insensitivity towards 25 µM MeJA on MS medium from the progeny of heterozygous *coi1* plants. After about two weeks of growth *coi1* mutant seedlings were transferred to soil together with wild-type and *ahk2 ahk3* seedlings (grown on MS medium without MeJA). The plants were continuously grown under SD rhythm and subjected to the CL regime after about five weeks. Control plants remained in SD rhythm and were not affected (for pictures see Appendix Fig. A.13). Pictures were taken two days after CL treatment and are representative for the observed phenotypes. **B**-**C**, The percentage of necrotic leaves counted in all mature leaves (**B**; n = 16; except *coi1*, n = 13) and the stress-induced decrease in F_v/F_m ratios (**C**; n = 16) measured one day after CL treatment. Experimental design corresponds to "32 h L/16 h D" in Fig. 3.6A. Asterisks indicate significant differences compared with wild-type plants (*t* test: ***, $p < 0.001$). Error bars represent SE.

This outcome was surprising and seems contradictory to the experiments involving *jar1-1* mutants. Since COI1 is the only (known) JA(-Ile) receptor and *coi1* loss-of-function mutants are impaired in every aspect of JA signal transduction and response (Feys *et al.*, 1994; Wasternack, 2007; Browse, 2009b) it is elusive how the JA signal was perceived and transmitted to promote cell death in cytokinin-deficient plants. A possible explanation for the result would be that an alternative COI1-independent signaling pathway exists which is activated under circadian stress conditions and mediates the JA(-Ile)-dependent promotion of cell death. This hypothesis will be evaluated in more detail in the Discussion (see 4.2.5.2).

3.7.5 Determination of lipid peroxidation and hydrogen peroxide levels

At late stages of cell death progression ("24 h" after CL treatment) ROS-induced lipid peroxidation (LPO) was strongly increased in cytokinin-deficient plants indicating that they encounter oxidative stress (Fig. 3.11C). Moreover, oxidative stress marker gene expression was increased very early already at "5 h" following the CL regime (see Fig. 3.23B-C). Oxidative stress results from a strong increase in ROS levels and affects the transcription of a large number of genes – the ROS response genes (op den Camp *et al.*, 2003; Gadjev *et al.*, 2006; Balazadeh *et al.*, 2012; see 1.4.3). Furthermore, ROS are among the key regulators of different types of developmentally and environmentally induced cell death in plants (Gechev *et al.*, 2006; De Pinto *et al.*, 2012; Brosché *et al.*, 2014; see 1.5.1 and 1.5.2). Therefore, the question had to be answered if oxidative stress was present in cytokinin-deficient plants already at early time points after CL treatment causing the induction of ROS-responsive genes and possibly also cell death initiation.

LPO analysis is a good tool to map oxidative stress. Since the oxidation of lipids is an immediate consequence of increased ROS levels, LPO can be considered as a "ROS footprint" (see also 3.3.1). Therefore, LPO measurements were carried out (Fig. 3.49) to answer the above question. However, instead of HOTE measurements (see Fig. 3.11C), malondialdehyde (MDA) was quantified. MDA is a secondary end product of the oxidation of polyunsaturated fatty acids (PUFAs) and, therefore, reflecting the extent of LPO (Heath and Packer, 1968). This method provides no detailed information about specific peroxidation products but is sufficient to allow an estimation of the overall oxidation of PUFAs.

Samples were collected in a 2.5-hour time interval starting directly after CL treatment or a normal SD light period (controls) and ending 10 hours later as well as after 16 and 18 hours following the CL regime (Fig. 3.49A). In control plants a significantly lower LPO was detected in cytokinin-deficient plants compared with wild-type plants at the end of the (SD) light and during the first half of the dark period (Fig. 3.49B-E). This is in accordance with the LPO data derived from HOTE measurements (see Fig. 3.11C). At the end of the CL treatment an increase in LPO was observed for all genotypes (Fig. 3.49B). Although the CL-treated wild type exhibited a significantly higher total LPO, the relative increase compared with the respective controls was similar for all investigated genotypes. The fact that prolonged CL treatment did not result in the development of cell death (see Fig. 3.15A) and that no profound induction of ROS response genes was recorded in the wild type or cytokinin-deficient plants directly after CL treatment (see Fig. 3.23B-C) indicates that the increase in LPO measured after 32 hours of CL (Fig. 3.49B) does not reflect a serious (oxidative) stress condition. It probably rather reflects the adaptation to the extended light treatment, which involves a prolonged photosynthetic activity, and hence, the generation of more ROS.

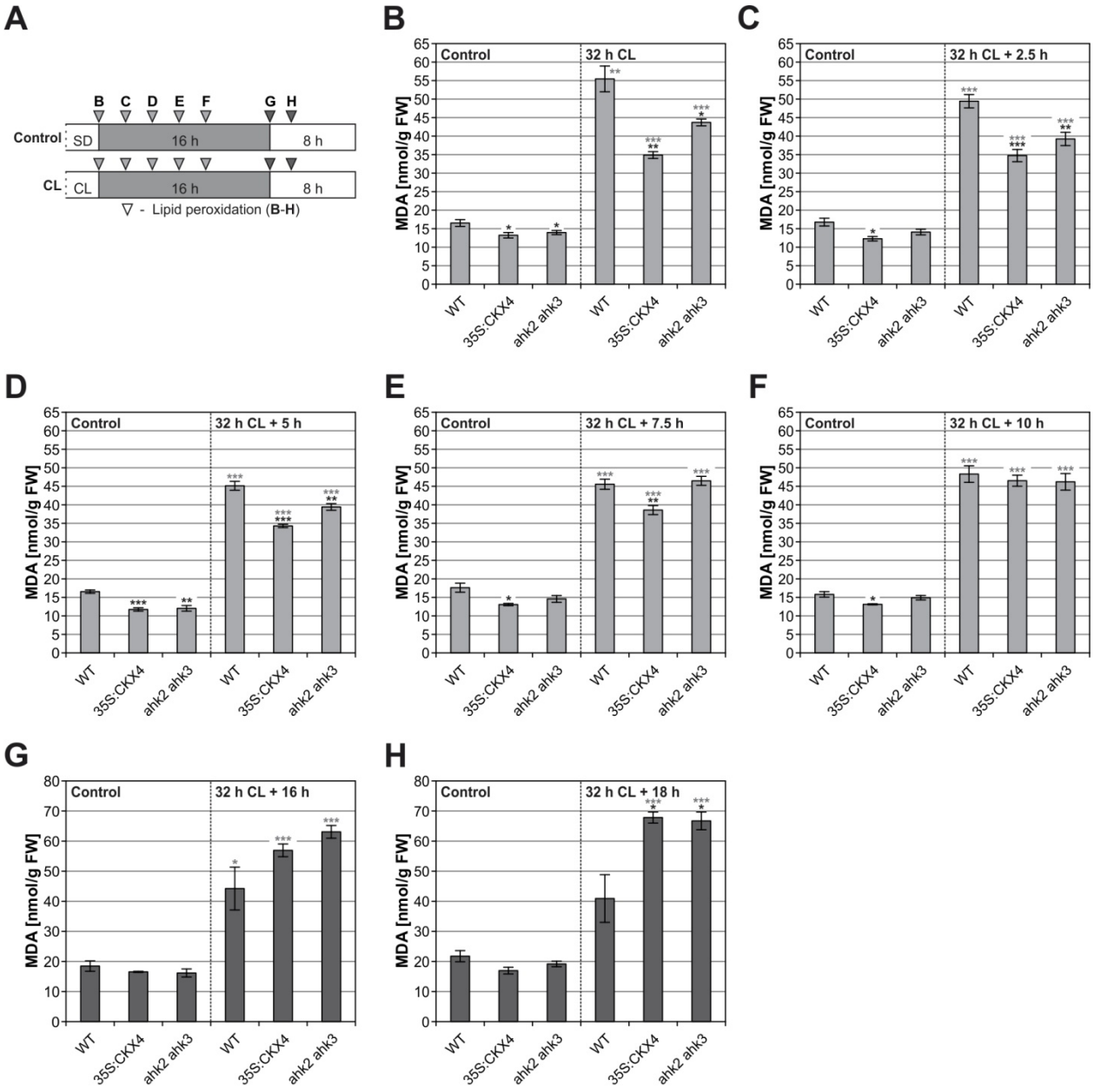

Figure 3.49: Determination of lipid peroxidation by malondialdehyde measurements after continuous light treatment.

A, Scheme represents the experimental design in **B**-**H**. White, light period; gray, dark period. Plants were grown under SD rhythm for five to six weeks prior to the indicated treatment. **B**-**H**, LPO expressed as MDA content. Leaf samples were collected directly after CL or a normal SD light period (**B**), as well as 2.5 h (**C**), 5 h (**D**), 7.5 h (**E**), and 10 h (**F**) later. In an independent experiment leaf material was harvested at later time points after 16 h (**G**) and 18 h (**H**), respectively (n = 4). Asterisks indicate significant differences compared with the respective wild type (black) and with the corresponding control (gray) (*t* test: *, $p < 0.05$; **, $p < 0.01$; ***, $p < 0.001$). Error bars represent SE.

Intriguingly, the extent of LPO did not change after "2.5 h" (Fig. 3.49C) and especially not after "5 h" (Fig. 3.49D) of darkness following CL treatment. In order to explain the strong upregulation of the ROS marker genes *BAP1* and *ZAT12* at "5 h" (see Fig. 3.23B-C) a drastic increase in LPO, corresponding to increased oxidative stress, would have been expected. Only after "7.5 h" (Fig. 3.49E) and more pronounced after "10 h" of darkness (Fig. 3.49F) LPO tended to increase in CL-treated cytokinin-

deficient plants but still to a low extent. The wild-type LPO levels were not exceeded and merely reached at "10 h". In conclusion, these results revealed that cytokinin-deficient plants did not (immediately) encounter strong oxidative stress in response to the circadian stress regime. Only at "16 h" and "18 h" after CL treatment, corresponding to later stages of cell death progression, oxidative stress increased in cytokinin-deficient plants, as reflected by elevated MDA levels that finally even exceeded wild-type levels (Fig. 3.49G-H). Therefore, these results already indicated that the upregulation of ROS response genes as well as the cell death initiation in cytokinin-deficient plants was not caused by oxidative stress.

To further evaluate this conclusion a second approach was conducted to study oxidative stress, this time by directly measuring ROS production. By using an Amplex Red-based assay, H_2O_2 levels were determined after "5 h" (coinciding with the upregulation of ROS response genes) as well as after "7.5 h" and "10 h" (coinciding with cell death initiation) of darkness following CL treatment. Consistent with the LPO data, H_2O_2 levels were not drastically increased in cytokinin-deficient plants compared with the wild type at "5 h" after CL treatment (Fig. 3.50A). They were rather slightly lower. Even after "7.5 h" and "10 h" following the CL regime the H_2O_2 content in cytokinin-deficient plants only slightly exceeded the levels in the corresponding wild type, though not statistically significant (Fig. 3.50B-C). A general increase in H_2O_2 levels was detected for all CL-treated plants in comparison with the respective control plants, reflecting the influence of the prolonged light treatment on ROS production as deduced from the LPO data (Fig. 3.50A-C). However, the absolute increase in H_2O_2 levels was still small in cytokinin-deficient plants compared with the wild type after the CL regime.

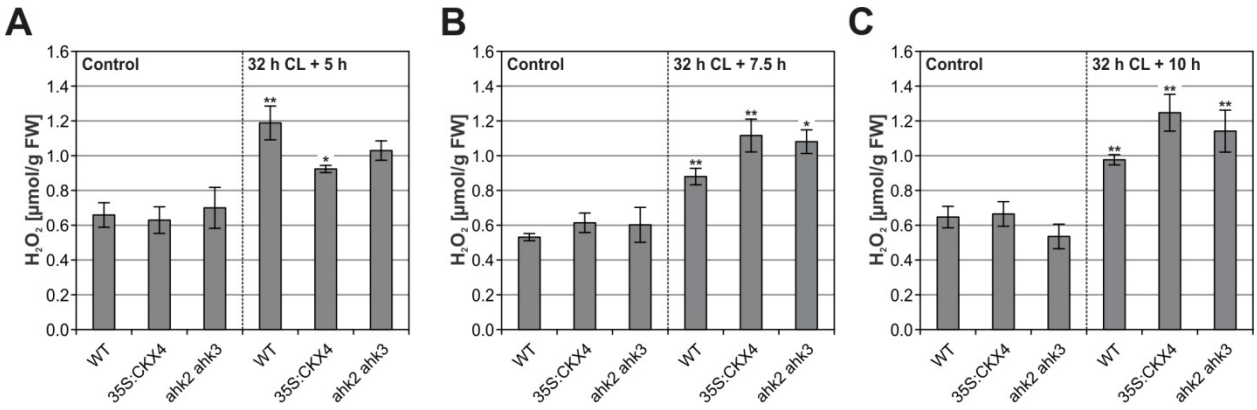

Figure 3.50: Hydrogen peroxide levels in response to continuous light treatment.

A-**C**, H_2O_2 content was determined by using an amplex red-based assay. The experimental design corresponds to the one explained in Fig. 3.49. Leaf samples were collected 5 h (**A**), 7.5 h (**B**), and 10 h (**C**) after CL treatment or a normal SD light period (n = 4). Asterisks indicate significant differences compared with the corresponding control (*t* test: *, $p < 0.05$; **, $p < 0.01$). Differences compared with the respective wild type were not significant ($p > 0.05$). Error bars represent SE. These experiments were performed in collaboration with Dr. Anne Cortleven (see 2.11).

Collectively, the LPO and H_2O_2 data revealed that the circadian stress regime did not immediately result in oxidative stress in cytokinin-deficient plants. An oxidative burst can, therefore, not explain the detected stress responses (on the molecular level) and the initiation of cell death. An eventual increase in ROS levels during cell death development can be deduced from the increase in LPO at later time

points (see Fig. 3.49G-H) and strong ROS-induced LPO one day after CL treatment (see Fig. 3.11C). The results, therefore, indicate that oxidative stress was accompanying cell death progression rather than being its cause.

3.7.6 The role of the NADPH oxidases RBOHD and RBOHF in the response to changed light-dark regimes

One essential source for ROS during development and under abiotic and biotic stress conditions are RESPIRATORY BURST OXIDASE HOMOLOGUES (RBOHs). These NADPH oxidases produce superoxide ($O_2^{\bullet-}$) in the apoplast which is (rapidly) dismutated to hydrogen peroxide (H_2O_2) by SOD (Sagi and Fluhr, 2006; Suzuki *et al.*, 2011). Interestingly, of the 10 *RBOH* genes in *Arabidopsis* only *RBOHD* and *RBOHF* are expressed throughout the whole plant, including leaves. Especially *RBOHD* plays a pivotal role in responses to diverse stimuli and is tightly controlled at the transcriptional level being highly stress-responsive (Mittler *et al.*, 2004; Miller *et al.*, 2009; Suzuki *et al.*, 2011). Together with *RBOHF* it is involved in pathogen responses, stomatal closure, and cell death regulation (Torres *et al.*, 2002; 2005; Kwak *et al.*, 2003). Furthermore, both genes were found to be important for JA-induced gene expression (Maruta *et al.*, 2011). The link to JA, their contribution to ROS production and their importance under various environmental stresses as well as for cell death regulation made them interesting candidates to study under circadian stress conditions.

First, the transcript profiles of *RBOHD* and *RBOHF* were recorded during the night following a normal SD light period and CL treatment (Fig. 3.51A-B; for experimental design see Fig. 3.23A). Interestingly, *RBOHD* was strongly induced in both *35S:CKX4* and *ahk2 ahk3* but not in wild-type plants after CL treatment (Fig. 3.51A). The upregulation of *RBOHD* in cytokinin-deficient plants (compared with the respective controls) started after "5 h" following the CL regime (see corresponding table in Fig. 3.51A). The changes in transcript abundance were again reminiscent of oscillation waves as was observed for the oxidative stress marker genes (see Fig. 3.23B-C) and the majority of JA-associated genes (see Fig. 3.42). Moreover, the induction of *RBOHD* could be prevented by re-entrainment similar to the induction of *JAZ1* (Fig. 3.44D and data not shown). For *RBOHF* no strong CL-induced changes in transcript levels were detected (Fig. 3.51B).

In order to further evaluate if RBOHD and/or RBOHF play a role in the response to altered light-dark regimes, the corresponding mutants were analyzed. Genetic crosses between the *rbohDF* double mutant and *35S:CKX4* or *ahk2 ahk3*, respectively, were carried out in order to obtain cytokinin-deficient plants carrying the *rbohD-3* or *rbohF-3* single as well as the *rbohDF* double knockout. This approach started at the final stage of my practical work and, therefore, only preliminary data are shown here (Fig. 3.51C-E; for controls see Appendix Fig. A.14).

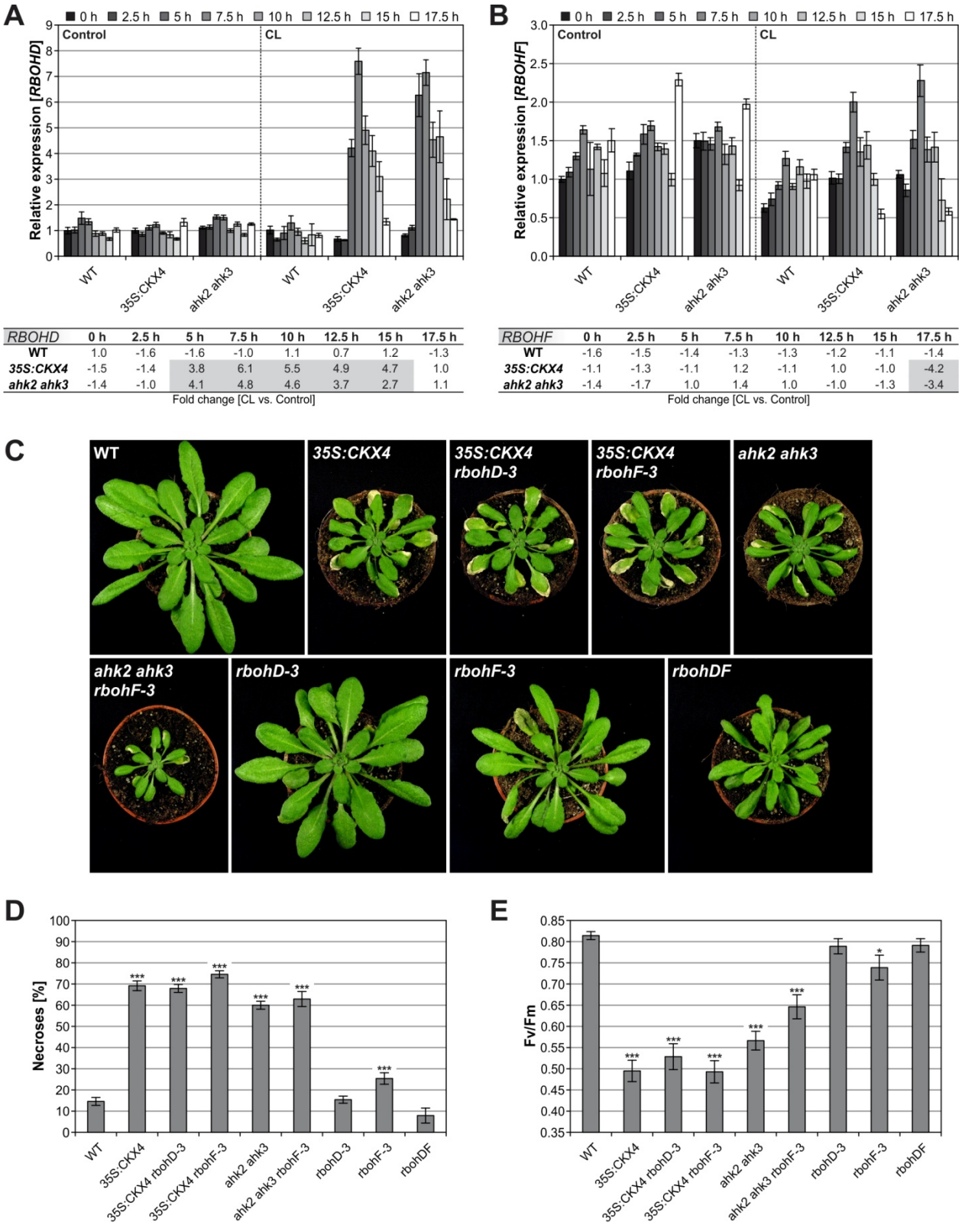

RBOHD	0 h	2.5 h	5 h	7.5 h	10 h	12.5 h	15 h	17.5 h
WT	1.0	-1.6	-1.6	-1.0	1.1	0.7	1.2	-1.3
35S:CKX4	-1.5	-1.4	3.8	6.1	5.5	4.9	4.7	1.0
ahk2 ahk3	-1.4	-1.0	4.1	4.8	4.6	3.7	2.7	1.1

Fold change [CL vs. Control]

RBOHF	0 h	2.5 h	5 h	7.5 h	10 h	12.5 h	15 h	17.5 h
WT	-1.6	-1.5	-1.4	-1.3	-1.3	-1.2	-1.1	-1.4
35S:CKX4	-1.1	-1.3	-1.1	1.2	-1.1	1.0	-1.0	-4.2
ahk2 ahk3	-1.4	-1.7	1.0	1.4	1.0	-1.0	-1.3	-3.4

Fold change [CL vs. Control]

Figure 3.51: The NADPH oxidases RBOHD and RBOHF play no major role in the development of the cell death phenotype in response to changed light-dark cycles.

Figure 3.51 continued.

A-**B**, Expression profiles of *RBOHD* (**A**) and *RBOHF* (**B**) were recorded in a 2.5-hour time interval starting directly after SD or CL (0h) and ending 17.5 hours later (for a schematic overview see Fig. 3.23A). The transcript levels are expressed as relative values compared with the respective 0-hour wild-type control, which was set to 1 (n = 4). *PP2AA2* and *MCP2D* served as reference genes. **C,** Plants carrying a mutation in *RBOHD* or *RBOHF* in wild-type and cytokinin-deficient (*35S:CKX4* and *ahk2 ahk3*) background. Five-week-old SD-grown plants were subjected to CL treatment and transferred back into SD rhythm afterwards. Control plants remained in SD rhythm continuously and were not affected (for pictures see Appendix Fig. A.14). Pictures were taken two days after CL treatment and are representative for the observed phenotypes. **B**-**C**, The percentage of necrotic leaves counted in all mature leaves (**D**; n = 18; except *ahk2 ahk3 rbohF-3*, n = 10) and the stress-induced decrease in F_v/F_m ratios (**E**; n = 16) measured one day after CL treatment. Experimental design corresponds to "32 h L/16 h D" in Fig. 3.6A. Asterisks indicate significant differences compared with wild-type plants (*t* test: *, $p < 0.05$; ***, $p < 0.001$). Error bars represent SE.

Analysis of *35S:CKX4* plants carrying either a *rbohD-3* or *rbohF-3* allele indicated that neither the *RBOHD* nor the *RBOHF* gene are required to establish the stress and cell death phenotype as *35S:CKX4* plants and the hybrids showed a similar phenotype (Fig. 3.51C-E). The same was observed for *ahk2 ahk3 rbohF-3* plants in comparison with *ahk2 ahk3* mutants. Due to the close proximity of *RBOHD* and *AHK2* on chromosome 5, no homozygotes for mutations in both genes could be selected in the F2 generation. Thus, plants segregating for *rbohD-3* but homozygous for *ahk2 ahk3* were chosen for analysis among the F3 progeny. These plants were exposed to the circadian stress regime (in total 66 plants) and the percentage of necroses was determined for each plant. 19 plants exhibiting the weakest cell death phenotype were selected and genotyped (out of the 66 segregating plants). Out of these only 3 plants were homozygous for the *rbohD-3* allele. This low proportion indicates that RBOHD is not required to induce cell death in *ahk2 ahk3* plants after CL treatment, which is consistent with the outcome for *35S:CKX4* plants.

Unfortunately, it was impossible to obtain seeds from *35S:CKX4* or *ahk2 ahk3* plants carrying both *RBOH* mutations because their survival rate was extremely low. The corresponding *rbohDF* double mutant showed already a stress phenotype under normal growth conditions (see also Torres *et al.*, 2002) which was even more pronounced in a cytokinin-deficient background. These mutants were severely dwarfed, developed strong chloroses and/or accumulated high amounts of anthocyanins. Finally, they stopped growing and died around bolting time (data not shown).

Together, the data on *rboh* mutants revealed that RBOHD and RBOHF play no prominent role in the response to circadian stress and, consequently, for the development of cell death although *RBOHD* was strongly induced in cytokinin-deficient plants after CL treatment. However, there are other potential sources for ROS which could explain increased ROS levels in these plants accompanying later stages of cell death progression.

4 Discussion

4.1 A protective function for cytokinin in the light stress response under HL

One aim of this work was to study the role of cytokinin under HL stress. For that, the light stress responses of *Arabidopsis* plants with a reduced cytokinin signaling or content have been examined. Intriguingly, plants with a reduced cytokinin status were more sensitive to light stress, reflected by stronger photoinhibition after prolonged HL treatment (Fig. 3.1). Photoinhibition is caused when the rate of photodamage to PSII is higher than its repair (Nishiyama *et al.*, 2006; Takahashi and Murata, 2008; Takahashi and Badger, 2011). Therefore, the balance between damage and repair was more strongly affected in cytokinin-deficient plants. Indeed, the results demonstrate that direct photodamage to PSII was more pronounced in these plants (Fig. 3.3). Furthermore, they exhibited a slower and incomplete recovery from photoinhibition and were highly depleted of the PSII reaction center D1 protein after HL stress (Fig. 3.2). These findings both indicate insufficient repair of PSII, which could be either due to a compromised D1 repair machinery and/or to a persistent or even irreversible photodamage. Additional analyses into the mechanisms revealed that the ROS scavenging capacity was significantly diminished in cytokinin-deficient plants. Their general deficiency in carotenoids was particularly pronounced (Fig. 3.4). These antioxidants are indispensable for the quenching of $^1O_2$ as well as for the dissipation of excess energy as heat *via* NPQ, thereby reducing the inhibition of the D1 repair by ROS and, albeit to a lesser extent, the direct photodamage to PSII (Nishiyama *et al.*, 2006; Murata *et al.*, 2012). Moreover, the data revealed that the protective function of cytokinin in the response to HL is mainly mediated by the cytokinin receptor AHK3, while AHK2 has an accessory function. The major results and conclusions are summarized in a comprehensive model (Fig. 4.1).

4.1.1 Accelerated photoinhibition in cytokinin-deficient plants due to greater imbalance between photodamage and repair

On the one hand, a stronger direct photodamage to PSII has been demonstrated for cytokinin-deficient plants (Fig. 3.3). This might in part be explained by the deficiency in carotenoids, especially xanthophylls (Fig. 3.4) which could result in a reduced NPQ and, hence, contribute to the higher photodamage (Li *et al.*, 2002; Sarvikas *et al.*, 2006). However, defective light avoidance mechanisms such as leaf or chloroplast movements and/or dramatic alterations in the chloroplast ultrastructure could also account for that (Lichtenthaler and Burkart, 1999; Takahashi and Badger, 2011). The chloroplast ultrastructure has been analyzed by Dr. Anne Cortleven and the results revealed no profound differences between the genotypes (Cortleven and Nitschke *et al.*, 2014). On the other hand, indications for an impaired D1 repair cycle in plants with a reduced cytokinin status were collected. One was their reduced capacity to recover from photoinhibition after relaxation (Fig. 3.2A). Moreover, the protein level of D1 was earlier and more strongly reduced following HL treatment in these plants in comparison with the wild type (Fig. 3.2B). This suggests an accelerated depletion of D1 (i.e. increased photodamage) and/or a decelerated D1 repair due to a lack of replenishment of D1 by *de novo*

synthesis. The decrease in D1 protein-encoding *PSBA* gene expression upon HL stress was strongest in the *ahk2 ahk3* mutant (Fig. 3.2C) which could be due to transcriptional control by the redox state of the chloroplast (Mulo *et al.*, 2012). The *PSBA* transcript level is increased under conditions leading to an oxidized plastoquinone pool (Allen and Pfannschmidt, 2000). HL treatment causes an over-reduction of the plastoquinone pool which may in turn lead to downregulation of *PSBA*. However, it should be noted that post-transcriptional mechanisms including mRNA processing and co-translational modifications are the major steps in the regulatory network controlling expression of the *PSBA* gene and production of the D1 protein (Mulo *et al.*, 2012). These mechanisms could also be affected in plants with a reduced cytokinin status. For instance, the reduction of the antioxidant capacity in these plants indicates that the *PSBA* translation might be compromised since ROS cause photoinhibition mainly by suppressing *de novo* synthesis of proteins (Nishiyama *et al.*, 2006; 2011b).

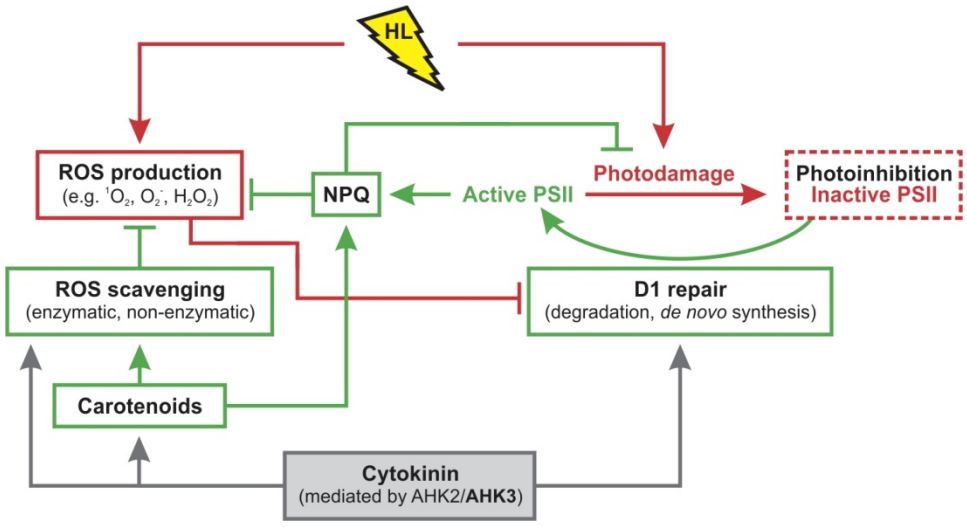

Figure 4.1: Model for the protective function of cytokinin in the light stress response upon high light.
HL causes photoinhibition by directly damaging PSII. Additionally, ROS production is increased upon excess of light. ROS inhibit the D1 repair, thereby indirectly accelerating photoinhibition through the accumulation of inactive PSII complexes (red, damaging impact of HL). Plants have evolved several mechanisms such as the dissipation of excitation energy as heat (NPQ), ROS scavenging, and the D1 repair cycle to counteract the detrimental effects of HL intensities (green, photo-protective mechanisms). Cytokinin plays a protective role in the light stress response which is mediated by the AHK2 and AHK3 receptors (gray). It promotes the D1 repair directly and/or indirectly by promoting ROS scavenging. Its positive effect on the formation of carotenoids strongly supports the ROS scavenging capacity but might also facilitate NPQ to prevent both ROS production and photodamage.

There are several important steps in the removal of damaged D1 and the replacement by novel D1 protein. ATP-dependent FTSH metalloproteases and ATP-independent DEG endopeptidases play predominant roles in D1 degradation (Kato and Sakamoto, 2009). *Arabidopsis* mutants of the major isoforms of FTSH (FTSH2 and FTSH5) displayed a high sensitivity to photoinhibition under HL and accumulated high levels of ROS (Sakamoto *et al.*, 2004). Also *deg5 deg8* mutants exhibited a HL-sensitive phenotype (Sun *et al.*, 2007). These reports clearly demonstrate that a proper degradation of the damaged D1 is important for protection against photoinhibition. The final step of the D1 repair cycle comprises the maturation of newly synthesized preD1 to mature D1 catalyzed by C-terminal processing peptidase (CTP) which enables the full reassembly of PSII (Anbudurai *et al.*, 1994; Roose

and Pakrasi, 2004). Consistently, the analysis of loss-of-function mutants of one of the three predicted *Arabidopsis CTP* homologs (AT4G17740) under HL showed that this gene is required for an efficient repair of D1 (Che *et al.*, 2013) and corroborated the necessity to incorporate a fully functional D1 protein to complete the D1 repair cycle. The results of this work showed that HL caused no major differences in the expression of genes encoding FTSH and DEG proteases between wild-type and cytokinin-deficient plants (Fig. 3.2D-E). Likewise, the functionally important *CTP* gene homolog (AT4G17740) was neither induced by HL nor differentially regulated among the investigated genotypes. One other *CTP* homolog (AT3G57680) exhibited a different expression pattern in cytokinin-deficient plants compared with wild-type plants (Fig. 3.2F). However, the corresponding loss-of-function mutant (Yin *et al.*, 2008) exhibited a wild-type-like HL response under the conditions of this study. This indicates that AT3G57680 is not indispensable under HL stress which is consistent with the report by Che *et al.* (2013). Together, the transcript data suggest that cytokinin does not predominantly act through transcriptional regulation of the analyzed genes but may act on a different level to positively influence the efficiency of the D1 repair cycle.

Collectively, the results indicate that the higher depletion of the D1 protein in cytokinin-deficient plants was very likely a consequence of both increased photodamage and an impaired D1 repair cycle which caused stronger photoinhibition in response to HL stress. The available data do not allow distinguishing whether (1) limited ROS scavenging causing enhanced ROS production and thereby indirectly inhibiting the D1 repair cycle, (2) reduced *de novo* production of D1, including transcription and translation, or (3) an impaired action of proteins (e.g. proteases) required for a functional D1 repair cycle contribute most to the reduction and compromised recovery of the D1 protein. However, the decreased antioxidant capacity in plants with a reduced cytokinin status points to an interference of ROS with the D1 repair cycle, which would include the blockage of *PSBA* translation, more specifically the elongation step during protein synthesis (Nishiyama *et al.*, 2011b).

4.1.2 Cytokinin deficiency is associated with a reduced antioxidant capacity under HL

Plants with a reduced cytokinin status exhibited a lower total antioxidant capacity compared with the wild type under HL. This reduction was probably mainly due to lower levels of carotenoids (Fig. 3.4). In contrast, no major differences between wild-type and cytokinin-deficient plants were found for ascorbate and glutathione, which also play an important role in redox homeostasis (Foyer and Noctor, 2011).

Under HL, carotenoids are of great importance for NPQ, the dissipation of excess excitation energy as heat (see 1.2.1.2), and the quenching of $^3Chl^*$ and $^1O_2$ (see also 1.4.2) (Gill and Tuteja, 2010; Jahns and Holzwarth, 2012). The main function of lutein is to efficiently quench $^3Chl^*$ (Dall'Osto *et al.*, 2006). Zeaxanthin is crucial for NPQ and *npq1* mutants that lack zeaxanthin are impaired in NPQ and exhibit a higher sensitivity to photoinhibition (Niyogi *et al.*, 1998). Neoxanthin was shown to particularly scavenge $O_2^{\bullet -}$ and detached leaves of neoxanthin-deficient *aba4-1* plants were more sensitive to oxidative stress under HL (Dall'Osto *et al.*, 2007). Lastly, β-carotene is decisive for the degradation of $^1O_2$ in the PSII reaction center (Telfer, 2014). These examples indicate the high relevance of different

carotenoids especially under conditions that increase ROS generation and photodamage such as HL. In cytokinin-deficient plants all carotenoids analyzed, including lutein, zeaxanthin, neoxanthin, and β-carotene, were less efficiently produced upon HL treatment resulting in levels that were 30 to 45 % lower compared with the wild type (Fig. 3.4B-C). Interestingly, *npq1* mutants that additionally lack neoxanthin (*aba4-1 npq1*) or lutein (*npq1 lut2.1*) display strongly aggravated stress phenotypes compared with the corresponding single mutants (Dall'Osto *et al.*, 2006; 2007) revealing their functional overlap and, hence, their cooperative effect for photo-protection. Therefore, the simultaneous deficiency of several important carotenoids might be one explanation for the increased sensitivity to photoinhibition in cytokinin-deficient plants.

In contrast, the content of tocopherols, in particular α-tocopherol, was increased in cytokinin-deficient plants (Fig. 3.4D). Accordingly, the amount of plastoglobuli was strongly increased in cytokinin-deficient plants, as revealed by analysis of the chloroplast ultrastructure performed by Dr. Anne Cortleven (Cortleven and Nitschke *et al.*, 2014). Plastoglobuli are storage sites for lipoprotein particles containing for example plastoquinone, α-tocopherol, and triacylglycerols (Lundquist *et al.*, 2012). They play a role in the synthesis of tocopherols and plastoquinone, and also in recycling of thylakoid catabolites (Vidi *et al.*, 2006; Ytterberg *et al.*, 2006). Numerous studies reported a strong increase in plastoglobuli size and amount under stress conditions which has been connected to the antioxidative effect of tocopherol (Bréhélin *et al.*, 2007). Tocopherols, especially α-tocopherol, are important antioxidants that protect PSII by scavenging $^1O_2$ and lipid radicals which are highly generated under HL (Trebst *et al.*, 2002; Trebst, 2003; Gill and Tuteja, 2010). However, their increased production in cytokinin-deficient plants could be part of a compensatory protective mechanism counteracting the deficiency in carotenoids and the higher degree of photodamage. Compensatory processes have been described in several studies analyzing antioxidant protection against photoinhibition. For example, *lut2.1* plants compensate for the lack of lutein by increased amounts of violaxanthin as well as antheraxanthin and zeaxanthin (Dall'Osto *et al.*, 2006). The *npq1 npq4 lut2* mutant compensates for the deficit in NPQ with increased α-tocopherol and ascorbate levels (Golan *et al.*, 2006) and the tocopherol-deficient *vte1* mutant accumulates more zeaxanthin under HL than the wild type (Havaux *et al.*, 2005).

Recycling enzymes of the Halliwell-Asada pathway (MDHAR, DHAR, and GR) showed no altered activity in response to HL, while the enzymes directly involved in scavenging of $O_2^{\bullet -}$ (SOD) and H_2O_2 (APX) were strongly activated upon HL (Fig. 3.5). Cytokinin-deficient plants exhibited only about half of the SOD activity of wild-type plants under control conditions and after HL treatment (Fig. 3.5A). A similar reduction in activity was also noted for APX under control conditions, which was however compensated upon HL treatment. These results indicate, on the one hand, that the scavenging capacity of cytokinin-deficient plants is generally lower than in wild-type plants and, on the other hand, that upon HL they seem to encounter more oxidative stress and try to deal with it by increasing the activities of APX and SOD. The hypothesis of a higher degree of stress is supported by the finding that cytokinin-deficient plants undergo increased photodamage as demonstrated by the lincomycin treatment (Fig. 3.3).

4.1.3 The function of cytokinin in the light stress response is mediated by AHK2 and AHK3

A strong HL effect was caused by the loss of AHK3 and was further enhanced by the additional loss of AHK2, which alone was ineffective (Fig. 3.1F). This indicates that AHK3 has a major role in the HL response while AHK2 has a cooperative function. Similar observations on cooperative or redundant functions of AHK2 and AHK3 have been made in other studies. For example, the combined loss of AHK2 and AHK3 but not the loss of each single receptor caused prominent morphological changes in roots and shoots, respectively (Higuchi *et al.*, 2004; Nishimura *et al.*, 2004, Riefler *et al.*, 2006). Interestingly, AHK2 and AHK3 are evolutionary closer related to each other than to CRE1/AHK4 and both receptors are predominantly expressed and active in shoot tissues (Ueguchi *et al.*, 2001a; Higuchi *et al.*, 2004; Stolz *et al.*, 2011). Several important functions during leaf development have been attributed to AHK2 and AHK3, including a role in leaf cell formation, chlorophyll metabolism and leaf senescence (Kim *et al.*, 2006; Riefler *et al.*, 2006). However, a role in the light stress response has not yet been listed among their various activities (Müller, 2011; Heyl *et al.*, 2012). An apparently higher relevance of AHK3 compared to AHK2 could be due to the different sensitivities of the receptors to various cytokinin metabolites (Spíchal *et al.*, 2004; Romanov *et al.*, 2006; Stolz *et al.*, 2011) and/or to differences in coupling to downstream signaling elements as indicated by distinct interacting proteins (Dortay *et al.*, 2008).

Additionally, the possible involvement of B-type ARRs has been investigated by Dr. Anne Corleven (Cortleven and Nitschke *et al.*, 2014). The fact that the *arr1 arr12* mutant (but not *arr1 arr10* or *arr10 arrr12*) displayed a strong HL effect indicates that cytokinin action in the light stress response is mediated at least partly through transcriptional regulation by ARR1 and ARR12. Both ARRs belong to subfamily 1 of the B-type ARR transcription factors (Heyl *et al.*, 2008; Hill *et al.*, 2013; Kieber and Schaller, 2014) and the corresponding genes are expressed in leaves (Mason *et al.*, 2004). Mutation of both genes was required to obtain an effect in response to HL indicating their redundant action, which is a common feature of B-type *ARR* genes (Müller, 2011). For ARR1 and ARR12, a combined action in regulating the expression of the sodium transporter gene *HKT1;1* and the accumulation of sodium in *Arabidopsis* shoots has been reported (Mason *et al.*, 2010). Interestingly, ARR10, as closest relative of ARR12, acts together with ARR1 and ARR12 to mediate the majority of typical cytokinin responses, including shoot and leaf development (Argyros *et al.*, 2008; Ishida *et al.*, 2008a). However, ARR10 seems to display no predominant function in the light stress response, indicating that it has functionally diverged.

The role of ARR1 and ARR12 in light stress protection links this activity to a specific transcriptional response, consistent with the great importance of a fine-tuned gene regulation to realize the many different biological activities of cytokinin (Brenner *et al.*, 2012). Cytokinin regulates numerous genes involved in light signaling and redox regulation (Rashotte *et al.*, 2003; Brenner *et al.*, 2005; Taniguchi *et al.*, 2007; Brenner and Schmülling, 2012; Bhargava *et al.*, 2013). For example, microarray meta-analyses placed genes encoding glutaredoxins, which have a role in protecting plants against photo-oxidative stress (Laporte *et al.*, 2012), among the top 20 cytokinin-regulated genes (Brenner *et al.*, 2012; Bhargava *et al.*, 2013). The emerging network of transcriptional regulation connecting the

actions of light, ROS, and cytokinin (Vandenbussche *et al.*, 2007; Chen *et al.*, 2013a) provides a starting point to unravel the molecular mechanisms linking cytokinin with its function in light stress protection.

4.2 A novel role for cytokinin under circadian stress

The results of the second project revealed that changes in the light-dark regime negatively affected the performance of the circadian clock, even in wild-type plants. Cytokinin-deficient plants, however, were particularly strongly affected. In the most extreme scenario the altered light-dark rhythm caused the initiation of pronounced stress responses followed by cell death development in leaves of plants with a reduced cytokinin status. Due to the coincidence between changes in the circadian core oscillator and the severe stress phenotype, the conditions leading to this previously unknown phenomenon were coined "circadian stress".

The obtained data indicated that circadian stress resulted in a profound perturbation of circadian timekeeping in cytokinin-deficient plants which coincided with a strong misregulation of JA-associated genes and genes of the ROS network. The early changes in gene expression were not associated with increased JA or ROS levels, respectively, but were found to be linked to a decreased clock performance. Since the circadian clock regulates JA-related genes and genes of the ROS network as well as JA and oxidative stress responses (Lai *et al.*, 2012; Shin *et al.*, 2012) these changes are considered to be part of a perturbed output regulation by a malfunctioning oscillator. One consequence was the activation of the JA pathway which was an essential determinant of the severity of cell death. Moreover, the misregulation of genes of the ROS network including general stress response (GSR) and plant core environmental stress response (PCESR) genes (see 1.4.3) is thought to be responsible for the activation of stress pathways as part of the "death signal". Oxidative stress, reflecting a disturbed ROS homeostasis, was accompanying cell death progression, probably being the consequence of the misregulated ROS gene network and not its cause. Intriguingly, a strong cell death phenotype was also observed in several clock mutants in response to the circadian stress regime pointing to an important role of specific components of the oscillator. The similarity of the phenotypes between cytokinin- and clock-deficient plants strongly supported the "circadian stress" hypothesis and, furthermore, suggested cytokinin as important input factor for the circadian clock. Therefore, it was concluded that cytokinin confers an adaptive advantage under circadian stress by directly or indirectly fine-tuning circadian clock function.

The main results and conclusions of the "circadian stress" project, as outlined in the previous paragraph, are summarized in a model (Fig. 4.2). In the following chapters I will discuss in more detail which observations underlie these conclusions and how they can be integrated into current scientific knowledge. Facts will be presented that qualify this new kind of stress as "circadian stress" and distinguish it from light stress. The associated cell death will be proposed as a form of programmed cell death. Furthermore, I will evaluate which components of cytokinin signaling are especially important under circadian stress and discuss if the cytokinin status alone determines the circadian stress response. The importance of specific circadian clock components will be emphasized as they constitute

a functional and robust oscillator that prevents a high degree of circadian stress. Moreover, I will discuss the hypothesis that a perturbed oscillator under circadian stress produces inadequate clock outputs which cause the stress and cell death response. The focus will be especially on the contribution of the JA pathway and the ROS network but other potential clock outputs will be considered as well. Lastly, I will address the question how cytokinin might support circadian clock function, thereby enabling a high circadian stress resistance.

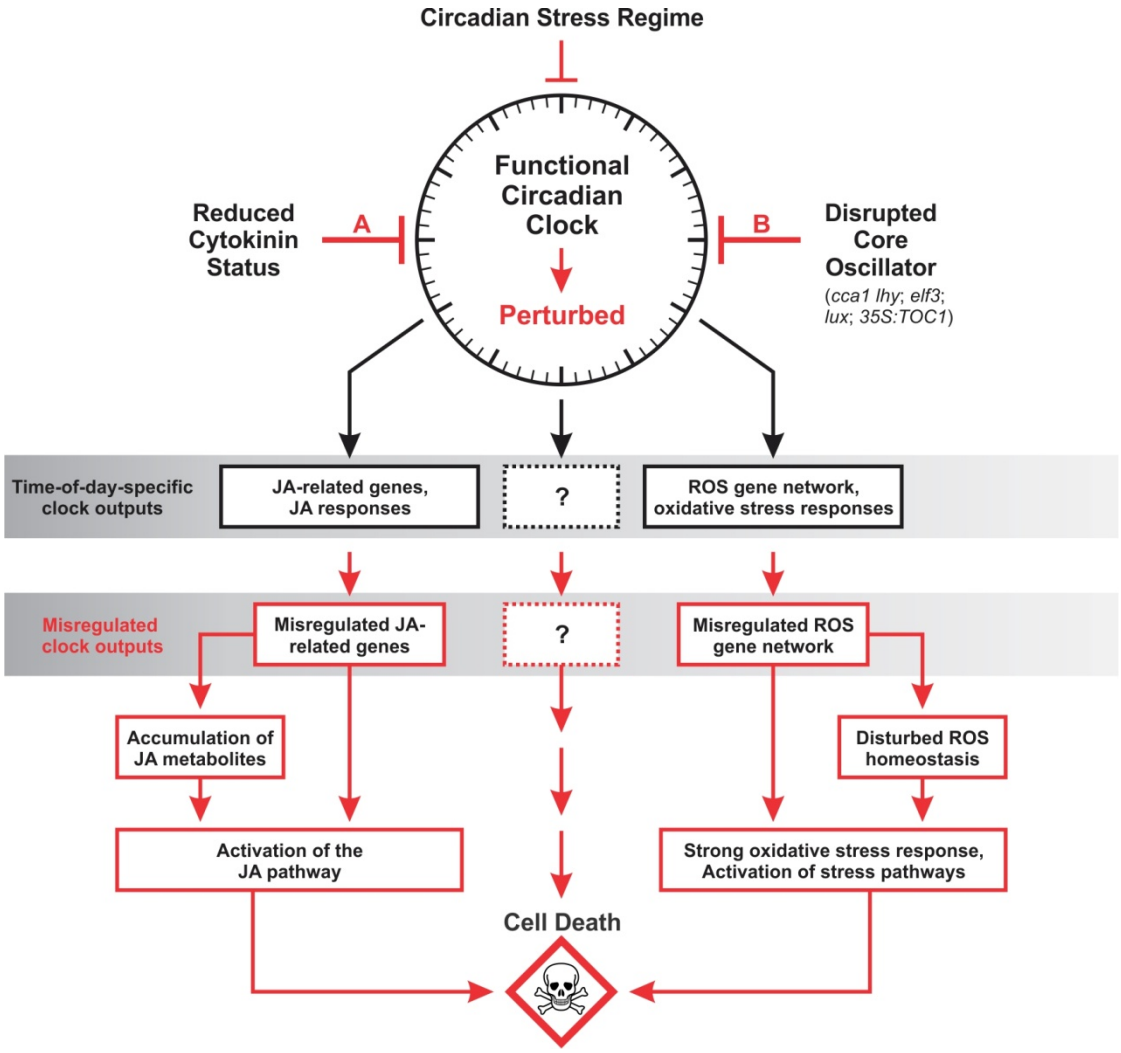

Figure 4.2: Model for the consequences of circadian stress regimes in combination with a reduced cytokinin status or an already disrupted core oscillator.

Figure 4.2 continued.

Changed light-dark regimes negatively affect the circadian clock causing a malfunction of circadian timekeeping, termed "circadian stress". Circadian stress is particularly severe in plants with a reduced cytokinin status (A) and mutants exhibiting a disrupted core oscillator (B) leading to pronounced stress responses and finally cell death development in these plants (red, consequences of circadian stress regimes in combination with A or B). The findings of this work indicate that a strong perturbation of the circadian clock under circadian stress results in a misregulation of clock outputs by the perturbed oscillator that fails to generate proper time-of-day-specific outputs. Accordingly, a strong misregulation of gene expression including JA-related genes and genes of the ROS network was detected, leading to strong JA and oxidative stress responses on the molecular level without initial increase in JA and ROS levels, respectively. These early changes in gene expression can be explained by a direct misregulation of clock-controlled genes and possibly also a perturbed gating of JA and oxidative stress responses by the circadian clock resulting in enhanced JA and ROS responsiveness. One consequence was the activation of the JA pathway and subsequently also the accumulation of JA metabolites amplifying JA signaling which altogether promoted cell death development. On the other hand, the misregulation of the ROS gene network included the upregulation of ROS-inducible genes probably sensed as strong oxidative stress as well as GSR/PCESR genes that are thought to be involved in core stress pathways that might be part of the "death signal" under circadian stress conditions. Moreover, the misregulation of genes encoding scavenging enzymes or ferritins might have contributed to a disturbed ROS homeostasis which accompanied later stages of cell death progression further amplifying oxidative stress responses and hence cell death development. It is possible that the misregulation of additional clock outputs might be involved under circadian stress as indicated by question marks. Taken together, the adaptation to circadian stress regimes requires a functional circadian clock to prevent inadequate clock outputs. Furthermore, clock mutant analyses pointed to an important role of specific clock components. An adaptive advantage in this response is conferred by cytokinin, achieved by directly or indirectly supporting circadian clock function.

4.2.1 Unraveling a new phenomenon – circadian stress

4.2.1.1 Circadian stress is distinct from light stress

Both HL and circadian stress responses were triggered by light. HL stress is indeed a direct consequence of excess light leading to an immediate stress response (Fig. 3.1). However, circadian stress was triggered by prolonged light (CL) treatment but only if succeeded by a long dark period (Figs. 3.15 and 3.16). Therefore, although dependent on the light treatment, this response is distinct from light stress because no signs of stress were detectable directly after the light regime. Even a substantial extension of the CL treatment (up to eight days) did not cause a decline in F_v/F_m ratios.

Low temperatures usually act synergistically with light stress and accelerate photoinhibition due to interference with the PSII repair, thereby aggravating light stress responses (Murata *et al.*, 2007; Fig. 3.3). In contrast, decreased temperatures during the CL treatment strongly reversed the later stress phenotype, supporting the conclusion that the circadian stress phenotype is distinct from light stress responses. Interestingly, HL stress was detected and examined in a detached leaf assay. The results were similar to the ones obtained from attached leaves on whole plants showing that HL acts locally, causing photodamage. Contrarily, the CL-associated cell death phenotype was only observed on whole plants and not in a detached leaf assay (data not shown). This implies that the response to circadian stress is not locally restricted and might rely on long-distance/systemic signals. By analyzing the cytokinin receptor double mutants an important role for CRE1/AHK4 (in concert with AHK3) in the response to the CL regime was revealed while the light stress response required AHK3 and, to a lesser extent, AHK2 but not CRE1/AHK4. This further distinguishes circadian stress from HL stress and, moreover, supports the idea that long-distance signals might be involved since CRE1/AHK4 is predominantly expressed and mainly acting in the root (Mähönen *et al.*, 2000; Higuchi *et al.*, 2004; Stolz *et al.*, 2011; see also 4.2.3.1).

Intriguingly, the 24-hour HL treatment (of whole plants) also resulted in a cell death phenotype if followed by a long (SD) night (data not shown). Thus, these plants encountered two kinds of stress,

the direct HL stress and the later occurring circadian stress. However, the severity of the cell death phenotype after continuous HL was comparable with the phenotype observed after continuous moderate light (CL), sometimes even less pronounced. The numerous different light-dark-temperature regimes (see 3.4) clearly indicated that the negative consequences of a prolonged light treatment depended on the overall change in the light-dark regime, characterized by the entrainment, light treatment, and the post-treatment regime (see Fig. 3.22). Consistently, even extended periods of growth under HL intensities in the SD rhythm did not result in stress-associated phenotypes such as chlorosis or cell death (data not shown).

4.2.1.2 Circadian stress is caused by specific changes in the light-dark regime

Substantial changes in the light-dark-regime caused a strong stress phenotype in plants with a reduced cytokinin status. The specific interplay between entrainment, light treatment, and post-treatment regime was crucial for the outcome (see Fig. 3.22). Short photoperiods followed by prolonged light treatments and succeeding long dark periods affected the plants most strongly. Moreover, changes in the temperature modulated the severity of the phenotype. This led to the conclusion that this stress phenotype is linked to a perturbation of the circadian clock, coining the phenomenon "circadian stress".

Among the different entrainments, SD entrainment prior to CL treatment resulted in stronger phenotypes compared with LD-entrained plants. Hence, the stress phenotype inversely correlated with the length of light periods prior to CL. The circadian clock is entrained by strong environmental signals such as light-dark rhythms which synchronize clock-driven rhythms with the environment (see 1.3.2). Besides structural, transcriptomic, and metabolic differences as well as changes in the redox state between SD- and LD-grown plants (Lepistö and Rintamäki, 2012), there are also substantial differences in the cycling of genes. In SD photocycles more transcripts oscillate than in LD conditions and phases of peak expression are shifted within a 24-hour period and relative to dawn and dusk, respectively (Michael *et al.*, 2008b). Therefore, it is conceivable that a strong alteration in the light-dark rhythm results in a strong discrepancy between the ongoing circadian (internal) rhythms and the new (external) conditions. This can have negative consequences. It is known that incorrect matching of endogenous rhythms with the environmental rhythms reduces plant fitness (Dodd *et al.*, 2005; see 1.3.1).

Interestingly, the (32 h) CL treatment interrupted the prior SD rhythm but the following dark period was still in-phase with the entrainment regime (see Fig. 3.6A). Cytokinin-deficient plants were unable to properly adjust to these changes. Hence, they might be impaired in the re-acclimation to SD after prolonged photoperiods and, therefore, failed to cope with the long nights associated with the SD regime. Genes that are associated with the acclimation of *Arabidopsis* plants to SD conditions include cell cycle genes as well as genes involved in the regulation of transcription and circadian rhythm (Lepistö and Rintamäki, 2012). One example is *CCR2*/*GRP7*, a clock-controlled gene, which is induced after transfer from longer photoperiods to SD conditions and repressed after transfer from SD to LD. Strikingly, CL-treated wild-type plants exhibited an increased expression of *CCR2*/*GRP7* in the second

half of the long (SD) night following the CL regime compared with cytokinin-deficient plants which could indicate a better acclimation to the recurring SD conditions (see Appendix Fig. A.15).

The circadian clock is involved in the measurement of daylength and, therefore, important for photoperiodic responses such as hypocotyl growth (Michael *et al.*, 2008a; Nomoto *et al.*, 2012; see 1.3.8) and flowering (Imaizumi, 2010; McWatters and Devlin, 2011). These responses involve coincidence mechanisms that are not only regulated by the circadian clock but also rely on light signaling – as many rhythmic events in plants (Dalchau *et al.*, 2010). Light signaling, however, may be very decisive for circadian timing during daytime but for the timing of nocturnal processes the circadian clock is of major importance (Dodd *et al.*, 2014). Therefore, it is striking that the dark period (as part of the post-treatment regime; see Fig. 3.22) was so crucial for the induction of cell death in cytokinin-deficient plants pointing to a misregulation of nighttime events. Re-entrainment experiments using different night lengths supported this view and, moreover, revealed that a resetting of the oscillator (by light) was linked to a rescued plant phenotype (Figs. 3.16 and 3.27).

The fact that a decrease of the ambient temperature was protective against circadian stress also indicated an involvement of the circadian clock. Temperature is an important entrainment factor for the circadian oscillator (Salomé and McClung, 2005b; McWatters and Devlin, 2011; see 1.3.6.2). Temperature cycles during the CL regime strongly reversed the stress phenotype of cytokinin-deficient plants. This indicated that they could at least in part substitute for the missing light-dark cycle during CL treatment providing sufficient input information to prevent a profound desynchronization of the circadian clock. On the other hand, it has to be noted that plant phenotypes could also be strongly reversed when the temperature was constantly low during CL treatment (data not shown). Low temperatures have a strong impact on oscillator function and were shown to cause complete arrhythmicity in clock gene expression under constant light conditions (at 4 °C; Bieniawska *et al.*, 2008). Bieniawska and colleagues also reported that in several cases, for example for *CCA1* and *LHY*, the stopped circadian oscillation was characterized by constantly high expression levels. This could be an explanation for the rescued phenotype under the alternative temperature regime because both morning genes, *CCA1* and *LHY*, were found to be decisive under circadian stress conditions (see also 4.2.4.1). It is possible that temperature cycles and constantly low temperatures during the CL regime reversed the circadian stress phenotype by different means. However, both explanations are based on the fact that low temperatures affect the circadian clock and hence might counteract an impairment of the circadian oscillator occurring under circadian stress.

One could argue that in nature plants would never encounter as strong changes in the light-dark regime as were applied experimentally and, therefore, ask whether there is any relevance for circadian stress under more physiological conditions. Moreover, one could ask whether the results obtained under rather "extreme" conditions (such as CL treatment interrupting a SD rhythm) are in any way informative or even transferable to plants grown under "natural" conditions. CL treatment is extensively used to study the circadian clock machinery and its performance and was crucial for the identification of clock mutants (Millar *et al.*, 1995a; Velez-Ramirez *et al.*, 2011; see 1.3.3). Constant conditions such as CL are indispensable for clock research because they enable to elucidate clock

defects which are usually masked by a daily resetting of the system *via* entrainment. Likewise, the circadian stress regime helped to unravel that cytokinin is able to regulate or fine-tune the circadian oscillator and that a perturbation of the clock during the dark period can have severe consequences, leading to a strong stress and cell death phenotype (see Fig. 4.2). This would have been impossible to observe with a fully functional clock and the externally induced disturbance of the oscillator by exposure to circadian stress regimes unmasked the connections existing between cytokinin, circadian clock, JA pathway, the ROS gene network, and cell death (see also later sections). Furthermore, smaller alterations in the light-dark regime also induced stress and cell death phenotypes in cytokinin-deficient plants, e.g. the transfer from SD to LD ("16 h L/8 h D", Fig. 3.6). This indicates that even within a more physiological range of changes in the light-dark regime plants encounter circadian stress.

The cell death phenotype after the "16 h L/8 h D" regime (SD to LD) was rather weak compared with the standard (32 h) CL regime ("32 h L/16 h D") used in this work (Fig. 3.6) but, on the other hand, was highly similar when a long dark period followed ("16 h L/16 h D", Fig. 3.6 or "16 h CL", Fig. 3.19). This confirmed that a long dark period (more than the exact duration of the preceding light treatment or a certain T-cycle) is very crucial for the severity of cell death and, moreover, that an earlier onset of light can suppress the upcoming circadian stress. Accordingly, after 7.5 hours of darkness following "16 h CL" or "32 h CL" the stress phenotype was highly comparable on the molecular level (Fig. 3.19E-F) but if the night ended after 7.5 h or 8 h, respectively, the highest possible degree of circadian stress (finally reflected by the extent of cell death) was not reached (see Figs. 3.6 and 3.16).

4.2.2 Circadian stress provokes an age-dependent programmed cell death

4.2.2.1 Programmed cell death under circadian stress

The term programmed cell death (PCD) is used to indicate an active cell suicide. PCD can be triggered both exogenously and endogenously and involves genetically regulated processes, including the activation of signaling pathways and metabolic changes (de Pinto *et al.*, 2012; Lord and Gunawardena, 2012; see 1.5). The data in this work support the view that the cell death upon circadian stress relies on an intracellular program and, therefore, is a kind of PCD.

Strong changes in gene expression were already recorded "5 h" after CL treatment (Figs. 3.23 and 3.42) and, therefore, preceded by far the detection of the first (still weak) visible symptoms at "10 h" (Fig. 3.14). Among the early upregulated genes were *BAP1* and *ZAT12* that both are well-known oxidative stress marker genes (op den Camp *et al.*, 2003; Gechev *et al.*, 2006) and *JAZ1*, a JA response gene (Thines *et al.*, 2007). Interestingly, the responsiveness of these three genes is not restricted to a specific stress. They are differentially regulated under many biotic and abiotic stress conditions and were, therefore, defined as general stress response (GSR) genes (Walley *et al.*, 2007) or even (true for *JAZ1* and *ZAT12*) as core environmental stress response (PCESR) genes (Kilian *et al.*, 2012; Hahn *et al.*, 2013). Also other PCESR genes were upregulated during cell death progression such as *ERF5* or *WRKY18* (data not shown). GSR or PCESR genes appear to be conserved between different plant species, such as rice, barley or wheat, and are thought to be crucial for general stress signaling

in plants that mediates stress tolerance and adaptation involving systemic signaling but also provokes alarm responses. Moreover, *BAP1* (together with *BAP2*) functions as cell death regulator (suppressor) in plants (Yang *et al.*, 2007). The same is true for *BI1* which is a highly conserved cell death regulator gene (Ishikawa *et al.*, 2011) and was also upregulated in cytokinin-deficient plants under circadian stress. *BI1* induction temporally correlated with the initiation of cell death in these plants (see Figs. 3.19, 3.23, 3.36 and 3.44). Together, the strongly altered expression of stress and cell death-related genes reflects the involvement of active signaling before cell death was phenotypically visible. Moreover, it could indicate that core stress pathways were activated triggering alarm responses which might be part of the "death signal" (Fig. 4.2).

Strikingly, gene expression levels correlated well with the severity of cell death. For instance, intermediate cell death phenotypes as visible after intermediate 7.5-hour nights and the rescue of the plants after 2.5- or 5-hour short nights (Fig. 3.16), were reflected by intermediate expression levels of *JAZ1* and *BI1* (7.5 h) and the lack of induction (2.5 h) or even consecutive downregulation (5 h) when induction had already started (Fig. 3.44; see also 3.7.2). This is consistent with a recent study which showed that quantitative differences in cell death-related gene expression better correlated with the observed cell death phenotypes than qualitative changes (Brosché *et al.*, 2014). Furthermore, it is generally accepted that the quantity of "death signals" determines the cell death response. Only if ROS levels increase above certain threshold levels they are able to induce cell death (Gechev *et al.*, 2010; Karuppanapandian *et al.*, 2011). Similarly, only if a certain threshold is reached during effector-triggered immunity (ETI) HR cell death is initiated (Jones and Dangl, 2006; Coll *et al.*, 2011).

Plants with a reduced cytokinin status in the JA-deficient background exhibited a strongly alleviated cell death phenotype upon circadian stress in comparison with cytokinin-deficient plants in the wild-type background (see Fig. 3.47). This outcome pointed to an active involvement of the JA pathway in cell death development. Additionally, the cell death response was age-dependent (see 4.2.2.2) which also supported the hypothesis that cell death in response to circadian stress is a form of PCD, being determined by the presence or absence of specific factors and active signaling.

4.2.2.2 Age-dependence of the cell death phenotype under circadian stress

Cell death upon circadian stress is age-dependent (see 3.3.3). The severity of cell death was strongest in five- to six-week-old plants (all experiments in this work) and less pronounced or even absent in three- to four-week-old plants or very young seedlings, respectively (data not shown). A very well-characterized form of age-dependent PCD is senescence (Lim *et al.*, 2007). However, several observations and data revealed that the circadian stress-associated cell death is rather distinct from senescence (see 1.5.2).

Firstly, natural senescence is a rather slow process and leaves are usually affected one after another, depending on their age (Lim *et al.*, 2007). Cell death under circadian stress was fastly progressing and affecting many leaves at once and in very severe cases even leaves that were not even fully expanded (e.g. in *ipt3,5,7*). Secondly, a decrease in *CAB2* expression accompanies chlorophyll degradation during senescence and *SAG12* is a frequently used marker gene that is expressed once the first signs

of senescence become visible (Gan and Amasino, 1995; Lim *et al.*, 2007). Circadian stress-associated cell death was also accompanied by *CAB2* downregulation (Figs. 3.12, 3.13, and 3.25) but the usually associated chlorosis, the yellowing of leaves typical for senescence, did not appear. Moreover, *SAG12* upregulation was observed at a late stage of cell death progression (Fig. 3.12) but not at early stages when the first symptoms were already detectable (Fig. 3.13). Thirdly, water-soaked lesions occurred during circadian stress-induced cell death and are reported for HR cell death (Greenberg *et al.*, 2000; Katagiri *et al.*, 2002; Su'udi *et al.*, 2011; Ishiga *et al.*, 2011) but are untypical for senescence.

In addition to the whole-plant age, the cell death phenotype under circadian stress was also dependent on the leaf age within one plant as reflected by strong cell death in the older mature leaves and no cell death response in very young developing leaves. One explanation could be that the emerging leaves including the shoot apical meristem (SAM) were somehow protected or insensitive to ensure optimal reproduction as during senescence (Lim *et al.*, 2007). During senescence the protection of younger tissues is due to the absence of age-related signals that are required to acquire the competence to senesce (Jibran *et al.*, 2013; Thomas, 2013). Similar signals determining the developmental stage might be involved in the cell death response under circadian stress which would imply that young leaves have not yet acquired the "competence to die". This is well studied for the inducibility of senescence by ethylene (Jing *et al.*, 2002; 2005). However, the gene expression data for *ERF1*, an ethylene response gene (Solano *et al.*, 1998; Lorenzo *et al.*, 2003), showed that it was not strongly induced early during the development of circadian stress (Fig. 3.42G) and, therefore, indicated that ethylene signaling was not desicive for the onset of stress.

In order to gain insight into why leaves of a different developmental stage behaved differently stress-, cell death-, and clock-related gene expression was studied in young and mature leaves. It turned out that stress- and cell death-related transcripts were solely altered in mature leaves (Fig. 3.13 and 3.44) while clock gene expression was similarly changed in all leaves (Fig. 3.28), indicating that the whole plant encountered circadian stress. However, the chosen time point for these experiments (16 h after CL treatment) did not allow evaluating whether the extent of circadian stress in cytokinin-deficient plants was comparable between young and mature leaves because the greatest differences in oscillator gene expression occurred earlier during the night (see *CCA1*/*LHY*; Fig. 3.24A-B). It is possible that the perturbation of *CCA1*/*LHY* expression and hence the extent of circadian stress was wild-type-like in young leaves. This would explain the absence of stress and cell death responses. Moreover, it could imply that there are differences in the sensing of photoperiodic changes between young and mature leaves which would be one explanation why the circadian oscillator was not affected in young leaves. Furthermore, there is strong experimental evidence that there are differences in oscillator mechanisms between different cell types or tissues (Para *et al.*, 2007; James *et al.*, 2008; Yakir *et al.*, 2011). Therefore, one could also think of differences in oscillator properties between young and mature leaves. According to that, differences in the molecular composition of the oscillator could explain different effects on circadian outputs and hence different consequences of circadian stress conditions. It is also conceivable that clock input pathways (e.g. depending on light and/or possibly cytokinin) might be differently regulated in young *versus* mature leaves.

The alternative would be that circadian stress was present to a similar extent in cytokinin-deficient young leaves compared with mature leaves. In this case, the difference in stress and cell death responses (Fig. 3.13) would result from a different sensitivity towards circadian stress. One possible explanation could be that certain metabolites or pathways that are under clock control and contribute to the cell death phenotype under circadian stress differ in their abundance, acitivity, or function in sink (young) and source (mature) leaves, respectively. One possible scenario could be a differential regulation of ROS homeostasis and signaling. On the one hand, strongly increased ROS levels lead to oxidative stress and can induce cell death (de Pinto *et al.*, 2012). On the other hand, the circadian clock regulates ROS homeostasis and the sensitivity to oxidative stress in part by extensively regulating the ROS gene network (Lai *et al.*, 2012). Moreover, it is known that similar to senescing leaves emerging leaves encounter strong oxidative stress. However, in contrast to senescing leaves this is not translated into oxidative damage or cell death but seems to support their development (Juvany *et al.*, 2013) indicating that there are indeed differences in downstream events/signaling following oxidative stress. So far, there are no studies that have focused in detail on ROS signaling and ROS-responsive gene expression in emerging leaves. Since a misregulation of genes of the ROS gene network (including GSR/PCESR genes, see 4.2.2.1) is one consequence of circadian stress in mature leaves and possibly part of the "death signal" (Fig. 4.2; see 4.2.6.1 and 4.2.6.2) differences in the regulation of the ROS gene network (by the clock) between young and mature leaves could be one possible explanation for their different behavior under circadian stress.

4.2.3 A reduced cytokinin status results in high sensitivity towards circadian stress

Circadian stress phenotypes including stress and cell death responses were observed in many plants with a reduced cytokinin status pointing to a redundant action of synthesis and signaling genes. Hence, cytokinin plays a pivotal role in the adaptive response to changing light-dark regimes. In the following I will discuss which cytokinin signaling components are of particular importance under circadian stress (see 4.2.3.1) and, moreover, whether it is the overall increase in cytokinin levels or signaling alone that rescues plants with a higher cytokinin status in contrast to cytokinin-deficient plants (see 4.2.3.2).

4.2.3.1 The circadian stress response is mediated by specific cytokinin signaling components

Each of the three cytokinin receptors contributes differently to the circadian stress response (Fig. 3.7). The AHK3 receptor turned out to be the most important mediator of cytokinin signaling under circadian stress since even single *ahk3* mutants exhibited a weak but distinct cell death phenotype. This circadian stress phenotype was strongly aggravated when combined with *AHK2* or *CRE1* loss-of-function, revealing an accessory role for AHK2 and CRE1, respectively. The strong phenotype of *ahk2 ahk3* plants is consistent with the predominant expression and function of *AHK2* and *AHK3* in shoot tissues including leaves (Higuchi *et al.*, 2004; Nishimura *et al.*, 2004; Kim *et al.*, 2006; Riefler *et al.*, 2006; Stolz *et al.*, 2011; see also 4.1.3). The rather synergistic effect of *cre1* on *AHK3* loss-of-function, however, was surprising and revealed a strong cooperative function of CRE1. *CRE1* is mainly expressed in the roots and several of its functions are associated with underground tissues (Mähönen *et al.*, 2000; Ueguchi *et al.*, 2001b; Birnbaum *et al.*, 2003; Higuchi *et al.*, 2004). The strongly

pronounced phenotype of *cre1 ahk3* mutants (even stronger than in *ahk2 ahk3*) either points to a so far underestimated or novel role for *CRE1* in aerial tissues or to an involvement of underground tissues in the development of circadian stress.

CRE1 transcripts exhibit a quite low overall abundance in *Arabidopsis* shoot tissues. However, its expression and activity in above-ground tissues is present in the vasculature and the SAM (Higuchi *et al.*, 2004; Nishimura *et al.*, 2004; Gordon *et al.*, 2009; Stolz *et al.*, 2011; Chickarmane *et al.*, 2012). Intriguingly, the vasculature plays an important role in the response to circadian stress regimes as will be discussed in more detail later (see 4.2.4.4). Due to the importance of vascular clock function under circadian stress the predominant expression of *CRE1* in the vasculature could explain an involvement of CRE1 in leaves. Interestingly, basal *ARR5:GUS* cytokinin reporter gene activity is dramatically reduced in the leaf vasculature of both *ahk2 ahk3* and *cre1 ahk3* plants, while basal cytokinin signaling is detected in *cre1 ahk2* plants that retain AHK3 activity (Stolz *et al.*, 2011). This is in line with the fact that exclusively the latter double mutant plants could cope with circadian stress. CRE1 has a high affinity and responsiveness to iP-type cytokinins in contrast to AHK3 (Romanov *et al.*, 2006; Stolz *et al.*, 2011; Lomin *et al.*, 2012). If a proper circadian stress response would depend on iP-type cytokinins CRE1 could support the less sensitive AHK3 receptor. The fact that the single *cre1* receptor mutant behaves like wild type (Fig. 3.7) indicates that CRE1 only acts together with AHK3. It has been shown that AHK3 and CRE1 can interact with each other (Dortay *et al.*, 2006; Caesar *et al.*, 2011). So far, it has not been investigated if or in which way such a hetero-dimerization (or oligomerization) influences the respective receptor properties.

As mentioned above, the role of CRE1 under circadian stress could also point to an involvement of underground tissues in this adaptive response. Since only the aerial parts are exposed to the changing light-dark regimes an involvement of cytokinin signaling in the roots would require long-distance signals (as already suggested in 4.2.1.1) to enable communication between shoot and root tissues. One potential long-distance signal could be cytokinin itself. iP-type cytokinins are mainly produced in above-ground tissues but transported basipetally in the phloem sap and, oppositely, tZ-type cytokinins are mainly synthesized in the root and transported acropetally in the xylem (Matsumoto-Kitano *et al.*, 2008; Hirose *et al.*, 2008; Kudo, 2010; Ko *et al.*, 2014; Zhang *et al.*, 2014). In this respect, it is striking that the circadian stress phenotype was almost fully rescued in *rock4 35S:CKX1* plants (Fig. 3.8). *rock4* represents a dominant *IPT3* gain-of-function allele and strongly reverses many phenotypic traits that are associated with the low cytokinin status of *35S:CKX1* plants (Jensen, 2012). Interestingly, *IPT3* is predominantly expressed in the vasculature, more specifically in the phloem (Miyawaki *et al.*, 2004), which is decisive for the basipetal cytokinin transport. This could indicate that IPT3-dependent cytokinin production in the vasculature contributes to the prevention of circadian stress and again highlights the relevance of vascular tissues for a proper circadian stress response (for more details see 4.2.4.4).

Of course, cytokinin itself is not the only possible systemic signal. Alternatively, shoot-derived carbohydrates as products of photosynthesis could act as systemic messengers. Carbohydrates, especially sucrose, are transported from shoot to root and act as signaling molecules (Rolland *et al.*,

2006; Smeekens *et al.*, 2010; Wind *et al.*, 2010; Hammond and White, 2011; Kircher and Schopfer, 2012). Interestingly, cytokinin-deficient plants (e.g. *ahk3* and *cre1 ahk3*) are hypersensitive to sucrose (Franco-Zorilla *et al.*, 2005). An ongoing supply with sucrose under CL could be a signal for the roots that photosynthetic processes are still active and hence that the light period is prolonged. Interestingly, addition of sucrose at dusk under diurnal conditions disrupts circadian rhythms in the root (but not in the shoot) in a similar manner as observed under circadian (constant light) conditions (James *et al.*, 2008). In addition, blocking photosynthesis with DCMU (3-(3,4-dichlorophenyl)-1,1-dimethylurea), an inhibitor of electron transport in chloroplasts, also negatively affected the expression of clock genes exclusively in the roots. These data led to the conclusion that, in contrast to the shoot circadian system, the root circadian clock relies on diurnal signals which presumably are photosynthesis-related (James *et al.*, 2008; Más and Yanovsky, 2009). This is reasonable because the root system lacks light input signals. At the present stage of the circadian stress project it is not clear if a desynchronization between the shoot and root circadian system is involved in the development of circadian stress. Yet, in cytokinin-deficient plants hypersensitivity to sucrose could cause a more pronounced perturbation of the root circadian system. However, it would require also a root-to-shoot feedback which would explain the stress and cell death responses in the leaves.

Testing B-type *arr* mutants under circadian stress conditions revealed that ARR2 and a combination of ARR10 and ARR12 are involved in the response to changing light-dark regimes (Fig. 3.10). However, the cell death phenotypes were much less pronounced than in *35S:CKX4* plants. Even the intermediate phenotype of *arr2* plants was not observed in all experiments. The rather weak phenotypes are in accordance with the strong functional redundancy among B-type *ARR* genes (Mason *et al.*, 2005; Argyros *et al.*, 2008; Ishida *et al.*, 2008a). In contrast to the HL response, *arr1,12* mutants exhibited the weakest cell death that was even less pronounced than in *arr10,12* plants which showed a wild-type-like HL response (Cortleven and Nitschke *et al.*, 2014). This indicates that the circadian stress response is probably mediated by a different set of B-type ARRs than the HL response. In future studies, additional double and triple mutants should be tested to gain more insight into which B-type *ARR* genes are required to counteract circadian stress. For example, *arr1,10* plants were not yet analyzed under circadian stress conditions and, moreover, double mutant combinations including *ARR2* loss-of-function could be promising since the *arr2* single mutant was already affected (at least in some experiments). Due to the severe growth defects of *arr1,10,12* triple mutants especially in the SD regime it was impossible to test these plants under circadian stress conditions. Interesting alternatives could be the *arr1,2,12* and *arr2,10,12* triple mutants, respectively (Mason *et al.*, 2005). Another reason for the rather weak circadian stress phenotypes in the so far tested B-type *arr* mutants (in addition to functional redundancy) could be that another branch of cytokinin signaling contributes to or even dominates in this response. Candidates could be the *CRF* genes (Rashotte *et al.*, 2006; Cutcliffe *et al.*, 2011).

4.2.3.2 A high cytokinin status is required but not sufficient to cope with circadian stress

Several results demonstrate that a high cytokinin status (involving functional signaling, see 4.2.3.1) is required to efficiently cope with circadian stress, even pointing to a dosage effect. For instance, the

severity of cell death was dependent on the number of *IPT* mutations revealing that the extent of circadian stress correlated with the increasing lack of cytokinin biosynthesis (Fig. 3.9). Furthermore, there were differences in the circadian stress response between *CKX* overexpressor lines. *35S:CKX1* plants exhibited a very severe phenotype whereas *35S:CKX2* and *35S:CKX4* plants both were slightly less affected (Fig. 3.8). In this respect, the extent of circadian stress correlates well with the severity of the cytokinin deficiency syndrome in these plants (Werner *et al.*, 2003). Although CKX2 and CKX4 are much more active on the bioactive iP- and tZ-type cytokinins than CKX1 (Galuszka *et al.*, 2007), the concentration of these substrates is stronger reduced in *35S:CKX1* plants (Nishiyama *et al.*, 2011a). This could explain the stronger circadian stress phenotype of *CKX1*-overexpressing plants and might be due to the different subcellular localization of the respective CKX enzymes. CKX1 is present in the vacuole while CKX2 and CKX4 are transported through the secretory pathway and targeted to the apoplast (Werner *et al.*, 2003). It is possible that the composition of the vacuolar cytokinin pool differs from that in other compartments (e.g. containing a higher portion of iP- and tZ-type cytokinins or other cytokinins that are relevant under circadian stress) or that the vacuolar degradation creates a stronger intracellular sink for cytokinins. In addition, it is not inconceivable that the vacuole itself might have a function under circadian stress. Vacuoles play a crucial role in plant cell death (Hara-Nishimura and Hatsugai, 2011) which could be a reason why the vacuolar cytokinin pool size might matter under cell death-inducing circadian stress conditions.

rock1 and *rock4* mutations, respectively, partially or almost fully reversed the circadian stress phenotype of *35S:CKX1* plants similar to their ability to reverse the stunted shoot phenotype in these plants (see 1.1.4; Figs. 3.8 and A.2). The partial reversion in *rock1 35S:CKX1* plants can be explained by a reduced CKX activity that is caused by *ROCK1* loss-of-function counteracting the effect of *CKX1* overexpression and increasing the cytokinin content (Niemann, 2013). *rock4* is a dominant gain-of-function allele of the *IPT3* gene that is capable of increasing the cytokinin status in shoots and roots (Jensen, 2012). Together, the presented data strongly support the view of an inverse relationship between the cytokinin status and the degree of circadian stress.

Surprisingly, two of the four tested *rock* mutants (in the *35S:CKX1* background) did not behave consistently with this conclusion. Although *35S:CKX1* suppressor mutants carrying the *rock2* or *rock3* allele also showed a strong reversion of the stunted shoot growth compared with *35S:CKX1* plants the circadian stress-associated cell death was not (*rock2 35S:CKX1*) or only very slightly (*rock3 35S:CKX1*) reversed (Figs. 3.8 and A.2). *rock2* and *rock3* are dominant gain-of-function alleles that result in constitutively active AHK2 and AHK3 receptors, respectively (Jensen, 2013). Although the slight reversion by introgression of *rock3* is in accordance with the major function of AHK3 under circadian stress compared with the minor impact of AHK2 (see 4.2.3.1) it is still striking that the effect of constitutive AHK3 activity is so small concerning the circadian stress response but very pronounced concerning the shoot phenotype. A similar discrepancy has been described before in a different context. *arr3,4* and *arr3,4,5,6* mutants exhibit a pronounced long-period phenotype (Salomé *et al.*, 2006, see 1.3.8.1). Although their cytokinin responsiveness can be restored by the presence of a genomic copy of *ARR5* (To *et al.*, 2004), their circadian phenotype is not reversed by the *ARR5* transgene (Salomé *et al.*, 2006). The conclusion has been that the long-period phenotype was

established in a cytokinin-independent manner. This, however, is not a legitimate explanation for the results shown in this work since the data on cytokinin synthesis and receptor mutants as well as *CKX* overexpressing plants revealed a positive correlation between the cytokinin status/cytokinin sensitivity and the severity of circadian stress. Nevertheless, this discrepancy might indicate that it is not sufficient to produce a constantly high cytokinin signal in order to rescue the circadian stress phenotype. In addition to an enhanced cytokinin status it might be crucial to also (re-)establish a modulation capability, thereby enabling time-of-day-specific alterations in the intensity of cytokinin responses.

So far, there is limited knowledge about a possible regulation of the cytokinin pathway by the circadian clock but there are indications for such a connection (see also 1.3.8.1). Among the A-type *ARR* genes several were found to oscillate diurnally with peaks during the night (Fig. 3.26; see 3.5.5; Ishida *et al.*, 2008b). Even circadian rhythms of cytokinin-induced genes exhibit phase enrichment during the night (Covington *et al.*, 2008). The strong repression of A-type *ARR* genes not only in cytokinin-deficient but also in clock-deficient plants under circadian stress (Fig. 3.36) strongly supports the view that these genes are additionally regulated in a clock-dependent fashion. As already shown for other hormones such as JA, ABA, or auxin (Covington and Harmer, 2007; Rawat *et al.*, 2009; Castells *et al.*, 2010; Seung *et al.*, 2012; Shin *et al.*, 2012) the circadian clock might also regulate cytokinin synthesis, sensitivity, and/or signaling to fine-tune the overall cytokinin output. This could, on the one hand, help the plant saving energy costs and, on the other hand, concentrate cytokinin outputs to a specific period of time when it is needed most. The data on *ARR* gene transcript abundance revealed that cytokinin-deficient plants are impaired in diurnal oscillations of *ARR* gene expression (reduced amplitude or no peak expression during the night; Fig. 3.26) that are present in wild-type control plants. A similar impairment in diurnal (or even circadian) rhythms of cytokinin outputs could be suggested for plants with constitutively active cytokinin signaling such as *rock2* or *rock3*. However, this might only be true for *rock2* and *rock3* plants in the *35S:CKX1* background since the extremely low cytokinin content strongly limits signaling through the other two available cytokinin receptors (CRE1/AHK4 and AHK3 or AHK2, respectively). *rock2* and *rock3* mutants in the wild-type background should sustain a modulation capability of cytokinin signaling through the unmodified receptors.

For future studies, it would be interesting to test a possible gating of cytokinin outputs by the circadian oscillator and its possible disruption in *rock2* or *rock3* (*35S:CKX1*) plants in order to find out if this is an additional feature needed to master circadian stress. For that, one could analyze cytokinin responsiveness under diurnal and circadian conditions by measuring A-type *ARR* gene expression in response to cytokinin treatment at different times of the (subjective) day. The prior entrainment regime could be very crucial for the outcome of these experiments since cytokinin might be of particular importance under SD conditions (Figs. 3.21 and 3.22).

In addition to the cycling of cytokinin-related genes, altered cytokinin responses (regarding root and hypocotyl elongation, or tissue culture) in clock mutants provide another indication that the circadian clock regulates cytokinin signaling outputs (Zheng *et al.*, 2006). The hypersensitivity towards cytokinin in *CCA1* or *LHY* gain-of-function plants and the reduced sensitivity in *cca1 lhy* loss-of-function plants,

respectively, could result from an impaired gating of cytokinin signaling by disruption of normal *CCA1* and/or *LHY* function. Circadian changes in cytokinin levels during the course of the day could be one way to achieve altered intensities of cytokinin outputs. So far, diurnal rhythms in the cytokinin content have been described in tobacco (Nováková *et al.*, 2005) but there are no available data for *Arabidopsis*. Another way to gate the cytokinin signal strength would be to directly influence cytokinin signaling. Potential targets could be the B-type ARRs. Their abundance and activity have a strong impact on cytokinin signal transduction since they control a high portion of cytokinin-responsive genes (Fig. 1.1). F-box proteins of the KMD family regulate the abundance of B-type ARRs by mediating the degradation of both inactive and activated forms of B-type ARRs through the ubiquitin proteasome pathway (Kim *et al.*, 2013). Interestingly, the expression of at least three of the four *KMD* genes is regulated by the circadian clock (Covington and Harmer 2007; Covington *et al.*, 2008; Kim *et al.*, 2013). To regulate the abundance of activated and non-activated B-type ARRs by the circadian control of KMDs would be a great tool to modulate cytokinin responsiveness in a clock-dependent manner.

4.2.4 Specific clock components are indispensable under circadian stress

Transcript and mutant analyses together supported the hypothesis that a perturbation of the circadian clock underlies the circadian stress phenotype in cytokinin-deficient plants. At the same time, they also revealed that it is decisive which part of the core oscillator is impaired pointing to specific clock components that determine the plant's fate under circadian stress.

4.2.4.1 CCA1 and LHY are important players during circadian stress

Transcription-based feedback loops are a critical part of the oscillatory mechanism and essential for circadian timekeeping (McClung, 2011; Carré and Veflingstad, 2013). Moreover, the control of gene transcription is an important tool used by the circadian clock to regulate clock output pathways (see 1.3.7.2). Therefore, it is striking that the analysis of clock gene expression revealed strong alterations in cytokinin-deficient plants during the dark period following CL treatment. Especially *CCA1*/*LHY* expression was affected (Fig. 3.24; see 3.5.2). All CL-treated plants, including the wild type, exhibited dampened *CCA1*/*LHY* oscillations but the attenuated cycling was severely aggravated in plants with a reduced cytokinin status. They were almost completely lacking peak expression indicating an impaired anticipation of dawn. In contrast, wild-type plants still exhibited *CCA1*/*LHY* peak expression, albeit slightly reduced and advanced in phase compared with the controls. The lack of sufficient nighttime *CCA1*/*LHY* expression in cytokinin-deficient plants reflected a substantial disruption of the circadian core oscillator and pointed to a predominant role of CCA1 and LHY in preventing circadian stress. Furthermore, strongly altered output gene expression confirmed the disruption of the circadian clock (Fig. 3.25). Strikingly, the divergence in oscillator gene expression between wild-type and cytokinin-deficient plants coincided with the upregulation of stress and cell death marker genes in the latter (Figs. 3.23 and 3.24). Additionally, re-entrainment experiments demonstrated that the reversion of the cell death phenotype was linked to a wild-type-like (or even higher) *CCA1*/*LHY* expression reflecting the resetting of the oscillator by light (Fig. 3.27).

In accordance with the idea that CCA1 and LHY are crucial for the circadian stress response, *CCA1*/*LHY*-deficient plants displayed a strong cell death phenotype upon exposure to the circadian stress regime whereas plants with high levels of *CCA1* and/or *LHY* were only slightly affected or completely unaffected, respectively. Some examples will be presented and discussed in the following sections.

cca1 lhy double mutants carrying the loss-of-function alleles *cca1-1* (Green and Tobin, 1999) and either *lhy-11* (Mizoguchi *et al.*, 2002) or *lhy-20* (Michael *et al.*, 2003a) are one example for *CCA1*/*LHY*-deficient plants that showed a circadian stress phenotype. However, it seems that *lhy-11* was the stronger allele under circadian stress compared with *lhy-20* as deduced from the phenotypes of the respective single mutants (see Fig. 3.30) as well as from the analyses of the corresponding double mutants with *cca1-1* (see 3.6.2). As already briefly outlined in the Results (see also 3.6.2), the mutant *LHY* alleles have different genetic backgrounds. In the following, three possible explanations for the differences between the two alleles are presented: 1) LHY proteins were not detectable in *lhy-11* plants, indicating that *lhy-11* is a null allele (Kim *et al.*, 2003). In contrast, LHY protein abundances have not been analyzed in *lhy-20* plants. However, *LHY* loss-of-function was confirmed by a short-period phenotype in *lhy-20* mutants (Michael *et al.*, 2003a; Salomé *et al.*, 2010) which is typical for plants lacking LHY (Mizoguchi *et al.*, 2002). This still does not exclude that the *lhy-20* mutation might result in an incomplete knockout which is not fully inconceivable since the T-DNA inserted into an intron (Michael *et al.*, 2003a). 2) *lhy-11* plants are derived from the L*er* accession (Mizoguchi *et al.*, 2002). Although backcrossed to Col-0 several times (Ito *et al.*, 2007), some phenotypical characteristics were still reminiscent of the L*er* background (observations during this work). L*er* plants were tested under the circadian stress regime and behaved like Col-0 plants. It still cannot be ruled out completely, that L*er*-specific alleles which may still be present in the *lhy-11* plants might – although not acting alone – amplify the effect of *LHY* loss-of-function acting synergistically with *lhy-11*. 3) *lhy-11* plants exhibit constantly high *LHY* transcript levels which are due to the still present *lhy-1* background causing *LHY* overexpression (Schaffer *et al.*, 1998). This has already been shown for the closely related *lhy-12* plants (Mizoguchi *et al.*, 2002) and the data in this work also revealed *LHY* overexpression in *lhy-11* carrying plants (Fig. 3.35; see 3.6.6). Interestingly, there are studies which point to a regulatory role of *LHY* transcripts. Wild-type plants that were transformed with a transgenic copy of the *lhy-1* mutant allele (called *lhy-1*^{TN104}) leading to constitutive expression of the *LHY* transgene exhibited arrhythmic expression (constant between preak and trough levels found in the wild type) of the endogenous *LHY* gene under constant light (Schaffer *et al.*, 1998) and strongly attenuated expression (close to trough levels found in the wild type) of both the endogenous *LHY* and the *CCA1* gene under a light-dark rhythm (Kim *et al.*, 2003). This was unlikely caused by constantly high LHY protein levels since these were shown to be highly rhythmic (albeit with a different pattern than in the wild type) in the presence of light-dark transitions (Kim *et al.*, 2003). Therefore, it is conceivable that the high *LHY* levels in *lhy-11* plants although not translatable into functional LHY proteins might be regulatory active thereby causing slightly stronger perturbations within the oscillator than solely caused by *LHY* loss-of-function. The period phenotypes of *cca1-1 lhy-11* and *cca1-1 lhy-20* plants, respectively, confirmed the view that *lhy-11* causes stronger clock defects than the *lhy-20*

allele. While the *cca1-1 lhy-20* mutant exhibits a short-period phenotype (Hong *et al.*, 2013b; Zhang *et al.*, 2013) *cca1-1 lhy-11* plants show extreme period shortening or even arrhythmicity of circadian rhythms (Mizoguchi *et al.*, 2002; Yamashino *et al.*, 2008). Although there are differences in the consequences of *lhy-11* or *lhy-20* mutation the presence of circadian stress phenotypes in both *cca1-1 lhy-11* and *cca1-1 lhy-20* plants confirms that the simultaneous mutation of *CCA1* and *LHY* is linked to the observed cell death phenotype supporting the hypothesis that CCA1 and LHY are important under circadian stress.

Plants such as *elf3-8*, *elf3-9*, *lux-1*, and *35S:TOC1* that are primarily impaired in a different part of the core oscillator also exhibited profound cell death phenotypes. Strikingly, an impaired EC in *elf3* or *lux* plants (Hazen *et al.*, 2005; Dixon *et al.*, 2011) as well as *TOC1* overexpression (Makino *et al.*, 2002; Gendron *et al.*, 2012; Huang *et al.*, 2012) also result in a profound *CCA1*/*LHY* deficiency as a consequence of the impaired oscillator function. The EC components ELF3, ELF4, and LUX act together (Nusinow *et al.*, 2011) to ensure proper clock gene expression especially at night (Pokhilko *et al.*, 2012). This includes the nocturnal regulation of *CCA1* and *LHY* (Doyle *et al.*, 2002; Hazen *et al.*, 2005; Kolmos *et al.*, 2009; Dixon *et al,* 2011). It is notable that the positive effect of the EC on *CCA1*/*LHY* expression is not accomplished by the regulation of their transcription. Instead, it is thought to be achieved by an indirect mechanism *via PRR9* (and probably also *PRR7*) repression (Dixon *et al.*, 2011; Helfer *et al.*, 2011; Herrero *et al.*, 2012; Carré and Veflingstad, 2013; see 1.3.5.5). In turn, the reduction of PRR9 (and PRR7) levels results in a derepression of *CCA1*/*LHY* (Nakamichi *et al.*, 2010; see Fig. 1.3A). Intriguingly, *PRR9* levels were elevated in cytokinin-deficient plants relative to wild type during the night following CL treatment (Fig. 3.38D). Moreover, *prr9* loss-of-function appeared to be protective at least in comparison with wild-type plants which exhibited a weak cell death phenotype. To further evaluate whether the main function of the EC during circadian stress is indeed to ensure sufficient *CCA1*/*LHY* nighttime expression *via* regulation of *PRR9* it would be interesting to test *prr9 elf3* double mutants. *elf3* plants exhibit increased levels of *PRR9* (and *PRR7*) (Dixon *et al.*, 2011). A reversion of the *elf3*-associated circadian stress phenotype by *PRR9* mutation would provide evidence that the EC-dependent suppression of *PRR9* expression to facilitate high-amplitude rhythms of both *CCA1* and *LHY* is important in this context. Additionally, the generation of cytokinin-deficient *prr9* plants would provide information about whether *PRR9* is also crucial for the development of circadian stress in plants with a reduced cytokinin status. This does not necessarily need to be the case. Due to the strong interconnection of clock components in a highly complex network of feedback relationships (Fig. 1.3A) it is possible that *CCA1*/*LHY* deficiency in cytokinin-deficient plants is caused in a different way than in EC-deficient plants.

Circadian timekeeping is not functioning as a unidirectional pathway but as an extensive regulatory network (Pruneda-Paz and Kay, 2010), which sometimes makes it difficult to predict clock-associated phenotypes and is also the reason why systems approaches and mathematical modeling have been very useful for clock research (Bujdoso and Davis, 2013). In the context of this work, a good example for the unpredictability of phenotypes and the requirement to take into account the complex relationships within the oscillator circuit was the attempt to decipher the role of *TOC1* under circadian stress. *35S:TOC1* plants exhibited a strong cell death phenotype upon circadian stress. However, it

could be excluded that the high *TOC1* expression itself was causing the phenotype because cytokinin-deficient plants were not rescued in the *toc1* background. This indicated that the elevated *TOC1* levels observed in CL-treated cytokinin-deficient plants were rather a secondary event and supported the idea that it could indeed be the strong reduction in *CCA1*/*LHY* expression, present in *35S:TOC1* plants due to repression by TOC1 (Makino *et al.*, 2002; Gendron *et al.*, 2012; Huang *et al.*, 2012), that might be decisive. Strikingly, *toc1* mutants also showed a weak but reproducible cell death phenotype and *TOC1* mutation in cytokinin-deficient plants significantly aggravated their already quite strong cell death phenotype. If sufficient *CCA1*/*LHY* levels are protective and TOC1 represses *CCA1*/*LHY* expression, why would *TOC1* loss-of-function cause a stronger stress response? Interestingly, *toc1* plants also exhibit reduced *CCA1*/*LHY* expression (Alabadí *et al.*, 2001; Más *et al.*, 2003a; Kikis *et al.*, 2005) which originally led to the conclusion that TOC1 is a positive regulator of *CCA1* and *LHY* (Locke *et al.*, 2005; Pokhilko *et al.*, 2010). This view has been revised. TOC1 acts as transcriptional repressor on *CCA1* and *LHY* but also on many other target genes (Gendron *et al.*, 2012; Huang *et al.*, 2012). Hence, the diminished *CCA1*/*LHY* expression in *toc1* plants has been explained by the derepression of genes that encode *CCA1*/*LHY* repressors such as *PRR9* and *PRR7* (Huang *et al.*, 2012; Pokhilko *et al.*, 2012). In conclusion, the cell death phenotypes observed in *toc1* loss-of-function mutants either in the wild-type or cytokinin-deficient background can be attributed to the repression of *CCA1*/*LHY* expression which, albeit in an indirect manner, is also occurring in these plants.

Lastly, *35S:CCA1* and *prr9 prr7 prr5* plants exhibited very weak or no cell death phenotypes, respectively, compared with the wild type. Their phenotypes following the circadian stress regime can also be explained by their respective *CCA1*/*LHY* levels. *35S:CCA1* plants constitutively express *CCA1* (Wang and Tobin, 1998) and *prr* triple mutants even exhibit constantly high levels of both *CCA1* and *LHY* (Nakamichi *et al.*, 2005b). Thus, the high morning gene levels in these plants might protect them against circadian stress especially when both *CCA1* and *LHY* are highly expressed. The weak circadian stress response in *35S:CCA1* plants might at least in part be due to the drastically reduced *LHY* levels (Wang and Tobin, 1998) that lead to severely diminished or even undetectable amounts of LHY protein in these plants (Kim *et al.*, 2003; Daniel *et al.*, 2004).

Among the plants with impaired clock function, *cca1-1 lhy-11* and *elf3-9* plants were selected for a more detailed analysis under circadian stress. Interestingly, both clock mutants not only showed a severe cell death phenotype but also showed highly similar perturbations on the molecular level compared with cytokinin-deficient plants. The expression of clock output and stress marker genes as well as of JA-associated and cytokinin-related genes was strongly and similarly misregulated. These results indicated that the observed impairments in gene expression were crucial for the development of the circadian stress phenotype and also emphasized that a malfunctioning circadian clock is the connecting link between cytokinin deficiency and the stress and cell death phenotype upon changed light-dark regimes.

4.2.4.2 A potential role for the gating of light inputs into the circadian clock under circadian stress

The mutation of each EC component resulted in a cell death phenotype under circadian stress. However, the severity of the circadian stress response was different. *elf3* and *lux* plants developed a very severe cell death while *elf4* plants only showed an intermediate response. This could indicate that each single EC component might be able to also contribute independently (without the requirement of the EC) to the mastering of circadian stress. This would imply that there might be additional factors than *CCA1*/*LHY* deficiency alone (see 4.2.4.1) which are decisive for the degree of circadian stress.

An important role of ELF3 and ELF4 is their function as so-called "gate-keepers" (see 1.3.6.1). This means that they are involved in regulating the light sensitivity of the circadian clock functioning as negative regulators of light input into the clock. The gating of light inputs enables a high sensitivity of the clock to dawn and dusk signals and, very importantly, a low sensitivity during the course of the day. It is, therefore, crucial for proper light entrainability and for the integration of daylength information into the oscillator (Devlin, 2002; Gardner *et al.*, 2006; McWatters and Devlin, 2011). It was concluded from the experiments using different light-dark regimes that the prolonged light (CL) treatment somehow changed the internal settings towards long photoperiods (see 3.4.2). This resetting must have been stronger or rather irreversible in cytokinin-deficient plants since they could not master anymore long dark periods associated with short photoperiods. *elf4* and even stronger *elf3* mutants are impaired in gate-keeping. They have an "open gate" which means that they are hypersensitive to resetting light stimuli (McWatters *et al.*, 2000; 2007; McWatters and Devlin, 2011). This particular defect correlates with their hypersensitivity towards CL treatment and also with the difference in the severity of their circadian stress phenotypes. In this respect, it is interesting that *tic* mutants which showed an intermediate cell death phenotype are also impaired in the gating of light responses that is characterized by a failure to anticipate light-dark transitions in long days (Hall *et al.*, 2003; McWatters and Devlin, 2011). On the other hand, *prr9 prr7 prr5* triple mutants that are highly light-insensitive and show impaired entrainment to light-dark cycles (Nakamichi *et al.*, 2005b; Ito *et al.*, 2007; Yamashino *et al.*, 2008) were insensitive to the circadian stress regime (Fig. 3.37). The *elf3 tic* and *elf4 tic* double mutants display extremely aggravated circadian defects compared with the respective single mutants becoming immediately arrhythmic after transfer to constant light and completely lacking anticipation of dawn and dusk under diurnal conditions (Ding *et al.*, 2007). Therefore, it would be interesting to test whether these plants also show aggravated circadian stress phenotypes. This would be informative about whether the proper regulation of light inputs into the circadian clock is decisive under circadian stress regimes and whether an enhanced responsiveness to light inputs contributes at least in part to the development of circadian stress.

Although the results strongly support the view that CCA1/LHY function is indispensable under circadian stress (see 4.2.4.1) it is possible that a functional EC contributes to a high circadian stress resistance by the gate-keeping properties of its components in addition to the support of *CCA1*/*LHY* expression. Intriguingly, TOC1 suppresses the EC by repressing gene expression of *ELF4* and *LUX* (Huang *et al.*, 2012; Fig. 1.3A). Therefore, it should be considered that the strong circadian stress phenotype in *35S:TOC1* plants might in fact be a combined effect of *CCA1*/*LHY* and EC deficiency. Even *cca1 lhy*

double mutants display a slightly diminished *ELF3* expression during the night under diurnal conditions and complete arrhythmicity in *ELF3* expression in constant light (Dixon *et al.*, 2011) which might contribute to the circadian stress phenotype in *cca1 lhy* plants. In this regard, it would be informative to analyze *cca1 lhy elf3* plants in order to evaluate if the *elf3*-associated circadian stress phenotype is indeed mainly caused by *CCA1*/*LHY* deficiency or, conversely, whether an additional EC/ELF3 deficiency further aggravates circadian stress in *cca1 lhy* plants confirming a specific role for the EC and/or ELF3, respectively.

4.2.4.3 A function for CHE under circadian stress

CHE is a clock-associated component that acts within the oscillator (Pruneda-Paz *et al.*, 2009, see 1.3.5.6). *CHE* expression was strongly downregulated in cytokinin-deficient plants during the night following CL treatment (Fig. 3.24). First experiments on *che-2* knockdown mutants revealed an intermediate cell death phenotype between wild-type and *35S:CKX4* plants (Fig. 3.34) pointing to a protective function of CHE against circadian stress. However, it is not clear how this protection was achieved because the results cannot be explained with the current model of CHE function which shows that CCA1 and LHY repress *CHE* expression and that CHE has a suppressive effect on *CCA1* expression (Fig. 1.3B). In accordance with this model, *cca1 lhy* plants exhibit constantly high *CHE* levels (Pruneda-Paz *et al.*, 2009). On the one hand, this argues against a contribution of *CHE* deficiency to the circadian stress phenotype in *cca1 lhy* double mutants. On the other hand, it raises the question how the deficiency in *CCA1*/*LHY* expression observed in cytokinin-deficient plants after CL treatment could be in agreement with the reduction of *CHE* expression in these plants. Moreover, *che-2* plants show an increased *CCA1* promoter activity (*CCA1:LUC*) indicating an overall increase in *CCA1* expression in these plants (Pruneda-Paz *et al.*, 2009). Therefore, the observed circadian stress phenotype of *che-2* plants cannot be attributed to a decreased *CCA1* expression. This supports the hypothesis that additional factors than *CCA1*/*LHY* deficiency alone might be involved in the development of circadian stress (as already suggested in 4.2.4.2). Moreover, CHE might be linked to the oscillator in an additional way than only as component acting within the CCA1/LHY-TOC1 loop since the perturbation of these oscillator components is not consistent with the *CHE* misregulation observed in cytokinin-deficient plants. Hence, the link between CHE and circadian stress raises general questions such as the position of CHE within the oscillator circuit and how *CHE* deficiency could contribute to circadian stress development.

4.2.4.4 The role of PRR3 under circadian stress indicates that the vasculature is important

Another clock component I want to discuss is PRR3 and its relevance under circadian stress. The *prr3* mutant exhibited an intermediate cell death phenotype upon circadian stress which indicated a protective role of PRR3 and was consistent with a strong downregulation of *PRR3* in CL-treated cytokinin-deficient plants (Figs. 3.37 and 3.38). Interestingly, the changes in *PRR3* gene expression in these plants coincided with the onset of stress responses on the molecular level and the divergence in *CCA1*/*LHY* expression compared with the wild type (Figs. 3.23 and 3.24). This strong temporal correlation in changes of expression patterns underpinned the close connection of PRR3 with the

development of circadian stress in cytokinin-deficient plants. Moreover, *PRR3* and *TOC1* expression profiles usually highly overlap temporally (Matsushika *et al.*, 2000; 2002; Para *et al.*, 2007; Fujiwara *et al.*, 2008) and, therefore, the diverging expression patterns of *PRR3* (down) and *TOC1* (unchanged and then up) in cytokinin-deficient plants after the CL regime indicate that this might be one of the critical perturbations in these plants. The fact that *prr9 prr7 prr5* triple mutants, that do not encounter circadian stress (Fig. 3.37), show constantly high *PRR3* expression (Nakamichi *et al.*, 2005b) is also in accordance with its protective role.

PRR3 is part of the PRR family but is its least characterized member and, therefore, often disregarded in current clock models (see 1.3.5.4 and 1.3.5.6). *PRR3* expression is restricted to the vascular tissue of leaves. Its restricted expression explains the rather modest effects on ubiquitously or broadly expressed clock or clock-regulated genes (e.g. *CCA1*, *LHY*, *CAB2*, and *CCR2*/*GRP7*) or leaf movements in *PRR3*-deficient (RNAi lines or *prr3*) plants (Michael *et al.*, 2003a; Para *et al.*, 2007). In contrast, the impact on the rhythms of clock or clock-regulated genes that are highly abundant in the vasculature (e.g. *PRR9* or *CDF1*) was much stronger and characterized by pronounced period shortening and/or phase advance (Para *et al.*, 2007). This confirmed the predominant action of PRR3 and its importance for clock performance in the vasculature. In the vascular tissue PRR3 supports TOC1 stability by prevention of ZTL-mediated proteasomal TOC1 degradation (Para *et al.*, 2007; Fig. 1.3C). The circadian stress phenotypes of *prr3* and *toc1-101* plants were similar (Figs. 3.31 and 3.37), indicating that the sensitivity towards circadian stress in *prr3* plants was mainly caused by reduced TOC1 levels.

Many cytokinin-related genes are strongly expressed in the vasculature including *IPT3*, *CKX6*, as well as B-type and A-type *ARR* genes (Mason *et al.*, 2004; To *et al.*, 2004; Werner *et al.*, 2006; Hirose *et al.*, 2008). Even cytokinin receptor expression and signaling is pronounced in vascular tissues and important for vascular tissue development (Mähönen *et al.*, 2000; 2006; Higuchi *et al.*, 2004; Nishimura *et al.*, 2004; Hejátko *et al.*, 2009; Stolz *et al.*, 2011). The crucial role for cytokinin synthesis and signaling in vascular tissues and the predominant function of PRR3 in the vasculature indicate that vascular processes and/or clock function might be very relevant under circadian stress. In this context, I would like to point out three connected thoughts: 1) The vascular expression of *PRR3* and its role under circadian stress are not the only observations pointing to the presence and relevance of tissue-specific clock mechanisms. There are more studies which strongly suggest that cell type- and tissue-specific clocks exist in plants – oscillators with different properties (Thain *et al.*, 2000; 2002; Hall *et al.*, 2002; Michael *et al.*, 2003b; James *et al.*, 2008; Yakir *et al.*, 2011). So far, very little was known about their particular functions and relevance for the whole plant because it is difficult to study clock mechanisms in specific tissues or cells. However, a very recent study not only confirmed the presence of tissue-specific clocks but also demonstrated that an asymmetric coupling between the vascular and the mesophyll clock exists (Endo *et al.*, 2014). The latter predominates quantitatively in *Arabidopsis* leaves but the performance of the quantitatively underrepresented vascular clock significantly influences the performance of the mesophyll clock but not *vice versa*. Furthermore, the vascular circadian clock is much more robust than the mesophyll clock. Circadian rhythms persist for a long time under constant conditions and are sustained even when the mesophyll clock has already lost rhythmicity due to the lack of resetting external stimuli (Endo *et al.*, 2014). This means that internal

factors probably regulate its robustness. One hypothesis could be that cytokinin signaling fine-tunes clock performance by specifically supporting the robustness of the vascular clock which in turn affects clock performance in other tissues. 2) Photoperiodic responses such as flowering require photoperiod measurement. Interestingly, in addition to *PRR3*, the expression of several genes that are involved in the clock-regulated photoperiodic control of flowering (e.g. *CO*, *CDF1*, *CDF2*, and *FT*) is restricted to vascular tissues (An *et al.*, 2004; Imaizumi and Kay, 2006; Para *et al.*, 2007; Imaizumi, 2010). The vasculature and a vascular-specific clock mechanism are highly relevant for precise daylength measurement with respect to flowering (Kobayashi and Weigel, 2007; Imaizumi, 2010). A similar kind of daylength sensing might also be crucial under changing light-dark regimes that can trigger circadian stress. 3) Since the vasculature is essential for the relay of long-distance signals it could also be suggested that systemic signaling plays a role in the management or prevention of circadian stress. This idea is in accordance with the conclusion drawn from the discrepancy between the outcome of whole-plant examinations and detached leaf assays resulting in pronounced circadian stress or the complete lack of a visible phenotype, respectively (data not shown, see 4.2.1.1). Also the involvement of CRE1 in the circadian stress response and the rescue of *rock4 35S:CKX1* plants compared with *35S:CKX1* plants could argue for this hypothesis (as discussed in 4.2.3.1).

4.2.4.5 General clock defects such as altered periodicity or arrhythmia do not comprehensively explain the severity of circadian stress phenotypes

A perturbation of the circadian oscillator could be linked to cell death phenotypes in response to changed light-dark (circadian stress) regimes. Therefore, I will discuss whether the severity of the circadian stress-associated cell death can be correlated with the extent of alteration in clock function, as reflected by changes in periodicity.

The circadian stress phenotype was detected in short-period (e.g. *cca1 lhy*, *toc1*, *prr3)* and not in the long-period mutants tested (e.g. *prr9, prr7*, *prr9 prr7; arr3,4*). Nevertheless, the severity of cell death did not in every case correlate with the degree of period shortening. The period shortening in *toc1-101* plants (Salomé *et al.*, 2010) is more pronounced than in *prr3* plants (Michael *et al.*, 2003a; Para *et al.*, 2007) but the cell death phenotypes upon circadian stress were similar in these plants (Figs. 3.31 and 3.37). Moreover, *prr5* mutants exhibit a short-period phenotype (Eriksson *et al.*, 2003; Michael *et al.*, 2003a; Yamamoto *et al.*, 2003) but in this work *prr5* mutants showed a wild-type-like circadian stress response (Fig. 3.37). Conversely, *cre1 ahk3* plants exhibited a very pronounced cell death phenotype upon circadian stress (Fig. 3.7) but no altered periodicity was detected in the leaf movements of these plants (Salomé *et al.*, 2006).

Arrhythmic clock mutants also did not consistently show a circadian stress phenotype although an arrhythmia phenotype reflects a very pronounced clock defect. Plants with arrhythmic circadian rhythms such as *cca1-1 lhy-11* (Mizoguchi *et al.*, 2002), *elf3* (Hicks *et al.*, 1996; 2001) and *lux* mutants (Hazen *et al.*, 2005) or *TOC1* overexpressors (Makino *et al.*, 2002; Más *et al.*, 2003a; Gendron *et al.*, 2012) exhibited strong stress phenotypes upon exposure to the circadian stress regime. However, the cell death phenotype was only weak in *CCA1* overexpressing plants and not

present in *prr9 prr7 prr5* plants which are both also highly arrhythmic (Wang and Tobin, 1998; Nakamichi *et al.*, 2005b; Yamashino *et al.*, 2008).

The incomplete congruence between the extent of circadian stress and the period (or arrhythmia) phenotype of the investigated plants supports the view that it is rather the deficiency in specific clock components (see 4.2.4.1 and 4.2.4.2) than an affected periodicity of the plants which makes them vulnerable to circadian stress. This is in good agreement with the results from alternative light-dark treatments. Although the robustness and periodicity is increasingly affected under extended constant conditions due to the lack of resetting stimuli, the cell death phenotype was still induced to a similar degree after four days of CL treatment (data not shown, see 3.4.1). Moreover, different durations of prolonged light (CL) treatment (16 h to 32 h, Fig. 3.19 and 24 h to 40 h, data not shown) did not substantially change the outcome. If the cell death phenotype would depend on the phase of certain circadian rhythms at the end of the CL regime and hence the subjective time, pronounced differences in the circadian stress responses would have been expected when shifting the onset of the death-inducing dark period. The comparability of cell death phenotypes after different lengths of CL indicated that the subjective time did not dramatically matter and, therefore, that periodicity or phase are of minor importance.

4.2.5 The activation of the JA pathway is one of the consequences of circadian stress and promotes cell death development in cytokinin-deficient plants

A strong upregulation of JA synthesis and response genes was associated with the stress and cell death responses in cytokinin-deficient plants under circadian stress and started early, before the plants showed any visible symptoms (Figs. 3.41 and 3.42). The molecular JA response was not caused by elevated JA (JA-Ile) levels which started to increase later when the first signs of cell death became phenotypically visible (Figs. 3.14 and 3.46). The induction of JA response genes was also detected in affected clock mutants (Fig. 3.43) and is, together with the upregulation of JA synthesis genes, considered to be one of the misregulated clock outputs due to a perturbed oscillator (Fig. 4.2).

4.2.5.1 Misregulation of JA-related genes by a perturbed oscillator

The circadian clock provides an anticipation mechanism which facilitates the prediction and response to daily external signals, including biotic and abiotic stresses (Roden and Ingle, 2009; Sanchez *et al.*, 2011; Bhardwaj *et al.*, 2011). One important tool to gain control of multiple clock outputs is to rhythmically regulate hormone pathways as has been demonstrated for auxin and ABA (Covington and Harmer, 2007; Rawat *et al.*, 2009; Castells *et al.*, 2010; Seung *et al.*, 2012; see 1.3.8). In the context of this work it is very interesting that also JA synthesis and JA signaling are under clock control (Shin *et al.*, 2012; Goodspeed *et al.*, 2012; 2013). Properly timed JA accumulation during the day increases the resistance against the herbivore *Trichoplusia ni* (*T. ni*), an adaptive advantage that is lost in arrhythmic clock mutants (e.g. *lux*) as well as in JA synthesis mutants (*aos* and *jar1*) (Goodspeed *et al.*, 2012; 2013). Moreover, JA signaling is a circadian-gated process, which means that JA sensitivity is regulated by the circadian clock and changes in a time-of-day-specific manner. The clock-associated component TIC (see 1.3.5.6) is a key regulator of this process and *tic* mutants are impaired in the

suppression of JA signaling. They exhibit JA hypersensitivity phenotypes, including enhanced inhibition of root growth, increased expression of MYC branch marker genes, and reduced resistance to pathogen infection (Shin *et al.*, 2012). Strikingly, many JA-related genes display robust diurnal and circadian oscillations (Mizuno and Yamashino, 2008; Covington *et al.*, 2008; Shin *et al.*, 2012). Up to 50 % of the JA (MeJA) response genes are circadian-regulated which provides yet another mechanism how the oscillator controls JA responsiveness.

Under circadian stress JA synthesis (*LOX3*, *LOX4*, and *OPR3*) and response (*MYC2* and *JAZ1*) genes were strongly upregulated in cytokinin-deficient plants (Fig. 3.42). This induction of JA-related gene expression coincided with a diminished *CCA1*/*LHY* expression (starting at "5 h") which reflected the perturbation of the circadian clock in these plants (Fig. 3.24; see 4.2.4.1). The re-entrainment of the oscillator by earlier onset of light (Fig. 3.27) reversed this molecular phenotype (shown for *JAZ1*, Fig. 3.44). The fact that the upregulation of *JAZ1* and *MYC2* was also observed in the strongly affected clock mutants *cca1-1 lhy-11* and *elf3-9* (Fig. 3.43) further supported the view that a perturbed oscillator was responsible for the misregulated gene expression. These JA-related genes displayed very low expression in the controls at the corresponding time points (Fig. 3.42) indicating that these genes should normally be minimally expressed during the SD night period. This is consistent with the low nighttime expression that was already shown for diurnal *MYC2* oscillations (Shin *et al.*, 2012). Therefore, it seems that circadian stress completely inversed the normal nighttime expression pattern turning trough into peak expression. In accordance with this, the opposite change in the expression profile was detected for *COI1* which is also diurnally and circadian-regulated (Covington *et al.*, 2008; Shin *et al.*, 2012). Some small perturbations in the normal expression pattern were observed in the CL-treated wild type (for *LOX4*, *COI1*, and *JAZ1*) which is in line with its weak circadian stress phenotype.

On the basis of the high similarity in the expression patterns between the clock-regulated gene *MYC2* and *LOX3*, *LOX4*, *OPR3*, and *JAZ1* expression it can be suggested that the expression of these genes is also under clock control and hence misregulated by a perturbed oscillator under circadian stress. Oscillations in JA accumulation are under clock control (Goodspeed *et al.*, 2012). One way to achieve a time-of-day-specific accumulation of JA could be to control the expression of essential JA synthesis genes. It is already well known that all JA synthesis genes are transcriptionally regulated (Wasternack and Hause, 2013) and, indeed, *AOS* and *OPR3* are included in the set of genes that are under clock control (Covington *et al.*, 2008).

An additional explanation for the upregulation of JA-related genes could be an enhanced JA responsiveness which is gated by the circadian clock (Shin *et al.*, 2012). This would also explain how JA synthesis genes that are JA-inducible (Wasternack, 2007) and other response genes are induced without the elevation of JA (JA-Ile) levels (Fig. 3.46). Consistently, *tic-2* plants exhibit an enhanced responsiveness to JA (Shin *et al.*, 2012) and show a circadian stress phenotype (Fig. 3.34). Together, the results indicate that the misregulation of JA-related genes under circadian stress reflects a perturbed output regulation by a malfunctioning oscillator. It could be explained by a direct regulation of transcript abundance and/or an impaired gating of JA signaling (Fig. 4.2).

4.2.5.2 Promotion of cell death development by activated JA signaling

Several results indicate that the JA pathway was activated in cytokinin-deficient plants upon circadian stress. The induction of JA response genes, including the JA-inducible JA synthesis genes (Wasternack, 2007), reflected active JA signaling. The molecular JA response in cytokinin-deficient plants was, albeit delayed, accompanied by elevated JA metabolite levels. This points to an activated JA pathway because JA signaling is known to positively feed back to JA synthesis to amplify downstream responses (Wasternack, 2007; Browse, 2009a). Since *COI1* expression is downregulated by JA treatment (Shin *et al.*, 2012) a negative feedback from JA signaling to receptor expression can be suggested. Thus, the reduced *COI1* expression in cytokinin-deficient plants upon circadian stress (Fig. 3.42) also supports the idea of an activated JA pathway.

But does an activated JA pathway contribute to cell death development? There are a number of studies that revealed a link between JA and cell death. One well-known example is the promotion of senescence by JA (Jibran *et al.*, 2013; Khan *et al.*, 2014; see 1.5.2). Moreover, JA promotes $^1O_2$-dependent cell death as was shown for the conditional *flu* mutant (Danon *et al.*, 2005) and the *chlorina 1* mutant (Ramel *et al.*, 2013). The former overaccumulates protochlorophyllides in the dark and, therefore, produces high amounts of $^1O_2$ upon re-illumination (Meskauskiene *et al.*, 2001; op den Camp *et al.*, 2003) and the latter overproduces $^1O_2$ under light stress (Ramel *et al.*, 2013). In both cases the accumulation of $^1O_2$ induces a JA-dependent cell death (Danon *et al.*, 2005; Ramel *et al.*, 2013). In addition, lesion development and spreading in the lesion mimic mutant *cpr5* (see 1.5.2) was also dependent on JA signaling (Clarke *et al.*, 2000; Love *et al.*, 2008). However, on the other hand there are also several studies that reported that JA was important for the suppression and containment of PCD (Rao *et al.*, 2000; Overmyer *et al.*, 2000; 2005; Devadas *et al.*, 2002). Thus, it appears that JA can play opposite roles in cell death development, probably depending on the form of cell death.

In this study, the coincidence between JA response and synthesis with stress and cell death responses suggests a positive role of JA in cell death development under circadian stress conditions. Several results support this view. Cell death initiation (as reflected by *BI1* induction; see Figs. 3.19G, 3.23D, 3.36D, and 3.44C) succeeded the activation of JA response genes such as *JAZ1* (Fig. 3.23 and 3.42). Interestingly, the expression levels of *JAZ1* correlated well with the severity of cell death (Figs. 3.16 and 3.44). Consistently, only mature affected and not young unaffected leaves exhibited an induction of *JAZ1* gene expression (Fig. 3.44B). Circadian stress-induced cell death in clock mutants was also accompanied by increased JA response gene expression (Fig. 3.43). Further, CL-treated *tic-2* plants which are hypersensitive to JA (Shin *et al.*, 2012) showed a cell death phenotype upon circadian stress (Fig. 3.34).

Possibly the strongest evidence for a positive role of JA in the cell death phenomenon came from *jar1-1* mutant analysis. JAR1 catalyzes the conjugation of JA to the biologically active form JA-Ile. Hence, *JAR1* loss-of-function results in JA-Ile deficiency (Suza and Staswick, 2008; see 1.6.1) and led to a strongly attenuated cell death in the cytokinin-deficient background (Fig. 3.47) clearly demonstrating that JA (JA-Ile) promotes cell death under circadian stress. The lack of a full rescue of cytokinin-deficient *jar1-1* plants can have different reasons: 1) The activation of the JA pathway might

only be one among several perturbations under circadian stress that promote cell death. 3) JA-Ile is not completely eliminated in the *jar1-1* mutant (Suza and Staswick, 2008). Hence, residual amounts of JA-Ile, enabling residual JA signaling, might explain the incomplete reversion of cell death phenotypes especially if JA responsiveness was indeed enhanced in cytokinin-deficient plants under circadian stress conditions (see 4.2.5.1). 2) JA signaling might not be required for cell death initiation but only determine cell death progression. Compromised JA signaling would, therefore, only result in a reduced severity but would not circumvent the induction of cell death. Although it is not clear whether JA (JA-Ile) also affects the initiation of cell suicide in this context, a predominant role of JA-Ile-dependent signaling in the progression of cell death can be concluded. This is in good accordance with the increase in JA-Ile levels after cell death initiation and the strong accumulation of JA metabolites at later stages of cell death progression (Fig. 3.46).

One possible explanation for the opposite roles JA can play in different forms of cell death (see examples above) could be the involvement of the two different branches of JA signaling which act antagonistically and are activated or inhibited, respectively, under specific conditions (see 1.6.2). From the gene expression data (Fig. 3.42), one could suggest that the early occurring activation of the MYC branch (reflected by upregulation of *MYC2*) promoted cell death. The later activation of the ERF branch (reflected by upregulation of *ERF1* and *ORA59*) might have been induced to counteract the MYC branch, thereby diminishing cell death progression for lesion containment. Since the ERF branch of the JA pathway requires both JA and ethylene signaling (Lorenzo and Solano, 2005; Pieterse *et al.*, 2012) it would be interesting to test the influence of the *etr1-1* allele under circadian stress conditions which renders the plants insensitive to ethylene (Bleecker *et al.*, 1988) and, therefore, compromises the ERF branch of the JA pathway. In the literature one can find opposite (Overmyer *et al.*, 2000) and overlapping (Clarke *et al.*, 2000) roles for JA and ethylene in cell death development presumably dependent on which branch was underlying JA action in the different contexts.

To further study the contribution of JA signaling to cell death development in cytokinin-deficient plants under circadian stress, *coi1 ahk2 ahk3* plants were examined (Fig. 3.48; see 3.7.4). Surprisingly, the cell death phenotype was not altered in these plants compared with *ahk2 ahk3* plants. The investigated *coi1* mutant carried a strong *coi1* allele as indicated by male sterility of *coi1* homozygous plants (Maruta *et al.*, 2011 and observations in this study). Therefore, the results indicate that COI1 does not have a predominant function under circadian stress pointing to an alternative COI1-independent signaling pathway that mediates the JA (JA-Ile)-dependent promotion of cell death in this context. However, COI1 is the only known JA-Ile receptor and *coi1* mutants are strongly impaired in every known aspect of JA signal transduction and response (Feys *et al.*, 1994; Wasternack, 2007; Browse, 2009b). Interestingly, there are JA-independent COI1-dependent responses (Adams and Turner, 2010; He *et al.*, 2012; Ralhan *et al.*, 2012) but COI1-independent JA (JA-Ile)-dependent pathways have not been elucidated so far. Nevertheless, there is a significant number of JA-responsive genes that are induced (~16 %) or repressed (~47 %) in a COI1-independent manner (Devoto *et al.*, 2005). Furthermore, several studies demonstrated that other oxylipins such as the JA precursor OPDA can act *via* COI1-independent pathways (Taki *et al.*, 2005; Mueller *et al.*, 2008; Ribot *et al.*, 2008; Stotz *et al.*, 2011; Park *et al.*, 2013). Thus, data from the literature as well as the results in this work support the

idea of an alternative COI1-independent pathway. Although COI1 seems to be the predominant JA (JA-Ile) receptor under many conditions it could be that the potential additional pathway/receptor acts redundantly or even independently only under very specific conditions such as the circadian stress regime used in this work.

Unraveling a novel mechanism for JA (JA-Ile) action would be striking. However, at first the COI1 independence of JA (JA-Ile) action under circadian stress should be confirmed by using alternative *coi1* loss-of-function alleles. Moreover, the importance of JA-Ile should be tested with other JA synthesis mutants (e.g. *fad3 fad7 fad8*, *aos*/*dde2*, *opr3*/*dde1*) in a cytokinin-deficient background. If the hypothesis of an alternative pathway/receptor is supported by these experiments it would be interesting to conduct a suppressor screen using cytokinin-deficient *coi1* plants. A technical difficulty is the male sterility of *coi1* loss-of-function mutants. One could try to generate cytokinin-deficient *coi1* plants that carry a *COI1* transgene under the control of an inducible promoter (e.g. by ethanol or estradiol). That way one could overcome sterility by *COI1* transgene induction when bolting starts, perform the EMS-mutagenesis on homozygous *coi1* (cytokinin-deficient) seeds and could screen for suppressors which then could be propagated by again inducing the *COI1* transgene. Nevertheless, it has to be noted that only a subgroup of suppressor mutants found in such a screen might be impaired in the potential alternative JA-Ile-dependent pathway. Since the circadian stress phenotype is dependent on cytokinin deficiency and a perturbation of the circadian clock it is very likely that cytokinin-related gain-of-function mutants and/or mutants with altered clock properties would be among the suppressor mutants and possibly also PCD signaling mutants.

4.2.5.3 Cytokinin deficiency may cause cell death progression through enhanced activation of the JA pathway

Next I will discuss the possibility of a direct crosstalk between cytokinin and JA and if such a connection could also explain the activation of the JA pathway in cytokinin-deficient plants under circadian stress. This would mean that the development of cell death is promoted also in a more direct manner than solely by the perturbation of the circadian clock that is caused by cytokinin deficiency. Very little is known about the crosstalk between cytokinin and JA. The results concerning cytokinin action on JA (synthesis, signaling, and responses) that have been described so far are not consistent. There are studies which show that cytokinin supports JA synthesis (Sano *et al.*, 1996; Dervinis *et al.*, 2010) but on the other hand an antagonistic relationship has been indicated by others (Naik *et al.*, 2002; Stoynova-Bakalova *et al.*, 2008). Therefore, it appears that the cytokinin-JA interaction is rather complex and probably strongly dependent on the conditions and potentially also on the levels of other hormones (O'Brien and Benková, 2013). For instance, it has been suggested that an antagonistic effect of cytokinin on JA responses could indirectly be caused by its positive effect on SA (Choi *et al.*, 2010; Robert-Seilaniantz *et al.*, 2011) since SA widely acts antagonistically to the JA pathway (Brooks *et al.*, 2005; Zheng *et al.*, 2012; Pieterse *et al.*, 2012; Van der Does *et al.*, 2013). Systems biology analysis and targeted experiments indicated that this might indeed be a mechanism how cytokinin suppresses JA-mediated responses in plant immunity (Naseem *et al.*, 2013). In this work, transcript data of CL-treated plants indicated enhanced SA responses in wild-type plants in comparison with cytokinin-

deficient plants (Fig. 3.40D-E) pointing to a protective function of SA signaling under circadian stress conditions. However, the kinetics of SA-responsive *PR1* gene expression (Fig. 3.40F), quantification of SA levels (Fig. 3.45) as well as mutant analysis (*npr1-1* and *npr1-2*, data not shown) did not support this hypothesis.

Interestingly, phytohormone measurements revealed that JA metabolites were increased in cytokinin-deficient control plants compared with the wild type at all analyzed time points (Fig. 3.46 and data not shown, see also 3.7.3). This elevation was not found for the AOS- and AOC-catalyzed products dinor-OPDA and OPDA. These results indicate that cytokinin might have a suppressive function on JA synthesis at the OPR3-catalyzed step in which the cyclopentenone ring is reduced to a cyclopentanone ring to form OPCs (see 1.6.1). In turn, this would imply that a lacking negative control of JA synthesis in plants with a reduced cytokinin status might have facilitated the accumulation of JA metabolites under circadian stress and hence contributed to the cell death phenotype.

4.2.6 Misregulation of the ROS gene network upon circadian stress contributes to cell death development in cytokinin-deficient plants

4.2.6.1 The misregulation of the ROS gene network is due to a perturbed oscillator under circadian stress

Circadian stress caused a strong oxidative stress response in cytokinin-deficient plants on the molecular level (Fig. 3.23). It was concluded that, similar to the JA response (see 4.2.5.1), this response is due to a disturbed output regulation by a perturbed oscillator under circadian stress conditions resulting in a misregulation of genes of the ROS gene network (Fig. 4.2). In this section I will discuss which results led to this conclusion and how they can be integrated into the current knowledge regarding the circadian clock and (oxidative) stress responses.

The early induction of ROS-inducible genes such as *BAP1* or *ZAT12* (Fig. 3.23; see 1.4.3) coincided with a diminished *CCA1*/*LHY* gene expression, reflecting a perturbed oscillator in cytokinin-deficient plants under circadian stress (Fig. 3.24; see 4.2.4.1), but not with (oxidative) stress in these plants. Neither LPO nor H_2O_2 levels were increased in comparison with the wild type at the corresponding early time points (Figs. 3.49 and 3.50). In addition, none of the tested stress hormones, including ABA, SA, and JA, initially (at "2.5 h" and "5 h") exhibited elevated levels which would have indicated a pronounced stress condition (Figs. 3.45 and 3.46). Moreover, the ROS-responsive genes did not behave consistently. For instance, although *BAP1* and *ZAT12* were strongly upregulated *FER1*, a well-known H_2O_2-inducible gene (op den Camp *et al.*, 2003), was strongly downregulated (Fig. 3.25) indicating that their expression might under these circumstances not depend on ROS levels. Interestingly, clock mutants (*cca1-1 lhy-11* and *elf3-9*) showed a highly similar phenotype on the molecular level in response to the circadian stress regime, including the upregulation of *BAP1* and *ZAT12* (Fig. 3.36). Furthermore, the expression pattern of many tested ROS/stress-related genes that were strongly induced in cytokinin-deficient plants was reminiscent of an oscillation wave (Figs. 3.23 and 3.42). The phase of peak expression appeared to be gene-specific and, strikingly, the expression was in many cases slightly reduced towards the end of the stress- and cell death-inducing dark period

although the stress and cell death phenotype was obviously not. Conversely, LPO as well as ion leakage were increasing towards "16 h" after CL treatment (Figs. 3.14 and 3.49) and cell death was continuously progressing (visual inspection).

Numerous genes of the ROS gene network, including genes encoding for ROS scavenging and producing enzymes as well as ROS-responsive genes, are oscillating. About 73 % are rhythmic under diurnal conditions, while on average 39 % cycle under circadian conditions, demonstrating their regulation by the circadian clock (Lai *et al.*, 2012). Similar results were obtained by Covington *et al.* (2008). Among the ROS-responsive genes are a high number of genes that are commonly induced under various stresses, which is in line with the fact that an increase in oxidative stress (ROS levels) is accompanying many if not all kinds of stresses (Gadjev *et al.*, 2006; Sharma *et al.*, 2012). Genes that are differentially expressed under almost any stress condition are called GSR (Walley *et al.*, 2007) or PCESR (Hahn *et al.*, 2013) genes. Examples are *BAP1*, *ZAT12*, and *JAZ1* as well as *ERF5* and *WRKY18* that were induced under circadian stress (Figs. 3.23, 3.42, and data not shown, see also 4.2.2.1). At least some GSR/PCESR genes are circadian-regulated. One prominent example is *ZAT12* (Fowler *et al.*, 2005; Lai *et al.*, 2012).

ZAT12 is one of the 56 identified PCESR genes (Hahn *et al.*, 2013), its expression oscillates under circadian conditions, and its cold- and paraquat-inducibility is gated by the circadian clock which means that its responsiveness changes in a time-of-day-specific-, clock-dependent manner (Fowler *et al.*, 2005; Lai *et al.*, 2012). Furthermore, other genes of the ROS network, such as *FER1* and *CAT2*, are also clock-regulated (Zhong and McClung, 1996; Duc *et al.*, 2009; Lai *et al.*, 2012; Hong *et al.*, 2013b). Interestingly, both genes exhibited a strongly diminished expression in response to circadian stress (Fig. 3.25). Since *ZAT12*, *FER1*, and *CAT2* are regulated by the circadian oscillator their up- or downregulation, respectively, might be caused by the perturbed oscillator under circadian stress and could, therefore, be considered as misregulated clock output (Fig. 4.2). The different regulation of these genes under circadian stress is consistent with their different phasing under non-stress conditions. For example, *ZAT12* usually shows minimal while *CAT2* shows maximal expression in the morning (Lai *et al.*, 2012), whereas *ZAT12* was induced and *CAT2* expression was reduced in response to circadian stress at that time. In the future it would be interesting to find out if their misregulation resulted from a direct regulation by oscillator components that act as transcription factors or was rather caused by impaired gating which could include intermediate transcription factors or pathways (Hotta *et al.*, 2007). It could even be a combination of both. For instance, the oscillator component CCA1 binds to *cis*-regulatory elements in promoters of a subset of ROS-related genes, including *ZAT12*, thereby directly regulating their expression. At the same time, *ZAT12* inducibility, as already mentioned, is gated by the circadian clock, changing its responsiveness during the course of the day (Fowler *et al.*, 2005; Lai *et al.*, 2012).

In addition to the gene expression data, clock mutant analyses also supported the view that a functional circadian clock is crucial for proper (oxidative) stress responses and, more specifically, their containment under circadian stress. Clock mutants strongly differ in their sensitivity to certain stresses. For example, *gi* mutants display a high tolerance to paraquat-induced oxidative stress

(Kurepa *et al.*, 1998), while hypersensitivity to paraquat treatment was observed in *cca1 lhy*, *elf3*, and *lux* mutants as reflected by pronounced cell death phenotypes (Lai *et al.*, 2012). The latter mutants were also highly vulnerable towards circadian stress. Moreover, *CCA1* overexpressing plants are highly tolerant to paraquat-induced oxidative stress (Lai *et al.*, 2012) and, intriguingly, the *prr9 prr7 prr5* triple mutant is extremely tolerant to various stresses (Nakamichi *et al.*, 2009). These stress phenotypes are also consistent with the high tolerance of *35S:CCA1* and *prr9 prr7 prr5* plants in this study. Lai and colleagues suggested CCA1 as master regulator of ROS homeostasis and oxidative stress responses (Lai *et al.*, 2012). Proper CCA1 function indeed was decisive for oscillations in H_2O_2 levels, circadian changes in catalase activity, and the gating of ROS responses on the transcript level, determining the time of day as well as the overall intensity. However, CCA1 function alone cannot fully explain the observed phenotypes in this study because *lhy* single mutants as well as EC-deficient plants (*elf3*, *lux*, but also *elf4* plants) also exhibited a pronounced paraquat-induced cell death phenotype, pointing to an additional role of LHY and the EC components. Interestingly, the same components were found to be crucial under circadian stress (for detailed discussion see 4.2.4.1 and 4.2.4.2). The overlap between oscillator components that are relevant under oxidative stress (Lai *et al.*, 2012) and under circadian stress (this study), respectively, supports the hypothesis that the circadian stress phenotype can be attributed to an inadequate control of the ROS gene network and (oxidative) stress responses which are usually tightly coordinated by the circadian clock (especially CCA1, but probably also LHY and EC components).

4.2.6.2 Cell death as a consequence of the misregulated ROS gene network

Among the genes of the ROS gene network that were strongly induced in cytokinin-deficient plants under circadian stress were GSR/PCESR genes such as *BAP1*, *JAZ1*, and *ZAT12* (Figs. 3.23 and 3.42). As discussed in 4.2.2.1, their increased expression might reflect the activation of core stress pathways and initiation of alarm responses that might have been sensed as "death signal".

At the same time, these genes are ROS-reponsive genes and their strong upregulation is probably perceived as strong oxidative stress. As described in the Introduction ROS production is closely linked to PCD processes (see 1.5.1 and 1.5.2). The increase of ROS levels above certain threshold levels is crucial to induce cell death (Gechev *et al.*, 2010; Karuppanapandian *et al.*, 2011). However, cell death is not only caused by destruction due to ROS toxicity and the significance of oxidative damage is even debatable (Foyer and Noctor, 2005; Van Breusegem and Dat, 2006; Van Breusegem *et al.*, 2008). Although ROS were shown to be decisive for the regulation of PCD (e.g. in *lsd1* and *rcd1* mutants, see 1.5.2), a functional signaling network downstream of the ROS signal is required. Initial experimental evidence was obtained in cell suspensions by demonstrating that the H_2O_2-induced cell death could be blocked by cycloheximide and protease inhibitors (Levine *et al.*, 1994). Another very prominent example is linked to the conditional *flu* mutant that undergoes $^1O_2$-induced cell death in response to dark-light shifts (Meskauskiene *et al.*, 2001; op den Camp *et al.*, 2003). This cell death response depends on the activity of the two proteins EXECUTER1 (EX1) and EX2. Although the triple mutant *ex1 ex2 flu* still generates similar amounts of $^1O_2$ compared with the parental *flu* line after the dark-light shift, the cell death phenotype is completely abolished (Wagner *et al.*, 2004; Lee *et al.*, 2007b;

Kim and Apel, 2013). These results demonstrate the existence of so-called execution pathways that need to operate to enable the execution of cell death.

On the one hand, cell death initation in reponse to circadian stress could not be attributed to increased ROS levels/oxidative stress (Figs. 3.49 and 3.50). On the other hand, ROS "footprints" (Gadjev *et al.*, 2006) were detected on the transcript level indicating increased oxidative stress and active ROS signaling. It is possible that the activation of a ROS-dependent execution pathway by transcriptional regulation of its signaling components can cause cell death induction even without ROS as trigger. As discussed in the previous section (see 4.2.6.1) the perturbation of the circadian clock under circadian stress was likely responsible for the strong oxidative stress response, by directly (mis)regulating ROS-related genes and/or by causing a gating defect leading to a changed responsiveness (e.g. hypersensitivity to ROS). Recent data show that HR cell death (which is also regulated by ROS, see 1.5.2) is controlled by the circadian clock. This means that the severity of cell death differs depending on the (circadian) time of infection (Korneli *et al.*, 2014). Together, these results support the view that the circadian clock might regulate death execution pathways.

It should be noted that an early increase in ROS levels/oxidative stress might have been overlooked. This could be due to a strong local restriction of ROS production, e.g. in vascular tissues, which makes possible changes rather undetectable when inspecting big parts of the leaves. An only transient increase in the ROS content could be another reason which is unlikely because ROS production is usually amplified and not attenuated once cell death is initiated (Gechev *et al.*, 2010; see also 1.5.1 and 1.5.2).

Nevertheless, the results document a later increase in oxidative stress accompanying and probably promoting later stages of cell death (Figs. 3.11C and 3.49H). A delayed ROS production could be a consequence of the substantial changes in ROS-related gene expression (Fig. 4.2) and/or might be part of the typical amplification of oxidative stress during cell death (Gechev *et al.*, 2010). Among the genes that were used as indicators for clock output regulation were *CAT2* and *FER1* (Fig. 3.25). Both genes were drastically downregulated in cytokinin-deficient plants during circadian stress and both, deficient *CAT2* and *FER1* expression, might have contributed to an increase in oxidative stress at later time points. *FER1* is a clock-regulated ROS-responsive gene (Duc *et al.*, 2009; Hong *et al.*, 2013b) connected to Fe homeostasis (Briat *et al.*, 2010). In general, Fe homeostasis is tightly linked to the circadian clock (Hong *et al.*, 2013b; Chen *et al.*, 2013b; Salomé *et al.*, 2013) and ferritins (including FER1) provide a link between Fe homeostasis and redox homeostasis protecting against oxidative stress (Ravet *et al.*, 2009; Briat *et al.*, 2010). Ferritin-deficient plants exhibit higher ROS levels (Ravet *et al.*, 2009) and also show an earlier onset of age-dependent leaf senescence (Murgia *et al.*, 2007). Similar to *FER1*, *CAT2* is also regulated on the transcript level in a clock-dependent fashion (Zhong and McClung, 1996; Lai *et al.*, 2012). Since CAT2 is the most important catalase in leaves, efficiently degrading H_2O_2 (Queval *et al.*, 2007), a decreased abundance could contribute to an increase in oxidative stress. Interestingly, a decreased *CAT2* expression and/or a decline in catalase activity has been reported for many forms of plant PCD including senescence (Smykowski *et al.*, 2010; Bieker *et al.*, 2012; de Pinto *et al.*, 2012). This seems to be one mechanism to amplify the ROS signal in order

to promote cell death progression (Gechev *et al.*, 2010). In this respect, it would be interesting for future studies to analyze the activities of catalase and other scavenging enzymes to evaluate their contribution to the circadian stress-associated cell death. However, the ROS-producing enzymes RBOHD and RBOHF were not required for cell death under circadian stress (Fig. 3.51).

4.2.7 A perturbed oscillator might cause a disturbance of multiple clock outputs in addition to misregulation of gene expression

The circadian clock controls many output pathways (see 1.3.7.1). Although circadian transcriptional regulation is an important mechanism to influence many outputs (see 1.3.7.2) it is certainly not the only one. In this work, the main focus was on gene expression as a crucial clock output that even strongly determines oscillator function itself. However, a possible perturbation of other outputs in response to circadian stress has to be considered as indicated in Figure 4.2. In this chapter I will discuss some potential alternative clock outputs that might have been misregulated under circadian stress. These would be an interesting focus for future research because they might either link circadian clock function with (oxidative) stress and cell death responses or the cytokinin status with clock performance.

4.2.7.1 Free cytosolic calcium concentration

A first clock output that I would like to contemplate is the circadian regulation of the cytosolic free calcium concentration ($[Ca^{2+}]_{cyt}$) (Johnson *et al.*, 1995; Love *et al.*, 2004; Dodd *et al.*, 2007). The clock component CCA1 is required for circadian oscillations of $[Ca^{2+}]_{cyt}$. *CCA1* overexpression results in constitutively low and *cca1-1* loss-of-function in constitutively high $[Ca^{2+}]_{cyt}$ (Dodd *et al.*, 2007; Xu *et al.*, 2007). Interestingly, a rapid increase in $[Ca^{2+}]_{cyt}$ is observed in response to many biotic and abiotic stresses (Bowler and Fluhr, 2000; Martí *et al.*, 2013; Zhu *et al.*, 2013). Hence, Ca^{2+} signaling is thought to act at a convergence point integrating different signals. Increases in $[Ca^{2+}]_{cyt}$ co-occur with ROS production (Bowler and Fluhr, 2000). It is still not clear whether the rise in $[Ca^{2+}]_{cyt}$ or ROS levels appear first after biotic and abiotic stresses, probably both can happen (Wrzaczek *et al.*, 2013). However, there are studies showing that ROS can activate Ca^{2+} channels (Mori and Schroeder, 2004), that Ca^{2+} signaling affects ROS-dependent gene expression (Short *et al.*, 2012), and that alterations in Ca^{2+} fluxes occur downstream of ROS and upstream of cell death development (Gadjev *et al.*, 2008; Gechev *et al.*, 2010). Therefore, a misregulation of $[Ca^{2+}]_{cyt}$ oscillations by a perturbed oscillator under circadian stress (leading to high $[Ca^{2+}]_{cyt}$ as observed in *cca1-1* plants, see above) might result in inadequate (oxidative) stress responses and hence promote cell death. Furthermore, circadian $[Ca^{2+}]_{cyt}$ oscillations as well as intracellular Ca^{2+} signals in response to different stimuli are tissue- and cell type-specific (Wood *et al.*, 2001; Martí *et al.*, 2013). Moreover, Ca^{2+} waves can be propagated as long-distance signals (Choi *et al.*, 2014) revealing these second messengers as interesting candidates to explain potential tissue- or even cell type-specificity or the involvement of systemic/long-distance signals under circadian stress (see 4.2.4.4). Strikingly, circadian $[Ca^{2+}]_{cyt}$ oscillations have been suggested to encode photoperiodic information (Love *et al.*, 2004) which additionally draws the attention to their potential function in response to changed light-dark regimes.

4.2.7.2 Catalase activity and glutathione levels

A second clock output I would like to consider is the regulation of catalase activity by the circadian clock (Lai *et al.*, 2012). Growth under different light-dark regimes revealed that the photoperiod is a critical determinant of the oxidative stress response and the associated cell death phenotype in the oxidative stress signaling mutant *cat2* (Queval *et al.*, 2007; 2011). H_2O_2-induced cell death in these plants was dependent on long photoperiods and not on the total light exposure or the severity of oxidative stress (Queval *et al.*, 2007). Strikingly, oxidative stress and redox profiling even revealed a stronger perturbation of the cellular redox state in *cat2* plants under SD conditions which is consistent with the higher levels of H_2O_2 in SD- *versus* LD-adapted leaves (Lepistö and Rintamäki, 2012). The authors, therefore, suggested that the LD-dependent cell death in *cat2* plants might be mediated through an execution pathway (similar to the *EX1*-dependent pathway in the *flu* mutant, see 4.2.6.2) that is absent or less active in SD conditions (Queval *et al.*, 2007). The results in this work indicated that cytokinin deficiency might lead to difficulties with the re-acclimation to SD conditions after prolonged light (CL) treatments (see 4.2.1.2). Hence, cell death induction in cytokinin-deficient plants might have been facilitated because they were still adapted to a long photoperiod under which the putative death execution pathway is active. In addition, *CAT2* gene expression was dramatically downregulated in cytokinin-deficient plants under circadian stress (Fig. 3.25; see also 4.2.6.2). It would be interesting to test if the reduced *CAT2* transcript levels indeed resulted in a lowered protein content and hence in a decreased CAT2 activity. Moreover, *cat2* mutants should be tested regarding their susceptibility to circadian stress in order to find out if the circadian stress phenotype at least in part can be attributed to CAT2 deficiency.

The total glutathione content was strongly elevated in *cat2* plants (Queval *et al.*, 2007). Glutathione is a key player in oxidative stress metabolism in plants (Foyer and Noctor, 2011). Recently, it was shown that glutathione accumulation was required for the activation of the JA pathway in *cat2* mutants (Han *et al.*, 2013). In another study transcript profiling revealed that glutathione application not only induces JA-related genes (e.g. *LOX3*) but also represses cytokinin-associated genes (e.g. *ARR7*) (Hacham *et al.*, 2014), which was also observed under circadian stress. Interestingly, *tic-2* plants that also show a circadian stress-associated cell death phenotype also exhibit elevated glutathione levels and are disturbed in oxidative stress responses (Fig. 1.3D; Sanchez-Villarreal *et al.*, 2013). Some authors suggest that glutathione levels might be regulated by the circadian clock since this is commonly observed in other organisms (e.g. Drosophila) but so far this has not been examined in plants (Spoel and van Ooijen, 2014). In future studies it would be informative to test this hypothesis. A disturbance in glutathione oscillations might lead to increased levels at inappropriate times of day which could explain some of the observations in cytokinin-deficient plants under circadian stress.

4.2.7.3 Sugar sensitivity and metabolism

Lastly, I would like to highlight the connection between the circadian clock and sugar metabolism as well as between cytokinin and sugar signaling and metabolism. The circadian clock regulates transcripts associated with chlorophyll biosynthesis and the photosynthetic apparatus, net carbon

assimilation, and starch metabolism, especially starch degradation and hence carbohydrate availability during the night (Harmer *et al.*, 2000; Dodd *et al.*, 2005; Lu *et al.*, 2005; Graf *et al.*, 2010; Noordally *et al.*, 2013). In addition to being a key metabolic output of the circadian clock, the production of sugars by photosynthesis strongly supports diurnal gene expression (Bläsing *et al.*, 2005; Usadel *et al.*, 2008) and is an important input signal for the circadian oscillator (Haydon *et al.*, 2013b). It was concluded that carbon starvation was unlikely the cause of the circadian stress phenotype because the starch content did not indicate limited carbohydrate availability (Fig. 3.18). However, it is still possible that the relative amounts of different soluble sugars (e.g. fructose, glucose, and sucrose) were altered in CL-treated cytokinin-deficient plants which could result in different input signals into the oscillator.

Strikingly, cytokinin-deficient plants (e.g. *ahk3* and *cre1 ahk3*) are hypersensitive to sugars (Franco-Zorilla *et al.*, 2005). Moreover, starch degradation during the 16-hour night following CL treatment was accelerated in all plants compared with the control plants (Fig. 3.18) and might have been sensed as sugar overload by the hypersensitive cytokinin-deficient plants. On the one hand, the hypersensitivity to sugars could accelerate the PCD program as sugar accumulation can also trigger senescence (Wingler *et al.*, 2006). On the other hand, it could simply be integrated differently as entraining signal into the clock which could contribute to the perturbed clock function in cytokinin-deficient plants under circadian stress.

To study if differences in sugar sensing might contribute to the circadian stress phenotype, one could test additional mutants that are hypersensitive to sugars (e.g. *cpr5* [allelic to *old1/hys1*], *etr1*, or *ein2* mutants) and, of course, also the impact of mutations that lead to sugar insensitivity (e.g. *hxk1*, *abi4*, or *kin10*) in the cytokinin-deficient background (Ramon *et al.*, 2008). Another interesting connection between cytokinin and sugar metabolism is the trehalose pathway. The overexpression of *TREHALOSE-6-PHOSPHATE-SYNTHASE 1* (*TPS1*), involved in trehalose synthesis, results in sugar insensitivity and increased stress tolerance (Avonce *et al.*, 2004). Intriguingly, cytokinin induces the expression of several *TPS* genes, including *TPS1*, while a repression of *TPS* genes is observed in the cytokinin-deficient *35S:CKX1* transgenic plants (Brenner *et al.*, 2005; Brenner *et al.*, 2012; Bhargava *et al.*, 2013). Moreover, genes of the trehalose metabolism, including *TPS* genes, are diurnally (by sugars) and circadian-regulated (Bläsing *et al.*, 2005; Usadel *et al.*, 2008). Since trehalose metabolism appears to be crucial for sugar sensing and stress resistance and, moreover, provides a link between cytokinin and circadian clock function it might be worthwhile to investigate its impact on circadian stress in future studies.

4.2.8 How does cytokinin prevent circadian stress?

The previous chapters dealt with the novel phenomenon circadian stress. It was discussed what kind of stress and cell death the plants were facing, how the stress and cell death responses might have been induced, which conditions trigger circadian stress, and which circadian components are of major importance. Since cytokinin-deficient plants encounter strong circadian stress and the cytokinin status is of great importance to counteract the development of circadian stress-associated cell death

phenotypes an essential question is how exactly cytokinin might confer such an adaptive advantage when it comes to changing light-dark regimes.

4.2.8.1 Cytokinin rather supports circadian clock function, thereby preventing circadian stress-induced cell death, than directly controlling cell death development

The perturbation of the circadian clock in cytokinin-deficient plants started before the onset of cell death and mutants with impaired clock function (e.g. *cca1-1 lhy-11*, *elf3-9*) also showed a cell death phenotype. Therefore, it is very likely that cytokinin mainly acts indirectly through the modulation of the circadian clock to prevent misregulated clock outputs and, hence, stress and cell death in response to circadian stress regimes (see Fig. 4.2). How this might be achieved will be discussed in the following chapter (see 4.2.8.2).

Data on the regulation of plant cell death by cytokinin are scarce which could indicate that cytokinin has no important role in directly controlling PCD programs. Cytokinin is well known for its delaying effect on senescence which means that it is protective against this form of developmentally induced PCD (Kim *et al.*, 2006; Lim *et al.*, 2007). On the other hand, high levels of cytokinin promote PCD in cell cultures, a process mediated by CRE1/AHK4 (Vescovi *et al.*, 2012; Kunikowska *et al.*, 2013). Under circadian stress a normal cytokinin status protects against circadian stress-induced cell death. One could argue, that cell death development in cytokinin-deficient plants might have been favored by a lacking suppression of JA synthesis (as discussed in 4.2.5.3) and/or by a decreased antioxidant capacity (as present under HL conditions; see 4.1.2). However, both consequences of a reduced cytokinin status might only have contributed to cell death progression and not its intiation since an actual increase in JA (JA-Ile) levels or oxidative stress accompanied later stages of cell death development (Figs. 3.11, 3.46, and 3.49). Thus, they by far cannot explain the complete cell death phenomenon under circadian stress and additionally would only represent an indirect mechanism of cytokinin action in the control of cell death.

4.2.8.2 Cytokinin supports circadian clock function

Cytokinin is able to cause phase delays in different circadian rhythms (Hanano *et al.*, 2006; Salomé *et al.*, 2006; Zheng *et al.*, 2006, see 1.3.8.1). The phase adjustment by cytokinin was shown to be dependent on ARR4 and PHYB function. Since neither *arr4* or *arr3,4* mutants nor *phyB* mutants exhibited a pronounced circadian stress phenotype (Fig. 3.29; see 3.6.1) it can be suggested that the phase-adjusting cytokinin-input to the clock is of minor importance for a proper circadian stress response. This is completely in line with the conclusion that it is rather the deficiency in specific oscillator components than a general clock defect which is decisive for the extent of circadian stress (see 4.2.4.5).

CCA1 and LHY are important players under circadian stress conditions (see 4.2.4.1) and cytokinin-deficient plants especially lacked sufficient nighttime *CCA1*/*LHY* expression (Fig. 3.24). There is evidence that cytokinin induces *CCA1* and *LHY* expression while repressing *TOC1* expression (Zheng *et al.*, 2006). On the contrary, available microarray data did not reveal a prominent cytokinin effect on

clock gene expression (Salomé *et al.*, 2006; Brenner *et al.*, 2012; Bhargava *et al.*, 2013). However, the inducibility by cytokinin might be conditional (e.g. dependent on the photoperiod, cytokinin type, length of treatment, temperature, or time of day). Experimental evidence for this hypothesis comes from results by Hanano and colleagues showing that cytokinin induced *CCA1* in the evening but not in the morning (Hanano *et al.*, 2006). Furthermore, Zheng and colleagues concluded that the induction of *CCA1* and *LHY* by cytokinin was light-dependent because they did not observe an upregulation in the dark (Zheng *et al.*, 2006). It is notable that the experimental setting they used does not fully allow drawing conclusions about the impact of cytokinin during a (subjective) night period under diurnal or circadian conditions because they grew the seedlings under constant light for three weeks before applying cytokinin without any prior entrainment. A sudden dark period which the seedlings never encountered before at an undefined subjective time could have multiple unforeseeable side effects. Therefore, it cannot be excluded that cytokinin might still influence clock gene expression during the (subjective) night.

A strong influence on clock gene expression during the dark period would be in accordance with the predominant influence of cytokinin on clock function in the darkness. For instance, the phase delay was more pronounced in constant darkness compared with constant light conditions and cytokinin also significantly supported *CAB2* rhythms in constant darkness which usually lose rhythmicity very quickly after transfer to darkness (Hanano *et al.*, 2006). An important role of cytokinin during nighttime is also reflected by the fact that stress and cell death responses in cytokinin-deficient plants upon circadian stress depended on a prolonged dark period (Figs. 3.15 and 3.16). Moreover, cytokinin-inducible genes such as A-type *ARRs* show maximal diurnal and circadian expression during the (subjective) night (Fig. 3.26; Ishida *et al.*, 2008b; Covington *et al.*, 2008).

Most of the microarray analyses were performed under light conditions (Brenner *et al.*, 2012; Bhargava *et al.*, 2013). Thus, it might be worthwhile to determine the cytokinin-dependence of clock gene expression at different times of the (subjective) day under diurnal (SD and LD) and circadian conditions. This could be part of investigating the potential gating of cytokinin responses by the circadian clock (see 4.2.3.2). For these experiments it could be decisive under which photoperiods the plants grow, which type of cytokinin is used, and how long the plants are exposed to cytokinin.

Alternatively, a positive effect of cytokinin on *CCA1*/*LHY* expression could be achieved by other means than direct transcriptional regulation. The overall transcript abundance does not only depend on the transcription rate but also on the transcript stability. It is known that light negatively affects *CCA1* transcript stability, while *CCA1* transcripts are relatively stable in the dark (Yakir *et al.*, 2007a). Therefore, one hypothesis could be that cytokinin promotes *CCA1*/*LHY* transcript stability in the dark to support a higher *CCA1*/*LHY* expression in wild-type plants under circadian stress. Alternative splicing (AS) is more and more emerging as important mechanism to influence transcript abundance and proteome diversity in a quantitative manner by post-transcriptionally generating various transcript isoforms that are either degraded by the nonsense-mediated mRNA decay (NMD) surveillance machinery, regulate the level of functional transcripts, or encode proteins with altered or impaired function (Filichkin *et al.*, 2010). AS is strongly influenced by external factors, including abiotic stress,

and in addition is a widespread phenomenon among plant circadian clock genes such as *CCA1*/*LHY* and *PRR* genes (McClung, 2011; Nagel and Kay, 2012; Filichkin and Mockler, 2012; James *et al.*, 2012; Staiger and Brown, 2013; Filichkin *et al.*, 2014). Therefore, AS is one important mechanism to mediate clock responses to the environment (Staiger and Green, 2011; Staiger and Brown, 2013) which makes it an interesting research topic in the context of circadian stress for future studies. A possible impact of cytokinin on alternative splicing mechanisms is so far unexplored in plants. However, cytokinin treatment rescued a human disease-causing mRNA splicing defect, revealing its potential to influence splicing events (Slaugenhaupt *et al.*, 2004). Furthermore, microarray analyses revealed that cytokinin induces the expression of *PRMT5* (*PROTEIN ARGININE METHYLTRANSFERASE 5*) (Kiba *et al.*, 2005; Bhargava *et al.*, 2013; and unpublished results, Dr. Wolfram Brenner). PRMT5 regulates alternative splicing globally and *PRMT5*-deficient plants have clock defects that could at least in part be attributed to changes in *PRR9* splicing (Hong *et al.*, 2010; Sanchez *et al.*, 2010).

Since EC-deficient plants showed strong circadian stress phenotypes and PRR9 function appeared to be protective under circadian stress conditions (Figs. 3.32 and 3.37; see 4.2.2.1) another scenario could be that cytokinin acts on EC and/or PRR function. Proper EC function during the night is crucial for nighttime clock gene expression including *CCA1*/*LHY* expression (Pokhilko *et al.*, 2012). This is thought to be achieved by the repression of *PRR9*, *PRR7*, and *TOC1* leading to a derepression of *CCA1*/*LHY* (Carré and Veflingstad, 2013). The increased expression of *PRR9* in combination with the decreased expression of *ELF3* in cytokinin-deficient plants compared with the wild type under circadian stress (Figs. 3.33 and 3.38; see also corresponding tables) could indicate that cytokinin promotes *CCA1*/*LHY* expression indirectly by controlling *ELF3* and/or *PRR9* transcript levels. In addition to the transcriptional regulation, PRRs are regulated post-transcriptionally by alternative splicing (see above) but also post-translationally by phosphorylation and proteasomal degradation (Fujiwara *et al.*, 2008; McClung, 2011; Nagel and Kay, 2012). In order to find out if cytokinin influences EC and/or PRR function to promote *CCA1*/*LHY* expression, an analysis of epistatic relationships would be useful. For instance, testing *cca1 lhy elf3*, *35S:CKX4 prr9* and *elf3 prr9* plants under circadian stress conditions would be informative (see also 4.2.4.1 and 4.2.4.2). A second important approach would be to analyze protein levels of EC components and PRRs in cytokinin-deficient plants compared with wild-type plants under circadian stress to clarify if cytokinin regulates the EC or PRRs on the protein level. Further, testing *cca1 lhy elf3* as well as cytokinin-deficient *elf3*, *35S:CCA1*, or *prr9 prr7 prr5* plants under circadian stress would help to elucidate whether cytokinin indeed mainly attenuates circadian stress by promoting *CCA1*/*LHY* expression or also by having an accessory function in the gating of light inputs into the circadian clock (see 4.2.4.2). Additional more indirect cytokinin functions such as the impact on sugar sensitivity and metabolism, which could influence sugar input information into the oscillator, have been addressed in section 4.2.7.3.

How is it that on the one hand cytokinin has such a strong influence on clock function under circadian stress regimes but on the other hand seems to be of moderate importance for clock performance under the conditions studied so far (see 1.3.8.1)? 1) One could argue that other input factors might predominate under many conditions, masking the impact cytokinin can have. This would mean that the importance of cytokinin is only revealed under very specific conditions when the aforesaid other factors

are missing or ineffective for some reason. 2) In plant chronobiological research clock performance is often evaluated by studying promoter-driven luciferase activity. However, there are several examples showing discrepancies between promoter activity of clock output genes and the corresponding mRNA profiles because circadian oscillations in transcript abundance result from transcriptional as well as post-transcriptional regulation (Staiger and Green, 2011). In case cytokinin acts on the post-transcriptional level (as discussed above) its effect on actual transcript levels might be stronger than its effect on bioluminescence rhythms which were for example measured by Hanano and colleagues to assess clock regulation by cytokinin (Hanano *et al.*, 2006). 3) There are tissue-specific clocks in *Arabidopsis* which contribute differently to clock performance on the whole-leaf level (Endo *et al.*, 2014). Endo and colleagues showed that approximately 77 % of the total leaf mRNA is derived from mesophyll cells while only about 8 % of the mRNA is derived from the vasculature, suggesting that results of circadian clock studies that were based on whole-leaf or whole-plant measurements mostly reflect mesophyll clock performance. If cytokinin indeed predominantly supports vascular clock function (as discussed in 4.2.4.4) it is possible that a strong impact of cytokinin on clock performance has been largely overlooked in previous studies. The very weak amplitude in oscillations of *ARR4* transcripts (Salomé *et al.*, 2006) might result from a predominant expression (To *et al.*, 2004) and circadian regulation in the vasculature. Moreover, *cre1 ahk3* plants exhibited no period phenotype when determined by leaf movement measurements (Salomé *et al.*, 2006). It could be that cytokinin signaling mainly influences the periodicity of the vascular clock, similar to PRR3 (Para *et al.*, 2007). Therefore, it would be helpful to measure circadian rhythms of vasculature-enriched transcripts (Para *et al.*, 2007; Endo *et al.*, 2014) and not whole-leaf responses or to study circadian oscillations in extracts of the isolated leaf vasculature (Endo *et al.*, 2014).

4.2.9 Future Perspectives

In this work two different types of abiotic stress – HL and circadian stress – have been investigated and the role of cytokinin in the respective stress response was studied.

It is already well known that cytokinin is an important player in various light-regulated processes, including chloroplast development, and moreover has an influence on photosynthesis (see 1.1.5). In this respect, it was intriguing to investigate a potential function of cytokinin in the response to HL. Under HL plants encounter light stress that strongly affects the photosynthesis-performing chloroplasts leading to photoinhibition (see 1.2.1.1) and cytokinin provides protection on different levels against this negative impact of light (Fig. 4.1). Several parameters contributing to HL resistance are affected by the cytokinin status. However, it is not clear which of these contributes the most or which might be indirect consequences of cytokinin deficiency. For instance, it could be that the stronger increase in the α-tocopherol content after HL is a consequence of the low overall carotenoid content in cytokinin-deficient plants. This could be a compensatory mechanism to counteract the lack of carotenoids in order to keep the scavenging capacity as high as possible (see 4.1.2). Further, this compensatory regulation probably strongly masks the full negative effect of the reduced carotenoid content in plants with a reduced cytokinin status under HL. To test this hypothesis, it could be informative to generate cytokinin-deficient plants that are deficient in tocopherols and compare the HL stress response of these

plants with the corresponding tocopherol mutants in the wild-type background. In addition, it could be valuable to generate cytokinin-deficient plants that overproduce carotenoids. This could be achieved for example by overexpressing beta-carotene hydroxylase (Davison *et al.*, 2002) or by introgressing the *szl1* (*suppressor of zeaxanthin-less 1*) allele into the cytokinin-deficient background (Li *et al.*, 2009). It could then be tested if the stronger HL stress response in cytokinin-deficient plants can be reversed to wild-type levels by overproduction of carotenoids. Moreover, tocopherol levels could be determined in these plants to find out if they are still stronger increased compared with the wild type in response to HL stress.

The carotenoid deficiency in plants with a reduced cytokinin status is consistent with their reduced ABA content (Nishiyama *et al.*, 2011a), since ABA biosynthesis requires carotenoids (Seo and Koshiba, 2002). Therefore, it should also be studied if ABA deficiency and/or ABA hypersensitivity (Nishiyama *et al.*, 2011a) contributes to the aggravated HL stress response in cytokinin-deficient plants. This is especially interesting because interplay between ABA and cytokinin signaling has already been reported for other forms of abiotic stress (Tran *et al.*, 2007; 2010; Nishiyama *et al.*, 2011a; Ha *et al.*, 2012). Besides, it has not been studied so far which step of ABA (carotenoid) synthesis might be promoted by cytokinin. Another interesting approach would be to test if the positive effect of cytokinin under HL might at least in part be due to its negative effect on JA synthesis (Fig. 3.46; see also 4.2.5.3). JA negatively affects photosynthesis (Weidhase *et al.*, 1987; Shan *et al.*, 2011; Attaran *et al.*, 2014). Furthermore, increased JA synthesis and hence an activated JA pathway could be correlated to aggravated photo-oxidative stress and cell death in response to HL (Ramel *et al.*, 2013). Levels of JA metabolites were not measured after 24 h HL treatment in this work. However, the much stronger accumulation of plastoglobuli in both *ahk2 ahk3* and *35S:CKX4* plants under HL conditions (Cortleven and Nitschke *et al.*, 2014) could indicate a stronger JA synthesis. Plastoglobuli contain triacylglycerols which comprise also α-linolenic acid (Bréhélin *et al.*, 2007; Bréhélin and Kessler, 2008; Lundquist *et al.*, 2012), the initial substrate for JA synthesis (see 1.6.1). It is known that substrate availability regulates JA synthesis (Wasternack, 2007). Additionally, proteomic analyses revealed that two lipases and the JA synthesis enzyme AOS are present in plastoglobuli (Vidi *et al.*, 2006; Ytterberg *et al.*, 2006). Therefore, it is believed that plastoglobuli accommodate the early steps of JA synthesis (Lundquist *et al.*, 2012). Hence, the stronger accumulation of plastoglobuli under HL might indicate a stronger stress-induced JA synthesis in cytokinin-deficient plants.

Studying the circadian stress response of cytokinin-deficient plants revealed a novel form of abiotic stress as was discussed in detail in the previous chapters. Concomitantly, it helped uncovering several so far underestimated or new connections between circadian clock, cytokinin function, JA pathway, ROS signaling, stress and cell death responses. For future investigations it could be very interesting to study at least some of the links found during the course of this work. In view of the current state-of-the-art cytokinin research it would be a very relevant and novel contribution to unravel the relationship between cytokinin and the circadian clock in more detail. The results indicated that it might be a reciprocal relationship (see 4.2.3.2 and 4.2.8.2) characterized by the regulation of cytokinin outputs by the circadian clock and, oppositely, by cytokinin inputs into the oscillator to support clock function. It is a frequently observed phenomenon that clock outputs serve as clock inputs at the same time (see

1.3.4). Thereby, the circadian clock not only altruistically enhances plant fitness by timing and modulating certain outputs (see 1.3.1) but simultaneously receives feedback signals to fine-tune clock function, e.g. by sugars, ABA, auxin, and the Fe status (Hanano *et al.*, 2006; Rawat *et al.*, 2009; Castells *et al.*, 2010; Seung *et al.*, 2012; Haydon *et al.*, 2013b; Hong *et al.*, 2013b; Chen *et al.*, 2013b; Salomé *et al.*, 2013). In this context it could be studied if cytokinin indeed predominantly influences vascular clock function (see 4.2.4.4). If so, this would necessitate a re-evaluation of previous results regarding cytokinin action on clock performance because the impact of cytokinin might have been largely overlooked by analyzing whole-leaf or whole-plant samples (see 4.2.8.2). Furthermore, it could be examined which clock components are regulated by cytokinin and on which level as well as under which conditions. Conversely, another line of future investigations could be to study the possible gating of cytokinin synthesis, signaling, and/or responses by the circadian clock because such a gating might strongly influence and fine-tune cytokinin signaling outputs.

Another connection that could be worthwhile to study is the cytokinin-JA interplay (see 4.2.5.3) which might be of particular importance under stress conditions such as HL stress (see above). Moreover, the contribution of the activated JA pathway to cell death development in cytokinin-deficient plants under circadian stress and the possible involvement of COI1-independent signaling are intriguing topics. In addition, rather large-scale approaches such as microarray analyses at specific time points (e.g. early between "5 h" and "7.5 h" or at later time points after CL treatment correlating with the strongest perturbation of oscillator function) could be informative as well. Finally, suppressor mutagenesis screens using cytokinin- or clock-deficient plants could be very useful in order to unravel yet unknown connections and potential components and signaling pathways that contribute to the development of circadian stress in plants with a reduced cytokinin status.

5 Summary

Cytokinins are plant hormones that regulate diverse processes in plant development and responses to biotic and abiotic stresses. In this study a novel protective function of cytokinin under high light (HL) stress as well as under circadian stress has been elucidated.

In the first part of this work plants with a reduced cytokinin status, i.e. cytokinin receptor mutants and *CKX4*-overexpressing transgenic plants, were analyzed regarding their response to HL conditions. A stronger decline in the photosystem II (PSII) maximum quantum efficiency (F_v/F_m) after HL treatment revealed stronger photoinhibition and hence a higher susceptibility to HL stress in these plants compared with wild-type plants. Receptor mutant analyses indicated that the cytokinin receptor AHK3 is the key player in mediating this light stress response, while AHK2 has an accessory function.

PSII, especially the D1 protein, is highly sensitive to the detrimental impact of light. Therefore, photoinhibition is always observed when the rate of photodamage exceeds the rate of D1 repair. In line with the stronger photoinhibtion, D1 protein levels were strongly decreased upon HL stress in cytokinin-deficient plants. On the one hand, experimentally induced inhibition of D1 repair indicated that this was a consequence of stronger photodamage in these plants. On the other hand, slow and incomplete recovery in these plants after HL treatment indicated insufficient D1 repair.

Plants have evolved a high number of photo-protective mechanisms to counteract the negative impact of light stress. Among them is the ROS scavenging system. The total antioxidant capacity was decreased in plants with a reduced cytokinin status. A more detailed analysis of different scavenging mechanisms revealed a pronounced deficiency in carotenoids after HL exposure. A lack of carotenoids could explain both a compromised D1 repair and a stronger photodamage. Carotenoids strongly support the ROS scavenging capacity through proper energy dissipation (NPQ) and the quenching of excited triplet chlorophylls ($^3Chl^*$) and singlet oxygen ($^1O_2$), thereby minimizing the inhibition of D1 repair. In addition, efficient NPQ helps reducing photodamage.

The second part of this work aimed to uncover a new phenomenon characterized by a pronounced cell death phenotype in plants with a reduced cytokinin status after exposure to changed light-dark regimes. Cytokinin synthesis mutants, *CKX*-overexpressing transgenic plants and cytokinin signaling mutants were affected upon these treatments, revealing the necessity of normal cytokinin levels as well as functional cytokinin signaling for this adaptive response. Also under this kind of stress the receptor AHK3 was found to be the key player, while AHK2 and, even more pronounced, CRE1/AHK4 played accessory roles.

Cell death progression in cytokinin-deficient plants was accompanied by necrotic and water-soaked lesions, loss of membrane integrity, and increased oxidative stress, correlating with a strong induction of stress- and cell death-related genes in the affected leaves. The exposure to different light-dark-temperature regimes clearly demonstrated that, although dependent on prolonged light periods, cell death initiation was not part of a light stress response since it required a dark period following the extended light treatment. Instead, the severity of cell death was determined by a specific interplay between entrainment, treatment, and post-treatment regime pointing to an involvement of the

circadian clock. Transcript profiles were recorded during the cell death-inducing dark period. The induction of stress- and JA-related genes in cytokinin-deficient plants coincided with a stronger misregulation in core oscillator gene expression compared with wild-type plants. Especially the morning genes *CCA1* and *LHY* exhibited a strongly diminished expression. Misregulated clock output gene expression also indicated a perturbation of the core oscillator. Intriguingly, the cell death phenotype was also observed in clock mutants lacking proper CCA1 and LHY function. Additionally, these plants exhibited a highly similar molecular phenotype compared with cytokinin-deficient plants regarding clock output, stress and cell death marker, and, interestingly, also A-type *ARR* gene expression. In conclusion, these results confirmed the hypothesis that a malfunction of circadian timekeeping – "circadian stress" – was responsible for the cell death phenotype in cytokinin-deficient plants in response to changed light-dark regimes.

A strong upregulation of JA-related genes and genes of the ROS network occurred prior to cell death initiation. However, these early changes in gene expression were not accompanied by increases in JA levels or oxidative stress. The data indicate that the strongly altered transcript levels result from a direct misregulation of clock-controlled genes by a perturbed oscillator and potentially also a disrupted gating of JA and oxidative stress responses resulting in enhanced JA and ROS responsiveness. One consequence was the activation of the JA pathway and, subsequently, also the accumulation of JA metabolites amplifying JA signaling. The partial rescue of cytokinin-deficient plants lacking proper JA synthesis confirmed an involvement of the JA pathway in the promotion of cell death development under circadian stress. The misregulation of genes of the ROS network, including the induction of ROS-inducible and plant core environmental stress response (PCESR) genes, was probably part of the "death signal". Furthermore, genes encoding scavenging enzymes or ferritins exhibited reduced expression in cytokinin-deficient plants which might have contributed to a disturbed ROS homeostasis which accompanied later stages of cell death progression presumably further amplifying oxidative stress responses and hence cell death development.

6 Zusammenfassung

Das Pflanzenhormon Cytokinin reguliert eine Vielzahl an Entwicklungsprozessen sowie die pflanzliche Reaktion auf biotischen und abiotischen Stress. In dieser Arbeit konnte eine bisher unbekannte Rolle von Cytokinin bei der Antwort auf Starklicht- (SL) und circadianen Stress gezeigt werden.

Im ersten Teil der Untersuchungen wurden Pflanzen mit reduziertem Cytokininstatus, d.h. Cytokinin-Rezeptor-Mutanten und *CKX4*-überexprimierende transgene Pflanzen, auf ihre SL-Antwort hin analysiert. Nach SL-Behandlung war die Effizienz der Photosystem II (PSII)-Aktivität (F_v/F_m) in diesen Pflanzen stärker vermindert als in Wildtyp-Pflanzen. Dies offenbarte eine stärkere Photoinhibition in Cytokinin-defizienten Pflanzen und demnach eine stärkere Empfindlichkeit gegenüber SL-Stress. Zudem konnte durch Analyse verschiedener Rezeptor-Mutanten die tragende Rolle des AHK3-Rezeptors in der Vermittlung dieser Lichtstress-Antwort aufgedeckt werden, wobei AHK2 eine Hilfsfunktion ausübt.

PSII, und insbesondere das D1-Protein, ist äußerst empfindlich gegenüber dem negativen Einfluss von Licht. Photoinhibition tritt demzufolge auf, wenn die Rate der Schädigung durch Licht die Rate der D1-Reparatur übersteigt. In der Tat waren die D1-Protein-Gehalte nach SL-Stress in Cytokinin-defizienten Pflanzen stark reduziert. Einerseits konnte durch experimentell induzierte Inhibition der D1-Reparatur gezeigt werden, dass dies aus einer stärkeren Schädigung resultierte. Andererseits deutete die langsame und unvollständige Regeneration von PSII nach SL-Behandlung auf eine unzureichende D1-Reparatur hin.

Pflanzen besitzen viele photo-protektive Mechanismen, um dem negativen Einfluss von Lichtstress entgegenzuwirken. Ein wichtiger Schutzmechanismus besteht in der effizienten Beseitigung reaktiver Sauerstoffspezies (englisch: *ROS scavenging*). Die antioxidative Kapazität war in Pflanzen mit reduziertem Cytokinin-Status vermindert. Eine detailliertere Analyse verschiedener *Scavenging*-Mechanismen nach Einfluss von SL offenbarte eine deutliche Defizienz an Carotenoiden. Carotenoid-Mangel könnte sowohl eine mangelhafte D1-Reparatur als auch stärkere Schädigung durch Licht erklären. Durch Dissipation von Energie (NPQ) und die Beseitigung von angeregtem Chlorophyll im Triplett-Zustand ($^3Chl^*$) und Singulett-Sauerstoff ($^1O_2$) erhöhen Carotenoide die *Scavenging*-Kapazität und minimieren so eine Inhibition der D1-Reparatur durch ROS. Zusätzlich trägt effizientes NPQ zur Reduktion der Schädigung von PSII bei.

Der zweite Teil der Untersuchungen hatte zum Ziel ein neuartiges Phänomen zu charakterisieren, welches durch einen starken Zelltod-Phänotyp in Cytokinin-defizienten Pflanzen nach Behandlung mit veränderten Licht-Dunkel-Rhythmen gekennzeichnet war. Pflanzen mit Mutationen im Cytokinin-Synthese oder -Signalweg sowie transgene Linien mit *CKX*-Überexpression waren sensitiv gegenüber diesen Regimes, was die Notwendigkeit normaler Cytokinin-Gehalte und eines funktionellen Cytokinin-Signalweges für diese adaptive Antwort verdeutlichte. Wie auch beim SL-Stress ist AHK3 hierbei Hauptvermittler, wohingegen AHK2 und noch entscheidender CRE1/AHK4 am AHK3-abhängigen Signal mitwirken.

Der Zelltod in Cytokinin-defizienten Pflanzen war begleitet von nekrotischen Läsionen, dem Verlust an Frischgewicht und Membranintegrität sowie der Entstehung von oxidativem Stress. Diese Veränderungen in den betroffenen Blättern gingen einher mit der starken Induktion von Stress- und Zelltodmarker-Genen. Verschiedene Licht-Dunkel-Temperatur-Regimes wurden getestet und zeigten, dass der Zelltod nicht durch Lichtstress induziert wurde. Obwohl der Zelltodphänotyp mit einer verlängerten Lichtphase in Zusammenhang stand, war eine anschließende Dunkelphase erforderlich, um den Zelltod auszulösen. Insgesamt hing der Schweregrad des Zelltodes vom synchronisierenden Licht-Dunkel-Regime während der Anzucht, der Behandlung selbst sowie von den nachfolgenden Bedingungen ab, was auf eine Beteiligung der circadianen Uhr (englisch: *clock*) hindeutete. Transkriptprofile wurden während der Zelltod-induzierenden Dunkelphase aufgezeichnet. Diese zeigten, dass die Induktion von Stress- und JA-assoziierten Genen in Cytokinin-defizienten Pflanzen mit einer stärkeren Fehlregulation von *Clock*-Genen im Vergleich zum Wildtyp korrelierte. Besonders drastisch reduziert war die Expression der Morgen-Gene *CCA1* und *LHY*, aber auch fehlregulierte circadian gesteuerte Gene (englisch: *output genes*) deuteten auf eine Störung des Hauptoscillators hin. *Clock*-Mutanten mit beeinträchtigter CCA1- und LHY-Funktion zeigten auch den in Cytokinin-defizienten Pflanzen beobachteten Zelltod-Phänotyp und wiesen zudem vergleichbare Veränderungen in den Transkriptmengen von *Output*-, Stress- und Zelltodmarker- sowie A-Typ *ARR*-Genen auf. Diese Ergebnisse bestätigten die Hypothese, dass eine Störung der circadianen Rhythmik – „circadianer Stress" – für den Zelltod durch veränderte Licht-Dunkel-Regimes in Cytokinin-defizienten Pflanzen verantwortlich war.

Die Hochregulation von JA-assoziierten Genen und Genen des ROS-Netzwerks wurde bereits vor Initiation des Zelltodes detektiert, war aber nicht begleitet von erhöhten JA-Gehalten oder oxidativem Stress. Die Daten deuten darauf hin, dass die stark veränderten Transkriptmengen aus einer direkten Fehlregulation von circadian regulierten Genen resultiert. Zusätzlich könnte die gestörte circadiane Uhr durch fehlerhaftes *Gating* eine Hypersensitivität gegenüber JA und oxidativem Stress ausgelöst haben. Eine Folge war die Aktivierung des JA-Weges und schließlich auch die Akkumulation von JA-Metaboliten, die das JA-Signal weiter verstärkten. Die partielle Rettung von Cytokinin-defizienten Pflanzen in einem genetischen Hintergrund mit gestörter JA-Synthese bestätigte eine Beteiligung des JA-Weges an der Förderung des Zelltodes unter circadianem Stress. Die Fehlregulation von Genen des ROS-Netzwerks schloss die Induktion von ROS-induzierbaren Genen und universellen Stress-Antwort-Genen, den PCESR-Genen (englisch: *plant core environmental stress response*), ein, was vermutlich Teil des Zelltod-auslösenden Signals war. Des Weiteren war die Expression von *Scavenging*- und Ferritin-Genen reduziert, was durch negativen Einfluss auf die ROS-Homöostase zu oxidativem Stress, der bei forgeschrittenem Zelltod zu beobachten war, und so zur Förderung des Zelltodes beigetragen haben könnte.

7 References

Abràmoff, M.D., Magalhães, P.J., and Ram, S.J. (2004). Image processing with ImageJ. Biophotonics International *11*, 36-42.

Acosta, I.F., and Farmer, E.E. (2010). Jasmonates. Arabidopsis Book *8*, e0129.

Adams, E., and Turner, J. (2010). COI1, a jasmonate receptor, is involved in ethylene-induced inhibition of *Arabidopsis* root growth in the light. J Exp Bot *61*, 4373-4386.

Adams, S., and Carré, I.A. (2011). Downstream of the plant circadian clock: output pathways for the control of physiology and development. Essays Biochem *49*, 53-69.

Adir, N., Zer, H., Shochat, S., and Ohad, I. (2003). Photoinhibition - a historical perspective. Photosynth Res *76*, 343-370.

Alabadí, D., Oyama, T., Yanovsky, M.J., Harmon, F.G., Más, P., and Kay, S.A. (2001). Reciprocal regulation between *TOC1* and *LHY/CCA1* within the *Arabidopsis* circadian clock. Science *293*, 880-883.

Alabadí, D., Yanovsky, M.J., Más, P., Harmer, S.L., and Kay, S.A. (2002). Critical role for CCA1 and LHY in maintaining circadian rhythmicity in *Arabidopsis*. Curr Biol *12*, 757-761.

Allen, J.F., and Pfannschmidt, T. (2000). Balancing the two photosystems: photosynthetic electron transfer governs transcription of reaction centre genes in chloroplasts. Philos Trans R Soc Lond B Biol Sci *355*, 1351-1359.

Alonso, J.M., Stepanova, A.N., Leisse, T.J., Kim, C.J., Chen, H., Shinn, P., Stevenson, D.K., Zimmerman, J., Barajas, P., Cheuk, R*., et al.* (2003). Genome-wide insertional mutagenesis of *Arabidopsis thaliana*. Science *301*, 653-657.

An, H., Roussot, C., Suárez-López, P., Corbesier, L., Vincent, C., Piñeiro, M., Hepworth, S., Mouradov, A., Justin, S., Turnbull, C*., et al.* (2004). CONSTANS acts in the phloem to regulate a systemic signal that induces photoperiodic flowering of *Arabidopsis*. Development *131*, 3615-3626.

Anbudurai, P.R., Mor, T.S., Ohad, I., Shestakov, S.V., and Pakrasi, H.B. (1994). The *ctpA* gene encodes the C-terminal processing protease for the D1 protein of the photosystem II reaction center complex. Proc Natl Acad Sci U S A *91*, 8082-8086.

Apel, K., and Hirt, H. (2004). Reactive oxygen species: metabolism, oxidative stress, and signal transduction. Annu Rev Plant Biol *55*, 373-399.

Arana, M.V., Marín-de la Rosa, N., Maloof, J.N., Blázquez, M.A., and Alabadí, D. (2011). Circadian oscillation of gibberellin signaling in *Arabidopsis*. Proc Natl Acad Sci U S A *108*, 9292-9297.

Argueso, C.T., Ferreira, F.J., and Kieber, J.J. (2009). Environmental perception avenues: the interaction of cytokinin and environmental response pathways. Plant Cell Environ *32*, 1147-1160.

Argyros, R.D., Mathews, D.E., Chiang, Y.H., Palmer, C.M., Thibault, D.M., Etheridge, N., Argyros, D.A., Mason, M.G., Kieber, J.J., and Schaller, G.E. (2008). Type B response regulators of *Arabidopsis* play key roles in cytokinin signaling and plant development. Plant Cell *20*, 2102-2116.

Aro, E.M., Suorsa, M., Rokka, A., Allahverdiyeva, Y., Paakkarinen, V., Saleem, A., Battchikova, N., and Rintamäki, E. (2005). Dynamics of photosystem II: a proteomic approach to thylakoid protein complexes. J Exp Bot *56*, 347-356.

Aro, E.M., Virgin, I., and Andersson, B. (1993). Photoinhibition of Photosystem II. Inactivation, protein damage and turnover. Biochim Biophys Acta *1143*, 113-134.

Asada, K. (2006). Production and scavenging of reactive oxygen species in chloroplasts and their functions. Plant Physiol *141*, 391-396.

Aschoff, J. (1979). Circadian rhythms: influences of internal and external factors on the period measured in constant conditions. Z Tierpsychol *49*, 225-249.

Attaran, E., Major, I.T., Cruz, J.A., Rosa, B.A., Koo, A.J., Chen, J., Kramer, D.M., He, S.Y., and Howe, G.A. (2014). Temporal dynamics of growth and photosynthesis suppression in response to jasmonate signaling. Plant Physiol *165*, 1302-1314.

Avonce, N., Leyman, B., Mascorro-Gallardo, J.O., Van Dijck, P., Thevelein, J.M., and Iturriaga, G. (2004). The *Arabidopsis* trehalose-6-P synthase *AtTPS1* gene is a regulator of glucose, abscisic acid, and stress signaling. Plant Physiol *136*, 3649-3659.

Baena-González, E., and Aro, E.M. (2002). Biogenesis, assembly and turnover of photosystem II units. Philos Trans R Soc Lond B Biol Sci *357*, 1451-1460.

Baker, N.R. (2008). Chlorophyll fluorescence: a probe of photosynthesis *in vivo*. Annu Rev Plant Biol *59*, 89-113.

Balazadeh, S., Jaspert, N., Arif, M., Mueller-Roeber, B., and Maurino, V.G. (2012). Expression of ROS-responsive genes and transcription factors after metabolic formation of H_2O_2 in chloroplasts. Front Plant Sci *3*, 234.

Balazadeh, S., Kwasniewski, M., Caldana, C., Mehrnia, M., Zanor, M.I., Xue, G.P., and Mueller-Roeber, B. (2011). ORS1, an H_2O_2-responsive NAC transcription factor, controls senescence in *Arabidopsis thaliana*. Mol Plant *4*, 346-360.

Bancos, S., Szatmári, A.M., Castle, J., Kozma-Bognár, L., Shibata, K., Yokota, T., Bishop, G.J., Nagy, F., and Szekeres, M. (2006). Diurnal regulation of the brassinosteroid-biosynthetic *CPD* gene in *Arabidopsis*. Plant Physiol *141*, 299-309.

Bannenberg, G., Martínez, M., Hamberg, M., and Castresana, C. (2009). Diversity of the enzymatic activity in the lipoxygenase gene family of *Arabidopsis thaliana*. Lipids *44*, 85-95.

Barber, J., and Andersson, B. (1992). Too much of a good thing: light can be bad for photosynthesis. Trends Biochem Sci *17*, 61-66.

Bartrina, I. (2006). Molekulare Charakterisierung von *ckx* Insertionsmutanten und Suppressormutanten des Cytokinindefizienzsyndroms in *Arabidopsis thaliana*. Dissertation. Institute of Biology/Applied Genetics Berlin, Freie Universität Berlin.

Bell, E., Creelman, R.A., and Mullet, J.E. (1995). A chloroplast lipoxygenase is required for wound-induced jasmonic acid accumulation in *Arabidopsis*. Proc Natl Acad Sci U S A *92*, 8675-8679.

Bhardwaj, V., Meier, S., Petersen, L.N., Ingle, R.A., and Roden, L.C. (2011). Defence responses of *Arabidopsis thaliana* to infection by *Pseudomonas syringae* are regulated by the circadian clock. PLoS One *6*, e26968.

Bhargava, A., Clabaugh, I., To, J.P., Maxwell, B.B., Chiang, Y.H., Schaller, G.E., Loraine, A., and Kieber, J.J. (2013). Identification of cytokinin-responsive genes using microarray meta-analysis and RNA-Seq in *Arabidopsis*. Plant Physiol *162*, 272-294.

Bieker, S., Riester, L., Stahl, M., Franzaring, J., and Zentgraf, U. (2012). Senescence-specific alteration of hydrogen peroxide levels in *Arabidopsis thaliana* and oilseed rape spring variety *Brassica napus* L. cv. Mozart. J Integr Plant Biol *54*, 540-554.

Bieniawska, Z., Espinoza, C., Schlereth, A., Sulpice, R., Hincha, D.K., and Hannah, M.A. (2008). Disruption of the *Arabidopsis* circadian clock is responsible for extensive variation in the cold-responsive transcriptome. Plant Physiol *147*, 263-279.

Bilyeu, K.D., Cole, J.L., Laskey, J.G., Riekhof, W.R., Esparza, T.J., Kramer, M.D., and Morris, R.O. (2001). Molecular and biochemical characterization of a cytokinin oxidase from maize. Plant Physiol *125*, 378-386.

Birnbaum, K., Shasha, D.E., Wang, J.Y., Jung, J.W., Lambert, G.M., Galbraith, D.W., and Benfey, P.N. (2003). A gene expression map of the *Arabidopsis* root. Science *302*, 1956-1960.

Bishopp, A., Help, H., El-Showk, S., Weijers, D., Scheres, B., Friml, J., Benková, E., Mähönen, A.P., and Helariutta, Y. (2011). A Mutually Inhibitory Interaction between Auxin and Cytokinin Specifies Vascular Pattern in Roots. Curr Biol *21*, 917-926.

Bläsing, O.E., Gibon, Y., Günther, M., Höhne, M., Morcuende, R., Osuna, D., Thimm, O., Usadel, B., Scheible, W.R., and Stitt, M. (2005). Sugars and circadian regulation make major contributions to the global regulation of diurnal gene expression in *Arabidopsis*. Plant Cell *17*, 3257-3281.

Bleecker, A.B., Estelle, M.A., Somerville, C., and Kende, H. (1988). Insensitivity to ethylene conferred by a dominant mutation in *Arabidopsis thaliana*. Science *241*, 1086-1089.

Boonman, A., Prinsen, E., Gilmer, F., Schurr, U., Peeters, A.J., Voesenek, L.A., and Pons, T.L. (2007). Cytokinin import rate as a signal for photosynthetic acclimation to canopy light gradients. Plant Physiol *143*, 1841-1852.

Bowler, C., and Fluhr, R. (2000). The role of calcium and activated oxygens as signals for controlling cross-tolerance. Trends Plant Sci *5*, 241-246.

Bowling, S.A., Clarke, J.D., Liu, Y., Klessig, D.F., and Dong, X. (1997). The *cpr5* mutant of *Arabidopsis* expresses both NPR1-dependent and NPR1-independent resistance. Plant Cell *9*, 1573-1584.

Bradford, M.M. (1976). A rapid and sensitive method for the quantitation of microgram quantities of protein utilizing the principle of protein-dye binding. Anal Biochem *72*, 248-254.

Bréhélin, C., and Kessler, F. (2008). The plastoglobule: a bag full of lipid biochemistry tricks. Photochem Photobiol *84*, 1388-1394.

Bréhélin, C., Kessler, F., and van Wijk, K.J. (2007). Plastoglobules: versatile lipoprotein particles in plastids. Trends Plant Sci *12*, 260-266.

Brenner, W.G., Ramireddy, E., Heyl, A., and Schmülling, T. (2012). Gene regulation by cytokinin in *Arabidopsis*. Front Plant Sci *3*, 8.

Brenner, W.G., Romanov, G.A., Köllmer, I., Bürkle, L., and Schmülling, T. (2005). Immediate-early and delayed cytokinin response genes of *Arabidopsis thaliana* identified by genome-wide expression profiling reveal novel cytokinin-sensitive processes and suggest cytokinin action through transcriptional cascades. Plant J *44*, 314-333.

Brenner, W.G., and Schmülling, T. (2012). Transcript profiling of cytokinin action in *Arabidopsis* roots and shoots discovers largely similar but also organ-specific responses. BMC Plant Biol *12*, 112.

Briat, J.F., Ravet, K., Arnaud, N., Duc, C., Boucherez, J., Touraine, B., Cellier, F., and Gaymard, F. (2010). New insights into ferritin synthesis and function highlight a link between iron homeostasis and oxidative stress in plants. Ann Bot *105*, 811-822.

Brooks, D.M., Bender, C.L., and Kunkel, B.N. (2005). The *Pseudomonas syringae* phytotoxin coronatine promotes virulence by overcoming salicylic acid-dependent defences in *Arabidopsis thaliana*. Mol Plant Pathol *6*, 629-639.

Brosché, M., Blomster, T., Salojärvi, J., Cui, F., Sipari, N., Leppälä, J., Lamminmäki, A., Tomai, G., Narayanasamy, S., Reddy, R.A*., et al.* (2014). Transcriptomics and functional genomics of ROS-induced cell death regulation by *RADICAL-INDUCED CELL DEATH1*. PLoS Genet *10*, e1004112.

Brownlee, B.G., Hall, R.H. und Whitty, C.D. (1975). 3-Methyl-2-butenal: an enzymatic degradation product of the cytokinin, N-6-(delta-2 isopentenyl)adenine. Can J Biochem *53*, 37-41.

Browse, J. (2009a). Jasmonate passes muster: a receptor and targets for the defense hormone. Annu Rev Plant Biol *60*, 183-205.

Browse, J. (2009b). The power of mutants for investigating jasmonate biosynthesis and signaling. Phytochemistry *70*, 1539-1546.

Brzobohaty, B., Moore, I., Kristoffersen, P., Bako, L., Campos, N., Schell, J., and Palme, K. (1993). Release of active cytokinin by a beta-glucosidase localized to the maize root meristem. Science *262*, 1051-1054.

Bujdoso, N., and Davis, S.J. (2013). Mathematical modeling of an oscillating gene circuit to unravel the circadian clock network of *Arabidopsis thaliana*. Front Plant Sci *4*, 3.

Caesar, K., Thamm, A.M., Witthöft, J., Elgass, K., Huppenberger, P., Grefen, C., Horak, J., and Harter, K. (2011). Evidence for the localization of the *Arabidopsis* cytokinin receptors AHK3 and AHK4 in the endoplasmic reticulum. J Exp Bot *62*, 5571-5580.

Cai, Y.M., Yu, J., and Gallois, P. (2014). Endoplasmic reticulum stress-induced PCD and caspase-like activities involved. Front Plant Sci *5*, 41.

Caldelari, D., Wang, G., Farmer, E.E., and Dong, X. (2011). *Arabidopsis lox3 lox4* double mutants are male sterile and defective in global proliferative arrest. Plant Mol Biol *75*, 25-33.

Cao, H., Glazebrook, J., Clarke, J.D., Volko, S., and Dong, X. (1997). The *Arabidopsis NPR1* gene that controls systemic acquired resistance encodes a novel protein containing ankyrin repeats. Cell *88*, 57-63.

Carabelli, M., Possenti, M., Sessa, G., Ciolfi, A., Sassi, M., Morelli, G., and Ruberti, I. (2007). Canopy shade causes a rapid and transient arrest in leaf development through auxin-induced cytokinin oxidase activity. Genes Dev *21*, 1863-1868.

Carré, I., and Veflingstad, S.R. (2013). Emerging design principles in the *Arabidopsis* circadian clock. Semin Cell Dev Biol *24*, 393-398.

Castells, E., Portolés, S., Huang, W., and Más, P. (2010). A functional connection between the clock component TOC1 and abscisic acid signaling pathways. Plant Signal Behav *5*, 409-411.

Čatský, J., Pospíšilová, J., Macháčková, I., Wilhelmová, N., and Šesták, Z. (1993). Photosynthesis and water relations in transgenic tobacco plants with T-DNA carrying gene 4 for cytokinin synthesis. Biol Plant *35*, 393-399.

Chang, L., Ramireddy, E., and Schmülling, T. (2013). Lateral root formation and growth of *Arabidopsis* is redundantly regulated by cytokinin metabolism and signalling genes. J Exp Bot *64*, 5021-5032.

Che, Y., Fu, A., Hou, X., McDonald, K., Buchanan, B.B., Huang, W., and Luan, S. (2013). C-terminal processing of reaction center protein D1 is essential for the function and assembly of photosystem II in *Arabidopsis*. Proc Natl Acad Sci U S A *110*, 16247-16252.

Chen, D., Xu, G., Tang, W., Jing, Y., Ji, Q., Fei, Z., and Lin, R. (2013a). Antagonistic basic helix-loop-helix/bZIP transcription factors form transcriptional modules that integrate light and reactive oxygen species signaling in *Arabidopsis*. Plant Cell *25*, 1657-1673.

Chen, Y.Y., Wang, Y., Shin, L.J., Wu, J.F., Shanmugam, V., Tsednee, M., Lo, J.C., Chen, C.C., Wu, S.H., and Yeh, K.C. (2013b). Iron is involved in the maintenance of circadian period length in *Arabidopsis*. Plant Physiol *161*, 1409-1420.

Cheng, C.Y., Mathews, D.E., Schaller, G.E., and Kieber, J.J. (2013). Cytokinin-dependent specification of the functional megaspore in the *Arabidopsis* female gametophyte. Plant J *73*, 929-940.

Chernyad'ev, I.I. (2000). Ontogenetic changes in the photosynthetic apparatus and effect of cytokinins. Appl Biochem Microbiol *36*, 527-539, translated from Prikl Biokhim Mikrobiol *36*, 611-625.

Chickarmane, V.S., Gordon, S.P., Tarr, P.T., Heisler, M.G., and Meyerowitz, E.M. (2012). Cytokinin signaling as a positional cue for patterning the apical-basal axis of the growing *Arabidopsis* shoot meristem. Proc Natl Acad Sci U S A *109*, 4002-4007.

Chini, A., Fonseca, S., Fernández, G., Adie, B., Chico, J.M., Lorenzo, O., García-Casado, G., López-Vidriero, I., Lozano, F.M., Ponce, M.R.*, et al.* (2007). The JAZ family of repressors is the missing link in jasmonate signalling. Nature *448*, 666-671.

Choi, J., Huh, S.U., Kojima, M., Sakakibara, H., Paek, K.H., and Hwang, I. (2010). The cytokinin-activated transcription factor ARR2 promotes plant immunity *via* TGA3/NPR1-dependent salicylic acid signaling in *Arabidopsis*. Dev Cell *19*, 284-295.

Choi, W.G., Toyota, M., Kim, S.H., Hilleary, R., and Gilroy, S. (2014). Salt stress-induced Ca^{2+} waves are associated with rapid, long-distance root-to-shoot signaling in plants. Proc Natl Acad Sci U S A *111*, 6497-6502.

Chory, J., Reinecke, D., Sim, S., Washburn, T., and Brenner, M. (1994). A role for cytokinins in de-etiolation in *Arabidopsis* (*det* mutants have an altered response to cytokinins). Plant Physiol *104*, 339-347.

Chow, B.Y., Helfer, A., Nusinow, D.A., and Kay, S.A. (2012). ELF3 recruitment to the *PRR9* promoter requires other Evening Complex members in the *Arabidopsis* circadian clock. Plant Signal Behav *7*, 170-173.

Chung, H.S., Koo, A.J., Gao, X., Jayanty, S., Thines, B., Jones, A.D., and Howe, G.A. (2008). Regulation and function of *Arabidopsis JASMONATE ZIM*-domain genes in response to wounding and herbivory. Plant Physiol *146*, 952-964.

Chung, H.S., Niu, Y., Browse, J., and Howe, G.A. (2009). Top hits in contemporary JAZ: an update on jasmonate signaling. Phytochemistry *70*, 1547-1559.

Clarke, J.D., Volko, S.M., Ledford, H., Ausubel, F.M., and Dong, X. (2000). Roles of salicylic acid, jasmonic acid, and ethylene in cpr-induced resistance in *Arabidopsis*. Plant Cell *12*, 2175-2190.

Coll, N.S., Epple, P., and Dangl, J.L. (2011). Programmed cell death in the plant immune system. Cell Death Differ *18*, 1247-1256.

Coll, N.S., Vercammen, D., Smidler, A., Clover, C., Van Breusegem, F., Dangl, J.L., and Epple, P. (2010). *Arabidopsis* type I metacaspases control cell death. Science *330*, 1393-1397.

Cortleven, A., Nitschke, S., Klaumünzer, M., Abdelgawad, H., Asard, H., Grimm, B., Riefler, M., and Schmülling, T. (2014). A novel protective function for cytokinin in the light stress response is mediated by the *Arabidopsis* histidine kinase2 and *Arabidopsis* histidine kinase3 receptors. Plant Physiol *164*, 1470-1483.

Cortleven, A., and Valcke, R. (2012). Evaluation of the photosynthetic activity in transgenic tobacco plants with altered endogenous cytokinin content: lessons from cytokinin. Physiol Plant *144*, 394-408.

Covington, M.F., and Harmer, S.L. (2007). The circadian clock regulates auxin signaling and responses in *Arabidopsis*. PLoS Biol *5*, e222.

Covington, M.F., Maloof, J.N., Straume, M., Kay, S.A., and Harmer, S.L. (2008). Global transcriptome analysis reveals circadian regulation of key pathways in plant growth and development. Genome Biol *9*, R130.

Covington, M.F., Panda, S., Liu, X.L., Strayer, C.A., Wagner, D.R., and Kay, S.A. (2001). ELF3 modulates resetting of the circadian clock in *Arabidopsis*. Plant Cell *13*, 1305-1315.

Cutcliffe, J.W., Hellmann, E., Heyl, A., and Rashotte, A.M. (2011). CRFs form protein-protein interactions with each other and with members of the cytokinin signalling pathway in *Arabidopsis via* the CRF domain. J Exp Bot *62*, 4995-5002.

D'Agostino, I.B., Deruère, J., and Kieber, J.J. (2000). Characterization of the response of the *Arabidopsis* response regulator gene family to cytokinin. Plant Physiol *124*, 1706-1717.

Dalchau, N., Hubbard, K.E., Robertson, F.C., Hotta, C.T., Briggs, H.M., Stan, G.B., Gonçalves, J.M., and Webb, A.A. (2010). Correct biological timing in *Arabidopsis* requires multiple light-signaling pathways. Proc Natl Acad Sci U S A *107*, 13171-13176.

Dall'Osto, L., Cazzaniga, S., North, H., Marion-Poll, A., and Bassi, R. (2007). The *Arabidopsis* aba4-1 mutant reveals a specific function for neoxanthin in protection against photooxidative stress. Plant Cell *19*, 1048-1064.

Dall'Osto, L., Lico, C., Alric, J., Giuliano, G., Havaux, M., and Bassi, R. (2006). Lutein is needed for efficient chlorophyll triplet quenching in the major LHCII antenna complex of higher plants and effective photoprotection *in vivo* under strong light. BMC Plant Biol *6*, 32.

Daniel, X., Sugano, S., and Tobin, E.M. (2004). CK2 phosphorylation of CCA1 is necessary for its circadian oscillator function in *Arabidopsis*. Proc Natl Acad Sci U S A *101*, 3292-3297.

Danon, A., Miersch, O., Felix, G., Camp, R.G., and Apel, K. (2005). Concurrent activation of cell death-regulating signaling pathways by singlet oxygen in *Arabidopsis thaliana*. Plant J *41*, 68-80.

Dave, A., and Graham, I.A. (2012). Oxylipin signaling: a distinct role for the jasmonic acid precursor *cis*-(+)-12-oxo-phytodienoic acid (*cis*-OPDA). Front Plant Sci *3*, 42.

Davison, P.A., Hunter, C.N., and Horton, P. (2002). Overexpression of beta-carotene hydroxylase enhances stress tolerance in *Arabidopsis*. Nature *418*, 203-206.

Davletova, S., Schlauch, K., Coutu, J., and Mittler, R. (2005). The zinc-finger protein Zat12 plays a central role in reactive oxygen and abiotic stress signaling in *Arabidopsis*. Plant Physiol *139*, 847-856.

Daxinger, L., Hunter, B., Sheikh, M., Jauvion, V., Gasciolli, V., Vaucheret, H., Matzke, M., and Furner, I. (2008). Unexpected silencing effects from T-DNA tags in *Arabidopsis*. Trends Plant Sci *13*, 4-6.

de Montaigu, A., Tóth, R., and Coupland, G. (2010). Plant development goes like clockwork. Trends Genet *26*, 296-306.

de Pinto, M.C., Locato, V., and De Gara, L. (2012). Redox regulation in plant programmed cell death. Plant Cell Environ *35*, 234-244.

de Pinto, M.C., Paradiso, A., Leonetti, P., and De Gara, L. (2006). Hydrogen peroxide, nitric oxide and cytosolic ascorbate peroxidase at the crossroad between defence and cell death. Plant J *48*, 784-795.

Demmig-Adams, B., and Adams, W.W. (1996). The role of xanthophyll cycle carotenoids in the protection of photosynthesis. Trends Plant Sci *1*, 21-26.

Dervinis, C., Frost, C., Lawrence, S., Novak, N., and Davis, J. (2010). Cytokinin primes plant responses to wounding and reduces insect performance. J Plant Growth Regul *29*, 289-296.

Devadas, S.K., Enyedi, A., and Raina, R. (2002). The *Arabidopsis hrl1* mutation reveals novel overlapping roles for salicylic acid, jasmonic acid and ethylene signalling in cell death and defence against pathogens. Plant J *30*, 467-480.

Devlin, P.F. (2002). Signs of the time: environmental input to the circadian clock. J Exp Bot *53*, 1535-1550.

Devlin, P.F., and Kay, S.A. (2000). Cryptochromes are required for phytochrome signaling to the circadian clock but not for rhythmicity. Plant Cell *12*, 2499-2510.

Devlin, P.F., and Kay, S.A. (2001). Circadian photoperception. Annu Rev Physiol *63*, 677-694.

Devoto, A., Ellis, C., Magusin, A., Chang, H.S., Chilcott, C., Zhu, T., and Turner, J.G. (2005). Expression profiling reveals *COI1* to be a key regulator of genes involved in wound- and methyl jasmonate-induced secondary metabolism, defence, and hormone interactions. Plant Mol Biol *58*, 497-513.

Dhindsa, R.S., Plumb-Dhindsa, P., and Thorpe, T.A. (1981). Leaf senescence: correlated with increased levels of membrane permeability and lipid peroxidation, and decreased levels of superoxide dismutase and catalase. J Exp Bot *32*, 93-101.

Ding, Z., Millar, A.J., Davis, A.M., and Davis, S.J. (2007). *TIME FOR COFFEE* encodes a nuclear regulator in the *Arabidopsis thaliana* circadian clock. Plant Cell *19*, 1522-1536.

Dixon, L.E., Knox, K., Kozma-Bognar, L., Southern, M.M., Pokhilko, A., and Millar, A.J. (2011). Temporal repression of core circadian genes is mediated through EARLY FLOWERING 3 in *Arabidopsis*. Curr Biol *21*, 120-125.

Dodd, A.N., Dalchau, N., Gardner, M.J., Baek, S.J., and Webb, A.A. (2014). The circadian clock has transient plasticity of period and is required for timing of nocturnal processes in *Arabidopsis*. New Phytol *201*, 168-179.

Dodd, A.N., Gardner, M.J., Hotta, C.T., Hubbard, K.E., Dalchau, N., Love, J., Assie, J.M., Robertson, F.C., Jakobsen, M.K., Goncalves, J.*, et al.* (2007). The *Arabidopsis* circadian clock incorporates a cADPR-based feedback loop. Science *318*, 1789-1792.

Dodd, A.N., Salathia, N., Hall, A., Kevei, E., Toth, R., Nagy, F., Hibberd, J.M., Millar, A.J., and Webb, A.A. (2005). Plant circadian clocks increase photosynthesis, growth, survival, and competitive advantage. Science *309*, 630-633.

Dong, M.A., Farré, E.M., and Thomashow, M.F. (2011). CIRCADIAN CLOCK-ASSOCIATED 1 and LATE ELONGATED HYPOCOTYL regulate expression of the C-REPEAT BINDING FACTOR (CBF) pathway in *Arabidopsis*. Proc Natl Acad Sci U S A *108*, 7241-7246.

Dortay, H., Mehnert, N., Bürkle, L., Schmülling, T., and Heyl, A. (2006). Analysis of protein interactions within the cytokinin-signaling pathway of *Arabidopsis thaliana*. FEBS J *273*, 4631-4644.

Dortay, H., Gruhn, N., Pfeifer, A., Schwerdtner, M., Schmülling, T., and Heyl, A. (2008). Toward an interaction map of the two-component signaling pathway of *Arabidopsis thaliana*. J Proteome Res *7*, 3649-3660.

Doyle, M.R., Davis, S.J., Bastow, R.M., McWatters, H.G., Kozma-Bognar, L., Nagy, F., Millar, A.J., and Amasino, R.M. (2002). The *ELF4* gene controls circadian rhythms and flowering time in *Arabidopsis thaliana*. Nature *419*, 74-77.

Duc, C., Cellier, F., Lobréaux, S., Briat, J.F., and Gaymard, F. (2009). Regulation of iron homeostasis in *Arabidopsis thaliana* by the clock regulator time for coffee. J Biol Chem *284*, 36271-36281.

Ducruet, J.M. (2003). Chlorophyll thermoluminescence of leaf discs: simple instruments and progress in signal interpretation open the way to new ecophysiological indicators. J Exp Bot *54*, 2419-2430.

Edelman, M., and Mattoo, A.K. (2008). D1-protein dynamics in photosystem II: the lingering enigma. Photosynth Res *98*, 609-620.

Endo, M., Shimizu, H., Nohales, M.A., Araki, T., and Kay, S.A. (2014). Tissue-specific clocks in *Arabidopsis* show asymmetric coupling. Nature *515*, 419-422.

Eriksson, M.E., Hanano, S., Southern, M.M., Hall, A., and Millar, A.J. (2003). Response regulator homologues have complementary, light-dependent functions in the *Arabidopsis* circadian clock. Planta *218*, 159-162.

Espinoza, C., Bieniawska, Z., Hincha, D.K., and Hannah, M.A. (2008). Interactions between the circadian clock and cold-response in *Arabidopsis*. Plant Signal Behav *3*, 593-594.

Falk, A., Feys, B.J., Frost, L.N., Jones, J.D., Daniels, M.J., and Parker, J.E. (1999). *EDS1*, an essential component of *R* gene-mediated disease resistance in *Arabidopsis* has homology to eukaryotic lipases. Proc Natl Acad Sci U S A *96*, 3292-3297.

Fankhauser, C., and Staiger, D. (2002). Photoreceptors in *Arabidopsis thaliana*: light perception, signal transduction and entrainment of the endogenous clock. Planta *216*, 1-16.

Farré, E.M., Harmer, S.L., Harmon, F.G., Yanovsky, M.J., and Kay, S.A. (2005). Overlapping and distinct roles of *PRR7* and *PRR9* in the *Arabidopsis* circadian clock. Curr Biol *15*, 47-54.

Farré, E.M., and Liu, T. (2013). The PRR family of transcriptional regulators reflects the complexity and evolution of plant circadian clocks. Curr Opin Plant Biol *16*, 621-629.

Farré, E.M., and Weise, S.E. (2012). The interactions between the circadian clock and primary metabolism. Curr Opin Plant Biol *15*, 293-300.

Feys, B., Benedetti, C.E., Penfold, C.N., and Turner, J.G. (1994). *Arabidopsis* mutants selected for resistance to the phytotoxin coronatine are male sterile, insensitive to methyl jasmonate, and resistant to a bacterial pathogen. Plant Cell *6*, 751-759.

Feys, B.J., Moisan, L.J., Newman, M.A., and Parker, J.E. (2001). Direct interaction between the *Arabidopsis* disease resistance signaling proteins, EDS1 and PAD4. EMBO J *20*, 5400-5411.

Filichkin, S.A., Cumbie, J.S., Dharmawadhana, J.P., Jaiswal, P., Chang, J.H., Palusa, S.G., Reddy, A.S., Megraw, M., and Mockler, T.C. (2014). Environmental stresses modulate abundance and timing of alternatively spliced circadian transcripts in *Arabidopsis*. Mol Plant [Epub ahead of print, doi: 10.1093/mp/ssu130]

Filichkin, S.A., and Mockler, T.C. (2012). Unproductive alternative splicing and nonsense mRNAs: a widespread phenomenon among plant circadian clock genes. Biol Direct *7*, 20.

Filichkin, S.A., Priest, H.D., Givan, S.A., Shen, R., Bryant, D.W., Fox, S.E., Wong, W.K., and Mockler, T.C. (2010). Genome-wide mapping of alternative splicing in *Arabidopsis thaliana*. Genome Res *20*, 45-58.

Fischer, B.B., Hideg, E., and Krieger-Liszkay, A. (2013). Production, detection, and signaling of singlet oxygen in photosynthetic organisms. Antioxid Redox Signal *18*, 2145-2162.

Fonseca, S., Chini, A., Hamberg, M., Adie, B., Porzel, A., Kramell, R., Miersch, O., Wasternack, C., and Solano, R. (2009). (+)-7-*iso*-jasmonoyl-L-isoleucine is the endogenous bioactive jasmonate. Nat Chem Biol *5*, 344-350.

Fowler, S., Lee, K., Onouchi, H., Samach, A., Richardson, K., Morris, B., Coupland, G., and Putterill, J. (1999). *GIGANTEA*: a circadian clock-controlled gene that regulates photoperiodic flowering in *Arabidopsis* and encodes a protein with several possible membrane-spanning domains. EMBO J *18*, 4679-4688.

Fowler, S.G., Cook, D., and Thomashow, M.F. (2005). Low temperature induction of *Arabidopsis CBF1*, *2*, and *3* is gated by the circadian clock. Plant Physiol *137*, 961-968.

Foyer, C.H., and Noctor, G. (2005). Redox homeostasis and antioxidant signaling: a metabolic interface between stress perception and physiological responses. Plant Cell *17*, 1866-1875.

Foyer, C.H., and Noctor, G. (2011). Ascorbate and glutathione: the heart of the redox hub. Plant Physiol *155*, 2-18.

Franco-Zorrilla, J.M., Martín, A.C., Leyva, A., and Paz-Ares, J. (2005). Interaction between phosphate-starvation, sugar, and cytokinin signaling in *Arabidopsis* and the roles of cytokinin receptors CRE1/AHK4 and AHK3. Plant Physiol *138*, 847-857.

Fujiwara, S., Wang, L., Han, L., Suh, S.S., Salomé, P.A., McClung, C.R., and Somers, D.E. (2008). Post-translational regulation of the *Arabidopsis* circadian clock through selective proteolysis and phosphorylation of pseudo-response regulator proteins. J Biol Chem *283*, 23073-23083.

Fukushima, A., Kusano, M., Nakamichi, N., Kobayashi, M., Hayashi, N., Sakakibara, H., Mizuno, T., and Saito, K. (2009). Impact of clock-associated *Arabidopsis* pseudo-response regulators in metabolic coordination. Proc Natl Acad Sci U S A *106*, 7251-7256.

Gadjev, I., Stone, J.M., Gechev, T.S., and Kwang, W.J. (2008). Chapter 3: Programmed cell death in plants: new insights into redox regulation and the role of hydrogen peroxide. *In:* International Review of Cell and Molecular Biology (Academic Press), 87-144.

Gadjev, I., Vanderauwera, S., Gechev, T.S., Laloi, C., Minkov, I.N., Shulaev, V., Apel, K., Inzé, D., Mittler, R., and Van Breusegem, F. (2006). Transcriptomic footprints disclose specificity of reactive oxygen species signaling in *Arabidopsis*. Plant Physiol *141*, 436-445.

Galichet, A., Hoyerova, K., Kamínek, M., and Gruissem, W. (2008). Farnesylation directs AtIPT3 subcellular localization and modulates cytokinin biosynthesis in *Arabidopsis*. Plant Physiol *146*, 1155-1164.

Galuszka, P., Popelková, H., Werner, T., Frébortová, J., Pospíšilová, H., Mik, V., Köllmer, I., Schmülling, T., and Frébort, I. (2007). Biochemical characterization of cytokinin oxidases/dehydrogenases from *Arabidopsis thaliana* expressed in *Nicotiana tabacum* L. J Plant Growth Regul *26*, 255-267.

Gan, S., and Amasino, R.M. (1995). Inhibition of leaf senescence by autoregulated production of cytokinin. Science *270*, 1986-1988.

Gardner, K.E., Allis, C.D., and Strahl, B.D. (2011). Operating on chromatin, a colorful language where context matters. J Mol Biol *409*, 36-46.

Gardner, M.J., Hubbard, K.E., Hotta, C.T., Dodd, A.N., and Webb, A.A. (2006). How plants tell the time. Biochem J *397*, 15-24.

Gechev, T., Petrov, V., and Minkov, I. (2010). Reactive oxygen species and programmed cell death. *In:* Reactive oxygen species and antioxidants in higher plants (Science Publishers), 65-78.

Gechev, T.S., Van Breusegem, F., Stone, J.M., Denev, I., and Laloi, C. (2006). Reactive oxygen species as signals that modulate plant stress responses and programmed cell death. Bioessays *28*, 1091-1101.

Gendron, J.M., Pruneda-Paz, J.L., Doherty, C.J., Gross, A.M., Kang, S.E., and Kay, S.A. (2012). *Arabidopsis* circadian clock protein, TOC1, is a DNA-binding transcription factor. Proc Natl Acad Sci U S A *109*, 3167-3172.

Gfeller, A., Dubugnon, L., Liechti, R., and Farmer, E.E. (2010). Jasmonate biochemical pathway. Sci Signal *3*, cm3.

Gill, S.S., and Tuteja, N. (2010). Reactive oxygen species and antioxidant machinery in abiotic stress tolerance in crop plants. Plant Physiol Biochem *48*, 909-930.

Gillespie, K.M., Chae, J.M., and Ainsworth, E.A. (2007). Rapid measurement of total antioxidant capacity in plants. Nat Protoc *2*, 867-870.

Gillette, M.U. [Editor] (2013). Chronobiology: Biological timing in health and disease. Progress in Molecular Biology and Translational Science *119*, 1-356.

Golan, T., Müller-Moulé, P., and Niyogi, K.K. (2006). Photoprotection mutants of *Arabidopsis thaliana* acclimate to high light by increasing photosynthesis and specific antioxidants. Plant Cell Environ *29*, 879-887.

Goodspeed, D., Chehab, E.W., Covington, M.F., and Braam, J. (2013). Circadian control of jasmonates and salicylates: the clock role in plant defense. Plant Signal Behav *8*, e23123.

Goodspeed, D., Chehab, E.W., Min-Venditti, A., Braam, J., and Covington, M.F. (2012). *Arabidopsis* synchronizes jasmonate-mediated defense with insect circadian behavior. Proc Natl Acad Sci U S A *109*, 4674-4677.

Gordon, S.P., Chickarmane, V.S., Ohno, C., and Meyerowitz, E.M. (2009). Multiple feedback loops through cytokinin signaling control stem cell number within the *Arabidopsis* shoot meristem. Proc Natl Acad Sci U S A *106*, 16529-16534.

Gould, P.D., Locke, J.C., Larue, C., Southern, M.M., Davis, S.J., Hanano, S., Moyle, R., Milich, R., Putterill, J., Millar, A.J.*, et al.* (2006). The molecular basis of temperature compensation in the *Arabidopsis* circadian clock. Plant Cell *18*, 1177-1187.

Graf, A., Schlereth, A., Stitt, M., and Smith, A.M. (2010). Circadian control of carbohydrate availability for growth in *Arabidopsis* plants at night. Proc Natl Acad Sci U S A *107*, 9458-9463.

Graf, A., and Smith, A.M. (2011). Starch and the clock: the dark side of plant productivity. Trends Plant Sci *16*, 169-175.

Green, R.M., Tingay, S., Wang, Z.Y., and Tobin, E.M. (2002). Circadian rhythms confer a higher level of fitness to *Arabidopsis* plants. Plant Physiol *129*, 576-584.

Green, R.M., and Tobin, E.M. (1999). Loss of the circadian clock-associated protein 1 in *Arabidopsis* results in altered clock-regulated gene expression. Proc Natl Acad Sci U S A *96*, 4176-4179.

Greenberg, J.T. (1996). Programmed cell death: a way of life for plants. Proc Natl Acad Sci U S A *93*, 12094-12097.

Greenberg, J.T., Silverman, F.P., and Liang, H. (2000). Uncoupling salicylic acid-dependent cell death and defense-related responses from disease resistance in the *Arabidopsis* mutant *acd5*. Genetics *156*, 341-350.

Grennan, A.K., and Ort, D.R. (2007). Cool temperatures interfere with D1 synthesis in tomato by causing ribosomal pausing. Photosynth Res *94*, 375-385.

Ha, S., Vankova, R., Yamaguchi-Shinozaki, K., Shinozaki, K., and Tran, L.S. (2012). Cytokinins: metabolism and function in plant adaptation to environmental stresses. Trends Plant Sci *17*, 172-179.

Hacham, Y., Koussevitzky, S., Kirma, M., and Amir, R. (2014). Glutathione application affects the transcript profile of genes in *Arabidopsis* seedling. J Plant Physiol *171*, 1444-1451.

Hahn, A., Kilian, J., Mohrholz, A., Ladwig, F., Peschke, F., Dautel, R., Harter, K., Berendzen, K.W., and Wanke, D. (2013). Plant core environmental stress response genes are systemically coordinated during abiotic stresses. Int J Mol Sci *14*, 7617-7641.

Hall, A., Bastow, R.M., Davis, S.J., Hanano, S., McWatters, H.G., Hibberd, V., Doyle, M.R., Sung, S., Halliday, K.J., Amasino, R.M.*, et al.* (2003). The *TIME FOR COFFEE* gene maintains the amplitude and timing of *Arabidopsis* circadian clocks. Plant Cell *15*, 2719-2729.

Hall, A., Kozma-Bognár, L., Bastow, R.M., Nagy, F., and Millar, A.J. (2002). Distinct regulation of *CAB* and *PHYB* gene expression by similar circadian clocks. Plant J *32*, 529-537.

Hammond, J.P., and White, P.J. (2011). Sugar signaling in root responses to low phosphorus availability. Plant Physiol *156*, 1033-1040.

Han, Y., Mhamdi, A., Chaouch, S., and Noctor, G. (2013). Regulation of basal and oxidative stress-triggered jasmonic acid-related gene expression by glutathione. Plant Cell Environ *36*, 1135-1146.

Hanano, S., Domagalska, M.A., Nagy, F., and Davis, S.J. (2006). Multiple phytohormones influence distinct parameters of the plant circadian clock. Genes Cells *11*, 1381-1392.

Hara-Nishimura, I., and Hatsugai, N. (2011). The role of vacuole in plant cell death. Cell Death Differ *18*, 1298-1304.

Hara-Nishimura, I., Hatsugai, N., Nakaune, S., Kuroyanagi, M., and Nishimura, M. (2005). Vacuolar processing enzyme: an executor of plant cell death. Curr Opin Plant Biol *8*, 404-408.

Harmer, S.L. (2009). The circadian system in higher plants. Annu Rev Plant Biol *60*, 357-377.

Harmer, S.L., Hogenesch, J.B., Straume, M., Chang, H.S., Han, B., Zhu, T., Wang, X., Kreps, J.A., and Kay, S.A. (2000). Orchestrated transcription of key pathways in *Arabidopsis* by the circadian clock. Science *290*, 2110-2113.

Harmer, S.L., and Kay, S.A. (2005). Positive and negative factors confer phase-specific circadian regulation of transcription in *Arabidopsis*. Plant Cell *17*, 1926-1940.

Havaux, M. (2003). Spontaneous and thermoinduced photon emission: new methods to detect and quantify oxidative stress in plants. Trends Plant Sci *8*, 409-413.

Havaux, M., Eymery, F., Porfirova, S., Rey, P., and Dörmann, P. (2005). Vitamin E protects against photoinhibition and photooxidative stress in *Arabidopsis thaliana*. Plant Cell *17*, 3451-3469.

Havaux, M., Ksas, B., Szewczyk, A., Rumeau, D., Franck, F., Caffarri, S., and Triantaphylidès, C. (2009). Vitamin B6 deficient plants display increased sensitivity to high light and photo-oxidative stress. BMC Plant Biol *9*, 130.

Havaux, M., Triantaphylidès, C., and Genty, B. (2006). Autoluminescence imaging: a non-invasive tool for mapping oxidative stress. Trends Plant Sci *11*, 480-484.

Haydon, M.J., Hearn, T.J., Bell, L.J., Hannah, M.A., and Webb, A.A. (2013a). Metabolic regulation of circadian clocks. Semin Cell Dev Biol *24*, 414-421.

Haydon, M.J., Mielczarek, O., Robertson, F.C., Hubbard, K.E., and Webb, A.A. (2013b). Photosynthetic entrainment of the *Arabidopsis thaliana* circadian clock. Nature *502*, 689-692.

Hazen, S.P., Schultz, T.F., Pruneda-Paz, J.L., Borevitz, J.O., Ecker, J.R., and Kay, S.A. (2005). *LUX ARRHYTHMO* encodes a Myb domain protein essential for circadian rhythms. Proc Natl Acad Sci U S A *102*, 10387-10392.

He, R., Drury, G.E., Rotari, V.I., Gordon, A., Willer, M., Farzaneh, T., Woltering, E.J., and Gallois, P. (2008). Metacaspase-8 modulates programmed cell death induced by ultraviolet light and H_2O_2 in *Arabidopsis*. J Biol Chem *283*, 774-783.

He, Y., Chung, E.H., Hubert, D.A., Tornero, P., and Dangl, J.L. (2012). Specific missense alleles of the *Arabidopsis* jasmonic acid co-receptor COI1 regulate innate immune receptor accumulation and function. PLoS Genet *8*, e1003018.

He, Y., Fukushige, H., Hildebrand, D.F., and Gan, S. (2002). Evidence supporting a role of jasmonic acid in *Arabidopsis* leaf senescence. Plant Physiol *128*, 876-884.

Heath, R.L., and Packer, L. (1968). Photoperoxidation in isolated chloroplasts. I. Kinetics and stoichiometry of fatty acid peroxidation. Arch Biochem Biophys *125*, 189-198.

Heintzen, C., and Liu, Y. (2007). The *Neurospora crassa* circadian clock. Adv Genet *58*, 25-66.

Hejátko, J., Ryu, H., Kim, G.T., Dobešová, R., Choi, S., Choi, S.M., Souček, P., Horák, J., Pekárová, B., Palme, K.*, et al.* (2009). The histidine kinases CYTOKININ-INDEPENDENT1 and ARABIDOPSIS HISTIDINE KINASE2 and 3 regulate vascular tissue development in *Arabidopsis* shoots. Plant Cell *21*, 2008-2021.

Helfer, A., Nusinow, D.A., Chow, B.Y., Gehrke, A.R., Bulyk, M.L., and Kay, S.A. (2011). *LUX ARRHYTHMO* encodes a nighttime repressor of circadian gene expression in the *Arabidopsis* core clock. Curr Biol *21*, 126-133.

Herrero, E., Kolmos, E., Bujdoso, N., Yuan, Y., Wang, M., Berns, M.C., Uhlworm, H., Coupland, G., Saini, R., Jaskolski, M.*, et al.* (2012). EARLY FLOWERING4 recruitment of EARLY FLOWERING3 in the nucleus sustains the *Arabidopsis* circadian clock. Plant Cell *24*, 428-443.

Heyl, A., Ramireddy, E., Brenner, W.G., Riefler, M., Allemeersch, J., and Schmülling, T. (2008). The transcriptional repressor ARR1-SRDX suppresses pleiotropic cytokinin activities in *Arabidopsis*. Plant Physiol *147*, 1380-1395.

Heyl, A., and Schmülling, T. (2003). Cytokinin signal perception and transduction. Curr Opin Plant Biol *6*, 480-488.

Heyl, A., Riefler, M., Romanov, G.A., and Schmülling, T. (2012). Properties, functions and evolution of cytokinin receptors. Eur J Cell Biol *91*, 246-256.

Hicks, K.A., Albertson, T.M., and Wagner, D.R. (2001). *EARLY FLOWERING3* encodes a novel protein that regulates circadian clock function and flowering in *Arabidopsis*. Plant Cell *13*, 1281-1292.

Hicks, K.A., Millar, A.J., Carré, I.A., Somers, D.E., Straume, M., Meeks-Wagner, D.R., and Kay, S.A. (1996). Conditional circadian dysfunction of the *Arabidopsis early-flowering 3* mutant. Science *274*, 790-792.

Higuchi, M., Pischke, M.S., Mähönen, A.P., Miyawaki, K., Hashimoto, Y., Seki, M., Kobayashi, M., Shinozaki, K., Kato, T., Tabata, S.*, et al.* (2004). *In planta* functions of the *Arabidopsis* cytokinin receptor family. Proc Natl Acad Sci U S A *101*, 8821-8826.

Hill, K., Mathews, D.E., Kim, H.J., Street, I.H., Wildes, S.L., Chiang, Y.H., Mason, M.G., Alonso, J.M., Ecker, J.R., Kieber, J.J.*, et al.* (2013). Functional characterization of type-B response regulators in the *Arabidopsis* cytokinin response. Plant Physiol *162*, 212-224.

Hirose, N., Takei, K., Kuroha, T., Kamada-Nobusada, T., Hayashi, H., and Sakakibara, H. (2008). Regulation of cytokinin biosynthesis, compartmentalization and translocation. J Exp Bot *59*, 75-83.

Hong, L.W., Yan, D.W., Liu, W.C., Chen, H.G., and Lu, Y.T. (2013a). TIME FOR COFFEE controls root meristem size by changes in auxin accumulation in Arabidopsis. J Exp Bot *65*, 275-286.

Hong, S., Kim, S.A., Guerinot, M.L., and McClung, C.R. (2013b). Reciprocal interaction of the circadian clock with the iron homeostasis network in *Arabidopsis*. Plant Physiol *161*, 893-903.

Hong, S., Song, H.R., Lutz, K., Kerstetter, R.A., Michael, T.P., and McClung, C.R. (2010). Type II protein arginine methyltransferase 5 (PRMT5) is required for circadian period determination in *Arabidopsis thaliana*. Proc Natl Acad Sci U S A *107*, 21211-21216.

Hotta, C.T., Gardner, M.J., Hubbard, K.E., Baek, S.J., Dalchau, N., Suhita, D., Dodd, A.N., and Webb, A.A. (2007). Modulation of environmental responses of plants by circadian clocks. Plant Cell Environ *30*, 333-349.

Hsu, P.Y., and Harmer, S.L. (2014). Wheels within wheels: the plant circadian system. Trends Plant Sci *19*, 240-249.

Huang, W., Perez-Garcia, P., Pokhilko, A., Millar, A.J., Antoshechkin, I., Riechmann, J.L., and Más, P. (2012). Mapping the core of the *Arabidopsis* circadian clock defines the network structure of the oscillator. Science *336*, 75-79.

Hubbard, K.E., Robertson, F.C., Dalchau, N., and Webb, A.A. (2009). Systems analyses of circadian networks. Mol Biosyst *5*, 1502-1511.

Hwang, I., Chen, H.C., and Sheen, J. (2002). Two-component signal transduction pathways in *Arabidopsis*. Plant Physiol *129*, 500-515.

Hwang, I., and Sheen, J. (2001). Two-component circuitry in *Arabidopsis* cytokinin signal transduction. Nature *413*, 383-389.

Hwang, I., Sheen, J., and Müller, B. (2012). Cytokinin signaling networks. Annu Rev Plant Biol *63*, 353-380.

Ihara-Ohori, Y., Nagano, M., Muto, S., Uchimiya, H., and Kawai-Yamada, M. (2007). Cell death suppressor *Arabidopsis* bax inhibitor-1 is associated with calmodulin binding and ion homeostasis. Plant Physiol *143*, 650-660.

Imaizumi, T. (2010). *Arabidopsis* circadian clock and photoperiodism: time to think about location. Curr Opin Plant Biol *13*, 83-89.

Imaizumi, T., and Kay, S.A. (2006). Photoperiodic control of flowering: not only by coincidence. Trends Plant Sci *11*, 550-558.

Inoue, T., Higuchi, M., Hashimoto, Y., Seki, M., Kobayashi, M., Kato, T., Tabata, S., Shinozaki, K., and Kakimoto, T. (2001). Identification of CRE1 as a cytokinin receptor from *Arabidopsis*. Nature *409*, 1060-1063.

Ishida, K., Yamashino, T., and Mizuno, T. (2008b). Expression of the cytokinin-induced type-A response regulator gene *ARR9* is regulated by the circadian clock in *Arabidopsis thaliana*. Biosci Biotechnol Biochem *72*, 3025-3029.

Ishida, K., Yamashino, T., Yokoyama, A., and Mizuno, T. (2008a). Three type-B response regulators, ARR1, ARR10 and ARR12, play essential but redundant roles in cytokinin signal transduction throughout the life cycle of *Arabidopsis thaliana*. Plant Cell Physiol *49*, 47-57.

Ishiga, Y., Ishiga, T., Uppalapati, S.R., and Mysore, K.S. (2011). Arabidopsis seedling flood-inoculation technique: a rapid and reliable assay for studying plant-bacterial interactions. Plant Methods *7*, 32.

Ishikawa, T., Watanabe, N., Nagano, M., Kawai-Yamada, M., and Lam, E. (2011). Bax inhibitor-1: a highly conserved endoplasmic reticulum-resident cell death suppressor. Cell Death Differ *18*, 1271-1278.

Ito, S., Matsushika, A., Yamada, H., Sato, S., Kato, T., Tabata, S., Yamashino, T., and Mizuno, T. (2003). Characterization of the APRR9 pseudo-response regulator belonging to the APRR1/TOC1 quintet in *Arabidopsis thaliana*. Plant Cell Physiol *44*, 1237-1245.

Ito, S., Nakamichi, N., Nakamura, Y., Niwa, Y., Kato, T., Murakami, M., Kita, M., Mizoguchi, T., Niinuma, K., Yamashino, T.*, et al.* (2007). Genetic linkages between circadian clock-associated components and phytochrome-dependent red light signal transduction in *Arabidopsis thaliana*. Plant Cell Physiol *48*, 971-983.

Jahns, P., and Holzwarth, A.R. (2012). The role of the xanthophyll cycle and of lutein in photoprotection of photosystem II. Biochim Biophys Acta *1817*, 182-193.

James, A.B., Monreal, J.A., Nimmo, G.A., Kelly, C.L., Herzyk, P., Jenkins, G.I., and Nimmo, H.G. (2008). The circadian clock in *Arabidopsis* roots is a simplified slave version of the clock in shoots. Science *322*, 1832-1835.

James, A.B., Syed, N.H., Bordage, S., Marshall, J., Nimmo, G.A., Jenkins, G.I., Herzyk, P., Brown, J.W., and Nimmo, H.G. (2012). Alternative splicing mediates responses of the *Arabidopsis* circadian clock to temperature changes. Plant Cell *24*, 961-981.

Jensen, H. (2013). Molecular characterisation of dominant repressors of the cytokinin deficiency syndrome. Dissertation. Institute of Biology/Applied Genetics Berlin, Freie Universität Berlin.

Jeon, J., and Kim, J. (2013). *Arabidopsis* response regulator1 and *Arabidopsis* histidine phosphotransfer protein2 (AHP2), AHP3, and AHP5 function in cold signaling. Plant Physiol *161*, 408-424.

Jeon, J., Kim, N.Y., Kim, S., Kang, N.Y., Novák, O., Ku, S.J., Cho, C., Lee, D.J., Lee, E.J., Strnad, M.*, et al.* (2010). A subset of cytokinin two-component signaling system plays a role in cold temperature stress response in *Arabidopsis*. J Biol Chem *285*, 23371-23386.

Jibran, R., Hunter, D.A., and Dijkwel, P.P. (2013). Hormonal regulation of leaf senescence through integration of developmental and stress signals. Plant Mol Biol *82*, 547-561.

Jing, H.C., Anderson, L., Sturre, M.J., Hille, J., and Dijkwel, P.P. (2007). *Arabidopsis CPR5* is a senescence-regulatory gene with pleiotropic functions as predicted by the evolutionary theory of senescence. J Exp Bot *58*, 3885-3894.

Jing, H.C., Hebeler, R., Oeljeklaus, S., Sitek, B., Stühler, K., Meyer, H.E., Sturre, M.J., Hille, J., Warscheid, B., and Dijkwel, P.P. (2008). Early leaf senescence is associated with an altered cellular redox balance in *Arabidopsis cpr5*/*old1* mutants. Plant Biol *10 Suppl 1*, 85-98.

Jing, H.C., and Nam, H.G. (2012). Leaf senescence in plants: from model plants to crops, still so many unknowns. J Integr Plant Biol *54*, 514-515.

Jing, H.C., Schippers, J.H., Hille, J., and Dijkwel, P.P. (2005). Ethylene-induced leaf senescence depends on age-related changes and *OLD* genes in *Arabidopsis*. J Exp Bot *56*, 2915-2923.

Jing, H.C., Sturre, M.J., Hille, J., and Dijkwel, P.P. (2002). *Arabidopsis onset of leaf death* mutants identify a regulatory pathway controlling leaf senescence. Plant J *32*, 51-63.

Johnson, C.H., Knight, M.R., Kondo, T., Masson, P., Sedbrook, J., Haley, A., and Trewavas, A. (1995). Circadian oscillations of cytosolic and chloroplastic free calcium in plants. Science *269*, 1863-1865.

Jones, J.D., and Dangl, J.L. (2006). The plant immune system. Nature *444*, 323-329.

Jones, M. (2009). Entrainment of the *Arabidopsis* circadian clock. J Plant Biol *52*, 202-209.

Jouve, L., Gaspar, T., Kevers, C., Greppin, H., and Degli Agosti, R. (1999). Involvement of indole-3-acetic acid in the circadian growth of the first internode of *Arabidopsis*. Planta *209*, 136-142.

Juvany, M., Müller, M., and Munné-Bosch, S. (2013). Photo-oxidative stress in emerging and senescing leaves: a mirror image? J Exp Bot *64*, 3087-3098.

Kaczorowski, K.A. (2004). Mutants in phytochrome-dependent seedling photomorphogenesis and control of the *Arabidopsis* circadian clock (University of California, Berkeley).

Kakimoto, T. (2001). Identification of plant cytokinin biosynthetic enzymes as dimethylallyl diphosphate:ATP/ADP isopentenyltransferases. Plant Cell Physiol *42*, 677-685.

Kang, N.Y., Cho, C., and Kim, J. (2013). Inducible expression of *Arabidopsis* response regulator 22 (ARR22), a type-C ARR, in transgenic *Arabidopsis* enhances drought and freezing tolerance. PLoS One *8*, e79248.

Kant, P., Gordon, M., Kant, S., Zolla, G., Davydov, O., Heimer, Y.M., Chalifa-Caspi, V., Shaked, R., and Barak, S. (2008). Functional-genomics-based identification of genes that regulate *Arabidopsis* responses to multiple abiotic stresses. Plant Cell Environ *31*, 697-714.

Kar, M., and Mishra, D. (1976). Catalase, peroxidase, and polyphenoloxidase activities during rice leaf senescence. Plant Physiol *57*, 315-319.

Karuppanapandian, T., Moon, J.C., Kim, C., Manoharan, K., and Kim, W. (2011). Reactive oxygen species in plants: their generation, signal transduction and scavenging mechanisms. Aust J Crop Sci *5*, 709-725.

Kasahara, H., Takei, K., Ueda, N., Hishiyama, S., Yamaya, T., Kamiya, Y., Yamaguchi, S., and Sakakibara, H. (2004). Distinct isoprenoid origins of *cis*- and *trans*-zeatin biosyntheses in *Arabidopsis*. J Biol Chem *279*, 14049-14054.

Katagiri, F., Thilmony, R., and He, S.Y. (2002). The *Arabidopsis thaliana*-pseudomonas syringae interaction. Arabidopsis Book *1*, e0039.

Kato, Y., and Sakamoto, W. (2009). Protein quality control in chloroplasts: a current model of D1 protein degradation in the photosystem II repair cycle. J Biochem *146*, 463-469.

Katsir, L., Schilmiller, A.L., Staswick, P.E., He, S.Y., and Howe, G.A. (2008). COI1 is a critical component of a receptor for jasmonate and the bacterial virulence factor coronatine. Proc Natl Acad Sci U S A *105*, 7100-7105.

Kawai-Yamada, M., Jin, L., Yoshinaga, K., Hirata, A., and Uchimiya, H. (2001). Mammalian Bax-induced plant cell death can be down-regulated by overexpression of *Arabidopsis Bax Inhibitor-1* (*AtBI-1*). Proc Natl Acad Sci U S A *98*, 12295-12300.

Kawai-Yamada, M., Ohori, Y., and Uchimiya, H. (2004). Dissection of *Arabidopsis* Bax inhibitor-1 suppressing Bax-, hydrogen peroxide-, and salicylic acid-induced cell death. Plant Cell *16*, 21-32.

Kazan, K., and Manners, J.M. (2012). JAZ repressors and the orchestration of phytohormone crosstalk. Trends Plant Sci *17*, 22-31.

Kazan, K., and Manners, J.M. (2013). MYC2: the master in action. Mol Plant *6*, 686-703.

Khan, M., Rozhon, W., and Poppenberger, B. (2014). The role of hormones in the aging of plants - a mini-review. Gerontology *60*, 49-55.

Khanna, R., Kikis, E.A., and Quail, P.H. (2003). *EARLY FLOWERING 4* functions in phytochrome B-regulated seedling de-etiolation. Plant Physiol *133*, 1530-1538.

Khanna-Chopra, R. (2011). Leaf senescence and abiotic stresses share reactive oxygen species-mediated chloroplast degradation. Protoplasma *249*, 469-481.

Kiba, T., Henriques, R., Sakakibara, H., and Chua, N.H. (2007). Targeted degradation of PSEUDO-RESPONSE REGULATOR5 by an SCF^{ZTL} complex regulates clock function and photomorphogenesis in *Arabidopsis thaliana*. Plant Cell *19*, 2516-2530.

Kiba, T., Naitou, T., Koizumi, N., Yamashino, T., Sakakibara, H., and Mizuno, T. (2005). Combinatorial microarray analysis revealing *Arabidopsis* genes implicated in cytokinin responses through the His→Asp phosphorelay circuitry. Plant Cell Physiol *46*, 339-355.

Kiba, T., Yamada, H., Sato, S., Kato, T., Tabata, S., Yamashino, T., and Mizuno, T. (2003). The type-A response regulator, ARR15, acts as a negative regulator in the cytokinin-mediated signal transduction in *Arabidopsis thaliana*. Plant Cell Physiol *44*, 868-874.

Kieber, J.J., and Schaller, G.E. (2014). Cytokinins. Arabidopsis Book *12*, e0168.

Kikis, E.A., Khanna, R., and Quail, P.H. (2005). ELF4 is a phytochrome-regulated component of a negative-feedback loop involving the central oscillator components CCA1 and LHY. Plant J *44*, 300-313.

Kilian, J., Peschke, F., Berendzen, K.W., Harter, K., and Wanke, D. (2012). Prerequisites, performance and profits of transcriptional profiling the abiotic stress response. Biochim Biophys Acta *1819*, 166-175.

Kim, C., and Apel, K. (2013). Singlet oxygen-mediated signaling in plants: moving from *flu* to wild type reveals an increasing complexity. Photosynth Res *116*, 455-464.

Kim, H.J., Chiang, Y.H., Kieber, J.J., and Schaller, G.E. (2013). SCF^{KMD} controls cytokinin signaling by regulating the degradation of type-B response regulators. Proc Natl Acad Sci U S A *110*, 10028-10033.

Kim, H.J., Ryu, H., Hong, S.H., Woo, H.R., Lim, P.O., Lee, I.C., Sheen, J., Nam, H.G., and Hwang, I. (2006). Cytokinin-mediated control of leaf longevity by AHK3 through phosphorylation of ARR2 in *Arabidopsis*. Proc Natl Acad Sci U S A *103*, 814-819.

Kim, J.Y., Song, H.R., Taylor, B.L., and Carré, I.A. (2003). Light-regulated translation mediates gated induction of the *Arabidopsis* clock protein LHY. EMBO J *22*, 935-944.

Kim, K., Ryu, H., Cho, Y.H., Scacchi, E., Sabatini, S., and Hwang, I. (2012). Cytokinin-facilitated proteolysis of ARABIDOPSIS RESPONSE REGULATOR 2 attenuates signaling output in two-component circuitry. Plant J *69*, 934-945.

Kim, W.Y., Fujiwara, S., Suh, S.S., Kim, J., Kim, Y., Han, L., David, K., Putterill, J., Nam, H.G., and Somers, D.E. (2007). ZEITLUPE is a circadian photoreceptor stabilized by GIGANTEA in blue light. Nature *449*, 356-360.

Kircher, S., and Schopfer, P. (2012). Photosynthetic sucrose acts as cotyledon-derived long-distance signal to control root growth during early seedling development in *Arabidopsis*. Proc Natl Acad Sci U S A *109*, 11217-11221.

Knowles, S.M., Lu, S.X., and Tobin, E.M. (2008). Testing time: can ethanol-induced pulses of proposed oscillator components phase shift rhythms in *Arabidopsis*? J Biol Rhythms *23*, 463-471.

Ko, D., Kang, J., Kiba, T., Park, J., Kojima, M., Do, J., Kim, K.Y., Kwon, M., Endler, A., Song, W.Y.*, et al.* (2014). *Arabidopsis* ABCG14 is essential for the root-to-shoot translocation of cytokinin. Proc Natl Acad Sci U S A *111*, 7150-7155.

Kobayashi, Y., and Weigel, D. (2007). Move on up, it's time for change - mobile signals controlling photoperiod-dependent flowering. Genes Dev *21*, 2371-2384.

Köllmer, I., Novák, O., Strnad, M., Schmülling, T., and Werner, T. (2014). Overexpression of the cytosolic cytokinin oxidase/dehydrogenase (CKX7) from *Arabidopsis* causes specific changes in root growth and xylem differentiation. Plant J *78*, 359-371.

Kolmos, E., Nowak, M., Werner, M., Fischer, K., Schwarz, G., Mathews, S., Schoof, H., Nagy, F., Bujnicki, J.M., and Davis, S.J. (2009). Integrating *ELF4* into the circadian system through combined structural and functional studies. HFSP J *3*, 350-366.

Kombrink, E. (2012). Chemical and genetic exploration of jasmonate biosynthesis and signaling paths. Planta *236*, 1351-1366.

Korneli, C., Danisman, S., and Staiger, D. (2014). Differential control of pre-invasive and post-invasive antibacterial defense by the *Arabidopsis* circadian clock. Plant Cell Physiol *55*, 1613-1622.

Kowalska, M., Galuszka, P., Frébortová, J., Šebela, M., Béres, T., Hluska, T., Šmehilová, M., Bilyeu, K.D., and Frébort, I. (2010). Vacuolar and cytosolic cytokinin dehydrogenases of *Arabidopsis thaliana*: heterologous expression, purification and properties. Phytochemistry *71*, 1970-1978.

Kreps, J.A., Wu, Y., Chang, H.S., Zhu, T., Wang, X., and Harper, J.F. (2002). Transcriptome changes for *Arabidopsis* in response to salt, osmotic, and cold stress. Plant Physiol *130*, 2129-2141.

Krieger-Liszkay, A. (2005). Singlet oxygen production in photosynthesis. J Exp Bot *56*, 337-346.

Krieger-Liszkay, A., Fufezan, C., and Trebst, A. (2008). Singlet oxygen production in photosystem II and related protection mechanism. Photosynth Res *98*, 551-564.

Kroemer, G., Galluzzi, L., Vandenabeele, P., Abrams, J., Alnemri, E.S., Baehrecke, E.H., Blagosklonny, M.V., El-Deiry, W.S., Golstein, P., Green, D.R.*, et al.* (2009). Classification of cell death: recommendations of the Nomenclature Committee on Cell Death 2009. Cell Death Differ *16*, 3-11.

Krysan, P.J., Young, J.C., Tax, F., and Sussman, M.R. (1996). Identification of transferred DNA insertions within *Arabidopsis* genes involved in signal transduction and ion transport. Proc Natl Acad Sci U S A *93*, 8145-8150.

Kudo, T., Kiba, T., and Sakakibara, H. (2010). Metabolism and long-distance translocation of cytokinins. J Integr Plant Biol *52*, 53-60.

Kunikowska, A., Byczkowska, A., Doniak, M., and Kaźmierczak, A. (2013). Cytokinins résumé: their signaling and role in programmed cell death in plants. Plant Cell Rep *32*, 771-780.

Kurakawa, T., Ueda, N., Maekawa, M., Kobayashi, K., Kojima, M., Nagato, Y., Sakakibara, H., and Kyozuka, J. (2007). Direct control of shoot meristem activity by a cytokinin-activating enzyme. Nature *445*, 652-655.

Kurepa, J., Smalle, J., Van Montagu, M., and Inzé, D. (1998). Oxidative stress tolerance and longevity in *Arabidopsis*: the late-flowering mutant *gigantea* is tolerant to paraquat. Plant J *14*, 759-764.

Kuroha, T., Tokunaga, H., Kojima, M., Ueda, N., Ishida, T., Nagawa, S., Fukuda, H., Sugimoto, K., and Sakakibara, H. (2009). Functional analyses of LONELY GUY cytokinin-activating enzymes reveal the importance of the direct activation pathway in *Arabidopsis*. Plant Cell *21*, 3152-3169.

Kusnetsov, V., Herrmann, R.G., Kulaeva, O.N., and Oelmüller, R. (1998). Cytokinin stimulates and abscisic acid inhibits greening of etiolated *Lupinus luteus* cotyledons by affecting the expression of the light-sensitive protochlorophyllide oxidoreductase. Mol Gen Genet *259*, 21-28.

Kwak, J.M., Mori, I.C., Pei, Z.M., Leonhardt, N., Torres, M.A., Dangl, J.L., Bloom, R.E., Bodde, S., Jones, J.D., and Schroeder, J.I. (2003). NADPH oxidase *AtrbohD* and *AtrbohF* genes function in ROS-dependent ABA signaling in *Arabidopsis*. EMBO J *22*, 2623-2633.

Lai, A.G., Doherty, C.J., Mueller-Roeber, B., Kay, S.A., Schippers, J.H., and Dijkwel, P.P. (2012). *CIRCADIAN CLOCK-ASSOCIATED 1* regulates ROS homeostasis and oxidative stress responses. Proc Natl Acad Sci U S A *109*, 17129-17134.

Laloi, C., Stachowiak, M., Pers-Kamczyc, E., Warzych, E., Murgia, I., and Apel, K. (2007). Cross-talk between singlet oxygen- and hydrogen peroxide-dependent signaling of stress responses in *Arabidopsis thaliana*. Proc Natl Acad Sci U S A *104*, 672-677.

Laporte, D., Olate, E., Salinas, P., Salazar, M., Jordana, X., and Holuigue, L. (2012). Glutaredoxin GRXS13 plays a key role in protection against photooxidative stress in *Arabidopsis*. J Exp Bot *63*, 503-515.

Lee, D.J., Park, J.Y., Ku, S.J., Ha, Y.M., Kim, S., Kim, M.D., Oh, M.H., and Kim, J. (2007a). Genome-wide expression profiling of *ARABIDOPSIS RESPONSE REGULATOR 7* (*ARR7*) overexpression in cytokinin response. Mol Genet Genomics *277*, 115-137.

Lee, K.P., Kim, C., Landgraf, F., and Apel, K. (2007b). EXECUTER1- and EXECUTER2-dependent transfer of stress-related signals from the plastid to the nucleus of *Arabidopsis thaliana*. Proc Natl Acad Sci U S A *104*, 10270-10275.

Legnaioli, T., Cuevas, J., and Más, P. (2009). TOC1 functions as a molecular switch connecting the circadian clock with plant responses to drought. EMBO J *28*, 3745-3757.

Leibfried, A., To, J.P., Busch, W., Stehling, S., Kehle, A., Demar, M., Kieber, J.J., and Lohmann, J.U. (2005). WUSCHEL controls meristem function by direct regulation of cytokinin-inducible response regulators. Nature *438*, 1172-1175.

Lepistö, A., and Rintamäki, E. (2012). Coordination of plastid and light signaling pathways upon development of *Arabidopsis* leaves under various photoperiods. Mol Plant *5*, 799-816.

Levine, A., Tenhaken, R., Dixon, R., and Lamb, C. (1994). H_2O_2 from the oxidative burst orchestrates the plant hypersensitive disease resistance response. Cell *79*, 583-593.

Li, G., Siddiqui, H., Teng, Y., Lin, R., Wan, X.Y., Li, J., Lau, O.S., Ouyang, X., Dai, M., Wan, J.*, et al.* (2011). Coordinated transcriptional regulation underlying the circadian clock in *Arabidopsis*. Nat Cell Biol *13*, 616-622.

Li, X.P., Müller-Moulé, P., Gilmore, A.M., and Niyogi, K.K. (2002). PsbS-dependent enhancement of feedback de-excitation protects photosystem II from photoinhibition. Proc Natl Acad Sci U S A *99*, 15222-15227.

Li, Z., Ahn, T.K., Avenson, T.J., Ballottari, M., Cruz, J.A., Kramer, D.M., Bassi, R., Fleming, G.R., Keasling, J.D., and Niyogi, K.K. (2009). Lutein accumulation in the absence of zeaxanthin restores nonphotochemical quenching in the *Arabidopsis thaliana npq1* mutant. Plant Cell *21*, 1798-1812.

Lichtenthaler, H.K., and Burkart, S. (1999). Photosynthesis and high light stress. Bulg J Plant Physiol *25*, 3-16.

Lim, P.O., Kim, H.J., and Nam, H.G. (2007). Leaf senescence. Annu Rev Plant Biol *58*, 115-136.

Lin, C. (2002). Blue light receptors and signal transduction. Plant Cell *14 Suppl*, S207-225.

Liu, X.L., Covington, M.F., Fankhauser, C., Chory, J., and Wagner, D.R. (2001). *ELF3* encodes a circadian clock-regulated nuclear protein that functions in an *Arabidopsis* PHYB signal transduction pathway. Plant Cell *13*, 1293-1304.

Lochmanová, G., Zdráhal, Z., Konečná, H., Koukalová, S., Malbeck, J., Souček, P., Válková, M., Kiran, N.S., and Brzobohatý, B. (2008). Cytokinin-induced photomorphogenesis in dark-grown *Arabidopsis*: a proteomic analysis. J Exp Bot *59*, 3705-3719.

Locke, J.C., Southern, M.M., Kozma-Bognar, L., Hibberd, V., Brown, P.E., Turner, M.S., and Millar, A.J. (2005). Extension of a genetic network model by iterative experimentation and mathematical analysis. Mol Syst Biol *1*, 2005 0013.

Lomin, S.N., Krivosheev, D.M., Steklov, M.Y., Osolodkin, D.I., and Romanov, G.A. (2012). Receptor properties and features of cytokinin signaling. Acta Naturae *4*, 31-45.

Lord, C.E., and Gunawardena, A.H. (2012). Programmed cell death in *C. elegans*, mammals and plants. Eur J Cell Biol *91*, 603-613.

Lorenzo, O., Chico, J.M., Sánchez-Serrano, J.J., and Solano, R. (2004). *JASMONATE-INSENSITIVE1* encodes a MYC transcription factor essential to discriminate between different jasmonate-regulated defense responses in *Arabidopsis*. Plant Cell *16*, 1938-1950.

Lorenzo, O., Piqueras, R., Sánchez-Serrano, J.J., and Solano, R. (2003). ETHYLENE RESPONSE FACTOR1 integrates signals from ethylene and jasmonate pathways in plant defense. Plant Cell *15*, 165-178.

Lorenzo, O., and Solano, R. (2005). Molecular players regulating the jasmonate signalling network. Curr Opin Plant Biol *8*, 532-540.

Lorrain, S., Vailleau, F., Balagué, C., and Roby, D. (2003). Lesion mimic mutants: keys for deciphering cell death and defense pathways in plants? Trends Plant Sci *8*, 263-271.

Love, A.J., Milner, J.J., and Sadanandom, A. (2008). Timing is everything: regulatory overlap in plant cell death. Trends Plant Sci *13*, 589-595.

Love, J., Dodd, A.N., and Webb, A.A. (2004). Circadian and diurnal calcium oscillations encode photoperiodic information in *Arabidopsis*. Plant Cell *16*, 956-966.

Lowry, O.H., Rosebrough, N.J., Farr, A.L., and Randall, R.J. (1951). Protein measurement with the Folin phenol reagent. J Biol Chem *193*, 265-275.

Lu, S.X., Knowles, S.M., Andronis, C., Ong, M.S., and Tobin, E.M. (2009). CIRCADIAN CLOCK ASSOCIATED1 and LATE ELONGATED HYPOCOTYL function synergistically in the circadian clock of *Arabidopsis*. Plant Physiol *150*, 834-843.

Lu, S.X., Webb, C.J., Knowles, S.M., Kim, S.H., Wang, Z., and Tobin, E.M. (2012). CCA1 and ELF3 Interact in the control of hypocotyl length and flowering time in *Arabidopsis*. Plant Physiol *158*, 1079-1088.

Lu, Y., Gehan, J.P., and Sharkey, T.D. (2005). Daylength and circadian effects on starch degradation and maltose metabolism. Plant Physiol *138*, 2280-2291.

Lundquist, P.K., Poliakov, A., Bhuiyan, N.H., Zybailov, B., Sun, Q., and van Wijk, K.J. (2012). The functional network of the *Arabidopsis* plastoglobule proteome based on quantitative proteomics and genome-wide coexpression analysis. Plant Physiol *158*, 1172-1192.

Macková, H., Hronková, M., Dobrá, J., Turečková, V., Novák, O., Lubovská, Z., Motyka, V., Haisel, D., Hájek, T., Prášil, I.T*., et al.* (2013). Enhanced drought and heat stress tolerance of tobacco plants with ectopically enhanced cytokinin oxidase/dehydrogenase gene expression. J Exp Bot *64*, 2805-2815.

Mähönen, A.P., Bonke, M., Kauppinen, L., Riikonen, M., Benfey, P.N., and Helariutta, Y. (2000). A novel two-component hybrid molecule regulates vascular morphogenesis of the *Arabidopsis* root. Genes Dev *14*, 2938-2943.

Mähönen, A.P., Bishopp, A., Higuchi, M., Nieminen, K.M., Kinoshita, K., Tormakangas, K., Ikeda, Y., Oka, A., Kakimoto, T., and Helariutta, Y. (2006). Cytokinin signaling and its inhibitor AHP6 regulate cell fate during vascular development. Science *311*, 94-98.

Makino, S., Matsushika, A., Kojima, M., Yamashino, T., and Mizuno, T. (2002). The APRR1/TOC1 quintet implicated in circadian rhythms of *Arabidopsis thaliana*: I. Characterization with APRR1-overexpressing plants. Plant Cell Physiol *43*, 58-69.

Martí, M.C., Stancombe, M.A., and Webb, A.A. (2013). Cell- and stimulus type-specific intracellular free Ca^{2+} signals in *Arabidopsis*. Plant Physiol *163*, 625-634.

Maruta, T., Inoue, T., Tamoi, M., Yabuta, Y., Yoshimura, K., Ishikawa, T., and Shigeoka, S. (2011). *Arabidopsis* NADPH oxidases, AtrbohD and AtrbohF, are essential for jasmonic acid-induced expression of genes regulated by MYC2 transcription factor. Plant Sci *180*, 655-660.

Más, P., Alabadí, D., Yanovsky, M.J., Oyama, T., and Kay, S.A. (2003a). Dual role of TOC1 in the control of circadian and photomorphogenic responses in *Arabidopsis*. Plant Cell *15*, 223-236.

Más, P., Kim, W.Y., Somers, D.E., and Kay, S.A. (2003b). Targeted degradation of TOC1 by ZTL modulates circadian function in *Arabidopsis thaliana*. Nature *426*, 567-570.

Más, P., and Yanovsky, M.J. (2009). Time for circadian rhythms: plants get synchronized. Curr Opin Plant Biol *12*, 574-579.

Mason, M.G., Li, J., Mathews, D.E., Kieber, J.J., and Schaller, G.E. (2004). Type-B response regulators display overlapping expression patterns in *Arabidopsis*. Plant Physiol *135*, 927-937.

Mason, M.G., Mathews, D.E., Argyros, D.A., Maxwell, B.B., Kieber, J.J., Alonso, J.M., Ecker, J.R., and Schaller, G.E. (2005). Multiple type-B response regulators mediate cytokinin signal transduction in *Arabidopsis*. Plant Cell *17*, 3007-3018.

Mason, M.G., Jha, D., Salt, D.E., Tester, M., Hill, K., Kieber, J.J., and Schaller, G.E. (2010). Type-B response regulators ARR1 and ARR12 regulate expression of *AtHKT1;1* and accumulation of sodium in *Arabidopsis* shoots. Plant J *64*, 753-763.

Matsumoto-Kitano, M., Kusumoto, T., Tarkowski, P., Kinoshita-Tsujimura, K., Václavíková, K., Miyawaki, K., and Kakimoto, T. (2008). Cytokinins are central regulators of cambial activity. Proc Natl Acad Sci U S A *105*, 20027-20031.

Matsushika, A., Makino, S., Kojima, M., and Mizuno, T. (2000). Circadian waves of expression of the APRR1/TOC1 family of pseudo-response regulators in *Arabidopsis thaliana*: insight into the plant circadian clock. Plant Cell Physiol *41*, 1002-1012.

Matsushika, A., Makino, S., Kojima, M., Yamashino, T., and Mizuno, T. (2002). The APRR1/TOC1 quintet implicated in circadian rhythms of *Arabidopsis thaliana*: II. Characterization with *CCA1*-overexpressing plants. Plant Cell Physiol *43*, 118-122.

Matyash, V., Liebisch, G., Kurzchalia, T.V., Shevchenko, A., and Schwudke, D. (2008). Lipid extraction by methyl-*tert*-butyl ether for high-throughput lipidomics. J Lipid Res *49*, 1137-1146.

McClung, C.R. (2006). Plant circadian rhythms. Plant Cell *18*, 792-803.

McClung, C.R. (2011). The genetics of plant clocks. Adv Genet *74*, 105-139.

McClung, C.R. (2014). Wheels within wheels: new transcriptional feedback loops in the *Arabidopsis* circadian clock. F1000Prime Rep *6*, 2.

McClung, C.R., and Davis, S.J. (2010). Ambient thermometers in plants: from physiological outputs towards mechanisms of thermal sensing. Curr Biol *20*, R1086-1092.

McGaw, B.A., and Horgan, R. (1983). Cytokinin catabolism and cytokinin oxidase. Phytochemistry *22*, 1103-1105.

McWatters, H.G., Bastow, R.M., Hall, A., and Millar, A.J. (2000). The *ELF3 zeitnehmer* regulates light signalling to the circadian clock. Nature *408*, 716-720.

McWatters, H.G., and Devlin, P.F. (2011). Timing in plants – a rhythmic arrangement. FEBS Lett *585*, 1474-1484.

McWatters, H.G., Kolmos, E., Hall, A., Doyle, M.R., Amasino, R.M., Gyula, P., Nagy, F., Millar, A.J., and Davis, S.J. (2007). *ELF4* is required for oscillatory properties of the circadian clock. Plant Physiol *144*, 391-401.

Meskauskiene, R., Nater, M., Goslings, D., Kessler, F., op den Camp, R., and Apel, K. (2001). FLU: a negative regulator of chlorophyll biosynthesis in *Arabidopsis thaliana*. Proc Natl Acad Sci U S A *98*, 12826-12831.

Mhamdi, A., Queval, G., Chaouch, S., Vanderauwera, S., Van Breusegem, F., and Noctor, G. (2010). Catalase function in plants: a focus on *Arabidopsis* mutants as stress-mimic models. J Exp Bot *61*, 4197-4220.

Michael, T.P., Breton, G., Hazen, S.P., Priest, H., Mockler, T.C., Kay, S.A., and Chory, J. (2008a). A morning-specific phytohormone gene expression program underlying rhythmic plant growth. PLoS Biol *6*, e225.

Michael, T.P., and McClung, C.R. (2003). Enhancer trapping reveals widespread circadian clock transcriptional control in *Arabidopsis*. Plant Physiol *132*, 629-639.

Michael, T.P., Mockler, T.C., Breton, G., McEntee, C., Byer, A., Trout, J.D., Hazen, S.P., Shen, R., Priest, H.D., Sullivan, C.M.*, et al.* (2008b). Network discovery pipeline elucidates conserved time-of-day-specific cis-regulatory modules. PLoS Genet *4*, e14.

Michael, T.P., Salomé, P.A., Yu, H.J., Spencer, T.R., Sharp, E.L., McPeek, M.A., Alonso, J.M., Ecker, J.R., and McClung, C.R. (2003a). Enhanced fitness conferred by naturally occurring variation in the circadian clock. Science *302*, 1049-1053.

Michael, T.P., Salomé, P.A., and McClung, C.R. (2003b). Two *Arabidopsis* circadian oscillators can be distinguished by differential temperature sensitivity. Proc Natl Acad Sci U S A *100*, 6878-6883.

Millar, A.J. (2004). Input signals to the plant circadian clock. J Exp Bot *55*, 277-283.

Millar, A.J., Carré, I.A., Strayer, C.A., Chua, N.H., and Kay, S.A. (1995a). Circadian clock mutants in *Arabidopsis* identified by luciferase imaging. Science *267*, 1161-1163.

Millar, A.J., and Kay, S.A. (1991). Circadian Control of *cab* Gene Transcription and mRNA Accumulation in *Arabidopsis*. Plant Cell *3*, 541-550.

Millar, A.J., Straume, M., Chory, J., Chua, N.H., and Kay, S.A. (1995b). The regulation of circadian period by phototransduction pathways in *Arabidopsis*. Science *267*, 1163-1166.

Miller, G., Schlauch, K., Tam, R., Cortes, D., Torres, M.A., Shulaev, V., Dangl, J.L., and Mittler, R. (2009). The plant NADPH oxidase RBOHD mediates rapid systemic signaling in response to diverse stimuli. Sci Signal *2*, ra45.

Miller, G., Shulaev, V., and Mittler, R. (2008). Reactive oxygen signaling and abiotic stress. Physiol Plant *133*, 481-489.

Mittler, R., Vanderauwera, S., Gollery, M., and Van Breusegem, F. (2004). Reactive oxygen gene network of plants. Trends Plant Sci *9*, 490-498.

Mittler, R., Vanderauwera, S., Suzuki, N., Miller, G., Tognetti, V.B., Vandepoele, K., Gollery, M., Shulaev, V., and Van Breusegem, F. (2011). ROS signaling: the new wave? Trends Plant Sci *16*, 300-309.

Miyawaki, K., Matsumoto-Kitano, M., and Kakimoto, T. (2004). Expression of cytokinin biosynthetic isopentenyltransferase genes in *Arabidopsis*: tissue specificity and regulation by auxin, cytokinin, and nitrate. Plant J *37*, 128-138.

Miyawaki, K., Tarkowski, P., Matsumoto-Kitano, M., Kato, T., Sato, S., Tarkowska, D., Tabata, S., Sandberg, G., and Kakimoto, T. (2006). Roles of *Arabidopsis* ATP/ADP isopentenyltransferases and tRNA isopentenyltransferases in cytokinin biosynthesis. Proc Natl Acad Sci U S A *103*, 16598-16603.

Mizoguchi, T., Wheatley, K., Hanzawa, Y., Wright, L., Mizoguchi, M., Song, H.R., Carré, I.A., and Coupland, G. (2002). *LHY* and *CCA1* are partially redundant genes required to maintain circadian rhythms in *Arabidopsis*. Dev Cell *2*, 629-641.

Mizuno, T., and Yamashino, T. (2008). Comparative transcriptome of diurnally oscillating genes and hormone-responsive genes in *Arabidopsis thaliana*: insight into circadian clock-controlled daily responses to common ambient stresses in plants. Plant Cell Physiol *49*, 481-487.

Mizuno, T., Nomoto, Y., Oka, H., Kitayama, M., Takeuchi, A., Tsubouchi, M., and Yamashino, T. (2014). Ambient temperature signal feeds into the circadian clock transcriptional circuitry through the EC night-time repressor in *Arabidopsis thaliana*. Plant Cell Physiol *55*, 958-976.

Mockler, T.C., Michael, T.P., Priest, H.D., Shen, R., Sullivan, C.M., Givan, S.A., McEntee, C., Kay, S.A., and Chory, J. (2007). The DIURNAL project: DIURNAL and circadian expression profiling, model-based pattern matching, and promoter analysis. Cold Spring Harb Symp Quant Biol *72*, 353-363.

Mohanty, P., Allakhverdiev, S.I., and Murata, N. (2007). Application of low temperatures during photoinhibition allows characterization of individual steps in photodamage and the repair of photosystem II. Photosynth Res *94*, 217-224.

Mohawk, J.A., Green, C.B., and Takahashi, J.S. (2012). Central and peripheral circadian clocks in mammals. Annu Rev Neurosci *35*, 445-462.

Mok, D.W., and Mok, M.C. (2001). Cytokinin Metabolism and Action. Annu Rev Plant Physiol Plant Mol Biol *52*, 89-118.

Mok, M.C. (1994). Cytokinins and plant development - an overview. *In:* Mok, DWS, Mok, MC (eds), Cytokinins: chemistry, activity, and function. CRC Press, 155-166.

Montillet, J.L., Cacas, J.L., Garnier, L., Montané, M.H., Douki, T., Bessoule, J.J., Polkowska-Kowalczyk, L., Maciejewska, U., Agnel, J.P., Vial, A.*, et al.* (2004). The upstream oxylipin profile of *Arabidopsis thaliana*: a tool to scan for oxidative stresses. Plant J *40*, 439-451.

Mori, I.C., and Schroeder, J.I. (2004). Reactive oxygen species activation of plant Ca^{2+} channels. A signaling mechanism in polar growth, hormone transduction, stress signaling, and hypothetically mechanotransduction. Plant Physiol *135*, 702-708.

Mueller, S., Hilbert, B., Dueckershoff, K., Roitsch, T., Krischke, M., Mueller, M.J., and Berger, S. (2008). General detoxification and stress responses are mediated by oxidized lipids through TGA transcription factors in *Arabidopsis*. Plant Cell *20*, 768-785.

Müller, B. (2011). Generic signal-specific responses: cytokinin and context-dependent cellular responses. J Exp Bot *62*, 3273-3288.

Müller, B., and Sheen, J. (2008). Cytokinin and auxin interaction in root stem-cell specification during early embryogenesis. Nature *453*, 1094-1097.

Mulo, P., Sakurai, I., and Aro, E.M. (2012). Strategies for *psbA* gene expression in cyanobacteria, green algae and higher plants: from transcription to PSII repair. Biochim Biophys Acta *1817*, 247-257.

Munné-Bosch, S., Queval, G., and Foyer, C.H. (2013). The impact of global change factors on redox signaling underpinning stress tolerance. Plant Physiol *161*, 5-19.

Murakami, M., Yamashino, T., and Mizuno, T. (2004). Characterization of circadian-associated APRR3 pseudo-response regulator belonging to the APRR1/TOC1 quintet in *Arabidopsis thaliana*. Plant Cell Physiol *45*, 645-650.

Murashige, T., and Skoog, F. (1962). A revised medium for rapid growth and bio assays with tobacco tissue cultures. Physiol Plant *15*, 473-497.

Murata, N., Allakhverdiev, S.I., and Nishiyama, Y. (2012). The mechanism of photoinhibition *in vivo*: re-evaluation of the roles of catalase, α-tocopherol, non-photochemical quenching, and electron transport. Biochim Biophys Acta *1817*, 1127-1133.

Murata, N., Takahashi, S., Nishiyama, Y., and Allakhverdiev, S.I. (2007). Photoinhibition of photosystem II under environmental stress. Biochim Biophys Acta *1767*, 414-421.

Murgia, I., Vazzola, V., Tarantino, D., Cellier, F., Ravet, K., Briat, J.F., and Soave, C. (2007). Knock-out of ferritin *AtFer1* causes earlier onset of age-dependent leaf senescence in *Arabidopsis*. Plant Physiol Biochem *45*, 898-907.

Murshed, R., Lopez-Lauri, F.I., and Sallanon, H. (2008). Microplate quantification of enzymes of the plant ascorbate-glutathione cycle. Anal Biochem *383*, 320-322.

Nagel, D.H., and Kay, S.A. (2012). Complexity in the wiring and regulation of plant circadian networks. Curr Biol *22*, R648-657.

Nagy, F., and Schäfer, E. (2002). Phytochromes control photomorphogenesis by differentially regulated, interacting signaling pathways in higher plants. Annu Rev Plant Biol *53*, 329-355.

Naik, G.R., Mukherjee, I., and Reid, D.M. (2002). Influence of cytokinins on the methyl jasmonate-promoted senescence in *Helianthus annuus* cotyledons. Plant Growth Regul *38*, 61-68.

Nakamichi, N., Kiba, T., Henriques, R., Mizuno, T., Chua, N.H., and Sakakibara, H. (2010). PSEUDO-RESPONSE REGULATORS 9, 7, and 5 are transcriptional repressors in the *Arabidopsis* circadian clock. Plant Cell *22*, 594-605.

Nakamichi, N., Kiba, T., Kamioka, M., Suzuki, T., Yamashino, T., Higashiyama, T., Sakakibara, H., and Mizuno, T. (2012). Transcriptional repressor PRR5 directly regulates clock-output pathways. Proc Natl Acad Sci U S A *109*, 17123-17128.

Nakamichi, N., Kita, M., Ito, S., Sato, E., Yamashino, T., and Mizuno, T. (2005a). The *Arabidopsis* pseudo-response regulators, PRR5 and PRR7, coordinately play essential roles for circadian clock function. Plant Cell Physiol *46*, 609-619.

Nakamichi, N., Kita, M., Ito, S., Yamashino, T., and Mizuno, T. (2005b). PSEUDO-RESPONSE REGULATORS, PRR9, PRR7 and PRR5, together play essential roles close to the circadian clock of *Arabidopsis thaliana*. Plant Cell Physiol *46*, 686-698.

Nakamichi, N., Kusano, M., Fukushima, A., Kita, M., Ito, S., Yamashino, T., Saito, K., Sakakibara, H., and Mizuno, T. (2009). Transcript profiling of an *Arabidopsis PSEUDO RESPONSE REGULATOR* arrhythmic triple mutant reveals a role for the circadian clock in cold stress response. Plant Cell Physiol *50*, 447-462.

Naseem, M., Kaltdorf, M., Hussain, A., and Dandekar, T. (2013). The impact of cytokinin on jasmonate-salicylate antagonism in *Arabidopsis* immunity against infection with *Pst* DC3000. Plant Signal Behav *8*, e26791.

Navabpour, S., Morris, K., Allen, R., Harrison, E., S, A.H.-M., and Buchanan-Wollaston, V. (2003). Expression of senescence-enhanced genes in response to oxidative stress. J Exp Bot *54*, 2285-2292.

Ni, Z., Kim, E.D., Ha, M., Lackey, E., Liu, J., Zhang, Y., Sun, Q., and Chen, Z.J. (2009). Altered circadian rhythms regulate growth vigour in hybrids and allopolyploids. Nature *457*, 327-331.

Niemann, M. (2013). Molekulare Charakterisierung des *ROCK1* Gens von *Arabidopsis thaliana*. Dissertation. Institute of Biology/Applied Genetics Berlin, Freie Universität Berlin.

Nishimura, C., Ohashi, Y., Sato, S., Kato, T., Tabata, S., and Ueguchi, C. (2004). Histidine kinase homologs that act as cytokinin receptors possess overlapping functions in the regulation of shoot and root growth in *Arabidopsis*. Plant Cell *16*, 1365-1377.

Nishiyama, R., Watanabe, Y., Fujita, Y., Le, D.T., Kojima, M., Werner, T., Vankova, R., Yamaguchi-Shinozaki, K., Shinozaki, K., Kakimoto, T.*, et al.* (2011a). Analysis of cytokinin mutants and regulation of cytokinin metabolic genes reveals important regulatory roles of cytokinins in drought, salt and abscisic acid responses, and abscisic acid biosynthesis. Plant Cell *23*, 2169-2183.

Nishiyama, R., Watanabe, Y., Leyva-Gonzalez, M.A., Ha, C.V., Fujita, Y., Tanaka, M., Seki, M., Yamaguchi-Shinozaki, K., Shinozaki, K., Herrera-Estrella, L.*, et al.* (2013). *Arabidopsis* AHP2, AHP3, and AHP5 histidine phosphotransfer proteins function as redundant negative regulators of drought stress response. Proc Natl Acad Sci U S A *110*, 4840-4845.

Nishiyama, Y., Allakhverdiev, S.I., and Murata, N. (2006). A new paradigm for the action of reactive oxygen species in the photoinhibition of photosystem II. Biochim Biophys Acta *1757*, 742-749.

Nishiyama, Y., Allakhverdiev, S.I., and Murata, N. (2011b). Protein synthesis is the primary target of reactive oxygen species in the photoinhibition of photosystem II. Physiol Plant *142*, 35-46.

Nishiyama, Y., Yamamoto, H., Allakhverdiev, S.I., Inaba, M., Yokota, A., and Murata, N. (2001). Oxidative stress inhibits the repair of photodamage to the photosynthetic machinery. EMBO J *20*, 5587-5594.

Niwa, Y., Ito, S., Nakamichi, N., Mizoguchi, T., Niinuma, K., Yamashino, T., and Mizuno, T. (2007). Genetic linkages of the circadian clock-associated genes, *TOC1*, *CCA1* and *LHY*, in the photoperiodic control of flowering time in *Arabidopsis thaliana*. Plant Cell Physiol *48*, 925-937.

Niyogi, K.K., Grossman, A.R., and Björkman, O. (1998). *Arabidopsis* mutants define a central role for the xanthophyll cycle in the regulation of photosynthetic energy conversion. Plant Cell *10*, 1121-1134.

Nomoto, Y., Kubozono, S., Yamashino, T., Nakamichi, N., and Mizuno, T. (2012). Circadian clock- and PIF4-controlled plant growth: a coincidence mechanism directly integrates a hormone signaling network into the photoperiodic control of plant architectures in *Arabidopsis thaliana*. Plant Cell Physiol *53*, 1950-1964.

Noordally, Z.B., Ishii, K., Atkins, K.A., Wetherill, S.J., Kusakina, J., Walton, E.J., Kato, M., Azuma, M., Tanaka, K., Hanaoka, M.*, et al.* (2013). Circadian control of chloroplast transcription by a nuclear-encoded timing signal. Science *339*, 1316-1319.

Nováková, M., Motyka, V., Dobrev, P.I., Malbeck, J., Gaudinová, A., and Vanková, R. (2005). Diurnal variation of cytokinin, auxin and abscisic acid levels in tobacco leaves. J Exp Bot *56*, 2877-2883.

Nusinow, D.A., Helfer, A., Hamilton, E.E., King, J.J., Imaizumi, T., Schultz, T.F., Farré, E.M., and Kay, S.A. (2011). The ELF4-ELF3-LUX complex links the circadian clock to diurnal control of hypocotyl growth. Nature *475*, 398-402.

O'Brien, J.A., and Benková, E. (2013). Cytokinin cross-talking during biotic and abiotic stress responses. Front Plant Sci *4*, 451.

Ochsenbein, C., Przybyla, D., Danon, A., Landgraf, F., Göbel, C., Imboden, A., Feussner, I., and Apel, K. (2006). The role of *EDS1* (enhanced disease susceptibility) during singlet oxygen-mediated stress responses of *Arabidopsis*. Plant J *47*, 445-456.

Onai, K., and Ishiura, M. (2005). *PHYTOCLOCK 1* encoding a novel GARP protein essential for the *Arabidopsis* circadian clock. Genes Cells *10*, 963-972.

op den Camp, R.G., Przybyla, D., Ochsenbein, C., Laloi, C., Kim, C., Danon, A., Wagner, D., Hideg, E., Göbel, C., Feussner, I.*, et al.* (2003). Rapid induction of distinct stress responses after the release of singlet oxygen in *Arabidopsis*. Plant Cell *15*, 2320-2332.

Overmyer, K., Brosché, M., and Kangasjärvi, J. (2003). Reactive oxygen species and hormonal control of cell death. Trends Plant Sci *8*, 335-342.

Overmyer, K., Brosché, M., Pellinen, R., Kuittinen, T., Tuominen, H., Ahlfors, R., Keinänen, M., Saarma, M., Scheel, D., and Kangasjärvi, J. (2005). Ozone-induced programmed cell death in the *Arabidopsis radical-induced cell death1* mutant. Plant Physiol *137*, 1092-1104.

Overmyer, K., Tuominen, H., Kettunen, R., Betz, C., Langebartels, C., Sandermann, H., Jr., and Kangasjärvi, J. (2000). Ozone-sensitive *Arabidopsis rcd1* mutant reveals opposite roles for ethylene and jasmonate signaling pathways in regulating superoxide-dependent cell death. Plant Cell *12*, 1849-1862.

Para, A., Farré, E.M., Imaizumi, T., Pruneda-Paz, J.L., Harmon, F.G., and Kay, S.A. (2007). PRR3 is a vascular regulator of TOC1 stability in the *Arabidopsis* circadian clock. Plant Cell *19*, 3462-3473.

Park, S.W., Li, W., Viehhauser, A., He, B., Kim, S., Nilsson, A.K., Andersson, M.X., Kittle, J.D., Ambavaram, M.M., Luan, S.*, et al.* (2013). Cyclophilin 20-3 relays a 12-oxo-phytodienoic acid signal during stress responsive regulation of cellular redox homeostasis. Proc Natl Acad Sci U S A *110*, 9559-9564.

Parthier, B. (1979). The role of phytohormones (cytokinin) in chloroplasts development. Biochem Physiol Pfl *174*, 173-214.

Perales, M., and Más, P. (2007). A functional link between rhythmic changes in chromatin structure and the *Arabidopsis* biological clock. Plant Cell *19*, 2111-2123.

Pérez, A.C., and Goossens, A. (2013). Jasmonate signalling: a copycat of auxin signalling? Plant Cell Environ *36*, 2071-2084.

Pieterse, C.M., Van der Does, D., Zamioudis, C., Leon-Reyes, A., and Van Wees, S.C. (2012). Hormonal modulation of plant immunity. Annu Rev Cell Dev Biol *28*, 489-521.

Pokhilko, A., Fernandez, A.P., Edwards, K.D., Southern, M.M., Halliday, K.J., and Millar, A.J. (2012). The clock gene circuit in *Arabidopsis* includes a repressilator with additional feedback loops. Mol Syst Biol *8*, 574.

Pokhilko, A., Hodge, S.K., Stratford, K., Knox, K., Edwards, K.D., Thomson, A.W., Mizuno, T., and Millar, A.J. (2010). Data assimilation constrains new connections and components in a complex, eukaryotic circadian clock model. Mol Syst Biol *6*, 416.

Potters, G., Horemans, N., Bellone, S., Caubergs, R.J., Trost, P., Guisez, Y., and Asard, H. (2004). Dehydroascorbate influences the plant cell cycle through a glutathione-independent reduction mechanism. Plant Physiol *134*, 1479-1487.

Procházková, D., Haisel, D., and Wilhelmová, N. (2008). Antioxidant protection during ageing and senescence in chloroplasts of tobacco with modulated life span. Cell Biochem Funct *26*, 582-590.

Pruneda-Paz, J.L., Breton, G., Para, A., and Kay, S.A. (2009). A functional genomics approach reveals CHE as a component of the *Arabidopsis* circadian clock. Science *323*, 1481-1485.

Pruneda-Paz, J.L., and Kay, S.A. (2010). An expanding universe of circadian networks in higher plants. Trends Plant Sci *15*, 259-265.

Quail, P.H. (2002). Phytochrome photosensory signalling networks. Nat Rev Mol Cell Biol *3*, 85-93.

Queval, G., Issakidis-Bourguet, E., Hoeberichts, F.A., Vandorpe, M., Gakière, B., Vanacker, H., Miginiac-Maslow, M., Van Breusegem, F., and Noctor, G. (2007). Conditional oxidative stress responses in the *Arabidopsis* photorespiratory mutant *cat2* demonstrate that redox state is a key modulator of daylength-dependent gene expression, and define photoperiod as a crucial factor in the regulation of H_2O_2-induced cell death. Plant J *52*, 640-657.

Queval, G., Neukermans, J., Vanderauwera, S., Van Breusegem, F., and Noctor, G. (2011). Day length is a key regulator of transcriptomic responses to both CO_2 and H_2O_2 in *Arabidopsis*. Plant Cell Environ *35*, 374-387.

Ralhan, A., Schöttle, S., Thurow, C., Iven, T., Feussner, I., Polle, A., and Gatz, C. (2012). The vascular pathogen *Verticillium longisporum* requires a jasmonic acid-independent COI1 function in roots to elicit disease symptoms in *Arabidopsis* shoots. Plant Physiol *159*, 1192-1203.

Ramel, F., Ksas, B., Akkari, E., Mialoundama, A.S., Monnet, F., Krieger-Liszkay, A., Ravanat, J.L., Mueller, M.J., Bouvier, F., and Havaux, M. (2013). Light-induced acclimation of the *Arabidopsis chlorina1* mutant to singlet oxygen. Plant Cell *25*, 1445-1462.

Ramireddy, E., Brenner, W.G., Pfeifer, A., Heyl, A., and Schmülling, T. (2013). *In planta* analysis of a *cis*-regulatory cytokinin response motif in *Arabidopsis* and identification of a novel enhancer sequence. Plant Cell Physiol *54*, 1079-1092.

Ramon, M., Rolland, F., and Sheen, J. (2008). Sugar sensing and signaling. Arabidopsis Book *6*, e0117.

Rao, M.V., Lee, H., Creelman, R.A., Mullet, J.E., and Davis, K.R. (2000). Jasmonic acid signaling modulates ozone-induced hypersensitive cell death. Plant Cell *12*, 1633-1646.

Rashotte, A.M., Carson, S.D., To, J.P., and Kieber, J.J. (2003). Expression profiling of cytokinin action in *Arabidopsis*. Plant Physiol *132*, 1998-2011.

Rashotte, A.M., Mason, M.G., Hutchison, C.E., Ferreira, F.J., Schaller, G.E., and Kieber, J.J. (2006). A subset of Arabidopsis AP2 transcription factors mediates cytokinin responses in concert with a two-component pathway. Proc Natl Acad Sci U S A *103*, 11081-11085.

Ravet, K., Touraine, B., Boucherez, J., Briat, J.F., Gaymard, F., and Cellier, F. (2009). Ferritins control interaction between iron homeostasis and oxidative stress in *Arabidopsis*. Plant J *57*, 400-412.

Rawat, R., Schwartz, J., Jones, M.A., Sairanen, I., Cheng, Y., Andersson, C.R., Zhao, Y., Ljung, K., and Harmer, S.L. (2009). REVEILLE1, a Myb-like transcription factor, integrates the circadian clock and auxin pathways. Proc Natl Acad Sci U S A *106*, 16883-16888.

Reed, J.W., Nagatani, A., Elich, T.D., Fagan, M., and Chory, J. (1994). Phytochrome A and phytochrome B have overlapping but distinct functions in *Arabidopsis* development. Plant Physiol *104*, 1139-1149.

Reed, J.W., Nagpal, P., Poole, D.S., Furuya, M., and Chory, J. (1993). Mutations in the gene for the red/far-red light receptor phytochrome B alter cell elongation and physiological responses throughout *Arabidopsis* development. Plant Cell *5*, 147-157.

Resco, V., Hartwell, J., and Hall, A. (2009). Ecological implications of plants ability to tell the time. Ecol Lett *12*, 583-592.

Ribot, C., Zimmerli, C., Farmer, E.E., Reymond, P., and Poirier, Y. (2008). Induction of the *Arabidopsis PHO1;H10* gene by 12-oxo-phytodienoic acid but not jasmonic acid via a CORONATINE INSENSITIVE1-dependent pathway. Plant Physiol *147*, 696-706.

Riefler, M., Novák, O., Strnad, M., and Schmülling, T. (2006). *Arabidopsis* cytokinin receptor mutants reveal functions in shoot growth, leaf senescence, seed size, germination, root development, and cytokinin metabolism. Plant Cell *18*, 40-54.

Rivero, R.M., Kojima, M., Gepstein, A., Sakakibara, H., Mittler, R., Gepstein, S., and Blumwald, E. (2007). Delayed leaf senescence induces extreme drought tolerance in a flowering plant. Proc Natl Acad Sci U S A *104*, 19631-19636.

Rizhsky, L., Davletova, S., Liang, H., and Mittler, R. (2004). The zinc finger protein Zat12 is required for cytosolic ascorbate peroxidase 1 expression during oxidative stress in *Arabidopsis*. J Biol Chem *279*, 11736-11743.

Robert-Seilaniantz, A., Grant, M., and Jones, J.D. (2011). Hormone crosstalk in plant disease and defense: more than just jasmonate-salicylate antagonism. Annu Rev Phytopathol *49*, 317-343.

Robertson, F.C., Skeffington, A.W., Gardner, M.J., and Webb, A.A. (2009). Interactions between circadian and hormonal signalling in plants. Plant Mol Biol *69*, 419-427.

Roden, L.C., and Ingle, R.A. (2009). Lights, rhythms, infection: the role of light and the circadian clock in determining the outcome of plant-pathogen interactions. Plant Cell *21*, 2546-2552.

Rolland, F., Baena-Gonzalez, E., and Sheen, J. (2006). Sugar sensing and signaling in plants: conserved and novel mechanisms. Annu Rev Plant Biol *57*, 675-709.

Romanov, G.A., Lomin, S.N., and Schmülling, T. (2006). Biochemical characteristics and ligand-binding properties of *Arabidopsis* cytokinin receptor AHK3 compared to CRE1/AHK4 as revealed by a direct binding assay. J Exp Bot *57*, 4051-4058.

Roose, J.L., and Pakrasi, H.B. (2004). Evidence that D1 processing is required for manganese binding and extrinsic protein assembly into photosystem II. J Biol Chem *279*, 45417-45422.

Sagi, M., and Fluhr, R. (2006). Production of reactive oxygen species by plant NADPH oxidases. Plant Physiol *141*, 336-340.

Sakakibara, H. (2006). Cytokinins: activity, biosynthesis, and translocation. Annu Rev Plant Biol *57*, 431-449.

Sakamoto, W., Miura, E., Kaji, Y., Okuno, T., Nishizono, M., and Ogura, T. (2004). Allelic characterization of the leaf-variegated mutation *var2* identifies the conserved amino acid residues of FtsH that are important for ATP hydrolysis and proteolysis. Plant Mol Biol *56*, 705-716.

Salomé, P.A., and McClung, C.R. (2005a). *PSEUDO-RESPONSE REGULATOR 7* and *9* are partially redundant genes essential for the temperature responsiveness of the *Arabidopsis* circadian clock. Plant Cell *17*, 791-803.

Salomé, P.A., and McClung, C.R. (2005b). What makes the *Arabidopsis* clock tick on time? A review on entrainment. Plant Cell Environ *28*, 21-38.

Salomé, P.A., Michael, T.P., Kearns, E.V., Fett-Neto, A.G., Sharrock, R.A., and McClung, C.R. (2002). The *out of phase 1* mutant defines a role for PHYB in circadian phase control in *Arabidopsis*. Plant Physiol *129*, 1674-1685.

Salomé, P.A., Oliva, M., Weigel, D., and Krämer, U. (2013). Circadian clock adjustment to plant iron status depends on chloroplast and phytochrome function. EMBO J *32*, 511-523.

Salomé, P.A., To, J.P., Kieber, J.J., and McClung, C.R. (2006). *Arabidopsis* response regulators ARR3 and ARR4 play cytokinin-independent roles in the control of circadian period. Plant Cell *18*, 55-69.

Salomé, P.A., Weigel, D., and McClung, C.R. (2010). The role of the *Arabidopsis* morning loop components CCA1, LHY, PRR7, and PRR9 in temperature compensation. Plant Cell *22*, 3650-3661.

Sanchez, A., Shin, J., and Davis, S.J. (2011). Abiotic stress and the plant circadian clock. Plant Signal Behav *6*, 223-231.

Sanchez, S.E., Petrillo, E., Beckwith, E.J., Zhang, X., Rugnone, M.L., Hernando, C.E., Cuevas, J.C., Godoy Herz, M.A., Depetris-Chauvin, A., Simpson, C.G.*, et al.* (2010). A methyl transferase links the circadian clock to the regulation of alternative splicing. Nature *468*, 112-116.

Sanchez, S.E., and Yanovsky, M.J. (2013). Time for a change. Elife *2*, e00791.

Sanchez-Villarreal, A. (2010). Genomic and physiological characterization of the mutant *time for coffee* within the *Arabidopsis thaliana* circadian clock. Dissertation. Max Planck Institute for Plant Breeding Research Köln, Universität zu Köln.

Sanchez-Villarreal, A., Shin, J., Bujdoso, N., Obata, T., Neumann, U., Du, S.X., Ding, Z., Davis, A.M., Shindo, T., Schmelzer, E.*, et al.* (2013). TIME FOR COFFEE is an essential component in the maintenance of metabolic homeostasis in *Arabidopsis thaliana*. Plant J *76*, 188-200.

Sano, H., Seo, S., Koizumi, N., Niki, T., Iwamura, H., and Ohashi, Y. (1996). Regulation by cytokinins of endogenous levels of jasmonic and salicylic acids in mechanically wounded tobacco plants. Plant Cell Physiol *37*, 762-769.

Santner, A., and Estelle, M. (2010). The ubiquitin-proteasome system regulates plant hormone signaling. Plant J *61*, 1029-1040.

Sarvikas, P., Hakala, M., Pätsikkä, E., Tyystjärvi, T., and Tyystjärvi, E. (2006). Action spectrum of photoinhibition in leaves of wild type and *npq1-2* and *npq4-1* mutants of *Arabidopsis thaliana*. Plant Cell Physiol *47*, 391-400.

Satoh, K., and Yamamoto, Y. (2007). The carboxyl-terminal processing of precursor D1 protein of the photosystem II reaction center. Photosynth Res *94*, 203-215.

Schaffer, R., Ramsay, N., Samach, A., Corden, S., Putterill, J., Carré, I.A., and Coupland, G. (1998). The late elongated hypocotyl mutation of *Arabidopsis* disrupts circadian rhythms and the photoperiodic control of flowering. Cell *93*, 1219-1229.

Schaller, A., and Stintzi, A. (2009). Enzymes in jasmonate biosynthesis - structure, function, regulation. Phytochemistry *70*, 1532-1538.

Schippers, J.H.M., Jing, H.-C., Hille, J., and Dijkwel, P.P. (2007). Developmental and hormonal control of leaf senescence. *In:* Annual Plant Reviews Volume 26: Senescence processes in plants (Blackwell Publishing Ltd), 145-170.

Schmitt, F.J., Renger, G., Friedrich, T., Kreslavski, V.D., Zharmukhamedov, S.K., Los, D.A., Kuznetsov, V.V., and Allakhverdiev, S.I. (2014). Reactive oxygen species: re-evaluation of generation, monitoring and role in stress-signaling in phototrophic organisms. Biochim Biophys Acta *1837*, 835-848.

Schmülling, T., Werner, T., Riefler, M., Krupková, E., and Bartrina y Manns, I. (2003). Structure and function of cytokinin oxidase/dehydrogenase genes of maize, rice, *Arabidopsis* and other species. J Plant Res *116*, 241-252.

Seltmann, M.A., Stingl, N.E., Lautenschlaeger, J.K., Krischke, M., Mueller, M.J., and Berger, S. (2010). Differential impact of lipoxygenase 2 and jasmonates on natural and stress-induced senescence in *Arabidopsis*. Plant Physiol *152*, 1940-1950.

Seo, M., and Koshiba, T. (2002). Complex regulation of ABA biosynthesis in plants. Trends Plant Sci *7*, 41-48.

Seung, D., Risopatron, J.P., Jones, B.J., and Marc, J. (2012). Circadian clock-dependent gating in ABA signalling networks. Protoplasma *249*, 445-457.

Shan, X., Wang, J., Chua, L., Jiang, D., Peng, W., and Xie, D. (2011). The role of *Arabidopsis* Rubisco activase in jasmonate-induced leaf senescence. Plant Physiol *155*, 751-764.

Sharma, P., Jha, A.B., Dubey, R.S., and Pessarakli, M. (2012). Reactive oxygen species, oxidative damage, and antioxidative defense mechanism in plants under stressful conditions. J Bot *2012*, 1-26.

Sheard, L.B., Tan, X., Mao, H., Withers, J., Ben-Nissan, G., Hinds, T.R., Kobayashi, Y., Hsu, F.F., Sharon, M., Browse, J.*, et al.* (2010). Jasmonate perception by inositol-phosphate-potentiated COI1-JAZ co-receptor. Nature *468*, 400-405.

Shin, J., Heidrich, K., Sanchez-Villarreal, A., Parker, J.E., and Davis, S.J. (2012). TIME FOR COFFEE represses accumulation of the MYC2 transcription factor to provide time-of-day regulation of jasmonate signaling in *Arabidopsis*. Plant Cell *24*, 2470-2482.

Short, E.F., North, K.A., Roberts, M.R., Hetherington, A.M., Shirras, A.D., and McAinsh, M.R. (2012). A stress-specific calcium signature regulating an ozone-responsive gene expression network in *Arabidopsis*. Plant J *71*, 948-961.

Slaugenhaupt, S.A., Mull, J., Leyne, M., Cuajungco, M.P., Gill, S.P., Hims, M.M., Quintero, F., Axelrod, F.B., and Gusella, J.F. (2004). Rescue of a human mRNA splicing defect by the plant cytokinin kinetin. Hum Mol Genet *13*, 429-436.

Smeekens, S., Ma, J., Hanson, J., and Rolland, F. (2010). Sugar signals and molecular networks controlling plant growth. Curr Opin Plant Biol *13*, 274-279.

Smith, A.M., and Zeeman, S.C. (2006). Quantification of starch in plant tissues. Nat Protoc *1*, 1342-1345.

Smith, S.M., Fulton, D.C., Chia, T., Thorneycroft, D., Chapple, A., Dunstan, H., Hylton, C., Zeeman, S.C., and Smith, A.M. (2004). Diurnal changes in the transcriptome encoding enzymes of starch metabolism provide evidence for both transcriptional and posttranscriptional regulation of starch metabolism in *Arabidopsis* leaves. Plant Physiol *136*, 2687-2699.

Smykowski, A., Zimmermann, P., and Zentgraf, U. (2010). G-Box binding factor1 reduces *CATALASE2* expression and regulates the onset of leaf senescence in *Arabidopsis*. Plant Physiol *153*, 1321-1331.

Solano, R., Stepanova, A., Chao, Q., and Ecker, J.R. (1998). Nuclear events in ethylene signaling: a transcriptional cascade mediated by ETHYLENE-INSENSITIVE3 and ETHYLENE-RESPONSE-FACTOR1. Genes Dev *12*, 3703-3714.

Somers, D.E., Devlin, P.F., and Kay, S.A. (1998). Phytochromes and cryptochromes in the entrainment of the *Arabidopsis* circadian clock. Science *282*, 1488-1490.

Spíchal, L., Rakova, N.Y., Riefler, M., Mizuno, T., Romanov, G.A., Strnad, M., and Schmülling, T. (2004). Two cytokinin receptors of *Arabidopsis thaliana*, CRE1/AHK4 and AHK3, differ in their ligand specificity in a bacterial assay. Plant Cell Physiol *45*, 1299-1305.

Spoel, S.H., and van Ooijen, G. (2014). Circadian redox signaling in plant immunity and abiotic stress. Antioxid Redox Signal *20*, 3024-3039.

Staiger, D., and Brown, J.W. (2013). Alternative splicing at the intersection of biological timing, development, and stress responses. Plant Cell *25*, 3640-3656.

Staiger, D., and Green, R. (2011). RNA-based regulation in the plant circadian clock. Trends Plant Sci *16*, 517-523.

Staswick, P.E., Su, W., and Howell, S.H. (1992). Methyl jasmonate inhibition of root growth and induction of a leaf protein are decreased in an *Arabidopsis thaliana* mutant. Proc Natl Acad Sci U S A *89*, 6837-6840.

Staswick, P.E., and Tiryaki, I. (2004). The oxylipin signal jasmonic acid is activated by an enzyme that conjugates it to isoleucine in *Arabidopsis*. Plant Cell *16*, 2117-2127.

Staswick, P.E., Tiryaki, I., and Rowe, M.L. (2002). Jasmonate response locus *JAR1* and several related *Arabidopsis* genes encode enzymes of the firefly luciferase superfamily that show activity on jasmonic, salicylic, and indole-3-acetic acids in an assay for adenylation. Plant Cell *14*, 1405-1415.

Stolz, A., Riefler, M., Lomin, S.N., Achazi, K., Romanov, G.A., and Schmülling, T. (2011). The specificity of cytokinin signalling in *Arabidopsis thaliana* is mediated by differing ligand affinities and expression profiles of the receptors. Plant J *67*, 157-168.

Stotz, H.U., Jikumaru, Y., Shimada, Y., Sasaki, E., Stingl, N., Mueller, M.J., and Kamiya, Y. (2011). Jasmonate-dependent and COI1-independent defense responses against *Sclerotinia sclerotiorum* in *Arabidopsis thaliana*: auxin is part of COI1-independent defense signaling. Plant Cell Physiol *52*, 1941-1956.

Stoynova-Bakalova, E., Petrov, P.I., Gigova, L., and Baskin, T.I. (2008). Differential effects of methyl jasmonate on growth and division of etiolated zucchini cotyledons. Plant Biol *10*, 476-484.

Strasser, B., Sánchez-Lamas, M., Yanovsky, M.J., Casal, J.J., and Cerdán, P.D. (2010). *Arabidopsis thaliana* life without phytochromes. Proc Natl Acad Sci U S A *107*, 4776-4781.

Strayer, C., Oyama, T., Schultz, T.F., Raman, R., Somers, D.E., Más, P., Panda, S., Kreps, J.A., and Kay, S.A. (2000). Cloning of the *Arabidopsis* clock gene *TOC1*, an autoregulatory response regulator homolog. Science *289*, 768-771.

Sun, X., Wang, L., and Zhang, L. (2007). Involvement of DEG5 and DEG8 proteases in the turnover of the photosystem II reaction center D1 protein under heat stress in *Arabidopsis thaliana*. Chin Sci Bull *52*, 1742-1745.

Su'udi, M., Kim, M.G., Park, S.R., Hwang, D.J., Bae, S.C., and Ahn, I.P. (2011). *Arabidopsis* cell death in compatible and incompatible interactions with *Alternaria brassicicola*. Mol Cells *31*, 593-601.

Suza, W.P., and Staswick, P.E. (2008). The role of JAR1 in jasmonoyl-L-isoleucine production during *Arabidopsis* wound response. Planta *227*, 1221-1232.

Suzuki, N., Miller, G., Morales, J., Shulaev, V., Torres, M.A., and Mittler, R. (2011). Respiratory burst oxidases: the engines of ROS signaling. Curr Opin Plant Biol *14*, 691-699.

Suzuki, T., Miwa, K., Ishikawa, K., Yamada, H., Aiba, H., and Mizuno, T. (2001). The *Arabidopsis* sensor His-kinase, AHK4, can respond to cytokinins. Plant Cell Physiol *42*, 107-113.

Sweere, U., Eichenberg, K., Lohrmann, J., Mira-Rodado, V., Bäurle, I., Kudla, J., Nagy, F., Schäfer, E., and Harter, K. (2001). Interaction of the response regulator ARR4 with phytochrome B in modulating red light signaling. Science *294*, 1108-1111.

Synková, H., Semorádová, S., Schnablová, R., Witters, E., Hušák, M., and Valcke, R. (2006). Cytokinin-induced activity of antioxidant enzymes in transgenic P*ssu-ipt* tobacco during plant ontogeny. Biol Plant *50*, 31-41.

Synková, H., Van Loven, K., Pospíšilová, J., and Valcke, R. (1999). Photosynthesis of transgenic P*ssu-ipt* tobacco. J Plant Physiol *155*, 173-182.

Takahashi, S., and Badger, M.R. (2011). Photoprotection in plants: a new light on photosystem II damage. Trends Plant Sci *16*, 53-60.

Takahashi, S., and Murata, N. (2008). How do environmental stresses accelerate photoinhibition? Trends Plant Sci *13*, 178-182.

Takei, K., Sakakibara, H., and Sugiyama, T. (2001). Identification of genes encoding adenylate isopentenyltransferase, a cytokinin biosynthesis enzyme, in *Arabidopsis thaliana*. J Biol Chem *276*, 26405-26410.

Takei, K., Ueda, N., Aoki, K., Kuromori, T., Hirayama, T., Shinozaki, K., Yamaya, T., and Sakakibara, H. (2004a). *AtIPT3* is a key determinant of nitrate-dependent cytokinin biosynthesis in *Arabidopsis*. Plant Cell Physiol *45*, 1053-1062.

Takei, K., Yamaya, T., and Sakakibara, H. (2004b). *Arabidopsis CYP735A1* and *CYP735A2* encode cytokinin hydroxylases that catalyze the biosynthesis of *trans*-Zeatin. J Biol Chem *279*, 41866-41872.

Taki, N., Sasaki-Sekimoto, Y., Obayashi, T., Kikuta, A., Kobayashi, K., Ainai, T., Yagi, K., Sakurai, N., Suzuki, H., Masuda, T.*, et al.* (2005). 12-oxo-phytodienoic acid triggers expression of a distinct set of genes and plays a role in wound-induced gene expression in *Arabidopsis*. Plant Physiol *139*, 1268-1283.

Taniguchi, M., Sasaki, N., Tsuge, T., Aoyama, T., and Oka, A. (2007). ARR1 directly activates cytokinin response genes that encode proteins with diverse regulatory functions. Plant Cell Physiol *48*, 263-277.

Telfer, A. (2014). Singlet oxygen production by PSII under light stress: mechanism, detection and the protective role of beta-carotene. Plant Cell Physiol *55*, 1216-1223.

Ternes, P., Feussner, K., Werner, S., Lerche, J., Iven, T., Heilmann, I., Riezman, H., and Feussner, I. (2011). Disruption of the ceramide synthase LOH1 causes spontaneous cell death in *Arabidopsis thaliana*. New Phytol *192*, 841-854.

Thain, S.C., Hall, A., and Millar, A.J. (2000). Functional independence of circadian clocks that regulate plant gene expression. Curr Biol *10*, 951-956.

Thain, S.C., Murtas, G., Lynn, J.R., McGrath, R.B., and Millar, A.J. (2002). The circadian clock that controls gene expression in *Arabidopsis* is tissue specific. Plant Physiol *130*, 102-110.

Thain, S.C., Vandenbussche, F., Laarhoven, L.J., Dowson-Day, M.J., Wang, Z.Y., Tobin, E.M., Harren, F.J., Millar, A.J., and Van Der Straeten, D. (2004). Circadian rhythms of ethylene emission in *Arabidopsis*. Plant Physiol *136*, 3751-3761.

Thayer, S.S., and Björkman, O. (1990). Leaf xanthophyll content and composition in sun and shade determined by HPLC. Photosynth Res *23*, 331-343.

Thines, B., Katsir, L., Melotto, M., Niu, Y., Mandaokar, A., Liu, G., Nomura, K., He, S.Y., Howe, G.A., and Browse, J. (2007). JAZ repressor proteins are targets of the SCF^{COI1} complex during jasmonate signalling. Nature *448*, 661-665.

Thomas, H. (2013). Senescence, ageing and death of the whole plant. New Phytol *197*, 696-711.

Tissier, A.F., Marillonnet, S., Klimyuk, V., Patel, K., Torres, M.A., Murphy, G., and Jones, J.D. (1999). Multiple independent defective *Suppressor*-mutator transposon insertions in *Arabidopsis*: a tool for functional genomics. Plant Cell *11*, 1841-1852.

To, J.P., Deruère, J., Maxwell, B.B., Morris, V.F., Hutchison, C.E., Ferreira, F.J., Schaller, G.E., and Kieber, J.J. (2007). Cytokinin regulates type-A *Arabidopsis* Response Regulator activity and protein stability *via* two-component phosphorelay. Plant Cell *19*, 3901-3914.

To, J.P., Haberer, G., Ferreira, F.J., Deruère, J., Mason, M.G., Schaller, G.E., Alonso, J.M., Ecker, J.R., and Kieber, J.J. (2004). Type-A *Arabidopsis* response regulators are partially redundant negative regulators of cytokinin signaling. Plant Cell *16*, 658-671.

Tokunaga, H., Kojima, M., Kuroha, T., Ishida, T., Sugimoto, K., Kiba, T., and Sakakibara, H. (2012). *Arabidopsis* lonely guy (LOG) multiple mutants reveal a central role of the LOG-dependent pathway in cytokinin activation. Plant J *69*, 355-365.

Torres, M.A., and Dangl, J.L. (2005). Functions of the respiratory burst oxidase in biotic interactions, abiotic stress and development. Curr Opin Plant Biol *8*, 397-403.

Torres, M.A., Dangl, J.L., and Jones, J.D. (2002). *Arabidopsis* $gp91^{phox}$ homologues *AtrbohD* and *AtrbohF* are required for accumulation of reactive oxygen intermediates in the plant defense response. Proc Natl Acad Sci U S A *99*, 517-522.

Torres, M.A., Jones, J.D., and Dangl, J.L. (2005). Pathogen-induced, NADPH oxidase-derived reactive oxygen intermediates suppress spread of cell death in *Arabidopsis thaliana*. Nat Genet *37*, 1130-1134.

Tóth, R., Kevei, E., Hall, A., Millar, A.J., Nagy, F., and Kozma-Bognár, L. (2001). Circadian clock-regulated expression of phytochrome and cryptochrome genes in *Arabidopsis*. Plant Physiol *127*, 1607-1616.

Tran, L.S., Shinozaki, K., and Yamaguchi-Shinozaki, K. (2010). Role of cytokinin responsive two-component system in ABA and osmotic stress signalings. Plant Signal Behav *5*, 148-150.

Tran, L.S., Urao, T., Qin, F., Maruyama, K., Kakimoto, T., Shinozaki, K., and Yamaguchi-Shinozaki, K. (2007). Functional analysis of AHK1/ATHK1 and cytokinin receptor histidine kinases in response to abscisic acid, drought, and salt stress in *Arabidopsis*. Proc Natl Acad Sci U S A *104*, 20623-20628.

Trebst, A. (2003). Function of beta-carotene and tocopherol in photosystem II. Z Naturforsch C *58*, 609-620.

Trebst, A., Depka, B., and Holländer-Czytko, H. (2002). A specific role for tocopherol and of chemical singlet oxygen quenchers in the maintenance of photosystem II structure and function in *Chlamydomonas reinhardtii*. FEBS Lett *516*, 156-160.

Triantaphylidès, C., and Havaux, M. (2009). Singlet oxygen in plants: production, detoxification and signaling. Trends Plant Sci *14*, 219-228.

Tyystjärvi, E. (2008). Photoinhibition of photosystem II and photodamage of the oxygen evolving manganese cluster. Coordination Chemistry Reviews *252*, 361-376.

Tyystjärvi, E., and Aro, E.M. (1996). The rate constant of photoinhibition, measured in lincomycin-treated leaves, is directly proportional to light intensity. Proc Natl Acad Sci U S A *93*, 2213-2218.

Ueguchi, C., Koizumi, H., Suzuki, T., and Mizuno, T. (2001a). Novel family of sensor histidine kinase genes in *Arabidopsis thaliana*. Plant Cell Physiol *42*, 231-235.

Ueguchi, C., Sato, S., Kato, T., and Tabata, S. (2001b). The *AHK4* gene involved in the cytokinin-signaling pathway as a direct receptor molecule in *Arabidopsis thaliana*. Plant Cell Physiol *42*, 751-755.

Usadel, B., Bläsing, O.E., Gibon, Y., Retzlaff, K., Höhne, M., Günther, M., and Stitt, M. (2008). Global transcript levels respond to small changes of the carbon status during progressive exhaustion of carbohydrates in *Arabidopsis* rosettes. Plant Physiol *146*, 1834-1861.

Van Breusegem, F., Bailey-Serres, J., and Mittler, R. (2008). Unraveling the tapestry of networks involving reactive oxygen species in plants. Plant Physiol *147*, 978-984.

Van Breusegem, F., and Dat, J.F. (2006). Reactive oxygen species in plant cell death. Plant Physiol *141*, 384-390.

Van der Does, D., Leon-Reyes, A., Koornneef, A., Van Verk, M.C., Rodenburg, N., Pauwels, L., Goossens, A., Körbes, A.P., Memelink, J., Ritsema, T.*, et al.* (2013). Salicylic acid suppresses jasmonic acid signaling downstream of SCF^{COI1}-JAZ by targeting GCC promoter motifs *via* transcription factor ORA59. Plant Cell *25*, 744-761.

van Doorn, W.G. (2011). Classes of programmed cell death in plants, compared to those in animals. J Exp Bot *62*, 4749-4761.

van Doorn, W.G., Beers, E.P., Dangl, J.L., Franklin-Tong, V.E., Gallois, P., Hara-Nishimura, I., Jones, A.M., Kawai-Yamada, M., Lam, E., Mundy, J.*, et al.* (2011). Morphological classification of plant cell deaths. Cell Death Differ *18*, 1241-1246.

Vandenbussche, F., Habricot, Y., Condiff, A.S., Maldiney, R., Van der Straeten, D., and Ahmad, M. (2007). HY5 is a point of convergence between cryptochrome and cytokinin signalling pathways in *Arabidopsis thaliana*. Plant J *49*, 428-441.

Vandesompele, J., De Preter, K., Pattyn, F., Poppe, B., Van Roy, N., De Paepe, A., and Speleman, F. (2002). Accurate normalization of real-time quantitative RT-PCR data by geometric averaging of multiple internal control genes. Genome Biol *3*, RESEARCH0034.

Velez-Ramirez, A.I., van Ieperen, W., Vreugdenhil, D., and Millenaar, F.F. (2011). Plants under continuous light. Trends Plant Sci *16*, 310-318.

Vescovi, M., Riefler, M., Gessuti, M., Novák, O., Schmülling, T., and Lo Schiavo, F. (2012). Programmed cell death induced by high levels of cytokinin in *Arabidopsis* cultured cells is mediated by the cytokinin receptor CRE1/AHK4. J Exp Bot *63*, 2825-2832.

Vidi, P.A., Kanwischer, M., Baginsky, S., Austin, J.R., Csucs, G., Dörmann, P., Kessler, F., and Bréhélin, C. (2006). Tocopherol cyclase (VTE1) localization and vitamin E accumulation in chloroplast plastoglobule lipoprotein particles. J Biol Chem *281*, 11225-11234.

Vogel, J.T., Zarka, D.G., Van Buskirk, H.A., Fowler, S.G., and Thomashow, M.F. (2005). Roles of the CBF2 and ZAT12 transcription factors in configuring the low temperature transcriptome of *Arabidopsis*. Plant J *41*, 195-211.

Wagner, D., Przybyla, D., Op den Camp, R., Kim, C., Landgraf, F., Lee, K.P., Würsch, M., Laloi, C., Nater, M., Hideg, E.*, et al.* (2004). The genetic basis of singlet oxygen-induced stress responses of *Arabidopsis thaliana*. Science *306*, 1183-1185.

Walley, J.W., Coughlan, S., Hudson, M.E., Covington, M.F., Kaspi, R., Banu, G., Harmer, S.L., and Dehesh, K. (2007). Mechanical stress induces biotic and abiotic stress responses *via* a novel cis-element. PLoS Genet *3*, 1800-1812.

Wang, W., Barnaby, J.Y., Tada, Y., Li, H., Tor, M., Caldelari, D., Lee, D.U., Fu, X.D., and Dong, X. (2011). Timing of plant immune responses by a central circadian regulator. Nature *470*, 110-114.

Wang, Y., Lin, A., Loake, G.J., and Chu, C. (2013). H_2O_2-induced leaf cell death and the crosstalk of reactive nitric/oxygen species. J Integr Plant Biol *55*, 202-208.

Wang, Z.Y., and Tobin, E.M. (1998). Constitutive expression of the *CIRCADIAN CLOCK ASSOCIATED 1* (*CCA1*) gene disrupts circadian rhythms and suppresses its own expression. Cell *93*, 1207-1217.

Wasternack, C. (2007). Jasmonates: an update on biosynthesis, signal transduction and action in plant stress response, growth and development. Ann Bot *100*, 681-697.

Wasternack, C. (2014). Action of jasmonates in plant stress responses and development - applied aspects. Biotechnol Adv *32*, 31-39.

Wasternack, C., Forner, S., Strnad, M., and Hause, B. (2013). Jasmonates in flower and seed development. Biochimie *95*, 79-85.

Wasternack, C., and Hause, B. (2013). Jasmonates: biosynthesis, perception, signal transduction and action in plant stress response, growth and development. An update to the 2007 review in Annals of Botany. Ann Bot *111*, 1021-1058.

Wasternack, C., and Kombrink, E. (2010). Jasmonates: structural requirements for lipid-derived signals active in plant stress responses and development. ACS Chem Biol *5*, 63-77.

Wasternack, C., Stenzel, I., Hause, B., Hause, G., Kutter, C., Maucher, H., Neumerkel, J., Feussner, I., and Miersch, O. (2006). The wound response in tomato - role of jasmonic acid. J Plant Physiol *163*, 297-306.

Watanabe, N., and Lam, E. (2006). *Arabidopsis* Bax inhibitor-1 functions as an attenuator of biotic and abiotic types of cell death. Plant J *45*, 884-894.

Watanabe, N., and Lam, E. (2008). Bax inhibitor-1 modulates endoplasmic reticulum stress-mediated programmed cell death in *Arabidopsis*. J Biol Chem *283*, 3200-3210.

Watanabe, N., and Lam, E. (2009). Bax Inhibitor-1, a conserved cell death suppressor, is a key molecular switch downstream from a variety of biotic and abiotic stress signals in plants. Int J Mol Sci *10*, 3149-3167.

Watanabe, N., and Lam, E. (2011). *Arabidopsis* metacaspase 2d is a positive mediator of cell death induced during biotic and abiotic stresses. Plant J *66*, 969-982.

Weidhase, R.A., Lehmann, J., Kramell, H., Sembdner, G., and Parthier, B. (1987). Degradation of ribulose-1,5-bisphosphate carboxylase and chlorophyll in senescing barley leaf segments triggered by jasmonic acid methylester, and counteraction by cytokinin. Physiol Plant *69*, 161-166.

Werner, T., Motyka, V., Strnad, M., and Schmülling, T. (2001). Regulation of plant growth by cytokinin. Proc Natl Acad Sci U S A *98*, 10487-10492.

Werner, T., Motyka, V., Laucou, V., Smets, R., Van Onckelen, H., and Schmülling, T. (2003). Cytokinin-deficient transgenic *Arabidopsis* plants show multiple developmental alterations indicating opposite functions of cytokinins in the regulation of shoot and root meristem activity. Plant Cell *15*, 2532-2550.

Werner, T., Köllmer, I., Bartrina, I., Holst, K., and Schmülling, T. (2006). New insights into the biology of cytokinin degradation. Plant Biol *8*, 371-381.

Werner, T., and Schmülling, T. (2009). Cytokinin action in plant development. Curr Opin Plant Biol *12*, 527-538.

Wind, J., Smeekens, S., and Hanson, J. (2010). Sucrose: metabolite and signaling molecule. Phytochemistry *71*, 1610-1614.

Wingler, A., Purdy, S., MacLean, J.A., and Pourtau, N. (2006). The role of sugars in integrating environmental signals during the regulation of leaf senescence. J Exp Bot *57*, 391-399.

Winter, D., Vinegar, B., Nahal, H., Ammar, R., Wilson, G.V., and Provart, N.J. (2007). An "Electronic Fluorescent Pictograph" browser for exploring and analyzing large-scale biological data sets. PLoS One *2*, e718.

Wood, N.T., Haley, A., Viry-Moussaïd, M., Johnson, C.H., van der Luit, A.H., and Trewavas, A.J. (2001). The calcium rhythms of different cell types oscillate with different circadian phases. Plant Physiol *125*, 787-796.

Wrzaczek, M., Brosché, M., and Kangasjärvi, J. (2013). ROS signaling loops - production, perception, regulation. Curr Opin Plant Biol *16*, 575-582.

Wu, X.Y., Kuai, B.K., Jia, J.Z., and Jing, H.C. (2012). Regulation of leaf senescence and crop genetic improvement. J Integr Plant Biol *54*, 936-952.

Wulfetange, K., Lomin, S.N., Romanov, G.A., Stolz, A., Heyl, A., and Schmülling, T. (2011). The cytokinin receptors of *Arabidopsis* are located mainly to the endoplasmic reticulum. Plant Physiol *156*, 1808-1818.

Xie, D.X., Feys, B.F., James, S., Nieto-Rostro, M., and Turner, J.G. (1998). *COI1*: an *Arabidopsis* gene required for jasmonate-regulated defense and fertility. Science *280*, 1091-1094.

Xu, X., Hotta, C.T., Dodd, A.N., Love, J., Sharrock, R., Lee, Y.W., Xie, Q., Johnson, C.H., and Webb, A.A. (2007). Distinct light and clock modulation of cytosolic free Ca^{2+} oscillations and rhythmic *CHLOROPHYLL A/B BINDING PROTEIN2* promoter activity in *Arabidopsis*. Plant Cell *19*, 3474-3490.

Yakir, E., Hassidim, M., Melamed-Book, N., Hilman, D., Kron, I., and Green, R.M. (2011). Cell autonomous and cell-type specific circadian rhythms in *Arabidopsis*. Plant J *68*, 520-531.

Yakir, E., Hilman, D., Harir, Y., and Green, R.M. (2007a). Regulation of output from the plant circadian clock. FEBS J *274*, 335-345.

Yakir, E., Hilman, D., Hassidim, M., and Green, R.M. (2007b). *CIRCADIAN CLOCK ASSOCIATED1* transcript stability and the entrainment of the circadian clock in *Arabidopsis*. Plant Physiol *145*, 925-932.

Yakir, E., Hilman, D., Kron, I., Hassidim, M., Melamed-Book, N., and Green, R.M. (2009). Posttranslational regulation of CIRCADIAN CLOCK ASSOCIATED1 in the circadian oscillator of *Arabidopsis*. Plant Physiol *150*, 844-857.

Yamada, H., Suzuki, T., Terada, K., Takei, K., Ishikawa, K., Miwa, K., Yamashino, T., and Mizuno, T. (2001). The *Arabidopsis* AHK4 histidine kinase is a cytokinin-binding receptor that transduces cytokinin signals across the membrane. Plant Cell Physiol *42*, 1017-1023.

Yamamoto, Y., Aminaka, R., Yoshioka, M., Khatoon, M., Komayama, K., Takenaka, D., Yamashita, A., Nijo, N., Inagawa, K., Morita, N.*, et al.* (2008). Quality control of photosystem II: impact of light and heat stresses. Photosynth Res *98*, 589-608.

Yamamoto, Y., Sato, E., Shimizu, T., Nakamichi, N., Sato, S., Kato, T., Tabata, S., Nagatani, A., Yamashino, T., and Mizuno, T. (2003). Comparative genetic studies on the *APRR5* and *APRR7* genes belonging to the APRR1/TOC1 quintet implicated in circadian rhythm, control of flowering time, and early photomorphogenesis. Plant Cell Physiol *44*, 1119-1130.

Yamashino, T., Ito, S., Niwa, Y., Kunihiro, A., Nakamichi, N., and Mizuno, T. (2008). Involvement of *Arabidopsis* clock-associated pseudo-response regulators in diurnal oscillations of gene expression in the presence of environmental time cues. Plant Cell Physiol *49*, 1839-1850.

Yan, Y., Stolz, S., Chételat, A., Reymond, P., Pagni, M., Dubugnon, L., and Farmer, E.E. (2007). A downstream mediator in the growth repression limb of the jasmonate pathway. Plant Cell *19*, 2470-2483.

Yang, H., Yang, S., Li, Y., and Hua, J. (2007). The Arabidopsis *BAP1* and *BAP2* genes are general inhibitors of programmed cell death. Plant Physiol *145*, 135-146.

Yanovsky, M.J., Mazzella, M.A., and Casal, J.J. (2000). A quadruple photoreceptor mutant still keeps track of time. Curr Biol *10*, 1013-1015.

Yaronskaya, E., Vershilovskaya, I., Poers, Y., Alawady, A.E., Averina, N., and Grimm, B. (2006). Cytokinin effects on tetrapyrrole biosynthesis and photosynthetic activity in barley seedlings. Planta *224*, 700-709.

Yerushalmi, S., and Green, R.M. (2009). Evidence for the adaptive significance of circadian rhythms. Ecol Lett *12*, 970-981.

Yerushalmi, S., Yakir, E., and Green, R.M. (2011). Circadian clocks and adaptation in *Arabidopsis*. Mol Ecol *20*, 1155-1165.

Yin, S.M., Sun, X.W., and Zhang, L.X. (2008). An *Arabidopsis ctpA* homologue is involved in the repair of photosystem II under high light. Chin Sci Bull *53*, 1021-1026.

Yokoyama, A., Yamashino, T., Amano, Y., Tajima, Y., Imamura, A., Sakakibara, H., and Mizuno, T. (2007). Type-B ARR transcription factors, ARR10 and ARR12, are implicated in cytokinin-mediated regulation of protoxylem differentiation in roots of *Arabidopsis thaliana*. Plant Cell Physiol *48*, 84-96.

Young, M.W., and Kay, S.A. (2001). Time zones: a comparative genetics of circadian clocks. Nat Rev Genet *2*, 702-715.

Ytterberg, A.J., Peltier, J.B., and van Wijk, K.J. (2006). Protein profiling of plastoglobules in chloroplasts and chromoplasts. A surprising site for differential accumulation of metabolic enzymes. Plant Physiol *140*, 984-997.

Yue, H., Nie, S., and Xing, D. (2012). Over-expression of *Arabidopsis* Bax inhibitor-1 delays methyl jasmonate-induced leaf senescence by suppressing the activation of MAP kinase 6. J Exp Bot *63*, 4463-4474.

Zagotta, M.T., Hicks, K.A., Jacobs, C.I., Young, J.C., Hangarter, R.P., and Meeks-Wagner, D.R. (1996). The *Arabidopsis ELF3* gene regulates vegetative photomorphogenesis and the photoperiodic induction of flowering. Plant J *10*, 691-702.

Zagotta, M.T., Shannon, S., Jacobs, C.I., and Meeks-Wagner, D.R. (1992). Early-flowering mutants of *Arabidopsis thaliana*. Aust J Plant Physiol *19*, 411-418.

Zhang, C., and Shapiro, A.D. (2002). Two pathways act in an additive rather than obligatorily synergistic fashion to induce systemic acquired resistance and *PR* gene expression. BMC Plant Biol *2*, 9.

Zhang, C., Xie, Q., Anderson, R.G., Ng, G., Seitz, N.C., Peterson, T., McClung, C.R., McDowell, J.M., Kong, D., Kwak, J.M.*, et al.* (2013). Crosstalk between the circadian clock and innate immunity in *Arabidopsis*. PLoS Pathog *9*, e1003370.

Zhang, K., Novák, O., Wei, Z., Gou, M., Zhang, X., Yu, Y., Yang, H., Cai, Y., Strnad, M., and Liu, C.J. (2014). *Arabidopsis* ABCG14 protein controls the acropetal translocation of root-synthesized cytokinins. Nat Commun *5*, 3274.

Zheng, B., Deng, Y., Mu, J., Ji, Z., Xiang, T., Niu, Q.-W., Chua, N.-H., and Zuo, J. (2006). Cytokinin affects circadian-clock oscillation in a phytochrome B- and *Arabidopsis* response regulator 4-dependent manner. Physiol Plant *127*, 277-292.

Zheng, X.Y., Spivey, N.W., Zeng, W., Liu, P.P., Fu, Z.Q., Klessig, D.F., He, S.Y., and Dong, X. (2012). Coronatine promotes *Pseudomonas syringae* virulence in plants by activating a signaling cascade that inhibits salicylic acid accumulation. Cell Host Microbe *11*, 587-596.

Zhong, H.H., and McClung, C.R. (1996). The circadian clock gates expression of two *Arabidopsis* catalase genes to distinct and opposite circadian phases. Mol Gen Genet *251*, 196-203.

Zhong, H.H., Painter, J.E., Salomé, P.A., Straume, M., and McClung, C.R. (1998). Imbibition, but not release from stratification, sets the circadian clock in *Arabidopsis* seedlings. Plant Cell *10*, 2005-2017.

Zhu, X., Feng, Y., Liang, G., Liu, N., and Zhu, J.K. (2013). Aequorin-based luminescence imaging reveals stimulus- and tissue-specific Ca^{2+} dynamics in *Arabidopsis* plants. Mol Plant *6*, 444-455.

Zubo, Y.O., Selivankina, S.Y., Yamburenko, M.V., Zubkova, N.K., Kulaeva, O.N., and Kusnetsov, V.V. (2005). Cytokinins activate transcription of chloroplast genes. Dokl Biochem Biophys *400*, 48-51.

Zubo, Y.O., Yamburenko, M.V., Selivankina, S.Y., Shakirova, F.M., Avalbaev, A.M., Kudryakova, N.V., Zubkova, N.K., Liere, K., Kulaeva, O.N., Kusnetsov, V.V.*, et al.* (2008). Cytokinin stimulates chloroplast transcription in detached barley leaves. Plant Physiol *148*, 1082-1093.

Zürcher, E., Tavor-Deslex, D., Lituiev, D., Enkerli, K., Tarr, P.T., and Müller, B. (2013). A robust and sensitive synthetic sensor to monitor the transcriptional output of the cytokinin signaling network *in planta*. Plant Physiol *161*, 1066-1075.

Publications

Cortleven, A.*, Nitschke, S.*, Klaumünzer, M., Abdelgawad, H., Asard, H., Grimm, B., Riefler, M., and Schmülling, T. (2014). A novel protective function for cytokinin in the light stress response is mediated by the *Arabidopsis* histidine kinase2 and *Arabidopsis* histidine kinase3 receptors. Plant Physiol *164*, 1470-1483.

* These authors contributed equally to the article.

Appendix

Figure A.1: Pictures of control plants corresponding to Figure 3.7.
Pictures of five-week-old SD-grown plants that served as controls for the experiment in Fig. 3.7 are shown.

Figure A.2: Pictures of control plants corresponding to Figure 3.8.
Pictures of six-week-old SD-grown plants that served as controls for the experiment in Fig. 3.8 are shown.

Figure A.3: Pictures of control plants corresponding to Figure 3.9.
Pictures of six-week-old SD-grown plants that served as controls for the experiment in Fig. 3.9 are shown.

Figure A.4: Pictures of control plants corresponding to Figure 3.10.
Pictures of six-week-old SD-grown plants that served as controls for the experiment in Fig. 3.10 are shown.

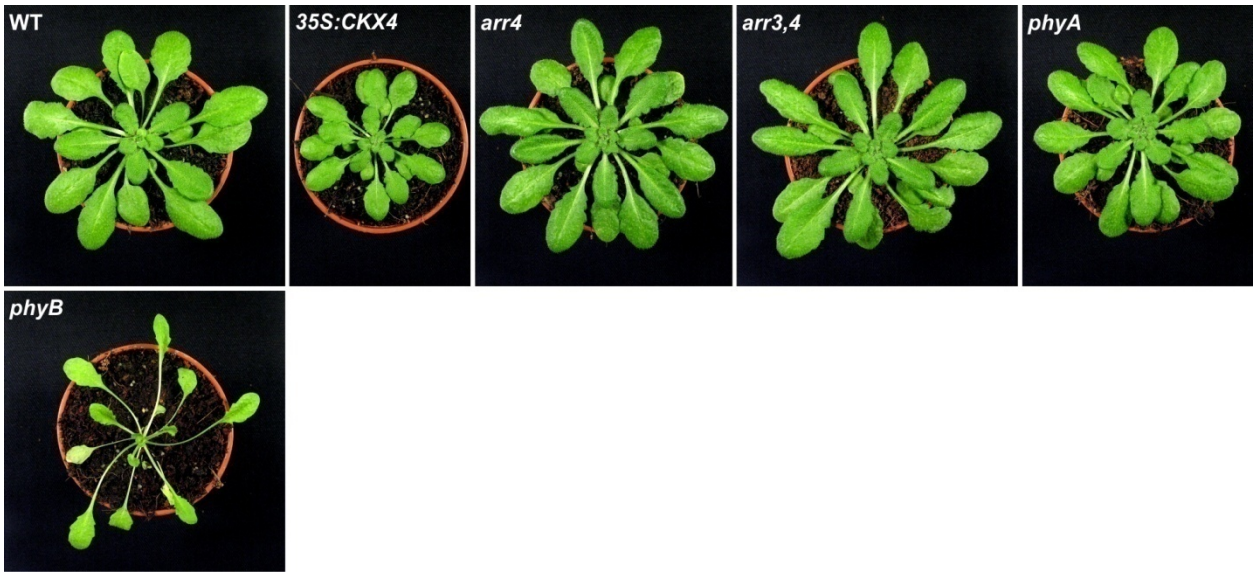

Figure A.5: Pictures of control plants corresponding to Figure 3.29.
Pictures of six-week-old SD-grown plants that served as controls for the experiment in Fig. 3.29 are shown.

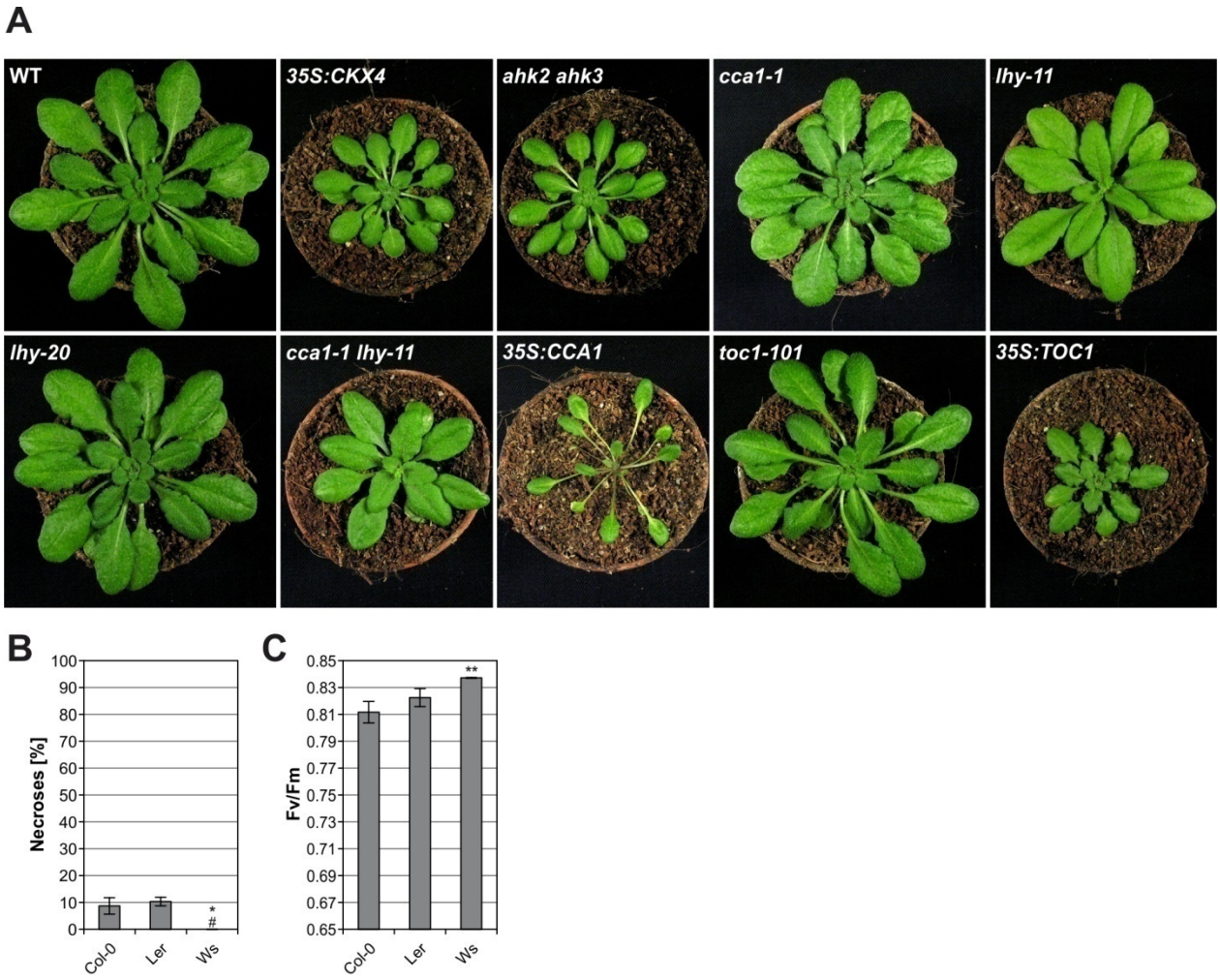

Figure A.6: Pictures of control plants corresponding to Figure 3.30 and CL responses of different *Arabidopsis* ecotypes.

A, Pictures of five-week-old SD-grown plants that served as controls for the experiment in Fig. 3.30 are shown. **B**-**C**, CL responses determined as percentage of necroses (**B**) and stress-induced decrease in F_v/F_m ratios (**C**). The experimental design corresponds to the one explained in Fig. 3.30. #, not detected.

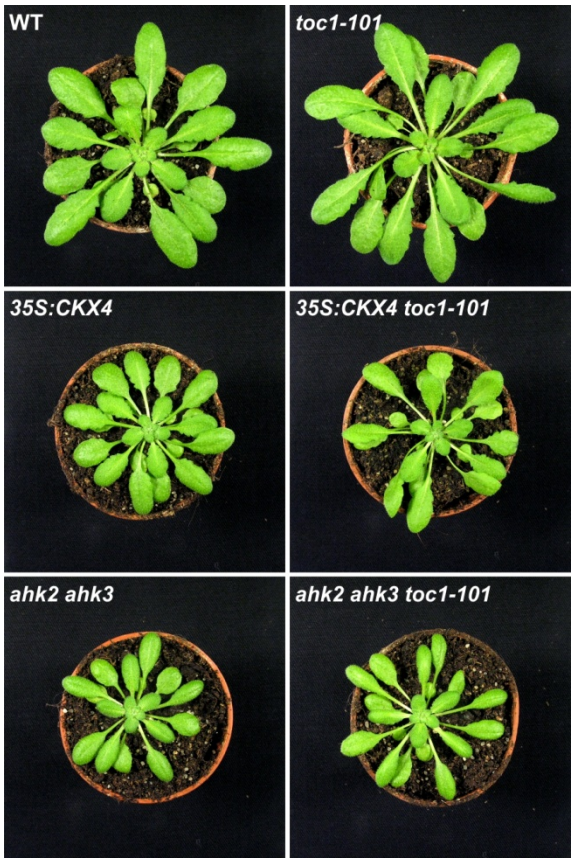

Figure A.7: Pictures of control plants corresponding to Figure 3.31.
Pictures of five-week-old SD-grown plants that served as controls for the experiment in Fig. 3.31 are shown.

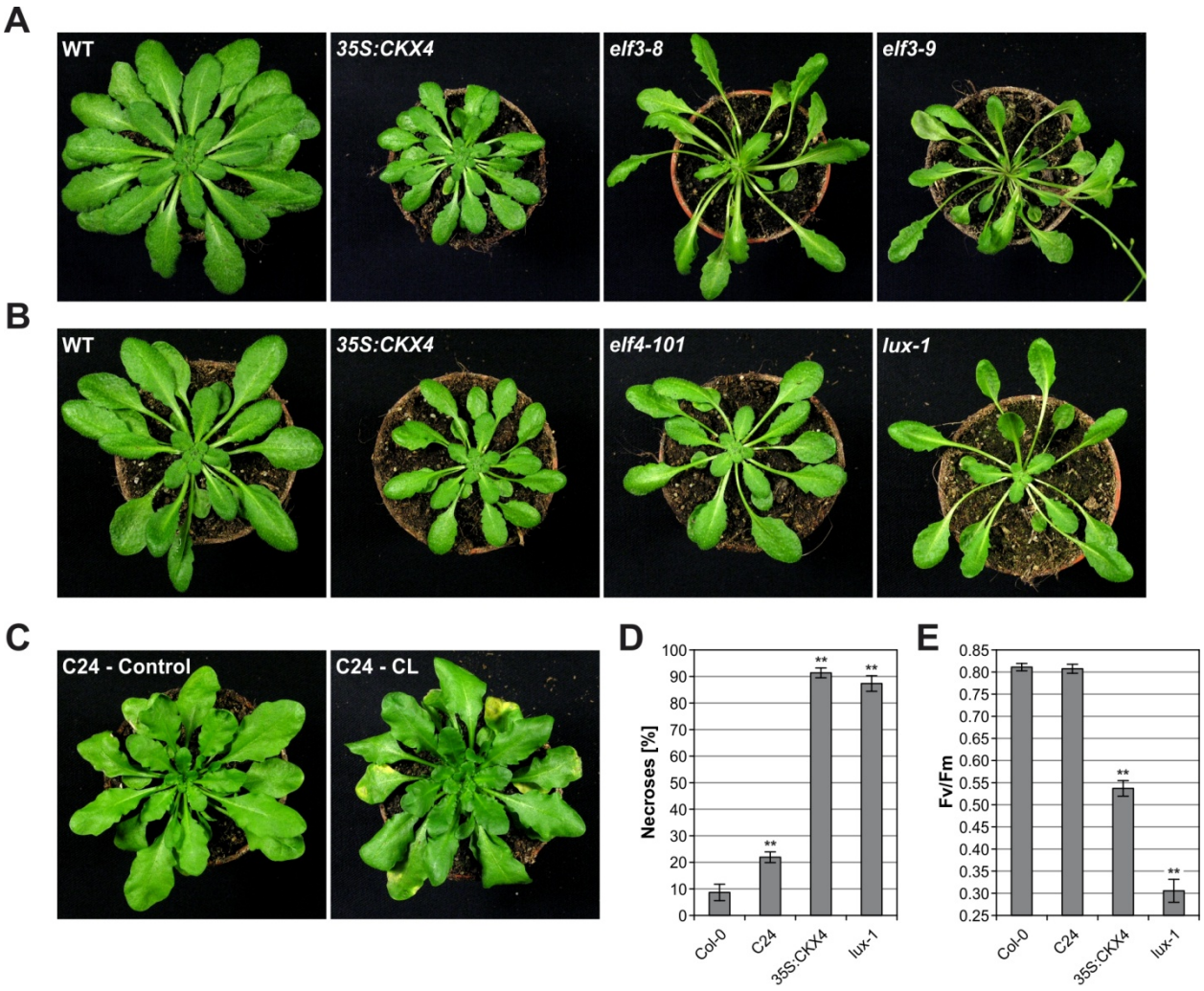

Figure A.8: Pictures of control plants corresponding to Figure 3.32 and CL responses of *35S:CKX4* and *lux-1* plants compared with their respective wild-type backgrounds Col-0 and C24.

A-**B**, Pictures of six- or five-week-old (**A** and **B**, respectively) SD-grown plants that served as controls for the experiments in Fig. 3.32 are shown. **C**, Six-week-old SD-grown control and CL-treated C24 plant. **D**-**E**, CL responses determined as percentage of necroses (**D**) and stress-induced decrease in F_v/F_m ratios (**E**).The experimental design corresponds to the one explained in Fig. 3.32 (*t* test: **, $p < 0.01$).

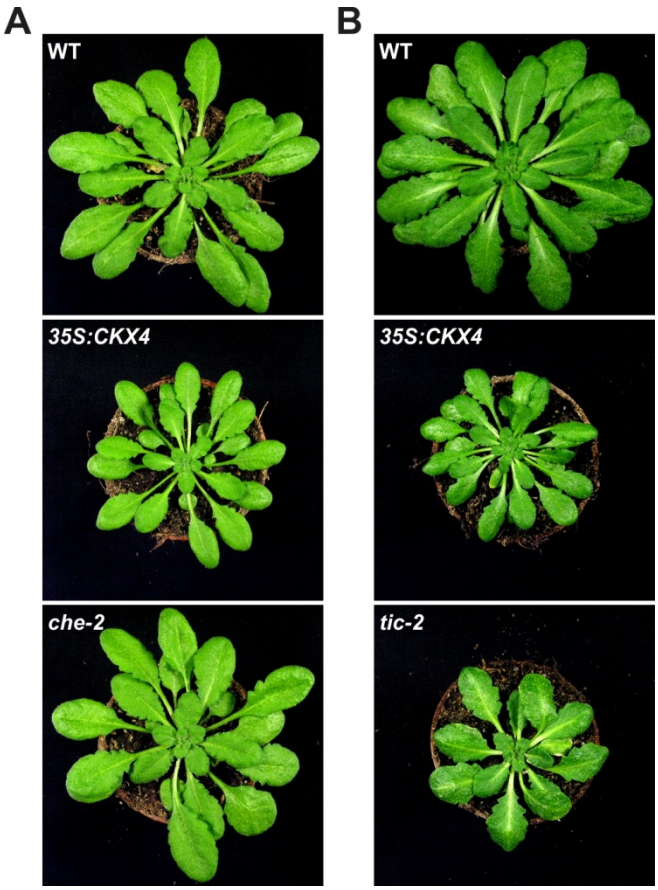

Figure A.9: Pictures of control plants corresponding to Figure 3.34.

Pictures of five- or six-week-old (**A** and **B**, respectively) SD-grown plants that served as controls for the experiments in Fig. 3.34 are shown.

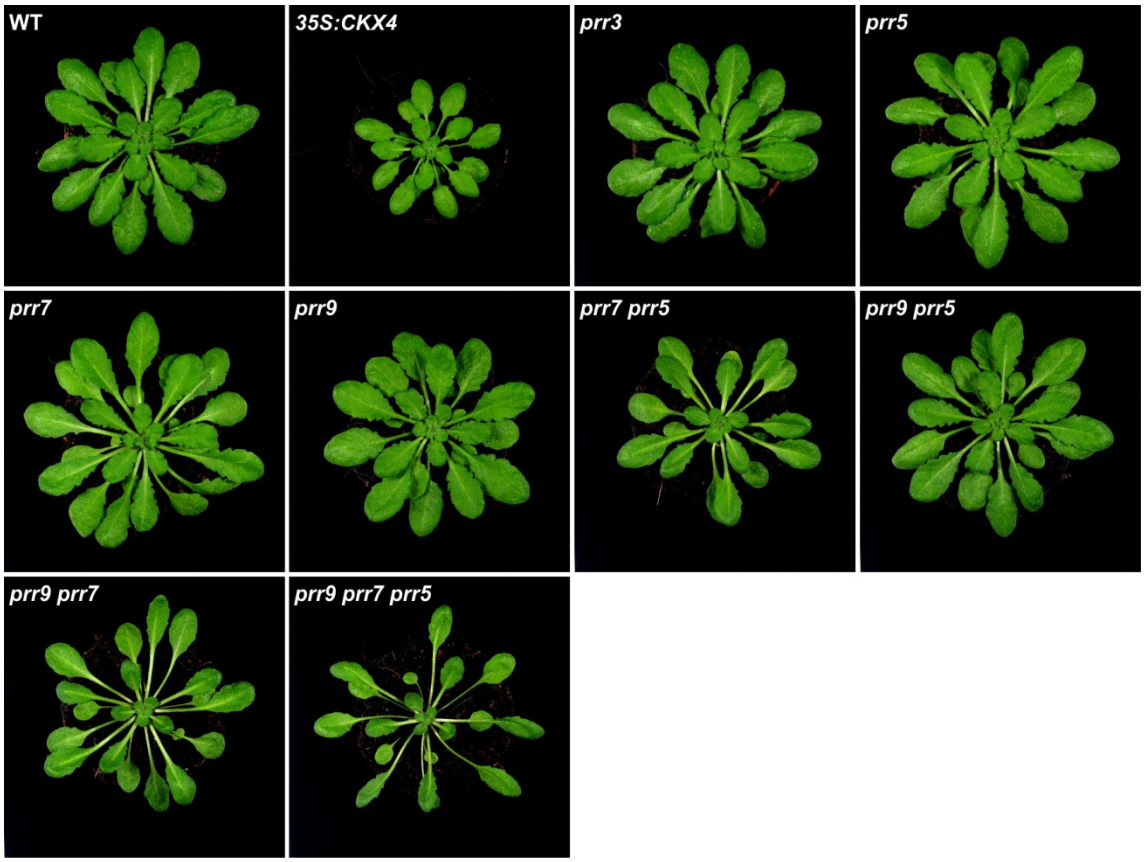

Figure A.10: Pictures of control plants corresponding to Figure 3.37.
Pictures of six-week-old SD-grown plants that served as controls for the experiment in Fig. 3.37 are shown.

A

LOX3	0 h	2.5 h	5 h	7.5 h	10 h	12.5 h	15 h	17.5 h
WT	-2.5	-1.2	-1.5	-1.1	-1.2	1.4	-1.3	1.1
35S:CKX4	-2.3	1.1	18.8	29.3	41.4	21.8	31.5	2.2
ahk2 ahk3	-4.6	-1.5	28.2	30.1	51.0	26.1	54.4	-1.7

B

LOX4	0 h	2.5 h	5 h	7.5 h	10 h	12.5 h	15 h	17.5 h
WT	-2.2	1.0	-1.2	3.6	9.1	5.0	8.5	-1.0
35S:CKX4	-2.2	-1.0	52.7	57.5	108.7	27.8	35.6	4.5
ahk2 ahk3	-3.4	1.2	73.8	124.1	89.5	47.3	67.0	2.1

C

OPR3	0 h	2.5 h	5 h	7.5 h	10 h	12.5 h	15 h	17.5 h
WT	-1.8	-1.8	-1.4	-1.2	-1.6	-1.0	2.1	1.3
35S:CKX4	-2.4	-1.4	3.2	2.6	3.6	3.8	5.6	1.4
ahk2 ahk3	-3.4	-1.9	3.3	3.3	3.5	5.8	8.6	-1.3

D

COI1	0 h	2.5 h	5 h	7.5 h	10 h	12.5 h	15 h	17.5 h
WT	1.1	-1.8	-1.1	-1.5	-1.8	-1.2	-1.9	-1.4
35S:CKX4	1.3	-1.3	-1.5	-2.3	-5.2	-5.3	-4.8	-2.8
ahk2 ahk3	-1.0	-1.7	-2.0	-3.0	-3.2	-4.8	-5.1	-2.8

E

MYC2	0 h	2.5 h	5 h	7.5 h	10 h	12.5 h	15 h	17.5 h
WT	-2.2	-2.6	-2.1	-1.3	-1.3	1.2	1.1	-2.0
35S:CKX4	-2.5	-1.2	2.9	1.5	4.5	2.4	1.7	-2.5
ahk2 ahk3	-3.6	-2.1	2.7	4.2	3.9	4.0	3.8	-4.3

F

JAZ1	0 h	2.5 h	5 h	7.5 h	10 h	12.5 h	15 h	17.5 h
WT	-1.4	-1.2	-1.3	1.4	3.5	3.6	2.8	2.8
35S:CKX4	-1.7	-1.0	8.0	7.7	18.2	10.3	9.8	9.3
ahk2 ahk3	-2.8	1.1	11.2	24.9	14.0	16.4	22.3	5.4

G

ERF1	0 h	2.5 h	5 h	7.5 h	10 h	12.5 h	15 h	17.5 h
WT	-1.6	-1.4	1.3	-1.1	2.6	4.4	2.3	-1.6
35S:CKX4	1.1	1.1	7.3	2.8	5.8	7.2	7.4	17.5
ahk2 ahk3	-1.2	2.1	7.2	5.4	5.0	14.6	17.2	8.0

Fold change [CL vs. Control]

H

ORA59	0 h	2.5 h	5 h	7.5 h	10 h	12.5 h	15 h	17.5 h
WT	-1.1	-2.0	-2.8	-5.2	1.5	1.8	-1.6	4.8
35S:CKX4	-1.0	-1.4	1.3	1.4	3.1	9.3	4.5	39.7
ahk2 ahk3	1.1	1.2	-1.2	1.8	3.9	7.7	9.9	29.6

Fold change [CL vs. Control]

Figure A.11: Fold-change tables corresponding to the gene expression data in Figure 3.42.
Tables display the respective fold changes in gene expression, comparing CL-treated plants with the corresponding control plants to facilitate the evaluation of CL-dependent changes in relative expression levels (shown in Fig. 3.42) between the genotypes. Highlighted in gray, most prominent CL-induced divergences in cytokinin-deficient plants compared with the wild type. Capital letters refer to the different panels in Fig. 3.42.

Figure A.12: Pictures of control plants corresponding to Figure 3.47.
Pictures of five-week-old SD-grown plants that served as controls for the experiment in Fig. 3.47 are shown.

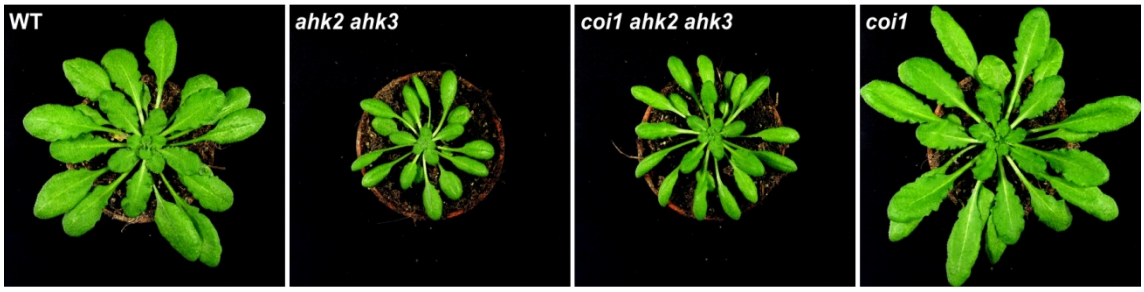

Figure A.13: Pictures of control plants corresponding to Figure 3.48.
Pictures of five-week-old SD-grown plants that served as controls for the experiment in Fig. 3.48 are shown.

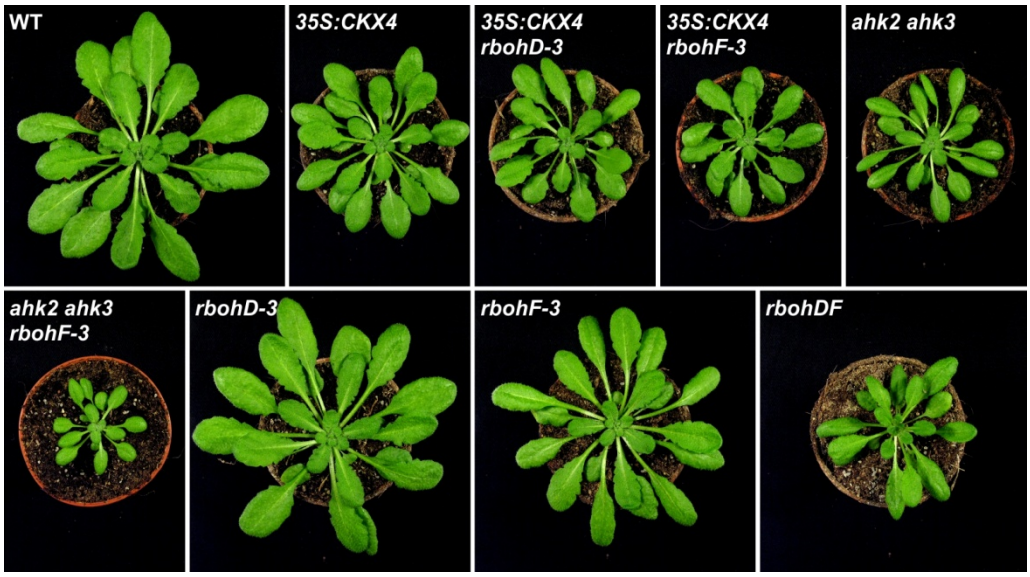

Figure A.14: Pictures of control plants corresponding to Figure 3.51.
Pictures of five-week-old SD-grown plants that served as controls for the experiment in Fig. 3.51 are shown.

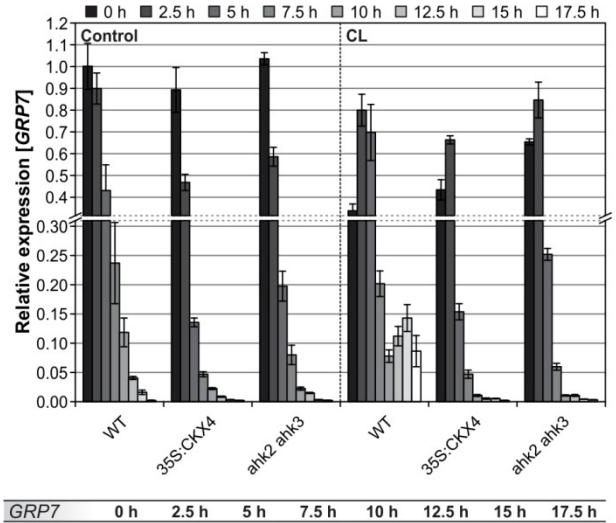

GRP7	0 h	2.5 h	5 h	7.5 h	10 h	12.5 h	15 h	17.5 h
WT	-3.0	-1.1	1.6	-1.2	-1.5	2.7	8.7	33.8
35S:CKX4	-2.1	1.4	1.1	1.0	-2.1	-1.5	1.8	-1.2
ahk2 ahk3	-1.6	1.4	1.3	-1.3	-2.1	-1.4	1.5	2.1

Fold change [CL vs. Control]

Figure A.15: Kinetics of *GRP7* (*CCR2*) expression during the dark period following continuous light treatment.
Relative expression data and the corresponding fold-change table for *GRP7* expression are shown. The experimental design corresponds to the one explained in Fig. 3.25 showing the expression profile of other clock output genes.

Acknowledgements

First of all I would like to express my gratitude to Prof. Dr. Thomas Schmülling for giving me the opportunity to join his lab although I came from a completely different field, for his supervision and guidance, and fruitful discussions. Thanks that you were persistent in asking about the "necrotic phenotype", gave me the freedom to investigate this peculiar phenomenon, and shared my enthusiasm for this topic. Thank you so much for all your support during the writing process.

I want to say thank you to Prof. Dr. Wolfgang Schuster of course for reviewing this work but also for being helpful in many other ways. Thanks for scientific discussions, your assistance with computer problems, for lending lab equipment, and for being friendly and encouraging.

I also want to say thanks to my supervisor Dr. Michael Riefler. Thank you for all support and advice during the past years. I am especially grateful for your continuous help, persistence (in dealing with the technicians), and creativity (key word "webcam") regarding the phytochambers. We both know how essential the functionality of these chambers was for my project and how unreliable and discontinuous it actually has been.

My deep thanks go to Dr. Anne Cortleven. Thank you for all the scientific discussions we had, for your constructive criticism, your advice, helpfulness and kindness. I enjoyed working with you. Thank you for the great collaboration on the HL project, for your patience and endurance in this respect and for bringing forward the manuscript.

I want to thank Prof. Dr. Han Asard and Hamada AbdElgawad (University of Antwerp, Belgium), Prof. Dr. Michel Havaux (CEA Cadarache, Saint-Paul-lès-Durance, France), and not least Prof. Dr. Ivo Feussner and Dr. Tim Iven (Albrecht-von-Haller-Institute for Plant Sciences, University of Göttingen) for the successful collaboration.

To Prof. Dr. Tatsuo Kakimoto, Prof. Dr. Takeshi Mizuno, Prof. Dr. Rachel Green, Prof. Dr. C. Robertson McClung, Dr. Jos Schippers, and Dr. Patrice Salomé: thank you for kindly providing seeds of mutant and transgenic plants that were valuable for the circadian stress project.

Many thanks to the Gardner team! Without you it would have been impossible. Special thanks to Frau Losensky! Thank you to everyone who helped sieving the vast amount of seeds.

I thank Dr. Diana Mutz not only for her work as DCPS coordinator – organizing many great meetings – but also for constantly supporting us, the PhD students, and for the marvelous idea to create the *Eltern-Kind-Zimmer*, which was a comfy haven during long-term experiments.

I am grateful to the DRS and the CRC973 for financing this work.

Special thanks to all present and former co-workers in Lab 104, office colleagues, and other members of the institute. You have provided a welcoming, warm, and fun atmosphere, were helpful in multiple ways, and have contributed to an enjoyable and memorable time at the institute.

There are no words to express my endless gratitude to my family. Thank you for believing in me, encouraging me, and supporting me, for your patience and for simply being there. Thank you Felix and Leila, you are so precious to me!